

## RESEARCH PAPER

# Assessment of Risk Behaviors and Toxic Heavy Metals Exposure of Car Dye Workers in Repairing Services in Erbil City, Kurdistan Region, Iraq

Hawraz Sami Khalid\*, Shokhan Sherzad Hamadamin, Hanan Salm Salih

Department of Chemistry, College of Education, Salahaddin University-Erbil, Erbil City, Kurdistan Region, Iraq

### ABSTRACT:

The main objective of this study was to determine blood cadmium (BCd) and blood lead (BPb) contents for 16 car dye workers in repairing service and compared to those of 16 controls (non-occupational exposed subjects) in Erbil City, Kurdistan Region, Iraq. Strong wet acid digestion method was applied to digest whole blood samples using a mixture H<sub>2</sub>O<sub>2</sub> (50% v/v) and HNO<sub>3</sub> (65% v/v) with a volume ration (1:2). Inductively coupled plasma - optical emission spectrometer (ICP-OES) was used to determine these toxic metals in collected whole blood samples. The recorded mean of BCd and BPb contents in subjected painters were higher levels compared to the control group. The mean  $\pm$  standard deviation (SD) contents of BCd and BPb of painters were 2.93 $\pm$ 2.35  $\mu$ g/L and 32.19 $\pm$ 16.95  $\mu$ g/L, respectively. The mean  $\pm$  SD contents of BCd and BPb of controls were 0.870 $\pm$ 0.34  $\mu$ g/L and 22.46 $\pm$ 12.55  $\mu$ g/L, respectively. A set of formal investigation questionnaire was performed to know participants history profile, smoking status, clinical profile, the risk behaviors at the workplace, and occurrence symptoms. The results showed that the percentages of occurrence of most investigated symptoms (especially respiratory and musculoskeletal) system on the experimental painters were significantly (p-value = 0.016) higher than those symptoms of the control group. The collected data on risk behaviors confirmed that personal protection equipment (PPE) had not been concerned by most of the experimental painters. Duration of work (years), and the use of PPE (wearing a respirator) were noticeably associated with BCd and BPb levels of painters.

KEY WORDS: Heavy metals, Blood, Painters, ICP-OES, Erbil City

DOI: <http://dx.doi.org/10.21271/ZJPAS.32.6.1>

ZJPAS (2020) , 32(6);1-13 .

## 1. INTRODUCTION

Due to the continuing of industrial activities, the presence of toxic heavy metals in the environment has become major pollution, health problem and widely released and detected in the air (Amin et al., 2017), water (Aziz and Rasheed, 2017), food (Al-Attar, 2016),

soil (Mwstefa and Ahmed, 2019), and many other natural and human-made samples. Lead and cadmium which are the most harmful heavy metals that are broadly used in the manufacture of batteries, the color pigment in paints, several alloys, piping, electrical systems, construction materials, industrial agents, stabilizers, and a variety of other occupational purposes (Järup, 2003). During the last decades, the toxic heavy metals exposure to the human body has been encountered in several ways such as water consumption, inhalation of polluted air, skin contact, food ingestion, and occupational exposure

### \* Corresponding Author:

Hawraz Sami Khalid

E-mail: [hawraz.khalid@su.edu.krd](mailto:hawraz.khalid@su.edu.krd)

### Article History:

Received: 02/06/2020

Accepted: 23/07/2020

Published: 20/12/2020

at the workplace. Thus, heavy metals could enter the human body, accumulate for a long half-life, and slowly released from the human compartment. Human blood and urine samples are the most common, known, and scientifically recommended matrices to bio-monitor and assess toxic heavy metal exposure in environmental and occupational (Ladeira and Viegas, 2016). These matrices could be used as the direct approach, provide prerequisite and unequivocal evidence for evaluating human exposure to natural and synthetic chemicals from surroundings (Schulz et al., 2011).

In the recent years, several biomonitoring studies have been intensively carried out on human immune (Marth et al., 2001), hematopoietic (Pyszal et al., 2005), diabetes mellitus (Akinloye et al., 2010), cardiovascular (Solenkova et al., 2014), renal (Lentini et al., 2017), prenatal (Taylor et al., 2018), and musculoskeletal (Rodríguez and Mandalunis, 2018) systems effects due to cadmium and lead metal exposure. To monitor heavy metals exposure, compare purposes, and evaluate risk behaviors, the establishment of reference values for blood metals have been early proposed and scientifically set by many countries including the different European community countries (Sabbioni et al., 1992), the Czech Republic (Černá et al., 2001), Germany (Wilhelm et al., 2004), and the United States (CDC, 2013) based on the investigation of their normal and healthy population.

More recent papers also prove the view that environmental and occupational exposures to the risk of toxic metals have been persisted to be a major public health concern in the world. Workers blood lead and cadmium levels were significantly associated with the occupation, environment, lifestyle, and risk behaviors (An et al., 2017, Ishola et al., 2017, Junaid et al., 2017, Khlifi et al., 2014, Mierna et al., 2015, Vitayavirasuk et al., 2005). There are numerous studies in the literature to assess blood heavy metals exposure of country workers such as batteries worker in Poland (Wasowicz et al., 2001), sanitary landfill and painter workers in Thailand (Decharat, 2016, Vitayavirasuk et al., 2005), steel and leather workers in Pakistan (Afridi et al., 2011, Junaid et al., 2017), welder workers in Indonesia (Mierna et al., 2015), changers, mechanics and metalworkers in Nigeria (Ishola et al., 2017, Sani and Abdullahi, 2017), e-waste workers in Ghana (Wittsiepe et al.,

2017), smelting workers in Korea (An et al., 2017) and different manufacturing workers in Iran (Nakhaee et al., 2019).

Paint is generally classified into two main types including industrial and decorative (domestic) paints which are broadly utilized to protect, decorate, and preserve surface or object by covering it with a varying pigmented coating. Decorative paints which are either oil-based or water-based are mainly applied for the exterior or interior decoration of homes and buildings surface. However, industrial paint products are commonly applied in automobile coatings, marine coatings, steel structures, and many other high-performance purposes (Kameti, 2013). Paints are mainly included four important components which are pigment, binder, solvent, and required additives. Pigments are generally categorized as either synthetic or natural solid granular which is added into the paint as a powder to contribute color, texture, and toughness (Buxbaum, 2008).

Heavy metals which are known as the most polluting chemicals in the environment have been commonly encountered and used in paints as pigments and recorded with a high amount in various paint samples (Apanpa-Qasim et al., 2016, Kameti, 2013, Ogilo et al., 2017, Okewole and Omin, 2013, Hsu et al., 2018). Lead and cadmium have been used as paint pigments as they speed drying, increase durability, retain a fresh appearance, and resist moisture that causes corrosion.

Kameti (2013) revealed that a high level of Pb metal in the oil-based paints with a range of 275.86 – 37084.48 mg/L was recorded and exceeded the set limit of 90 mg/L by far. However, the recorded level range for Pb in water-based paint was 48.53 – 298.38 mg/L and lower than this metals level in oil-based paint. Okewole and Omin (2013) stated that in both oil and water-based paints manufactured in the city of Lagos, Nigeria, Pb contents ranged from 4.271 to 49.609 mg/L and 0.391 to 2.194 mg/L respectively while the corresponding Cd contents were recorded to be 0.733 – 0.991 mg/L and 0.810 – 1.334 mg/L. Apanpa-Qasim et al. (2016) verified that the levels of lead and cadmium in the 174 various dry paint samples sold in Lagos and Ibadan ranged from 170–3231 mg/Kg and 98–1999 mg/Kg, respectively. They also mentioned that the levels of the selected metals in all the examined samples were exceeded permissible

limits (90 mg/Kg for Pb and 100 mg/Kg for Cd in dry paint) of the US and EU Consumer Product Safety Commission respectively. According to a recent study in Nairobi City County, Kenya, the recorded mean concentrations (ranges) of Cd, Cr, Pb, and Zn were 73.45 mg/Kg (3.07 to 89.87 mg/Kg), 77.54 mg/Kg (12.39 to 189.01 mg/Kg), 289.59 mg/Kg (16.86 to 740.52 mg/Kg), and 321.77 mg/Kg (38.63 to 1056.37 mg/Kg) for the house paint chip samples respectively (Ogilo et al., 2017). Hsu et al. (2018) mentioned that the recorded levels of lead in a car refinishing solvent-based paints were two to three orders of magnitude higher than these found levels in water-based paints, especially in yellow and red paints. They suggested that water-based paints can be used as eco-friendly paints and to decrease the exposure potential of refinishing painters to lead metal. Hsu et al. (2018) found that lead levels ranged from 0.25 mg/Kg to 107,928 mg/Kg in solvent-based paints, while the Lead levels in water-based paints were low and ten times lower than that in the solvent-based paints.

During spray painting, the paint can easily cause aerosolization, disperses in the air, and consequent inhalation exposure to these ingredients by painters. Thus, painters in automobile painting services may inhale paint and are potentially exposed to toxic chemical and safety hazards during spray painting at their workplace (Kim et al., 2013). In a particular case study, Kim et al. (2013) investigated that the developed lung cancer of bumper spray painter in an automobile body shop for 15 years seems to have been affected by yellow paint, which causes increasing the level of heavy metals in the workplace air. They suggested that the uses of eco-friendly paint are better than the normal paint due to the present low levels of hexavalent chromium and lead chromate.

The main objective of the study was to assess the concentration of heavy metals, including cadmium and lead in blood samples of experimental automobile dye workers/painters group and control group (non-painters) in Erbil city; evaluating of the history profile, clinical profile, and work characterization of the study subjects; and surveying of the automobile painters risk behaviors during spray painting; comparing selected metals level in the experimental control group with other world countries group.

## 2. MATERIALS AND METHODS

### 2.1. Chemicals and Instruments

All chemicals were of analytical grades including nitric acid ( $\text{HNO}_3$  65% v/v) and Hydrogen peroxide ( $\text{H}_2\text{O}_2$  50% v/v) (Scharlau, Spain, Extra Pure). Distilled water was used to wash glassware and dilute samples. Inductively coupled plasma - optical emission spectrometer (ICP-OES, Spectro Arcos FHS22, GmbH, Kleve, Germany) was utilized as an advanced instrument during metal analysis. Classical Digestion-Heater (Gerhardt) with digestive Kjeldal's flask was used during blood digestion.

### 2.2. Sample Collection

During sampling (December 2019), a blood sample for metal analysis was collected from two different worker groups in Erbil city, Kurdistan Region, Iraq. The first group was sixteen automobile dye workers (exposed group) in the different automobile repairing services workplace, while the second group was sixteen control workers (none exposed group). None exposed group was control workers who have not used and worked with any chemical products yet. After sampling, whole blood samples were directly and individually kept in the special clean blood test tube, labeled and preserved in a refrigerator till the digestion process. To collect informative data on participants, a set of formal investigation questionnaire was performed and directly asked participants to know their history profile, smoking status, clinical profile, risk behaviors at the workplace, and symptoms occurrence.

### 2.3. Sample Digestion

Prior to sample digestion, all glassware equipment was cleaned and washed with dilute nitric acid solution and distilled water to avoid contamination. A strong wet acid digestion method was applied according to common previous applied studies (Alrobaian and Arida, 2019, Badran et al., 2018, Lech, 2013, Junaid et al., 2016) for completing the whole blood digestion. During digestion, 2.5 mL of the blood sample was quantitatively added to digestive Kjeldal's flask and then treated with 2 mL of  $\text{H}_2\text{O}_2$  (50% v/v) and 4 mL of  $\text{HNO}_3$  (65% v/v) by using Classical Digestion-Heater until completing the digestion process. After cooling, the clear solution was quantitatively transferred; diluted to 5 mL with distilled water, and then labeled before

being analyzed by ICP-OES instrument. In the same conditions, digestion processes were repeated three times for the collected blood samples and blank. The blank solution which contains only the digested chemicals was individually used for calibration purposes or zeroed the absorbance of all the other presented components in the sample solution except the component of interest.

#### 2.4. Metal Analysis

Inductive capable plasma - optical emission spectrometer (ICP-OES, Spectro Arcos) was used as an advanced instrument to detect blood cadmium (BCd) and blood lead (BPb) contents in collected whole blood samples. Optimum operating conditions for the instrument were easily selected and conducted because all operating parameters are software controlled. The detailed fundamental features of the instrument, applied operating conditions in the analysis, and selected wavelengths (lines) with a limit of detection (LOD) for the investigated metals were chosen according to instrument manufacture (AMETEK, FHS22) and are presented in **Tables 1** and **2**. The instrument was also calibrated against multi-element standards. The accuracy and precision of the method were investigated in excellent agreement for the analyzed elements using the standard reference material SRM 1640 (Trace Elements in Natural Water) (AMETEK, FHS22). A limit of detection (LOD) for the analyzed metals is calculated according to **Equation 1** as follows.

$$\text{LOD} = \frac{3 \text{ RSDb} \cdot c}{\text{SBR}} \quad (\text{Equation 1})$$

Where, RSDb, c, and SBR denote relative standard deviation of 10 replicates of the blank, concentration of the standard, and signal to background ratio.

**Table 1:** shows ICP Operating Conditions

Parameters	Condition
Power	1280 W
Coolant flow	13 L/min
Auxiliary flow	0.8 L/min
Nebulizer flow	0.75 L/min
Plasma Torch	Quartz, demountable, 1.8 mm injector tube
Spray Chamber	Cyclonic

Nebulizer	SeaSpray
Sample aspiration rate	2.0 mL/min
Replicate read time	48 sec per replicate

**Table 2:** shows LOD for selected lines (nm)

Metal (Symbol)	Wavelength Line (nm)	LOD 3 $\sigma$ ( $\mu\text{g/L}$ )
Cadmium (Cd)	214.438	0.333
Lead (Pb)	220.351	3.44

#### 2.5. Statistical Analysis

Results data of the BCd and BPb contents were calculated and expressed as parts per billion ( $\mu\text{g/L}$ ) and are shown as mean  $\pm$  standard deviations (SD) in tables. The data were subjected to statistical significance analysis by using GraphPad Prism 6 and Microsoft Excel 2010 software program. Statistical analysis was conducted using Student's t-test and the significance level was set to 0.05.

### 3. RESULTS AND DISCUSSIONS

#### 3.1. History Profile and Work Characteristics

In the present study, the participated subjects were sixteen automobile spray painters (exposed group); sixteen control workers (non-exposed group) who have not used or worked with any chemical's product yet. All attended subjects were Kurdish, male gender, workers, 42 $\pm$ 6 years old, and lived in Erbil city, Kurdistan Region, Iraq.

Detailed information on the participant's profile and work characteristics including gender, age, occupation, weight, education, smoking status, and working experience, were collected through conducting the formal questionnaire and are shown (as mean $\pm$ SD & %) in **Table 3**. In the same table, the given results of the study were also compared with the previously reported studies (Vitayavirasuk et al., 2005). Note that statistical data of an analysis of variance (ANOVA) showed that there is no significant difference (p-value = 0.403) among the recorded results between the participated study profile information with the compared study (Vitayavirasuk et al., 2005) excluding their education profile. Although painters age, weight, and work experience duration data (means  $\pm$ SD) for the present study were 42 $\pm$ 6 yrs, 77 $\pm$ 12 Kg, and 21.0 $\pm$ 8.3 yrs, respectively, while the data for the previously

reported painters were noticeably lower and equal to  $27\pm7$  yrs,  $56\pm9$  Kg, and  $8.3\pm5.6$  yrs,

respectively (Vitayavirasuk et al., 2005).

**Table 3:** compares history profile of this study subjects with a previous study (Vitayavirasuk et al., 2005)

History profile	This study		(Vitayavirasuk et al., 2005)	
	Exposed subjects	Controls	Exposed subjects	Controls
<b>Kinds of occupation</b>	Painters*	Non-painters*	Painters*	Non-painters*
<b>Nationality</b>	Kurdish/Iraqi	Kurdish/Iraqi	Thai	Thai
<b>Sex (%male)</b>	100	100	100	100
<b>Age (years old) <sup>m</sup></b>	42.0±6	42.0±7	27.0±7	26.0±7
<b>Weight (Kg) <sup>m</sup></b>	77.0±12	79.0±13	56.0±9	57.0±7
<b>Work duration (years) <sup>m</sup></b>	21.0±8	13.5±6	8.3±5.6	7.8±5
<b>Daily working (hours) <sup>m</sup></b>	9.0±2	10.0±2	8.0±1	8.0±1
<b>Smoker (%)</b>	68.8	56.2	64.3	31.4
<b>Non-smoker (%)</b>	31.2	43.8	35.7	68.6
<b>Education (%)</b>				
<b>Under graduated (%)</b>	12.5	12.5	0.0	0.0
<b>12<sup>th</sup> grade (%)</b>	0.0	18.75	15.7	20.0
<b>9<sup>th</sup> grade (%)</b>	18.75	25.0	24.3	25.7
<b>6<sup>th</sup> grade (%)</b>	56.25	12.5	60.0	54.3
<b>Illiteracy (%)</b>	12.5	31.25	0.0	0.0

\*; no significant difference as  $p$ -value = 0.403, Non-painters; controls or workers who have not used and worked with any chemical products yet, <sup>m</sup> : represented results as mean ±SD,

### 3.2. Occupational Risk Behaviors

Due to conducting a formal questionnaire, detailed information on hygiene and risk behaviors in this study were only collected on participated painters. Data on the painter's risk behavior were compared with another previously examined study (Vitayavirasuk et al., 2005) and are presented in **Table 4**. According to data in the present study, in the worst situation, all the painters stated that they are not wearing a protective hat and cloth during spray painting in the automobile repairing services workplace in Erbil City. The whole painters also declared that they do not have the isolated laundry for clothes worn at work; they are not always taking a shower immediately after work; they are not going home with the same working clothes. In the present study, note that 37.5% of the painter's subjects were also not wearing respirator equipment during spray painting. Thus, the

collected data on risk behaviors confirm that personal protection equipment (PPE) was not concerned by most of the experimental painters. Statistical data (paired t-test) proved that there is no significant difference ( $p$ -value = 0.337) between the painter's risk behaviors among these two compared studies (**Table 4**). Painters may face harmful chemicals because spray paint can easily cause aerosolization and consequent inhalation exposure to hazardous chemical ingredients by the painter (Vitayavirasuk et al., 2005). Tahir et al. (2010) mentioned that workers, air, plants, soil, and all environments around the "Auto body refinishing" service shops were potentially exposed to aerosolized organic solvents, noise, dust, and metal pigments.

**Table 4:** Comparison of Frequencies of the study subjects (painters) risk behaviors

Risk behaviors at work	Frequency (%)	
	This study*	(Vitayavirasuk et al., 2005)*
Not wearing a protective hat at work	100	87.2
Not wearing protective clothing at work	100	91.4
Not wearing a respirator while spraying	37.5	72.8
Smoking without washing hands first	68.8	64.3
Eating food/drinking water without washing face first	12.5	74.3
Eating food/drinking water without washing hands first	12.5	30.0
Not always taking a shower immediately after work	100	85.7
No separate laundry for clothes worn at work	100	92.9
Going home the same working clothes	100	87.1
Always living at the workplace	0.0	30.0

\*; no significant difference as p-value = 0.337

### 3.3. Occurrence Symptoms

Frequency data of occurrence of symptoms related to painters digestive, respiratory, musculoskeletal, and nervous systems are shown in **Table 5** amongst this study and earlier reported study (Vitayavirasuk et al., 2005). Finding data in this study showed that the percentages of occurrence of most investigated symptoms (especially respiratory and musculoskeletal system) on the experimental painters were significantly (paired t-test, p-value = 0.016) higher than those symptoms

of the study control group. Statistical data also showed that the frequencies of evaluated painters symptoms reported in the previous study (Vitayavirasuk et al., 2005) were also significantly (paired t-test,  $p < 0.0001$ ) different and higher than that symptoms result on the present control group. Thus, results reveal that the presence of high symptoms of diseases on experimental painters could come from the effects of their occupation (painting), risk behaviors, and workplace environment.

**Table 5:** Comparison studies data of occurrences of symptoms between subjects group

Symptoms	Frequency (%)			
	This study		(Vitayavirasuk et al., 2005)	
	Study subjects (Painters)**	Controls** (Non-painters)	Study subjects (Painters)**	Controls (Non-painters)
<b>Digestive system</b>				
Dry mouth	37.5	18.75	54.3	32.4
Sore throat	12.5	25	54.3	20.3
<b>Respiratory system</b>				
Nasal congestion	25	18.75	44.3	32.4
Cough	25	0.0	30.0	18.9
Sneezing	25	12.5	38.6	24.3
Asthma	37.5	0.0	4.3	1.4
Nasal irritation	12.5	12.5	32.9	8.1
Phlegm discharge	25	18.75	34.3	17.5
<b>Musculoskeletal system</b>				

Muscle pain	43.75	25	44.3	24.3
Tremor	25	6.25	30.0	14.8
Joint pain	37.5	25	34.3	13.5
<b>Nervous system</b>				
Poor co-ordination	31.25	6.25	35.7	5.4
Insomnia	12.5	25	30	14.8
Numbness of extremities	12.5	31.25	32.9	10.8
<b>Forgetting</b>	50	18.75	NA	NA
<b>Angry</b>	37.5	31.25	NA	NA

NA: none available, \*\* significant difference as p-value < 0.05

### 3.4. Heavy Metals Level

Blood cadmium (BCd) and blood lead (BPb) contents were determined for sixteen automobile painters (exposed group) and compared to those of sixteen control group (non-occupational exposed subjects) in this study. Detailed information on the recorded BCd and BPb contents in the present study are shown in **Table 6**. The detected mean±SD (range) for BCd and BPb contents of overall examined painters were 2.93±2.35 µg/L (ND – 7.52 µg/L), and 32.19±16.95 µg/L (ND – 61.64 µg/L), respectively. However, the recorded mean±SD (range) for BCd and BPb contents of overall controls group were 0.870±0.34 µg/L (ND – 1.46 µg/L), and 22.46±12.55 µg/L (ND – 26.15 µg/L), respectively. Findings data verify that the documented contents of BCd and BPb in automobile painters were increased due to the increase in subjects' work experience (working

years). Data also confirmed that both BCd and BPb contents were noticeably increased ongoing to not using and wearing respirator equipment by participated painters (PNWR).

The mean with a standard deviation of BCd and BPb concentrations (µg/L) in the study was clearly illustrated in **Figure 1**. Statistical data (Unpaired t-test, Assuming Unequal Variance) confirmed that the recorded mean content of BCd (2.93±2.35 µg/L) in the participated painters was three times significantly (p-value = 0.044) higher than that content (0.870±0.34 µg/L) in the study control group. However, the detected mean content of BPb (32.19±16.95 µg/L) in the examined painters was also higher (not significantly, p-value = 0.205) than that content (22.46±12.55 µg/L) in the examined control group due to using a statistical Unpaired t-test and assuming both populations have the same variance (**Table 6**).

**Table 6:** Variables related to study subjects blood Cd levels and blood Pb levels

Characteristics	Comparison of blood metal level (µg/L)			
	Cd	p-value	Pb	p-value
<b>Overall painters group</b>				
Mean ± SD	2.93±2.35**	<b>0.044</b>	32.19±16.95*	0.205
(Range)	(ND – 7.52)		(ND – 61.64)	
n	16		16	
<b>Overall controls group</b>				
Mean ± SD	0.870±0.34**		22.46±12.55*	
(Range)	(ND – 1.46)		(ND – 26.15)	
n	16		16	
<b>Painters Subject</b>				
<b>Work experience (yrs)</b>				
< 15	1.66±1.70*	0.424	26.0±16.70*	0.596
≥ 15	3.25±2.50*		33.4±17.60*	
<b>Wearing respirator</b>		0.214		0.148

Wearing (PWR)	1.76±1.40*		22.00±10.10*	
Not wearing (PNWR)	3.72±2.60*		37.30±17.90*	

SD; standard deviation, ND; not detectable, \*; no significant difference, \*\* significant difference, PNWR: painters not wearing a respirator, PWR: painters wearing a respirator

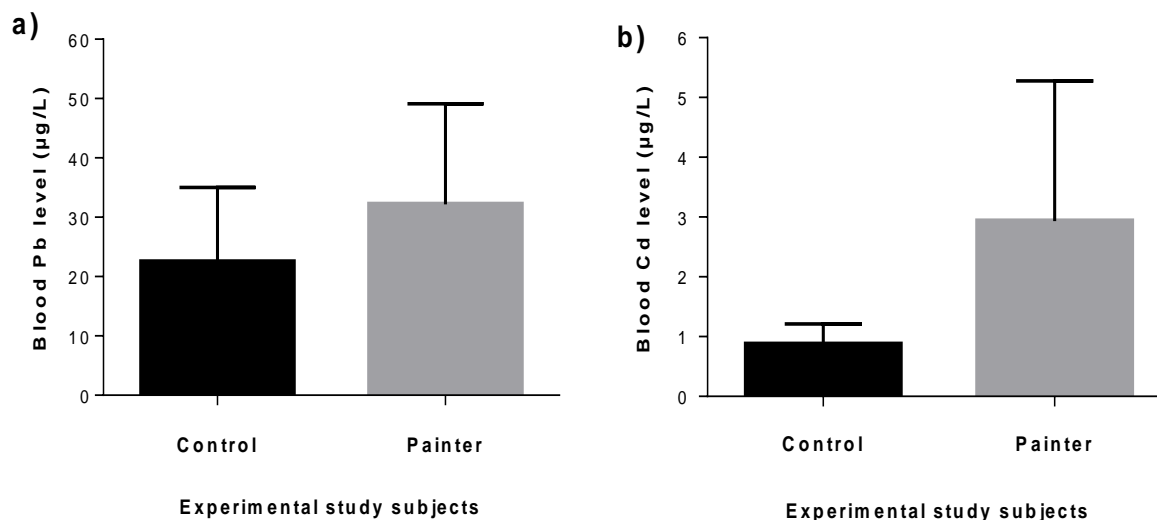


**Figure 1:** Illustrates study subject's comparison as mean±SD (µg/L) for a) BPb content and b) BCd content

The recorded average for BCd and BPb contents in the study control group (Kurdish people) and the other sixteen different country controls previously reported for different healthy nationalities in the world are clearly ordered, compared and shown in **Figures 2** and **3**, respectively. The compared and previous reported world controls were Thai (Sirivarasai et al., 2002), Czech (Batáriová et al., 2006), German (Heitland

and Köster, 2006), American (Crinnion, 2010), Italian (Forte et al., 2011), Pakistani (Shafique et al., 2011), Korean (Kim and Lee, 2011), Iraqi (Hassan et al., 2011) Emirati (Yousef et al., 2013), Chinese (Zhang et al., 2015), Turkish (Akinci et al., 2016), Iranian (Aliomrani et al., 2016), Nigerian (Ishola et al., 2017), Ghanaian (Wittsiepe et al., 2017), Serbian (Stojsavljević et al., 2019), and Saudi (Alrobaian and Arida, 2019) people.



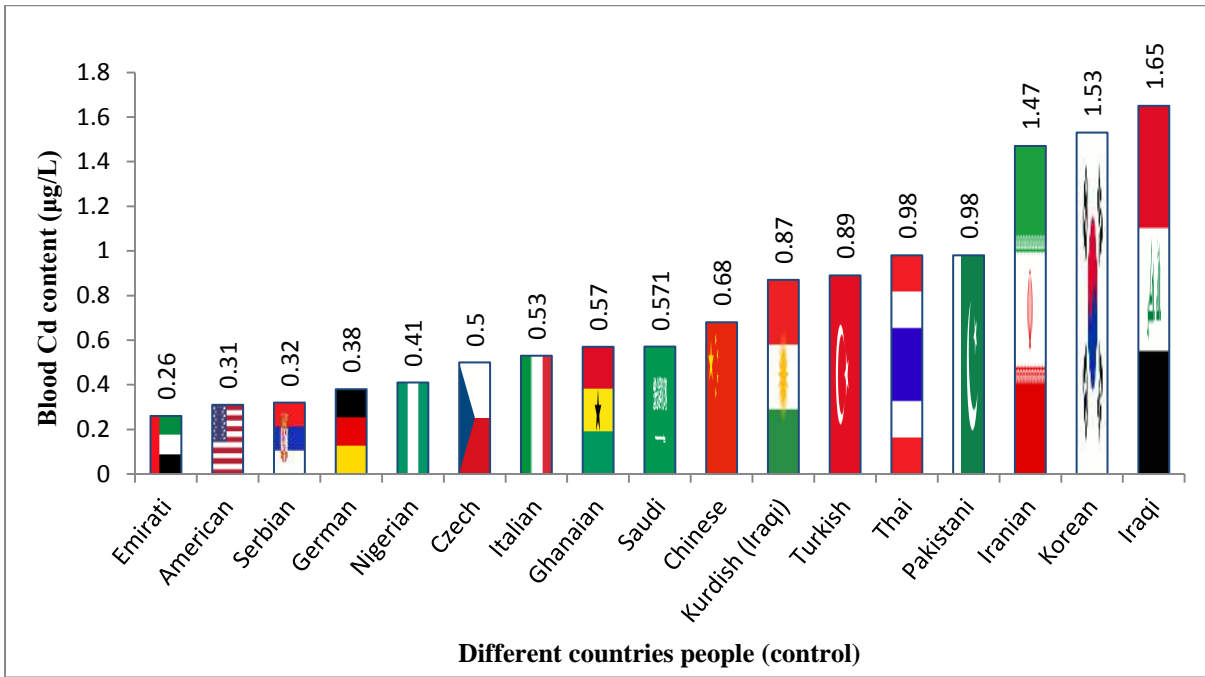


Figure 2: shows a comparison of the recorded average of BCd level (µg/L) of different countries control people

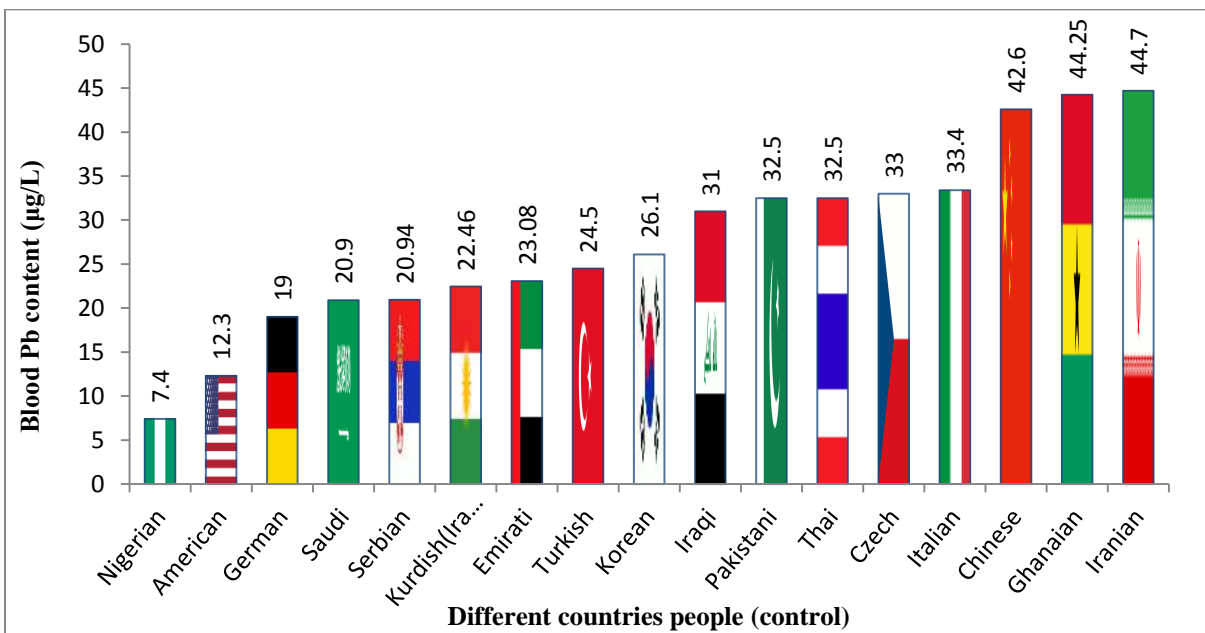


Figure 3: shows a comparison of the recorded average of BPb level (µg/L) of different countries control people

Statistical data (One-Sample t-test) showed that there is no significant difference (p-value = 0.315) between the whole compared controls (16 world controls) with this study control group for the recorded average of BCd level. A comparison of statistical data showed that there is also no significant difference (p-value = 0.058) between the recorded contents of BPb level in this study (Kurdish people) with all the sixteen mentioned

world controls. Thus, results verify that there is a good agreement between the recorded mean of

BCd and BPb contents in the control group in this study with the recorded data of sixteen previously reported controls in the world. Consequently, the recorded average of each BCd and BPb contents in the present study for the experimental control group can be seen as a normal resident baseline, reference value for healthy Kurdish residents and used to monitor heavy metals exposure, compare

purposes, and evaluate occupational risk behaviors.

The detected average for BCd and BPb contents in the participated study painters were compared with that previously reported data in the other different countries worker and are shown in **Table 7**. According to data in the **Table 7**, the detected mean for BPb content in the present study was lower than that previously reported content from painters (Vitayavirasuk et al., 2005), welders (Mierna et al., 2015), sanitary landfill (Decharat, 2016), spray painters, battery chargers, mechanics (Ishola et al., 2017), metal workers (Sani and Abdullahi, 2017), leather (Junaid et al., 2017), smelting (An et al., 2017) e-waste (Wittsiepe et

al., 2017), and painting, printing, rubber, mining and mechanics (Nakhaee et al., 2019) workers occupation.

However, the recorded mean for BCd content in the overall examined painters in this study was higher than that content previously reported from (**Table 7**) welder workers (Mierna et al., 2015), sanitary landfill workers (Decharat, 2016), spray painters, battery chargers, mechanics (Ishola et al., 2017), metal workers (Sani and Abdullahi, 2017), e-waste workers occupation (Wittsiepe et al., 2017). High BCd contents (8.39  $\mu\text{g/L}$  and 10.53  $\mu\text{g/L}$ ) were detected from leatherworkers (Junaid et al., 2017) and smelting workers (An et al., 2017) occupation respectively.

**Table 7:** Comparison of the recorded BCd and BPb contents ( $\mu\text{g/L}$ ) for various occupational workers

Location	Study subjects Worker	Cd	Pb	References
Erbil, Iraq	Overall Painters	2.93±2.35	32.19±16.95	This study
	Painters (PNWR)	3.72±2.60	37.3±17.90	
	Painters (PWR)	1.76±1.40	22.00±10.10	
Hat Yai Thailand	Painters (PWR)	0.57±0.26 †	86.2±27.2	(Vitayavirasuk et al., 2005)
	Painters (PNWR)	0.76±0.54 †	104.2±40.7	
Benin, Nigeria	Spray Painters	1.16 ± 0.67	47.2 ± 19.2	(Ishola et al., 2017)
	Battery Chargers	0.97 ± 0.33	62.0 ± 21.2	
	Mechanics	1.17 ± 0.52	47.4 ± 23.5	
Khorasan, Iran	Painting, printing, rubber, mining & mechanics	NT	65.0±81	(Nakhaee et al., 2019)
Ulsan, Korea	Smelting worker	10.53	58.39	(An et al., 2017)
Kano, Nigeria	Metal worker	2.50±1.4	190.7±16.9	(Sani and Abdullahi, 2017)
Songkhla, Thailand	Sanitary landfill workers	2.95±0.58	85.8±25.8	(Decharat, 2016)
Ghanian	e-waste worker	0.55	101.9	(Wittsiepe et al., 2017)
Jakarta, Indonesia	Welder worker	0.9	45.12	(Mierna et al., 2015)
Sialkot, Pakistan	Leather worker	8.39 ± 4.87	119.04 ± 59.32	(Junaid et al., 2017)

PWR: painters wearing a respirator, PNWR: painters not wearing a respirator, NT: not tested, †: urinary cadmium (mg/Kg creatinine) for painters

The results in the present study (**Table 6 & 7**) showed that the detected averages for both BCd and BPb contents in the participated painters wearing a respirator (PWR) were higher than that contents in the subjected painters not wearing a respirator (PNWR). Vitayavirasuk et al. (2005) also reported that the detected blood lead and urine cadmium contents were increased in the subjected automobile painters who were not wearing a respirator (PNWR) during spray

painting (**Table 7**). The presented high amount of BCd and BPb contents from participated painters could come from their occupation because the paint can easily cause aerosolization, disperses in the air, and consequent inhalation exposure to these ingredients by painters during spray painting. Thus, painters in automobile painting services may inhale paint and are potentially exposed to toxic chemical and safety hazards during spray painting at their workplace (Kim et

al., 2013). Tahir et al. (2010) stated that the process of spray painting is continuously deposited and affects the environment including workers, air, plants, and exposed soil. Thus, the soil around the auto body refinishing services is exponentially contaminated with the released chemicals. Tahir et al. (2010) announced that 36 soil samples collected around 26 different auto body refreshing workplaces were generally contaminated due to the exposure of metals pigment. Thus, the study confirms that more precaution needs to be taken by painters during spray painting.

#### 4. CONCLUSION

Occupational exposure at a workplace can be classified as one of the most important diverse forms to exposure of heavy metals to humans. This study revealed that pigment spray of the automobile body is such a kind of occupation that can affect car dye workers, and cause to the presence of high symptom diseases on painters. The results confirmed that the levels of BCd and BPb contents from the subjected painters were higher than that contents from the control group. The study suggested that more precaution needs to be taken by painters during spray painting.

#### ACKNOWLEDGEMENT

I would like deeply thank the participated painters and control group at Erbil city who allowed us to take blood sampling during this research project.

#### References

AFRIDI, H. I., KAZI, T. G., KAZI, A. G., SHAH, F., WADHWA, S. K., KOLACHI, N. F., SHAH, A. Q., BAIG, J. A. & KAZI, N. 2011. Levels of arsenic, cadmium, lead, manganese and zinc in biological samples of paralysed steel mill workers with related to controls. *Biological trace element research*, 144, 164-182.

AKINCI, I., TUTKUN, E., TURKSOY, V., YILMAZ, H., YUKSEL, B., KAYAALTI, Z., SOYLEMEZOGLU, T., YILMAZ, H. & ABUSOGLU, S. 2016. Toxic metal and essential trace element levels of blood donors. *J Clin Anal Med*, 7, 816-9.

AKINLOYE, O., OGUNLEYE, K. & OGUNTIBEJU, O. O. 2010. Cadmium, lead, arsenic and selenium levels in patients with type 2 diabetes mellitus. *African Journal of Biotechnology*, 9, 5189-5195.

AL-ATTAR, M. S. 2016. Effects of Nickel and Cadmium Contaminated Fish Meat on Chromosomal Aberrations and Sperm Morphology of Swiss Albino Mice. *ZANCO Journal of Pure and Applied Sciences*, 28.

ALIOMRANI, M., SAHRAIAN, M. A., SHIRKHANDLOO, H., SHARIFZADEH, M., KHOSHAYAND, M. R. & GHAREMANI, M. H. 2016. Blood concentrations of cadmium and lead in multiple sclerosis patients from Iran. *Iranian journal of pharmaceutical research: IJPR*, 15, 825.

ALROBAIAN, M. & ARIDA, H. 2019. Assessment of Heavy and Toxic Metals in the Blood and Hair of Saudi Arabia Smokers Using Modern Analytical Techniques. *International journal of analytical chemistry*, 2019, 1-8.

AMETEK. FHS22. *Spectro ICP Report; Analysis of Aqueous Solutions by ICP-OES with Radial Plasma Observation. Spectro Arcos, Spectro Analytical Instruments GmbH Germany* [Online]. Germany. Available: <https://extranet.spectro.com/-/media/31793ADA-B987-4D37-B597-04AFB66C7C22.pdf> [Accessed 20 Jan 2020].

AMIN, J. K. M., JALAL, S. S. & JARJEES, F. Z. 2017. The Elemental Composition of Atmospheric Particles and Dust Fall Rate in Erbil Governorate. *ZANCO Journal of Pure and Applied Sciences*, 29, 38-48.

AN, H. C., SUNG, J. H., LEE, J., SIM, C. S., KIM, S. H. & KIM, Y. 2017. The association between cadmium and lead exposure and blood pressure among workers of a smelting industry: a cross-sectional study. *Annals of occupational and environmental medicine*, 29, 47.

APANPA-QASIM, A. F., ADEYI, A. A., MUDLIAR, S. N., RAGHUNATHAN, K. & THAWALE, P. 2016. Examination of lead and cadmium in water-based paints marketed in Nigeria. *Journal of Health and Pollution*, 6, 43-49.

AZIZ, F. H. & RASHEED, R. O. 2017. Heavy metals in water, fishes and sediments in Derbendikhan reservoir, kurdistan Region-Iraq. *ZANCO Journal of Pure and Applied Sciences*, 29, 19-27.

BADRAN, M., MORSY, R., SOLIMAN, H. & ELNIMR, T. 2018. Assessment of wet acid digestion methods for ICP-MS determination of trace elements in biological samples by using multivariate statistical analysis. *Journal of Elementology*, 23, 179-189.

BATÁRIOVÁ, A., SPĚVÁČKOVÁ, V., BENEŠ, B., ČEJCHANOVÁ, M., ŠMÍD, J. & ČERNÁ, M. 2006. Blood and urine levels of Pb, Cd and Hg in the general population of the Czech Republic and proposed reference values. *International journal of hygiene and environmental health*, 209, 359-366.

BUXBAUM, G. 2008. *Industrial inorganic pigments*, John Wiley & Sons.

CDC. 2013. *Fourth National Report on Human Exposure to Environmental Chemicals, Updated Tables. Centers for Disease Control and Prevention National Center for Environmental Health Division of Laboratory Sciences Mail Stop F-20 4770 Buford Highway* [Online]. NE Atlanta, p. 30341-3724. Available: <https://www.cdc.gov/exposurereport/> [Accessed 10 March 2020].

ČERNÁ, M., SPĚVÁČKOVÁ, V., BENEŠ, B., ČEJCHANOVÁ, M. & ŠMÍD, J. 2001. Reference values for lead and cadmium in blood of Czech

- population. *Int J Occup Med Environ Health*, 14, 189-92.
- CRINNION, W. J. 2010. The CDC Fourth National Report on Human Exposure to Environmental Chemicals: What it Tells Us About our Toxic Burden and How it Assists Environmental Medicine Physicians. *Alternative medicine review*, 15.
- DECHARAT, S. 2016. Heavy metals exposure and hygienic behaviors of workers in sanitary landfill areas in Southern Thailand. *Scientifica*, 2016, 1-9.
- FORTE, G., MADEDDU, R., TOLU, P., ASARA, Y., MARCHAL, J. A. & BOCCA, B. 2011. Reference intervals for blood Cd and Pb in the general population of Sardinia (Italy). *International journal of hygiene and environmental health*, 214, 102-109.
- HASSAN, M. K., ALFHADY, N. H. & ALJUMAILY, M. A. 2011. Serum heavy metals in patients with fragments and shells of improvised explosive devices. *Annals of the College of Medicine Mosul*, 37, 8-13.
- HEITLAND, P. & KÖSTER, H. D. 2006. Biomonitoring of 37 trace elements in blood samples from inhabitants of northern Germany by ICP-MS. *Journal of Trace Elements in Medicine and Biology*, 20, 253-262.
- HSU, D.-J., CHUNG, S.-H., DONG, J.-F., SHIH, H.-C., CHANG, H.-B. & CHIEN, Y.-C. 2018. Water-based automobile paints potentially reduce the exposure of refinish painters to toxic metals. *International journal of environmental research and public health*, 15, 899.
- ISHOLA, A. B., OKECHUKWU, I. & ASHIMEDUA, U. 2017. Serum level of lead, zinc, cadmium, copper and chromium among occupationally exposed automotive workers in Benin city. *Int J Environ Pollut Res*, 5, 70-79.
- JÄRUP, L. 2003. Hazards of heavy metal contamination. *British medical bulletin*, 68, 167-182.
- JUNAID, M., HASHMI, M. Z. & MALIK, R. N. 2016. Evaluating levels and health risk of heavy metals in exposed workers from surgical instrument manufacturing industries of Sialkot, Pakistan. *Environmental Science and Pollution Research*, 23, 18010-18026.
- JUNAID, M., HASHMI, M. Z., TANG, Y.-M., MALIK, R. N. & PEI, D.-S. 2017. Potential health risk of heavy metals in the leather manufacturing industries in Sialkot, Pakistan. *Scientific reports*, 7, 1-13.
- KAMETI, C. M. 2013. *Determination of lead and cadmium levels in decorative paints sold in Nairobi Kenya*. Master Thesis, Kenyatta University, Kenya.
- KHLIFI, R., OLMEDO, P., GIL, F., FEKI-TOUNSI, M., HAMMAMI, B., REBAI, A. & HAMZA-CHAFFAI, A. 2014. Biomonitoring of cadmium, chromium, nickel and arsenic in general population living near mining and active industrial areas in Southern Tunisia. *Environmental monitoring and assessment*, 186, 761-779.
- KIM, B., YOON, J.-H., CHOI, B.-S. & SHIN, Y. C. 2013. Exposure assessment suggests exposure to lung cancer carcinogens in a painter working in an automobile bumper shop. *Safety and health at work*, 4, 216-220.
- KIM, N.-S. & LEE, B.-K. 2011. National estimates of blood lead, cadmium, and mercury levels in the Korean general adult population. *International archives of occupational and environmental health*, 84, 53-63.
- LADEIRA, C. & VIEGAS, S. 2016. Human Biomonitoring—An overview on biomarkers and their application in Occupational and Environmental Health. *Biomonitoring*, 3.
- LECH, T. 2013. Application of ICP-OES to the determination of barium in blood and urine in clinical and forensic analysis. *Journal of analytical toxicology*, 37, 222-226.
- LENTINI, P., ZANOLI, L., GRANATA, A., SIGNORELLI, S. S., CASTELLINO, P. & DELL'AQUILA, R. 2017. Kidney and heavy metals-The role of environmental exposure. *Molecular medicine reports*, 15, 3413-3419.
- MARTH, E., JELOVCAN, S., KLEINHAPPL, B., GUTSCHI, A. & BARTH, S. 2001. The effect of heavy metals on the immune system at low concentrations. *International journal of occupational medicine and environmental health*, 14, 375-386.
- MIERNA, R., CYNTHIA, N., AFRIYANTI, W., FERRY, C., NEVITA, P. T., DORETHEA, K., MARLISAWATI, S., INDAH, R., AGUS, P. T. & DINA, R. 2015. Biomonitoring for iron, manganese, chromium, aluminum, nickel and cadmium in workers exposed to welding fume: a preliminary study. *Russian Open Medical Journal*, 4.
- MWSTEFAN, S. B. & AHMED, I. T. 2019. Effect of Phosphorus Fertilization on Phytoremediation efficacy of Heavy Metals by Wheat and Bean Plants. *ZANCO Journal of Pure and Applied Sciences*, 31, 18-27.
- NAKHAEE, S., AMIRABADIZADEH, A., NAKHAEE, S., ZARDAST, M., SCHIMMEL, J., AHMADIAN-MOGHADAM, J., AKBARI, A., DARMIAN, H. M., MOHAMMADI, M. & MEHRPOUR, O. 2019. Blood lead level risk factors and reference value derivation in a cross-sectional study of potentially lead-exposed workers in Iran. *BMJ open*, 9, e023867.
- OGILO, J., ONDITI, A., SALIM, A. & YUSUF, A. 2017. Assessment of Levels of Heavy Metals in Paints from Interior Walls and Indoor Dust from Residential Houses in Nairobi City County, Kenya. *Chemical Science International Journal*, 1-7.
- OKEWOLE, A. & OMIN, B. 2013. Assessment of Heavy Metal Contents of Some Paints Produced in Lagos, Nigeria. *Polytech. J. Sci. Tech*, 8, 60-66.
- PYSZEL, A., WROBEL, T., SZUBA, A. & ANDRZEJAK, R. 2005. Effect of metals, benzene, pesticides and ethylene oxide on the haematopoietic system. *Medycyna pracy*, 56, 249-255.
- RODRÍGUEZ, J. & MANDALUNIS, P. M. 2018. A review of metal exposure and its effects on bone health. *Journal of toxicology*, 2018, 10-11.
- SABBIONI, E., MINOIA, C., PIETRA, R., FORTANER, S., GALLORINI, M. & SALTELLI, A. 1992.

- Trace element reference values in tissues from inhabitants of the European Community. II. Examples of strategy adopted and trace element analysis of blood, lymph nodes and cerebrospinal fluid of Italian subjects. *Science of the total environment*, 120, 39-61.
- SANI, A. & ABDULLAHI, I. L. 2017. Evaluation of some heavy metals concentration in body fluids of metal workers in Kano metropolis, Nigeria. *Toxicology Reports*, 4, 72-76.
- SCHULZ, C., WILHELM, M., HEUDORF, U. & KOLOSSA-GEHRING, M. 2011. Update of the reference and HBM values derived by the German Human Biomonitoring Commission. *International journal of hygiene and environmental health*, 215, 26-35.
- SHAFIQUE, U., ANWAR, J. & ALI, S. Z. 2011. Assessment of concentration of lead, cadmium, chromium and selenium in blood serum of cancer and diabetic patients of Pakistan. *J. Chem. Soc. Pak*, 33, 869.
- SIRIVARASAI, J., KAOJAREN, S., WANANUKUL, W. & SRISOMERANG, P. 2002. Non-occupational determinants of cadmium and lead in blood and urine among a general population in Thailand. *Southeast Asian Journal of Tropical Medicine and Public Health*, 33, 180-187.
- SOLENKOVA, N. V., NEWMAN, J. D., BERGER, J. S., THURSTON, G., HOCHMAN, J. S. & LAMAS, G. A. 2014. Metal pollutants and cardiovascular disease: mechanisms and consequences of exposure. *American heart journal*, 168, 812-822.
- STOJSAVLJEVIĆ, A., BORKOVIĆ-MITIĆ, S., VUJOTIĆ, L., GRUJIĆIĆ, D., GAVROVIĆ-JANKULOVIĆ, M. & MANOJLOVIĆ, D. 2019. The human biomonitoring study in Serbia: background levels for arsenic, cadmium, lead, thorium and uranium in the whole blood of adult Serbian population. *Ecotoxicology and environmental safety*, 169, 402-409.
- TAHIR, H., ZEB, Q. J. & SULTAN, M. 2010. Assessment of heavy metal exposure around auto body refinishing shops. *African Journal of Biotechnology*, 9, 7862-7869.
- TAYLOR, C. M., EMOND, A. M., LINGAM, R. & GOLDING, J. 2018. Prenatal lead, cadmium and mercury exposure and associations with motor skills at age 7 years in a UK observational birth cohort. *Environment international*, 117, 40-47.
- VITAYAVIRASUK, B., JUNHOM, S. & TANTISAERANEE, P. 2005. Exposure to lead, cadmium and chromium among spray painters in automobile body repair shops. *Journal of occupational health*, 47, 518-522.
- WASOWICZ, W., GROMADZINSKA, J. & RYDZYNSKI, K. 2001. Blood concentration of essential trace elements and heavy metals in workers exposed to lead and cadmium. *International journal of occupational medicine and environmental health*, 14, 223-229.
- WILHELM, M., EWERS, U. & SCHULZ, C. 2004. Revised and new reference values for some trace elements in blood and urine for human biomonitoring in environmental medicine. *International journal of hygiene and environmental health*, 207, 69-73.
- WITTSIEPE, J., FELDT, T., TILL, H., BURCHARD, G., WILHELM, M. & FOBIL, J. N. 2017. Pilot study on the internal exposure to heavy metals of informal-level electronic waste workers in Agbogbloshie, Accra, Ghana. *Environmental Science and Pollution Research*, 24, 3097-3107.
- YOUSEF, S., EAPEN, V., ZOUBEIDI, T., KOSANOVIC, M., MABROUK, A. A. & ADEM, A. 2013. Learning disorder and blood concentration of heavy metals in the United Arab Emirates. *Asian journal of psychiatry*, 6, 394-400.
- ZHANG, L.-L., LU, L., PAN, Y.-J., DING, C.-G., XU, D.-Y., HUANG, C.-F., PAN, X.-F. & ZHENG, W. 2015. Baseline blood levels of manganese, lead, cadmium, copper, and zinc in residents of Beijing suburb. *Environmental research*, 140, 10-17.

## RESEARCH PAPER

# Nutrient imbalance diagnosis in walnut orchards by using DRIS and PCA Approaches in the northern part of Erbil governorate-Iraq.

Pakhshan Mustafa Maulood<sup>1\*</sup>, Dalshad Azeez Darwesh<sup>2</sup>

<sup>1</sup>Biology Department, College of Science, Salahaddin University -Erbil, Iraq

<sup>2</sup>Environmental Sciences and Health Department, College of Science, Salahaddin University-Erbil, Iraq

### ABSTRACT:

The use of Diagnosis and Recommendation Integrated System (DRIS) in studying the concept of a plant's nutritional balance has become an efficient method for assessing plant nutritional status; this method limits nutrient location depending on plant demand, enabling the nutritional balance between the nutrients in the leaf sample. Aim of this study is to establish walnut DRIS norms and diagnosis nutrient imbalance by using DRIS and PCA (Principal component analysis) methods. One hundred four leaf samples were collected during two consecutive years (2016 and 2017) from three walnut orchards in Erbil governorate/ Iraq. The results showed that the smallest average NBI (Nutrient Balance Index) values are 125.6 and 27.2 respectively for both studied years which was coincided by high walnut productivity. The most limiting nutrient descending order as Fe>Na>Ca>K>P>N>Mg respectively for first-year samples, and N>Na>P>Fe>Mg>Ca>K respectively for the second year. From the result of PCA reveal that the nutrient concentration was explained in the low and high yield subgroups and the DRIS index by 61.95%, 87.75% and 58.67% respectively for first-year and 79.22%, 60% and 65.95% respectively for second-year sampling. Several nutrient interventions in a single PC indicate that no nutrient imbalance in isolation could be diagnosed.

KEY WORDS: Walnut; Foliar nutrient concentration; Nutrient imbalance; Diagnosis and Recommendation Integrated System (DRIS); Principal Component Analysis (PCA).

DOI: <http://dx.doi.org/10.21271/ZJPAS.32.6.2>

ZJPAS (2020) , 32(6);14-24. .

## 1. INTRODUCTION

Common walnut species (*Juglans regia* L.) belongs to the Juglandaceae family, one of the most important horticultural crops in northern Iraq (Townsend and Guest, 1980). It is a valuable tree attained great concern from the farmers and villagers in the region from their economically and ecologically importance (Gauthier and Jacobs, 2011, Sytykiewicz *et al.*, 2019).

Leaf analysis plays the main role in the physiological processes of the plants. Therefore, it becomes a successful tool for diagnosing the nutritional requirement of forest tree and crops (Carneiro *et al.*, 2015). Nutritional diagnosis is an appropriate way of detecting deficiencies and allowing more efficient application of fertilizers (Carneiro *et al.*, 2015, Silveira *et al.*, 2005).

Diagnosis and Recommendation Integrated System (DRIS) is regarded as an accurate system that uses pairwise relationship among nutrients and compare it with the high population productivity (references norm) which represented by the mean, variance and coefficient of variance (Silveira *et al.*, 2005, Matos *et al.*, 2018, Dias *et*

### \* Corresponding Author:

Pakhshan Mustafa Maulood

E-mail: [pakhshan.maulood@su.edu.krd](mailto:pakhshan.maulood@su.edu.krd)

### Article History:

Received: 06/04/2020

Accepted: 10/08/2020

Published: 20/12 /2020

*al.*, 2011). Many studies urge to established regional DRIS norm, that adapted for varieties of crops (Carneiro *et al.*, 2015), that driven from the same local soil and climate condition (Talpur, 2015). The mean of the deviations from the DRIS norm compose nutrient index (Bailey *et al.*, 1997, Yao *et al.*, 2013). The sum of absolute values of nutrient indices forms nutrient balance index (NBI) (Yao *et al.*, 2013). Their value ranges from negative to positive with always the sum value of zero. The excessive nutrient contents of crops are expressed by (positive indices), deficient (negative indices) and adequate (zero indices) (Geiklooi *et al.*, 2018, Darwesh, 2011).

Principal component analysis (PCA) is a multivariate mathematical reduction procedure, which reduced a large data set of variables (Principal component- PC) that contains most of the information in the original data set. PCA has been performed on DRIS indices by many investigators (Wairegi and Van Asten, 2011). However, several authors in Iraq have successfully used the DRIS method to interpret the results of leaf analysis for a wide range of plants such as lentils (Darwesh, 2011), wheat (Esmail, 2012, Esmail *et al.*, 2019), soybean (Darwesh and Mustafa, 2012), barley (Dizayee and Hussein, 2017), Broccoli (Dizayee and Saleh, 2017), . Whereas, there is not the availability of such information about nutrient balance for a walnut tree for local agriculture manager and orchard farmers who complain about the lack of production of these trees. The aims of this study is to establish the norm of walnut and assess nutrient balance index.

## 2. MATERIALS AND METHODS

### 2.1 Samples collection

For this study, three areas in the northern part of Erbil province / Iraq were selected. In the following counties with their geographical coordinates, plant samples were collected using (GPS) a Global Positioning System (UTM): Shaqlawa District (38s E0439944 latitude N4028711 , elevation 963m above sea level ); Malakan village (38s E0463373 N4035073, elevation 1366 above sea level ); Choman (Warda village) (38s E0489275 N4057261, elevation 1514m above sea level) (Figure 1). The climate in the area is semi-arid and, characterised by wet,

cold winter (December- March) and hot summer (Al-Kubaisi and Gardi, 2012).

In each studied area a specific walnut orchard selected after previous obtained permission from the orchard owners. Two consecutive years of plant sampling were conducted in June 2016 and June 2017. Eighteen samples per study orchards were taken.

### 2.2 Laboratory analysis

The leaves samples have been dried at 65°C for 48 hrs., ground and wet digested using H<sub>2</sub>SO<sub>4</sub>: H<sub>2</sub>O<sub>2</sub> method (Cotteine, 1980). From the digestive samples N were determined using the Micro - Kjeldahl method ; P was determined using the Molybdenum Blue method and measured by the Spectrophotometer; K using the Flame Photometer, while Ca and Mg was assayed by EDTA titrimetric method (Allen *et al.*, 1974).

### 2.3 DRIS calculation

According to Beauflis (1971), the mean, variance and coefficient of variation (CV) for each possible nutrient pair ratio were calculated for both high and low yield populations. For each pair of nutrients, the mean and CV ratios that maximized the variance ratio between the low and high population were selected as norms for that pair of nutrients as described by Walworth and Sumner (1987). For current study the reference population was defined as 12.6 Kg.tree<sup>-1</sup> or 3.54 t.ha<sup>-1</sup>, a population exceeded this limit considered as high yield and lower of this point regarded as low yielding population.

DRIS provides a means of ordering nutrient ratios or products into a meaningful expression called the DRIS index. A nutrient index is the mean of deviations of the ratios containing a given nutrient from their respective optimum or norms value. All indices were balanced to nearly zero. Therefore, nutrient indices to sum zero. The more negative an index is the more insufficient nutrient compared to other nutrients being used in the diagnosis. Alternatively, a positive index showed that the corresponding nutrients were found in relatively excessive quantities. DRIS indices could be calculated for nutrients from following generalized equation as an example:

$$N \text{ index} = [f\left(\frac{N}{P}\right) + f\left(\frac{N}{Ca}\right) + \dots - f\left(\frac{Na}{N}\right) - f\left(\frac{Fe}{N}\right)]$$

$$\text{When } \frac{N}{P} > \frac{n}{p} \text{ then } f(N/P) = \left(\frac{N}{P} - 1\right) \left(\frac{1000}{CV}\right)$$

$$\text{When } \frac{N}{P} < \frac{n}{p} \text{ then } f(N/P) = \left(1 - \frac{n}{P}\right) \left(\frac{1000}{CV}\right)$$

$$\text{When } \frac{N}{P} = \frac{n}{p} \text{ then } f\left(\frac{N}{P}\right) = 0$$

Where N/P is the ratio of nutrient from analyzed leaves tissue n/p is the ratio of nutrient from DRIS norm of paired nutrients from the population CV is the coefficient of variance(n/p) of the references (high yield population).

Nutrient imbalance index (NBI) calculated from the sum of absolute values of the nutrient indices. The smaller the absolute sum (NBI), the lesser imbalance among nutrients. Whereas the larger the sum index, the more imbalance within nutrients (Agbangba *et al.*, 2011, Wairegi and Van Asten, 2011, Snyder and Kretschmer Jr, 1988).

## 2.4 Principal component analysis (PCA)

The PCA was performed separately on the nutrient concentration data for low and high yield populations and DRIS indices (Sharma *et al.*, 2005). PCs with eigenvalues greater >1 regarded as significant. Only PC loadings in the eigenvectors having values greater than the selection criterion (SC) were considered as the significant loads. The selection criterion was as follows (Raghupathi *et al.*, 2005, Geiklooi *et al.*, 2018):

$$SC = 0.5/(PC \text{ eigen values})^{0.5}$$

## 2.5 Statistical analysis

Descriptive, multivariate (Principal component analysis), normal distribution and DRIS calculation for parameters were performed by using (SPSS version 25) program and Excell spreadsheets.

## 3. RESULTS AND DISCUSSION

### 3.1 Diagnosis and Recommendation Integrated System (DRIS)

The results show the descriptive statistics for leaf tissues of the walnut tree (Table 1). The data for the high and low yielding population was relatively less skewed, with most nutrients having a skewed value of less than 1. It is an indication

that most data is normally distributed, therefore, suitable for the deriving the DRIS norm (Chanan *et al.*, 2019). Because the symmetrical data provided a realistic approximation of the possibility of interactive effect variations in the productivity of walnut of different nutrients. The only marginal difference was noticed throughout the study period in the concentration of various nutrients between high and low yielding plants. More than 66% of walnut trees in first year sampling considered as high yielding population coincided with higher nutrients concentration compared with only 55% of high yield population for second year samples with decreases in nutrients concentration for most cases.

All ratios of nutrients are presented in Tables (2 and 3 ) for both studying years with their mean, variance and coefficient of variance. Twenty - one ratios of nutrients were chosen as those with the highest ratio variants between the high and low yielding population and became the DRIS norm. These norms were used to calculate nutrient indices and nutrient imbalance indices. The choice of nutrient ratio with maximum variants of high and low yielding populations was used to maximize the potential of differentiated walnut with high yielding compared to inadequate yielding populations. The variant of the ratio indicated the importance of certain nutrient ratios against the results parameter with a very high ratio, which shows that the nutrient is essential for the plant (Raghupathi *et al.*, 2005). The similar selected nutrient ratios for both studying years are: N/P, N/K, Fe/N, Mg/Na, Fe/Mg; and K/Na had greater physiological effects in leaf tissue. Photosynthesis rate influences K content through involvement in osmoregulation, protein synthesis and enzymes activation (Gardner *et al.*, 2017). Among the essential functions of Fe in the plant, the body is the constituent of the enzyme as a metal activator. The Fe deficiency causes chlorophyll formation to fail because Fe is essential for chlorophyll molecule biosynthesis through decreasing chloroplast size (Barker and Pilbeam, 2015). On the other hand, the intensive review of the literature showed that no study had been done to establish the DRIS walnut norms. However, the use of universal DRIS norms is suitable for several factors, such as soil type, climate and crop genotypes (Talpur, 2015).



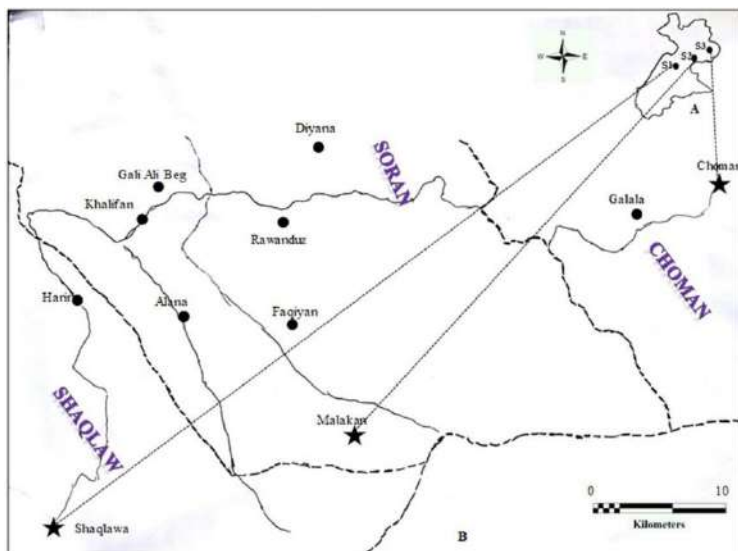


**Figure 1:** A. Locations of the studied area in northern part of Erbil province/Iraq. B. Study sites.

**Table 1:** Descriptive statistics of nutrients in the walnut leaves from high and low yielding population for two consequence years 2016 and 2017.

		2016					
		High yielding population (n=36)					
	N (%)	P (mg/kg)	Fe (mg/kg)	Ca (mg/kg)	Mg (mg/kg)	Na (mg/kg)	K (mg/kg)
Minimum	1.371	4.070	24.70	2.511	2.500	11.52	83.26
Maximum	3.530	22.96	445.3	5.000	7.330	31.45	169.6
Mean	2.299	14.21	174.9	3.862	4.479	10.84	130.6
SD	0.579	4.125	12.81	0.673	1.208	3.509	17.03
Skewness	-0.021	0.098	0.943	0.178	0.895	1.176	-0.431
		Low yielding population (n=18)					
	N (%)	P (mg/kg)	Fe (mg/kg)	Ca (mg/kg)	Mg (mg/kg)	Na (mg/kg)	K (mg/kg)
Minimum	2.274	11.60	90.59	2.500	3.333	10.41	2.509
Maximum	2.901	21.11	153.5	3.333	6.667	27.02	153.1
Mean	2.626	15.76	110.9	3.160	4.458	15.57	122.9
SD	0.163	2.5610	17.52	0.254	1.245	4.093	34.82
Skewness	-0.583	0.381	0.506	0.441	1.132	0.641	1.016
		2017					
		High yielding population (n=30)					
	N (%)	P (mg/kg)	Fe (mg/kg)	Ca (mg/kg)	Mg (mg/kg)	Na (mg/kg)	K (mg/kg)
Minimum	0.744	1.272	64.71	1.333	1.833	14.62	127.8
Maximum	1.803	14.81	235.3	3.333	5.000	22.15	180.6
Mean	1.152	8.116	153.2	2.172	3.322	19.53	151.7
SD	0.356	3.465	49.95	0.552	0.947	2.187	13.58
Skewness	0.548	0.678	0.123	0.698	0.548	-0.671	0.488
		Low yielding population (n=24)					
	N (%)	P (mg/kg)	Fe (mg/kg)	Ca (mg/kg)	Mg (mg/kg)	Na (mg/kg)	K (mg/kg)
Minimum	0.235	3.457	42.94	1.667	1.333	15.06	121.1
Maximum	1.411	10.99	505.9	3.000	5.833	22.15	158.6
Mean	1.111	6.008	157.4	2.257	3.316	17.54	140.1
SD	0.342	2.169	107.4	0.408	1.421	1.952	9.876
Skewness	-1.921	0.291	0.961	0.022	0.288	1.114	0.053

Table

2:

Comparison of leaf nutrients, nutrient ratio means and coefficient of variance (CV), variance between high and low yielding population in walnut during June 2016.

Nutrients ratios	High yielding population			Low yielding population			S <sup>2</sup> <sub>y</sub> /S <sup>2</sup> <sub>e</sub>	Selected ratios
	Mean	CV %	Variance (S <sup>2</sup> <sub>y</sub> )	Mean	CV %	Variance (S <sup>2</sup> <sub>e</sub> )		
N/P	0.16	4.13	0.000447	0.17	2.09	0.000012	0.268	*
P/N	6.19	4.13	0.06534	6	2.09	0.015698	0.240	
N/Ca	0.6	9.75	0.003388	0.83	4.64	0.00149	0.440	*
Ca/N	1.68	9.68	0.02658	1.2	4.54	0.002986	0.112	
N/Mg	0.51	1.22	0.000394	0.59	4.83	0.000813	20.635	*
Mg/N	1.95	1.22	0.0005614	1.7	4.82	0.0067	11.934	
K/N	56.9	4.95	7.92	49.9	0.34	0.0295	0.004	
N/K	0.02	4.98	0.000008	0.02	0.34	0.00003	3.750	*
N/Na	0.12	2.76	0.0000114	0.17	3.53	0.000036	3.158	*
Na/N	8.18	2.74	0.050292	5.93	3.53	0.0437	0.869	
N/Fe	0.01	1.14	0.00001	0.02	2.08	0.00001	1.000	
Fe/N	76.1	1.13	0.74509	42.2	2.08	0.7749	1.040	*
P/Ca	3.69	5.61	0.04276	4.99	2.79	0.01943	0.454	*
Ca/P	0.27	5.58	0.000229	0.2	2.75	0.00003	0.131	
P/Mg	3.17	3	0.00908	3.54	6.92	0.06015	6.624	*
Mg/P	0.32	2.98	0.000885	0.28	6.9	0.000382	4.316	
P/K	0.11	0.87	0.000009	0.12	2.43	0.000009	1.000	
K/P	9.19	0.87	0.006355	8.31	2.43	0.0407	6.404	*
P/Na	0.76	6.88	0.002711	1.01	5.62	0.003246	1.197	*
Na/P	1.33	6.83	0.008189	0.99	5.61	0.00307	0.375	
P/Fe	0.08	3.07	0.000062	0.14	0	0.000006	0.968	*
Fe/P	12.3	3.06	0.14148	7.04	0	0.000062	0.00004	
Ca/Mg	0.86	8.55	0.00545	0.71	9.14	0.004231	0.776	
Mg/Ca	1.16	8.55	0.009893	1.41	9.37	0.017555	1.774	*
Ca/K	0.03	4.76	0.000002	0.02	4.86	0.000001	0.500	
K/Ca	33.9	4.77	2.61	41.5	4.97	4.26	1.632	*
Ca/Na	0.21	12.4	0.000655	0.2	7.89	0.000258	0.394	
Na/Ca	4.9	12.41	0.3691	4.94	8.09	0.1593	0.432	*
Ca/Fe	0.02	8.62	0.000036	0.03	2.76	0.000001	0.028	
Fe/Ca	45.4	8.63	15.256	35.1	2.8	0.9645	0.063	*
Mg/K	0.03	3.79	0.000017	0.03	4.48	0.000002	1.176	*
K/Mg	29.2	3.79	145.26	29.4	4.49	168.53	1.160	
Mg/Na	0.24	3.88	0.000853	0.29	1.3	0.000014	0.164	*
Na/Mg	4.2	3.87	0.02647	3.49	1.3	0.00206	0.078	
Mg/Fe	0.03	0.08	0.00004	0.04	6.9	0.000001	0.025	
Fe/Mg	39	0.08	0.00102	24.9	6.92	2.9758	2917.451	*
K/Na	6.96	7.67	0.285	8.42	3.19	0.0719	0.252	*
Na/K	0.14	7.66	0.000122	0.12	3.18	0.000014	0.115	
K/Fe	0.75	3.87	0.000837	1.18	2.43	0.000822	0.982	*
Fe/K	1.34	3.8	0.00268	0.85	2.43	0.000423	0.158	
Na/Fe	0.11	3.8	0.000017	0.14	5.61	0.000062	3.647	*
Fe/Na	9.3	12.4	0.12506	7.13	5.62	0.16057	1.284	

**Table 3:** Comparison of leaf nutrients, nutrient ratio means and coefficient of variance (CV), variance between high and low yielding population in walnut during June 2017.

Nutrients ratios	High yielding population			Low yielding population			S <sup>2</sup> <sub>y</sub> /S <sup>2</sup> <sub>e</sub>	Selected ratios
	Mean	CV %	Variance (S <sup>2</sup> <sub>y</sub> )	Mean	CV %	Variance (S <sup>2</sup> <sub>e</sub> )		
N/P	0.14	10.52	0.00078	0.18	1.86	0.000012	0.015384615	*
P/N	7.06	9.93	1.44	5.41	1.87	0.010216	0.007094444	
N/Ca	0.33	3.17	15.34	0.02	27.99	0.00037	0.0000241	
Ca/N	1.88	3.21	0.083	49	33.31	266.39	3209.518072	*
N/Mg	0.35	0.89	7.05	0.34	1.68	0.000032	0.000004539	
Mg/N	2.88	0.88	0.2032	2.98	1.67	0.002481	0.012209646	*
K/N	131.64	0.87	431.88	126.05	1.51	3.6	0.008335649	
N/K	0.01	0.87	0.003529	0.01	1.52	0.004	1.133465571	*
N/Na	0.06	0.86	0.2125	0.06	1.94	0.000002	0.00000941	
Na/N	16.95	0.86	7.16	15.79	1.94	0.09344	0.013050279	*
N/Fe	0.01	1.97	0.00354	0.01	29.08	0.00005	0.014124294	
Fe/N	132.99	1.99	444.534	140.6	34.88	2404.658	5.409390508	*
P/Ca	2.47	79.94	1027.87	0.12	29.02	0.001172	0.00000141	
Ca/P	0.27	13.81	0.00294	9.09	34.86	10.04	3414.965986	*
P/Mg	2.45	10.64	469.71	0.34	0.41	0.003968	0.00000844	
Mg/P	0.41	11.28	0.00717	0.55	3.41	0.000353	0.049232915	*
P/K	0.05	9.23	0.23	0.04	1.28	0.0082	0.035652174	*
K/P	18.78	9.74	15.23	23.31	1.29	0.08977	0.005894288	
P/Na	0.42	9.25	14.11	0.34	0.41	0.000002	0.00000141	
Na/P	2.42	9.77	0.25	2.92	0.41	0.000141	0.000564	*
P/Fe	0.05	8.53	0.23	0.04	30.11	0.000155	0.000673913	
Fe/P	18.96	8.96	15.682	26.09	36.44	90.3509	5.761439867	*
Ca/Mg	0.65	2.42	0.00025	16.41	32.67	28.75	115000	*
Mg/Ca	1.53	2.39	0.001336	0.06	27.69	0.000322	0.241017964	
Ca/K	0.01	4.05	0.0003	0.39	35	0.01864	62.13333333	*
K/Ca	69.95	4	7.84	2.75	29.17	0.64	0.081632653	
Ca/Na	0.11	4.03	0.00002	3.12	35.19	1.2	60000	*
Na/Ca	9.01	3.99	0.13	0.34	29.26	0.010166	0.0782	
Ca/Fe	0.01	5.06	0.000001	0.35	1.4	0.000024	24	
Fe/Ca	70.68	5.04	12.673	2.86	1.41	0.001626	0.000128304	
Mg/K	0.02	1.75	0.000004	0.02	2.6	0.000003	0.75	
K/Mg	46.68	1.75	476.18	42.27	2.61	389.89	0.818787013	*
Mg/Na	0.17	1.74	0.000009	0.19	3.38	0.000041	4.555555556	*
Na/Mg	5.88	1.75	0.0106	5.3	3.43	0.032980321	3.111351067	
Mg/Fe	0.02	2.85	0.000005	0.02	28.8	0.000043	8.6	
Fe/Mg	46.15	2.88	1.7636	47.09	43.23	259.8944	147.3658426	*
K/Na	7.76	0.05	0.000013	7.98	1.01	0.00649	499.2307692	*
Na/K	0.13	0.05	0.000003	0.13	1.01	0.00002	6.666666667	
K/Fe	0.99	1.13	0.000124	0.96	30.25	0.0851	686.2903226	
Fe/K	1.01	1.13	0.00013	1.12	36.57	0.16763	1289.461538	*
Na/Fe	0.13	1.12	0.000002	0.12	30.34	0.001344	672	
Fe/Na	7.84	1.13	0.0078	8.94	36.76	10.8027	1384.961538	*

Depending on DRIS chart Figures (2 and 3), the origin point in the center of the chart is the mean of each expression N/P, N/K and K/P for the population of high yielding plants, this is the composition required to increase the possibility of gaining a high yield. In another word, the ratio within the origin (in the center of the small circle) represents the optimum (balance) values of the studied nutrient concentrations for high yield of the plant. The nutrient ratio values situated between the two circles represented the critical value (imbalance). The outer values of both circles are high sufficiency or high deficiency depending on the direction of the arrow. Arrow points up as an index to sufficiency, while the downward arrow represents deficiency and the right the optimum or adequacy. The results in Figure 2 explain that, if the ratio between N/P is greater than 0.1776, the concentration of nitrogen increases while the concentration of phosphorus decreases, in this case, the phosphorus requirement of the plant increases. Moreover, if the N/P ratio is lower than 0.1424 the plant requirement for nitrogen increases, the same explanation for other nutrient ratios is true (Beaufils, 1971, Beaufils, 1973).

The results of DRIS indices are shown in Tables ( 4 and 5). The most limiting nutrient descending order are as Fe>Na>Ca>K>P>N>Mg respectively for first-year samples, and are arranged as N>Na>P>Fe>Mg>Ca>K respectively for the second-year samples. Nitrogen deficiency is claimed to be the lack of the main nutrient that curbs plant growth and can also regulate forest ecosystem succession patterns (Kirchmann *et al.*, 2007). Compost or manure is commonly used biofertilizer as a source of N to minimize the input on the system. Adding these nutrients can give a positive effect on the soil's availability of P (Ohno *et al.*, 2005). Residues of plant deciduous leaves and animal waste decomposed as elements fulfil the need for essential nutrients for walnut productivity.

The smallest NBI value was 879 with an average NBI 125.6 for sample 8 during 2016, which produced from DRIS indices 219.9, 118.9, -8.06, 80.79, 19.99, -48.03 and -383.5 for N, P, Ca, Mg, K, Na and Fe respectively and gave a yield of 15.54 Kg.tree<sup>-1</sup>. While, sample 4 for second-year samples 2017 was more close to zero with NBI value 192.4 and an average NBI 27.2, which attained from DRIS indices 22, 2.51, -10.2, -

75.94, 32.6, 39.12 and -10.1 for N, P, Ca, Mg, K, Na and Fe respectively and produce a yield of 13.27 Kg.tree<sup>-1</sup>. The highest NBI values for both years were 19063.4 and 4137.3 respectively for samples 2 and 18 respectively with deficiencies Fe for the first year and each of N and Fe for the second-year sample. Generally, increases in Fe deficiency during second-year sampling were observed compared to first-year sampling.

### 3.2 Principal component analysis (PCA):

PCA was performed for high and low yield population and DRIS indices as shown in Table (6). Retained PCs with eigenvalue more than one represented the greatest variability in the data set was consist of the first three PCs for high yield, and two PCs for low yield and DRIS indices with explained 61.95%, 87.75% and 58.67% respectively for first-year sampling 2016. Under each PC, the nutrient with eigenvector larger than the selection score (SC) was selected. The first PC of the high yield population had a positive correlation with N, P, and K and negative loading for Ca and Na, and it designated as (N+P+Ca-Na-K+). The fundamental role of calcium in membrane stability and cell integrity by bridging phosphate and carboxylate groups of phospholipids and proteins, preferably on membrane surfaces, may involve an exchange of calcium at these binding sites with other cations (K<sup>+</sup> and Na<sup>+</sup>) (Marschner, 2011). A very high correlation in PC1 represented by N, K and P respectively. there is an inverse relationship between foliage nutrients (N, P, K) in one direction and Ca and Na on the opposite direction. For the second PC, was expressed as loading for (Fe+Mg+Na+). All variables were changed in the same direction. While PCA conducted on the low yield population produced three PCs with eigenvalues up to 3.22 and total variance of 87.75%. The first three PCs variances were explained by 46.11%, 24.47% and 17.16% respectively. PC1 had positive loading with N, P and inverse negative loading with Fe and Mg, as it designed (N+P+Fe-Mg-Na+). The contrasting relationship between N+P+Na and Mg+Fe was obtained. Fe deficiency may occur in plants grown on alkaline soils rich in Ca and Mg (Darwesh, 2011). While (Havlin *et al.*, 1999) stated that excessive phosphate anions could prevent Fe uptake and used by plants.

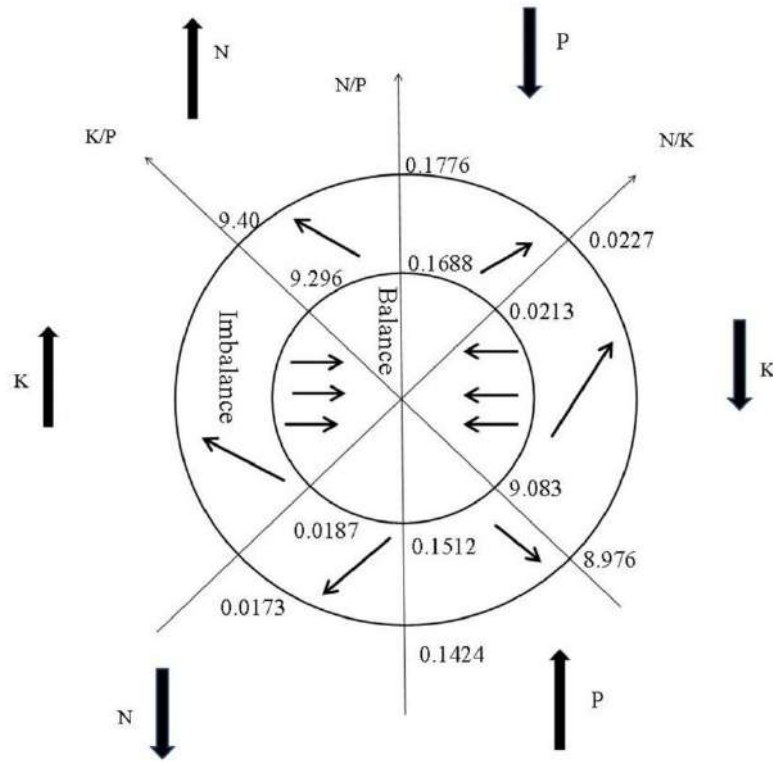


**Figure 2:** DRIS indices chart explain the optimum and critical values of some nutrients ratio for first-year samples 2016.

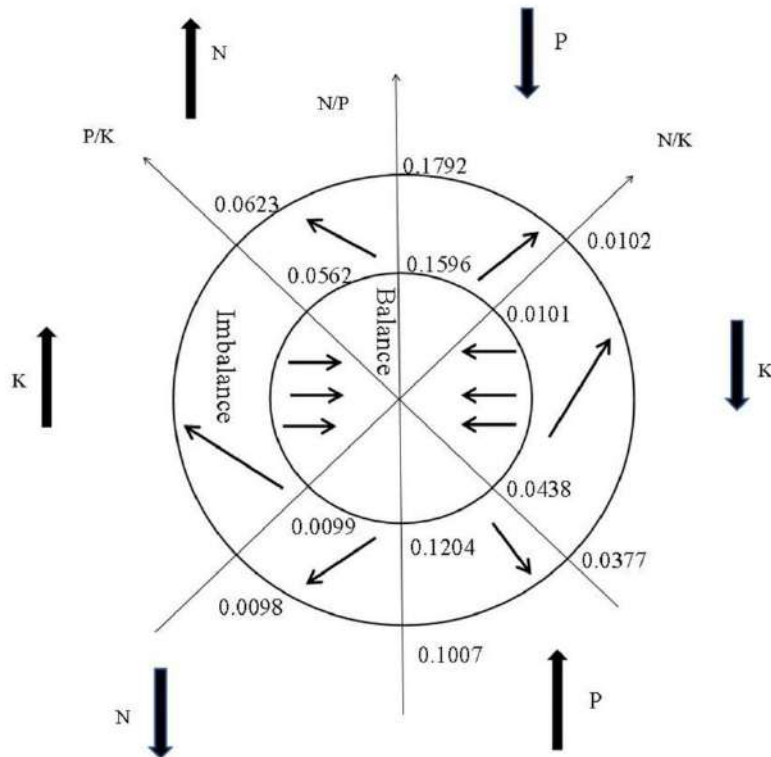


**Figure 3:** DRIS indices chart explain the optimum and critical values of some nutrients ratio for second-year samples 2017.

**Table 4:** Diagnosis of nutrient imbalance by DRIS indices in walnut during June 2016.

	NI	PI	CaI	MgI	KI	NaI	FeI	NBI	Average NBI
1.00	-70.87	-17.33	28.70	1413.84	43.33	27.22	-1424.88	3026.16	432.31
2.00	140.31	99.70	139.86	8686.13	215.87	249.83	-9531.70	19063.40	2723.34
3.00	70.77	-160.41	109.74	1973.71	87.86	152.98	-2234.64	4790.10	684.30
4.00	-193.87	-157.67	21.13	-2843.15	-93.40	-74.85	3341.82	6725.90	960.84
5.00	-368.11	-339.57	20.72	-1144.20	16.40	15.44	1799.32	3703.76	529.11
6.00	-145.74	-48.58	-62.60	-289.28	-82.18	-37.35	665.74	1331.47	190.21
7.00	61.07	-65.52	-9.59	1938.09	31.59	-171.71	-1783.93	4061.50	580.21
8.00	219.93	118.89	-8.06	80.79	19.99	-48.03	-383.51	879.20	125.60
9.00	98.33	-17.90	-18.19	-600.49	2.67	-40.99	576.58	1355.15	193.59
10.00	381.14	23.80	-35.97	1105.27	119.41	-31.73	-1561.92	3259.24	465.61
11.00	214.85	71.50	-11.37	1451.88	10.37	-30.65	-1706.59	3497.21	499.60
12.00	225.44	73.96	-9.59	1309.74	19.31	-28.09	-1590.77	3256.90	465.27
13.00	144.25	194.21	17.97	759.27	-22.67	0.33	-1093.37	2232.07	318.87
14.00	163.50	237.69	-32.97	1277.08	-22.57	49.93	-1672.66	3456.39	493.77
15.00	47.83	102.94	18.30	480.67	-10.52	20.75	-659.96	1340.95	191.56
16.00	243.30	107.21	-24.97	339.21	63.13	49.90	-777.79	1605.52	229.36
17.00	291.82	159.08	-19.15	1501.62	13.98	-3.35	-1944.00	3933.00	561.86
18.00	198.74	265.28	-4.67	636.73	-112.23	-25.06	-958.79	2201.50	314.50

**Table 5:** Diagnosis of nutrient imbalance by DRIS indices in walnut during June 2017.

	NI	PI	CaI	MgI	KI	NaI	FeI	NBI	Average NBI
1.00	-232.64	-25.36	240.15	-214.93	-695.89	966.49	-37.83	2413.27	344.75
2.00	50.92	-13.97	-27.69	80.50	684.82	-666.46	-108.13	1632.49	233.21
3.00	198.71	-17.43	-37.71	-197.28	154.62	-322.31	221.39	1149.44	164.21
4.00	22.03	2.51	-10.21	-75.94	32.60	39.12	-10.10	192.49	27.50
5.00	-131.20	-116.20	-72.84	359.84	-760.26	589.51	131.16	2161.02	308.72
6.00	-474.66	-21.00	-32.47	418.92	872.28	-927.40	164.33	2911.07	415.87
7.00	-72.99	-121.11	85.18	-16.56	533.93	-482.10	73.66	1385.53	197.93
8.00	-187.05	-0.53	13.35	234.53	48.99	-1.55	-107.74	593.74	84.82
9.00	-238.61	-77.58	153.63	-166.70	-317.59	385.15	261.70	1600.96	228.71
10.00	-526.19	-39.96	10.48	335.10	-75.23	263.49	32.31	1282.77	183.25
11.00	83.64	-71.64	71.33	140.96	-74.36	-187.96	38.04	667.94	95.42
12.00	-168.56	-57.34	31.54	239.99	-275.52	194.65	35.23	1002.84	143.26
13.00	286.60	-14.59	-3.63	-118.95	255.50	-264.19	-140.73	1084.19	154.88
14.00	-214.74	122.23	-33.29	133.47	-279.85	926.01	-653.83	2363.42	337.63
15.00	474.78	84.59	-54.36	-343.11	1042.99	-956.25	-248.64	3204.72	457.82
16.00	244.05	-27.20	82.45	-336.25	629.93	-716.64	123.67	2160.18	308.60
17.00	366.54	52.78	152.40	-745.74	-268.51	183.50	259.04	2028.50	289.79
18.00	-1827.70	63.80	211.76	153.11	1371.37	268.66	-240.99	4137.39	591.06

**Table 6:** Principal component analysis of nutrient concentration for high and low yield population, as well as DRIS indices in walnut during June 2016.

Nutrient	High yield		Low yield			DRIS index	
	PC1	PC2	PC1	PC2	PC3	PC1	PC2
N	0.825*	0.140	0.280*	0.849*	-0.252	-0.182	0.744*
P	0.767*	-0.130	0.905*	-0.180	-0.016	0.087	0.760*
Fe	0.115	0.840*	-0.754*	-0.009	0.482*	0.896*	0.261
Ca	-0.754*	0.019	0.025	0.002	0.963*	0.625*	-0.294
Mg	-0.030	0.845*	-0.965*	-0.144	-0.014	0.838*	0.036
Na	-0.458*	0.435*	0.791*	0.431*	0.145	0.635*	-0.063
K	0.793*	0.027	-0.136	0.927*	0.194	0.502*	0.475*
Eigen value	2.702	1.635	3.228	1.713	1.202	2.631	1.477
% Variance	38.59	23.36	46.11	24.47	17.16	37.58	21.09
Total variance %	38.59	61.95	46.11	70.58	87.75	37.58	58.67
Selection Criteria	0.304	0.391	0.278	0.382	0.456	0.308	0.411
	PC1=N+P+Ca-Na-K+		PC1=P+Fe-Mg-Na+			PC1= Fe+Ca+Mg+Na+K+	
	PC2=Fe+Mg+Na+		PC2= N+Na+K+			PC2=N+P+K+	
			PC3= Fe+Ca+				

The PC2 and PC3 (N+Na+K) and (Fe+Ca) was performed with a positive relationship and concentration changes in one direction. PCA on DRIS indices indicated of nutrients in two PCs that was designated as (N+P+Fe+Ca+Na+K) and (N+Fe+Mg+) respectively with total variance explained by 37.58% and 21.09% respectively. The positive relationship between nutrients obtained with highest loads for Fe and Mg in PC1 and P, N in PC2. The positive interaction between P and N become commonly held view (Raghupathi *et al.*, 2005).

For second-year sampling 2017, PCA conducted on high yield population produced three PCs that represented by 33.84%, 25.33% and 20.05% of the variances respectively Table (7). Several nutrients involvement in PC1 indicated an interaction between foliar nutrients, with positive loading for both N(0.936) and K(0.892) and negative loading for each one Ca (-0.330) and Mg(-0.387) as designated (N+Ca-Mg-K+). Deficiency of Ca and Mg in leaf tissues leads to a decrease in plant productivity. Ca play an essential role in membrane permeability, protein synthesis and carbohydrate transfer; while Mg is the main component in chlorophyll structure (Hirons and Thomas, 2018, Taiz and Zeiger, 2006). On the other hand, PC2 had shown positive loading for Fe and Ca with opposite change direction for P with high negative loading (-0.825). The third PC related to a positive

correlation with Ca and Na and negative correlation to Mg(-0.75).

For the low yielding population, only two PCs were retained with explaining 60% of total variance. The PC1 was effective in separating chemical nutrients into two groups based on their mobility. Phosphorus behaves in one direction with negative correlation (-0.841), while N, Fe, Mg, Na and K designated as (N+Fe+Ca+Na+) in the other direction with 22.44% of total variance. All these nutrients are essential in plant metabolic processes, such as synthesis protein, enzymes activity, chlorophyll, osmoregulation, phosphorylation and enzyme activation (Duca, 2015). The calcareous soil is widely distributed worldwide including soils in the Kurdistan region. The availability of phosphorus in this soil is low due to the high content of calcium carbonate (CaCO<sub>3</sub>), which has led to phosphorus being chemically fixed (Esmail, 2012).

Finally, PCA was performed on DRIS indices which produced two PCs with 45.73% and 20.23% of explained total variance. Both PCs was designated as (N+P+Fe+Ca+Na+K+) and (N+Fe+Mg) respectively, in positive correlation and one direction change. Mg (a component of the chlorophyll molecule) and P and Fe play a direct role in photosynthesis. If these elements are not present in sufficient levels, photosynthetic activity will be significantly reduced (Jones Jr, 2012, Barker and Pilbeam, 2015).

**Table 7:** Principal component analysis of nutrient concentration for high and low yield population, as well as DRIS indices in walnut during June 2017.

Nutrient	High yield			Low yield		DRIS index	
	PC1	PC2	PC3	PC1	PC2	PC1	PC2
N	0.936*	-0.081	0.138	0.349*	0.604*	0.296*	0.829*
P	0.219	-0.825*	0.003	-0.841*	0.254	0.869*	0.065
Fe	0.220	0.880*	-0.175	0.622*	0.465*	0.541*	0.559*
Ca	-0.330*	0.707*	0.477*	0.086	0.763*	0.520*	0.209
Mg	-0.387*	0.039	-0.750*	0.883*	0.035	-0.109	0.849*
Na	-0.101	-0.004	0.837*	0.623*	0.626*	0.846*	-0.059
K	0.892*	-0.061	-0.031	0.359*	-0.62	0.815*	0.216
Eigenvalue	2.369	1.773	1.404	2.629	1.571	3.201	1.416
% Variance	33.84	25.33	20.05	37.56	22.44	45.73	20.23
Total variance %	33.84	59.17	79.22	37.56	60.00	45.73	65.96
Selection Criteria	0.325	0.376	0.422	0.308	0.399	0.279	0.42
	PC1=N+Ca-Mg-K+			PC1=N+P-Fe+Mg+Na+K+		PC1=N+P+Fe+Ca+Na+K+	
	PC2=P-Fe+Ca+			PC2=N+Fe+Ca+Na+K-		PC2=N+Fe+Mg+	
	PC3=Ca+Mg-Na+						

#### 4. CONCLUSIONS

By developing the first DRIS walnut standards for northern Iraq, the results indicated that the local or regional DRIS norm is more convenient for local areas derived from special environmental conditions. It enables DRIS to demonstrate more reliable nutrient diagnosis deficiencies in the walnut tree. The obtained results from PCA reveal that it gives an opportunity for more accurate nutrient diagnosis deficiencies which confirm the DRIS approach. Depending on the average NBI values of the second-year samples were closer to adequate condition than the first-year samples. Generally, Fe was the most deficient nutrient. The amount of nutrient inputs back to the soil comes only from leaves falling plants it is not sufficient to a fulfilled deficit of nutrients. Application of bio-fertilizer compost and manure may be the best choice to compensate for nutrient deficiencies.

#### Acknowledgements

We would like to thank the owners of walnut orchards for giving as the permission to take plant leaf samples. We express our gratitude to villagers for their good hospitality. Finally, we are grateful to Professor Dr Yahya A. Shekha in Environmental Sciences Department/ College of Science/ Salahaddin University- Erbil for allowing us to use the equipment tools and his laboratory for plant analysis.

#### Conflict of Interest (1)

There is no conflict of interest among the authors.

#### REFERENCES

- AGBANGBA, E. C., SOSSA, E. L., DAGBENONBAKIN, G. D., DIATTA, S. & AKPO, L. E. 2011. DRIS model parameterization to access pineapple variety 'Smooth Cayenne' nutrient status in Benin (West Africa). *Journal of Asian Scientific Research*, 1, 254.
- AL-KUBAISI, Q. Y. & GARDI, L. M. 2012. Dust storm in Erbil city as a result of climatic change in Kurdistan Region Iraq. *Iraqi Journal of Science*, 53, 40-44.
- ALLEN, S. E., GRIMSHAW, H. M., PARKINSON, J. A. & QUARMBY, C. 1974. *Chemical analysis of ecological materials*, Blackwell Scientific Publications.
- BAILEY, J., BEATTIE, J. & KILPATRICK, D. 1997. The diagnosis and recommendation integrated system (DRIS) for diagnosing the nutrient status of grassland swards: I. Model establishment. *Plant and Soil*, 197, 127-135.
- BARKER, A. V. & PILBEAM, D. J. 2015. *Handbook of plant nutrition*, CRC press.
- BEAUFILS, E. 1971. Physiological diagnosis-a guide for improving maize production based on principles developed for rubber trees. *Fertilizer Society of South Africa Journal*, 1, 1-28.
- BEAUFILS, E. R. 1973. Diagnosis and recommendation integrated system (DRIS).
- CARNEIRO, A., PEREIRA, Ó., CUNHA, M. & QUEIROZ, J. 2015. The Diagnosis and Recommendation Integrated System (DRIS)–First Approach for the Establishment of Norms for Vineyards in Portugal. *Ciência e Técnica Vitivinícola*, 30, 53-59.
- CHANAN, M., HARDIWINOTO, S., AGUS, C., HADI PURWANTO, R. & PURWANTA, S. 2019. The identification of macro nutrient status of superior teak plantation (*Tectona grandis* Lin. F) by means of DRIS norms (Diagnosis and Recommendation Integrated System) in Indonesia. *Forest Science and Technology*, 1-6.
- COTTEINE, A. 1980. Soil Management for Conservation and Production. *New York*, 245-250.
- DARWESH, D. A. 2011. Effect of soil and foliar application of iron chelate on nutrient balance in lentil (*Lens esculenta* L.) by using modified DRIS equation. *Mesopotamia Journal of Agriculture*, 39, 39-49.
- DARWESH, D. A. & MUSTAFA, K. K. 2012. Influence of fungicides and vesicular arbuscular mycorrhiza on growth and nutrient balance of soybean by used DRIS equation. *Agricultural Sciences*, 3, 738-744.
- DIAS, J. R. M., WADT, P. G. S., PEREZ, D. V., SILVA, L. M. D. & LEMOS, C. D. O. 2011. DRIS formulas for evaluation of nutritional status of cupuaçu trees. *Revista Brasileira de Ciência do Solo*, 35, 2083-2091.
- DIZAYEE, A. & SALEH, H. 2017. Effect of different levels of nitrogen and potassium fertilizers application on nutrient balance and yield of Broccoli (*Brassica oleraceae*). *The Iraqi Journal of Agricultural Science*, 48, 107.
- DIZAYEE, A. T. & HUSSEIN, A. A. 2017. Early Diagnosis and Best Nutrient Balance for Barley Crop, As Influenced By Application of Different Levels of Nitrogen, Phosphorus and Potassium Using DRIS Methodology. *Muthanna Journal of Agricultural Science*.
- DUCA, M. 2015. Mineral nutrition of plants. *Plant Physiology*. Springer.
- ESMAIL, A. O. 2012. Effect of Soil Phosphorus Chemical Equilibrium on P-availability for Wheat using Solubility Diagram and (DRIS-Chart) Methods. *Journal Of Kirkuk University For Agricultural Sciences*, 3, 43-51.
- ESMAIL, A. O., SHEIKH-ABDULLAH, S. M. & MARUF, M. T. 2019. Phosphorus Availability in Entisols, Inceptisols, and Mollisols of Iraqi Kurdistan. *Soil Science*, 184, 95-100.

- GARDNER, F. P., PEARCE, R. B. & MITCHELL, R. L. 2017. *Physiology of crop plants*, Scientific Publishers.
- GAUTHIER, M.-M. & JACOBS, D. F. 2011. Walnut (*Juglans* spp.) ecophysiology in response to environmental stresses and potential acclimation to climate change. *Annals of Forest Science*, 68, 1277-1290.
- GEIKLOOI, A., REYHANITABAR, A., NAJAFI, N. & HOMEI, H. 2018. Diagnosis of Nutrient Imbalance in Wheat Plant by DRIS and PCA Approaches. *Journal of Plant Physiology & Breeding*, 7, 1-9.
- HAVLIN, J., BEATON, J., TISDALE, S. & NELSON, W. 1999. Soil fertility and fertilizers: an introduction to nutrient management. *Soil fertility and fertilizers: an introduction to nutrient management*.
- HIRONS, A. & THOMAS, P. A. 2018. *Applied Tree Biology*, John Wiley & Sons.
- JONES JR, J. B. 2012. *Plant nutrition and soil fertility manual*, CRC press.
- KIRCHMANN, H., BERGSTRÖM, L., KÄTTERER, T., MATTSSON, L. & GESSLEIN, S. 2007. Comparison of long-term organic and conventional crop-livestock systems on a previously nutrient-depleted soil in Sweden. *Agronomy Journal*, 99, 960-972.
- MARSCHNER, H. 2011. *Marschner's mineral nutrition of higher plants*, Academic press.
- MATOS, G. S. B. D., FERNANDES, A. R., WADT, P. G. S., FRANZINI, V. I., SOUZA, E. M. D. C. & RAMOS, H. M. N. 2018. Dris calculation methods for evaluating the nutritional status of oil palm in the Eastern Amazon. *Journal of plant nutrition*, 41, 1240-1251.
- OHNO, T., GRIFFIN, T. S., LIEBMAN, M. & PORTER, G. A. 2005. Chemical characterization of soil phosphorus and organic matter in different cropping systems in Maine, USA. *Agriculture, ecosystems & environment*, 105, 625-634.
- RAGHUPATHI, H., REDDY, Y., REJU, M. K. & BHARGAVA, B. 2005. Diagnosis of nutrient imbalance in mango by DRIS and PCA approaches. *Journal of plant nutrition*, 27, 1131-1148.
- SHARMA, J., SHIKHAMANY, S., SINGH, R. & RAGHUPATHI, H. 2005. Diagnosis of nutrient imbalance in Thompson Seedless grape grafted on Dog Ridge rootstock by DRIS. *Communications in soil science and plant analysis*, 36, 2823-2838.
- SILVEIRA, C. P., NACHTIGALL, G. R. & MONTEIRO, F. A. 2005. Norms for the diagnosis and recommendation integrated system for signal grass. *Scientia Agricola*, 62, 513-519.
- SNYDER, G. & KRETSCHMER JR, A. 1988. A DRIS analysis for bahiagrass pastures. *Proceedings-Soil and Crop Science Society of Florida (USA)*.
- SYTYKIEWICZ, H., KOZAK, A., ŁUKASIK, I., SEMPRUCH, C., GOŁAWSKA, S., MITRUS, J., KUROWSKA, M., KMIEĆ, K., CHRZANOWSKI, G. & LESZCZYŃSKI, B. 2019. Juglone-Triggered Oxidative Responses in Seeds of Selected Cereal Agrosystem Plant Species. *Polish Journal of Environmental Studies*, 28, 2389-2397.
- TAIZ, L. & ZEIGER, E. 2006. *Plant Physiology* Sinauer Associates. Inc., Sunderland, MA.
- TALPUR, N. 2015. Evaluating the DRIS norms for wheat belt of district Hyderabad, Pakistan. *Pakistan Journal of Agricultural Sciences*, 52, 767-774.
- TOWNSEND, C. & GUEST, E. 1980. *Flora of Iraq:(Hutchinson, 1959). Cornaceae to Resedaceae*, Ministry of agriculture & agrarian reform.
- WAIREGI, L. & VAN ASTEN, P. 2011. Norms for multivariate diagnosis of nutrient imbalance in the East African highland bananas (*Musa* spp. AAA). *Journal of plant nutrition*, 34, 1453-1472.
- WALWORTH, J. & SUMNER, M. 1987. The diagnosis and recommendation integrated system (DRIS). *Advances in soil science*. Springer.
- YAO, L., ZHAO, C. X., GU, X., ZHANG, W. W., WEN, J., REN, C., CHEN, Y., LI, J., ZHANG, R. & MENG, Q. 2013. Nephropathy Effects of Intravenous Contrast, Iodixanol, on db/db and eNOSKnockoutMice. *Life Science Journal*, 10.



## RESEARCH PAPER

# Computational Modeling, Docking, Synthesis, Characterization, and in vitro Cyclooxygenase Inhibitory Activity of Some Novel Non-Steroidal Anti-inflammatory Prodrugs

Dana Muhammad Hamad Ameen<sup>1</sup>, Sara Ramzi Abdulhameed<sup>2</sup>

1Department of Pharmaceutical Chemistry, College of Pharmacy, Halwer Medical University, Hawler, Kurdistan Region, Iraq

2Department of Pharmaceutical Chemistry, College of Pharmacy, University of Sulaimani, Sulaimani, Kurdistan Region, Iraq

### ABSTRACT:

Non-steroidal anti-inflammatory drugs (NSAIDs) are among the most prescribed analgesic and anti-inflammatory drugs. However, inhibition of cyclooxygenase1 and acidic groups such as carboxylic groups in most NSAIDs cause gastrointestinal (GI) side effects. Therefore, masking the acidic groups till it pass through the GI tract will decrease the direct GI side effects and because *N*-(2,6-dimethylphenyl)-acetamide **1** also has anti-inflammatory activity so the synthesized ester prodrugs might act as mutual prodrugs.

2-Chloro-*N*-(2,6-dimethylphenyl)-acetamide **1** was utilized to synthesize ester prodrug of various NSAIDs **2a-e**. The 2-Chloro-*N*-(2,6-dimethylphenyl)-acetamide **1** undergo substitution reaction at  $\alpha$  position with various sodium carboxylate of NSAIDs **2a-e** in DMSO. The constitution of the newly synthesized ester prodrugs of NSAIDs **3a-e** had been confirmed depending on their IR, <sup>1</sup>H and <sup>13</sup>C-NMR spectral analysis. The synthesized ester prodrugs **3a-e** were screened for their *in vitro* inhibitory activities of COX-1 as well as COX-2 however, their COX inhibition activity increased compared with their starting **1** and **2a-e**.

Physicochemical properties and "Lipinski's rule of five" were assessed for compounds **3a-e**, and they all satisfied the rule. Furthermore molecular docking for compounds **3a-e** into COX-1 and COX-2 was done, in which they showed binding free energies  $\Delta G_b$  in the range of (-8.9 to -9.8 kcal/mol) when docked into COX-1 and (-10.4 to -12.4 kcal/mol) into COX-2 enzymes.

KEY WORDS: NSAIDs; docking; prodrug; cyclooxygenase; acetamide.

DOI: <http://dx.doi.org/10.21271/ZJPAS.32.6.3>

ZJPAS (2020) , 32(6);25-39 .

## 1. INTRODUCTION

The fact that non-steroidal anti-inflammatory drugs (NSAIDs) are considered to be among the most commonly prescribed medications is attributed to their broad range of medical indications, as they can be used as analgesic, anti-inflammatory, antirheumatic and antipyretic agents (Al-Turki *et al.*, 2017). Despite being commonly used; NSAIDs were shown to have extensive adverse effects, including gastrointestinal (GI) complications,

hypertension, edema, renal disease, and cardiovascular risk. The most frequent among these are the gastrointestinal adverse effects such as dyspepsia, ulcers, bleeding and other associated GI complications (Pountos *et al.*, 2011). Hence, the need for designing new NSAIDs having less GI complications has become of a great importance. It has been approved that converting the acidic carboxylic groups into their corresponding amides and esters can effectively reduce the NSAIDs associated GI damage without changing their anti-inflammatory properties (Makhija, Somani and Chavan, 2013; Qasir, 2013; Ashraf *et al.*, 2016)(Ameen, 2020).

### \* Corresponding Author:

Dana Muhammad Hamad Ameen

E-mail: [sarahramzi1@gmail.com](mailto:sarahramzi1@gmail.com)

### Article History:

Received: 11/06/2020

Accepted: 09/08s/2020

Published:2 0/12 /2020

One approach was to use amino acids such as L-glycine, L-histidine, and L-tryptophan for synthesizing new amide and ester derivatives by masking the acidic carboxylic group of some NSAIDs. The synthesized derivatives can also be considered as mutual prodrugs since these amino acids possess some anti-inflammatory properties as well (Meyers, Moonka and Davis, 1979). Other NSAID mutual prodrugs were synthesized by combining two anti-inflammatory and analgesic agents, for example acetylsalicylic acid and paracetamol were esterified to give Benorylate; a mutual prodrug with better gastric tolerability (Croft, Cuddigan and Sweetland, 1972). Prodrugs of flurbiprofen (Gairola *et al.*, 2005), diclofenac, and ketoprofen (Dhaneshwar *et al.*, 2009) were synthesized by esterification using phenylalanine, alanine, histidine, tryptophan, and glycine. They showed reduced ulcerogenic effect with improved analgesic and anti-inflammatory activity. Ibuprofen, naproxen, and mefenamic acid mutual prodrugs were synthesized as they were linked to chlorzoxazone through an ester linkage with the objective of ameliorating the GI adverse effects. After evaluating their anti-inflammatory activity, these prodrugs were comparable to the starting NSAIDs. They also showed an improved gastro-sparing profile. Docking study was also performed for predicting the binding free energy ( $\Delta G_b$ ) and configuration of the synthesized prodrugs. Ibuprofen and naproxen prodrugs exhibited the highest binding free energy ( $\Delta G_b$ ) scores when docked into COX-2 enzyme; as ibuprofen showed -11.69 while naproxen showed -12.65 kcal/mol (Abdel-Azeem *et al.*, 2009). Other mefenamic acid and ibuprofen ester prodrugs were designed and synthesized using 4-(4-substituted benzylideneamino) phenol Schiff base for condensation with the acidic NSAIDs. These ester prodrugs showed significant anti-inflammatory effect. Interestingly, when studying their GI toxicity profile they were all non-ulcerogenic. This result proves that modifying the acidic carboxylic group of NSAIDs reduces their ulcerogenicity while retaining their anti-inflammatory activity. Molecular docking study was performed for the synthesized prodrugs into both COX-1 and COX-2 enzymes and they exhibited higher binding free energies ( $\Delta G_b$ ) when docked into COX-2 than COX-1 (Hegazy and Ali, 2012).

The interest in synthesizing poly-functional molecules is increasing nowadays. Acetamides can be considered as a poly-functional molecules since their derivatives were found to possess various bioactive properties such as; anthelmintic (Sawant and Kawade, 2011), anticonvulsant (Kamiński *et al.*, 2011) (Jawed *et al.*, 2010), antioxidant (Ayhan-Kilcigil *et al.*, 2012) (Autore *et al.*, 2010), anti-inflammatory (Jain *et al.*, 2013)(Autore *et al.*, 2010), anti-arthritic (Jain *et al.*, 2013), anti-bacterial (Kanagarajan and Gopalakrishnan, 2012) (Nayak *et al.*, 2014), antifungal (Bardiot *et al.*, 2015) (Kidwai *et al.*, 2012) (Kanagarajan, Thanusu and Gopalakrishnan, 2010), and anti-viral properties (Babkov *et al.*, 2015) (Kai *et al.*, 2001).

In view of the mentioned reports, this study was aimed to design and synthesize new ester prodrugs of *N*-(2,6-dimethylphenyl)-acetamide **1** and NSAIDs **2a-e** in an attempt to reduce the gastric irritation of acidic NSAIDs. Using *N*-(2,6-dimethylphenyl)-acetamide **1** for masking the acidic group will form a mutual prodrug, since it also works as a mild anti-inflammatory agent (Autore *et al.*, 2010; Ayhan-Kilcigil *et al.*, 2012).

## 2.MATERIALS AND METHODS

This experimental study was designed for modelling of some NSAIDs prodrugs and docking them into the PDB models of COX-1 and COX-2 receptors to compare their binding affinity ( $\Delta G_b$ ) in order to decide which models should be synthesized. MarvinSketch 19.7 was used to draw the chemical structures of these models as 2D structures and convert them to 3D structures. SwissADME web tool was used to check the compliance of the designed compounds with "Lipinski's rule of five". For the preparation of COX-1 and COX-2 macromolecules (proteins); AutoDockTools 1.5.6 was used, while ligand preparation and docking were both performed using PyRx (Python Prescription 0.8). For molecular visualization; "The PyMOL Molecular Graphics System (Version 2.3.2 Schrödinger)" was used.

Importantly, the study was aimed to synthesize those prodrugs of NSAIDs which had higher docking score and to evaluate the ability of the synthesized compounds **3a-e** of inhibiting COX enzyme. All the synthetic procedures were done at Hawler Medical University, College of Pharmacy, Pharmaceutical Chemistry and Organic Chemistry

Lab, between 1<sup>st</sup> of June 2019 to 15<sup>th</sup> of August 2019. The NSAIDs **2a-e** were purchased from (Sigma Aldrich, UK and Apollo Healthcare Resources, Singapore) the 2-Chloro-*N*-(2,6-dimethylphenyl)-acetamide **1** purchased from (Apollo Healthcare Resources, Singapore). All the chemicals were used directly without being purified in advance. For the determination of the melting points a Gallenkamp electro-thermal apparatus was used through an open capillary method and the results were recorded without correction. Pre-coated TLC plates 60 F254 (Merck, Germany) were used to check the purity of the compounds, with a solvent system of toluene: acetone (2:1). For visualizing the developed chromatographic plates; UV (254 nm) was used. JASCO FTIR Spectrophotometer was used to record IR spectra, (at Hawler Medical University, College of Pharmacy, Pharmaceutical Chemistry Department). Bruker Ultra shield 400 MHz with internal TMS was used to measure <sup>1</sup>H and <sup>13</sup>C-NMR spectra with the chemical shifts represented as ppm (at University of Science and Technology/ Irbid- Jordan). Finally, *in vitro* inhibitory properties (of COX-1 and COX-2 enzymes) for compounds **3a-e** and their starting **1** and **2a-e** were assessed at Central University of Lancashire, College of Pharmacy and Biomedical Science, Physiology and Biology Lab.

### 2.1 Computational and docking study

Docking into both COX-1 and COX-2 enzymes was studied. X-ray Crystallographic Structures for these enzymes were retrieved from "Protein Data Bank" website (<https://www.rcsb.org/>); COX-1 bound with ibuprofen (PDB: 1EQG) and COX-2 bound with meclufenamic acid (PDB: 5IKQ). For identifying the main amino acids involved in the ligand-receptor interactions which form the binding site of a receptor; data from "PDBsum" website was used as a reference (<http://www.ebi.ac.uk/thornton-srv/databases/cgi-bin/pdbsum/>) (Abdel-Aziz, Eltahir and Asiri, 2011).

#### Preparation of proteins

AutoDockTools 1.5.6 was used for the preparation of the protein structures. In this step the polar hydrogens were placed back to the protein. To avoid masking the enzyme surface with the water molecules which can affect the binding of the ligand; water molecules were removed. Ligands,

cofactors, and all the molecules bound to the protein were also removed from the protein structure (Hegazy and Ali, 2012; Dhingra *et al.*, 2014).

#### Preparation of ligands

MarvinSketch 19.7 was used to draw the Structures of ligands **3a-e**. They were primarily sketched as 2D structures and then converted to the 3D format (pdb) using the same program. Then they were energetically minimized by using PyRx (Python Prescription 0.8) (Dallakyan and Olson, 2015).

#### Docking study

PyRx (Python Prescription 0.8) docking program was used to perform the docking of ligands **3a-e** into the previously prepared proteins: COX-1 (1EQG) and COX-2 (5IKQ) (Dallakyan and Olson, 2015). For the molecular visualization of the docked conformations (poses) and the receptor-ligand interactions; "The PyMOL Molecular Graphics System (Version 2.3.2 Schrödinger)" was used.

#### Prediction of ADME properties

Ligands **3a-e** were all tested for their compliance to "Lipinski's rule of five". Physicochemical descriptors of these compounds were computed to predict their ADME parameters, pharmacokinetic properties, and druglike nature. To perform all these calculations SwissADME web tool was used (Daina, Michielin and Zoete, 2017).

### 2.2 Chemical Synthesis

#### Synthesis of the ester prodrugs of attempted NSAIDs with 2-Chloro-*N*-(2,6-dimethylphenyl)-acetamide

2-Chloro-*N*-(2,6-dimethylphenyl)-acetamide **1** (2.5 mmol) was added to a mixture of NSAIDs **2a-e** (2.5 mmol) and sodium bicarbonate (NaHCO<sub>3</sub>) (2.5

mmol) in 20 ml of dimethyl sulfoxide (DMSO), followed by stirring for 24 hours (Scheme 1).

After the completion of the reaction, this mixture was cooled by adding it to an ice-water (100 ml), then the formed precipitate was collected through suction filtration and left to dry. After drying, the obtained solid residue was recrystallized using absolute ethanol (Hamad *et al.*, 2017)(hamadameen and Ameen, 2019). Table 4 shows the physical properties of these synthesized prodrugs **3a-e**.

## 2.3 Biological study

### General procedure for the *in vitro* COX inhibitor screening

“Cayman's COX activity assay kit” was used for screening the COX inhibitory activity of the starting compounds **1** and **2a-e** as well as the synthesized compounds **3a-e**. This assay is a fluorescence-based technique in which ovine COX-1 and human recombinant COX-2 enzymes are used to screen for COX inhibiting properties (Nile *et al.*, 2016) (Aboaraia *et al.*, 2017)(Salih *et al.*, 2020).

1. Preparation of initial activity wells: 10  $\mu$ l of DMSO, 10  $\mu$ l of enzyme (COX-1 or COX-2), 10  $\mu$ l of ADHP (10-acetyl-3,7-dihydroxyphenoxazepine), 10  $\mu$ l of heme, and 150  $\mu$ l of assay buffer were mixed.
2. Preparation of background wells: 10  $\mu$ l of DMSO, 10  $\mu$ l of ADPH, 10  $\mu$ l of heme, and 160  $\mu$ l of assay buffer were mixed.
3. Preparation of Inhibitor wells: 10  $\mu$ l of inhibitors\*, 10  $\mu$ l of enzyme (COX-1 or COX-2), 10  $\mu$ l of ADPH, 10  $\mu$ l of heme, and 150  $\mu$ l of assay buffer were mixed.
4. For initiating the reactions; 10  $\mu$ l of arachidonic acid solution were added to all the used wells.
5. Followed by two minutes incubation of the wells at room temperature.
6. An excitation wavelength of (530-540 nm) and an emission wavelength of (585-595 nm) were used for reading the plate.

7. For each sample the average fluorescence was calculated.
8. The next step was subtracting the fluorescence of the background wells from the fluorescence of the inhibitor and the initial activity wells.
9. To calculate the percentage of inhibition; the value of each inhibitor sample was subtracted from the value of initial activity sample, followed by dividing this result by the value of initial activity and multiplying it by %100.

\* Solutions of 10, 100 and 1000 nm of each Inhibitor (compounds **1**, **2a-e** and **3a-e**) were prepared using DMSO as a solvent.

## 3.RESULTS

### 3.1 Computational study

#### Docking accuracy validation

For validating the molecular docking program which has been used; COX-1 enzyme bound with ibuprofen crystal structure (1EQG) was retrieved from “Protein Data Bank” website, then by re-docking ibuprofen into the binding site of the same enzyme, the best docking configuration was very close to the experimentally proven configuration showing a root-mean-square deviation (RMSD) of 0.45 Å (Fig. 1, a).

For COX-2 enzyme; meclufenamic acid was used as a reference (PDB code: 5IKQ). Meclofenamic acid was again docked into COX-2 enzyme binding site, and it gave a binding mode that seemed to be closely similar to the originally bound ligand, with an RMSD of 0.34 Å (Fig. 1, b).

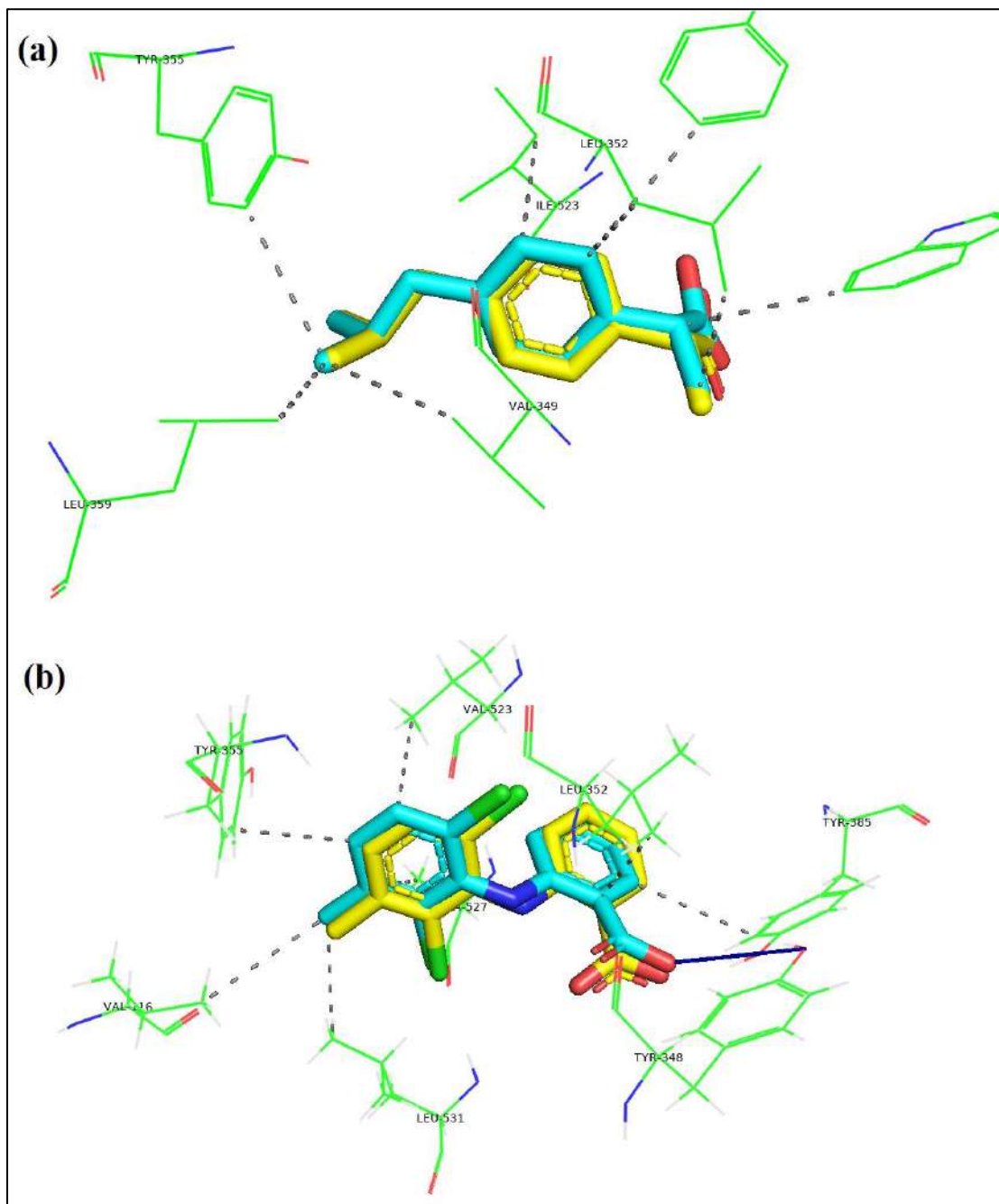


**Figure 1.** Validation of the docking accuracy. **(a)** Ibuprofen bound to COX-1. **(b)** Meclofenamic acid bound to COX-2. The native co-crystallized ibuprofen and Meclofenamic acid are shown in yellow, while the docked ligands are shown in cyan blue. All structures are colored by element. The hydrogen bonds are shown as dark blue lines. The docked ligands seem exactly superimposed on the native ones.

### Docking results of compounds 3a-e

Ester prodrugs of NSAIDs with 2-chloro-N-(2,6-dimethylphenyl)-acetamide (**3a-e**) were docked into COX-1 and COX-2 crystal structures for comparing their binding affinities. The binding free energy ( $\Delta G_b$ ) measured in (kcal/mol) was

used to compare the binding affinity. Table 1 and Table 2 show all the docking results for compounds **3a-e**. (Fig. 2) shows the best docked conformations of compounds **3a-e** bound to COX-1 (1EQG), while (Fig. 3) shows their best docked conformations bound to COX-2 (5IKQ).

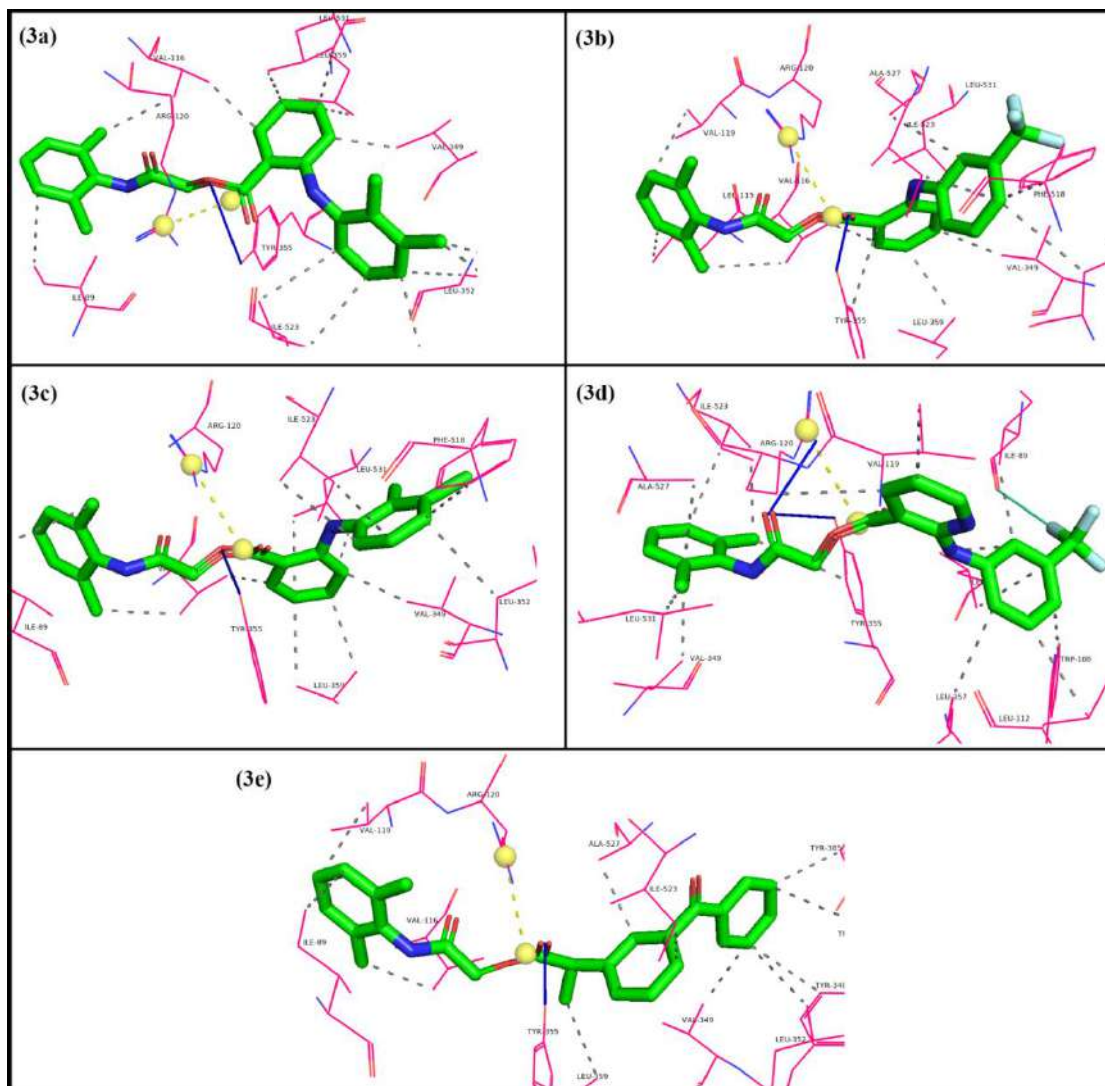


**Figure 2.** The best docking modes of compounds **3a-e** (colored in green) are shown in their binding site of COX-1 (1EQG). All structures are colored by element. The hydrogen bonds are shown as dark blue lines. The binding site of COX-1 is shown with labeled amino acids.

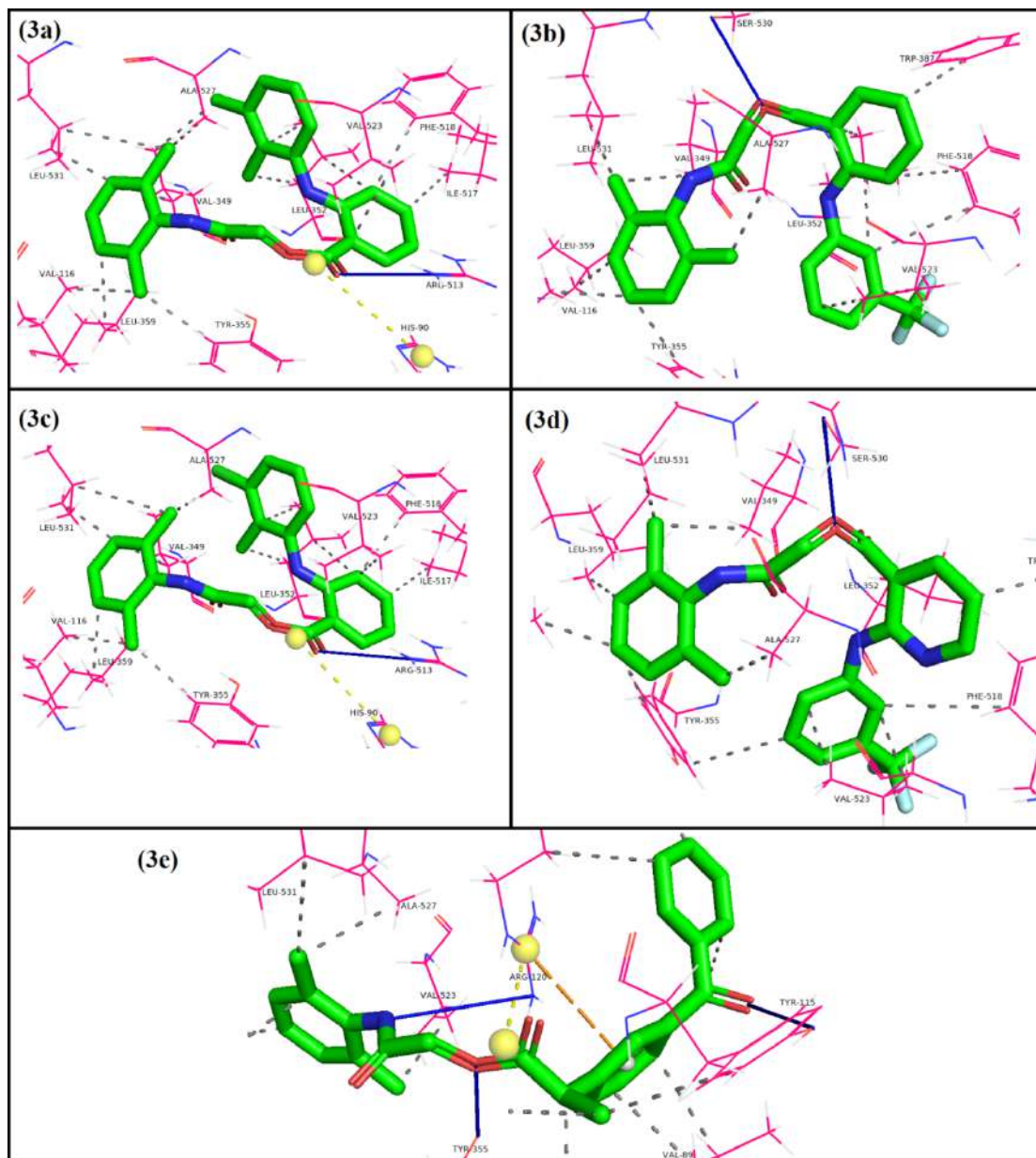


**Figure 3.** The best docking modes of compounds **3a-e** (colored in green) are shown in their binding site of COX-2 (5IKQ). All structures are colored by element. The hydrogen bonds are shown as dark blue lines. The binding site of COX-2 is shown with labeled amino acids.

### ADME properties

SwissADME web tool was used to evaluate the physicochemical properties of compounds **3a-e**; these properties can affect their oral bioavailability, metabolism, and druggability. They were also checked for their “Lipinski’s rule of five” compliance. All these results are shown in Table 3.

### 3.2 Synthesis

The synthetic procedures that resulted in the generation of compounds **3a-e** are represented in

Scheme 1. Characterization and purity of these compounds were monitored by measuring some of their physicochemical parameters such as their physical appearance, melting points,  $R_f$  values, and percent yields which are shown in Table 4. Identification and characterization of these compounds was also done using spectral analysis such as FT-IR,  $^1\text{H-NMR}$ , and  $^{13}\text{C-NMR}$  spectroscopy as shown in Table 5.

**Table 1: Docking results of compounds 3a-e docked into COX-1 (1EQG)**

Compound	$\Delta G_b$ (kcal/mol)	No. of HB	Residue	Amino Acid	Distance ( $\text{\AA}^\circ$ )
3a	-9.1	1	355A	TYR	3.10
3b	-9.3	1	355A	TYR	1.82
3c	-9.1	1	355A	TYR	3.19
3d	-9.8	2	120A	ARG	2.18
			355A	TYR	3.03
3e	-8.9	1	355A	TYR	1.97

**Table 2: Docking results of compounds 3a-e docked into COX-2 (5IKQ)**

Compound	$\Delta G_b$ (kcal/mol)	No. of HB	Residue	Amino Acid	Distance ( $\text{\AA}^\circ$ )
3a	-11	1	513A	ARG	2.86
3b	-10.4	1	530A	SER	2.54
3c	-11	1	513A	ARG	2.97
3d	-12.4	1	530A	SER	2.72
			115A	TYR	3.22
3e	-10.8	3	120A	ARG	3.85
			355A	TYR	2.11

**Table 3: Calculation of various molecular properties of test compounds 3a-e**

Compound	Mol. weight (MW) <sub>a</sub>	Rotatable bonds <sup>b</sup>	HB Donor <sup>c</sup>	HB Acceptors <sup>d</sup>	CLogP <sup>e</sup>	Lipinski violations <sup>f</sup>	TPSA <sup>g</sup>
3a	402.49	8	2	3	3.94	0	67.43
3b	442.43	9	2	6	3.92	0	67.43
3c	422.9	8	2	3	4.13	0	67.43
3d	443.42	9	2	7	3.29	0	80.32
3e	415.48	9	1	4	3.71	0	72.47

<sup>a</sup> (150 - 500 g/mol), <sup>b</sup> ( $\leq 9$ ), <sup>c</sup> ( $\leq 5$ ), <sup>d</sup> ( $\leq 10$ ), <sup>e</sup> ( $< 5$ ), <sup>f</sup> ( $\leq 1$ ), and <sup>g</sup> (20 - 130  $\text{\AA}^2$ )

**Table 4: Physical properties of synthesized compounds 3a-e**

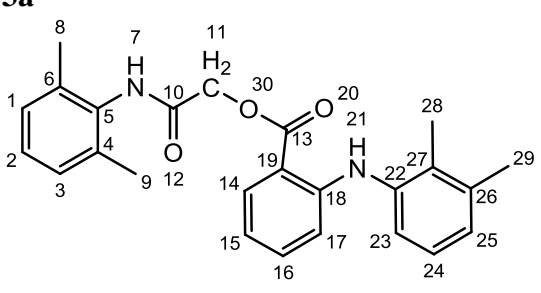
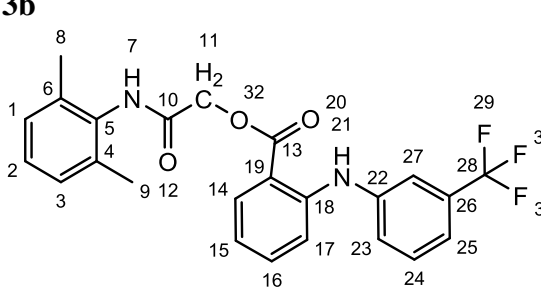
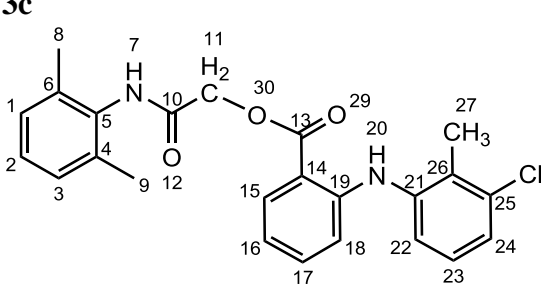
Compounds	Physical appearance	Yield (%)	Melting point $^\circ\text{C}$	Rf value *
3a	Colorless	67	217-219	0.82

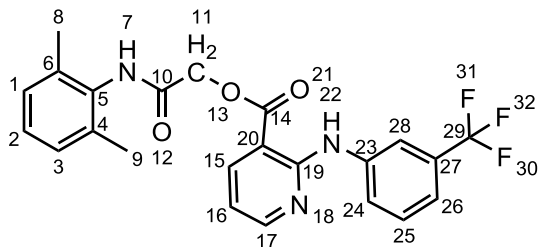
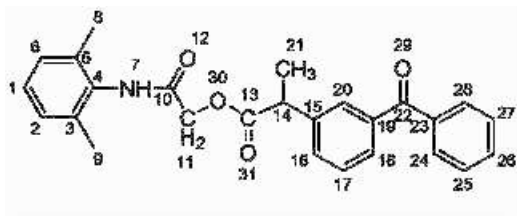


<b>3b</b>	powder Colorless powder	82	159-161	0.81
<b>3c</b>	Colorless powder	66	205-207	0.81
<b>3d</b>	Colorless powder	74	215-216	0.78
<b>3e</b>	Colorless powder	77	105-107	0.78

\*R<sub>f</sub> value, toluene: acetone (2:1) used as eluent.

**Table 5: Spectroscopic data of the synthesized compounds (3a-e)**

Compounds	Spectroscopic data
<p><b>3a</b></p> 	<p><b>IR in cm<sup>-1</sup>:</b> 3319, 3244 (NH str. amine and amide), 1689 (C=O ester), 1660 (C=O amide), 1222 (C-O ester).</p> <p><b><sup>1</sup>HNMR</b> (400 MHz, DMSO- <i>d</i><sub>6</sub>): δ 1.24(s, 3H, <sub>29</sub>CH<sub>3</sub>), 1.31(s, 6H, <sub>8</sub>CH<sub>3</sub>, <sub>9</sub>CH<sub>3</sub>), 1.44 (s, 3H, <sub>28</sub>CH<sub>3</sub>), 4.13 (s, 2H, <sub>11</sub>CH<sub>2</sub>), ((6.68, d, 1H, <i>J</i>=8Hz), (6.75, t, 1H), (7.08,s, 4H), (7.13,s,2H),( 7.36, t, 1H), (8.04, d, 1H, <i>J</i>=4Hz ) 10Ar-H), 9.12(s, 1H, Ar-NH), 9.57(s, 1H, Ar-NHCO).</p> <p><b><sup>13</sup>CNMR</b> (101 MHz, DMSO-<i>d</i><sub>6</sub>): δ C<sub>29</sub>-14.09, C<sub>8</sub>,C<sub>9</sub>- 18.46, , C<sub>28</sub>-20.69, C<sub>11</sub>-63.41, Ar (C) -110.69-149.16, C<sub>10</sub>-166.00, C<sub>13</sub>-167.98.</p>
<p><b>3b</b></p> 	<p><b>IR in cm<sup>-1</sup>:</b> 3323, 3201 (NH str. amine and amide), 1685 (C=O ester), 1658 (C=O amide), 1228 (C-O ester).</p> <p><b><sup>1</sup>HNMR</b> (400 MHz, DMSO- <i>d</i><sub>6</sub>): δ 2.17 (s, 6H, <sub>8</sub>CH<sub>3</sub>, <sub>9</sub>CH<sub>3</sub>), 5.01 (s, 2H, <sub>11</sub>CH<sub>2</sub>), ((9.98, t, 1H) (7.08, s, 3H) (7.34, d, 2H, <i>J</i>=8Hz)(7.50, m, 4H) (8.06, d, 1H, <i>J</i>=8Hz) 11Ar-H), 9.29 (s, 1H, Ar-NH), 9.60 (s, 1H, Ar-NHCO).</p> <p><b><sup>13</sup>CNMR</b> (101 MHz, DMSO-<i>d</i><sub>6</sub>): δ C<sub>8</sub>,C<sub>9</sub>- 17.80, C<sub>11</sub>-62.76, C<sub>28</sub>- 114.16, Ar (C) -115.45-144.76, C<sub>10</sub>-165.22, C<sub>13</sub>-166.58.</p>
<p><b>3c</b></p> 	<p><b>IR in cm<sup>-1</sup>:</b> 3313, 3246 (NH str. amine and amide), 1691 (C=O ester), 1666 (C=O amide), 1222 (C-O ester).</p> <p><b><sup>1</sup>HNMR</b> (400 MHz, DMSO- <i>d</i><sub>6</sub>): δ 2.18 (s, 6H, <sub>8</sub>CH<sub>3</sub>, <sub>9</sub>CH<sub>3</sub>), 2.26 (s, 3H, <sub>27</sub>CH<sub>3</sub>), 5.00 (s, 2H, <sub>11</sub>CH<sub>2</sub>), ((6.84, t, 2H) (7.09, s, 3H) (7.25, m, 3H)(7.43, t, 1H) (8.06, d, 1H, <i>J</i>=8Hz) 10Ar-H), 9.20</p>

**3d****3e**

(s, 1H, Ar-NH), 9.59 (s, 1H, Ar-NHCO).

<sup>13</sup>CNMR (101 MHz, DMSO-*d*<sub>6</sub>): δ C<sub>27</sub>-14.46, C<sub>8</sub>,C<sub>9</sub>-17.80, C<sub>11</sub>-62.84, Ar (C) -111.16-147.25, C<sub>10</sub>-165.25, C<sub>11</sub>-167.17.

**IR in cm<sup>-1</sup>:** 3265 (NH str. amine and amide overlaped), 1697 (C=O ester), 1668 (C=O amide), 1116 (C-O ester).

**<sup>1</sup>HNMR (400 MHz, DMSO-*d*<sub>6</sub>):** δ 2.18 (s, 6H, <sub>8</sub>CH<sub>3</sub>, <sub>9</sub>CH<sub>3</sub>, 5.07 (s, 2H, <sub>11</sub>CH<sub>2</sub>), ((7.02, d, 4H, *J*=20Hz) (7.35 ,s, 1H)(7.55, s, 1H) (7.89, s, 1H) (8.29, s, 1H) (8.43, d, 2H, *J*=28Hz) 10Ar-H), 9.63 (s, 1H, Ar-NH), 10.15 (s, 1H, Ar-NHCO).

<sup>13</sup>CNMR (101 MHz, DMSO-*d*<sub>6</sub>): C<sub>8</sub>,C<sub>9</sub>-17.89, C<sub>11</sub>-63.30, C<sub>29</sub>-107.85, Ar (C) -114.81-154.45, C<sub>10</sub>-165.10, C<sub>14</sub>-166.11.

**IR in cm<sup>-1</sup>:** 3346 (NH str. amide), 1747 (C=O str. ester), 1697 (C=O str. amide), 1116 (C-O str. ester).

**<sup>1</sup>HNMR (400 MHz, DMSO):** δ 1.49 (d, 3 H, <sub>2 1</sub> CH<sub>3</sub> ), 2.12 (s, 6 H, <sub>8</sub> CH<sub>3</sub> , <sub>9</sub> CH<sub>3</sub> ), 4.13 (q, 1 H, <sub>1 4</sub> CH), 4.73 (dd, 2 H, <sub>1 1</sub> CH<sub>2</sub> ), (7.08 (s, 3 H), 7.56 (t, 3 H), 7.64 (m, 6 H), 12 Ar-H), 9.40 (s, 1 H, Ar-NHCO).

<sup>13</sup>CNMR (101 MHz, DMSO): C<sub>8</sub> ,C<sub>9</sub> -17.50, C<sub>2 1</sub> -18.16, C<sub>1 4</sub> -43.57, C<sub>1 1</sub> -62.38, Ar (C) -126.22-140.42, C<sub>1 0</sub> -164.75, C<sub>1 3</sub> -172.87, C<sub>2 2</sub> -195.12.

**3.3COX inhibition activity**

Screening for the COX inhibition activity of compounds **1**, **2a-e** and **3a-e** was done using Cayman's assay kit. Results of COX-1 inhibition

screening are shown in Table 6, while results of COX-2 inhibition screening are shown in Table 7.

**Table 6: *In vitro* ovine COX I assay results**

Compounds	COX I % inhibition					
	F	10 nM	F	100 nM	F	1000 nM
<b>1</b>	13884±363	14	17452±378	17	1751±279	18
<b>2a</b>	24004±274	37	23118±251	39	22841±218	40
<b>3a</b>	29187±666	23	27534±445	27	26993±234	29
<b>2b</b>	27149±612	28	26601±184	30	232621±265	39
<b>3b</b>	33823±567	11	25695±408	33	23080±53	40
<b>2c</b>	31612±404	17	27505±499	28	24247±160	37
<b>3c</b>	28413±258	26	27191±112	29	24935±325	35
<b>2d</b>	29818±625	22	28602±407	25	25839±169	32
<b>3d</b>	33622±444	12	25693±213	33	22824±160	41

<b>2e</b>	33312±240	13	29051±234	24	25244±116	34
<b>3e</b>	32252±105	16	30295±501	21	26852±79	30

F= Mean±SD of the initial fluorescence activity. nM= Nano-molar concentrations of the synthesized prodrugs **3a-e** and their precursor **2a-e**.

**Table 7: *In vitro* human recombinant COX-2 assay results**

Compounds	COX II % inhibition					
	F	10 nM	F	100 nM	F	1000 nM
<b>1</b>	7255±247	10	12354±392	13	10124±582	16
<b>2a</b>	29428±353	22	24895±417	35	22225±235	41
<b>3a</b>	29551±583	23	25401±324	33	22323±209	42
<b>2b</b>	30511±442	22	26895±897	32	24279±531	39
<b>3b</b>	29506±597	23	25489±572	33	22863±528	40
<b>2c</b>	27556±386	26	27293±664	28	23987±266	35
<b>3c</b>	28099±21	27	26725±208	29	24729±292	37
<b>2d</b>	27047±437	32	26625±461	33	23780±408	40
<b>3d</b>	24931±459	37	22437±697	44	21063±680	47
<b>2e</b>	29167±444	23	25670±347	31	21229±81	35
<b>3e</b>	28158±63	26	26725±208	32	24557±287	44

F= Mean±SD of the initial fluorescence activity. nM= Nano-molar concentrations of the synthesized prodrugs **3a-e** and their precursor **2a-e**.

#### 4.DISCUSSION

In this study; new NSAIDs ester prodrugs were designed and synthesized by modifying some acidic NSAIDs with the main goals of decreasing side effects, increasing tolerability, and increasing efficacy. As mentioned in many literatures, masking the carboxylic acid group of an NSAID, gives less gastrototoxic prodrugs, with comparable or higher anti-inflammatory activity (Kalgutkar *et al.*, 2000; Le Borgne *et al.*, 2000).

Before using the docking program, its reliability should be investigated. Validating the docking program showed excellent results since the obtained RMSD values from redocking ibuprofen and meclufenamic acid into their binding sites of proteins 1EQG and 5IKQ respectively were both  $\leq 2$ , which according to literatures (Dhingra *et al.*, 2014)(Hegazy and Ali, 2012); if the RMSD value is within this range it means that the used scoring method is accurate and very reliable. The smaller RMSD values we get, the more confident we are in the applied docking program, because this means that the used program could reproduce the same binding mode (pose) of the native ligand, and as close as possible to the binding mode found experimentally. We can clearly see in (Fig. 1) how ibuprofen and meclufenamic acid ligands'

theoretically predicted conformations looked almost identical with the experimentally found ligand conformations of proteins 1EQG and 5IKQ respectively.

Docking of compounds **3a-e**, which were both the most potent and the most selective ones, showed that they were able to bind at the conventional binding site of COX-1 and COX-2 receptors as described in many literatures (Limongelli *et al.*, 2010)(Zarghi and Arfaei, 2011).

All the docked compounds (**3a-e**) showed higher binding affinities when docked into COX-2 than COX-1 (Table 1 and Table 2). These results indicate that these compounds (**3a-e**) are more likely to be selective COX-2 inhibitors which might be due to becoming bulkier after modifying their chemical structures and this has made them fit more easily in the bigger active site of COX-2 than COX-1 (Aboraia *et al.*, 2017).

Comparing the docking results; compound **3d** showed the highest binding affinity as it had the highest binding free energy ( $\Delta G_b$ : -12.4 kcal/mol) when it was docked into COX-2 (5IKQ) binding site (Table 2), and exhibited one hydrogen bond with Ser530 (Fig. 3). This predicts compound **3d** to have the highest ant-inflammatory activity among the evaluated compounds.

Computerized ADME predicting tool was used to determine certain parameters that can affect the bioavailability, cell permeability, and metabolism of the test compounds (**3a-e**). Their druglike nature was tested by measuring their compliance with “Lipinski’s rule of five”. This rule works as a guideline to assess the druglikeness of a certain molecule and mainly to predict its oral bioavailability profile (Lipinski *et al.*, 2012). It states that for a molecule to have good oral bioavailability; its molecular weight should not be more than 500 (g/mol), number of H-bond donors not exceeding five, number of H-bond acceptors not more than ten, and (CLogP) value should not be greater than five. If a molecule violates more than one of the mentioned rules, then it’s more probably going to have bad oral bioavailability (Barret, 2018).

Another predicted parameter was TPSA (topological polar surface area). TPSA measures the polarity of a molecule, more specifically its hydrogen bond forming ability, which is also associated with the bioavailability profile (Ertl, Rohde and Selzer, 2000). In order to have good oral bioavailability from passive absorption; the molecule’s TPSA should be between (20 and 130 Å<sup>2</sup>). ADME prediction results of compounds **3a-e** fall within the ideal ranges (Table 3).

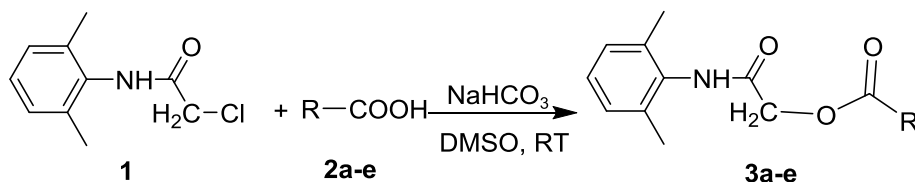
The reaction of the synthesis of compounds **3a-e** is demonstrated in Scheme 1, it is an esterification by S<sub>N</sub>2 reaction, which is a nucleophilic substitution reaction (Bruice, 2007); in this study it involves the substitution of the halide group (leaving group) of a primary alkyl halide with a carboxylate anion (nucleophile), as a result an ester is formed (Hamad *et al.*, 2017)(Hamlin, Swart and Bickelhaupt, 2018).

The main aim was to mask the carboxylic groups of the NSAIDs molecules to be modified (**2a-e**), through esterifying them using *N*-(2,6-dimethylphenyl)-acetamide **1**. At first the carboxylic groups of NSAIDs (**2a-e**) were converted to their sodium carboxylate salts by mixing them with sodium bicarbonate using dimethyl sulfoxide (DMSO) as a solvent. These sodium carboxylate salts provide the carboxylate anion (nucleophile). After the addition of 2-

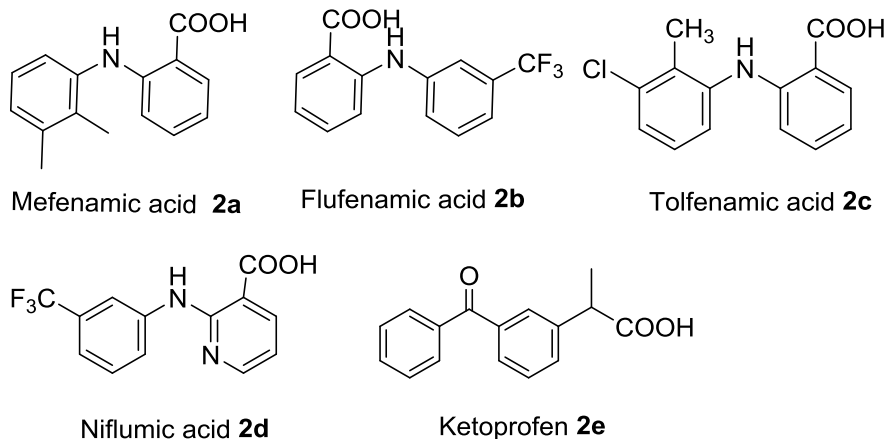
Chloro-*N*-(2,6-dimethylphenyl)-acetamide **1**; the carboxylate anion, prepared previously, substitutes the chloride group at the alpha position. The negatively charged oxygen of the carboxylate anion attacks the alpha carbon; at that point a transition-state is formed. This transition-state ends up by forming the alpha carbon-nucleophile bond and breaking the alpha carbon-chloride bond instantaneously producing the target compounds (**3a-e**). The target compounds (**3a-e**) were formed in high yields (66-82%).

The progress of the reaction was monitored using thin layer chromatography technique. FT-IR, <sup>1</sup>H-NMR, and <sup>13</sup>C-NMR spectroscopy were used for authenticating the final products chemical structures and to determine their purity. IR spectra of the synthesized compounds showed expected values. Correspondingly, peaks for <sup>1</sup>H and <sup>13</sup>C-NMR appeared at expected  $\delta$  values (Table 5). The observed IR, <sup>1</sup>H-NMR, and <sup>13</sup>C-NMR values showed a good agreement with the ones reported in the literature (Silverstein, Webster and Kiemle, 2005)(Smith and March, 2006) which accordingly confirm the structures of the synthesized compounds.

For evaluating the ability of these synthesized compounds (**3a-e**) as well as the starting compounds **1** and **2a-e** for inhibiting COX-1 and COX-2 enzymes, they were screened using “Cayman's COX activity assay kit”. Results of their COX-1 and COX-2 inhibitory activity are shown in Table 6 and Table 7 respectively. Compounds **3a-e** showed COX-1 inhibition activity which was comparable with the starting compounds (**1** and **2a-e**), while their COX-2 inhibition activity was superior to that of the starting compounds. Importantly, compound **3d** showed maximum *in vitro* COX-2 inhibition (37-47%) due to its better ability to fit with COX-2 enzyme. These results moreover confirm the theoretical predictions which were obtained from the molecular docking study as compound **3d** showed the highest binding free energy  $\Delta G_b$  (-12.4 kcal/mol) among the designed compounds when it was docked into COX-2 (5IKQ) binding site.



R= the following NSAIDs



**Scheme 1: synthesis of prodrugs of NSAIDs 3a-e**

## 5. CONCLUSIONS

An efficient and simple approach as well as an easy work-up had been applied for the synthesis of prodrugs of NSAIDs **3a-e** which was helpful in masking the irritating carboxylate moiety, to increase *in vitro* COX inhibitory activity i.e. anti-inflammatory activity of the parent NSAIDs **2a-e**. The approach and the reaction condition were mild to afford in suitable time the desired products with good yields. A simple recrystallization technique had been applied to separate conveniently the prepared products **3a-e** from the reaction mixture in high purity. Docking study was performed for the designed compounds **3a-e** showing binding free energies  $\Delta G_b$  of (-8.9 to -9.8 kcal/mol) when docked into COX-1 and (-10.4 to -12.4 kcal/mol) into COX-2 enzymes. Compound **3d** showed the highest binding free energies  $\Delta G_b$  (-9.8 and -12.4 kcal/mol) when it was docked into COX-1 and COX-2 binding sites, respectively. The synthesized prodrugs **3a-e** were screened for their COX inhibition activity which revealed that they possess greater inhibitory activity than the parent NSAIDs **2a-e**. Compound **3d** exhibited the highest COX-2 inhibition (37-47%) and this further supports the docking result.

## Acknowledgements

Deepest thanks to assistant professor Dr. Aras Hamad, Mrs. Banaz Ameen for their kind guidance and help.

## REFERENCES

- Abdel-Azeem, A. Z. *et al.* (2009) 'Chlorzoxazone esters of some non-steroidal anti-inflammatory (NSAI) carboxylic acids as mutual prodrugs: design, synthesis, pharmacological investigations and docking studies', *Bioorganic & medicinal chemistry*, 17(10), p. 3665—3670. doi: 10.1016/j.bmc.2009.03.065.
- Abdel-Aziz, A. A. M., Eltahir, K. E. H. and Asiri, Y. A. (2011) 'Synthesis, anti-inflammatory activity and COX-1/COX-2 inhibition of novel substituted cyclic imides. Part 1: Molecular docking study', *European Journal of Medicinal Chemistry*. doi: 10.1016/j.ejmech.2011.02.013.
- Aboria, A. S. *et al.* (2017) 'DESIGN, SYNTHESIS AND COX1/2 INHIBITORY ACTIVITY OF NEW QUINAZOLINE-5-ONE DERIVATIVES', *JOURNAL OF ADVANCES IN CHEMISTRY*. doi: 10.24297/jac.v13i12.6019.
- Al-Turki, D. A. *et al.* (2017) 'Design, synthesis, molecular modeling and biological evaluation of novel diaryl heterocyclic analogs as potential selective cyclooxygenase-2 (COX-2) inhibitors', *Saudi*

- Pharmaceutical Journal*. King Saud University, 25(1), pp. 59–69. doi: 10.1016/j.jpsps.2015.07.001.
- Ameen, D. (2020) ‘Synthesis, gastroprotective and acute toxicity of bio-isosteric derivative of diclofenac’, *Zanco Journal of Medical Sciences*. doi: 10.15218/zjms.2020.017.
- Ashraf, Z. *et al.* (2016) ‘Flurbiprofen–antioxidant mutual prodrugs as safer nonsteroidal anti-inflammatory drugs: Synthesis, pharmacological investigation, and computational molecular modeling’, *Drug Design, Development and Therapy*. doi: 10.2147/DDDT.S109318.
- Autore, G. *et al.* (2010) ‘Acetamide derivatives with antioxidant activity and potential anti-inflammatory activity’, *Molecules*. doi: 10.3390/molecules15032028.
- Ayhan-Kilcigil, G. *et al.* (2012) ‘Synthesis and Evaluation of Antioxidant Properties of Novel 2-[2-(4-chlorophenyl) benzimidazole-1-yl]-N-(2-arylmethylene amino) acetamides and 2-[2-(4-chlorophenyl) benzimidazole-1-yl]-N-(4-oxo-2-aryl-thiazolidine-3-yl) acetamides-I’, *Chemical Biology and Drug Design*. doi: 10.1111/j.1747-0285.2012.01347.x.
- Ayhan-Kilcigil, G. *et al.* (2012) ‘Synthesis and Evaluation of Antioxidant Properties of Novel 2-[2-(4-chlorophenyl) benzimidazole-1-yl]-N-(2-arylmethylene amino) acetamides and 2-[2-(4-chlorophenyl) benzimidazole-1-yl]-N-(4-oxo-2-aryl-thiazolidine-3-yl) acetamides-I’, *Chemical Biology & Drug Design*. John Wiley & Sons, Ltd, 79(5), pp. 869–877. doi: 10.1111/j.1747-0285.2012.01347.x.
- Babkov, D. A. *et al.* (2015) ‘2-(2,4-Dioxy-1,2,3,4-Tetrahydropyrimidin-1-yl)-N-(4-Phenoxyphenyl)-Acetamides as a Novel Class of Cytomegalovirus Replication Inhibitors’, *Acta naturae*. A.I. Gordeyev, 7(4), pp. 142–145. Available at: <https://pubmed.ncbi.nlm.nih.gov/26798502>.
- Bardiot, D. *et al.* (2015) ‘2-(2-Oxo-morpholin-3-yl)-acetamide derivatives as broad-spectrum antifungal agents’, *Journal of Medicinal Chemistry*, 58(3), pp. 1502–1512. doi: 10.1021/jm501814x.
- Barret, R. (2018) ‘Lipinski’s Rule of Five’, in *Therapeutical Chemistry*. doi: 10.1016/b978-1-78548-288-5.50006-8.
- Le Borgne, M. *et al.* (2000) ‘Synthesis and biological evaluation of indole derivatives acting as anti-inflammatory or antitumoral drugs | Derives indoliques a activites anti-inflammatoire ou antitumorale’, *Annales Pharmaceutiques Francaises*. doi: APF-10-2000-58-5-0003-4509-101019-ART4.
- Bruice, P. Y. (2007) *The SN2 Reaction, Organic Chemistry*.
- Croft, D. N., Cuddigan, J. H. P. and Sweetland, C. (1972) ‘Gastric Bleeding and Benorylate, a New Aspirin’, *British Medical Journal*, 3(5826), pp. 545–547. doi: 10.1136/bmj.3.5826.545.
- Daina, A., Michielin, O. and Zoete, V. (2017) ‘SwissADME: A free web tool to evaluate pharmacokinetics, drug-likeness and medicinal chemistry friendliness of small molecules’, *Scientific Reports*. doi: 10.1038/srep42717.
- Dallakyan, S. and Olson, A. J. (2015) ‘Small-molecule library screening by docking with PyRx’, *Methods in Molecular Biology*. doi: 10.1007/978-1-4939-2269-7\_19.
- Dhaneshwar, S. S. *et al.* (2009) ‘Evaluation of the chondroprotective effect of mutual prodrug of diacerein in monosodium iodoacetate-induced osteoarthritis in Wistar rats’, *Journal of Drug Delivery Science and Technology*. doi: 10.1016/S1773-2247(09)50087-1.
- Dhingra, M. S. *et al.* (2014) ‘Synthesis, evaluation, and molecular docking studies of cycloalkyl/aryl-3,4,5-trimethylgallates as potent non-ulcerogenic and gastroprotective anti-inflammatory agents’, *Medicinal Chemistry Research*. doi: 10.1007/s00044-013-0620-6.
- Ertl, P., Rohde, B. and Selzer, P. (2000) ‘Fast calculation of molecular polar surface area as a sum of fragment-based contributions and its application to the prediction of drug transport properties’, *Journal of Medicinal Chemistry*. doi: 10.1021/jm000942e.
- Gairola, N. *et al.* (2005) ‘Synthesis, Hydrolysis Kinetics and Pharmacodynamic Profile of Novel Prodrugs of Flurbiprofen. Neha Gairola, Deepika Nagpal, Suneela. S. Dhaneshwar, S. R. Dhaneshwar and S. C. Chaturvedi; Indian Journal of Pharmaceutical Sciences, 2005,67, 369-373.’, *Indian Journal of Pharmaceutical Sciences*, 67, pp. 369–373.
- Hamad, A. *et al.* (2017) ‘Synthetic Approaches and Pharmacological Evaluation of Some New Acetamide Derivatives and 5-Benzylidene-2-(2, 6-dimethyl-phenylimino)-thiazolidin-4-ones’, *ZANCO Journal of Pure and Applied Sciences*, (August), pp. 29(4):13–24.
- hamadameen, B. and Ameen, D. M. H. (2019) ‘Synthesis, Characterization, and Antibacterial Activity of Novel Mutual Non-Steroidal Anti-inflammatory Prodrugs’, *Zanco Journal of Pure and Applied Sciences*, 31(6 SE-Biology and Medical Researches). doi: 10.21271/zjpas.31.6.7.
- Hamlin, T. A., Swart, M. and Bickelhaupt, F. M. (2018) ‘Nucleophilic Substitution (SN2): Dependence on Nucleophile, Leaving Group, Central Atom, Substituents, and Solvent’, *ChemPhysChem*. doi: 10.1002/cphc.201701363.
- Hegazy, G. H. and Ali, H. I. (2012) ‘Design, synthesis, biological evaluation, and comparative Cox1 and Cox2 docking of p-substituted benzylidenamino phenyl esters of ibuprofenic and mefenamic acids’, *Bioorganic and Medicinal Chemistry*. doi: 10.1016/j.bmc.2011.12.030.
- Jain, N. *et al.* (2013) ‘Synthesis and anti-inflammatory activity of N-(Alkyl or Aryl)-2-(1H-benzotriazol-1-yl)acetamide derivatives’, *Research Journal of Pharmaceutical, Biological and Chemical Sciences*, 4, pp. 1470–1480.
- Jawed, H. *et al.* (2010) ‘N-(2-hydroxy phenyl) acetamide inhibits inflammation-related cytokines and ROS in adjuvant-induced arthritic (AIA) rats’, *International Immunopharmacology*. doi: 10.1016/j.intimp.2010.04.028.
- Kai, H. *et al.* (2001) ‘Anti-influenza virus activities of 2-alkoxyimino-N-(2-isoxazolin-3-

- ylmethyl)acetamides', *Bioorganic and Medicinal Chemistry Letters*. doi: 10.1016/S0960-894X(01)00362-6.
- Kalgutkar, A. S. *et al.* (2000) 'Ester and amide derivatives of the nonsteroidal antiinflammatory drug, indomethacin, as selective cyclooxygenase-2 inhibitors', *Journal of Medicinal Chemistry*. doi: 10.1021/jm000004e.
- Kamiński, K. *et al.* (2011) 'Synthesis and anticonvulsant properties of new acetamide derivatives of phthalimide, and its saturated cyclohexane and norbornene analogs', *European Journal of Medicinal Chemistry*. doi: 10.1016/j.ejmech.2011.07.043.
- Kanagarajan, V. and Gopalakrishnan, M. (2012) 'Pyrimidino piperazinyl acetamides: Innovative class of hybrid acetamide drugs as potent antimicrobial and antimycobacterial agents', *Pharmaceutical Chemistry Journal*. doi: 10.1007/s11094-012-0729-9.
- Kanagarajan, V., Thanusu, J. and Gopalakrishnan, M. (2010) 'Synthesis and in vitro microbiological evaluation of an array of biolabile 2-morpholino-N-(4,6-diarylpyrimidin-2-yl)acetamides', *European Journal of Medicinal Chemistry*. doi: 10.1016/j.ejmech.2009.12.068.
- Kidwai, M. *et al.* (2012) 'Cancer Chemotherapy and Heterocyclic Compounds', *Current Medicinal Chemistry*. doi: 10.2174/0929867023370059.
- Limongelli, V. *et al.* (2010) 'Molecular basis of cyclooxygenase enzymes (COXs) selective inhibition', *Proceedings of the National Academy of Sciences of the United States of America*. doi: 10.1073/pnas.0913377107.
- Lipinski, C. A. *et al.* (2012) 'Experimental and computational approaches to estimate solubility and permeability in drug discovery and development settings', *Advanced Drug Delivery Reviews*. doi: 10.1016/j.addr.2012.09.019.
- Makhija, D. T., Somani, R. R. and Chavan, A. V. (2013) 'Synthesis and pharmacological evaluation of antiinflammatory mutual amide prodrugs', *Indian Journal of Pharmaceutical Sciences*. doi: 10.4103/0250-474X.117399.
- Meyers, B. E., Moonka, D. K. and Davis, R. H. (1979) 'The effect of selected amino acids on gelatin-induced inflammation in adult male mice', *Inflammation*, 3(3), pp. 225–233. doi: 10.1007/BF00914179.
- Nayak, P. S. *et al.* (2014) 'Design and synthesis of novel heterocyclic acetamide derivatives for potential analgesic, anti-inflammatory, and antimicrobial activities', *Medicinal Chemistry Research*. doi: 10.1007/s00044-014-1003-3.
- Nile, S. H. *et al.* (2016) 'Screening of ferulic acid related compounds as inhibitors of xanthine oxidase and cyclooxygenase-2 with anti-inflammatory activity', *Brazilian Journal of Pharmacognosy*. doi: 10.1016/j.bjp.2015.08.013.
- Pountos, I. *et al.* (2011) 'Nonsteroidal anti-inflammatory drugs: Prostaglandins, indications, and side effects', *International Journal of Interferon, Cytokine and Mediator Research*. doi: 10.2147/IJICMR.S10200.
- Qasir, A. J. (2013) 'Synthesis of NSAID with Sulfonamide Conjugates as Possible Mutual Prodrugs using Amino Acid Spacer', *Der Pharma Chemica*, 2(1), pp. 241–248.
- Salih, K. *et al.* (2020) 'Synthesis and pharmacological profile of some new 2-substituted-2, 3-dihydro-1H-perimidine', *Zanco Journal of Medical Sciences*, 24(1), pp. 68–79. doi: 10.15218/zjms.2020.010.
- Sawant, R. and Kawade, D. (2011) 'Synthesis and biological evaluation of some novel 2-phenyl benzimidazole-1-acetamide derivatives as potential anthelmintic agents', *Acta Pharmaceutica*. doi: 10.2478/v10007-011-0029-z.
- Silverstein, R. M., Webster, F. X. and Kiemle, D. J. (2005) 'Spectrometric identification of organic compounds 7ed 2005 - Silverstein, Webster & Kiemle.pdf', *Microchemical Journal*. doi: 10.1016/0026-265X(76)90069-2.
- Smith, M. B. and March, J. (2006) *March's Advanced Organic Chemistry: Reactions, Mechanisms, and Structure, Wiley-Interscience A John Wiley & Sons*.
- Zarghi, A. and Arfaei, S. (2011) 'Selective COX-2 inhibitors: A review of their structure-activity relationships', *Iranian Journal of Pharmaceutical Research*. doi: 10.22037/ijpr.2011.1047.

## RESEARCH PAPER

# Histological Impacts of L-Arginine, Vitamin C and Their Combination on Liver and Kidney of Paracetamol Treated Rats

Dlshad H. Hassan<sup>1</sup>, Ali Z. Omar<sup>2</sup>, Dler Q. Gallaly<sup>3</sup>, Sundus R. Ahmad<sup>4</sup>, Ismail M. Maulood<sup>5</sup>

<sup>1</sup>Department of Biology, Faculty of Science, Soran University, Erbil-Soran, Kurdistan Region, Iraq

<sup>2</sup>Department of medical laboratory technology, Shaqlawa technical institute/Erbil Polytechnic University/ Kurdistan region/Iraq

<sup>3</sup>Department of Physiotherapy, College of health science, Hawler Medical University, Erbil, Kurdistan region, Iraq

<sup>4</sup>Physiology Unit, Department of Basic Science, College of Medicine, Hawler Medical University, Erbil, Kurdistan region, Iraq

<sup>5</sup>Biology department, College of science, Salahaddin university-Erbil, Erbil, Kurdistan region, Iraq

### ABSTRACT:

Paracetamol as analgesic drugs makes hepatotoxicity and kidney damage in overdose situations. The present study investigates the protective effects of L-arginine and vitamin c against paracetamol toxicity. Thirty male rats with age of eight weeks divided into five groups: Control group with normal diet, Model animals received 500 mg/kg of Paracetamol. The Third group received 1% of L-arginine and same dose of paracetamol. Forth group received 1% of vitamin c plus paracetamol and the last group treated with a combination of all three chemicals. All drugs administrated orally in drinking water for 28 days. Liver and kidneys of the control group rats showed increasing in the weight while non-significant result was observed in the other groups. Histological investigation of the kidney of the model group shows inflammatory cell infiltration, tubular dilation and glomerulus damage, while liver sections shows sinusoid dilation inflammatory cell accumulation hepatocytes degeneration. L-arginine and vitamin C showed some protective effects when administrated alone but their combination has no good effects when compared with control group. In conclusion, L-Arginine administration has good protective effects against toxicity of liver and kidney induced by Paracetamol.

KEY WORDS: L-Arginine; Vitamin c; hepatotoxicity; nephrotoxicity

DOI: <http://dx.doi.org/10.21271/ZJPAS.32.6.4>

ZJPAS (2020) , 32(6);40-45 .

## 1. INTRODUCTION

Paracetamol (Par.), as a pain reducing drug, is considered safe at convenient doses. Par. overdose makes liver damage and necrosis in laboratory animals and humans (Kaplowitz, 2005, Jaeschke et al., 2010). Basically, Par. metabolism is done by glucuronidation and sulphation; and a small amount changes to N-acetyl-p-benzoquinimine (NAPQI) by cytochrome P450, which is quickly neutralized by glutathione (James et al., 2003).

However, kidney damage is not more common than hepatotoxicity, but there is a chance for the development of acute renal failure without liver damage by Par. Indications. (McGill et al., 2012).

L-arginine (L- Arg.) as a semi-essential amino acid is utilized by all types of cells (Wu and Morris Jr, 1998). L-Arg. constitutes 7–5% of the total amino acids in the human's normal food intake and absorption process is in the jejunum and ileum portions of small intestine. L-Arg. participates in protein synthesis, tissue repair, urea cycle and immunity functions (White, 1985, Hendler and Rorvik, 2008). Immune system converts L-Arg. to Nitric oxide in the presence of enzyme nitric oxide synthase that has a role in cell signaling and oxidative bactericidal actions (Popovic et al., 2007). So, L-arginine can reduce infection rates, especially in

### \* Corresponding Author:

Dlshad H. Hassan

E-mail: [dlshad.hassan@soran.edu.iq](mailto:dlshad.hassan@soran.edu.iq)

### Article History:

Received: 21/03/2020

Accepted: 10/08/2020

Published: 20/12/2020



circumstances like surgery or critical illness (Böger, 2008).

Vitamin C (Vit. C), or ascorbic acid, plays roles in many biological functions. Vit. C participates in the production of collagen by taking a role in proline and lysine hydroxylation (Rebouche, 1991). Vit. C as a co-factor is used in different reactions of hydroxylation, for example, biological synthesis of cholesterol, catecholamines, and some hormones (Chatterjee *et al.*, 1975). Moreover, Vit. C is a strong antioxidant that prevents oxidation of low-density lipoproteins, boosts iron absorption and reduces free radicals in the stomach (Buettner and Jurkiewicz, 1996).

The aims of the experiment are to study the protective effect of L-Arg., Vit. C and their combination against paracetamol toxicity in kidney and liver of rats from histological points of view.

## 2. MATERIALS AND METHODS

### 2.1 Animal Grouping and Experimental Design

This study completed with thirty healthy male rats weighted between 200–250g with 8 weeks old. They harbored in polypropylene cage in the animal house belongs to the college of medicine, Hawler Medical University. All animals were bred under room temperature 25 °C with 12 hours of light and 12 hours dark pattern. Rats have had access to standard food and water *ad libitum*. The rats were distributed into five groups, each with six rats. Group I treated as control and receive only tap water (Control group). Other groups were treated as experimental groups. Group II was treated by paracetamol 500mg/kg (Model Group). Group III was receiving a combination of paracetamol (500mg/kg) and L-Arg. 1%, while group (Par.+L-Arg. group). Group IV were receiving a combination of paracetamol (500mg/kg) and vitamin C 1% (Par+ Vit. C group). Group V will be treated with a combination of all three substances (Par.+ L-Arg. + Vit. C Group). all drugs were dissolved in tap water and administered orally in drinking water (Chaudhary *et al.*, 2019). The experiment conducted for 28 days.

### 2.2 Animal Dissecting and Tissue Processing

The animals were anaesthetized by intraperitoneal injection of combination Xylazine (12mg/Kg) and Ketamine hydrochloride (80mg/Kg). After scarification, livers and kidneys removed, weighted by digital balance then fixed in formal saline. Dehydration process was done by series of ascending concentrations of ethanol (50%, 70%, 95% and 100%), followed by clearing process by using of xylene then after paraffin infiltration and embedding completed. Samples have been sectioned by using rotary microtome in five micrometer thickness (Bright, MIC) following hematoxylin and Eosin staining protocols (H&E) (Suvarna *et al.*, 2018). Light microscopy examination is completed by digital binocular compound microscope.

### 2.3. Statistical Analysis

Statistical analysis was done by GraphPad Prism program version 8.3 using one-way ANOVA analysis and Tukey as recommended post hoc test.

## 3. RESULTS AND DISCUSSION

### 3.1 Organs' weights

As shown in fig.1. A, liver weight in Model group increased significantly in compare of the control group while no significant difference between three other groups when compared with the control and Paracetamol group. Par. + L-Arg. group, demonstrated better liver weight improvement in respect of mean when compared to the model group. The hepatomegaly in Par. treated rats suggested liver tissue lesions and liver injury as a side effect for indications of Par. Accumulation of collagen and extracellular protein in hepatic tissue may be the main cause of increasing liver weight (Mahmood *et al.*, 2014). Liver weight of rats treated with Par. + L. Arg. shown closer results to control and it's maybe due to role of arginine in decreasing liver damage (Engin *et al.*, 2006) and lipid peroxidation, inflammation and free radicals (Butterworth and Canbay, 2019).

Both right and left kidneys weight (fig. 1 B & C) have not shown statistical change and there is a physiological increase of both kidneys weight belongs to Par. model group. There is a correlation between kidney damage and increasing kidney weight (Nematbakhsh *et al.*, 2013). The Third

group of experimental rats that treated with L. Arg. Have shown kidneys' weight close to the control group and it's maybe due to a role of arginine in decreasing oxidative stress(Kaul et al., 2008, Suschek et al., 2003).

### 3.2 Kidney and liver histology

As illustrates in figure 2A, the kidney section of control group has normal histological and structural appearance while the Par. model group showed glomerular shrinkage and degeneration, destruction of bowman capsule, inflammatory cells, tubular dilation, casts, cell debris in kidney tubules (fig. B 1,2&3).

The results are similar to previous researches that have reported kidney damage by Paracetamol inductions (ROSITA, 2018, Moshai-Nezhad et al., 2019). The nephrotoxic effects of paracetamol may due to interfering with apoptotic pathways including activation of caspases and decreasing Bcl-xL protein. It's reported that Par. Can makes oxidative stress and inflammation in the kidney (Lorz et al., 2005). Free radicals that produce as byproducts of Par. Metabolism could make glomerular damage and inflammatory cell infiltration (Singh et al., 2006). Renal tubule necrosis is one of the side effects of Par. Overdose (Goodman and Gilman, 2006).

glutathione and cytochrome p450 system have had a critical role in toxicity of Paracetamol. However toxic materials are concentrated in proximal tubule as a result of secretion and reabsorption activities, Cytochrome p450 is generally situated in the proximal tubule and in less amount in the distal convoluted tubule, glomerulus and collecting duct. (McGill et al., 2012, Mazer and Perrone, 2008).

Light microscopy examination of kidneys treated with Par.+L-Arg. Shown good improvement and histological protection but still, some tubular dilations and cell debris observed (fig. 3.A).

L-Arg. supplementation effect against paracetamol induced nephrotoxicity. L-Arg. has a role in the immune system for cell signaling and oxidative action therefore it can reduce inflammation (Popovic et al., 2007, Kalil and Danner, 2006).more ever It's reported that L-Arg. could reduce oxidative stress (Dawoud and Malinski, 2020) and improve the antioxidant system in rats(Silva et al., 2017).

Paraffin sections of kidneys belong to Par.+Vit. C group have shown some protective results

overall but tubular dilation, glomerular degeneration observed as well (fig. 3.B). The protective effect of Vit. C may due to its antioxidant activity(Grosso et al., 2013). Vitamin C has a role in reducing allergic reaction, boosting of the immune system and participates in infection elimination (Chambial et al., 2013).

Cross section of kidneys treated with Par. & combined L. Arg./Vit. C showed few protective effects, glomerular degeneration, tubular dilation and debris (fig. 3.C). surprisingly the combined L. Arg. And Vit. C supplementation could not show better protective result and its controversy with the previous finding that their combinations shown better anti-inflammatory and antioxidant features(Suliburska et al., 2014)

Paraffin section through the liver of control group shown normal structural and histological view (Fig. 4. A). As illustrated in Fig. 4. B 1,2 & 3, several histological alterations like inflammatory cells infiltration, central vein congestion, sinusoid dilation, hepatic tissue dissociation, necrotic cells and shading of cells have been noticed. The results are similar to previous researches(Jarsiah et al., 2017, Singh et al., 2015). In liver as a major organ of par. Metabolism , most of Par. is converted to sulfate and glucuronide, and the rest, converted to N-acetyl-p-benzoquinone imine (NAPQI) (Ayca et al., 2014). NAPQI is a reactive chemical and detoxified by enzyme glutathione peroxidase. Excessive production of NAPQI causes liver damage as a result of decline in the concentration of glutathione (Ayca et al., 2014, Omidi et al., 2014). At the time of glutathione deficiency and presence of NAPQI, the production of free radicals like hydrogen peroxide, superoxide and hydroxyl radicals has been increased and leads to oxidative stress (Merhi et al., 2019).

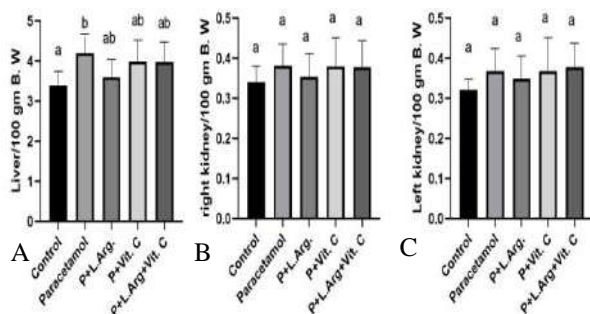
As shown in Fig. 5. A 1&2, the liver sections of liver treated with Par.& L.-Arg. were in approximately normal tissue structure regarding to hepatocyte and Central vein arrangements and appearance but a few inflammatory cell infiltrations have been noticed.

The observed results may due to the power of L-Arg. in the improvement of antioxidant system and reducing free radicals(De Nigris et al., 2003). L-Arg. act as a precursor for nitric oxide that plays a role in scavenging of reactive chemical species.(Ahmad et al., 2015). More ever It's been reported that L. Arginine can promotes cellular

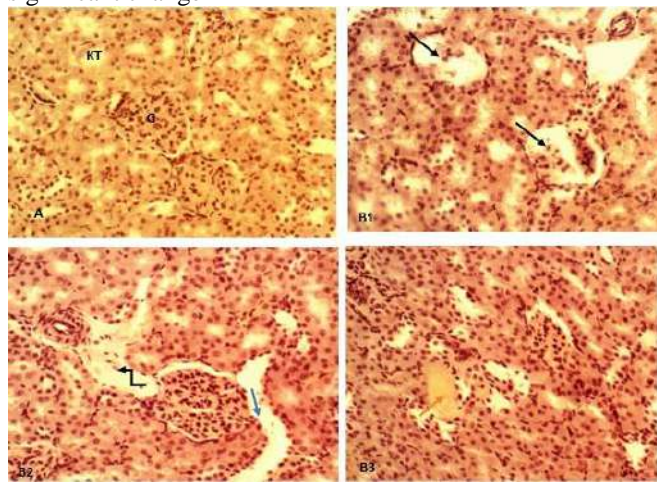
proliferation and decreases cell death (Greene et al., 2013)

Figure 5.B 1&2 illustrated liver sections of Par.+ Vit. C treated group with inflammatory cells and congested central veins but protected from other damages. The protective results may refer to the potential of Vit. C to decreasing cell damages and its role in boosting of glutathione antioxidant.

In Liver sections of Par.+ L-Arg.+Vit. C treated group some Inflammatory cells, congested central vein and sinusoid dilations observed (Fig. 5. C1&2). Vitamin C can act as a strong antioxidant whereas at the same time it can show free radical promoter activities and produce reactive substances (Pehlivan, 2017). Chemical interactions could not be neglected as a cause for the elimination of combined Vit. C and L. Arg. effects.



**Figure 1.** showing the weight of liver (A), right(B) and left kidney (C)per 100gm of body weight. Different letters on bars mean significant change and the same letters means no significant change



**Figure 2.** showing cross section through kidneys of the control group (A) and paracetamol group (B 1,2 and 3). Control group showing normal appearance in the glomerulus (G) and kidney tubules (KT). Paracetamol group showing glomerular shrinkage and degeneration (black arrow), tubular dilation (blue arrow), cellular debris (elbow arrow) and casts (red arrow). H and E stain 400 X

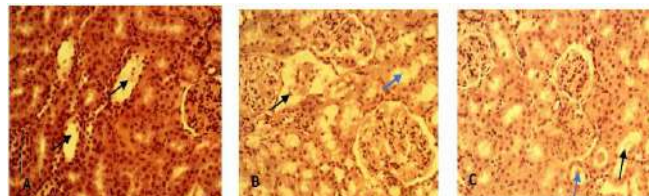


**Figure 3.** cross section through kidneys of rats treated with Par. & L. Arg. (A), P& vit. C (B) and P& L. Arg./Vit. C (C). Arg. group shows some tubular dilation and cell debris inside kidney tubules (black arrow) with normal glomerulus. Vit-c group shows some glomerular degeneration (black arrow) and tubular dilation (blue arrow). Arg.-Vit-c group shows some tubular dilation (black arrow) and cell debris (blue arrow) with deformed glomerulus. H&E stain, 400 X

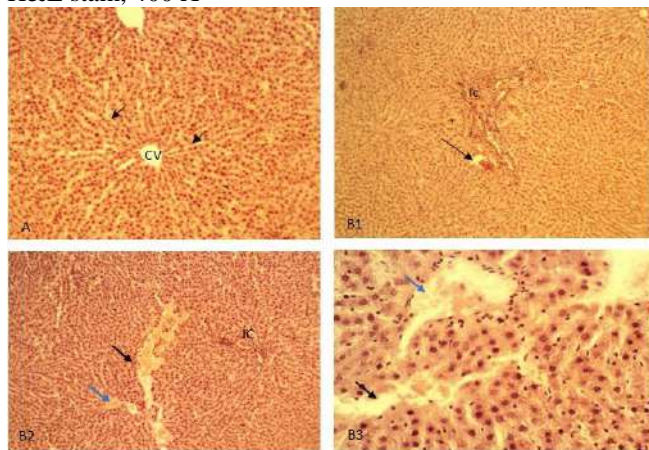


**Figure 4.** Figure 4 A, shows section of the liver belong to the control group with normal central vein (CV) and sinusoids (s). H & E stain. 100x. Histological sections through liver of the Paracetamol treated group (B1,2,3) show Inflammatory cells (IC), congested central veins (blue arrow) and sinusoid dilation (black arrow) filled with shaded hepatocytes. B1,2 H &E. 100x, B3 H &E 400X.

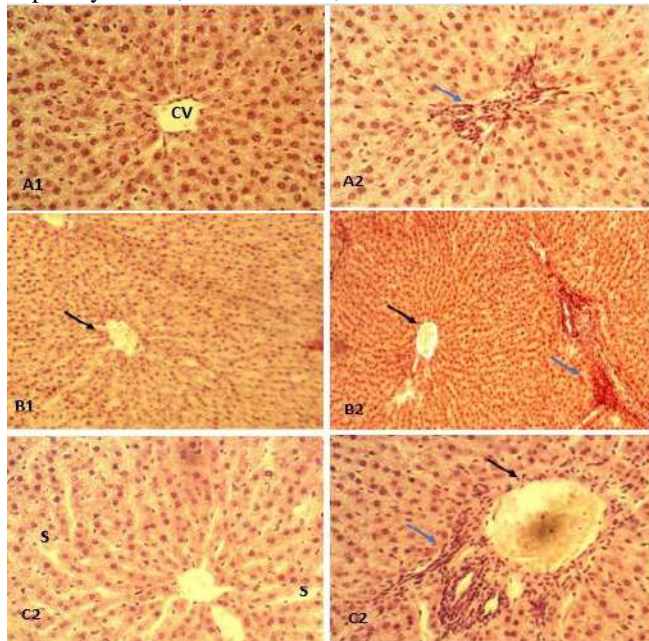


**Figure 5.** A1,2 show cross section of rat liver treated with Paracetamol and Arg. with approximately normal hepatic structure and central vein (CV), some inflammatory cells

(blue arrow) were seen. H& E stain 400 X. B1,2 cross section of liver belongs to Paracetamol and Vit. C group show central vein congestion (black arrow) and inflammatory cells (blue arrow) H& E stain 100 X. fig. C1,2 show liver section of rats treated with paracetamol, Arg, and Vit. C. Inflammatory cells (blue arrow), congested central vein (black arrow) and dilated sinusoids observed. H& E stain 400X

#### 4. CONCLUSIONS

From the present study, it can be understood that L. arginine shows a good protective effect against Paracetamol toxicity. Vitamin C also shows some positive effect as well. Both Vit. C and L. Arg. show better result compared to their combination.

#### Acknowledgements

Many thanks to Dr. Falah M. Aziz and Dr. Chnar Najmaddin for their technical supports.

#### References

AHMAD, A., SATTAR, M., RATHORE, H. A., HUSSAIN, A. I., KHAN, S. A., FATIMA, T., AFZAL, S., ABDULLAH, N. A. & JOHNS, E. J. 2015. Antioxidant activity and free radical scavenging capacity of L-arginine and NaHS: A comparative in vitro study. *Acta Pol Pharm*, 72, 245-52.

AYCAN, İ. Ö., TUFEK, A., TOKGÖZ, O., EVLIYAOĞLU, O., FIRAT, U., KAVAK, G. Ö., TURGUT, H. & YUKSEL, M. U. 2014. Thymoquinone treatment against acetaminophen-induced hepatotoxicity in rats. *International Journal of Surgery*, 12, 213-218.

BÖGER, R. H. 2008. L-Arginine therapy in cardiovascular pathologies: beneficial or dangerous? *Current Opinion in Clinical Nutrition & Metabolic Care*, 11, 55-61.

BUETTNER, G. R. & JURKIEWICZ, B. A. 1996. Catalytic metals, ascorbate and free radicals: combinations to avoid. *Radiation research*, 145, 532-541.

BUTTERWORTH, R. F. & CANBAY, A. 2019. Hepatoprotection by L-Ornithine L-Aspartate in Non-Alcoholic Fatty Liver Disease. *Dig Dis*, 37, 63-68.

CHAMBIAL, S., DWIVEDI, S., SHUKLA, K. K., JOHN, P. J. & SHARMA, P. 2013. Vitamin C in disease prevention and cure: an overview. *Indian Journal of Clinical Biochemistry*, 28, 314-328.

CHATTERJEE, I., MAJUMDER, A., NANDI, B. & SUBRAMANIAN, N. 1975. Synthesis and some major functions of vitamin C in animals. *Annals of the New York Academy of Sciences*, 258, 24-47.

DAWOUD, H. & MALINSKI, T. 2020. Vitamin D<sub>3</sub>, L-Arginine, L-Citrulline, and antioxidant supplementation enhances nitric oxide bioavailability and reduces oxidative stress in the vascular endothelium &#8211; Clinical

implications for cardiovascular system. *Pharmacognosy Research*, 12, 17-23.

DE NIGRIS, F., LERMAN, L. O., IGNARRO, S. W., SICA, G., LERMAN, A., PALINSKI, W., IGNARRO, L. J. & NAPOLI, C. 2003. Beneficial effects of antioxidants and L-arginine on oxidation-sensitive gene expression and endothelial NO synthase activity at sites of disturbed shear stress. *Proceedings of the National Academy of Sciences*, 100, 1420-1425.

ENGIN, A., ZEMHERI, M., BUKAN, N. & MEMIS, L. 2006. Effect of nitric oxide on the hypoglycaemic phase of endotoxaemia. *ANZ J Surg*, 76, 512-7.

GOODMAN, L. S. & GILMAN, A. 2006. *The pharmacological basis of therapeutics.*, McGraw-Hill.

GREENE, J. M., FEUGANG, J. M., PFEIFFER, K. E., STOKES, J. V., BOWERS, S. D. & RYAN, P. L. 2013. L-arginine enhances cell proliferation and reduces apoptosis in human endometrial RL95-2 cells. *Reproductive Biology and Endocrinology*, 11, 15.

GROSSO, G., BEI, R., MISTRETTA, A., MARVENTANO, S., CALABRESE, G., MASUELLI, L., GIGANTI, M. G., MODESTI, A., GALVANO, F. & GAZZOLO, D. 2013. Effects of vitamin C on health: a review of evidence. *Front Biosci (Landmark Ed)*, 18, 1017-29.

HENDLER, S. S. & RORVIK, D. M. 2008. *PDR for nutritional supplements*, Thomson Reuters.

JAESCHKE, H., WILLIAMS, C. D., MCGILL, M. R. & FARHOOD, A. 2010. Herbal extracts as hepatoprotectants against acetaminophen hepatotoxicity. *World journal of gastroenterology: WJG*, 16, 2448.

JAMES, L. P., MAYEUX, P. R. & HINSON, J. A. 2003. Acetaminophen-induced hepatotoxicity. *Drug metabolism and disposition*, 31, 1499-1506.

JARSIAH, P., NOSRATI, A., ALIZADEH, A. & HASHEMI-SOTEH, S. M. B. 2017. Hepatotoxicity and ALT/AST enzymes activities change in therapeutic and toxic doses consumption of acetaminophen in rats. *International Biological and Biomedical Journal*, 3, 119-124.

KALIL, A. C. & DANNER, R. L. 2006. L-Arginine supplementation in sepsis: beneficial or harmful? *Current opinion in critical care*, 12, 303-308.

KAPLOWITZ, N. 2005. Idiosyncratic drug hepatotoxicity. *Nature reviews Drug discovery*, 4, 489-499.

KAUL, D. K., ZHANG, X., DASGUPTA, T. & FABRY, M. E. 2008. Arginine therapy of transgenic-knockout sickle mice improves microvascular function by reducing non-nitric oxide vasodilators, hemolysis, and oxidative stress. *American Journal of Physiology-Heart and Circulatory Physiology*, 295, H39-H47.

LORZ, C., JUSTO, P., SANZ, A. B., EGIDO, J. & ORTIZ, A. 2005. Role of Bcl-xL in paracetamol-induced tubular epithelial cell death. *Kidney international*, 67, 592-601.

MAHMOOD, N., MAMAT, S., KAMISAN, F., YAHYA, F., KAMAROLZAMAN, M., NASIR, N., MOHTARRUDIN, N., TOHID, S. & ZAKARIA, Z. 2014. Amelioration of paracetamol-induced

- hepatotoxicity in rat by the administration of methanol extract of *Muntingia calabura* L. leaves. *BioMed research international*, 2014.
- MAZER, M. & PERRONE, J. 2008. Acetaminophen-induced nephrotoxicity: pathophysiology, clinical manifestations, and management. *Journal of Medical Toxicology*, 4, 2-6.
- MCGILL, M. R., WILLIAMS, C. D., XIE, Y., RAMACHANDRAN, A. & JAESCHKE, H. 2012. Acetaminophen-induced liver injury in rats and mice: comparison of protein adducts, mitochondrial dysfunction, and oxidative stress in the mechanism of toxicity. *Toxicology and applied pharmacology*, 264, 387-394.
- MERHI, Z., GARG, B., MOSELEY-LARUE, R., MOSELEY, A. R., SMITH, A. H. & ZHANG, J. 2019. Ozone therapy: a potential therapeutic adjunct for improving female reproductive health. *Medical gas research*, 9, 101.
- MOSHAIE-NEZHAD, P., HOSSEINI, S. M., YAHYAPOUR, M., IMAN, M. & KHAMESIPOURE, A. 2019. Protective effect of ivy leaf extract on paracetamol-induced oxidative stress and nephrotoxicity in mice. *Journal of Hermed Pharmacology*, 8.
- NEMATBAKHASH, M., ASHRAFI, F., NASRI, H., TALEBI, A., PEZESHKI, Z., ESHRAGHI, F. & HAGHIGHI, M. 2013. A model for prediction of cisplatin induced nephrotoxicity by kidney weight in experimental rats. *Journal of research in medical sciences: the official journal of Isfahan University of Medical Sciences*, 18, 370.
- OMIDI, A., RIAHINIA, N., TORBATI, M. B. M. & BEHDANI, M.-A. 2014. Hepatoprotective effect of *Crocus sativus* (saffron) petals extract against acetaminophen toxicity in male Wistar rats. *Avicenna journal of phytomedicine*, 4, 330.
- PEHLIVAN, F. E. 2017. Vitamin C: An antioxidant agent. *Vitamin C*, 23-35.
- POPOVIC, P. J., ZEH III, H. J. & OCHOA, J. B. 2007. Arginine and immunity. *The Journal of nutrition*, 137, 1681S-1686S.
- REBOUCHE, C. J. 1991. Ascorbic acid and carnitine biosynthesis. *The American journal of clinical nutrition*, 54, 1147S-1152S.
- ROSITA, Y. 2018. Nephroprotective Activity of Ethanol Extract of *Curcuma Mangga* val. In paracetamol-Induced Male Mice.
- SILVA, E. P., BORGES, L. S., MENDES-DA-SILVA, C., HIRABARA, S. M. & LAMBERTUCCI, R. H. 2017. L-Arginine supplementation improves rats' antioxidant system and exercise performance. *Free Radical Research*, 51, 281-293.
- SINGH, A., KUMAR, G. R., GUPTA, S. S., SINGH, S., RAWAT, A. & RAO, C. V. 2015. Hepatoprotective Potential of *Ziziphus oenoplia* (L.) Mill Roots against Paracetamol-Induced Hepatotoxicity in Rats. *AJPCT*, 3, 64-78.
- SINGH, D., KAUR, R., CHANDER, V. & CHOPRA, K. 2006. Antioxidants in the prevention of renal disease. *Journal of medicinal food*, 9, 443-450.
- SULIBURSKA, J., BOGDANSKI, P., KREJPCIO, Z., PUPEK-MUSIALIK, D. & JABLECKA, A. 2014. The effects of L-arginine, alone and combined with vitamin C, on mineral status in relation to its antidiabetic, anti-inflammatory, and antioxidant properties in male rats on a high-fat diet. *Biological trace element research*, 157, 67-74.
- SUSCHEK, C. V., SCHNORR, O., HEMMRICH, K., AUST, O., KLOTZ, L.-O., SIES, H. & KOLB-BACHOFEN, V. 2003. Critical role of L-arginine in endothelial cell survival during oxidative stress. *Circulation*, 107, 2607-2614.
- SUVARNA, K. S., LAYTON, C. & BANCROFT, J. D. 2018. *Bancroft's theory and practice of histological techniques E-Book*, Elsevier Health Sciences.
- WHITE, M. F. 1985. The transport of cationic amino acids across the plasma membrane of mammalian cells. *Biochimica et biophysica acta*, 822, 355-374.
- WU, G. & MORRIS JR, S. M. 1998. Arginine metabolism: nitric oxide and beyond. *Biochemical Journal*, 336, 1-17

## RESEARCH PAPER

# Molecular identification of some earthworm species (Annelida; Oligochaeta) In Kurdistan-Iraq

<sup>1</sup>Hawre Husamulddin Othman, <sup>2</sup>Sherwan Taeb Ahmad

<sup>1</sup>Department of Biology, Collage of Science, Salahaddin University - Erbil, Kurdistan Region, Iraq

<sup>2</sup>Department of Biology, Collage of Science, Salahaddin University - Erbil, Kurdistan Region, Iraq

### ABSTRACT:

A total of 256 specimens of earthworms were collected from four provinces in Kurdistan region of Iraq includes Erbil, Sulaymaniyah, Duhok and Halabja, during a period from July 2018 to April 2019.

DNA barcoding was used for the first time in Iraq for identification of earthworms to species level. A modified CTAB method was used for isolation and extraction of DNA. Mitochondrial COI region was amplified and sequenced to determine the differences among species.

Results revealed that six species belong to three genera of two families; Lumbricidae and Megascolecidae were successfully identified and the similarity of all species was 95% or more. which are *Amyntas morissi* (Beddard, 1892) ; *A. luridus* (Shen et al., 2019) ; *A. gracilis* (Kinberg, 1867) ; *Aporrectodea trapezoids* (Duges, 1828) ; *A. longa* (Ude, 1888) ; and *Healyella syriaca* (Rosa, 1893). Depending on the present results the species (*Haelyella syriaca*, *Amyntas gracilis* and *Amyntas luridus*) are considered as new records to Iraqi fauna. The phylogenetic tree analysis using maximum likelihood programs shown that there are seven clades. This study could be a suitable research program for future studies on the earthworms in Iraq.

KEY WORDS: Earthworms, COI, Lumbricidae; Megascolecidae.

DOI: <http://dx.doi.org/10.21271/ZJPAS.32.6.5>

ZJPAS (2020) , 32(6);46-53 .

## 1. INTRODUCTION

Earthworms belong to the phylum Annelida, class Oligochaete, they are widely distributed and more than 5500 aquatic and terrestrial species have been identified (Escudero et al., 2019). Their body is cylindrical and divided into segments by intersegmental grooves (Ahmed, 2015). The body cavity filled with coelomic fluid that extended from head to the anus; externally they bear little setae or short bristles (Dominguez and Edwards, 2011, Xiao, 2019).

Clitellum which found in adult worms only is a glandular swelling and saddle-shape usually occupying some segments and has a role in reproduction process (Brusca and Brusca, 1990, Csuzdi and Zicsi, 2003). These characteristics are important for morphological identification to species level.

Although, this worms have great role in soil studies and as soil biomarkers, recently many researchers proved that they have a helpful role in therapeutic processes of human diseases like treatment of diabetes, some types of cancer or as antibiotics (Liu et al., 2011, Liu et al., 2017, Augustine et al., 2017, Cooper et al., 2004). The earthworm glycolipoprotein (as known G-90) is a blend of macromolecules with some biological properties including mitogenicity, anticoagulation, fibrinolysis, bacteriostatic and antioxidation (Goodarzi et al., 2016).

### \* Corresponding Author:

Hawre Husamulddin Othman

E-mail: [hawre.hussam@gmail.com](mailto:hawre.hussam@gmail.com)

### Article History:

Received: 02/06/2020

Accepted: 23/07/2020

Published: 20/12/2020

Researchers which use the morphological characteristics for identification of earthworms, they critics the DNA barcodes for taxonomical studies because depended on a single mitochondrial region for identification and it can be misleading, but mitochondrial DNA(mtDNA) can be officiated at any stage of life cycle and the codes not change easily (Will and Rubinoff, 2004).

Phylogenetic studies for identification of animals verified that mtDNA have been widely used because it evolves more rapidly than nuclear DNA, thereby resulting in the accumulation of differences between closely related species (Moore, 1995, Mindell, 1997). Divergence of sequences among species is much higher than within species and mtDNA genealogies generally capture the biological discontinuities recognized by taxonomists as species. Cytochrome-C oxidase I gene (COI) describe as a DNA barcode for identification species of which is usually found in all animals, and comparison of sequences are simple because insertion and deletion are rare (Hebert et al., 2003, Azeez and Mohammed, 2017). Several phylogenetic analyses of Oligochaete taxa included a combination of several molecular markers (for instance nuclear18S, 28S rDNA, mitochondrial 12S rDNA, COI) and morphological features also confirmed for species identification (Bozorgi et al., 2019).

This present study aimed to introduce the use of molecular techniques for identification of

earthworm species in Iraq. It was constructed on an earthworm collection from samplings in different soils in Kurdistan/Iraq.

## 2.MATERIAL AND METHODES

### 2.1. Sample collection

During July 2018 to April 2019 a total of 256 specimens of earthworms were collected from four provinces in Kurdistan region of Iraq (Erbil, Sulaymaniyah, Duhok and Halabja) (Fig. 1). Collection was carried out by using Hand-storing method (Sims and Gerard, 1985, Farhadi et al., 2013), which the worms can be obtained simply by digging up the soil. The adult earthworms obtained from sites with their activity such as moist soil near ponds, gardens, farm areas, and forests. The samples of earthworms spread in plastic jars with the same soil from the area where the worms were obtained. Ten to fifteen worms were collected from each area, after that the worms were transported to laboratory and placed in bigger plastic jars. Leaf litters and manure added frequently to each plastic jars and the humidity of the plastic jars was kept between 70% to 80% by rushing water daily. However, each plastic jar was covered by textile net to avoid worm escaping. The adult worms were washed with tap water to remove soil particles and placed in Petri dishes (Ansari and Saywack, 2011). Finally, the worms killed in 30% ethanol and preserved in 95% ethanol for DNA extraction (Klinth et al., 2019).



**Figure 1.** Distribution of earthworm species in Kurdistan Region of Iraq.

## 2.2. DNA Extraction

After morphological identification of the specimens (Fig. 2.) the molecular study performed, the isolation of high quality of DNA is an essential for molecular study. In present study a modified CTAB (Cetyltrimethyl ammonium bromide) method for isolate high quality of DNA from different species of earthworm's tissue (Agustí et al., 2000, Juen and Traugott, 2006). The CTAB method generally used for extraction DNA from plant tissue which described by Murray and Thompson (1980) (Murray and Thompson, 1980). The CTAB genomic DNA isolation method include a cell lysis along with Chloroform; Isoamyl and use of proteinase K (Doyle and Doyle, 1987).

In present study the DNA extraction for amplification of the mitochondrial COI gene

region was performed in Ankara university, science college, Biology faculty. The mitochondrial COI region was amplified with primer LCO1490 and HCO2198 (Vrijenhoek, 1994, Huang et al., 2007, Escudero et al., 2019).

The preserved earthworms were placed on slides and 1 cm from caudal tissue at anterior part appended to prevent contamination by gut content (Huang et al., 2007). These tissues were divided to smaller pieces and transferred to clean and dry Eppendorf tubes. After adding 3ml of CTAB solution to each tube the tissues were crashed as much as possible, however more CTAB solution (3ml) were added. BME (Beta-mercatoethanol) a lysis buffer used to remove and destroy all proteins, lipids and other content (Ince et al., 2011, Horne et al., 2004), Fifty ml of BME buffer was added and placed in water bath for 1hr. to destroy the tissues and extract all mitochondria.



To each tube 500ml of CIAA (Chloroform: Isoamyl alcohol) were added and shaken so it became milky. All samples centrifuged for 15min. at 13,000 rpm at 4c° to add extra stability to DNA. The DNA extractions poured into other Eppendorf tubes with 500ml of CIAA and centrifuged again for best results.

At next step we add 500ml of Isopropanol to each sample and placed in -80c°, after freezing all samples centrifuged at 13,000rpm for 10min.,

when the centrifugation ended the supernatant and the DNA located at bottom of the tube were discharged.

For cleaning the DNA, 500ml of 100% alcohol added, centrifuged at 13,000 rpm for 3min., this step repeated twice. After all the supernatant discharged. Finally, the DNA diluted with TE buffer (PH 8) and left overnight.



**Figure 2:** Earthworm species identified in this study; *Aporrectodea longa* (A), *Aporrectodea trapezoides* (B), *Haelyella syriaca* (C), *Amyntas morissi* (D), *Amyntas gracilis* (E), *Amyntas luridus* (F).

### 2.3. PCR (Polymerase chain reaction)

The extracted DNA was amplified using PCR machine. Amount of 12.5 ml was added of PCR mixture into a tube with 9.5 ml of water, 1 ml of primer will be added and mix it well, after that 1 ml of extracted DNA added. The solution must mix well and take 1 ml of it, putted in an Eppendorf tube for PCR running, however the run for 30 cycles at 94 c° for 45s, at 49-52 c° for 40-60s, while at 72 c° for 90s (Huang et al., 2007).

Electrophoresis was used to ensure that the DNA completely extracted from earthworms. Both TAE (Tris-acetate- Ethylenediaminetetraacetic acid) buffer and agaroses prepared to run the electrophoreses, 50 ml of TAE buffer diluted in 950 ml of distal water, after that 0.8 % of agarose gel was dissolved in diluted TAE buffer. The

solution was heated until boiling and shaken well. When the solution reached the boiling degree, transferred to an electrophoresis glass and let to solidify. After that the solidified gel added into electrophoresis machine and 5 ml DNA also added with the marker.

Finally, the gel stained with bromide (1 mg per 1 ml of D.W) and was observed under the U.V. light, if there is a band meaning the extraction is perfect and there was DNA. The band on the gel clearly seen so there were a sufficient amount of DNA, finally the extractions sent to BM Labosis company in Ankara/Turkey for complete sequencing.

### 3.RESULTS

The DNA sequencing process results subjected to Nucleotide Basic Local Alignment Search Tool

(BLAST) in NCBI GenBank. The best match species are shown in Table 1. The results were three genera and six species belong to two families; Lumbricidae and Megascolecidae (Asian family).

The results of phylogenetic tree analyses using maximum likelihood method revealed in (Fig.3.) shows seven clades, two other results taken from NCBI for each species for compare. The first clade was *Amyntas luridus* having a moderate support bootstrap value reaches 67%. *Aporrectodea longa* is the second clade with a high bootstrap value reaches 100%. While *Haelyella syriaca* include two clades, each with 97% bootstrap value. The fourth clade *Amyntas*

*gracilis* with bootstrap reaches 90% and at fifth clade *Amyntas morrissi*, the bootstrap with marked sample that got from GenBank reaches 100%. The last clade includes *Aporrectodea trapezoides* has a high bootstrap reaches 99%.

According to above results Lumbricidae family involve three species; *Aporrectodea longa*, *Aporrectodea trapezoids* and *Haelyella syriaca*. Megascolecidae family also comprise three species; *Amyntas morrissi*, *Amyntas gracilis* and *Amyntas luridus*. Depending on the present results the species (*Haelyella syriaca*, *Amyntas gracilis* and *Amyntas luridus*) are first records in Iraq.

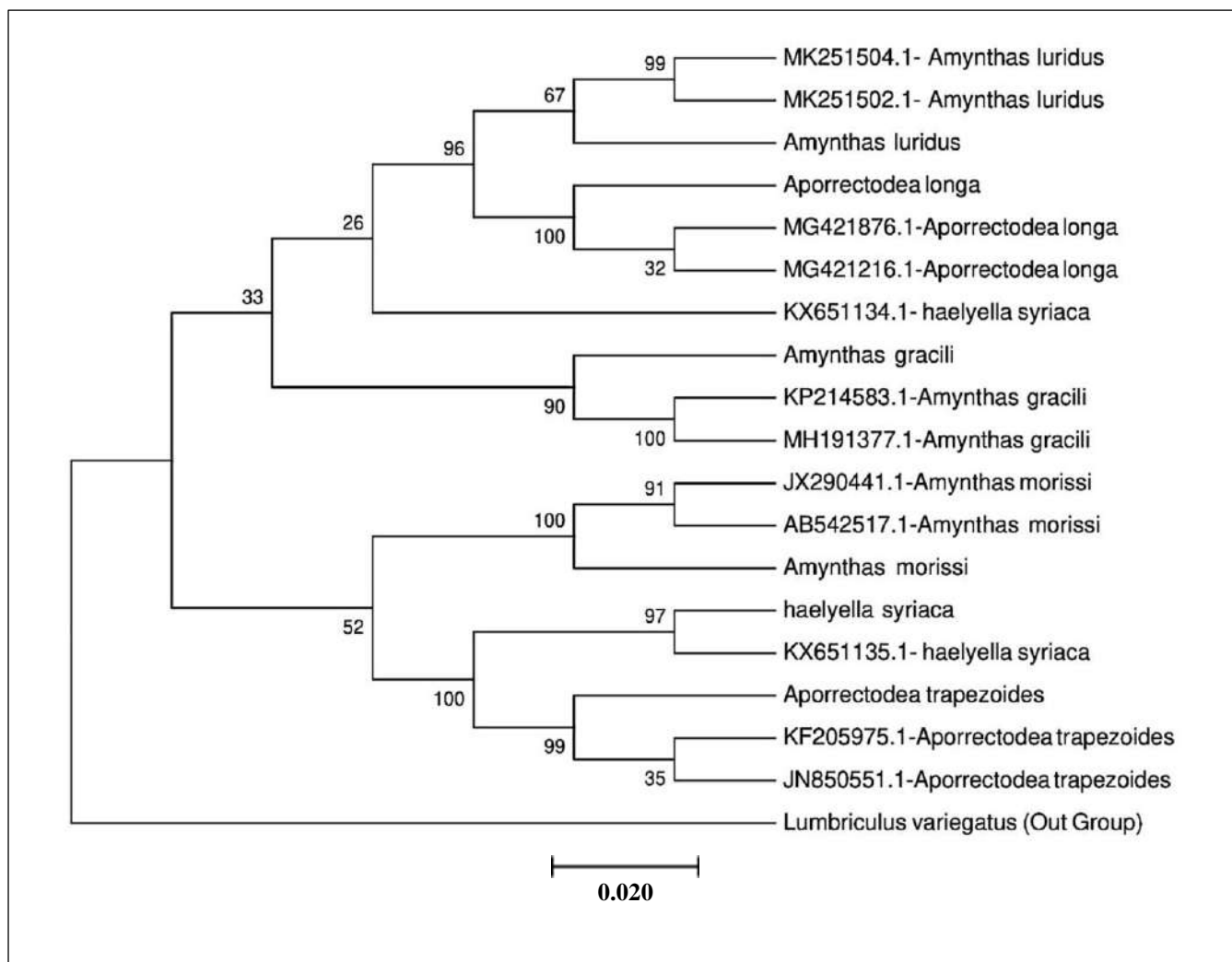


**Figure 3.** Molecular Phylogenetic analysis by Maximum Likelihood method. The evolutionary history was inferred by using the Maximum Likelihood method based on the Tamura-Nei model (Tamura and Nei, 1993). The tree with the highest log likelihood (-6713.35) is shown. The percentage of trees in which the associated taxa clustered together is shown next to the branches. Initial tree(s) for the heuristic search were obtained automatically by applying Neighbor-Join and BioNJ algorithms to a matrix of pairwise distances estimated using the Maximum Composite Likelihood (MCL) approach, and then selecting the topology with

superior log likelihood value. The analysis involved 19 nucleotide sequences. Codon positions included were 1st+2nd+3rd+Noncoding. All positions containing gaps and missing data were eliminated. There were a total of 557 positions in the final dataset. Evolutionary analyses were conducted in MEGA7 (Kumar et al., 2016).

**Table 1:** Representative of specimen collected in sampling sites in Kurdistan Region/Iraq with annotated sequences in GenBank.

Earthworm species	Province	Query Cover %	Identic Number %	GENBank Accession Number	GENBank earthworm Species Identification	Country Identification
<i>Amyntas morissi</i>	Sulaymaniyah Duhok Erbil	100	96.49	JX290441.1	<i>Amyntas morissi</i>	Taiwan
		99	96.49	AB542517.1	<i>Amyntas morissi</i>	Japan
<i>Healyella syriaca</i>	Duhok Erbil	100	95.13	KX651135.1	<i>Healyella syriaca</i>	USA
		99	90.45	MG941001.1	<i>Healyella syriaca</i>	USA
<i>Amyntas luridus</i>	Sulaymaniyah Halabja	100	95.09	MK251502.1	<i>Amyntas luridus</i>	Taiwan
		100	95.09	MK251504.1	<i>Amyntas luridus</i>	Taiwan
<i>Aporrectodea trapezoides</i>	Duhok Erbil	100	100	KF205975.1	<i>Aporrectodea trapezoides</i>	China
		100	100	JN850551.1	<i>Aporrectodea trapezoides</i>	Portugal
<i>Amyntas gracilis</i>	Sulaymaniyah Duhok Erbil Halabja	100	94.79	KP214583.1	<i>Amyntas gracilis</i>	UK
		100	94.61	MH191377.1	<i>Amyntas gracilis</i>	India
<i>Aporrectodea longa</i>	Sulaymaniyah Duhok Erbil Halabja	100	100	MG421876.1	<i>Aporrectodea longa</i>	Canada
		100	100	MG421216.1	<i>Aporrectodea longa</i>	Canada

#### 4.DISCUSSION

This study based on DNA barcodes for identification of earthworms, it represents the results of the first molecular based study for identification of earthworms in Iraq. Our results reveal that DNA barcoding is an auspicious tool for studying earthworm biodiversity: previous studies in the area reported three species from Kurdistan region, while our rather limited sample yielded nine (only six of them are represents here because the other three species gave inadequate DNA sequencing results, so they must be undergoing further molecular studies to confirm their classification accurately). There are two explanations for this, first, barcoding permits

identify juvenile or scantily preserved specimens. Second, many earthworm species look alike, and so the species indicating small minority of the sample bend to be grouped with more numerous species and unobserved.

In the study of BLAST, *Aporrectodea longa* (Ude, 1888) and *Aporrectodea trapezoides* (Duges, 1828), analysis of similarity in BLAST showed 100% similarity with those sequences annotated in GenBank at COI region. Conversely, *Amyntas morissi* (Beddard, 1892) showed only 96% similarity with annotated sequences. While, *Amyntas gracilis* (Kinberg, 1867) and *Amyntas luridus* (Shen et al., 2019) showed lower similarity which both of them 95%. The last

species is *Haelyella syriaca*, (Rosa, 1893) the result of analysis is between 90% and 95% similarity with annotated sequences in GenBank. Those species belong into two families Lumbricidae and Megascolecidae. These two families ranked as a first and second most widely distributed and abundant families in temperate zones (Simberloff and Rejmánek, 2011). *Amyntas gracilis* is highly associated with *Amyntas corticis* (Sims and Gerard, 1985).

The evolutionary divergence based on the Maximum Likelihood method shows different clade groups, regarding the present study the tree divided into seven clades. *Amyntas luridus*, related with annotated sample from Taiwan at bootstrap 67% (which a moderate value) and this may be due to the geographical distribution differences between them (Shen et al., 2019) Environment and mutation also have role in divergence among species and individual of same species at different habitat and countries (Csuzdi et al., 2017, Escudero et al., 2019).

However, *Aporrectodea longa* and *Amyntas morissi* included into different clades and this has agreement with results obtained by each of (Porco et al., 2018, Chang et al., 2009). *Amyntas gracilis* also located fourth clade with bootstrap reaches 90% , results obtained from NCBI which carried out by (Pop et al., 2005) were similar with ours . *Haelyella syriaca* included into two clades, the local species and one species from NCBI which located at sixth clades related at high bootstrap value reaches 97 %. The present findings confirmed that the suggestive bootstrap values of the attained tree were previously documented with same COI mtDNA marker which is existing in NCBI.

## 5.CONCLUSION

Six species belong to three genera of two families; Lumbricidae and Megascolecidae were successfully identified and the similarity of all species was 95% or more. *Haelyella syriaca*, *Amyntas gracilis* and *Amyntas luridus* are first records in Iraq. The phylogenetic tree analysis using maximum likelihood programs revealed that there are seven clades. This study could be a suitable research program for future studies on the earthworms in Iraq.

## ACKNOWLEDGMENT

We will express our gratitude to those who helped us, and special thanks to Salahaddin University- College of Science/Biology department for their support during the period of achievement of this research.

## REFERENCES

- AHMED, S. T. 2015. The impact of four pesticides on the earthworm *Lumbricus terrestris* (Annelida: Oligochaeta). *ZANCO Journal of Pure and Applied Sciences*, 27, 5-10.
- AGUSTÍ, N., DE VICENTE, M. & GABARRA, R. 2000. Developing SCAR markers to study predation on *Trialeurodes vaporariorum*. *Insect Molecular Biology*, 9, 263-268.
- ANSARI, A. A. & SAYWACK, P. 2011. Identification and classification of earthworm species in Guyana. *Int. J. Zool. Res*, 7, 93-99.
- AUGUSTINE, D., RAO, R. S., ANBU, J. & MURTHY, K. C. 2017. In vitro antiproliferative effect of earthworm coelomic fluid of *eudrilus eugeniae*, *eisenia foetida*, and *perionyx excavatus* on squamous cell carcinoma-9 cell line: a pilot study. *Pharmacognosy research*, 9, S61.
- AZEEZ, D. M. & MOHAMMED, S. I. 2017. Molecular identification and Phylogenetic tree of some fish (Cyprinidae) in Dukan Lake, Kurdistan of Iraq. *ZANCO Journal of Pure and Applied Sciences*, 29, 140-145.
- BEDDARD, F. E. 1892. XI.—Anatomical Description of Two New Genera of Aquatic Oligochaeta. *Earth and Environmental Science Transactions of The Royal Society of Edinburgh*, 36, 273-305.
- BOZORGI, F., SEIEDY, M., MALEK, M., AIRA, M., PÉREZ-LOSADA, M. & DOMÍNGUEZ, J. 2019. Multigene phylogeny reveals a new Iranian earthworm genus (Lumbricidae: Philomontanus) with three new species. *PloS one*, 14.
- BRUSCA, R. C. & BRUSCA, G. J. 1990. Invertebrates Sinauer Associates. *Inc. Sunderland, Massachusetts*, 922.
- CHANG, C.-H., ROUGERIE, R. & CHEN, J.-H. 2009. Identifying earthworms through DNA barcodes: Pitfalls and promise. *Pedobiologia*, 52, 171-180.
- COOPER, E. L., RU, B. & WENG, N. 2004. Earthworms: sources of antimicrobial and anticancer molecules. *Complementary and Alternative Approaches to Biomedicine*. Springer.
- CSUZDI, C., CHANG, C.-H., PAVLÍČEK, T., SZEDERJESI, T., ESOP, D. & SZLÁVECZ, K. 2017. Molecular phylogeny and systematics of native North American lumbricid earthworms (Clitellata: Megadrili). *PloS one*, 12.
- CSUZDI, C. & ZICSI, A. 2003. *Earthworms of Hungary (Annelida: Oligochaeta, Lumbricidae)*, Hungarian Natural History Museum Budapest.
- DOMINGUEZ, J. & EDWARDS, C. A. 2011. Biology and ecology of earthworm species used for vermicomposting. *Vermiculture technology: earthworms, organic wastes, and environmental*

- management. CRC Press USA. Elvira, C., Sampedro.
- DOYLE, J. J. & DOYLE, J. L. 1987. A rapid DNA isolation procedure for small quantities of fresh leaf tissue.
- ESCUADERO, G. J., LAGERLÖF, J., DEBAT, C. M. & PÉREZ, C. A. 2019. Identification of Earthworm Species in Uruguay Based on Morphological and Molecular Methods. *Agrociencia Uruguay*, 23, 1-10.
- FARHADI, Z., MALEK, M. & ELAHI, E. 2013. Review of the earthworm fauna of Iran with emphasis on Kohgiluyeh & Boyer-Ahmad Province. *Zootaxa*, 3670, 440-448.
- GOODARZI, G., QUJEQ, D., ELMI, M. M., FEIZI, F. & FATHAI, S. 2016. The effect of the glycolipoprotein extract (G-90) from earthworm *Eisenia foetida* on the wound healing process in alloxan-induced diabetic rats. *Cell biochemistry and function*, 34, 242-249.
- HEBERT, P. D., CYWINSKA, A., BALL, S. L. & DEWAARD, J. R. 2003. Biological identifications through DNA barcodes. *Proceedings of the Royal Society of London. Series B: Biological Sciences*, 270, 313-321.
- HORNE, E. C., KUMPATLA, S. P., PATTERSON, K. A., GUPTA, M. & THOMPSON, S. A. 2004. Improved high-throughput sunflower and cotton genomic DNA extraction and PCR fidelity. *Plant Molecular Biology Reporter*, 22, 83-84.
- HUANG, J., XU, Q., SUN, Z. J., TANG, G. L. & SU, Z. Y. 2007. Identifying earthworms through DNA barcodes. *Pedobiologia*, 51, 301-309.
- INCE, A. G., YILDIZ, F. & KARACA, M. 2011. The MAGi DNA extraction method for fresh tissues and dry seeds. *J Med Plants Res*, 5, 5458-5464.
- JUEN, A. & TRAUGOTT, M. 2006. Amplification facilitators and multiplex PCR: Tools to overcome PCR-inhibition in DNA-gut-content analysis of soil-living invertebrates. *Soil Biology and Biochemistry*, 38, 1872-1879.
- KINBERG, J. 1867. *Annulata nova. Ofversigt af K. Vetenskapsakademiens förhandlingar*, 23, 337-357.
- KLINTH, M., KREILING, A.-K. & ERSEUS, C. 2019. Investigating the Clitellata (Annelida) of Icelandic springs with alternative barcodes. *Fauna norvegica*, 39, 119-132.
- KUMAR, S., STECHER, G. & TAMURA, K. 2016. MEGA7: molecular evolutionary genetics analysis version 7.0 for bigger datasets. *Molecular biology and evolution*, 33, 1870-1874.
- LIU, C., CHEN, X., PAN, Y., LIANG, H., SONG, S. & JI, A. 2017. Antitumor studies of earthworm fibrinolytic enzyme component a from *Eisenia foetida* on breast cancer cell line MCF-7. *Indian Journal of Pharmaceutical Sciences*, 79, 361-368.
- LIU, L., WEN, X. & XU, M. 2011. Effects of zhenqing recipe and earthworm on the expressions of transforming growth factor-beta1 and plasminogen activator inhibitor 1 in renal tissues of type 2 diabetic rats. *Zhongguo Zhong xi yi jie he za zhi Zhongguo Zhongxiyi jiehe zazhi= Chinese journal of integrated traditional and Western medicine*, 31, 967-972.
- MINDELL, D. P. 1997. Phylogenetic relationships among and within select avian orders based on mitochondrial DNA. *Avian molecular evolution and systematics*, 211-247.
- MOORE, W. S. 1995. Inferring phylogenies from mtDNA variation: mitochondrial-gene trees versus nuclear-gene trees. *Evolution*, 49, 718-726.
- MURRAY, M. & THOMPSON, W. F. 1980. Rapid isolation of high molecular weight plant DNA. *Nucleic acids research*, 8, 4321-4326.
- POP, A. A., CSUZDI, C. & WINK, M. 2005. Remarks on the molecular phylogeny of Crassiclitellata families using the mitochondrial 16S rDNA gene (*Oligochaeta*, *Opisthophora*). *Cluj Univ. Press; Cluj*, 155-166.
- PORCO, D., CHANG, C.-H., DUPONT, L., JAMES, S., RICHARD, B. & DECAËNS, T. 2018. A reference library of DNA barcodes for the earthworms from Upper Normandy: Biodiversity assessment, new records, potential cases of cryptic diversity and ongoing speciation. *Applied soil ecology*, 124, 362-371.
- ROSA, D. 1893. Viaggio del Dr. E. Festa in Palestina, nel Libano e regioni vicine. II. Lumbricidi. *Bollettino dei Musei di Zoologia ed Anatomia comparata della R. Università di Torino*, 8, 1-14.
- SHEN, H.-P., CHANG, C.-H. & CHIH, W.-J. 2019. Two new earthworm species of the genus *Amyntas* (*Oligochaeta*: *Megascolecidae*) from central Taiwan, with comments on some recent species assignments in *Amyntas* and *Metaphire*. *Zootaxa*, 4658, 101-123.
- SIMBERLOFF, D. & REJMÁNEK, M. 2011. *Encyclopedia of biological invasions*, Univ of California Press.
- SIMS, R. W. & GERARD, B. M. 1985. *Earthworms: keys and notes for the identification and study of the species*, Brill Archive.
- TAMURA, K. & NEI, M. 1993. Estimation of the number of nucleotide substitutions in the control region of mitochondrial DNA in humans and chimpanzees. *Molecular biology and evolution*, 10, 512-526.
- UDE, H. J. H. 1888. Über die rückenporen der terricolen oligochaeten, nebst beiträgen zur histologie des leibeschlauches und zur systematik der lumbriciden.
- VRIJENHOEK, R. 1994. DNA primers for amplification of mitochondrial cytochrome c oxidase subunit I from diverse metazoan invertebrates. *Mol Mar Biol Biotechnol*, 3, 294-9.
- WILL, K. W. & RUBINOFF, D. 2004. Myth of the molecule: DNA barcodes for species cannot replace morphology for identification and classification. *Cladistics*, 20, 47-55.
- XIAO, N. 2019. *Terrestrial Earthworms (Oligochaeta: Opisthophora) of China*, Academic Press.

## RESEARCH PAPER

# Glutathione S-Transferase Mu 1 and Glutathione S-transferase theta 1 Genes Polymorphism and Susceptibility to Chronic Myeloid Leukemia in Erbil-Iraq Kurdistan Region

Mukhlis H. Aali<sup>1</sup>, Govand M. Qader<sup>1</sup>, Mustafa S. Al-Attar<sup>1</sup>, Mustafa F. Rajab<sup>1</sup>, Mudhir S. Shehka<sup>1</sup>

<sup>1</sup>Department of Biology, College of Science, Salahaddin University-Erbil, Kurdistan Region, Iraq

### ABSTRACT:

Chronic myeloid leukemia (CML) result from many reactions of heredity non-heredity factors. The null genotype for glutathione S-transferase (GSTM1 or GSTT1) is regarded a risk agent leukemia, especially on CML in various inhabitants. The current study focused on evaluating association of two polymorphic identified genes Glutathione S-Transferase Mu 1 and glutathione S-transferase null genotypes that respect to CML patients from Erbil province, hence this work was performed a case-control study that composed of 51 samples (62% males, 39% females) with CML included and 45 healthy controls (22% male and 78% females) have participated. Multiplex PCR was used to ascertain GSTM1 and GSTT1 null genotypes. The chi-square test was done to show any link between GSTM1 and GSTT1 null genotypes that might be occurred in CML. There are significant statistical differences between incidence of GSTM1 null genotypes among CML cases and the increased CML risk was showed in patients bearing any of the GSTM1 null genotypes (OR = 2.196, 95%CI = (0.6017-6.806), P-value = 0.2108). While there is no statistical relation of GSTT1 null genotype with the risk of CML and exhibited lower risk initiation of CML occurrence (OR: 0.391, 95% CI: 0.1741-0.9033, P-value = 0.0304). Our findings demonstrate that GSTM1 null genotype is linked with the risk of CML patient development. The statements are helpful for formulating different investigation including GSTM1, GSTT1 variation genes and comparing research outputs with geography zone diverse in Iraq.

KEY WORDS: GSTM1; GSTT1; Gene polymorphism; CML; Multiplex PCR.

DOI: <http://dx.doi.org/10.21271/ZJPAS.32.6.6>

ZJPAS (2020) , 32(6);54- 59.

## 1. INTRODUCTION

Chronic myelogenous leukaemia (CML) belong to blood cancer specifically formed due to chromosome called Philadelphia resulting by reciprocal translocation t (9; 22) (q34; q11) or BCR-ABL gene fusion that lead to the constitutive activation BCR-ABL tyrosine kinase which increase blood cells proliferation and malignancy. CML prevalence yearly accounts one to two cases per hundred thousand people and fifteen percentage leukaemia type in mature individual (Faderl, Talpaz et al. 1999, Deininger, Goldman et al. 2000, Al-Attar and Qader 2017).

Most of the cancers, including CML and stomach formed by a massive environmental interference, for instance, exposing to ionizing and nonionizing radiation, exist cancer leading agents in the habitat like benzene, alcohol, smoke and pesticides. This mutagenic substance refers to genotoxic and have act on the biotransformation of xenobiotics. It leads to genetic alteration in haemogenesis which rise the susceptibility of cancer like CML (Bhat, Bhat et al. 2012, Kassogue, Dehbi et al. 2015, Sulaiman 2016).

The DNA damages eliminated by activation and detoxification of carcinogens repair of genomic mistake errors and program cell death for mutant cells, apoptosis (Hayes and Pulford

### \* Corresponding Author:

Govand Musa Qader

E-mail: [govand.qader@su.edu.krd](mailto:govand.qader@su.edu.krd)

### Article History:

Received: 06/04/2020

Accepted: 10/08/2020

Published: 20/12 /2020

1995, Belitsky and Yakubovskaya 2008, Fang, Wang et al. 2013).

Several metabolic cancer susceptibility genes show DNA polymorphisms in the germline. These genes encode enzymes that have a role in exogenous and endogenous toxic substances and xenobiotics metabolism (Taioli 1999). Glutathione S-transferases (GSTs) are enzymes of phase II, have role in xenobiotics metabolism which share in cell detoxification by changing the activated carcinogenic metabolites of phase I enzymes (cytochrome P450) to inactivated metabolites and soluble glutathione, ease executable. There are eight categories of GSTs have been founded such as alpha (GSTA), mu (GSTM) theta (GSTT), pi (GSTP), zeta (GSTZ), sigma (GSTS), omega (GSTO) and kappa (GSTK) (Mannervik, Awasthi et al. 1992, Jancova, Anzenbacher et al. 2010, Rabab 2013). There are many studies on the assigned locus of GSTM1 and GSTT1 genes on chromosome 1p13.3 and 22q11.2 respectively. The long-term exposure to urban air pollution increase chromosome aberration like gap and break in human somatic cells (Pearson, Vorachek et al. 1993, Webb, Vaska et al. 1996, Knudsen et al. 1999).

The various research found that there is a link between enzyme inactivity in GSTM1 and GSTT1 and the susceptibility to form many sorts of malignancy like stomach, bladder and chronic myeloid leukemia (Bajpai, Tripathi et al. 2007, Ma, Zhuang et al. 2013, Sharma, Jain et al. 2013). The GSTM and GSTT genes are multifunctional enzymes groups that have a role in antioxidant activity interfere in cell differentiation drug detoxification, and anticancer drug resistance (Marchewka, Piwowar et al. 2017). The present study focuses on two polymorphic identified genes GSTM1 and GSTT1 null genotypes that respect to CML patients. Illustration the frequencies of these polymorphisms in Kurdish people from Erbil province, Kurdistan Region of Iraq and compare it to other population has benefit to show the exact role of GST genes in cancer formation.

## 2. MATERIALS AND METHODS

### 2.1. Sample Collection:

Three ml of blood samples were collected in EDTA tube of fifty-one CML patients collected from Nanakali Hospital, which was diagnosed by physicians. The age of patient suffered CML ranged (9-80) years, 62% were male, and 39% were female, and forty-five control group age ranged from 16 to 60 years, 22% male and 78% of samples were female.

#### 2.1.1 Molecular Technique Analysis

#### 2.1.2 Genomic DNA Extraction from blood sample

The genetic material was isolated from blood specimens in College of Science-Salahaddin University, using the Genomic DNA kit (GenetBio, Korea), depending on the manufacturer's instructions. Glutathione S-Transferase genes polymorphisms identified by running multiplex polymerase chain reaction.

### 2.2. Genotyping of GSTM1 and GSTT1 Polymorphism

The total of 25 µl volume of PCR master mix reaction performed containing 3µl of template, 12.5 µl of 2X GoTaqGreen PreMix (Promega, USA) and 1µl was added for each forward and reverse primers of both GSTM1, GSTT1 genes, GSTM1:forward5'GAACTCCCTGAAAAGCTA AAGC3',GSTM1:reverse5'GTTGGGCTCAAAT ATACGGTGG3',GSTT1:forward5'TTCCTTAC TGGTCCTCACATCTC-3' and GSTT1 reverse 5'-TCACCGGATCATGGCCAGCA-3' Albumin forward 5'-GCCCTCTGCTAACAAGTCCTAC-3'Albumin:reverse5'GCCCTAAAAAGAAAATC GCCAATC-3'(Sharma et al., 2012) then the mixture was completed by adding 3.5µl DNase free water.

The target gene amplification was done using PCR started by initial denaturation at 95°C for 5 min, continued by 35 cycles at 94°C for 1 min, 56°C for 1 min, 72°C for 1 min and eventually elongation at 72°C for 7 minutes. After PCR amplification, the PCR amplicon separated on two percentage agarose then the separated bands were stained with ethidium bromide to visualize under UV light (Brown 2016). The bands of (219, 459 and 350) base pair mean the appearance of GSTM1, GSTT1 gene polymorphism and albumin respectively. The existence of albumin without GSTT1 or GSTM1

means its deletion and used as a control (Sharma et al., 2012).

### 3. Statistical Analysis

The graph pad prism 8.0.1 used. The chi-square test was done to illustrate the risk between GSTM1 and GSTT1 null genotypes and incidence of CML, corresponding the genotype distribution between cancer and healthy inhabitants. A *p*-value of lower than 0.05 reflected statistically significant. Odds ratio (OR) with a confidence interval (CI) of 95% was counted.

GST Polymorphism	CML N=51 (%)	Control N=45 (%)	Genetic Models	OR 95% CI	P Value
GSTM1 Recessive					
Present	9(17.7)	4(8.9)		1	-
Null	42(82.3)	41(91.1)		2.196 (0.6017-6.806)	<b>0.2108</b>
GSTT1 Recessive					
Present	13(25.5)	21(46.7)		1	-
Null	38(74.5)	24(53.3)		0.391 (0.1741-0.9033)	<b>0.0304</b>

### 4. RESULTS AND DISCUSSION

The current work consists of fifty-one CML patients from 9 to 80 years' age, (62% males, 39% females) and healthy blood cases collected from forty-five (22% males, 78% females; age ranged from 16 to 60 years).

In the present study, we found frequency of GSTM1 and GSTT1 genotypes in CML and control group, and CML risk belong to the effect of GST polymorphism as illustrated in Table 1.

The ratio of GSTM1 and GSTT1 genotypes revealed in 51 chronic myelogenous leukemia and 45 healthy persons. There are significant statistical differences between incidence of GSTM1 null genotypes among CML cases and the increased CML risk was showed in patients bearing any of the GSTM1 null genotypes (OR = 2.196, 95%CI = (0.6017-6.806), *P*-value = 0.2108). While there is no any statistical relation of GSTT1 null genotype with the risk of CML and exhibited lower risk initiation of CML occurrence (OR: 0.391, 95% CI: 0.1741-0.9033, *P*-value = 0.0304).

There was a statistically significant relation between GSTM1 null genotype and CML incidence. Forty-two percentage of the CML cases and 41 % of health belong to homozygous

deletion in the *GSTM1* referring a high variation with an (OR, 95% CI, 2.196, 0.6017-6.806; *P*-value = 0.2108). Although GSTT1 null genotypes exhibited a reduce risk producing CML cancer incidence, it was statistically not significant (OR: 0.391, 95% CI: 0.1741-0.9033, *P*-value = 0.0304). The DNA Polymorphisms did not show a significant association with CML disease when disposes oddly, an association may appear when CML genotypes of these various polymorphisms are fused. Hence we examined the combination of GSTM1 versus GSTT1 their relation with CML occurrence as in Table 1.

**Table (1).** The Distribution of GSTM1 and GSTT1 genotypes in CML patients and healthy controls and evaluation of the risk of CML.

Abbreviations: CML: Chronic Myelogenous Leukemia; \**P* value < 0.05; OR: Odds ratio; CI: Confidence interval.

Two percentage agarose gel electrophoresis illustrating multiplex PCR genotyping of DNA samples for identifying of GSTM1 and GSTT1 gene deletion (null genotype). The (219, 459 and 350) base pair bands mean the existence of GSTM1, GSTT1 (non-null alleles) and albumin consecutively. The lake of GSTM1 or GSTT1 represents homozygous null genotype of that gene shown in Figure 1.

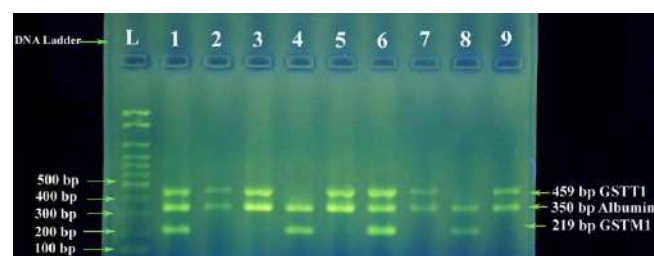


**Figure 1.** Agarose gel electrophoresis (2%) illustrating multiplex PCR genotyping of human genomic DNA samples for detection of GSTM1 and GSTT1 gene deletion (null genotype). The 219 bp, 459 bp and 350bp means the presence of GSTM1, GSTT1 (non-null alleles) and Albumin respectively. The absence of 219 bp band shows GSTM1 null genotype; absence of 459 bp band shows GSTT1 null genotype; albumin co-amplified in all samples. Absence of GSTM1 or GSTT1 product represents homozygous null



genotype of that gene. Lanes 1, 4, 6, and 8 GSTM1 and GSTT1 positive genotypes (non-null alleles). Lanes 2, 3, 5, 7,9: GSTM1 null genotypes. L: 100 bp DNA ladder.

Chronic myeloid leukemia is one the most of common studied human malignancy, and it is a myeloproliferative disturbance. Still, precise mechanism leading to this carcinogenesis is yet to be understood the risk of CML (Deininger, Goldman et al. 2000, Bhat, Bhat et al. 2012). The unequilibrium between expose to carcinogens (endogenous and exogenous) consequence lead to development of cancer and the ability of different enzymes involved in activation or in detoxification of xenobiotics (Kassogue, Dehbi et al. 2015). Metabolizing enzymes have role in cancer development of inter-individual genetic variation in xenobiotics. The genetic variation and level of expression of these carcinogen metabolizing enzymes are important in identifying the susceptibility of cancer initiation (Bhat, Bhat et al. 2012).

Hence, in a genetic case-control study, the relation between xenobiotic metabolizing gene polymorphisms and susceptibility were examined to CML patients in Erbil Province, Kurdistan Region of Iraq. There are many studies that reported the role of GSTT1 and GSTM1 gene polymorphisms in the formation of carcinogenesis like CML (Kassogue, Dehbi et al. 2015)

Genetic differences that decrease the activity of the phase II glutathione transferase enzymes or increase the level of the phase I cytochrome P450 enzymes associated with elevating risk of cancer because polymorphism lead to stop enzymatic activity and inhibit the detoxification role for GSTs (Makhtar, Husin et al. 2017). Although polymorphisms in detoxification genes have essential role in determining cancer risk, relatively little is known about their genetics and expression. (Pearson, Vorachek et al. 1993).

Two DNA polymorphisms that comprise deletions in GSTM1 and GSTT1 were described that results in enzyme missing or absence activity (Kassogue, Dehbi et al. 2015), therefore, we analyzed and realize the association between the GSTs (GSTT1 and GSTM1) gene polymorphisms and CML intensively. Nowadays, several studies have suggested that susceptibility to Acute myeloid leukemia and Chronic myeloid leukemia

may associate GSTT1 and or GSTM1 deletions (Souza, Barbosa et al. 2008).

The current results pointed out that polymorphic variants in the glutathione S-transferase (GSTs) are associated the CML cancer susceptibility. Moreover, regarding the GST genes, we noticed that GSTM1 null genotype people expose more at risk to be affected with CML by conceiving higher risk (OR= 2.196) for CML as compared to healthy controls as shown in table 1 and describing a statistically significant positive association with CML patients. Similarly, the results were also clearly reported about the elevated risk of CML for the GSTM1 null genotype by Al-Achkar et al. (2017), Bhat et al., (2012), and Lordelo et al. (2012) showed that the GSTM1 null genotype frequency was higher in CML than in control (Bhat, Bhat et al. 2012, Lordelo, Miranda-Vilela et al. 2012, Al-Achkar, Moassass et al. 2017, Rostami, Assad et al. 2019).

The concurring results from different populations depicted. Depending to the references, various epidemiological studies have represented the role of GSTM1 and GSTT1 null in predisposing individuals to different cancer types including CML. There are some studies elucidated that the GSTM1 null whether, alone or with GSTT1, increased disease risk in Indian, Brazilian and Syrian people (Al-Achkar, Moassass et al. 2017). Besides, Sharma et al., (2012) who stated that the existence of homozygous null GSTM1 genotype is substantially higher in Caucasians and Asians as compared to Indian population (Sharma, Pandey et al. 2012).

Disconcordance research are demonstrated in the relationship between GSTM1 null genotype and CML, and some studies remarked no association of the GSTM1 gene polymorphism with CML (Taspinar, Aydos et al. 2008, Özten, Sunguroğlu et al. 2012, Al-Achkar, Azeiz et al. 2014).

Alternatively, our analyses show that the GSTT1 gene deletion (null genotype) was not a significant association among CML patients with control sample. The findings of the current study are in accord with the previous investigation of Kassogue et al., (2015) who submit that the GSTT1 null genotype not found to be associated with the development of CML (Kassogue, Dehbi et al. 2015). Likewise, in the current study, Our results were similar to the results which concluded

by Rostami et al., (2019) consistent with Weich et al. (2016) report (Weich, Ferri et al. 2016, Rostami, Assad et al. 2019).

Furthermore, a research approved in Japan that did not report the association between GSTT1 null genotype and CML patient (Hishida, Terakura et al. 2005)a. In contrast, the conflicting results with an association were achieved such as the studies in Caucasian, Indian, Chinese Syrian populations that find an increase in the GSTT1null genotype in CML cases (Al-Achkar, Moassass et al. 2017). There is abundantly manifest and apparent that polymorphism in individual GST genes is important modulators of CML cancer susceptibility.

## 5. CONCLUSIONS

To the best of our comprehension and knowing, this is the first genetic variation in Kurdish people from Erbil Province, Kurdistan Region of Iraq for evaluating of association the risk of GSTM1 and GSTT1 null genotype carrier in the development of CML. This study has allowed determining the frequency of GSTM1 and GSTT1 gene polymorphism in a sample of our population. Besides, we have distinguished that the GSTM1 null genotype is associated with the development of CML patients. These statements have role in study many populations including allele variation of GSTM1, GSTT1 genes and comparing the data with many geographical zones in Iraq.

## Acknowledgements

We want to thank the University of Salahaddin-College of Science/Biology Department, for helping us and providing facilities. Furthermore, we thank all the patients, family members and staff from all the units of Nanakali Hospital for Blood Diseases and Cancer in Erbil city that assisted and participated in the present study.

## References

- AL-ACHKAR, W., AZEIZ, G., MOASSASS, F. & WAFI, A., 2014. Influence of CYP1A1, GST polymorphisms and susceptibility risk of chronic myeloid leukaemia in Syrian population. *Medical Oncology*, 31, 889.
- AL-ACHKAR, W., MOASSASS, F., AROUTIOUNIAN, R., HARUTYUNYAN, T., LIEHR, T. & WAFI, A. 2017. Effect of Glutathione S-transferase mu 1 (GSTM1) gene polymorphism on chronic myeloid leukaemia risk and Imatinib treatment response. *Meta Gene*, 12, 113-117.
- Al-Attar M. & Qader M. 2017. Cytogenetic and molecular genetic studies of number of chronic myelogenous leukemia in Erbil province. *ZANCO Journal of Pure and Applied Sciences*, 29 (2); 1-17.
- BAJPAI, P., TRIPATHI, A. K. & AGRAWAL, D. 2007. Increased frequencies of glutathione-S-transferase (GSTM1 and GSTT1) null genotypes in Indian patients with chronic myeloid leukemia. *Leuk Res*, 31, 10,1359-1363.
- BELITSKY, G. A. & YAKUBOVSKAYA, M. G. 2008. Genetic polymorphism and variability of chemical carcinogenesis. *Biochemistry (Mosc)*, 73, 543-54.
- BHAT, G., BHAT, A., WANI, A., SADIQ, N., JEELANI, S., KAUR, R., MASOOD, A. & GANAI, B. 2012. Polymorphic variation in glutathione-S-transferase genes and risk of chronic myeloid leukaemia in the Kashmiri population. *Asian Pac J Cancer Prev*, 13, 69-73.
- BROWN, T. A. 2016. *Gene cloning and DNA analysis: an introduction*, John Wiley & Sons.
- DEININGER, M. W. N., GOLDMAN, J. M. & MELO, J. V. 2000. The molecular biology of chronic myeloid leukemia. *Blood*, 96, 3343-3356.
- FADERL, S., TALPAZ, M., ESTROV, Z., O'BRIEN, S., KURZROCK, R. & KANTARJIAN, H. M. 1999. The Biology of Chronic Myeloid Leukemia. *New England Journal of Medicine*, 341, 164-172.
- FANG, J., WANG, S., ZHANG, S., SU, S., SONG, Z., DENG, Y., CUI, H., WANG, H., ZHANG, Y., QIAN, J., GU, J., LIU, B., LI, P., ZHANG, R., LIU, X. & WANG, Z. 2013. Association of the glutathione s-transferase m1, t1 polymorphisms with cancer: evidence from a meta-analysis. *PLoS One*, 8, e78707.
- HAYES, J. D. & PULFORD, D. J. 1995. The glutathione S-transferase supergene family: regulation of GST and the contribution of the isoenzymes to cancer chemoprotection and drug resistance. *Crit Rev Biochem Mol Biol*, 30, 445-600.
- HISHIDA, A., TERAKURA, S., EMI, N., YAMAMOTO, K., MURATA, M., NISHIO, K., SEKIDO, Y., NIWA, T., HAMAJIMA, N. & NAOE, T. 2005. GSTT1 and GSTM1 deletions, NQO1 C609T polymorphism and risk of chronic myelogenous leukemia in Japanese. *Asian Pacific Journal of Cancer Prevention*, 6, 251.
- JANCOVA, P., ANZENBACHER, P. & ANZENBACHEROVA, E. 2010. Phase II drug metabolizing enzymes. *Biomedical papers of the Medical Faculty of the University Palacký, Olomouc, Czechoslovakia*, 154, 103-116.
- KNUDSEN, L., NORPPA, H., GAMBORG, M., NIELSEN, P., OKKELS, HENRIK., SOLL-JOHANNING, H., RAFFIN, E., JARVENTAUS, H. & AUTRUP, H. 1999. Chromosomal Aberrations in Humans Induced by Urban Air Pollution: Influence of DNA Repair and Polymorphisms of Glutathione S-Transferase M1 and N-Acetyltransferase. *Cancer*

Epidemiology, Biomarkers & Preventio, 8, 303–310.

- KASSOGUE, Y., DEHBI, H., QUACHOUH, M., QUESSAR, A., BENCHEKROUN, S. & NADIFI, S. 2015. Association of glutathione S-transferase (GSTM1 and GSTT1) genes with chronic myeloid leukemia. *Springerplus*, 4, 210.
- SULAIMAN M. 2016. Cytogenetic study of Stomach cancer in Erbil City. *ZANCO Journal of Pure and Applied Sciences*, 28 (4); 56-65
- LORDELO, G. S., MIRANDA-VILELA, A. L., AKIMOTO, A. K., ALVES, P. C. Z., HIRAGI, C. O., NONINO, A., DALDEGAN, M. B., KLAUTAU-GUIMARÃES, M. N. & GRISOLIA, C. K. 2012. Association between methylene tetrahydrofolate reductase and glutathione S-transferase M1 gene polymorphisms and chronic myeloid leukemia in a Brazilian population. *Genet Mol Res*, 11 (2): 1013-1026
- MA, W., ZHUANG, L., HAN, B. & TANG, B. 2013. Association between glutathione S-transferase T1 null genotype and gastric cancer risk: a meta-analysis of 48 studies. *PLoS One*, 8, e60833.
- MAKHTAR, S. M., HUSIN, A., BABA, A. A. & ANKATHIL, R. 2017. Association of GSTM1, GSTT1 and GSTP1 Ile105Val polymorphisms with clinical response to imatinib mesylate treatment among Malaysian chronic myeloid leukaemia patients. *Journal of genetics*, 96, 633-639.
- MANNERVIK, B., AWASTHI, Y. C., BOARD, P. G., HAYES, J. D., DI ILIO, C., KETTERER, B., LISTOWSKY, I., MORGENSTERN, R., MURAMATSU, M., PEARSON, W. R. & ET AL. 1992. Nomenclature for human glutathione transferases. *Biochem J*, 282 (Pt 1), 305-6.
- MARCHEWKA, Z., PIWOWAR, A., RUZIK, S. & DŁUGOSZ, A. 2017. Glutathione S - transferases class Pi and Mi and their significance in oncology. *Postępy Higieny i Medycyny Doświadczalnej*, 71.
- ÖZTEN, N., SUNGUROĞLU, A. & BOSLAND, M. C. 2012. Variations in glutathione- S- transferase genes influence risk of chronic myeloid leukemia. *Hematological oncology*, 30, 150-155.
- PEARSON, W. R., VORACHEK, W. R., XU, S. J., BERGER, R., HART, I., VANNAIS, D. & PATTERSON, D. 1993. Identification of class-mu glutathione transferase genes GSTM1-GSTM5 on human chromosome 1p13. *Am J Hum Genet*, 53, 220-33.
- RABAB, A. 2013. GSTM1 and GSTT1 Polymorphism in Egyptian Sickle Cell Anemia Patients. *UHOD International Journal of Hematology and Oncology*, 23, 269-275.
- ROSTAMI, G., ASSAD, D., GHADYANI, F., HAMID, M., KARAMI, A., JALAEIKHOO, H. & KALAHROODI, R. A. 2019. Influence of glutathione S- transferases (GSTM1, GSTT1, and GSTP1) genetic polymorphisms and smoking on susceptibility risk of chronic myeloid leukemia and treatment response. *Molecular genetics & genomic medicine*, e717.
- SHARMA, A., PANDEY, A., SARDANA, S., SEHGAL, A. & SHARMA, J. K. 2012. Genetic polymorphisms of GSTM1 and GSTT1 genes in Delhi and comparison with other Indian and global populations. *Asian Pac J Cancer Prev*, 13, 5647-52.
- SHARMA, T., JAIN, S., VERMA, A., SHARMA, N., GUPTA, S., ARORA, V. K. & DEV BANERJEE, B. 2013. Gene environment interaction in urinary bladder cancer with special reference to organochlorine pesticide: a case control study. *Cancer Biomark*, 13, 243-51.
- SOUZA, C. L., BARBOSA, C. G., MOURA NETO, J. P. D., BARRETO, J. H., REIS, M. G. & GONÇALVES, M. S. 2008. Polymorphisms in the glutathione S-transferase theta and mu genes and susceptibility to myeloid leukemia in Brazilian patients. *Genetics and Molecular Biology*, 31, 39-41.
- TAIOLI, E. 1999. International collaborative study on genetic susceptibility to environmental carcinogens. *Cancer Epidemiol Biomarkers Prev*, 8, 727-8.
- TASPINAR, M., AYDOS, S., COMEZ, O., ELHAN, A. H., KARABULUT, H. G. & SUNGUROĞLU, A. 2008. CYP1A1, GST gene polymorphisms and risk of chronic myeloid leukemia. *Swiss medical weekly*, 138.
- WEBB, G., VASKA, V., COGGAN, M. & BOARD, P. 1996. Chromosomal localization of the gene for the human theta class glutathione transferase (GSTT1). *Genomics*, 33, 121-3.
- WEICH, N., FERRI, C., MOIRAGHI, B., BENGIÓ, R., GIERE, I., PAVLOVSKY, C., LARRIPA, I. B. & FUNDIA, A. F. 2016. GSTM1 and GSTP1, but not GSTT1 genetic polymorphisms are associated with chronic myeloid leukemia risk and treatment response. *Cancer epidemiology*, 44, 16-21.

## RESEARCH PAPER

# Effect of oxidative stress on tumor suppressor protein p53 and some biochemical markers in breast cancer patients in Erbil governorate

Ashtee A. Ahmad<sup>1</sup>, Kamaran Abdourahman<sup>2</sup>

<sup>1,2</sup>Department of Chemistry, College of Science, Salahaddin University-Erbil, Kurdistan Region, Iraq

### ABSTRACT:

The present study was conducted to observe the effect and association of oxidative stress on breast cancer, as well as evaluate the alteration of the serum lipid profile, hepatic and kidney biomarkers and serum tumor suppressor protein p53 in breast cancer patients in female as an important objective and determine the relationship between serum p53 with nitric oxide NO, malondialdehyde MDA, superoxide dismutase SOD, lipid profile, liver and kidney functions. In this study 80 subjects were conducted 50 women who had breast cancer as a patient group, and 30 healthy women were conducted as a control group. Blood samples were taken from both patients and control group, who were aged between (18-75) years old. The results of this study revealed that the median levels of serum NO, creatinine and the mean level of serum HDL are significantly lower in patients group with breast cancer than those in control group. Whereas, the median levels of serum MDA, TG, LDL, ALT, AST, and the mean level of serum CH are significantly higher in patients group with breast cancer rather than in control group. While, there are negative weak significant correlations between p53 with MDA, CH, TG and ALT. ROC curve analysis exhibit that serum NO, MDA, TG, HDL, ALT and AST are excellent biomarkers for the diagnostic accuracy of breast cancer in female as a result of the high level of AUC. Whereas, this study demonstrates that serum p53 is not a good biomarker for female breast cancer with AUC value 0.5636. Although, it is known that serum p53 is a tumor suppressor protein that plays a crucial role in the inhibition of cancer development.

In conclusion, the results revealed that patients with breast cancer have a systemic oxidative stress rising due to human tumor cells produce large quantity of ROS, which plays a crucial role in liver diseases, abnormality of renal function and hyperlipidemia. Most possibly due to the endothelial dysfunction which consequently is risk factor for patient's health.

KEY WORDS: Oxidative stress; breast cancer; tumor suppressor protein p53; Liver function.

DOI: <http://dx.doi.org/10.21271/ZJPAS.32.6.7>

ZJPAS (2020) , 32(6);60-71 .

## 1. INTRODUCTION:

Oxidative stress (OS) is a biochemical state that is considered as the inequality between the existence of relatively high levels of toxic reactive species, mainly involving of reactive oxygen species (ROS), reactive nitrogen species (RNS), and mechanisms of the antioxidative defense (Thannickal and Fanburg, 2000).

Oxidative stress cause an extreme formation of ROS that overcomes the system of antioxidant defense or while there is a substantial decrease or absence of antioxidant agents (Kang, 2002). There are Higher ROS formations in a number of pathological states such as myeloid leukemias, diabetes, rheumatoid arthritis and atherosclerosis have been related with defective functions of neutrophil (Karaa et al., 2005).

Breast cancer could be defined as the most prevalent cancers of women worldwide (Organization, 1998). In the Middle East, the most ubiquitous malignancy in women was breast cancer (Kahan et al., 1997). The precise reason of

### \* Corresponding Author:

Kamaran Abdourahman

E-mail: [kamaran.abdourahman@su.edu.krd](mailto:kamaran.abdourahman@su.edu.krd)

### Article History:

Received: 15/05/2020

Accepted: 25/08/2020

Published: 20/12 /2020

breast cancer is not exactly recognized but at present it characterizes a complex interaction of environmental and genetic factors (Wesseling et al., 1999). Substantial breast cancer risk factors consist of: age, early age menarche, late age menopause, first pregnancy at late age, obesity, intense breast tissue, using oral contraception, hormone surrogate treatment, alcohol, diet, tobacco smoke, lactation, family history and previous history of benign breast illness (Göncü et al., 2006). Several genes, such as BRCA1 and BRCA2, HER2/neu, and p53, have been related to breast cancer receptivity and improvement (Yeh et al., 2005).

The p53 protein is produced by a tumor suppressor gene situated on the human seventeenth chromosome that encodes a 53-kilodalton nuclear protein (P53) establish in scant magnitudes in normal tissue. Through the production of this protein, the gene applies an inhibitory influence on proliferation of cell and transformation (Ostrowski et al., 1991). Since tumor suppressor protein p53 works as a transcription factor which able to induce G1 cell cycle stay or apoptosis in reply to DNA damage (Clarke et al., 1993), also adjust normal cells proliferation through controlling initiation and/or adjusting of DNA replicating and programming of cell death (Montenarh, 1992).

H<sub>2</sub>O<sub>2</sub> is recognized to breaks DNA in unbroken cells and purified DNA. The damage of DNA as a result of ROS has been revealed in the base damage form (Baker and He, 1991). malondialdehyde (MDA) is an aldehyde which the lipid peroxidation (LPO) final product arising from polyunsaturated fatty acids degradation via free radical, and lead to cross-linking in lipids, nucleic acids and proteins (Flohe et al., 1985). Superoxide anion radical (O<sub>2</sub><sup>-•</sup>) is not highly toxic prime free radical produced in the cell via the molecular oxygen reduction, as seen in (Figure 1). Superoxide anion radical (O<sub>2</sub><sup>-•</sup>) dismutation catalyzed by the spontaneous or mitochondrial superoxide dismutase (SOD) and produces hydrogen peroxide (H<sub>2</sub>O<sub>2</sub>), that produces a highly toxic free radical as hydroxyl radical (•OH) which is in the existence of reduced iron or copper through the reactions of Fenton or Haber–Weiss (Freeman and Crapo, 1982).

Definitely, hypercholesterolemia motivates the production of superoxide anion radical (O<sub>2</sub><sup>-•</sup>) of vascular smooth muscle cells, that could do further oxidation of LDL (O'Hara et al., 1993). Moreover, superoxide anion radical may result in endothelial dysfunction through scavenging of endothelial-derived nitric oxide NO cause limitations of bioavailability of NO and results in nitrate tolerance, hypertension and vasoconstriction (Münzel et al., 1995). Superoxide speed up the NO destruction because NO binds superoxide radical (O<sub>2</sub><sup>-•</sup>) to produce the effective oxidant peroxynitrite anion (ONOO<sup>-</sup>) and also its conjugate acid peroxynitrous acid (Saran et al., 1990). Actually, the reaction rate for the peroxynitrite production is nearly six times quicker than the Superoxide anion radical (O<sub>2</sub><sup>-•</sup>) scavenging via SOD, indicating that peroxynitrite production can take place in vivo (Beckman and Koppenol, 1996). Reactive species can react with cellular macromolecules, such as lipids, DNA and proteins to which cause irreversible damaging by oxidative and interpose to indispensable cellular functions. DNA can be attacked directly by ROS and RNS and lead to mutagenic lesions (Aydin et al., 2006).

Liver is a main organ hit by ROS (Apel and Hirt, 2004). Parenchymal cells are essential cells exposed to oxidative stress resulted damage in the liver. As well as, in hepatic stellate cells proliferation and collagen synthesis is induced via lipid peroxidation made by oxidative stress (Weiss, 1992). Also, oxidative stress is considered as one of the pathological mechanisms that causes instigation and progress of different liver diseases, for instance alcoholic liver diseases, chronic viral hepatitis and steatohepatitis (Singal et al., 2011). The oxidative stress not only causes hepatic injury via inducing irreversible variation of lipids, DNA and proteins and more significantly modifying pathways which regulate normal biological functions. Furthermore, systemic oxidative stress rising in liver disease can also result in damage to other organs, for example kidney failure and brain impairment (Palma et al., 2014). As regards kidney failure, systemic oxidative stress is deliberated to play a serious role in the various kidney diseases pathophysiology (Valente et al., 2012).

There is quite of indication for rising levels of oxidative stress markers with declining

renal function, launch from early stages of chronic kidney disease CKD (Tbahriti et al., 2013). While, systemic oxidative stress could considerably participate to endothelial dysfunction (Annuk et al., 2005) with overstatement of atherosclerosis (Esper et al., 2006) and also progress of CVD (Paoletti et al., 2005). while extreme ROS are genotoxic (Stopper et al., 2004), oxidative stress might be a cause participate to higher rates of malignancy in patients with end-stage renal disease ESRD (Shang et al., 2016).

The present study was conducted to observe the effect and association of oxidative stress on breast cancer, as well as evaluate the alteration of the serum lipid profile, hepatic and kidney biomarkers and serum total tumor suppressor protein p53 in breast cancer patients in female as an important objective. In addition to, evaluate the relation between all of them with serum p53 (tumor suppressor p53).

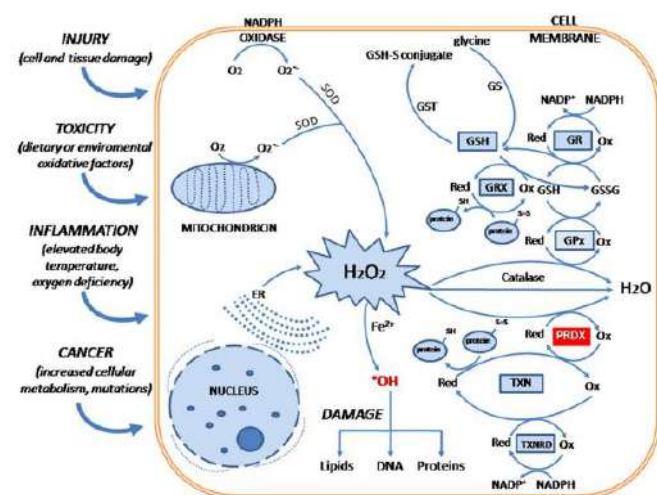


Figure 1: Cellular mechanisms related to oxidative stress.

## 2. MATERIALS AND METHODS

### 2.1 Study population

This study was conducted at Nanakali Hospital in Erbil Governorate during the period from March to June in 2019. Blood samples included 80 individuals; they were drawn in 50 women who had breast cancer as a patient group. The other samples were taken from 30 subjects (women) as a control group who had no breast cancer. Both patient and control groups were aged between (18-75) years old. The file of patients was used to get information about the stages of breast cancer of patients.

### 2.2 Procedures and measurements

In this study, nearly 5 ml of blood sample was taken from each individual and put into the collection tube containing gel and clot activator but no anticoagulant. Also, blood samples were left for around 20 minutes and allowed to clot at room temperature. Furthermore, serum samples were prepared through centrifugation of blood samples for about ten minutes at 4000 rpm and kept frozen at (-86 C°) until further analysis. The biochemical test parameters of serum p53 was assessed with human total p53 (Tumor Protein p53) ELISA Kit (mybiosource) via fully automated enzyme-Linked Immunosorbent Assay (ELISA) of USA origin. Moreover, nitric oxide (NO), malodialdehyde (MDA) and superoxide dismutase (SOD) were assessed with NO, MDA and SOD ELISA Kit (ZellBio GmbH assay kit) respectively via fully automated enzyme-Linked Immunosorbent Assay (ELISA) of Germany origin. As well as, serum total cholesterol (CH), triglyceride (TG), low density lipoprotein (LDL), high density lipoprotein (HDL), ALP, ALT, AST, uric acid, creatinine and blood urea measured by using fully automated chemical analyzer of Cobas c 111 with diagnostic kits (Roche/Hitachi Cobas), of Germany origin.

### 2.3 Statistical analysis

The whole statistical analyses are implemented by applying computer program as Graph pad-prism version. The data consequences existing as either mean  $\pm$  standard error of mean (Mean  $\pm$  SEM) or median with interquartile ranges. In the comparison of nonparametric (not normally distributed data) and parametric values (normally distributed data) between two groups used Mann-Whitney U test and independent student's t-test (unpaired t-test) correspondingly. P-values which ( $P < 0.05$ ) have been considered as significant and P-values that ( $P > 0.05$ ) regarded as no significant (NS). ROC curve (Receiveroperating characteristic) analysis was implemented to determine the area under the curve (AUC) for the diagnostic accuracy in patients with breast cancer in women. The Pearson and Spearman correlation analysis for normally distributed and not normally distributed data were done respectively to indicate the relationship between two groups, when serum p53 represented as dependent variables, while other parameters presented as independent variables.

## 3. RESULTS AND DISCUSSION

These data demonstrate that median serum levels of MDA, TG, LDL, ALT, AST, and the mean serum level of CH are significantly increased in patients group with breast cancer rather than in control group. The median level of serum SOD, ALP, uric acid and the mean levels of blood urea in patients group with breast cancer for female are insignificantly increased when compared with control group. While the median levels of serum NO, creatinine and the mean level of serum HDL are significantly decreased in patients group with breast cancer than those in control group. It is also observed that the median level of serum p53 in patients group with breast cancer for female are insignificantly decreased when compared with control group, as seen in (Table 1) and (Figure 2).

Our study demonstrates that serum levels of MDA exhibit significant increasing in patients group with breast cancer. This is in agreement with previous studies that exhibited the prevalence of ROS in patients group with breast cancer disease is much higher than those in control group because human tumor cells produce large quantity of  $H_2O_2$  (Cheeseman and Slater, 1993). The results of the present study demonstrate that the oxidative stress biomarker of serum NO and MDA are indeed potential oxidative stress biomarkers for breast cancer, due to the high levels of AUC (table 3). Since, the oxidative stress rising in breast cancer disease due to human tumor cells produce large quantity of RONS. Similar observations have been shown in the recent studies. Additionally, our study reveals that serum levels of p53 display insignificant dropping in patients group with breast cancer than those in control group. This is in agreement with earlier Experimental study exposes that ROS are contributed in cancer beginning and progression wherever certain tumor suppressor genes inactivation or loss is happened (Harris, 1989). Because DNA can be attacked directly by ROS and RNS and lead to mutagenic lesions (Aydin et al., 2006).

As well as, These antineoplastic agents that used to treating most of the breast cancer patients result in a decrease in the levels of antioxidant due to their toxicity raises the peroxidation reaction of the unsaturated fatty acids in the membrane phospholipids (Conklin, 2004), which in the case of dyslipidemia, inflammation,

human tumor cells and other pathological, high quantities of  $H_2O_2$  are produced via stimulated polymorphonuclear leukocytes and monocytes in respiratory burst pattern (Cheeseman and Slater, 1993). Our data display that serum TG, LDL and CH significantly increased and also serum HDL are significantly decreased. This is in agreement with Diniz et al., 2004, Furberg et al., 2005 and O'Hara et al., 1993. Hypercholesterolemia is illustrated as a rise in cholesterol level with rising in plasma levels of LDL and VLDL. The hypercholesterolemia enhances oxidative stress via rising lipid peroxidation and reducing antioxidant enzymes (O'Hara et al., 1993). Additionally, hypercholesterolemia is related to enhanced superoxide anion radical ( $O_2^{\cdot-}$ ) production and NO deactivation (Diniz et al., 2004, O'Hara et al., 1993). Moreover, Superoxide anion radical ( $O_2^{\cdot-}$ ) may result in endothelial dysfunction through scavenging of endothelial-derived nitric oxide cause limitations of NO bioavailability, as shown in (Figure 3).

Our study demonstrates that serum levels of NO exhibit significant dropping in patients group with breast cancer. This is in agreement with Gryglewski et al., 1986 and Hamadamin et al., 2016. Thus, increased production of ROS decreases NO bioavailability, leading to advancement of vasoconstriction, platelet aggregation inhibition reducing, and neutrophil adhesion to endothelium initiating. These variations result in endothelial dysfunction and might contribute to modification of intracellular signaling passageway and transcription factors intermediated gene expression in endothelial cells (Münzel et al., 1995). Convincing evidence identifies that while cellular levels of Superoxide anion radical ( $O_2^{\cdot-}$ ) or NO are raised, the effective oxidant, peroxynitrite is rapidly produced that speed up Nitric oxide (NO) destruction (Gryglewski et al., 1986, Hamadamin et al., 2016). Actually, the reaction rate for the peroxynitrite production is nearly six times quicker than the Superoxide anion radical ( $O_2^{\cdot-}$ ) scavenging via SOD, indicating that peroxynitrite production can take place in vivo (Beckman and Koppenol, 1996).

**Table (1)** Comparison the serum levels of p53, nitric oxide NO, malondialdehyde MDA, superoxide dismutase SOD, lipid profile and liver function renal function parameters in patients group with breast cancer and control group.

Parameters	Patient group(n=50)	Control group(n=30)	P value
p53 (pg/ml)	0.426 (0.31, 0.5545)	0.4955 (0.35 ,0.536)	0.3582
NO (nmol/ml)	9 (6.95, 12.55)	23.9 (20.05, 27.65)	< 0.0001
MDA (nmol/ml)	1.765 (1.42, 2.173)	1.45 (1.245, 1.7)	0.0013
SOD (IU/mg)	5.1 (4.8, 5.35)	4.95 (4.525, 5.25)	0.1327
CH (mg/dl)	172.0 ± 5.694	147.9 ± 4.407	0.0048
HDL (mg/dl)	40.16 ± 1.160	54.00 ± 2.421	< 0.0001
TG (mg/dl)	194.7 (146.2, 297)	102.1 (72.28, 156.7)	< 0.0001
LDL (mg/dl)	87 (74, 108)	74 (58.5, 92.5)	0.0041
ALP(U/L)	83.45 (67.7-102.6)	76.6 (63.8-88.2)	0.0565
ALT(U/L)	16 (9.5-25.5)	8 (6-10.5)	< 0.0001
AST(U/L)	20 (16-25.25)	15 (12-17)	< 0.0001
Creatinine (mg/dl)	0.6 (0.5, 0.65)	0.6 (0.6, 0.75)	0.0054
Uric acid (mg/dl)	4 (3.5, 4.6)	3.6 (3.2, 4.55)	0.2204
Urea (mg/dl)	26.67 ± 1.055	25.45 ± 1.069	0.4462
Age (year)	50.54 ± 1.662	52.66 ± 2.341	0.4550

The values expressed as (Mean ± SEM) for urea, HDL, cholesterol but all others expressed as mean with interquartile range.



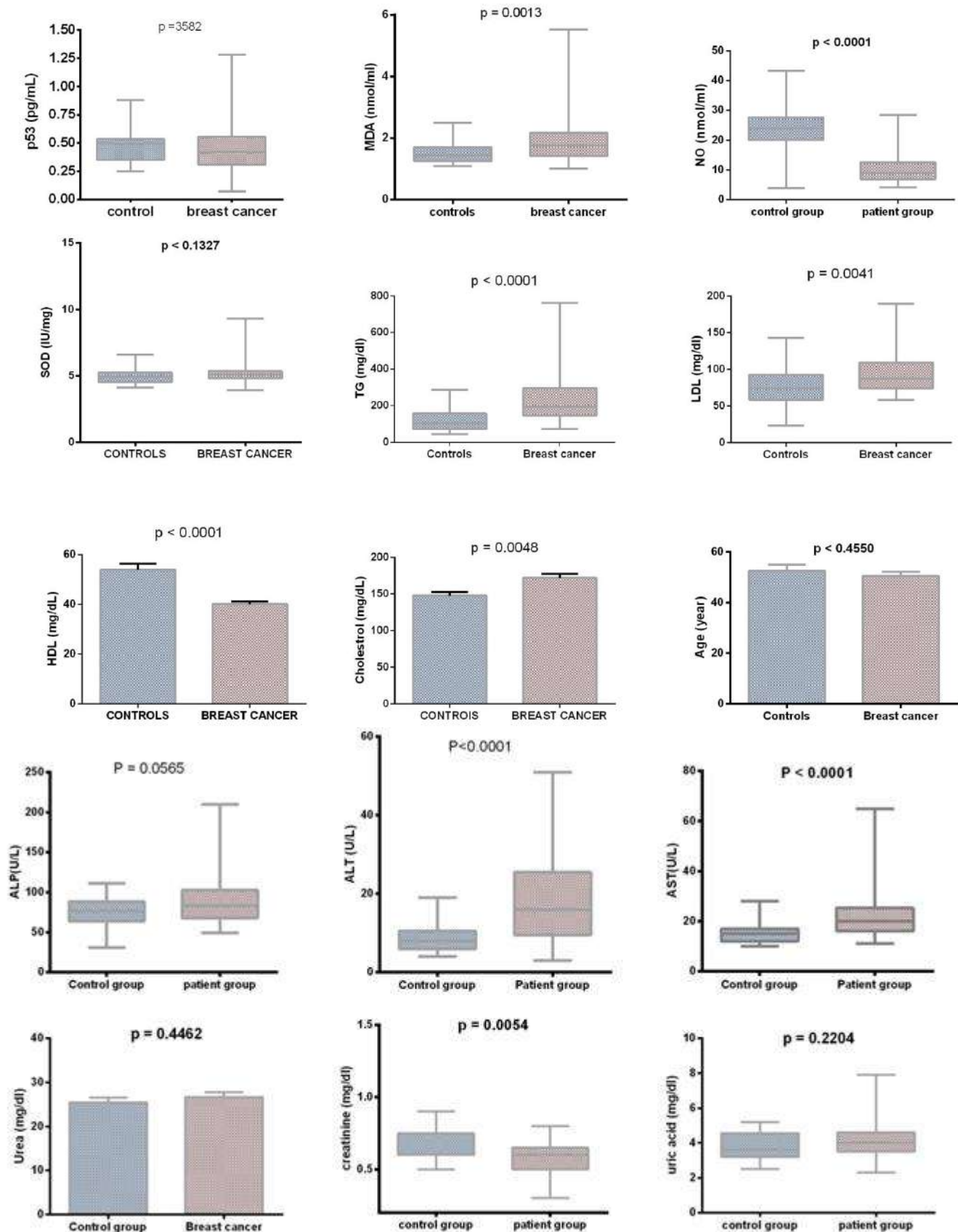


**Figure 2:** Serum levels of p53, MDA, NO, SOD, TG, LDL, HDL, CH, Age, ALP, ALT, AST, urea, creatinine and uric acid parameters in patients group with breast cancer and control group in women.

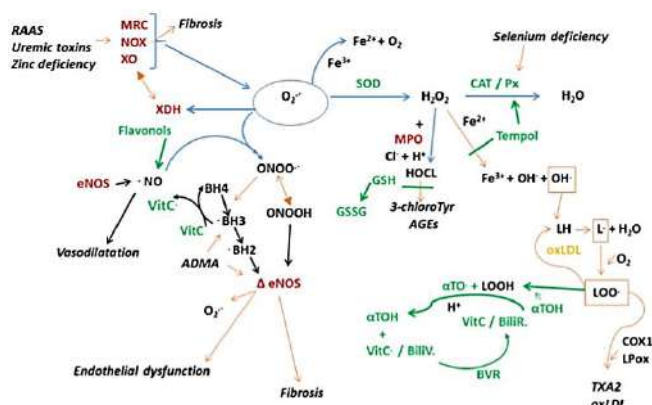


**Figure 3:** Mechanisms of oxidative stress damage to cellular targets and the defense of antioxidant. Where antioxidative reactions were indicated by Green arrow; inhibition of the oxidating reaction by antioxidative mechanism were written by green line; pro-oxidative reactions by red arrow. Abbreviations: ADMA is asymmetric dimethylarginine;  $\alpha$ TOH is alpha tocopherol; AGEs is advanced glycation end products; BiliR is bilirubin; BVR is biliverdin reductase; biliV is biliverdin; BH4 is (6R)-5,6,7,8-tetrahydro-l- biopterin; CAT is catalase; eNOS is endothelial NO synthase; COX is cyclooxygenase;  $\Delta$  eNOS is eNOS uncoupling;  $\text{Fe}^{2+}$  is iron;  $\text{H}_2\text{O}_2$  is hydrogen peroxide; GSH/GSSG is glutathione; LOOH is fatty acid chain; HOCL is hypochlorous acid; LOO $^-$  is lipid peroxy radical; MRC is mitochondrial respiratory complex; MPO is myeloperoxidase; NOX is NADPH oxidase; ONOO is peroxynitrite; NO is nitric oxide;  $\text{O}_2^{\bullet-}$ , superoxide anion radical;  $\text{O}_2$ , oxygen; PX is peroxidase; TXA is thromboxane; SOD is superoxide dismutase; VitC is vitamin C; XO is xanthine oxidase; XDH is xanthine dehydrogenase.

Several researches have explored whether the lipid metabolism is related to risk of evolving breast cancer, specified their relationship to obesity and overweight (Kulie et al., 2011). In the case of breast cancer alterations in the normal lipid metabolism specifically of serum triglycerides have been detected. Previous studies demonstrated the evidence for a positive relation between triglycerides and evolving these cancers riskiness (Das et al., 1987, Capasso et al., 2010). And also It has been proposed for both ovarian cancer and breast cancer that low levels of HDL (a communal obesity comorbid) can be reflective of a critical profile of hormone that, in sequence, would rise the risk (Furberg et al., 2005).

The results of the present study exhibit that the liver function parameters ALT and AST are elevated in patients with breast cancer disease in comparison with healthy group. This is in agreement with Li et al., 2014. Also, this study demonstrates that there is no significant elevation of ALP in patients with breast cancer disease compared to healthy group. This is also in agreement with Keshaviah et al., 2007 that

revealed that ALP is not a potential biomarker for breast cancer disease prediction. While, CA15-3 has been better capable of expect recurrence of breast cancer than ALP, however utilize both of them with each other provided a better previous indicator of recurrence (Keshaviah et al., 2007). While the ROS is extreme, the homeostasis will be troubled, causing oxidative stress that plays a crucial role in liver sicknesses and other prolonged and degenerative diseases (Li et al., 2014).

Our study demonstrates that serum levels of urea and uric acid exhibit insignificant increasing in patients group with breast cancer although serum creatinine is significantly decreased in patients group with breast cancer than those in control group. This is in agreement with previous studies of both Himmelfarb, 2005 and Tbahriti et al., 2013. ROS play a significant role in the regulating kidney function which subsequently makes the kidney specifically susceptible to redox inequalities and oxidative stress. The influence of oxidative stress to the progress of kidney disease and consequent renal function forfeiture has been comprehensively studied (Himmelfarb, 2005, Abdourahman, 2017). Additionally, There is quite of indication for rising levels of oxidative stress markers with declining renal function, launch from early stages of chronic kidney disease CKD (Tbahriti et al., 2013). Abnormality of renal function is associated with endothelial dysfunction, which leads to progression of atherosclerosis in patients with CKD.

Moreover, NO and MDA are represented as specific and sensitive oxidative stress biomarkers of breast cancer. The most vital problem factors of breast cancer are the risk of systemic oxidative stress rising in the existence of tumor cells that produce large quantity of  $\text{H}_2\text{O}_2$  (Cheeseman and Slater, 1993), which can also result in damage to other organs, for example liver disease, kidney failure and brain impairment (Palma et al., 2014). As well as, nitrate tolerance, hypertension, vasoconstriction (Münzel et al., 1995). and dyslipidemia (Diniz et al., 2004). Most possibly due to the endothelial dysfunction. The parameters of oxidative stress in this study such as decreased NO, increased MDA and insignificantly increased SOD values revealed that there was

**Table (2)** Correlation analysis between total serum p53 with NO, MDA, SOD, CH, TG, HDL, LDL, ALP, ALT, AST, age, creatinine, uric acid and urea in patients group with breast cancer.

<b>Parameters</b>	<b>Correlation coefficient (r) (spearman correlation)</b>	<b>P value</b>
serum p53 and MDA	-0.2656	0.0213
serum p53 and CH	-0.2715 (Pearson correlation)	0.0177
serum p53 and TG	-0.3349	0.0031
serum p53 and ALT	-0.2495	0.0297
serum p53 and SOD	-0.1076	N.S
serum p53 and LDL	-0.1454	N.S
serum p53 and ALP	-0.02882	N.S
serum p53 and AST	-0.05836	N.S
serum p53 and uric acid	-0.0344	N.S
serum p53 and age	-0.08389 (Pearson correlation)	N.S
serum p53 and NO	0.01766	N.S
serum p53 and HDL	0.1148 (Pearson correlation)	N.S
serum p53 and urea	0.0091 (Pearson correlation)	N.S
serum p53 and creatinine	0.0772	N.S

more production of free radicals when compared with their scavenging activity resulting in more oxidative stress in breast cancer. The present study shows that serum levels of creatinine are elevated in breast cancer patients compared to healthy subjects. This is agreement with studies. Whereas, there is no significant elevation of serum urea and uric acid levels in breast cancer patients.

In a correlation analysis, the results of this research illustrate that there are negative with significant weak correlations between serum p53 with MDA, CH, TG and ALT which the correlation (r) values for MDA ( $r = -0.2656$ ), CH ( $r = -0.2715$ ), TG ( $r = -0.3349$ ) and ALT ( $r = -0.2495$ ). Also, there are negative non-significant correlations between serum p53 with SOD, LDL, ALP, AST, uric acid and age. While, there are positive non-significant correlations among serum p53 with NO, HDL, urea, creatinine. The p values for SOD, LDL, ALP, AST, uric acid, age, NO, HDL, urea and creatinine are ( $P = 0.0213, 0.0031, 0.0297, 0.6214, 0.7709, 0.4712, 0.8796, 0.3234, 0.9385$  and  $0.5101$ ), respectively, as seen in (Table 2).

The ROC curve analysis was proposed for determination the diagnostic accuracy of NO, MDA, CH, TG, HDL, LDL, ALT, AST and p53. The consequences of current study exhibit that the value of AUC for serum nitric oxide NO is 0.8846, the value of S.E is 0.05062 and the 95% CI value is 0.7853 to 0.9838, ( $< 0.0001$ ). And also, the value of AUC for serum MDA is 0.7145, the value of S.E is 0.05757 and the 95% CI value is 0.6016 to 0.8273, ( $p = 0.001570$ ). Also, The AUC value for serum TG is 0.8317 which has a high range that showed the high sensitivity than specificity. The S.E value is 0.04544 and the 95% CI value is 0.7426 to 0.9208, ( $P < 0.0001$ ), and also, the AUC value for serum HDL is 0.8176, also S.E and 95% CI values are (0.04951 and 0.7205 to 0.9147) respectively, ( $P < 0.0001$ ). As well as, The AUC value in serum LDL is 0.6928, S.E has been recognized with a value of 0.06167 and the 95% CI value is 0.5719 to 0.8137, also The AUC value in serum CH is 0.6721, S.E has been recognized with a value of 0.06003 and the 95% CI value is 0.5545 to 0.7898. As well as The AUC value in serum ALT is 0.7988 which has a high range that showed the high sensitivity than specificity. The S.E value is 0.05054 and the 95% CI value is 0.6998 to 0.8979, ( $P < 0.0001$ ). Also, the AUC value for serum AST is 0.7803, as well

S.E and 95% CI values are (0.05312 and 0.6762 to 0.8845) respectively, ( $P < 0.0001$ ). And also, The AUC value in serum p53 is 0.5636, S.E has been recognized with a value of 0.06583 and the 95% CI value is 0.4345 to 0.6926, ( $P < 0.3539$ ). ROC curve analysis exhibit that serum NO, MDA, TG, HDL, ALT and AST are excellent biomarkers for the diagnostic accuracy of breast cancer in female as a result of the high level of AUC. Although, LDL and CH are good but not potential biomarker for the breast cancer diagnostic accuracy. Whereas, this study demonstrates that serum p53 is not a good biomarker for female breast cancer with AUC value 0.5636. Although, it is known that serum p53 is a tumor suppressor protein that plays a crucial role in the inhibition of cancer development. The data are shown in Table 3.

**Table (3):** ROC curve analysis for determination the diagnostic accuracy of NO, MDA, CH, TG, HDL, LDL, ALT and AST in patients group with breast cancer.

Parameters	AUC	S.E	95% CI	P value
NO (nmol/ml)	0.8846	0.05062	0.7853 to 0.9838	< 0.0001
MDA(nmol/ml)	0.7145	0.05757	0.6016 to 0.8273	0.001570
TG (mg/dl)	0.8317	0.04544	0.7426 to 0.9208	< 0.0001
HDL (mg/dl)	0.8176	0.04951	0.7205 to 0.9147	< 0.0001
LDL (mg/dl)	0.6928	0.06167	0.5719 to 0.8137	0.0045
CH (mg/dl)	0.6721	0.06003	0.5545 to 0.7898	0.01209
ALT(U/L)	0.7988	0.05054	0.6998 to 0.8979	< 0.0001
AST(U/L)	0.7803	0.05312	0.6762 to 0.8845	< 0.0001
p53 (pg/ml)	0.5636	0.06583	0.4345 to 0.6926	0.3539

#### 4. CONCLUSIONS

This work focused on the impacts of oxidative stress in patients with breast cancer as the oxidative stress rising in breast cancer disease due to human tumor cells produce large quantity of ROS. The results of this study reveal that the pervasiveness of the oxidative stress is a risk factor in patients group with breast cancer and it's much higher than in control group. The potential risk factors of liver diseases, abnormality of renal function and hyperlipidemia in patients with breast cancer exhibit the high levels. While, the results from the existent study show that systemic oxidative stress is raised to a greater degree in breast cancer disease and this oxidative stress causes damage to most of the cellular targets and has the highest side effect of lipid profile, hepatic and renal damage thus plays a crucial role in liver diseases, abnormality of renal function and

endothelial dysfunction which consequently is risk factor for patients health. hyperlipidemia most possibly due to the This study demonstrates that serum p53 is not a good biomarker for female breast cancer. Although, it is recognized that p53 is a tumor suppressor protein that plays a crucial role in the inhibition of cancer development.

#### Acknowledgements

Authors would like to thank Department of Chemistry, College of Science- Salahaddin University. We want to acknowledge all stuffs of oncology unit in Nanakali Hospital in Erbil Governorate and the patients who provided for us an opportunity to take them a blood samples. We thank Prof. Dr. Ismail Mustafa Mawlood at Department of Chemistry, college of Science, Salahaddin University for his help during statistical data analysis.

## References

- ABDOULRAHMAN, K. 2017. Lipid profile, oxidative stress and homocysteine in chronic renal failure CRF patients pre- and post-hemodialysis in Erbil city. *ZANCO JOURNAL OF PURE AND APPLIED SCIENCES*, 29, 65-73.
- ANNUK, M., SOVERI, I., ZILMER, M., LIND, L., HULTHE, J. & FELLSTRÖM, B. 2005. Endothelial function, CRP and oxidative stress in chronic kidney disease. *JN. Journal of Nephrology (Milano. 1992)*, 18, 721-726.
- APEL, K. & HIRT, H. 2004. Reactive oxygen species: metabolism, oxidative stress, and signal transduction. *Annu. Rev. Plant Biol.*, 55, 373-399.
- AYDIN, K., GUVEN, K. & OZBAY, E. Two-dimensional left-handed metamaterial with a negative refractive index. *Journal of Physics: Conference Series*, 2006. IOP Publishing, 6.
- BAKER, M. A. & HE, S. 1991. Elaboration of cellular DNA breaks by hydroperoxides. *Free Radical Biology and Medicine*, 11, 563-572.
- BECKMAN, J. S. & KOPPENOL, W. H. 1996. Nitric oxide, superoxide, and peroxynitrite: the good, the bad, and ugly. *American Journal of Physiology-Cell Physiology*, 271, C1424-C1437.
- CAPASSO, I., ESPOSITO, E., PENTIMALLI, F., CRISPO, A., MONTELLA, M., GRIMALDI, M., DE MARCO, M. R., CAVALCANTI, E., D'AIUTO, M. & FUCITO, A. 2010. Metabolic syndrome affects breast cancer risk in postmenopausal women: National Cancer Institute of Naples experience. *Cancer biology & therapy*, 10, 1240-1243.
- CHEESEMAN, K. & SLATER, T. 1993. An introduction to free radical biochemistry. *British medical bulletin*, 49, 481-493.
- CLARKE, A., PURDIE, C., HARRISON, D., MORRIS, R., BIRD, C., HOOPER, M. & WYLLIE, A. 1993. Thymocyte apoptosis induced by p53-dependent and independent pathways. *Nature*, 362, 849-852.
- CONKLIN, K. A. 2004. Chemotherapy-associated oxidative stress: impact on chemotherapeutic effectiveness. *Integrative cancer therapies*, 3, 300-294.
- DAS, N., MA, C. & SALMON, Y. 1987. The relationship of serum vitamin A, cholesterol, and triglycerides to the incidence of ovarian cancer. *Biochemical medicine and metabolic biology*, 37, 213-219.
- DINIZ, Y. S., FERNANDES, A. A., CAMPOS, K. E., MANI, F., RIBAS, B. O. & NOVELLI, E. L. 2004. Toxicity of hypercaloric diet and monosodium glutamate: oxidative stress and metabolic shifting in hepatic tissue. *Food and Chemical Toxicology*, 42, 313-319.
- ESPER, R. J., NORDABY, R. A., VILARINHO, J. O., PARAGANO, A., CACHARRÓN, J. L. & MACHADO, R. A. 2006. Endothelial dysfunction: a comprehensive appraisal. *Cardiovascular diabetology*, 5, 4.
- FLOHE, L., BECKMANN, R., GIERTZ, H. & LOSCHEN, G. 1985. Oxygen-centered free radicals as mediators of inflammation. *Oxidative stress*. Academic Press London.
- FREEMAN, B. A. & CRAPO, J. D. 1982. Biology of disease: free radicals and tissue injury. *Laboratory investigation; a journal of technical methods and pathology*, 47, 412-426.
- FURBERG, A.-S., JASIENSKA, G., BJURSTAM, N., TORJESEN, P. A., EMAUS, A., LIPSON, S. F., ELLISON, P. T. & THUNE, I. 2005. Metabolic and hormonal profiles: HDL cholesterol as a plausible biomarker of breast cancer risk. The Norwegian EBBA Study. *Cancer Epidemiology and Prevention Biomarkers*, 14, 33-40.
- GÖNENC, A., ERTEN, D., ASLAN, S., AKINCI, M., ŞİMŞEK, B. & TORUN, M. 2006. Lipid peroxidation and antioxidant status in blood and tissue of malignant breast tumor and benign breast disease. *Cell biology international*, 30, 376-380.
- GRYGLEWSKI, R., PALMER, R. & MONCADA, S. 1986. Superoxide anion is involved in the breakdown of endothelium-derived vascular relaxing factor. *Nature*, 320, 454-456.
- HAMADAMIN, P., SALIHI, A., ABDOULRAHMAN, K., ALI QADIR, F., KHASRO, R., NAJDAT, J., HAMAD, N. & NAJMADDIN, H. 2016. Screening of Oxidative Stress and Prostate Cancer Biomarkers among Rural and Urban Elderly People in Erbil Governorate-Kurdistan Region. *ZANCO Journal of Pure and Applied Sciences*, 28, 202-208.
- HARRIS, C. C. 1989. Interindividual variation among humans in carcinogen metabolism, DNA adduct formation and DNA repair. *Carcinogenesis*, 10, 1563-1566.
- HIMMELFARB, J. 2005. Relevance of oxidative pathways in the pathophysiology of chronic kidney disease. *Cardiology clinics*, 23, 319-330.
- KAHAN, E., IBRAHIM, A. S., NAJJAR, K. E., RON, E., AL-AGHA, H., POLLIACK, A. & EL-BOLKAINY, M. N. 1997. Cancer patterns in the Middle East special report from the Middle East Cancer Society. *Acta oncologica*, 36, 631-636.
- KANG, D.-H. 2002. Oxidative stress, DNA damage, and breast cancer. *AACN Advanced Critical Care*, 13, 540-549.
- KARAA, S., ZHANG, J. & YANG, F. 2005. A numerical study of a 3D bioheat transfer problem with different spatial heating. *Mathematics and Computers in Simulation*, 68, 375-388.
- KESHAVIAH, A., DELLAPASQUA, S., ROTMENSZ, N., LINDTNER, J., CRIVELLARI, D., COLLINS, J., COLLEONI, M., THURLIMANN, B., MENDIOLA, C. & AEBI, S. 2007. CA15-3 and alkaline phosphatase as predictors for breast cancer recurrence: a combined analysis of seven International Breast Cancer Study Group trials. *Annals of oncology*, 18, 701-708.
- KULIE, T., SLATTENGREN, A., REDMER, J., COUNTS, H., EGLASH, A. & SCHRAGER, S. 2011. Obesity and women's health: an evidence-based review. *The Journal of the American Board of Family Medicine*, 24, 75-85.
- LI, A. N., LI, S., ZHANG, Y. J., XU, X. R., CHEN, Y. M. & LI, H. B. 2014. Resources and biological activities of natural polyphenols. *Nutrients*, 6, 6020-47.

- MONTENARH, M. 1992. Biochemical properties of the growth suppressor/oncoprotein p53. *Oncogene*, 7, 16.1680-73
- MUNZEL, T., SAYEGH, H., FREEMAN, B. A., TARPEY, M. M. & HARRISON, D. G. 1995. Evidence for enhanced vascular superoxide anion production in nitrate tolerance. A novel mechanism underlying tolerance and cross-tolerance. *The Journal of clinical investigation*, 95, 187-194.
- O'HARA, P. J., SHEPPARD, P. O., THÓGERSEN, H., VENEZIA, D., HALDEMAN, B. A., MCGRANE, V., HOUAMED, K. M., THOMSEN, C., GILBERT, T. L. & MULVIHILL, E. R. 1993. The ligand-binding domain in metabotropic glutamate receptors is related to bacterial periplasmic binding proteins. *Neuron*, 11, 41-52.
- ORGANIZATION, W. H. 1998. *Quality control methods for medicinal plant materials*, World Health Organization.
- OSTROWSKI, J., SAWAN, A., HENRY, L., WRIGHT, C., HENRY, J., HENNESSY, C., LENNARD, T., ANGUS, B. & HORNE, C. 1991. p53 expression in human breast cancer related to survival and prognostic factors: an immunohistochemical study. *The Journal of pathology*, 164, 75-81.
- PALMA, H. E., WOLKMER, P., GALLIO, M., CORREA, M. M., SCHMATZ, R., THOME, G. R., PEREIRA, L. B., CASTRO, V. S., PEREIRA, A. B., BUENO, A., DE OLIVEIRA, L. S., ROSOLEN, D., MANN, T. R., DE CECCO, B. S., GRACA, D. L., LOPES, S. T. & MAZZANTI, C. M. 2014. Oxidative stress parameters in blood, liver, and kidney of diabetic rats treated with curcumin and/or insulin. *Mol Cell Biochem*, 386, 199-210.
- PAOLETTI, E., BELLINO, D., CASSOTTANA, P., ROLLA, D. & CANNELLA, G. 2005. Left ventricular hypertrophy in nondiabetic predialysis CKD. *American journal of kidney diseases*, 46, 320-327.
- SARAN, M., MICHEL, C., BORS, W. & CZAPSKI, G. 1990. Reaction of NO with O<sub>2</sub><sup>-</sup>. Implications for the action of endothelium-derived relaxing factor (EDRF). *Free radical research communications*, 10, 221-226.
- SHANG, W., HUANG, L., LI, L., LI, X., ZENG, R., GE, S. & XU, G. 2016. Cancer risk in patients receiving renal replacement therapy: a meta-analysis of cohort studies. *Molecular and clinical oncology*, 5, 315-325.
- SINGAL, A. K., JAMPANA, S. C. & WEINMAN, S. A. 2011. Antioxidants as therapeutic agents for liver disease. *Liver Int*, 31, 1432-48.
- STOPPER, H., SCHUPP, N., BAHNER, U., SEBEKOVA, K., KLASSEN, A. & HEIDLAND, A. Genomic damage in end-stage renal failure: potential involvement of advanced glycation end products and carbonyl stress. *Seminars in nephrology*.2004 , Elsevier, 474-478.
- TBAHRITI, H. F., KADDOUS, A., BOUCHENAK, M. & MEKKI, K. 2013. Effect of different stages of chronic kidney disease and renal replacement therapies on oxidant-antioxidant balance in uremic patients. *Biochemistry research international*, 2013.
- THANNICKAL, V. J. & FANBURG, B. L. 2000. Reactive oxygen species in cell signaling. *American Journal of Physiology-Lung Cellular and Molecular Physiology*, 279, L1005-L1028.
- VALENTE, M. J., CARVALHO, F., BASTOS, M., DE PINHO, P. G. & CARVALHO, M. 2012. Contribution of oxidative metabolism to cocaine-induced liver and kidney damage. *Curr Med Chem*, 19, 5601-6.
- WEISS, R. B. The anthracyclines: will we ever find a better doxorubicin? *Seminars in oncology*, 1992. 670-686.
- WESSELING, C., ANTICH, D., HOGSTEDT, C., RODRÍGUEZ, A. C. & AHLBOM, A. 1999. Geographical differences of cancer incidence in Costa Rica in relation to environmental and occupational pesticide exposure. *International journal of Epidemiology*, 28, 365-374.
- YEH, C.-C., HOU, M.-F., TSAI, S.-M., LIN, S.-K., HSIAO, J.-K., HUANG, J.-C., WANG, L.-H., WU, S.-H., HOU, L. A. & MA, H. 2005. Superoxide anion radical, lipid peroxides and antioxidant status in the blood of patients with breast cancer. *Clinica chimica acta*, 361, 104-111.

## RESEARCH PAPER

# Mutational analysis of the Janus kinase II (V617F) gene in patients with $\beta$ -Thalassemia major

Salar A. Ahmed\*

\*Department of Basic Sciences, College of Medicine, Hawler Medical University, Erbil- Iraq.

### ABSTRACT:

$\beta$ -Thalassemia is a group of congenital hemolytic anemia that characterized by the underproduction of the indispensable hemoglobin molecule, the oxygen and carbon dioxide carrying protein inside the red cells. With our current study, we've screened if some extent mutation at Valine 617 Phenylalanine of Janus kinase II genes detectable in  $\beta$ -thalassemia major in our region.

The present study for the screening of JAK II V617F mutation was conducted on (50) patients with  $\beta$ -thalassemia major, restriction fragment length polymorphism with restriction endonuclease enzyme AflIII was used to identify a flanking region of 617 for JAK II gene.

In the existing study, no mutation has been detected within the patients suffering from  $\beta$ -thalassemia major. Our results indicate that *JAK II*<sup>V617F</sup> mutation appears to not be associated with thromboembolic complications related to  $\beta$ -Thalassemia and therefore the incidence of  $\beta$ -Thalassemia. To the best of our knowledge, this study is the first evidence to determine the status of *JAK II*<sup>V617F</sup> mutation in patients with Thalassemia major in our region and expands the international published literature on it.

KEYWORDS:  $\beta$ -Thalassemia, *JAK II*, *V617F* mutation, Thromboembolic complications.

DOI: <http://dx.doi.org/10.21271/ZJPAS.32.6.8>

ZJPAS (2020), 32(6); 72-75 .

## 1. INTRODUCTION

Thalassemia is a congenital nonspherocytic hemolytic disorder that arises from  $\beta$ -globin chain abnormality or mutation, requiring regular blood transfusions to sustain life. However, excess body iron overload develops and may accumulate in heart, liver and endocrine glands, leading to progressive failure of those organs (Melchiori, 2010, Sipahi, *et al.*, 2009, Nihad, A. 2016)

It has long been known that chronic hemolytic anemia particularly  $\beta$ -thalassemia, is characterized by a hypercoagulable state (Ali, T *et al.*, 2008.

patients with hemolytic anemia are implicated in the existence of a prothrombotic hemostatic anomalies, which is found almost in half patients with  $\beta$ -thalassemia (Eldor, *et al.*, 2002, Ataga, 2009, Ahmed, *et al.* 2019).

Furthermore, the manifestation of thromboembolic complications, including recurrent arterial occlusion, venous thromboembolism which resulting in deep venous thrombosis, pulmonary embolism and stroke (Ataga, 2009, Cappellini, 2007).

Several other risk factors are also contributing to the hypercoagulable state, like abnormal RBCs formation and high expression of negatively charged phosphatidylserine at the outer surface, results from specific changes within the lipid membrane, which can cause post-splenectomy, liver, and cardiac dysfunction, subsequently

---

### \*Corresponding Author:

Salar Adnan Ahmed  
E-mail: [salar.adnan@hmu.edu.krd](mailto:salar.adnan@hmu.edu.krd)

### Article History:

Received: 16/03/2020

Accepted: 27/08/2020

Published: 20/12 /2020



resulting in protein C and protein S reduction (Cappellini, 2007)

Janus kinase II (JAK II) is a cytoplasmic tyrosine kinase that has a vital role in signal transduction triggered by hemopoietic growth factors (Karaköse, *et al.*, 2005). The domain structure of Janus kinase is organized with 2 homologous kinase domains: One among these JAK homology JH1 is an activating domain while the other JH2 lacks kinase activity (Al-Thwani *et al.*, 2010)

Previous studies revealed that the JAK II mutation in healthy individuals is extremely rare and is found on chromosome 9p. During this mutation, guanine is substituted to thymidine (G to T mutation), causes an amino acid substitution of valine with phenylalanine at codon 617 in JH2 pseudokinase domain of the JAK II gene (Al-Thwani *et al.*, 2010). As a result of point mutation leading to growth factor hypersensitivity and dependence which results in up-regulated constitutive kinase activity causing enhanced hematopoiesis (Amarapurkar, *et al.*, 2011).

Abnormalities in *Janus kinase II* (*V617F*) mutation has been implicated during a several disease disorders including essential thrombocythemia, polycythemia Vera and idiopathic Myelofibrosis, while it's contribution to the  $\beta$ -thalassemic patients complications is still unknown and it remains unclear if the V617F mutation is related to blood clots and embolus (Alabdulaali, 2009, Steensma, 2006, Steensma, *et al.*, 2005).

In this prospective cohort study, we evaluated the prevalence and the incidence of the *Janus kinase II* (*V617F*) mutation and its clinical correlation in patients with  $\beta$ -Thalassemia.

## 2. MATERIALS AND METHODS

### 2.1. Patient specimens

The present screening study for non-receptor protein tyrosine kinases ( Janus kinase II) mutation was carried out on (50) patients with  $\beta$ -Thalassemic major with the mean age (24) years, ranging from (5-45) years of age, all examined samples were collected from previously diagnosed patients with  $\beta$ -thalassemia by a clinician using electrophoresis and the WHO 2008 criteria.

For genomic DNA extraction, the patient specimens were obtained using venous blood (5 ml), the blood samples were collected into EDTA

blood collection tubes. After separation, the samples were either used directly for the study or kept frozen (-20 °C) until further analysis.

### 2.2. Molecular detection assay protocol for JAK2 V617F mutation

#### DNA extraction

The human genomic DNA was isolated from whole blood samples using a efficient genomic DNA Mini kit (Geneaid Biotech Ltd) according to manufacturer recommendations. The purity and the concentration of the extracted DNA samples were assessed by thermo scientific Nano drop 1000 spectrophotometer and the results were checked by 1% Agarose gel electrophoresis.

#### PCR/RFLP analysis

The V617F mutation analysis of JAK2 gene was assessed by restriction site generating polymerase chain reaction (RG-PCR). The full coding sequence of Janus kinase II gene at exon 14 was amplified by using forward primer (5'-TTT GGT TTT AAA TTA TGG AGT ACG-3') and Reverse primer (5'-CTA TTG TTT GGG CAT TGT AAC C-3').

RG-PCR was then performed in a total reaction volume of 50  $\mu$ l, containing 15  $\mu$ l extracted genomic DNA (30 ng/ $\mu$ l), 2.5 $\mu$ l reverse primer (42.8pmol/ $\mu$ l), 2.5 $\mu$ l forward primer (59 pmol/ $\mu$ l), 1 $\mu$ l buffer (10X(200 mM Tris-HCl (pH 8.4), 500 mM KCl.)), 2 $\mu$ l MgCl<sub>2</sub> (50mM), 0.2  $\mu$ l dNTPs (10mM), 1.25  $\mu$ l Taq polymerase (5U/ $\mu$ l) and 25.55  $\mu$ l dH<sub>2</sub>O.

The samples were amplified on the thermal cycler starting with an initial denaturing phase for 5 min at 94°C. The run consisted of 30 cycles, containing a step at 94 °C for 30 sec., Tm (Melting temperature) 59°C for 35 sec. and 72°C for 1 minute. The samples were held at 72°C for 10 min. afterward. The PCR product was stored at -70 °C until it had been loaded and analyzed on a 1% W/V Agarose gel.

Restriction fragment length polymorphism (RFLP) was used to assess the V617F mutation in a total volume of 20 $\mu$ l, as the following: 5  $\mu$ l amplicon products were digested overnight with 20 units/ 2 $\mu$ l *AflIII* restriction endonuclease enzyme in appropriate buffer (Acetylated BSA 0.4  $\mu$ l and 2  $\mu$ l buffer) at 37°C. Then the digested products were analyzed by visualization of

digested amplicon after separation by 2% (w/v) agarose gel electrophoresis at 100V current for 30 min and then staining with ethidium bromide.

When only wild type DNA is present, two fragments of 242 bp and 22 bp are generated, whereas mutated DNA (V617F-positive) JAK II allele) remains undigested (264 bp) fragment (Vlackaki, et al., 2012).

### 2.3. Ethical consideration

Ethics approval was granted by the professional research committee of the College of Medicine -HMU. The patient's venous blood was used for our prospective study, Informed consent and permission were obtained from the patients before phlebotomy and the sample taking.

### 3. RESULTS

A total of fifty  $\beta$ -thalassemia patients with the mean age (24) years, ranging from (5-45) years of age were enclosed into the study

A 264 bp fragment from exon 14 of the Janus kinase II gene among patients with  $\beta$ -thalassemia major were successfully amplified with the precise primers containing *AflIII* endonuclease restriction sites as shown in Fig (1).



**Figure 1:** Agarose gel analysis of PCR products corresponding to 264 (bp) fragment of the Janus kinase II gene. DNA markers are shown on the right (Bp). Whereas lines from 1 to 7 correspond to PCR products of the amplified DNA from 7 different samples of patients with  $\beta$ -thalassemia major.

In our study for mutational region screening, we demonstrate that none of the  $\beta$ -thalassemic patients was positive and carried any of the described *kinase II* (<sup>V617F</sup>) mutation, as shown in Fig 2.

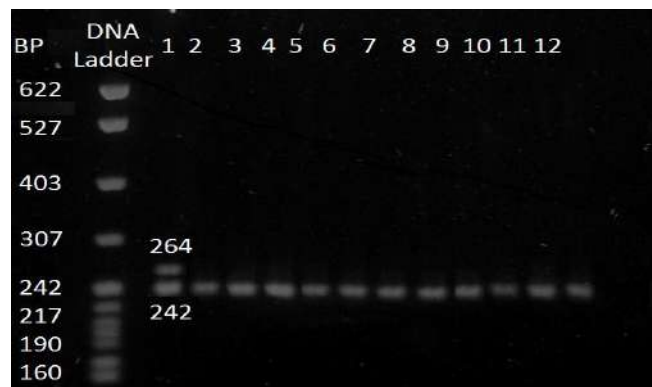


**Figure 2:** Agarose gel electrophoresis pattern of some RFLP products of the Janus kinase II gene. DNA markers are shown on the right (Bp), Line no. 1 control positive for *JAK2* <sup>V617F</sup> mutation, The other lanes are negative and did not have *JAK2* <sup>V617F</sup> mutation

### 4. DISCUSSION

It is well established that homozygous carriers of  $\beta$ -globin gene mutation suffer from severe hematological, thromboembolic complications, biochemical, and other serious complications from an early child (Eldor, *et al.*, 2002, Faris, *et al.*, 2019). Although, the life expectancy of patients has markedly improved over the previous couple of decades but patients are still suffer from many complications of this hereditary disease (Syed, *et al.*, 2018). Of something, additional complications are now being recognized. Especially, an increased risk of hypercoagulability and thrombosis (Hadeer, *et al.*, 2017)

Despite longstanding evidence the pathophysiology of blood clots and embolus remain unclear (Ataga, 2019, Gregory, *et al.*, 2017).

So, in Beta-Thalassimia, The mechanisms responsible for the increased thrombotic risk are probable multifactorial. Several factors are identified. While the likelihood of a genetic basis is still not very clear (Amiram, *et al.*, 2002, Maria-Domenica *et al.*, 2011).

In our prospective study, we focused on the *JAK II* <sup>V617F</sup> mutation in patients with  $\beta$ -Thalassemic major because a better rate of thrombotic complications has been reported in some non thalassemic patients with the *JAK II* <sup>V617F</sup> mutation; however, It remains unclear if the V617F mutation of Janus kinase is related to an increased risk of blood clots and embolus in thalassemic patients

To the best of our knowledge, ours is that the first molecular study in this region. no other group has done any work about the V617F mutation of the *JAK II* gene and  $\beta$ -Thalassemia major.

In our analysis for  $\beta$ -Thalassemic major individuals, we observed that the *JAK II*<sup>V617F</sup> mutation was completely absent among the study subjects and *JAK II*<sup>V617F</sup> point mutation doesn't related to thrombotic complications in thalassemic patients, Our results are in agreement with the results obtained by Vlackaki *et al'* which they found that there is no association between *JAK II*<sup>V617F</sup> mutation and  $\beta$ - Thalassemia major.

## 5. CONCLUSIONS

In our study, we found no evidence for an association between *JAK II*<sup>V617F</sup> mutation and  $\beta$ -Thalassemia major, and that's means in patients with  $\beta$ - Thalassemia mutation at Valine 617 Phenylalanine of *Janus kinase II* genes does not seem to play a role in the blood clotting, hematological and thrombotic complications.

### Conflict of Interest

The author declares that he has no conflicts of interest.

## References

Ahmed, A., Güldal, M. 2019. Estimation of MDA, CRP and Some hematological parameters in the mature Cypriot Thalassemia patients. ZANCO Journal of Pure and Applied Sciences, 31(s4);143-149

Alabdulaali, MK. 2009. The role of JAK2 abnormalities in hematologic neoplasms. Hematology Reviews, 1(10): 56-61.

Ali, T., Zaher, K., Imad, U. and Maria, D. 2008. Thalassemia and hypercoagulability, Blood Reviews, 22(5):283-92. DOI: 10.1016/j.blre.2008.04.001

Al-Thwani, AN., Yaseen, NY. and Khaleel, KJ. 2010. The Role of JAK2 Mutation in Polycythaemia Vera in Some Iraqi Patients. Iraqi Journal of Cancer and Medical Genetics, 3(2): 42-45.

Amarapurkar, D., Punamiya, S., Patel, N., Parekh, S., Mehta, SH. And Shah, N. 2011. Prevalence of JAK2V617F mutation in intra-abdominal venous thrombosis. Tropical Gastroenterology, 32(4): 279–284.

Amiram, E. and Eliezer, A. 2002. The hypercoagulable state in thalassemia. Blood, 99(1):36-43.

Ataga, KI. 2009. Hypercoagulability and thrombotic complications in hemolytic anemias. Haematologica, 94(11): 1481-1484.

Cappellini, MD. 2007. Coagulation in the Pathophysiology of Hemolytic Anemias. American Society of Hematology, (1)74-78. DOI: 10.1182/asheducation-2007.1.74

Eldor, A., Rachmilewitz, EA. 2002. The hypercoagulable state in thalassemia. Blood, 99(1): 36-44. DOI: 10.3324/haematol.2009.013672

Faris, Q., and Dalal, S. 2019. Biochemical and Molecular analysis of the beta-globin gene on Saudi sickle cell anemia. Saudi Journal of Biological Science. 26(7):1377–1384. DOI: 10.1016/j.sjbs.2019.03.003.

Gregory, J., Martin, H., and Mark, T., 2017. Intravascular hemolysis and the pathophysiology of sickle cell disease. Journal of Clinical Investigation, 127(3): 750–760. DOI: 10.1172/JCI89741

Hadeer, A. and Omar, M. 2017. Ghallab Candidate markers for thromboembolic complications in adult Egyptian patients with  $\beta$ -thalassemia . The Egyptian Journal of Haematology, 42 (2):64-69. DOI: 10.4103/ejh.ejh\_12\_17

Karaköse, S., Oruç, N., Zengin, M., Akarca, US. and Ersöz, G. 2015. Diagnostic value of the JAK2 V617F mutation for latent chronic myeloproliferative disorders in patients with budd-chiari syndrome and/or portal vein thrombosis. Turkish Journal Gastroenterology, 26: 42-8.

Maria-Domenica, C., Khaled, M. and , Ali, T. 2011. Thalassemia as a Hypercoagulable State. Oncology & Hematology,7(2):157-60 DOI: doi.org/10.17925/OHR.2011.07.2.157

Melchiori, L. 2010, Jak2 eritropoeisi inefficacy in Beta-Talassemia. PhD. thesis. Università degli Studi di Padova.

Nihad, A. 2016. A study of some factors and certain hematological parameters in transfusion dependent beta thalassemia patients in Erbil Province, ZANCO Journal of Pure and Applied Sciences, 28 (s6); s89-s96

Sipahi, T., Kara, A., Kuybulu, A., Egin, Y. and Akar, N. 2009. Congenital Thrombotic Risk Factors in  $\beta$ -thalassemia. Clinical and Applied Thrombosis/Hemostasis,15(5): 581-584. DOI: 10.1177/1076029608316170.

Steensma, DP. 2006. JAK2 V617F in Myeloid Disorders: Molecular Diagnostic Techniques and Their Clinical Utility. Journal of Molecular Diagnostics, 8(4): 397-411.

Steensma, DP., Dewald, GW., Lasho, TL., Powell, HL., McClure, RF. and Levine, RL. 2005. The JAK2 V617F activating tyrosine kinase mutation is an infrequent event in both “atypical” myeloproliferative disorders and myelodysplastic syndromes. Blood, 106(4): 1207-1210.

Syed, R., Sanjida S., and Islam, A. 2018. Clinical and Molecular Studies on Thalassemia . International Journal of Current Research and Review, 10(4). DOI: 10.7324/IJCRR.2018.1047

Vlackaki, E., Kalogeridis, A., Neokleous, N., Perifanis, V., Klonizakis, F., Ioannidou, E. and Klonizakis, L. 2012. Absence of Jak II ( V617F) mutation in patients with beta thalassemia major and thrombocytosis due to splenectomy, Molecular Biology Report, 39:6101-6105. DOI: 10.1007/s11033-011-1425-7.

## RESEARCH PAPER

# Protective roles of melatonin on Hematological Parameters and Thyroid Hormone Levels in rats treated with Aluminum Chloride

Zrar Saleem Kareem Almarzany

Department of Biology, Faculty of Science and Health, Koya University Koya KOY45, Kurdistan Region – F.R. Iraq

### ABSTRACT:

**Background:** Aluminum exists in numerous produced foods, medicines and likewise added to drinking water for refining purpose. Its existence has so heavily contaminated with the surroundings that exposed to it is almost inescapable.

**Goal:** This survey was aimed at evaluating effect of Melatonin for inhibiting effect of Aluminum Chloride.

**Methods:** Randomly selected rats were grouped separately into three groups for 40 days: ( $n = 5$ /group): healthy key group, Aluminum Chloride ( $AlCl_3$ ) group (Urged with 1000mg/L of  $AlCl_3$  in administrated water) and The last group were awarded (1000mg/L) of  $AlCl_3$  in water plus melatonin (50mg/kg diet). The estimated haematological parameters were leukocytes, erythrocytes, haemoglobin concentration and thrombocytes count. Also serum and brain supernatant beta amyloid and serum levels of  $T_3$ ,  $T_4$  and TSH were also measured.

**Results:** At the end of this study, statistical analysis showed that the some haematological parameters (RBC count Hb, PCV, WBC count, granulocyte and lymphocyte differential leucocyte counts, platelet count) serum and brain beta amyloid and thyroid hormone values in  $AlCl_3$  with melatonin at a dosage of 50mg/kg diet has aroused the rats to stay approximately near to the standards.

**Conclusion:** From the results of this study it was discovered that melatonin has a therapeutic effect on  $AlCl_3$  induced in albino rats.

KEY WORDS: Melatonin,  $AlCl_3$ , Hematology,  $\beta$  amyloid, Thyroid Hormones.

DOI: <http://dx.doi.org/10.21271/ZJPAS.32.6.9>

ZJPAS (2020) , 32(6);76-86 .

## 1. INTRODUCTION

The toxic effects of Aluminum have been studied on a variety of different body organs, including brain and circulatory system. It effects, as an environmental factor, also contributes to some neurodegenerative disease and effects on several enzymes and biomolecules relevant to Alzheimer's disease (Kadhum, 2017). Melatonin, as an eminent endogenous antioxidant, suggest that defended to the central nervous system (CNS) by propelling free radicals and consequently enhances the employment of further antioxidants.

Additionally, its metabolites have the capability to shield tissues versus oxidative destruction created by a diversity of toxic agents and metabolic behaviours (Peyrot and Ducrocq, 2008).

Previous *in vivo* and *in vitro* investigations have proposed the protective effects of melatonin against metal-induced oxidative damage, with high lipophilicity, if supplied exogenously it can swiftly cross the blood brain barrier to reach neurons and glial cells (Daniel et al., 2004). It is concluded that Melatonin acts as a hunter of free radicals, that is especially important in the brain, the most sensitive organ for oxidative stress and have ability to limit the generation of free radicals at the mitochondrial level by a mechanism which not fully understood (Reiter et al., 2005).

---

### \* Corresponding Author:

Zrar Saleem Kareem Almarzany

E-mail: [zrar.saleem@koyauniversity.org](mailto:zrar.saleem@koyauniversity.org)

### Article History:

Received: 11/08/2020

Accepted: 13/09/2020

Published: 20/12/2020

One strategy to restrict or diminish the advancement of AD is completely the attack in the A $\beta$  gathering process. Melatonin, by communicating beside A $\beta$  peptide, can inhibit the progressive creation or displacement of  $\beta$ -sheet and/or amyloid fibrils (Poeggeler et al., 2001). The mechanization of this activity is that melatonin could boost the conversion of  $\beta$ -sheets into random coils by obstructing the imidazole-carboxylate salt bridges thus, block A $\beta$  fibrillogenesis and gathering. In the aforementioned design, executes moulding the formation of the secondary  $\beta$ -sheet compatibility possible. It, hence, is not diminishing neurotoxicity alone but further benefits the clearance of the peptide via enhanced proteolytic degradation (Masilamoni et al., 2008).

On the other hand, the occurrence of remarkable variations in the blood of the cases with AD and influence the blood hemostasis assigns to the development of A $\beta$  plaques in the circulatory vessels and brain parenchyma (Smith and Greenberg, 2009). Abnormal haematological factors such as lower levels of erythrocyt, haemoglobin, and hematocrit also have been recognized as varied to ordinary individuals. This survey was aimed at evaluating the possible effects that Aluminum chloride could have on some blood parameters and thyroid hormones and the role of melatonin for inhibiting persuaded Aluminum Chloride of adult Albino rats.

## 1. Materials and Methods

### 2.1 Animals and Housing

This study consisted of fifteen adult male albino rats (*Rattus norvegicus*) each weighing of 190-240 g B.W. and 10-12 weeks old. The study was conducted in the animal house in Biology Department / Education College / Salahaddin University-Erbil, between October 2019 to January 2020. The rodents lived in plastic enclosures bedded with wooden chips supporting by official lab specifications, about 12:12 light/dark photoperiod (LD) at 22 $\pm$ 4 °C (Coskun et al., 2004). An automatic light-switching pattern was

used for preserving conventional 12-hours daytime cycles.

### 1.2 Experimental Design

This study involved fifteen adult male rats. They implied randomly categorized into three cohorts each consisting of five animals. The first cohort was supplied with standard rat chow and tap water which was considered as a controller cohort. The second ones were supplied (1000mg/L) of AlCl<sub>3</sub> in water and the latest ones were given (1000mg/L) of AlCl<sub>3</sub> in water plus melatonin (50mg/kg diet). The treatments were engrossed for 40 days and then the data were earned.

### 1.3 Anesthesia, Dissection and Removal of Brain

Following the procedure of Laird et al., (1996), Ketamine (35mg/kg B.W.) and xylazine (5mg/kg B.W.) were used to anesthetize all animals then they sacrificed at the end of experiment. Brain of each rat was divided into two equal parts, in which one part cut into small pieces (less than 0.5cm<sup>3</sup> thickness) then kept in fixative, while the other part stored at -80 °C in freezer until they were needed for estimation of A $\beta$  (1-42) peptide levels.

### 1.4 Tissue Homogenate Preparation

Brain tissues washed with cold saline, dried then weighed as asserted to a modified method elaborated by Dhuha and Ali (2020). Half of each brain used for homogenization by 10 mm cold phosphate buffer saline pH 7.4. The brain tissues homogenized (10 % w/v) using an electrical homogenizer at 20000 rpm for 6 seconds, while healthy cells and cell rubble were separated by centrifugation at 3000 rpm for 20 minutes by practicing a refrigerated centrifuge at (4°C). The supernatants were utilized for A $\beta$  (1-42) peptide analyses

### 1.5 Blood Collection

After 40 days of continuous treatment, blood specimens were obtained from the heart of the animals and then anaesthetize by diethyl ether. Tubes have ethylene diamine trichloroacetic acid (EDTA) were utilised for accumulating blood and directly were applied for estimating haematological determinants. Tubes without

anticoagulants were also utilized for serum preparation and centrifuged at 3000 rpm for 15 minutes for A $\beta$  (1-42) peptide and hormonal estimation (Cheng, 2002).

## 2.6 Determination of Serum and Brain Supernatant Beta Amyloid (1-42) Peptide Level

The kit assay, A $\beta$  (1-42) peptide (model No. SL0049Ra), was used to purify rat A $\beta$  (1-42) antibody to coat microtiter plate wells and to make a solid-phase antibody. Then A $\beta$  (1-42) added to the wells to combine A $\beta$  (1-42) antibody with Horse Radish Peroxidase (HRP) labeled to form antibody - antigen - enzyme-antibody complex. After thoroughly washing, the Tetra Methyl Benzene (TMB) substrate solution was added turning the TMB substrate into blue and then the HRP enzyme-catalyzed reaction was terminated by the addition of sulphuric acid solution. The colour change measured with the plate reader at a wavelength of 450 nm. The concentrations of the peptide for the samples were determined by comparing their optical density with the standard curve.

## 2.7. Estimation of haematological parameters

Automated parameter haematology analyzer (Mythic 22) was used to analyze erythrocyte count and additional haematological data.

## 2.8. Estimation of Hormone

Automated Immunoassay Analyzer (Biomerieux, France) nominated applied to appraise serum values of triiodothyronine, thyroxine and thyroid

stimulating hormone beside a chemiluminescence immunoassay.

## 3. Statistical Analysis

Statistical software (Graph pad Prizm, version 8) was used. Data are represented as mean  $\pm$  standard errors of means (SEM) of the number of animals used in each group. To compare the individual means in each group with the control group, ordinary one-way analysis of variation (ANOVA) for compared within control and studied treatments were applied and Tukey post hoc test was used to compare individual means. After analysis of variance (ANOVA).  $P < 0.05$  was considered statistically significant.

## Results

### Effect of melatonin on serum and brain $\beta$ amyloid level

As illustrated in Fig. 1 and Table 1, Urged of AlCl<sub>3</sub> in a dosage of (1000mg/L) generated a significant increase ( $P < 0.001$ ) in serum and brain  $\beta$ -Amyloid in compared to standard and melatonin with ALCL<sub>3</sub> cohort rats, while no important ( $p \leq 0.05$ ) alteration in the serum and brain  $\beta$  Amyloid values mentioned in melatonin with ALCL<sub>3</sub> cohort's rats.

**Table 1: Effect of melatonin on serum and brain  $\beta$  amyloid parameters:**

Parameters	Control	AlCl <sub>3</sub>	AlCl <sub>3</sub> + Melatonin
Serum $\beta$ Amyloid ug/L	24.780 $\pm$ 0.871	44.83 $\pm$ 1.100***	25.440 $\pm$ 1.307###
Brain $\beta$ Amyloid ug/L	73.66 $\pm$ 0.886	92.510 $\pm$ 2.092***	78.410 $\pm$ 1.994###

All data represent means  $\pm$  standard errors (SE),

n = 5,

\*\*\* =  $P < 0.001$

### =  $P < 0.0001$  significant differences between induced AlCl<sub>3</sub> and melatonin treated parameters

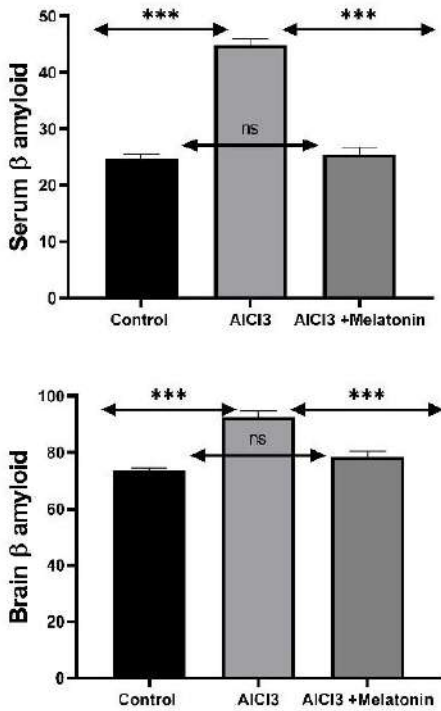


Figure 1. Effect of melatonin on the serum and brain  $\beta$  amyloid level

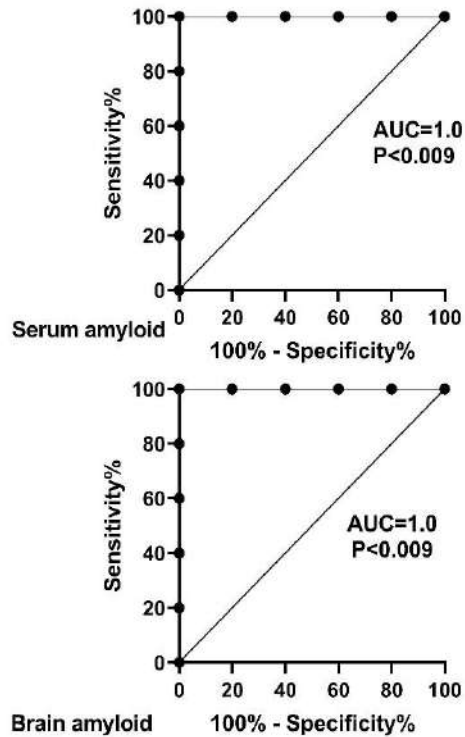


Figure 2. ROC curve shows the sensitivity of melatonin as a bio marker

The results in figure 2 showed improves in the ROC curve sensitivity of  $\beta$  amyloid in both serum and brain  $AlCl_3$  induced rats, (with the value of  $AUC= 1.0$  and  $P<0.009$ ).

**Effect of melatonin on serum  $T_3$ ,  $T_4$  and TSH levels:**

The effects of  $AlCl_3$  in albino induced rats on  $T_3$ ,  $T_4$  and TSH secretion levels were displayed in Table 2 and figure 3. The outcomes appear that  $T_3$  is altered improved ( $P<0.01$ ) between control and  $AlCl_3$  induced rats, while there are obvious changes between the values of  $AlCl_3$  melatonin

treated and both control and  $AlCl_3$  induced rats, nevertheless there were no statistical ( $p>0.05$ ) changes occur among them. The  $T_4$  values of  $AlCl_3$  induced rats are affected significantly ( $P<0.001$ ) with both control and  $AlCl_3$  melatonin treated rats, with none notable changes happen between control and  $AlCl_3$  with melatonin treated rat values. TSH values showed, that there are no statistical changes among control and both  $AlCl_3$  induced and  $AlCl_3$  melatonin treated rats.

**Table 2. Effect of melatonin on serum  $T_3$ ,  $T_4$  and TSH levels:**

Parameters	Control mean $\pm$ S.E n = 5	$AlCl_3$ mean $\pm$ S.E n = 5	$AlCl_3$ + Melatonin mean $\pm$ S.E n = 5
$T_3$ nmol/l	141.195 $\pm$ 10.692	96.451 $\pm$ 6.524**	123.800 $\pm$ 5.892
$T_4$ nmol/l	1.996 $\pm$ 0.365	16.200 $\pm$ 1.689***	4.404 $\pm$ 0.633####

TSH uIU/ml	2.488 ± 0.309	2.488 ± 0.337	2.400 ± 0.387
------------	---------------	---------------	---------------

- Data presented as mean ± S.E
- n = number of observation
- \*\* = P<0.01 \*\*\* = P<0.001
- ### = P<0.0001 significant differences between induced AlCl<sub>3</sub> and melatonin treated parameters

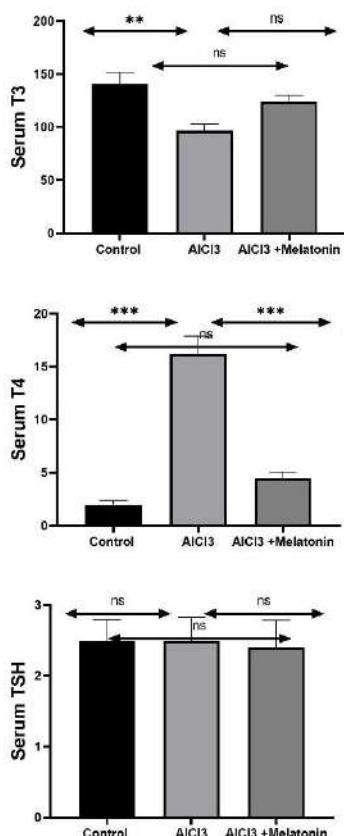


Figure 3 Effect melatonin on serum T3, T4 and TSH parameters

### Effect of melatonin on some hematological parameters:

#### a-Effect of melatonin on RBC indices parameters

From Table 3, revealed a meaningful (P<0.05) decrease in RBC count within AlCl<sub>3</sub> rat's cohort during vied with of normal cohort. After administration of melatonin, the improvement in the count of RBC is observed, but statistically (P<0.05) not changed. Otherwise, the Hb values of AlCl<sub>3</sub> cohort diminished statistically (P<0.001) when viewed with the control cohort. Also, the Hb values of melatonin treated cohort were

significantly (P<0.05) raised during viewed with AlCl<sub>3</sub> effected rat cohort. However, PCV values of AlCl<sub>3</sub> stimulated rats were lowered at (P<0.001) if observed with the normal cohort. Moreover, the melatonin treated rats were statistically (P<0.01) improved when compared with AlCl<sub>3</sub> stimulated rat cohorts. On the other hands, the other inquired RBC indices data of the current study, particularly MCV, MCH and MCHC values, were not altered at (P<0.05) if



viewed in stimulated rats with control cohort and  $AlCl_3$  with melatonin treated animals.

**Table 3: Effect of melatonin on RBC indices parameters:**

Parameters	Control mean $\pm$ S.E n = 5	$AlCl_3$ mean $\pm$ S.E n = 5	$AlCl_3$ + Melatonin mean $\pm$ S.E n = 5
R.B.C. $\times 10^{12}/L$	5.460 $\pm$ 0.258	4.525 $\pm$ 0.131*	5.109 $\pm$ 0.903
Hb g/dL	13.510 $\pm$ 0.258	10.721 $\pm$ 0.386***	12.180 $\pm$ 0.883 <sup>#</sup>
PCV %	40.841 $\pm$ 1.496	33.060 $\pm$ 1.491***	36.967 $\pm$ 1.373 <sup>##</sup>
MCV fL	75.095 $\pm$ 3.137	69.364 $\pm$ 1.109	72.583 $\pm$ 1.879
MCH Pg	24.883 $\pm$ 0.825	22.811 $\pm$ 1.347	23.732 $\pm$ 1.184
MCHC g/dL	33.159 $\pm$ 0.594	32.553 $\pm$ 1.031	32.758 $\pm$ 0.875

Data presented as mean  $\pm$  S.E.

- n = number of observations.
  - \* =  $P < 0.05$  \*\* =  $P < 0.01$  \*\*\* =  $P < 0.001$ .
  - # =  $P < 0.05$  ## =  $P < 0.01$  significant between  $AlCl_3$  induced and melatonin treated rats.
- b- Effect of melatonin on WBC, differential and platelet count parameters:

The results obtained from the table (4) revealed important ( $P < 0.05$ ) improvement in the WBC, Granulocyte differential count and platelet counts, with the notable ( $P < 0.05$ ) reduction in the lymphocyte differential counts rates of  $AlCl_3$  induced rat's cohort when compared with a control cohort. But the values of WBC, Granulocyte differential Count platelet count and lymphocyte differential

counts from melatonin treated cohorts were not affected at ( $P < 0.05$ ) with both control and  $AlCl_3$  stimulated cohorts. Finally, the monocyte values not changed within  $AlCl_3$  influenced rats, melatonin treated and normal cohorts' rats

**Table 4: Effect of melatonin on WBC, differential and platelet counts levels:**

Parameters	Control mean $\pm$ S.E n = 5	$AlCl_3$ mean $\pm$ S.E n = 5	$AlCl_3$ + Melatonin mean $\pm$ S.E n = 5
W.B.C. $\times 10^9/L$	766.465 $\pm$ 22.239	807.613 $\pm$ 27.410*	785.807 $\pm$ 19.128
Granulocyte Count %	50.600 $\pm$ 5.749	55.000 $\pm$ 4.871*	54.300 $\pm$ 3.920
Lymphocyte %	47.800 $\pm$ 6.010	43.200 $\pm$ 5.43*	44.100 $\pm$ 4.970

<b>Monocyte %</b>	<b>1.600 ± 1.244</b>	<b>1.800 ± 0.200</b>	<b>1.600 ± 0.258</b>
<b>Platelet ×10<sup>9</sup>/L</b>	<b>422.573 ± 19.452</b>	<b>544.310 ± 23.078*</b>	<b>458.213 ± 23.421</b>

- **Data presented as mean ± S.E**
- **n = number of observation**
- **\* =P<0.05**

## **Discussion:**

### **Effect of melatonin on serum and brain $\beta$ amyloid levels**

As indicated by the current study, AlCl<sub>3</sub> caused a significant increase in  $\beta$  amyloid level both in serum and brain supernatant of male rats which is supported by Castronia et al., (2010), they published that extreme consumption of aluminium (Al) may provoke the deposition of amyloids in the neurons and deficits memory as well as learning confusions in rats.

Increased  $\beta$  amyloid level in serum and brain supernatant of AlCl<sub>3</sub> cohort may be associated with the point that Al may attack the nucleus and may create nuclear vacuolation as proved by the current investigation creating gene mutation consequently starting to the disposition of this peptide which is firmly adhered with Al and deposited there. (Castronia et al., 2010).

In this analysis melatonin decreased  $\beta$ -amyloid values in serum and brain supernatant of male rats, the finding agreed with the data sustained by Millan-Plano et al. (2003), they documented that melatonin inhibits Al stimulated disposition of  $\beta$  amyloid and oxidative end products in the synaptosomal membranes, by merging with Al such adhesive may shed light into the role of this factor in the a etiology of AD (Lack et al., 2001).

Melatonin could advance the exchange of  $\beta$ -sheets into random coils by breaking the imidazole-carboxylate salt bridges thus, obstruct A $\beta$  fibrillogenesis and aggregation. Therefore, it does that achievable by preventing the creation of the secondary  $\beta$ -sheet conformation; it is not only

diminishing neurotoxicity but also help the withdrawal of the peptide via enhanced proteolytic degradation (Kurhaluk et al.,2017).

### **Effect of melatonin on serum T<sub>3</sub>, T<sub>4</sub> and TSH levels:**

Our study, examined the relationships between serum levels of thyroid hormones and TSH in AlCl<sub>3</sub> induced and melatonin treated rats. Serum T<sub>3</sub> levels were decreased, while having high serum T<sub>4</sub> levels were connected with an increase in cerebral  $\beta$  amyloid deposition. These results supported by the findings of Christopher et al., (2016), in which they proved that in patients with AD, T<sub>4</sub> levels are about 10 folds higher than normal, showing that a reduction in expression of isoform of the enzyme type 2 deiodinase (D2) or oxidative neurodegeneration cholinergic accompanying this disease occurs alongside the development, which contributes to a reduction of the enzymatic activity D2. Until today there isn't a full understanding of the mechanisms underlying the relationship between serum levels of T<sub>4</sub> and cerebral  $\beta$  amyloid (Choi et al., 2017). The conversion of serum T<sub>4</sub> to T<sub>3</sub> by type 2 deiodinase occurs after serum T<sub>4</sub> crosses BBB (Blood-brain barrier) by mono carboxylate transporter 8 and reaches the astrocytes (Morte & Bernal, 2014). The cerebral gene expression of  $\beta$  amyloid precursor protein are suppressed by brain T<sub>3</sub> (Belakavadi et al., 2011). In the present study, due to small contribution to brain T<sub>3</sub>, the serum T<sub>3</sub> was not associated with brain amyloid burden. Serum T<sub>3</sub> seems to be degraded by tyrosyl ring deiodinase before it reaches the neuronal space that is why in the cerebral cortex, active T<sub>3</sub> is predominantly derived from serum T<sub>4</sub> rather than serum T<sub>3</sub> (Choi et al., 2017). Negative association between brain T<sub>3</sub> and  $\beta$  amyloid

precursor protein expression was found from the preclinical studies by using a transgenic mouse model of AD (Contreras-Jurado, and Pascual, 2012). On the other hand, there was a decrease in the AlCl<sub>3</sub> melatonin treated albino rat cohorts T4 levels of our study, and it is because of the potent antioxidant role of melatonin which decreases the effects of AlCl<sub>3</sub> in deposition of  $\beta$  amyloid (Khidhir, and Ismail, 2016).

### **Effect of melatonin on some hematological parameters:**

#### **a- Effect of melatonin on RBC indices parameters:**

The results of current study showed changes in RBC indices parameters of rat's exposure to AlCl<sub>3</sub>. A decreased number of RBCs, Hb concentration and PCV value after 40 days of AlCl<sub>3</sub> exposure were observed. There was a development of normocytic normochromic anemia in the rat's RBC in our study. This kind of anemia has occurred in most of the studies regarding the effects of AlCl<sub>3</sub> on erythrocyte parameters (Farina et al., 2002). Our results show improvement of rat's RBC indices after treating them with the melatonin plus AlCl<sub>3</sub>. In the study achieved by Turgut et al. (2004), noted the alterations of RBC parameters were noticed after 3 months of the oral exposure to aluminum sulfate in mice.

In the biological system, the hem synthesis is disturbed as the aluminum Ions replace Iron and magnesium Ions then reduce Fe<sup>+2</sup> binding to ferritin (Yakubu; 2017). The other inhibition cause of hem-oxygenase is that this enzyme which is necessary for hemoglobin formation series, would be stopped by the toxicity of Aluminum and increase the destruction of RBCs then RBCs are transformed to bilirubin (Kalaiselve et al., 2015). As a result of Aluminum toxicity, the free radicals are accumulated in the target organs such as liver and it causes the inhibition of glutathione enzyme there. This is an important way of maintaining the hemoglobin in red blood cell and increase the removal of hydrogen peroxide (H<sub>2</sub>O<sub>2</sub>), also increases the lifetime of red blood cell (Buraimoh et

al., 2011). The reduction of some enzyme such as glutathione reductase, catalase, glucose-6-phosphate dehydrogenase were lead to accumulate of toxins inside red cells (Kalaiselve et al., 2015). da Rosa et al., (2010) showed that melatonin decreases the oxidative stress by acting as scavenger of free radicals and provides antioxidant protection of biomolecules. Melatonin reduces the lipoperoxidation levels in liver and erythrocytes and increases the antioxidant enzyme Superoxide dismutase activity in erythrocytes.

#### **b- Effect of melatonin on WBC, differential and platelet count:**

Current study showed that AlCl<sub>3</sub> has a significant effect in increasing white blood cell, differential granulocyte counts and platelet counts, also a significant effect in decreasing lymphocyte differential counts. This is because of the effect of Aluminum chloride in inducing infections in the target organs such as liver, brain, kidney, spleen and smooth muscle (Kadhum, 2017). In a histopathological study of spleen of AlCl<sub>3</sub> induced rats which was conducted by (Buraimoh et al., 2012) showed the same results as it noted the increase in white pulp, bleeding and degeneration of spleen tissues. It's known as this destruction is caused by the effects of free radicals and increase in lipid peroxidation which is the process of initiating tumor formation in target organs. The antioxidant properties of melatonin against AlCl<sub>3</sub> induced toxicity in the WBC and platelet count of rats can be explained by two different mechanisms. The Melatonin scavenges hydroxyl radicals (Kim et al., 2005), which are considered as the highest reactive ROS and, thus, diminish damage of cell structures, including DNA. The second method shows that the Melatonin also reduces oxidative stress by stimulating antioxidant enzymes (Reiter et al., 2003). Monocytes have shown playing critical roles in the pathogenesis of AD (Gu et al., 2016). However, we could not find any significant discrepancy between AD patients and NCs. Given that, we can say that the effect of monocyte playing in pathogenesis of

AD is mainly determined by its functions rather than its quantity. The defective phagocytosis of monocytes in AD have been confirmed in previous studies, and enrichment of levels of functionally normal monocytes resulted in substantial remission of disease progression in animal models of AD (Fiala et al., 2005). The decreased number of lymphocytes in AD were recorded by Shad et al., (2013) in which the mechanisms related to the decreased lymphocyte count in AD is the entry of peripheral lymphocytes into the brain and it was induced by elevated neuro inflammations, production of inflammatory mediators, and facilitated by increasing permeability of blood-brain barrier in AD (Chen et al., 2017). From the results of this study it was discovered that melatonin has a therapeutic effect on  $AlCl_3$  induced in albino rats which it decreased amount of brain  $\beta$  amyloid, improved, some hematological parameters (RBC count Hb, PCV, WBC count, granulocyte and lymphocyte differential leucocyte counts, platelet count) and  $T_4$  parameters.

## References

- BELAKAVADI, M., DELL, J., GROVER, G.J. & FONDELL, J.D. (2011). Thyroid hormone suppression of beta-amyloid precursor protein gene expression in the brain involves multiple epigenetic regulatory events. *Mol Cell Endocrinol.* 339,72–80.
- BURAIMOH, A.A., OJO, S.A., HAMBOLU, J.O. & ADEBISI, S.S. (2011). Effects of oral administration of Aluminum chloride on the histology of hippocampus of Wistar rats. *Curr. Res. J. Biol. Sci.*, 3, 509-515.
- BURAIMOH, A.A., OJO, S.A., HAMBOLU, J.O. & ADEBISI, S.S. (2012). Effects of Aluminum chloride exposure on the histology of the liver adult Wistar rats. *IOSR Journal of Pharmacy*; 2 (3),525-533.
- CASTORINA, A., TIRALONGO, A., GIUNTA, S., LISA, C. M. & SCAPAGNINI, G. (2010). Early effects of aluminum chloride on beta-secretase mRNA expression in a neuronal model of  $\beta$ -amyloid toxicity. *Cell Biology and Toxicology.* 26 (4) ,367-377.
- CHEN, S.H., XIAN-LE, B. & WANG-SHENG, J. M.D. (2017). Altered peripheral profile of blood cells in Alzheimer disease. *Medicine*, 96(21), 1-7.
- CHENG, Z. (2002). Angiotensin-induced inflammation and vascular dysfunction. Academic dissertation. University of Helsinki.
- CHOI, H.J., MIN, S.B., DAHYUN, Y.B., KYUNG, S., JUN, H.L., JUN-YOUNG, L., & YU, K.K. (2017). Associations of thyroid hormone serum levels with in-vivo Alzheimer's disease pathologies. *Alzheimer's Research & Therapy.* 9(64), 1-9.
- CHRISTOPHER, C. R., DAVID, A., VICTOR, L. V. & COLIN, L. M. (2016). Multilevel analysis of biomarker pool for Alzheimer's disease. *Aandd journal. Poster Presentations.* ,878.
- CONTRERAS-JURADO, C. & PASCULA, A. (2012). Thyroid hormone regulation of APP (beta-amyloid precursor protein) gene expression in brain and brain cultured cells. *Neurochem. Int.* 60,484–7.
- COSKUN, O., OCAKCL, A., BAYRAKTAROGLU, T. & KANTER, M. (2004). Exercise training prevents and protects streptozotocin-induced oxidative stress and beta-cell damage in rat pancreas. *Experimental Medicine.* 203 (3),145-154.
- DA ROSA, D. P., SILVIA, B., DOUGLAS, S., CLAUDIO, Z., CLAUDIO, A. M. & NORMA, P. M. (2010). Melatonin protects the liver and erythrocytes against oxidative stress in cirrhotic rats. *Arq. Gastroenterol.* 47 (1), 0004-2803.
- DANIEL,S., LIMSON, J., DAIRAM, A., WATKINS, G. & DAYA, S. (2004). Through metal binding, curcumin protects against lead and cadmium-induced lipid peroxidation in rat brain homogenates and against lead-induced tissue damage in rat brain. *Inorganic Biochemistry.*98 (2),266-275.
- DE JONG, F.J., MASAKI, K., CHEN, H., REMALEY, A.T., BRETELER, M.M. & PETROVITCH, H. (2009). Thyroid function, the risk of dementia and neuropathologic changes: The Honolulu-Asia aging study. *Neurobiol Aging.* 30,600–6.
- DHUHA, Q. K. & Ali, K. A. (2020). Study of the protective effect of green tea against bisphenol A-induced amyloid aggregation in the brain of male albino rats. *ZJPAS.*, 32 (2), 192-202.
- FARINA, M., LARA, F.S., BRANDAO, R., JACQUES, R. & ROCHA, J.B. (2002). Effects of aluminum sulfate on erythropoiesis in rats. *Toxicol. Lett.* 132, 131–139.
- FIALA, M., LIN, J. & RINGMAN, J. (2005). Ineffective phagocytosis of amyloid-beta by macrophages of Alzheimer's disease patients. *J Alzheimers Dis.*,7,221–32.

- GU, B.J., HUANG, X.D. & OU, A. (2016). Innate phagocytosis by peripheral blood monocytes is altered in Alzheimer's disease. *Acta Neuropathol.*, 132,377–89.
- KADHUM, S.A. (2017). Effects of Aluminum Chloride on some Blood Parameters and Histological Spleen in White Male Rats. *J Babylon UV.*,25 (5), 1886-1895.
- KALAISELVE, A., AADHINAATH, R. G. & RAMALINGAM, V. (2015). Effect of Aluminum chloride and protective effects of Ginger extract on hematological profiles in male Wistar rats. *Int J Phytopharmacol Res.*, 4 (4),218-222.
- KHIDHIR, S. M. & ISMAAIL, M.M. (2016). Mechanism of the relaxant effects of melatonin via cyclooxygenase and epoxygenase pathways in male rat isolated aorta and trachea. *ZJPAS*, 28(1),70-79.
- KIM, C. KIM, N. & JOO, H. (2005). Modulation by melatonin of the cardiotoxic and antitumor activities of adriamycin. *J Cardiovasc Pharmacol.*, 46,200–10.
- KLUNK, W.E. (2004). Imaging brain amyloid in Alzheimer's disease with Pittsburgh Compound-B. *Ann Neurol.*, 55,306–319.
- KOSENKO, E., LYUDMILA, T., GUBIDAT, A., AMPARO, U. & CARMINA, M. (2020). The Erythrocytic Hypothesis of Brain Energy Crisis in Sporadic Alzheimer Disease: Possible Consequences and Supporting Evidence. *J Clin Med.*, 9 (206),1-19.
- KURHALUK, N., ALINA, S., SVITLANA, K. & PAWEL, J. (2017). Melatonin Restores White Blood Cell, Diminishes Glycated Hemoglobin Level and Prevent Liver, Kidney and Muscle Oxidative Stress in Mice Exposed to Acute Ethanol Intoxication. *Alcohol and Alcoholism.*, 52(5), 521–528.
- LACK, B., DAYA, S. & NYOKONG, T. (2001). Interaction of serotonin and melatonin with sodium, potassium, calcium, lithium and aluminum. *Pineal Research.*, 31 (2), 102-108.
- LAIRD, K., SWINDLE, M. & FLECKNEELL, P. (1996). Rodent and Rabbit Medicine. *Wheatons Ltd: Exeter*.
- MASILAMONI, J., JESUDASON, E., DHANDAYUTHAPANI, S., ASHOK, B., VIGNESH, S., JEBARAJ, W., PAUL, S. & JAYAKUMAR, R. (2008). The neuroprotective role of melatonin against amyloid beta peptide injected mice. *Free Radical Research.*,42 (7), 661-673.
- MILLAN-PLANO, S., GARCIA, J., MARTINEZ-BALLARIN, E., REITER, R., ORTEGA-GUTIERREZ, S., LAZARO, R. & ESCANERO, J. (2003). Melatonin and pinoline prevent aluminum-induced lipid peroxidation in rat synaptosomes. *Trace Element Medicine Biology.*,17 (1), 39-44.
- MIRZAEI, F., KHAZAEI, M., KOMAKI, A., AMIRI, I. & JALILI, C. (2019). The Effects of virgin coconut oil on prevention of Alzheimer's Disease. *J Nat Pharm Prod.*,14(4), e67747.
- MORTE, B., BERNAL, J. (2014). Thyroid hormone action: astrocyte-neuron communication. *Front Endocrinol Lausanne.*, 5,82.
- MUFSON, E.J., MA, S.Y., COCHRAN, E.J., BENNETT, D.A., BECKETT, L.A., JAFFAR, S., SARAGOVI, H.U. & KORDOWER, J.H. (2000). Loss of nucleus basalis neurons containing trkA immunoreactivity in individuals with mild cognitive impairment and early Alzheimer's disease. *J Comp Neurol.*,427,19–30.
- PEYROT, F. & DUCROCQ, C. (2008). Potential role of tryptophan derivatives in stress responses characterized by the generation of reactive oxygen and nitrogen species. *Pineal Research.*, 45 (3),235-246.
- POEGGELER, B., MIRAVALLE, L., ZAGORSKI, M., WISNIEWSKI, T., CHYAN, Y., ZHANG, Y., SHAO, H., BRYANT-THOMAS, T., VIDAL, R. & FRANGIONE, B. (2001). Melatonin reverses the profibrillogenic activity of apolipoprotein E4 on the Alzheimer's amyloid Abeta peptide. *Biochemistry.*, 40 (49), 4995-5001.
- REITER, R.J., TAN, D.X. & MAYO, J.C. (2003). Melatonin as an antioxidant: biochemical mechanisms and pathophysiological implications in humans. *Acta Biochim Pol.*, 50,1129–46.
- REITER, R, DUN-XIAN, T, JOSEFA, L, ULKAN, K. & ERTUGRUL, K. (2005). When melatonin gets on your nerves: its beneficial actions in experimental models of stroke. *Bio Med.*, (5),1535-3702.
- SHAD, K.F., AGHAZADEH, Y. & AHMAD, S. (2013). Peripheral markers of Alzheimer's disease: surveillance of white blood cells. *Synapse.*, 67,541–3.
- SMITH E.E. & GREENBERG, S.M. (2009). Beta-amyloid, blood vessels, and brain function. *Stroke.*, 40(7),2601-6.
- TURGUT, G., KAPTANOGLU, B., TURGUT, S., ENLI, Y. & GENC, O. (2004). Effects of chronic aluminum administration on blood and liver iron-related parameters in mice. *Yonsei Med J.*, 45, 135–139.

YAKUBU, O.E., NWODO, O.F.C., IMO, C. & OGWONI, H.A. (2017). Spermatogenic and haematological effects of aqueous and ethanolic extracts of

Hymenocardia acid stem bark on aluminum-induced toxicity in male Wistar rats. *Inter med Pub J*, 2 (1),1-5.

## RESEARCH PAPER

# Clinical Diversity of Multiple Myeloma at the First Presentation through the Time Lapse to Diagnosis in Kurdistan Region, Iraq

Truska A. Amin<sup>1</sup>, Zeki A. Mohamed<sup>2</sup>, Ali I. Mohammed<sup>3</sup>, Diveen J. Hussein<sup>4</sup>, Nawsherwan S. Mohammed<sup>5</sup>, Rezhin N. Rajab<sup>6</sup>, Firiad Hiwaizi<sup>7</sup>, Kanar J. Karim<sup>8</sup>, Abid M. Hassan<sup>9</sup>, Hisham A. Getta<sup>10</sup>, Najmaddin S.H. Khoshnaw<sup>11</sup>, Sana D. Jalal<sup>12</sup>, Akram M. Mohammed<sup>13</sup>, Kawa M. Hasan<sup>14</sup>, Dana A. Abdullah<sup>15</sup>, Ameer I.A. Badi<sup>16</sup>, Ahmed K. Yassin<sup>17</sup>, Banaz M. Safar<sup>18</sup>, Basil K. Abdulla<sup>19</sup>, Rawand P. Shamoon<sup>20</sup>

<sup>1</sup>MBChB, KBMS-candidate, Department of Hematology, Hiwa Cancer hospital, Sulaymaniyah, Kurdistan Region, Iraq, [truska.hem@gmail.com](mailto:truska.hem@gmail.com)

<sup>2</sup>MBChB, MRCP, FIBMS, Department of Medicine, College of Medicine, University of Duhok, Duhok, Kurdistan Region, Iraq, [barwari65@yahoo.com](mailto:barwari65@yahoo.com)

<sup>3</sup>MBChB, FICMS, Department of Pathology, College of Medicine, University of Sulaymaniyah, Sulaymaniyah, Kurdistan Region, Iraq, [alibty2010@yahoo.com](mailto:alibty2010@yahoo.com)

<sup>4</sup>MBChB, KBMS-candidate, Department of Hematology, Nanakali Hospital, Erbil, Kurdistan Region, Iraq, [diveen.jelal@gmail.com](mailto:diveen.jelal@gmail.com)

<sup>5</sup>MBChB, FIBMS-path, Department of Pathology, College of Medicine, Hawler Medical University, Erbil, Kurdistan Region, Iraq, [nawsherwan.sadiq@med.hmu.edu.iq](mailto:nawsherwan.sadiq@med.hmu.edu.iq) <sup>6</sup>MBChB, KBMS-candidate, Department of Hematology, Nanakali Hospital, Erbil, Kurdistan Region, Iraq, [rezhenbotany@gmail.com](mailto:rezhenbotany@gmail.com)

<sup>7</sup>MBChB, MRCP UK, FRCPath, Department of Hematology, Nanakali Hospital, Erbil, Kurdistan Region, Iraq, [drfiriad@hotmail.com](mailto:drfiriad@hotmail.com)

<sup>8</sup>MBChB, FKBMS, KBMS-candidate, department of Hematology, Hiwa Cancer hospital, Sulaymaniyah, Kurdistan Region, Iraq, [kanarj@gmail.com](mailto:kanarj@gmail.com)

<sup>9</sup>MBChB, MD, FIMBS, Department of Medicine, College of Medicine, University of Duhok, Duhok, Kurdistan Region, Iraq, [dr.abid.hassan@yahoo.com](mailto:dr.abid.hassan@yahoo.com)

<sup>10</sup>MBChB, FIBMS-path, Department of Pathology, College of Medicine, University of Sulaymaniyah, Sulaymaniyah, Kurdistan Region, Iraq, [haalrawi@yahoo.com](mailto:haalrawi@yahoo.com)

<sup>11</sup>MBChB, HDH, KBMS-candidate, Department of Hematology, Hiwa Cancer hospital, Sulaymaniyah, Kurdistan region, Iraq, [najmaddin.salih@gmail.com](mailto:najmaddin.salih@gmail.com)

<sup>12</sup>MBChB, FIBMS-path, FRCPath, Department of Pathology, College of Medicine, University of Sulaymaniyah, Sulaymaniyah, Kurdistan Region, Iraq, [dr.sanajalal612@gmail.com](mailto:dr.sanajalal612@gmail.com)

<sup>13</sup>MBChB, KBMS-candidate, Department of Hematology, Hiwa Cancer hospital, Sulaymaniyah, Kurdistan Region, Iraq, [akram.mahmood8590@gmail.com](mailto:akram.mahmood8590@gmail.com)

<sup>14</sup>MBChB, FRCP, PhD, Department of Medicine, College of Medicine, Hawler Medical University, Erbil, Kurdistan Region, Iraq, [mah\\_kawa@yahoo.com](mailto:mah_kawa@yahoo.com)

<sup>15</sup>MBChB, MSc, PhD hematopathology, Department of Pathology, College of Medicine, University of Sulaymaniyah, Sulaymaniyah, Kurdistan Region, Iraq, [dr\\_dana73@hotmail.com](mailto:dr_dana73@hotmail.com)

<sup>16</sup>MBChB -KBMS-candidate, MSc. molecular hemato, FIBMS-hematopath, Department of Pathology, College of Medicine, University of Duhok, Duhok, Kurdistan Region, Iraq, [ameer.ibrahim@uod.ac](mailto:ameer.ibrahim@uod.ac)

<sup>17</sup>MBChB, DM, CABM, FIBMS, FRCPath, Department of Medicine, College of Medicine, Hawler Medical University, Erbil, Kurdistan Region, Iraq, [dahmedk@yahoo.com](mailto:dahmedk@yahoo.com)

<sup>18</sup>MBChB, HDH, KBMS-candidate, Department of Hematology, Hiwa Cancer hospital, Sulaymaniyah, Kurdistan Region, Iraq, [banaz\\_mu@yahoo.com](mailto:banaz_mu@yahoo.com)

<sup>19</sup>MBChB, FIMS-hemato-oncology, Department of Hematology, Hiwa Cancer hospital, Sulaymaniyah, Kurdistan Region, Iraq, [basilonc@yahoo.com](mailto:basilonc@yahoo.com)

<sup>20</sup>MBChB, PhD-hematopathology, Department of Pathology, College of Medicine, Hawler Medical University, Erbil, Kurdistan Region, Iraq, [rawand.shamoon@med.hmu.edu.iq](mailto:rawand.shamoon@med.hmu.edu.iq)

## ABSTRACT:

Multiple myeloma (MM) is a malignancy of the plasma cells. The study aimed to know the clinical diversity of MM at presentation, the time lapse from the first symptoms to diagnosis, and the association of this time lapse with the International Staging System (ISS) of MM. This is a retrospective observational study that was performed on 176 patients who had MM and were admitted to Hiwa Hospital in Sulaimani, Nanakaly Hospital in Hawler, and Azadi Hematology - Oncology Center in Duhok, from October 2010 to December 2019. Demographic and detailed clinical features were recorded, and the ISS of MM was used to assess possible effects of time lapse on patients' outcomes. The mean  $\pm$  SD (standard deviation) of patients' age was 60.58  $\pm$  11.54 years, and the majority of the patients (52.27%) were from Sulaimani. Most of them had an O+ blood group and a body mass index (BMI) of more than normal (30.68%, and 63.63%, respectively). Most of the patients had bone pain,  $\geq 2$  lytic lesions,

hypocalcemia and hypercalcemia, and renal impairment and stage II and III of ISS of MM at the time of diagnosis (78.98%, 32.39%, 49.43%, 89.77%, and 75.1%, respectively). Furthermore, their mean  $\pm$  SD of time lapse from the first symptom to diagnosis was  $3.01 \pm 3.18$  months, and its association with ISS was none significant. The clinical features of MM at diagnosis are mostly nonspecific, and may be shared by a wide range of clinical conditions. However, patients who have fatigue, bone pain, renal impairment, pallor, and infective events should arouse the clinical suspicion of MM.

KEY WORDS: International Staging System (ISS); Kurdistan; Multiple myeloma; Time lapse

DOI: <http://dx.doi.org/10.21271/ZJPAS.32.6.10>

ZJPAS (2020) , 32(6):87- 99.

## 1. INTRODUCTION

Multiple myeloma (MM) is a malignancy of plasma cells preceded by its asymptomatic premalignant monoclonal gammopathy of undetermined significance (MGUS) (Eslick and Talaulikar, 2013; Shephard et al., 2015; Goldschmidt et al., 2016; Rajkumar, 2018; Koshiaris et al., 2018; Li et al., 2019). The plasma cells proliferate and accumulate in the bone marrow and locally destroy bones due to their secretion of monoclonal paraproteins, which signifies end-organ damage (Eslick and Talaulikar, 2013; Shephard et al., 2015; Goldschmidt et al., 2016; Koshiaris et al., 2018). It represents 1% of all cancers, and 10-20% of all hematological malignancies and its incidence increases with aging (Shephard et al., 2015; Goldschmidt et al., 2016; Rajkumar, 2018; Koshiaris et al., 2018). In the United States, more than 30000 patients per year are diagnosed with MM, the annual age-adjusted incidence is nearly 4 per 100000, and more than 12000 are dying due to this disease (Rajkumar, 2018). Also, MM accounts for 2% of all newly diagnosed cancers with an incidence of 5500 patients per year in the United Kingdom (Li et al., 2019). Multiple Myeloma is slightly more common in males; the male to female ratio is 1.3:1, and it is twice as common in African-Americans as compared with Caucasians (Shephard et al., 2015; Rajkumar, 2018). Moreover, the median of age at diagnosis is 64-65 years, and in adults, it is the second common hematological malignancy (Eslick and Talaulikar, 2013; Shephard et al., 2015; Goldschmidt et al., 2016; Rajkumar, 2018; Koshiaris et al., 2018).

The clinical features of MM are ill-defined and broad, especially the initial symptoms which may be nonspecific and pose difficulties for the patients and the clinicians in differentiating it from prodromes of other self-limiting benign diseases (Howell et al., 2013). Moreover, MM presents with a wide range of symptoms and signs, including anemia, hypercalcemia, renal impairment, bone pains, and increased risk of infection, and any combination of these symptoms should arouse the attention of MM diagnostic evaluation and workup (Eslick and Talaulikar, 2013; Rajkumar, 2018). Bone lesions are the leading cause of morbidity in MM, and characteristically osteolytic bone lesions of MM do not exhibit new bone formations. Further, nearly 1-2% of the patients at the time of diagnosis have an extramedullary disease, and later during the disease course, 8% will also develop it (Rajkumar, 2018).

The diagnosis of MM can be challenging due to the possible extended time between the onset of the symptoms, consulting frequent and different medical professionals, and then the diagnosis (Friese et al., 2009; Howell et al., 2013; Shephard et al., 2015; Howell et al., 2018). Some of the patients are diagnosed after emergency admissions to hospitals with a poorer prognosis (Howell et al., 2013; Friese et al., 2009). This time lapse between the onsets of the symptoms to the diagnosis is important because early diagnosis can improve the outcome, including less complication and decreased mortality, as well as better quality of life and satisfaction with care (Friese et al., 2009; Howell et al., 2013; Neal et al., 2015). Therefore, measures should be taken in order to aware patients and professionals in the primary care units for the sake of early diagnosis (Friese et al., 2009; Howell et al., 2013).

### \* Corresponding Author:

Truska Awat Amin

E-mail: [truska.hem@gmail.com](mailto:truska.hem@gmail.com)

### Article History:

Received: 05/08/2020

Accepted: 27/08/2020

Published: 20/12 /2020



The diagnostic workup of plasma cell abnormalities is by identifying the presence of monoclonal paraprotein, baseline hematological, and radiological assessments, as well as bone marrow biopsy (Eslick and Talaulikar, 2013). The radiological assessment of bone lesions can be performed through routine radiographs, low dose whole-body computed tomography (CT) scan, magnetic resonance imaging (MRI), and sometimes fluorodeoxyglucose positron emission tomography (PET) scans (Rajkumar, 2018).

The diversity of the clinical features of MM and, therefore, the difference in the time lapse between first symptoms and signs till diagnosis can be managed by educating the patients and medical professionals of the primary health care (Friese et al., 2009; Howell et al., 2013; Neal et al., 2015). Therefore, in the current study, we aimed to know the clinical diversity of MM at presentation, time lapse from the first symptoms to the diagnosis, and the association of this time lapse with the International Staging System (ISS) of patients afflicted with MM in Kurdistan Region, Iraq.

### Patients and Methods

The current study is a retrospective observational study that included 176 patients who had MM. The patients were hospital admitted to Hiwa Hematological and Oncological Hospital in Sulaimani, Nanakaly Hospital in Hawler, and Azadi Hematology - Oncology Center in Duhok, Kurdistan Region, Iraq, during the period from October 13, 2010, to December 3, 2019.

Research Ethical Committee of the Kurdistan Board of Medical Specialties (KBMS) approved the study proposal.

The inclusion criteria included all patients who had been diagnosed with MM, and the exclusion criteria were patients with MGUS, amyloidosis, and Smoldering myeloma.

The recorded information about the patients was collected from the electronic databases of the mentioned hospitals. The demographic features, including age, gender, body mass index (BMI), residency, and detailed history and clinical features, including the time lapse from the first symptoms and signs, were recorded. Also, the ISS

of MM was used to assess the effect of time lapse on the disease outcomes.

The "IBM SPSS Statistics version 25" program was used for the analysis of the data, and both descriptive and inferential statistics were used. Further, means and standard deviation (SD) were used for continuous variables, and frequencies, as well as percentages, were used for categorical variables. Also, the Chi-Square test was used to find out the significance of the association between categorical independent and dependent variable pairs. Besides, a *p*-value of ( $\leq 0.05$ ) was considered statistically significant associations.

### Results

The mean  $\pm$  SD (standard deviation) of the patients' age was  $60.58 \pm 11.54$  (ranged from 35 to 89 years), and the majority of the patients were in their fifth and sixth decades of life (Figure 1). Also, most of the patients were Kurdish males from the Sulaimani governorate (Figures 2-3). Further,

most of the patients had O+, followed by A+ and B+ blood groups, and a BMI of more than normal (i.e.,  $>25$ ) (Figures 4-5).

The majority of the patients were referred by internal medicine, orthopedics, followed by rheumatology and neurosurgery specialties (Table 1).

Most of the patients had bone pain, fatigue, and pallor (78.98%, 71.02%, and 53.98%, respectively).

Further, other clinical features are shown in Table 2.

The majority of the patients had two or more lytic lesions on skeletal radiographs, which were mostly affected skull, spine, and pelvis (Table 3).

The laboratory findings of the patients' investigation are shown in Tables 4 and 5. Peripheral blood plasma cells presence is shown in Table 6. Besides, the majority of the patients had a hypercellular feature on bone marrow aspiration and biopsy (Table 7). The serum and urine protein electrophoresis, serum and urine

immunofixation assessments of the MM patients at diagnosis are shown in Tables 5 and 8 respectively. Most of the patients had stage II and III of the International Staging of MM at diagnosis (Table 9).

The mean  $\pm$  SD of time lapse from the first clinical feature to the diagnosis was  $3.01 \pm 3.18$  months (ranged from 0.25 to 18 months). Furthermore, the study results showed statistically none significant association between the time lapse from the first clinical feature to the diagnosis assessed by the International Staging system of MM (Table 10).

### Discussion

Multiple myeloma (MM) is a cancer of the plasma cells of the bone marrow and its incidence increases among older ages; the median of age at diagnosis is 64-65 years (Eslick and Talaulikar, 2013; Shephard et al., 2015; Goldschmidt et al., 2016; Rajkumar, 2018; Koshiaris et al., 2018). In contrast, the mean age of the patients in the current study was about 60.6 years old, and the majority of them were in the fifth and sixth decade of their lives (Figure 1). Besides, the population in the developed world is getting older due to the advances in health care and stable lifestyles; the average life span in the west is about 77.5 years (WHO, 2020). However, this slight difference in the ages of the patients may be due to the differences in demographic and genetic backgrounds of our population to theirs.

Previous studies have shown that, MM was more common among males with a male to female ratio of 1.3:1 (Shephard et al., 2015; Rajkumar, 2018). And although a slight increase in the frequency of MM in males was comparatively observed in the current study, however the results were almost about the same; with a male to female ratio of 1.4:1 (Figure 2).

A study by Ino-Ekanem et al. (2018) in Nigeria showed no significant association between hematological cancers and ABO blood type of patients, although most of their patients had O blood type. Further, patients with MM had group III ABO discrepancies, i.e., discrepancies between forward and reverse groupings due to protein or plasma abnormalities that result in the rouleaux formation or pseudo-agglutination (Wilson and Jacobs, 2002). Therefore, ABO blood types are not reliable predictors for the diagnosis of MM,

although most of our patients had group O followed by group A and group B (Figure 4).

Significantly increased body weight has been identified as a risk factor for many malignant tumors. The majority (63.6%) of the patients in the current study had a BMI of more than normal (Figure 5). This finding is in accordance with the finding of the meta-analysis performed by Wallin et al., (2011), who found excessive body weight as a risk factor for MM.

The clinical features of MM are nonspecific and diverse in such a way that they usually pose difficulties in diagnosis, and the patients may seek different specialties to manage their suffering (Howell et al., 2013). This may be the reason in the current study for the referral of the patients by different specialties (Table 1). Besides, the majority of this study's patients complained of fatigue, followed by pallor, bone pain and pathological fractures, renal impairment and hypercalcemia, and infective events (Table 2). These symptoms were considered as arousal signals for suspecting MM in the literature (Eslick and Talaulikar, 2013; Rajkumar, 2018). Moreover, bone pain and pathological fractures are due to the osteolytic bone lesions that do not show new bone formation (Rajkumar, 2018). The radiographic bone scans of our patients showed about the same; the majority of our patients were afflicted with lytic bone lesions and osteopenia that caused multiple bone fractures (Table 3). The fractures of the bones had been suggested to be due to the proliferation and accumulation of the plasma cells and its secretion of monoclonal paraprotein in the bone marrow of the bones that are hematopoietically active in adults, such as vertebrae, ribs, and sternum, skull, pelvis, proximal epiphyseal regions of femur and humerus bones (Shephard et al., 2015; Koshiaris et al., 2018).

Most of the laboratory results of our patients showed anemia, renal impairment, high Beta-2 microglobulin, high ESR, leukocytosis, hypercalcemia, and bone marrow plasma cells (Tables 4 and 5). Peripheral blood plasma cells were not detected in 130 (73.86%) of the study patients and were present in 46 (5.11%) of them (Table 6). These laboratory findings were in accordance with the laboratory findings of previous studies (Eslick and Talaulikar, 2013;

Willrich MA, Katzmann, 2016; Rajkumar, 2018; Chowdhury, 2018; Hussain et al., 2019).

Further, most of the patients had hypercellularity on bone marrow aspiration and biopsy (Table 7) due to plasma cell proliferation in bone marrow (Eslick and Talaulikar, 2013; Shephard et al., 2015; Goldschmidt et al., 2016; Rajkumar, 2018; Koshiaris et al., 2018; Li et al., 2019). Also, the majority of the patients had high serum and urine IgG of 51.71% and 29.54%, respectively (Table 8). These findings were also in accordance with the study of Willrich et al. (2016) in which they found 52% of IgG in their patients who were diagnosed with MM.

We used ISS for the classification of MM in the patients, and the majority of the patients had grade II followed by grade III and grade I (Tables 9 and 10). These results were different from the results found by Goldschmidt et al. (2016), who could calculate the ISS for only 43 of their patients; the majority of their patients had grade I followed by grade II and grade III. However, the study of Byun et al. (2019) showed that the majority of their patients were in grade II followed by grade I and grade III. These differences in the frequencies of the stages of MM according to the ISS may be due to the differences in the study populations and the variability of the time lapse from the first symptom and sign to the diagnosis. Although the majority of the patients who had ISS stage II followed by stage III were diagnosed within five consecutive months' time lapse from the start of symptoms to the diagnosis, the association of this time lapse with the staging of MM was statistically none significant (Table 10). Besides, the majority of patients (85.5%) were diagnosed within five months from the first symptom, with an average of 3.01 months (about 91 days) (Table 10). This time lapse is less than what had been found in the study of Howell et al. (2013), who found an average time lapse of 163 days (about 5.4 months) from the first symptom to the diagnosis of MM. As it is shown in Table 10, this time lapse was quite variable and dispersed, and this may be the reason that its association with MM staging was not statistically significant.

**Table (1):** The clinical units where the MM patients referred from

The clinical area referred from	Frequency	Percent
Rheumatology	26	14.77
Neurosurgery	19	10.80
Internal medicine	42	23.86
Neuro-Medicine	2	1.14
Gynecology	2	1.14
Orthopedic	43	24.44
General surgery	2	1.14
Nephrology	10	5.68
Him/Herself	2	1.14
Cardiology	2	1.14
Oncology	2	1.14
Outpatient consultation	23	13.7
Total	176	100

**Table (2):** The clinical features of the MM patients

Clinical features	Frequency	Percent
Fatigue	125	71.02
Pallor	95	53.98
Bone pain	139	78.98
Pathological fracture	37	21.02
Renal involvement	36	20.46
Hypercalcemia	16	9.09
Infective event	8	4.55
Weight loss	3	1.70
Multiple vertebral bone lesion	2	1.14
Throat mass	1	0.57
Hepatomegaly	1	0.57
Portal vein thrombosis	1	0.57
Melena and weight loss	1	0.57
Pleural effusion	1	0.57
Advanced osteoporosis with multiple lytic lesion	1	0.57
Excessive sweating	1	0.57
Cervical lymphadenopathy	1	0.57
Joint pain	1	0.57

**Table (3):** Radiographic findings of the MM patients

Radiological findings		Frequency	Percent
	Lytic lesion	108	61.36
	Osteopenia	45	25.57
	Extraseous plasmacytoma of tonsil	1	0.57
	Degenerative change with disc prolapse	1	0.57
	Lumbosacral spine and right radius bone plasmacytoma	1	0.57
	Osteoporosis	3	1.70
Frequency of bone lesion	0	28	15.91
	1	42	23.86
	2	36	20.45
	>2	56	31.82
	>3	1	0.57
Site of Bone lesion	Spine	53	30.11
	Skull and spine	28	15.91
	Skull	10	5.68
	Skull and pelvis	5	2.84
	Skull, spine, and pelvis	12	6.8
	Pelvis and spine	12	6.8
	Spine and thoracic cage	4	2.27
	Pelvis	4	2.27
	Skull, spine, and humerus	3	1.70
	Skull, spine, and femur	2	1.14
	Femur	2	1.14
	Not recorded	41	23.30

**Table (4):** Laboratory hematological findings of the MM patients

Investigation results		Frequency	Percent
Hemoglobin (g/dl)	Mean $\pm$ SD (range)	10.01 $\pm$ 2.07 (4.9 to 16)	
	Anemia	155	88.07
Mean cell volume (MCV) in fL		90.4 $\pm$ 53.73 (8.4 to 769)	
White blood cell (WBC) ( $10^9$ cell/L)	Mean $\pm$ SD (range)	7.66 $\pm$ 5.54 (2.3 to 54)	
	Leukopenia (< 4)	26	14.77
	Normal (4 - 11)	126	71.59
	Leukocytosis (>11)	24	13.64
Platelet ( $10^9$ cell/L)	Mean $\pm$ SD (range)	211.09 $\pm$ 91.14 (13 to 615)	
	Thrombocytopenia (<150)	37	21.0
	Normal (150-450)	134	76.1
	Thrombocytosis (>450)	5	2.8
Erythrocyte sedimentation rate (ESR) (mm/hr)	Mean $\pm$ SD (range)	92.65 $\pm$ 40.92 (3 to 162)	
	Normal	7	3.98
	High	160	90.91
	Unknown	9	5.11
Bone marrow aspiration plasma cell	Mean $\pm$ SD (range)	35.45 $\pm$ 20.08 (4 to 85)	
Bone marrow biopsy plasma cell	Mean $\pm$ SD (range)	45.14 $\pm$ 21.99 (0 to 97)	

SD = Standard deviation

**Table (5):** Laboratory Biochemical and Metabolic findings of the patients

Investigation results		Frequency	Percent
S.Creatinine (mg/dl)	Mean $\pm$ SD (range)	1.83 $\pm$ 2.94 (0.1 to 31)	
	Low	9	5.11
	Normal	96	54.54
	High	71	40.34
B.Urea (mg/dl)	Mean $\pm$ SD (range)	52.77 $\pm$ 34.38 (2.6 to 200)	
	Low (<7)	5	2.84
	Normal (7-20)	13	7.39
	High (>20)	158	89.77
S.Ca <sup>++</sup> (mg/dl)	Mean $\pm$ SD (range)	10.03 $\pm$ 6.39 (4.4 to 90)	
	Low (<8.6)	44	25.00
	Normal (8.6-10.2)	89	50.57
	High (>10.2)	43	24.43
Total serum protein (g/dl)	Mean $\pm$ SD (range)	7.97 $\pm$ 2.34 (0.4 to 13.6)	
	Low (<6)	25	14.20
	Normal (6-8.3)	86	48.86
	High (>8.3)	65	36.93
S.Albumin (g/dl)	Mean $\pm$ SD (range)	3.91 $\pm$ 3.4 (1.9 to 36)	
	Low (<3.4)	74	42
	Normal (3.4-5.4)	98	55.7
	High (>5.4)	4	2.27
Beta-2 microglobulin ( $\mu$ g/mL)	Mean $\pm$ SD (range)	6.7 $\pm$ 25.64 (0.4 to 340)	
	Normal (0-3)	55	31.3
	High (>3)	118	67
	Unknown	3	1.7
Lactate Dehydrogenase (U/L)	Mean $\pm$ SD (range)	296.58 $\pm$ 171.46 (4.2 to 1055)	
	Low (<140)	26	14.77
	Normal (140-280)	53	30.11
	High (>280)	80	45.45
Serum uric acid (mg/dL)	Mean $\pm$ SD (range)	10.14 $\pm$ 30.67 (1.09 to 341)	
	Low	9	5.11
	Normal	78	44.32
	High	46	26.14
Serum protein electrophoresis (g/dL)	Mean $\pm$ SD (range)	2.86 $\pm$ 2.69 (0 to 24)	
	Mean $\pm$ SD (range)	57.12 $\pm$ 116.28 (0 to 970)	
	Urine protein electrophoresis (mg/dL)		

SD = Standard deviation

**Table (6):** Peripheral blood plasma cells

Status:	Frequency	Percent
Present:	46	5.11%
Absent:	130	73.86 %

**Table (7):** Bone marrow cellularity findings on aspiration and biopsies

Bone marrow cellularity	Frequency	Percent
<b>BM aspiration cellularity</b>		
Normocellular	46	26.14
Hypercellular	78	44.32
Hypocellular	6	3.41
Diluted	5	2.84
Not done	41	23.30
<b>BM Biopsy cellularity</b>		
Normocellular	34	19.32
Hypercellular	114	64.77
Hypocellular	4	2.27
Not done	24	13.64

**Table (8):** Immunofixation of patients' serum and urine

Immunofixation at diagnosis	Frequency	Percent
<b>Serum immunofixation</b>		
IgG	11	6.25
IgG and kappa	56	31.82
IgA and kappa	10	5.68
IgA and lambda	16	9.09
Kappa	6	3.41
IgG and lambda	23	13.07
Negative	15	8.52
Lambda	3	1.70
IgG, IgA and kappa	1	0.57
IgM and kappa	1	0.57
Unknown	34	19.32
<b>Urine immunofixation</b>		
IgG	4	2.27
IgG and kappa	32	18.18
IgA and kappa	4	2.27
IgA and lambda	7	3.98
Kappa	13	7.39
IgG and lambda	15	8.52
Negative	41	23.30
Lambda	6	3.41
IgG, IgA and kappa	1	0.57
IgM and kappa	1	0.57
Lambda and biconal	1	0.57
Not done	51	28.98

**Table (9):** Multiple myeloma staging of the MM patients

International Staging	Frequency	Percent
I	41	23.3
II	77	43.8
III	55	31.3

Unknown	3	1.7
Total	176	100

**Table (10):** Association of time lapse to the outcome assessed by the International Staging System

Time lapse to diagnosis (month)	International Staging of multiple myeloma			Total (%)	p-value*
	Stage I (%)	Stage II (%)	Stage III (%)		
0.25 - 5	34 (19.7)	71 (41)	43 (24.9)	148 (85.5)	0.349
6-10	5 (2.9)	4 (2.3)	8 (4.6)	17 (9.8)	
12	1 (0.6)	2 (1.1)	2 (1.1)	5 (2.9)	
18	1 (0.6)	0 (0)	2 (1.1)	3 (1.7)	
Total	41 (23.7)	77 (44.5)	55 (31.8)	173 (100)	

\* Measured by Chi-Squared test

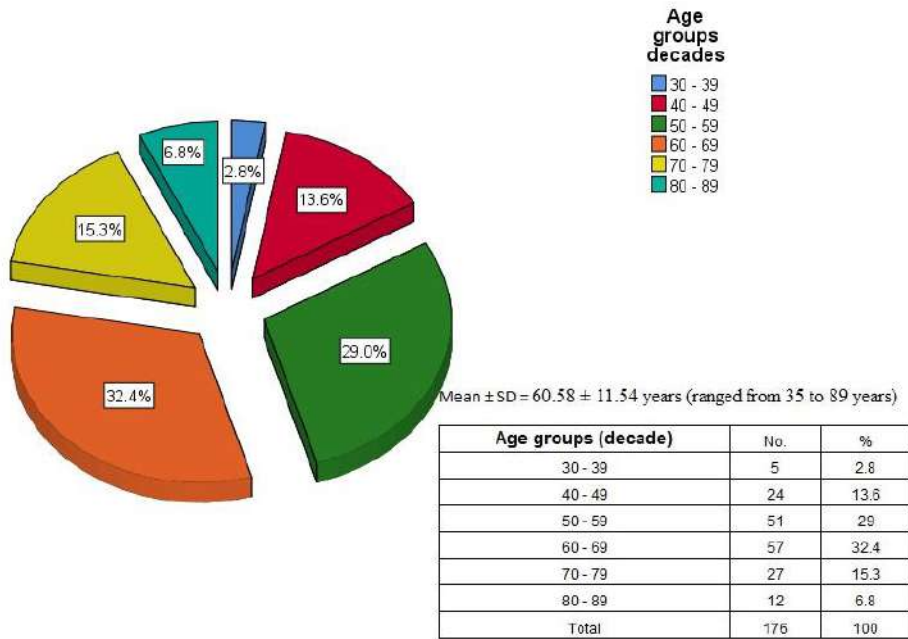


**Figure 1:** Age distribution of the MM patients



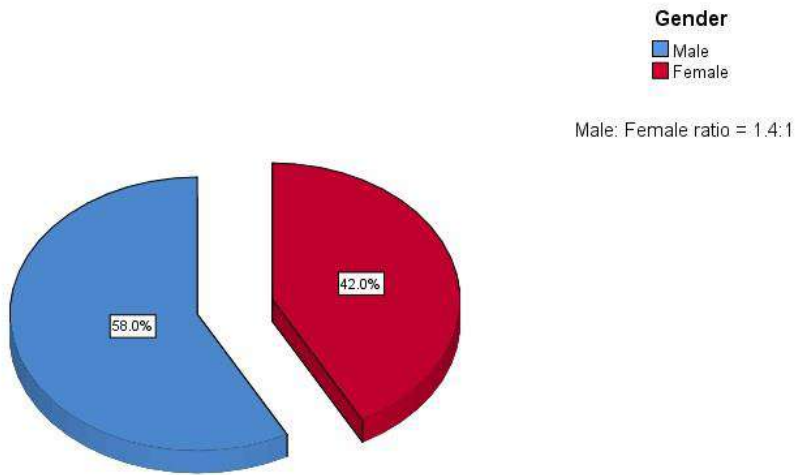


**Figure 2:** Gender distribution of the MM patients

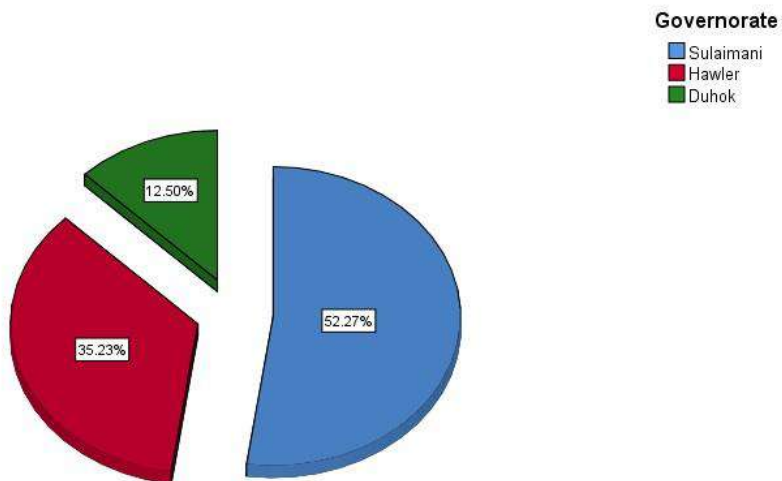


**Figure 3:** Residency of the MM patients

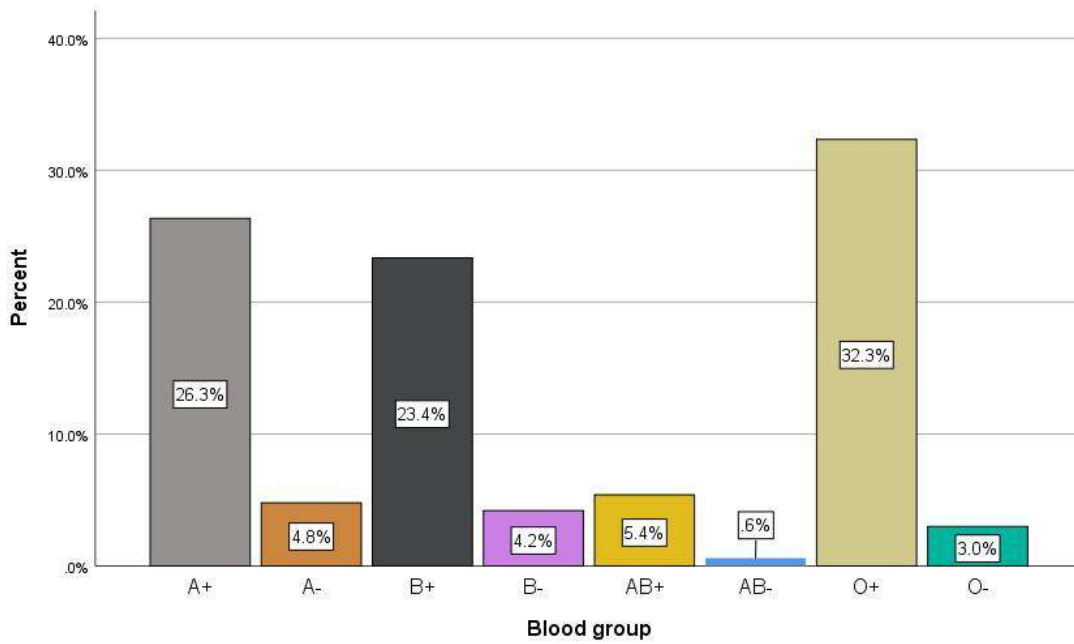


**Figure 4:** Blood groups distribution of the MM patients

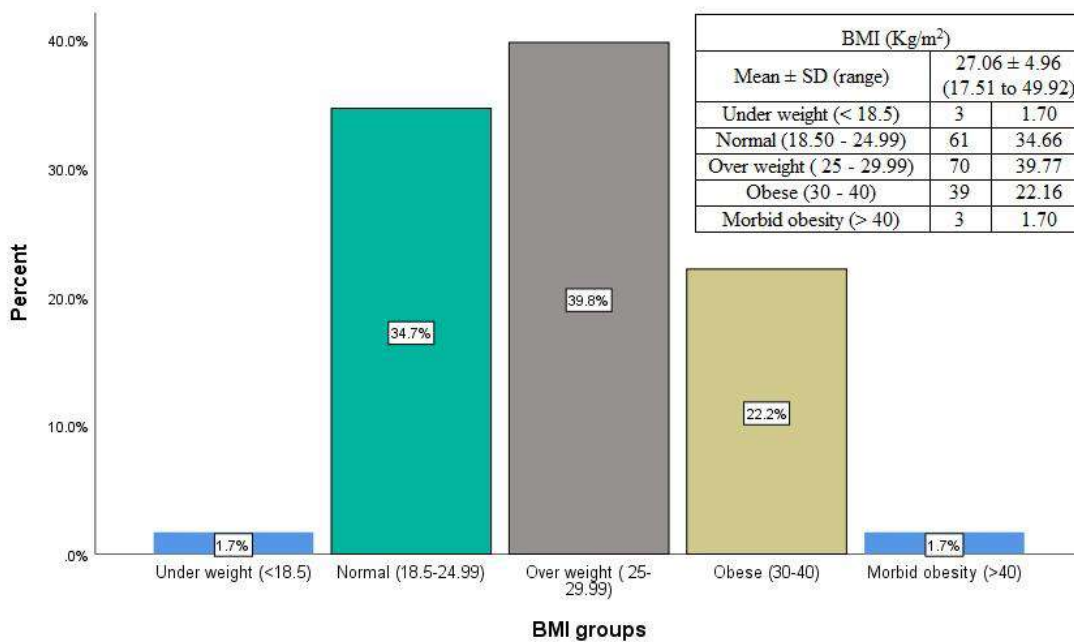


**Figure 5:** Body mass index (BMI) distribution of the MM patients

**Conclusions**

The clinical features of multiple myeloma (MM) are broad and nonspecific, which makes its diagnosis difficult. Furthermore, any patient who had fatigue, bone pain, renal impairment pallor, and infective events should arouse the possibility of MM diagnosis. We found no significant

association of the time lapse from the first symptom with the stages of MM, and we have the shortage of following the patients up after their treatment. Therefore, we suggest following up on the patients in order to know the effect of this time lapse on the patients' outcome after treatment

**Conflict of interest**

The authors declare no conflict of interest.

## References

- Byun JM, Kim D, Shin DY, Kim I, Koh Y, Yoon SS. Combination of Genetic Aberration With International Staging System Classification for Stratification of Asian Multiple Myeloma Patients Undergoing Autologous Stem Cell Transplantation. *In Vivo*. 2019;33(2):611-619.
- Chowdhury RK. A Clinical and Laboratory Profile of Multiple Myeloma. *J Enam Med Col*. 2018;8(3):159-64.
- Eslick R, Talaulikar D. Multiple myeloma: from diagnosis to treatment. *Aust Fam Physician*. 2013;42(10):684-8.
- Friese CR, Abel GA, Magazu LS, Neville BA, Richardson LC, Earle CC. Diagnostic delay and complications for older adults with multiple myeloma. *Leuk Lymphoma*. 2009;50(3):392-400.
- Goldschmidt N, Zamir L, Poperno A, Kahan NR, Paltiel O. Presenting Signs of Multiple Myeloma and the Effect of Diagnostic Delay on the Prognosis. *J Am Board Fam Med*. 2016;29(6):702-9.
- Howell DA, Hart RI, Smith AG, Macleod U, Patmore R, Cook G, et al. Myeloma: Patient accounts of their pathways to diagnosis. *PLoS ONE*. 2018;13(4):e0194788.
- Howell DA, Smith AG, Jack A, Patmore R, Macleod U, Mironska E, et al. Time-to-diagnosis and symptoms of myeloma, lymphomas and leukaemias: a report from the Haematological Malignancy Research Network. *BMC Hematol*. 2013;13(1):9.
- Hussain A, Almenfi HF, Almeddewi AM, Hamza MS, Bhat MS, Vijayashankar NP. Laboratory Features of Newly Diagnosed Multiple Myeloma Patients. *Cureus*. 2019 May 22;11(5):e4716.
- Ino-Ekanem MB, Ekwere TA, Ekanem AM. The Frequency and Distribution of ABO Blood Groups in Patients with Haematological Cancers in Uyo, Nigeria: A Hospital Based Retrospective Study. *IBRR*, 8(3): 1-8, 2018; Article no.IBRR.42665.
- Koshariis C, Oke J, Abel L, Nicholson BD, Ramasamy K, Van den Bruel A. Quantifying intervals to diagnosis in myeloma: a systematic review and meta-analysis. *BMJ Open*. 2018;8(6):e019758.
- Li J, Wang Y, Liu P. The impact on early diagnosis and survival outcome of M-protein screening-driven diagnostic approach to multiple myeloma in China: a cohort study. *J Cancer*. 2019;10(20):4807-4813.
- Neal RD, Tharmanathan P, France B, Din NU, Cotton S, Fallon-Ferguson J, et al. Is increased time to diagnosis and treatment in symptomatic cancer associated with poorer outcomes? Systematic review. *Br J Cancer*. 2015;112 Suppl 1(Suppl 1):S92-107.
- Rajkumar SV. Multiple myeloma: 2018 update on diagnosis, risk-stratification, and management. *Am J Hematol*. 2018;93(8):981-1114.
- Shephard EA, Neal RD, Rose P, Walter FM, Litt EJ, Hamilton WT. Quantifying the risk of multiple myeloma from symptoms reported in primary care patients: a large case-control study using electronic records. *Br J Gen Pract*. 2015;65(631):e106-13.
- Wallin A, Larsson SC. Body mass index and risk of multiple myeloma: a meta-analysis of prospective studies. *Eur J Cancer*. 2011;47(11):1606-15.
- Willrich MA, Katzmann JA. Laboratory testing requirements for diagnosis and follow-up of multiple myeloma and related plasma cell dyscrasias. *Clin Chem Lab Med*. 2016;54(6):907-19.
- Wilson JA, Jacobs A. ABO discrepancy in a multiple myeloma patient: a case study. *Clin Lab Sci* 2002;15(4):204-7.
- World Health Organization. Global Health Observatory (GHO) data; Life expectancy. Available from:[https://www.who.int/gho/mortality\\_burden\\_disease/life\\_tables/situation\\_trends\\_text/en/](https://www.who.int/gho/mortality_burden_disease/life_tables/situation_trends_text/en/). [Accessed July 26, 2020].

## RESEARCH PAPER

# Comparative effect of scarification and non-scarification of (*Pistacia atlantica*) seed in different media and environmental conditions.

Shilan Abdurrahman Mirsar<sup>1</sup>, Payman Hussein Aliehsan Pasha<sup>2\*</sup> and Hardy Kakakhan Awla Shekhany<sup>3</sup>

<sup>1,2,3</sup>Department of Forestry - College of Agricultural Engineering Sciences/ Salahaddin University-Erbil, Kurdistan region, Iraq

### ABSTRACT:

The effect of mechanical scarification on *Pistacia atlantica* seeds was studied on two different sites (indoor and outdoor) which has different environmental conditions in different media. The study examined 360 seeds (180 scarified and 180 non-scarified), 90 seeds were scarified on each site. Seeds sowed in three different media; Sandy soil, Compost and Peat moss. The statistical analysis applied on seedling parameters showed highly significant variation within-site level and between-site variation. The results of this study showed peat moss had best performance in most of parameters such as stem length 211.17mm, stem diameter 4.23mm, stem wet weight 6.04 mm, stem dry weight 2.59g, root length 484.42mm, root diameter 4.08mm, root wet weight 2.36g and root dry weight 1.08g. Also, interaction effect of scarification, indoor and Peat moss significantly increased all growth parameters.

KEY WORDS: scarification and non-scarification; *Pistacia atlantica* seed; different media.

DOI: <http://dx.doi.org/10.21271/ZJPAS.32.6.11>

ZJPAS (2020) , 32(6);100-107 .

## 1. INTRODUCTION

*Pistacia atlantica* is one of the most broadly distributed species of *Pistacia* which belongs to Anacardiaceae family. It is a deciduous tree which is drought resistance and very tolerant to dry and hot weather. The key roots grow vertically over the soil 2 to 6m or more in depth which allow plant to absorb water profound in the soil during drought period (Chelli-Chaabouni et al., 2010) It is native to North Africa and southern Europe into Turkey, Iran and the Middle East at elevations from sea level to 5,000 feet. According to the number of *Pistacia* cultivars and genotypes, one of the rich resources of *Pistacia* in the world is Iran (Mahmoodabadi et al., 2012).

*Pistacia atlantica* is mainly used for a variety traditional and industrial uses, including medicine and food such as blood clotting, throat infections , renal stones and gastralgia, periodontal disease (Farhoosh et al., 2008, Duru et al., 2003, Delazar et al., 2004). Also, tree nuts and their oils contain numerous bioactive and health-promoting components (Pourreza et al., 2008). According to Satil et al. (2003) fundamental oils of plants and their other products from minor metabolism have a great usage in food flavoring, folk medicine (Shekhany and Ahmed, 2018), fragrance, and pharmaceutical industries. *Pistacia* is typically propagated from seeds, and it might require more than 200 years for plants to reach one meter diameter and 25 meter in height (Zangeneh, 2003, Arefi et al., 2006). It is considered the greatest characteristic plant species of the pre-Saharan areas of the country (Yousfi et al., 2002). Stem elongation, leaf expansion and

### \* Corresponding Author:

Payman Hussein Aliehsan Pasha

E-mail: [payman.aliehsan@su.edu.krd](mailto:payman.aliehsan@su.edu.krd)

### Article History:

Received: 13/09/2019

Accepted: 10/08/2020

Published: 20/12 /2020

bud break occur during spring, level growth between late March and mid-May (Crane and Iwakiri, 1981). However, *Pistacia* is sensitive to spring frost, and it might fall flowers and new vegetative growth in April frost.

As different pretreatments were used to break seed dormancy of the seeds that have hard seed coat to enhance germination (Hamad and Ali, 2011), seed scarification has been widely studied to clarify its influence on germination and growth speed. It is noted that scarification was critically significant for seed germination (John et al., 2015). Chaodumrikul et al. (2016) stated that scarification has an advantage that can break dormancy and enhance seed germination, Yet, scarification also might lead to abnormal seedlings, embryo damage, and dead seeds (Bradbeer, 1988). The objective of this study was to evaluate the effect of scarification, different growing media (peat moss, compost and sandy soil) and environmental condition (indoor and outdoor) on growth of *Pistacia atlantica* seeds.

## 2. MATERIALS AND METHODS

### 2.1 Experiment Site

This study was conducted from 25th January 2018 to 25 August 2018 in Grdarasha research field, college of Agriculture, Salahaddin University-Erbil-Iraq at an altitude 436 meters above sea level (Latitude North 36.16°, longitude East 44.03°). Monthly averages of air temperature and relative humidity in this area were recorded throughout the experiments period and shown in Table 1.

**Table 1: Average of air temperature and relative humidity in outdoor during the period of the research.**

Year	Month	Average of air temperature °C	Average of air humidity %
2018	January	10.4	54.0
	February	12.5	63.0
	March	16.7	48.3
	April	21.3	39.1
	May	26.2	36.5
	June	32.7	17.9
	July	35.2	14.7
	August	35.2	16.7

### 2.2 Treatment and experimental design

The experiment was arranged in RCBD design with 36 treatment units, three replications and three factors. The first factor was included manually scarification and was carried out by clipping 180 out of 360 seeds, and the seeds were clipped opposite the embryo using a scalpel. The second factor was involved utilizing three types of soil; peat moss, compost and sandy soil, and the third factor included two different environmental conditions (indoor (under tunnel) and outdoor). Under tunnel, condition of average of air temperature (26.4°C) and air humidity (33.10 %) were recorded throughout the experiment period. In the experiment, seeds were put in polyethylene bags its size (30× 30× 45) (10 seeds planted into plastic bag). After rainfall season, the irrigation was performed for two days per week for all plants.

### 2.3 Parameters measurement

Length and diameter of stem and root for treatments were measured by (digital vernier caliper). The wet weight of stem and root was immediately measured by digital weighing after harvesting. In the lab, plants were dried in a hot air oven at 105 degrees oC, for at least 48 hours. Root and stem dry weight was obtained by weighing scale with accuracy of 0.0 g.

### 2.4 The statistical analysis

The results analyzed based on randomized complete block design (RCBD). The application treatments for the seedling growth experiment contain three media (peat moss, compost and sandy soil) with three replications; each replicate was contained ten seeds. All growth parameters were submitted to analysis of variance, the means were compared by least significant difference (L.S.D.) at probability level 0.05 for field, using (SAS Institute, 2005).

## 3. RESULTS AND DISCUSSION

### 3.1 Effect of seed scarification on the growth of *Pistacia atlantica*

Comparison between scarification and non-scarification seeds had no significantly differed for stem and root growth (Table 2). However,

Tigabu and Oden (2001) found that scarification treatment improve germination capacity and vigor of *Albizia gummifera* seeds, and mechanical scarification gave the highest germination and growth of plants. According to Valbuena and Vera (2002) germination of *Erica arborea* seeds can be increased by scarifying treatment.

### 3.2 Effect of growing media on the growth of *Pistacia atlantica*

A significantly positive effect of media on growth parameters was shown in Table 3. The seedlings which planted in peat moss were greater growth in term of stem length, stem diameter, stem wet weight, stem dry weight, root diameter, root wet weight and root dry weight (211.17mm, 4.23mm, 6.04g, 2.59g, 4.08mm, 2.36g, 1.08g respectively). However, root length was longer in compost soil (484mm) comparing with peat moss. This probably because compost does not keep water through it as peat moss keeps (Hasan et al., 2014); therefore, root in compost was longer attempting to find water. Although *Pistacia atlantica* gave the highest growth in peat moss, it is able to adopt with sandy soil. This is due to *Pistacia atlantica* is valuable species and can adopt with difficult environmental circumstances such as poor soil, low moisture in soil, hot and dry conditions (Hosseini et al., 2007).

### 3.3 Interaction effect of seed scarification and growing media on the growth of *Pistacia atlantica*

Scarified seeds in different media significantly differed in stem length, stem diameter, stem wet weight, root length, root diameter, root wet weight and root dry weight of seedlings (Table 4). Stem length in peat moss with non-scarification showed important difference (224.50mm), while the lowest stem length was observed in compost with non-scarification (97.00mm). However, stem diameter, stem wet weight, stem dry weight, root wet weight and root dry weight were highest in peat moss with scarification treatment (4.34mm, 6.32g and 2.68g, 2.57g and 1.12g respectively), and lowest in compost with scarification (2.40mm, 0.73g and 0.28g, 0.46g and 0.20g respectively). Root length was highest in peat moss with scarification (553.50mm), and lowest in sandy soil with non-scarification (282.17mm). Root diameter was highest in peat moss with non-scarification (4.09mm), nevertheless the lowest

was in compost with scarification (2.37mm). In general, soil type is an important factor that can be influenced on physical and morphological traits of seedlings (Gholami et al., 2007).

### 3.4 Interaction effect of seed scarification and environmental condition on the growth of *Pistacia atlantica*

Statistical analysis of interaction between environmental condition and scarification has shown strong differences in growth parameters (Table-5). The highest stem length, stem diameter, stem wet weight and stem dry weight was obtained at indoor with scarification treatment (179.78mm, 3.93mm, 5.02g and 2.06g respectively), but the lowest was observed in outdoor with scarification (86.22mm, 2.38mm, 0.70g and 0.25g respectively). Root length was highest outdoor with non-scarification (479.33mm), yet the lowest length of root was indoor with non-scarification (289.78mm). Root diameter was highest indoor with non-scarification (3.81mm) and the lowest diameter was outdoor with scarification treatment (2.36mm). Root wet weight and root dry weight were highest indoor with scarification (2.07g and 0.93g respectively), and they were lowest in outdoor with scarification treatment (0.41g and 0.16g respectively). It has been displayed that temperature is one of the most significant environmental factors which can affect *Pistacia* seeds during growth stages (Hedhly et al., 2005). Further, temperature regulates both germination and dormancy and also light regulates germination. Generally, high temperatures reinforce dormancy or it may even induce it, and low temperatures could also induce seed dormancy in some circumstances, yet in numerous species they are stimulatory (Pons, 2000, Baskin and Baskin, 2004). In addition, mechanical scarification is also considered as an efficient factor in promoting seed germination for growth (Medina-Sanchez and Lindig-Cisneros, 2005).

### 3.5 Interaction effect of growing media and environmental condition on the growth of *Pistacia atlantica*

The interaction effect between environmental condition and growing media displayed high differences on plant growth under tunnel and outdoor (Table-6). Stem length and stem diameter

were highest under tunnel with peat moss (304.50mm and 5.27mm respectively) and they were lowest in outdoor with sandy soil (85.00mm and 2.47mm respectively). Stem wet weight and stem dry weight also were highest at indoor with peat moss (10.59g and 4.55g respectively), however, they were lowest at indoor with compost (0.59g and 0.26g respectively). However, root length was highest outdoor with peat moss (542.50mm), but the lowest of root length was at indoor with sandy soil (227.50mm). Root diameter, root wet weight and root dry weight were highest at indoor with peat moss (5.10mm, 3.82g and 1.81g respectively), and they were lowest in outdoor with sandy soil (2.51mm, 0.47g and 0.19g respectively). These results of the seedlings growth illustrated the importance of media and climate during plant growth. Vilela and Ravetta (2011) stated that soil types strongly affect survival and growth of plants, for instance, nitrogen concentration in soil tends to raise allocation of carbon to stem and foliage that improves a species and makes plant a better competitor for light. It can be said that, *Pistacia atlantica* requires special conservation during the early stages of growth (Gholami et al., 2007), though this species can adopt with different environmental conditions (Jazireai and Rastaghi, 2003, Vargas et al., 1998).

### **3.6 Interaction effect of seed scarification, growing media and environmental condition on the growth of *Pistacia atlantica***

Statistically, significant differences were observed in growth parameters with different climate, media and scarification treatment (Table-7). Stem length was highest at indoor with peat moss and scarification (321mm), while lowest length of stem was in outdoor with peat moss and scarification (74.67mm). Stem diameter showed the highest at indoor with peat moss and scarification (6.08mm), but the lowest was outdoor with sandy soil and scarification (2.07mm). Stem wet weight and stem dry weight were highest at indoor with peat moss and scarification (12.13g and 5.22g respectively),

however, stem wet weight was lowest under tunnel with compost and scarification (0.44g). Stem dry weight was lowest in outdoor with scarification and peat moss (0.14g). Root length was greatest outdoor with compost and non-scarification (610.33mm), yet the lowest length of root showed at under tunnel with sandy soil and non-scarification (223mm). Root diameter was greatest under tunnel with peat moss and scarification (5.69mm), but it was lowest in outdoor with scarification and compost (2.31mm). Root wet weight and root dry weight were greatest under tunnel with peat moss and scarification (4.77g and 2.14g respectively), and they were lowest in outdoor with peat moss and scarification treatment (0.37g and 0.10g respectively). It is widely accepted that temperature is considered as an important factor controlling growth and development of plant, and seed germination is usually stimulated by temperature which interact positively and strongly with light and often with other factors including nitrate ions in the soil (Kakani et al., 2005). These results suggested that scarification with suitable environmental condition enhanced germination and growth because they may promote breaking of seed dormancy.

## **4. CONCLUSIONS**

This study presented that media is significant factor which can affect growth parameters of seed and seedlings of *Pistacia atlantica* in terms of stem length, stem diameter, root length, root diameter, stem dry weight, stem wet weight, and root wet weight and root dry weight). Using peat moss and scarification treatment under tunnel (indoor) have shown remarkable growth for parameters. The results have indicated that scarification treatments and environmental condition are important factors to enhance development and growth of *Pistacia atlantica* seed.

**Table 2: Effect of seed scarification on the growth of *Pistacia atlantica***

Treatment	Stem length (mm)	Stem diameter (mm)	Stem wet weight (g)	Stem dry weight (g)	Root Length (mm)	Root diameter (mm)	Root wet weight (g)	Root dry weight (g)
Scarification Seeds	133.00	3.15	2.86	1.16	381.06	3.06	1.24	0.54
Non-Scarification Seeds	141.67	3.50	2.64	1.14	384.56	3.46	1.29	0.60
L.S.D.> 0.05	N.S	N.S	N.S	N.S	N.S	N.S	N.S	N.S

**Table 3: Effect of selected media on the growth characteristics of *Pistacia atlantica***

Treatment	Stem length (mm)	Stem diameter (mm)	Stem wet weight (g)	Stem dry weight (g)	Root length (mm)	Root diameter (mm)	Root wet weight (g)	Root dry weight (g)
Sandy soil	97.08	2.77	0.81	0.35	280.00	2.64	0.69	0.31
Peat moss	211.17	4.23	6.04	2.59	384.42	4.08	2.36	1.08
Compost	103.75	2.98	1.39	0.51	484.00	3.07	0.76	0.35
L.S.D.> 0.05	48.62	0.57	1.60	0.71	139.47	0.52	0.52	0.24

**Table 4: Interaction effect of media and seed scarification on the growth of *Pistacia atlantica***

Treatment		Stem length (mm)	Stem diameter (mm)	Stem wet weight (g)	Stem dry weight (g)	Root length (mm)	Root diameter (mm)	Root wet weight (g)	Root dry weight (g)
Sandy soil	Scarification	104.00	2.72	1.54	0.52	285.83	2.76	0.71	0.32
	Non-Scarification	103.50	3.24	1.25	0.50	282.17	3.38	0.81	0.34
Peat moss	Scarification	197.83	4.34	6.32	2.68	553.50	4.07	2.57	1.12
	Non-Scarification	224.50	4.11	5.77	2.51	415.33	4.09	2.14	1.03
Compost	Scarification	97.17	2.40	0.73	0.28	303.83	2.37	0.46	0.20
	Non-Scarification	97.00	3.15	0.90	0.42	456.17	2.92	0.92	0.44
L.S.D. > 0.05		98.39	1.25	4.09	1.77	203.12	1.18	1.40	0.67



**Table 5: Interaction effect of environmental condition and seed scarification on the growth of *Pistacia atlantica***

Treatment		Stem length (mm)	Stem diameter (mm)	Stem wet weight (g)	Stem dry weight (g)	Root length (mm)	Root diameter (mm)	Root wet weight (g)	Root dry weight (g)
Indoor	Scarification	179.78	3.93	5.02	2.06	361.11	3.77	2.07	0.93
	Non-Scarification	164.89	3.66	3.83	1.61	289.78	3.81	1.61	0.82
Outdoor	Scarification	86.22	2.38	0.70	0.25	401.00	2.36	0.41	0.16
	Non-Scarification	118.44	3.33	1.44	0.67	479.33	3.11	0.97	0.39
L.S.D.> 0.05		88.96	1.06	3.60	1.58	177.17	0.97	1.21	0.56

**Table 6: Interaction effect of environmental condition and growing media on the growth of *Pistacia atlantica***

Treatment		Stem length (mm)	Stem diameter (mm)	Stem wet weight (g)	Stem dry weight (g)	Root length (mm)	Root diameter (mm)	Root wet weight (g)	Root dry weight (g)
Indoor	Soil	122.50	3.48	2.10	0.70	227.50	3.63	1.05	0.47
	Peat moss	304.50	5.27	10.59	4.55	426.33	5.10	3.82	1.81
	Compost	90.00	2.63	0.59	0.26	322.50	2.64	0.67	0.34
Outdoor	Soil	85.00	2.47	0.69	0.32	340.50	2.51	0.47	0.19
	Peat moss	117.83	3.18	1.49	0.64	542.50	3.06	0.89	0.34
	Compost	104.17	2.91	1.03	0.44	437.50	2.64	0.71	0.29
L.S.D.> 0.05		56.57	0.96	2.24	0.99	204.08	0.86	0.88	0.38

**Table 7: Interaction effect of environmental condition, growing media and seed scarification on the growth of *Pistacia atlantica***

Treatment	Stem length (mm)	Stem diameter (mm)	Stem wet weight (g)	Stem dry weight (g)	Root length (mm)	Root diameter (mm)	Root wet weight (g)	Root dry weight (g)
-----------	------------------	--------------------	---------------------	---------------------	------------------	--------------------	---------------------	---------------------

In Door	Soil	Scarification	129.00	3.36	2.49	0.79	232.00	3.19	0.98	0.43
		Non-Scarification	116.00	3.60	1.70	0.60	223.00	4.07	1.11	0.51
	pet moss	Scarification	321.00	6.08	12.13	5.22	508.33	5.69	4.77	2.14
		Non-Scarification	288.00	4.45	9.04	3.88	344.33	4.50	2.87	1.48
	Compost	Scarification	89.33	2.34	0.44	0.18	343.00	2.42	0.46	0.22
		Non-Scarification	90.67	2.93	0.74	0.34	302.00	2.86	0.87	0.46
Out Door	Soil	Scarification	79.00	2.07	0.58	0.24	339.67	2.32	0.43	0.20
		Non-Scarification	91.00	2.87	0.79	0.39	341.33	2.69	0.51	0.17
	Pet moss	Scarification	74.67	2.60	0.50	0.14	598.67	2.45	0.37	0.10
		Non-Scarification	161.00	3.76	2.49	1.13	486.33	3.67	1.42	0.58
	Compost	Scarification	105.00	2.45	1.02	0.38	264.67	2.31	0.45	0.17
		Non-Scarification	103.33	3.36	1.05	0.49	610.33	2.97	0.97	0.42
L.S.D.> 0.05			81.23	1.15	3.20	1.41	278.94	1.04	1.04	0.48

## 5. REFERENCES

- AREFI, H., ABDI, A., SAYDIAN, S., NASIRZADEH, A., NADUSHAN, H. M., Rad, M. H., AZDOO, Z. & ZIEDABADI, D. 2006. Genetics and breeding of *Pistacia atlantica* in Iran. *Acta Horti*, 726, 77–81.
- BASKIN, J. & BASKIN, C. 2004. A classification system for seed dormancy. *Seed Science Research*, 14, 1–16.
- BRADBEER, J. W. 1988. *Seed Dormancy and Germination*. Springer Verlag.
- CHAODUMRIKUL, S., KAEWSORN, P., CHULAKA, P. & CHANPRASERT, W. 2016. Breaking seed dormancy in smooth loofah (*Luffa cylindrica* (L.) M. Roem.) using scarification and dry heat treatment. *Agriculture and Natural Resources*, 85–88.
- CHELLI-CHAABOUNI, A., BEN MOSBAH, A., MAALEJ, M., GARGOURI BOUZID, R. & DRIRA, N. 2010. In vitro salinity tolerance of two pistachio rootstocks: *Pistacia vera* L. and *P. atlantica* Desf. *Environmental and Experimental Botany*, 69, 302–312.
- CRANE, J. & IWAKIRI, B. 1981. Morphology and reproduction in pistachio. *Hort.*, 3, 379–393.
- DELAZAR, A., REID, R. & SARKER, S. 2004. GC-MS analysis of the essential oil from the oleoresin of *Pistacia atlantica* var. *Mutica*. *Chem. Nat. Compd*, 40, 24–27.
- DURU, M. E., CAKIR, A., KORDALI, S., ZENGİN, H., HARMANDAR, M., IZUMI, S. & HIRATA, T. 2003. Chemical composition and antifungal properties of essential oils of three *Pistacia* species. *Fitoterapia*, 74, 170–176.
- FARHOOSH, R., TAVAKOLI, J. & KHODAPARAST, M. H. H. 2008. Chemical composition and oxidative stability of kernel oils from two current subspecies of *Pistacia atlantica* in Iran. *Journal of the American Oil Chemists' Society*, 85, 723–729.
- GHOLAMI, S., S, H. & SAYAD, E. 2007. Effect of soil, sowing depth and sowing date on growth and

- survival of *Pistacia atlantica* seedlings. *Pak. J. Biol. Sci.*, 10, 245-249.
- HAMAD, S. & ALI, O. 2011. Effect of Some Pretreatments and Sowing Periods on Seed Germination Percentage of *Acacia farnesiana*, *Gleditsia Triacanthos* and *Robinia Pseudoacacia* in the Plastic House. *Zanco Journal of Pure and Applied Science*, 23, 44-50.
- HASAN, A. E., BHIAH, K. M., & AL-ZURFY, M. T. 2014. The impact of peat moss and sheep manure compost extracts on marigold (*Calendula officinalis* L.) growth and flowering. *Journal of Organic Systems*, 9, 56-622.
- HEDHLY, A., HORMAZA, J. I. & HERRERO, M. 2005. Influence of genotype-temperature interaction on pollen performance. *J. Evol. Biol.*, 18, 1494-1502.
- HOSSEINI, S., GHOLAMI, S. & SAYAD, E. 2007. Effect of Weed Competition, Planting Time and Depth on *Pistacia atlantica* Seedlings in a Medi-terranean Nursery in Iran. *Silva Lusitana* 15, 189-199.
- JAZIREAI, M. H. & RASTAGHI, M. E. 2003. Silviculture of Zagros forests.
- JOHN, L., WILLIS, M. B., WALTERS, K. W. B. & J, G. 2015. Scarification and gap size have interacting effects on northern temperate seedling establishment. *Forest Ecology and Management*, 347, 237-247.
- KAKANI, V. G., REDDY, K. R., KOTI, S., WALLACE, T. P., PRASAD, P. V. V., REDDY, V. R. & ZHAO, D. 2005. Differences in in vitro pollen germination and pollen tube growth of cotton cultivars in response to high temperature. *Ann. Bot.*, 96, 59-67.
- MAHMOODABADI, S., PANAHI, B., AGHARAHIMI, J. & SALAJEGHEH, F. 2012. *Environ. Sci.*, 6, 81-86.
- MEDINA-SANCHEZ, E. & LINDIG-CISNEROS, R. 2005. Effect of scarification and growing media on seed germination of *Lupinus elegans* H.B.K. *International Seed Testing Association*, 33, 237-241.
- PONS, T. 2000. Seed responses to light. In: Fenner M, ed. *Seeds-the ecology of regeneration in plant communities*. 237-260.
- POURREZA, M., SHAW, J. & ZANGENEH, H. 2008. Sustainability of wild pistachio (*Pistacia atlantica* Desf.) in Zagros forests, Iran. *Forest Ecology and Management*, 255, 3667-3671.
- SAS INSTITUTE, C. N., USA, 2005.
- SATIL, F., AZCAN, N. & BASER, K. H. C. 2003. Fatty acid composition of pistachio nuts in Turkey. *Chemistry of natural compounds*, 39, 322-324.
- SHEKHANY, H. & AHMED, H. 2018. The study of chemical composition of gum in *Pistacia atlantica* in Erbil region. *Zanco Journal of Pure and Applied Science*, 30, 26-32.
- TIGABU, M. & ODEN, P. C. 2001. Effect of scarification, gibberellic acid and temperature on seed germination of two multipurpose *Albizia* species from Ethiopia. *Seed Sci. and Technol.*, 29.
- VALBUENA, L. & VERA, M. L. 2002. The effects of thermal scarification and seed storage on germination of four heathland species. *Plant ecology*, 161, 137-144.
- VARGAS, F. J., ROMERO, M. A. & CLAVE, J. 1998. Nursery behaviour of Pistachio rootstocks. Second international symposium on pistachio and Almonds, ISHS, Davis (California. USA). *Acta Hort.*, 470, 231-236.
- VILELA, A. E. & RAVETTA, D. A. 2011. The effect of seed scarification and soil media on germination, growth, storage and survival of seedlings of five species of *prosopis* L.(mimosacea). *Arid Environ.*, 48, 171-184.
- YOUSIF, M., NADJEMI, B., BELLAL, R., BEN BERTAL, D. & PALLA, G. 2002. Fatty acids and sterols of *Pistacia atlantica* fruit oil. *JAOCs*, 79, 1049-1050.
- ZANGENEH, H. 2003. Ecological requirements of *Pistacia atlantica* in Kermanshah Province, Iran. *J. For. Poplar Res. Special issue: The Second National Symposium on Wild Pistachio*, 122-130.

## RESEARCH PAPER

# Straw Throwing Method and Tractors Forward Speed Impacts on the Straw Picking Up and Chopping Machine's Performance

Affan O. Hussein\*

\* Department of Plant Protection, Khabat Technical Institute, Erbil Polytechnic University, Erbil, Kurdistan Region, Iraq.

### ABSTRACT

Wheat straw is a valuable by-product of grain harvesting in Kurdistan region basically for livestock feeding. It is thrown behind the harvester on the ground in different forms like heaps, windrows or spread in the field. Straw collecting in the field needs a lot of labor; it is also a costly and time-consuming operation. Recently, there has been a new operation in the field of straw chopping machines which picks up the straw from the ground, cuts and blows it to a trolley and all of this in one operation. This study was conducted to find the effect of some operational factors on the machines performance. The results show that collecting the straw as windrows in the field by the straw chopping machine gives better performance than the heaps. A tractor with 72 HP is sufficient for operating the straw picking-up and chopping machine with a trolley behind. Five different forward speeds (S1=3.12, S2=4.22, S3=5.21, S4=6.31 and S5=7.51) km/h were examined for straw picking-up and chopping as windrows to find their effects on the performance of the machine, it was found that with S3 or S4, the machine shows the best performance in terms of fuel and time consumption, throughput capacity, straw recovery, throughput efficiency and acceptable slippage percentage.

KEY WORDS: straw chopping machine, straw heaps, wheat straw, windrow.

DOI: <http://dx.doi.org/10.21271/ZJPAS.32.6.12>

ZJPAS (2020) , 32(6);108-115 .

### 1. INTRODUCTION

Wheat straws are an agricultural by-products consisting of the dry stalks after the grain and chaff have been removed. The grain ratio to the straw is about 1:1.5 to 1:2.0 Chandrasekaran *et al.* (2010). Straws have a number of different uses such as a fodder for livestock and bedding or for the paper industries and as biomass fuels (Vink, 2015).

In the Kurdistan region of Iraq, the main use of straws is as a livestock fodder which are produced as there are about 0.75 million hectares of

cultivated area annually with cereal crops consisting mainly of wheat and barley, and its yield is around 1 million tons (Ministry of planning, 2017). This results in nearly about 1.5 million tons of straw. Straws are always thrown behind the combine harvester in three forms: (1) directly on the ground as windrows, (2) thrown as heaps on the ground by a gathering mechanism equipped onto the harvester and it is pre-adjustable to a desired weight - which is the most common method used by farmers in the Kurdistan region of Iraq, and (3) cutting and spreading the straws in the field in one operation by the harvester for conservative agriculture Suradi *et al.* (2020). Loose straws are low in bulk density, irregular in size and shape, difficult to handle manually and difficult to transport and store. The straw in its original form is labor-intensive and costly as it should be transformed to a regular and dense form to facilitate its transportation and storage Gummert *et al.* (2020).

#### \* Corresponding Author:

Affan Othman Hussein

E-mail: [affan@epu.edu.iq](mailto:affan@epu.edu.iq)

#### Article History:

Received:29/05/2020

Accepted: 24/08/2020

Published:20/12/2020

Whenever combined harvesters are being used for crop harvesting, the straw which is left behind has a disposal problem. This is for the fact that it should either be collected manually, which is a laborious and a time-consuming job, or balers could be used to make bundles later to be copped to smaller particles according to the purpose of use. Recently, farmers have adopted an in-field straw picking-up and chopping machine which in one operation collects, cuts into the desired forms, and blows the straw through a tunneled pipe to a closed trolley trailing behind it. The straw chopping machine is power operated, gets its drive from tractor's PTO shaft and a small multi-purpose tractor of 75HP is sufficient to run a straw combine harvesting machine, this type of machines in addition to the three tasks (picking up, chopping, and blowing) it also cuts the remained stables in the field Mahmood *et al.* (2016).

Straw picking-up and chopping machine's performance is affected by many factors including straw moisture content during the time of collecting, straw density on the field and the forward working speed of the mechanical units Ankit *et al.* (2018). The field capacity and fuel consumption of any farm machines is considered as an important economic indicator for a successful work performance Gursoy *et al.* (2015). The forward speed of the in-field straw picking-up and chopping machine has a significant effect on the field capacity, field efficiency and fuel consumption. In other words, by increasing the forward speed, the field capacity and field efficiency decrease. On the other hand, the stability of the machine on the ground will be affected by the extra forward speed causing high rate of slippage percentage which leads to power and time losses Mahmood *et al.* (2016). Fuel consumption in most farm machines depends on the forward speed. Sometimes the various manufacturing designs of the same functioning machines affect the fuel consumption Kumar *et al.* (2017). The method of picking up straws affects the quality and quantity of the work done Afify *et al.* (2002).

The slippage percentage is one of the indicators of the performance of the tractor and the straw picking-up and chopping machines; limitation or reducing the slippage percentage leads to a good, economic and effortless work (Al-Auobi and Taha,

2009). The tractor driver's skills can decrease the slippage ratio according to the type of the agricultural operation Thakur *et al.* (2018). From an economic perspective, the cost of fuel represents at least 16% and it could reach a 45% of the hourly costs of an agricultural tractor, and this represents the largest share of the total cost of an hour of machine work Farias *et al.* (2017).

The objective of this study was to obtain the best combination of working parameters in the field for best performance of the straw picking up and chopping machine, because it is recently introduced to the region and no scientific studies have been done on it yet.

## 2. MATERIALS AND METHODS

The experiment was carried out after the wheat harvesting process in 10/6/2019 in a private field in Kharabadraw village, located 18 km northwest from Erbil city center in the Kurdistan Region of Iraq, the field was planted with wheat (*Triticum spp.*). The field was a normal leveled land with some natural girders. Crop harvested (10) cm above the ground by a combined harvester when the grain moisture content reached around 16%, the moisture content was determined according to the ASABE standard S358.2, (2008).

Two areas in the same field had been selected for the experiment; the first area was 0.4 hectare for throwing the straw behind the combine harvester in heaps forms on the ground (STH), the second area was 2 hectare for throwing the straw as windrows (STW), to study their effects on the performance of the straw picking up and chopping machine drawn by the tractor. The travelling distance of the tractor with the straw chopping machine and the trolley were limited by 200 m line long by placing guide poles in the beginning and the end of the distance as indicators.

Two experiments were conducted. First one was for comparing between picking up and chopping straws as heaps and picking up and chopping as windrows by a straw picking up and chopping machine with closed trolley trailing behind the chopping machine and both are drawn by a tractor with a forward speed limited by 3 km/h according to the straw density situation on the ground Mahmood *et al.*, (2016). Second experiment

was applied for comparing different forward speeds ( $S_1=3$ ,  $S_2=4$ ,  $S_3=5$ ,  $S_4=6$  and  $S_5=7$ ) measured in km/h for selecting the ideal forward speed for wheat straw picking up and chopping as windrows. All the experiments were conducted using a straw picking up and chopping machine type (Özen iş) Turkish made. The technical specifications of the chopping machine were (pickup reel width 175cm, cutting unit is rotary drum with blade system, 48HP need for operating, field capacity 1.9 ton/h and 540 rpm need from the P.T.O). The straw picking up and chopping machine and the trolley are drawn by a universal tractor (New Holland TD75D, 2004, Turkish made, pneumatic, 4 wheel drive, 4 cylinder, 72HP at 2500 rpm and P.T.O single speed of 540 rpm at 1800 engine rpm) figure (1).



**Figure 1.** Tractor, straw picking up and chopping machine, and trolley.

The mechanical units moved 10 m before reaching the guide poles toward the experimental lines to take its stability and desired speed for each treatment. The time spend for cutting the distance was recorded by a digital stopwatch in the starting pole and at the end of the line without any loads and later with loads to calculate the slippage percentage of the mechanical units. The chopped straws in the trolley for each line were collected and weighed and converted to tons in hectare area base.

The performance of the straw picking up and chopping machine was evaluated according to the following indicators:

- 1) Mechanical units stopping numbers measured by normal counting.
- 2) Straw recovery percentage calculating equation driven from the equation formed by Ankit *et al.* (2018) as follows:

$$SR = \frac{SPU}{SOG}$$

Where: **SR** = straw recovery (%), **SPU** = straw picked up (g/m) and **SOG** = straw on the ground (g/m). For the heaps form the straw recovery were determined by weighing 4 heaps from 4 straw lines as heaps and the average weight was calculated, as for determining the windrow straw form recovery, the straw weight of 4 times of 5m long in 4 straw line as windrows was taken and their average weight has been calculated. The chopped straw in the trolley for each line collected and weighed and converted to tons in one-hectare area base (the area containing loose straw were excluded in this operation).

- 3) Effective throughput capacity, the concepts of theoretical and effective capacity are also applicable to throughput capacity. Throughput is based on time, but because the throughput usually refers to the flow of material through a machine, the units may be different from those used for capacity. For example, the performance of a baler could be evaluated using units of bales per hour or tons per hour, the principles of field working of straw chopping machine is the same as for the balers in the picking up mechanism and the feeding inside the machine; hence, the same equation formed by (Field and John, 2007) is applied as follow:

$$ETC = \frac{WSR}{T}$$

Where: **ETC**= Effective throughput capacity (ton/h), **WSR**= weight of straw picked up (ton) and **T**= time (h).

- 4) Slippage percentage calculated according to the equation formed by (Albanna, 1990) as follow:

$$S.P = \frac{Vt - Vp}{Vt} \times 100$$

Where S.P= slippage percentage (%).  
**Vt** = Theoretical speed (without load), km/h.  
**Vp** = Practical speed (with load), km/h.

- 5) Fuel consumption was determined using the volumetric method by refilling the fuel tank with a graduated cylinder (Hunt, 2001), fuel consumption calculated according to the

equation suggested by (Jasim and Jebur, 2015) as follow:

$$F.C. = \frac{q.d \times 10000}{B.p \times s \times 1000}$$

Where  $F.C.$  = fuel consumption (L/ha),  $q.d$  = fuel consumed in one round (ml).  $B.p$  = actual working width (m) and  $S$  = distance of one round (m).

6) Throughput efficiency is used instead of field efficiency to describe machines that handle or process a product, such as grain augers, balers, forage harvesters, and combines. The throughput efficiency was determined according to the equation formed by (Field and John, 2007) as follows:

$$TE = \frac{ETC}{TTC} \times 100$$

Where:  $TE$  = throughput efficiency (%),  $ETC$  = effective throughput capacity (ton/h),  $TTC$  = theoretical throughput capacity (ton/h).

Theoretical throughput capacity was given in the technical specification brochure of the straw picking up and chopping machine.

Statistically the experiments were carried out by applying the randomized complete block design (RCBD) with four replicates for each treatment. 24 lines were specified, each line considered as a block and replicate, 4 lines for heap form and 20 lines for windrow form. The data was analyzed using SAS program according to the

applied design, and the least significant differences test (LSD test) and T. test applied to compare between the means at ( $p \leq 0.01$ ) and ( $p \leq 0.05$ ).

### 3. RESULTS AND DISCUSSION

#### 3.1. Experiment 1

Table (1) shows the effect of the wheat straw throwing method on some performance parameters of the straw picking up and chopping machine. Significant differences ( $P < 0.01$ ) were found in the stopping number of the mechanical units between (STH) and (STW), the means were (112, 5) stop/ha respectively, reducing the number of stopping during working leads to extending of machines and mechanical parts lifespan as well as a reduction in the total working time as it is shown also in the table which the average time taken for straw picking up and chopping machine was (01:38, 01:19) h/ha for (STH) and (STW) respectively.

The straw chopping machine throughput capacity was also significantly lower when using (STH) method compared to the (STW) method and the averages were (1.565, 1.685) ton/h respectively, this increase is due to continually picking up straw from the ground when it is thrown as windrows. For the same reason, there were significant differences in the mean of throughput efficiency of straw picking up and chopping machine, the values were (82%, 88.5%) for (STH) and (STW) respectively. The table shows that there were non-significant differences in straw recovery percentages between both methods.

**Table 1:** Effect of straw throwing method on the performance of the straw picking up and chopping machine

Parameters	Straw throwing form as	
	Heaps (STH)	Windrows (STW)
Number of mechanical working units stop per hectare	112±3.2	5**±0.51
Time required for straw picking up and chopping, (h/ha)	01:38±0:06	01:19*±0.05
Throughput capacity, (ton/h)	1.565±19	1.685*±23.9
Throughput efficiency, (%)	82±1.8	88.5*±1.96
Straw recovery, (%)	83±1.6	86±2.1

<b>Fuel consumption, (L/ha)</b>	5.9±0.12	4.6*±0.1
<b>Slippage percentage, (%)</b>	N	1.9 ±0.09

(\*), (\*\*) within the rows indicates to significant differences between means under probability level of ( $P \leq 0.05$ ), ( $P \leq 0.01$ )

Fuel consumption was significantly higher for (STH) compared with (STW) as it shown in the table, the averages were (5.9, 4.6) L/ha respectively, the reason of increasing in the fuel consumption is having an increase in the number of stops when using (STH) method which requires more working time to complete the specified area. Generally, the fuel consumption was within the acceptable ranges which were determined by Grisso *et al.* (2010) for the hay pickup and chopping machines.

### 3.2. Experiment 2

The actual forward speeds in the field without any breakage and clogging were ( $S_1=3.12$ ,  $S_2=4.22$ ,  $S_3=5.21$ ,  $S_4=6.31$  and  $S_5=7.51$ ) km/h; working speeds were not exactly like as proposed in the methods of the experiment. Effects of forward speeds on the time spent by the straw picking-up and chopping machine as windrows in the field are shown in the figure (2). In general, the time spent for straw picking up and chopping machine decreased as the forward speed increased and the averages were (1:19, 1:09, 0:54, 0:43, and 0:34) h/ha for all forward speeds respectively. The shortest time recorded with  $S_5$  and the longest time spend was with  $S_1$ ; the reason of reduction was that there were not any stops during the work process, so it's common sense to say that the faster speed will complete its task sooner. There were non-significant differences between  $S_4$  and  $S_5$ .

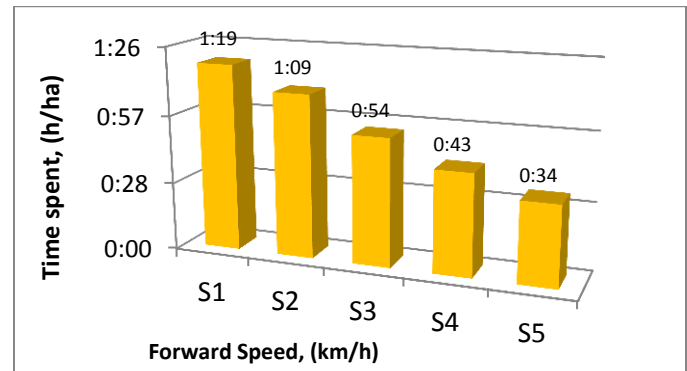


**Figure 2.** Effect of forward speed on the time spent for straw picking up and chopping machine.

Figure (3) shows the effect of the forward speed on the straw picking up and chopping machine's throughput capacity. As it can be seen that increasing the forward speed of the machine from  $S_1$  to ( $S_2$ ,  $S_3$ ,  $S_4$ , and  $S_5$ ) gradually did not cause any significant differences on the throughput capacity. The means of the throughput capacities were (1.685, 1.680, 1.678, 1.675 and 1.645) ton/h respectively, although there was a mathematical decrement with  $S_5$  when compared with other speeds: this decreasing is attributed to the instability of the mechanical units in high speeds and non-synchronization between the tractor forward speed and the picking up reel fingers of the straw picking up and chopping machine which leads to skipping of some straw stems on the ground and losses occur due to it. These results contradict the results found by Ankit *et al.* (2018).



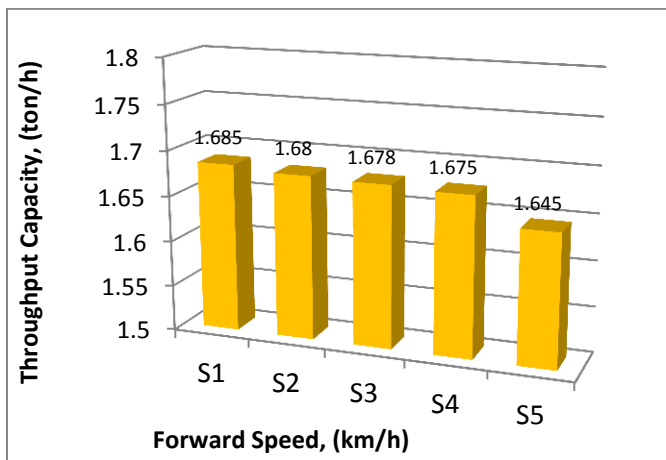


**Figure 3.** Effect of forward speed on the throughput capacity of straw picking up and chopping machine.

The effect of the forward speed on the throughput efficiency of the straw picking up and chopping machine is shown in figure (4). As it can be seen there is a slight mathematical gradually decreasing in the throughput efficiency of the straw picking up and chopping machine by increasing the forward speed from  $S_1$  to  $S_5$ , the averages were (81, 81, 80, 79, and 77) % respectively. The reason of having a drop in the straw chopping machine throughput efficiency is due to the reduction of throughput capacity when the forward speed increased because the throughput efficiency basically depends on the theoretical throughput capacity and effective throughput capacity as a numerator in the equation, and it is usually lower than theoretical throughput capacity Mahmood *et al.* (2016).

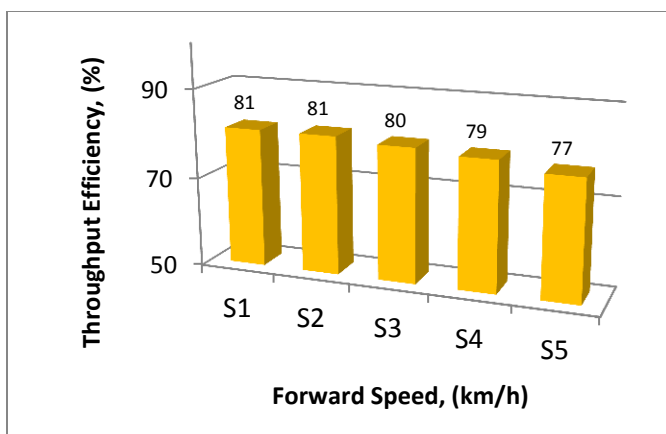


**Figure 4.** Effect of forward speed on the throughput efficiency of straw picking up and chopping machine

The straw recovery of the picking up and chopping machine was not statistically affected by the forward speed as it shown in figure (5). The straw recovery means for the speeds were (86, 86, 85, 85, 83),

85, 85 and 83) % respectively. Increasing the forward speed to  $S_5$  caused a slight mathematical decreasing in straw recovery of the machine. These results contradict the results obtained by Ankit *et al.* (2018) because the range of the forward speed they used for straw combining harvester was (1.5 to 2.5) km/h, this range was smaller than the least speed in this study.

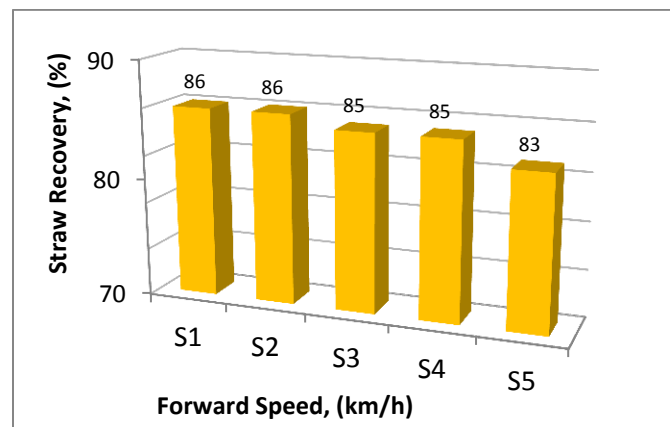


**Figure 5.** Effect of forward speed on the straw recovery of straw picking up and chopping machine

Figure (6) illustrates the effect of forward speed on the fuel consumption of the straw picking up and chopping machine. Increasing the forward speed significantly affected on the fuel consumption of straw picking up and chopping process. Fuel consumption averages for the forward speeds were (4.6, 4.2, 3.8, 3.3 and 3) L/ha respectively. The main reason of this reduction in fuel consumption was the constant speed of the tractor engine rpm for all operations for all treatments which was limited by 1800 rpm to keep the PTO shaft running at 540 rpm. These results agree with Anjum *et al.* (2015). The least amount of fuel consumption was with the  $S_4$  and  $S_5$ .

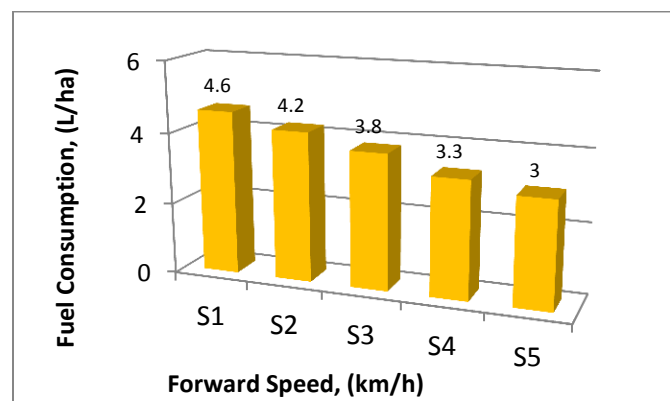


**Figure 6.** Effect of forward speed on the fuel consumption of straw chopping machine.

Figure (7) shows the forward speed effects on the straw picking up and chopping machine drawn by the tractor on the slippage percentage. The slippage percentage increased with increasing the forward speed. The averages were (3.4, 3.9, 4.5, 5.1, and 6.1) % for all speeds respectively. The highest slippage percentage recorded was with S<sub>5</sub> while the lowest slippage percentage recorded was with S<sub>1</sub>. The reason of slippage percentage occurrence is the instability of the mechanical units of the wheels on the ground with high speed operations which reduces the chances of tires cohesion with the ground. These results are in line with the results obtained by Al-Ayoubi and Taha, (2009).

#### 4. CONCLUSIONS

Since the straw picking up and chopping machine is a newly adapted in the region, it needs to be studied for economical usage. According to the results obtained from this study, throwing the straw

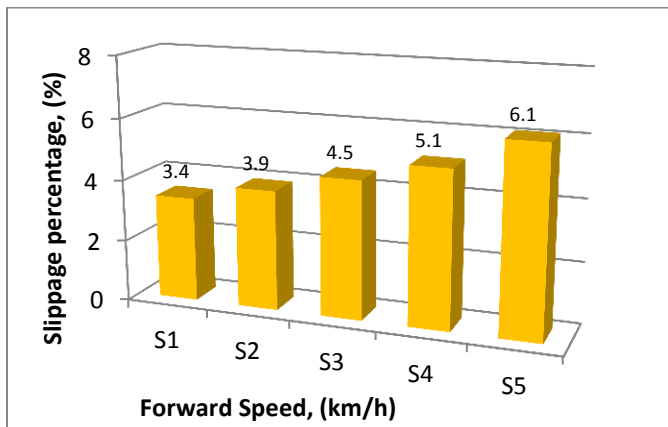


**Figure 7.** Effect of forward speed on the slippage percentage of straw chopping machine.

as heaps (which is the most common method used by farmers in Kurdistan region) and picking them up by the machine is not practical at all because of its negative effects. Straw picking up and chopping as windrows by the straw chopping machine give positive results for most studied parameters. The forward speed of the machine has many effects on the performance of the straw picking up and chopping machine. Operating the mechanical units with forward speed of (5.21 or 6.31) km/h gives the best results in terms of fuel and time consumption, throughput capacity and efficiency, and straw recovery. For these reasons, our recommendation to

the farmers is to get away from throwing the straw behind the harvester as heaps on the ground; instead, they are recommended to throw the straw as windrows with the mentioned forward speed for obtaining best results when it is collected by a straw picking up and chopping machine.

#### REFERENCES

- Afify, M. T., A. H. Bahnasawy and S. A. Ali. 2002. Effect of rice straw picking up method on the performance of a rectangular baler. *AIC 2002 meeting CSAE/SCGR program. Saskatoon, Saskatchewan.* July 14-17, 2002. Paper No. 02-217.
- Al-Auobi T.H.M and Taha S.Y. 2009. Effect of baler type and tractor speed on slippage percentage, baler productivity and baler field efficiency. *Raffidain. J. Agr. sci* 1(4): 183-188.
- Al-Banna, A. R. 1990. *Tillage Equipment.* Dar al kutub for press and publishing. Mosul University.
- Anjum A., Ghafoor A., Munir A., Iqbal M. and Ahmed M. 2015. Design modification of conventional wheat straw chopper. *CIGR Journal* 17(1): 50-58.
- Ankit Kr. U., Singh V. and Moses S. C. 2018. To study of effective speeds for harvesting of wheat straw by straw combine. *International Journal of Agriculture Engineering* 11(1): 54-59.
- ASABE Standard. 2008. S358.2: *Moisture measurement – forages.* St. Joseph, Mich.: ASABE.
- Chandrasekaran, B., K. Annadurai and E. Somasundaram. 2010. *A textbook of agronomy.* New age international publishers. New Delhi.
- Farias M. S., J. F. Schlosser, P. Linares, J. P. Barbieri, G. M. Negri, L. F. V. Oliveira and I. I. P. Rüdell. 2017. Fuel consumption efficiency of an agricultural tractor equipped with continuously variable transmission. *Ciência Rural*, 47:(6). 1-7.
- Field H. L and John B. So. 2007. *Introduction to Agricultural Engineering Technology. A Problem Solving Approach.* Springer. Third edition. Springer Science and Business Media, LLC.
- Grisso R.B., Perumpral J.V., Vaughan D., Roberson G.T. and Pitman R. 2010. Predicting tractor diesel fuel consumption. *Virginia cooperative extension. Publication* 442-073.
- Gummert, Martin, NguyenVan Hung, Pauline Chivenge and Boru Douthwaite. 2020. *Sustainable rice straw management [e-book].* Springer Open. This Springer imprint is published by the registered company Springer Nature Switzerland AG. Accessed date 21/3/2020. <https://link.springer.com/content/pdf/10.1007%2F978-3-030-32373-8.pdf>
- Gursoy S., Kolay B., Avsar O. and Sessiz A. 2015. Evaluation of wheat stubble management practices in terms of the fuel consumption and field capacity. *Res. Agr. Eng.* 61(3): 116-121.

- Jain S. C. and Philip G. 2003. *Farm machinery – an approach*. First edition. A.k. Jain for standard publishers distributors. Delhi. India.
- Jasim A.A and H.A. Jebur. 2015. Impact of primary tillage system on fuel consumption, management and total tractor costs. *The Iraqi Journal of Agricultural Science*. 46(1): 31-35.
- Kumar A. N., Kumar V., Rani V., Mukesh S. and Poonia R. 2017. Comparative performance of paddy straw chopper-cum-spreader of different designs. *Annals of Agri-Bio Research* 22(1): 60-63.
- Mahmood H. S., Ahmed T., Zulfiqar A., Ahmed M. and Amjed N. 2016. Field evaluation of a wheat straw chopper. *Pakistan J. Agric. Res.* 29(3): 301-314.
- Ministry of planning report, 2017. *A survey of winter planted crops in Kurdistan region, (area , yield , production and cost)*. Kurdistan region government, Ministry of planning, Foundation of statistics of Kurdistan region.
- SAS, 2009. *SAS/STAT 9.2 user's guide*. 2<sup>nd</sup> edn, SAS Institute Inc., SAS Campus Drive, Cary, North Carolina 27513.
- Suradi A., Stefanoni W., Alfano V., Bergonzoli S. and Pari L. 2020. Equipping a Combine Harvester with Turbine Technology Increases the Recovery of Residual Biomass from Cereal Crops via the Collection of Chaff. *Energies*. 13(7): 1572 . Available online. . Accessed date. 10/5/2020; <https://doi.org/0.3390/en13071572>
- Thakur S. S., Chandel R. and Narang M. K. 2018. Studies on straw management techniques using paddy-straw chopper cum spreader along with various tillage practices and subsequent effect of various sowing techniques on wheat yield and economics. *AMA* 49(2): 52-67.
- Vink A. 2015. *Crop residues for animal feed*. Netherlands. CTA. Publications Distribution Service.

# RESEARCH PAPER

## REDESCRIPTION OF FROGHOPPERS, *Cercopis intermedia* Kirschbaum, 1868 (HOMOPTERA: CERCOPIDAE) FROM ERBIL GOVERNORATE KURDISTAN REGION– IRAQ

Mudhafar I. Hamad\* ,Nabeel A. Mawlood\*\* , Abdul-Qadir S. Khidhir\*\*\*

\*Department of Plant Protection, Khabat Technical Institute Erbil Polytechnic University, Erbil-Iraq.

\*\* College of Agriculture engineering Science, Salahaddin University, Erbil- Iraq

\*\*\* Erbil Research Center, Insect Museum, Ministry of Agricultural, Erbil-Iraq

### ABSTRACT

The present work includes a details description of froghoppers, *Cercopis intermedia* Kirschbaum,1868 from Erbil Governorate Kurdistan Region– Iraq. The specimens were collected from the wheat field and the flower of some weeds during the period of March to June- 2018. The taxon is easily distinguishable, where the antenna dark brown, filliform, flagellum is the smallest, 0.8 times as long as pedicel, basal body of the flagellum conic with an arista nearly 5 times longer than pedicel. Forewing black, with four dark red pattern. Pygophore which encloses two pairs of hook- like processes neighboring the hook shaped Aedeagus hook shaped, moderately thick, the blade bear four needle-like process. Some important body parts such as mouthparts, antenna, forewing and male genitalia were illustrated and drawn. Localities, date of collection and plant hosts were mentioned.

KEY WORDS: *Cercopis intermedia*, Description, (Homoptera:Cercopidae), Kurdistan region – Iraq.

DOI: <http://dx.doi.org/10.21271/ZJPAS.32.6.13>

ZJPAS (2020) , 32(6);116-122 .

### 1. INTRODUCTION

Cercopidae belong to the suborder Auchenorrhyncha of the order Hemiptera which have piercing and sucking mouth parts style and feed on the xylem-sap of host plants, this family forms a large group of xylem feeding insects with approximately 1500 worldwide species included in 150 genera. Most species are distributed in the tropical and subtropical regions. Adults feed on leaves or stems of a wide variety of plants,

nymphs can feed on roots and in some cases they complete their development above the ground, the nymphs covered themselves with sputum produce frothy excreta which that serves as a means of protection and a means of reducing evaporation. Adults with bright color patterns ([Carvalho and Webb, 2005](#)).

, in the last revision lists 416 species collected in the New World, It is mostly tropical, with the exception of two species, *Prosapia bicincta* (Say,1830) and *Prosapia ignipectus* (Fitch,1851), founded in northern Mexico, two Genera, *Cercopis* Fabricius, 1775, and *Haematoloma* Haupt,1919, identified in Europe ([Carvalho et al., 2016](#), [Peck and Thompson, 2008](#)). The nymphs covered

#### \* Corresponding Author:

Mudhafar I. Hamad

E-mail: [mudhafar.hamad@epu.edu.iq](mailto:mudhafar.hamad@epu.edu.iq)

#### Article History:

Received:05/02/2020

Accepted: 18/08/2020

Published:20/12/2020

themselves with sputum produce frothy excreta which that serves as a means of protection and a means of reducing evaporation. Adults with bright color patterns (Carvalho and Webb, 2005). *C. intermedia* is one of the species of the *Cercopidae* collected on herbaceous plants in Antalya-Tukey, (Dmir,2919). Taxonomic works have often relied upon mainly superficial appearance, with the result that taxonomists have described and illustrated 10% of the species in sufficient detail, but tropical species are poorly known and in four Pacific island areas only 67 species from a 127 species were undescribed (Hamilton, 1980a,b; 1981 a,b and 2001).

These insects feed on shrubs, herbaceous plants and many other plants, some of them are economic importance because they cause plant dwarf especially clover plants (Johnson and Triplehorn, 2005, Demir, 2019). [Dolling \(1991\)](#) indicated that some species of froghoppers are polyphagous, feeding on grasses, broad-leaved weeds, and shrubs. Nymph are found in the soil cracks, under the stone ([Paladini and Carvalho, 2013](#)). [Hamilton and Morales \(1992\)](#) studied fifteen *Cercopidae* species belongs to four genera from New Zealand with keys for identifying the species. [Costes and Webb \(2004\)](#) indicated that four new species recorded in South America, which were described and illustrated withdrawing the male genitalia. [Dinardo-Miranda et al. \(2008\)](#) mentioned that sugarcane spittlebug, *Mahanarva fimbriolata* (Stål), is affected the sugarcane crop in Brazil, despite of its economic importance and reducing stalk productivity, ([Le Quesne, 1969](#)). [Holzinger \(2008\)](#) formulated a key to genera and species of the *Cercopidae* of Europe and gives an overview of the color morphs of Central European *Cercopis* taxa. In Iraq, the family isn't studied except ([Derwesh, 1965](#)) recorded *Triecphora septemmaculata* Mel., and ([Al-Hasnawy and Al-Asady, 2015](#)), described external morphology of a new record species of *Cercopis*

*vulnerata* (Rossi, 1807), male and female genitalia were discussed and illustrated.

## MATERIALS AND METHODS

The specimens were collected by net from the period of March to June - 2018 on the flower of some weeds from different Erbil-Iraq localities Girderashe village, Mallow weed on 28 /3 /2018 and 2/4/2018; Ainkawa, wild mint on 15/4/2018; Hiran, Mallow weed on 7/5/2018; Shaqlawa, Hollyhock and Mallow weed on 5/6/2018; Shaqlawa:Kore village, wild mint on 25/6/2013; Khelifan, Mallow weed on 28/6/2018. The specimens separated to three parts; head, thorax and abdomen under dissecting microscope, Head and abdomen soaks in a beaker contained 10% KOH and placed on hotplate with shaking for about 10 minutes for dissolving lipids, After that placed in distilled water for 5 minutes in order to neutralize the alkali. The parts were placed in a glass petri dish containing an amount of ethyl alcohol 25% and dissected under microscope. Then the parts placed in ethyl alcohol, 50%, 75% and 100% for dehydration for 2 minutes, then they placed in xylol for 2 minutes ,for translucency then places on slides with a drop of dpx and covered by cover slides.; ([Mawlood et al., 2016](#)). The body and some photographs were taken using a Canon MP-E 65mm/ 2.8 1–5× Macro on bellows attached to a Canon Digital IXUS 9515 camera. The species was identified with the help of available literatures ([Le Quesne, 1969](#)). The specimens were deposited in the Insects Museum at the Department of Plant protection, College of Agriculture/ Salahaddin University, Erbil, Iraq.

## RESULTS

### Body (Pictures 1. a, b and c)

Oval, black with four red patterns on fore wing; Length 7.1-9.2 mm, width 3.0-4.2 mm.

### Head

Semi-triangular shaped with width across eyes 1.3 times of pronotal length. Vertex and face

shinning black, smooth with fine pale pilosity. Fronto-clypeus strongly convex. Eyes black nearly spherical shaped; ocelli very small, reddish, 1.3-1.4 times as far from base of head, each other separated by 0.3-0.4 times their own width; Labrum triangular shaped with pointer apex. Mandibles (picture 2a) needle-like. Maxilla (picture 2b) needle-like slightly longer than the mandible; Labium (picture 2c) nearly tubular shaped, 2<sup>nd</sup> and 3<sup>rd</sup> segment are the same length and longer than the 1<sup>st</sup> segment. Antenna (picture 2 c) dark brown, filliform, 1<sup>st</sup> segment cylindrical, 1.1 times as long as the 2<sup>nd</sup> segment, 2<sup>nd</sup> segment nearly rectangular, 2.1 times as long as the 3<sup>rd</sup> segment, arista nearly two times as long as the 3<sup>rd</sup> segment.

### Thorax

Pronotum smooth, shining black with high dense of short yellow setae and fine shallowly punctures, the anterior margin straight width 1.7-1.8 mm. Scutellum triangular, shiny black. Forewing (Fig. 1E) black, with four dark red patterns and fine pale pilosity. Hind wings translucent, smoky brown, with fine pilosity. Vein Cu1 not thickened at the base, r-m situated at 0.65 length, m-cu at 0.55 length, proximal costal process at 0.20 length. fore legs red-black, fore coxae and trochanter black, fore femur cylindrical, the basal half is black and the apical half is red, fore tibia black tubular shaped with length slightly less than twice that of femur, 1/5<sup>th</sup> of apical is red bearing a pair of short spurs with 9-10 apical spines; Tarsus black with four segments, metatarsus with apical spines obscured by long setae; Mid legs nearly similar to fore leg; hind legs resemble to forelegs except the coxal plate shaped, the tibia tubular with two spines at the antero-dorsal margin.

### Abdomen

Composed of seven visible red-black segments, length is 5.2- 6.3 mm, surface covered with moderate dense of black setae. The sternites red with black spot, 1<sup>st</sup> - 6<sup>th</sup> tergites rectangular.

7<sup>th</sup> sternite oval. The tergites narrowly reddish posteriorly. (picture 3 a)

### Male genitalia

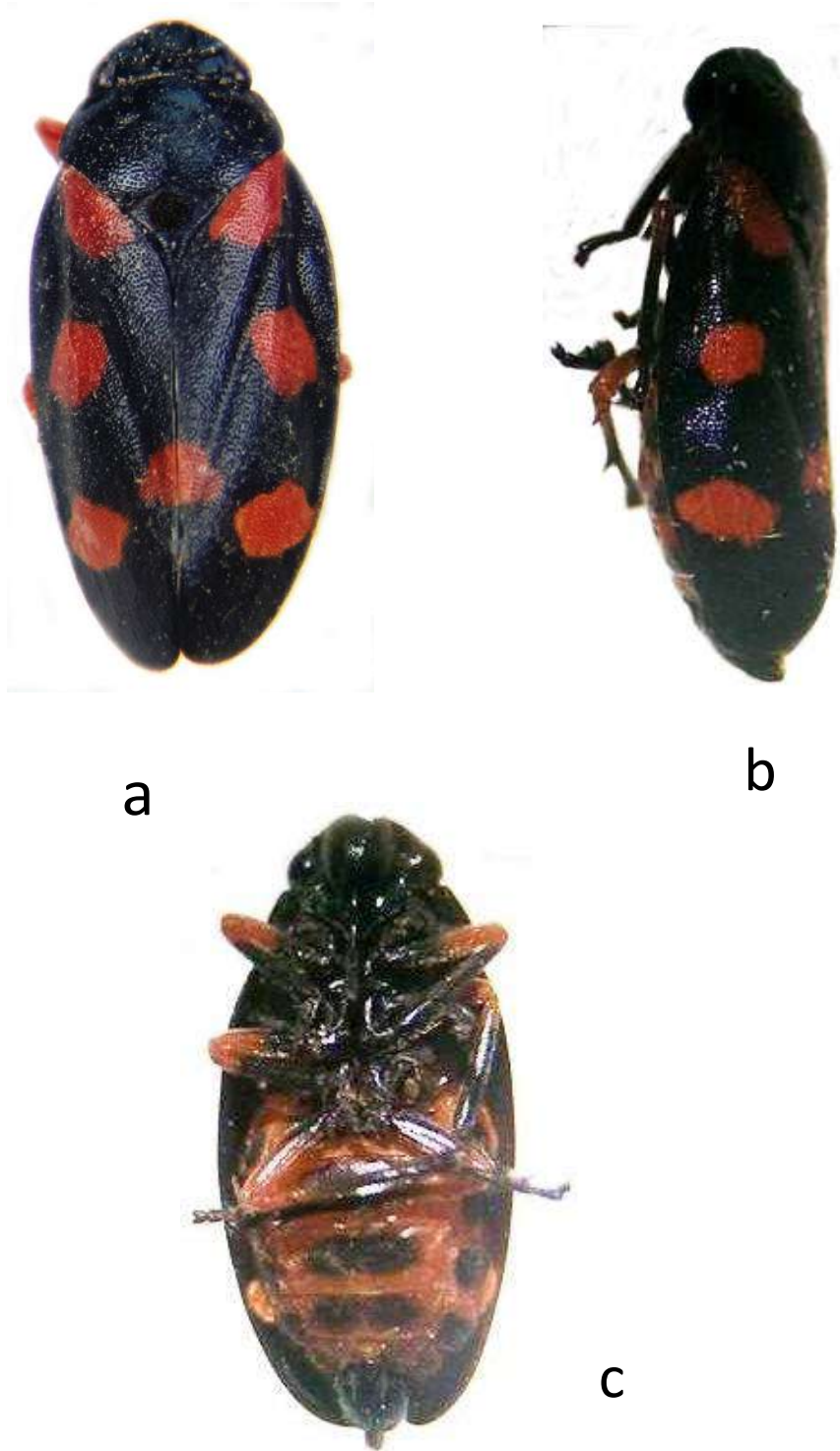
The 8<sup>th</sup> abdominal segment (picture 3a) nearly ovoid, highly sclerotized, laterally covered with moderate dense of short, brown setae. The genital capsule, Pygophore (picture 3a) encloses two pair of hook-like styles neighboring the penis nearly cup shaped, anterior margin slightly concave, prominent at the middle, half of anterior part highly sclerotized, basal half membranous, laterally with moderate dense of short, brown setae. Subgenital plates (picture 3 e) which are short pair of blunt or tapered, nearly cylindrical shaped processes serve to protect the copulatory apparatus and arise from the ventral margin of the pygophore and form the side walls of the genital capsule, these plates are highly sclerotized, covered with high dense of short, brown setae. Parameres (picture 3 b) irregular shaped, with short swollen apical process. Above the aedeagus the slender terminal segments of the abdomen form anal tube. Aedeagus (picture 3 f) hook shaped, moderately thick. The blade bear four needle-like process, two of these are long, the penis divided into a globular phallobase and a distal, tubular or leaf-like aedeagus, which in turn may be composed of a sclerotized theca ending in a membranous, often extensile vesica surrounding the gonopore.

### Female genitalia

Ovipositor yellow, composed of four long, slender styles bent at the middle, toothed dorsally, blunt, knife-like process, length 0.8-0.9 mm.

### Acknowledgments

We are grateful to Dr. Guido Sabatinelli (Natural History Museum of Geneva, Switzerland) and Dr. Unal Zeybekoglu, Department of Biology, Faculty of Art and Science, Ondokuz Mayıs University, Samsun, Turkey for their support to identify the specimen.

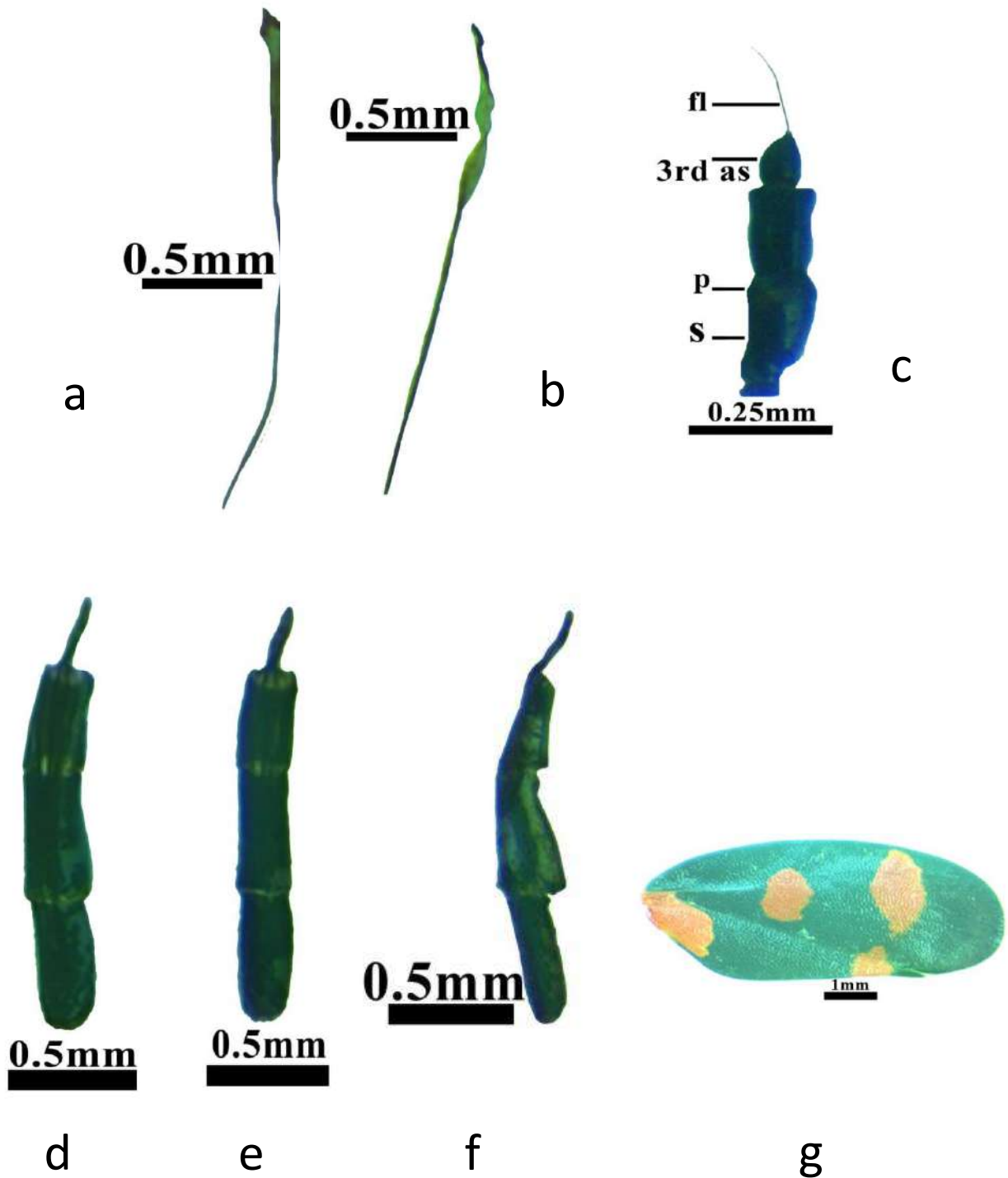


**Picture 1. Adult of *Cercopis intermedia* Kirschbaum, 1868 ( 10 X )**

**a. Dorsal view**

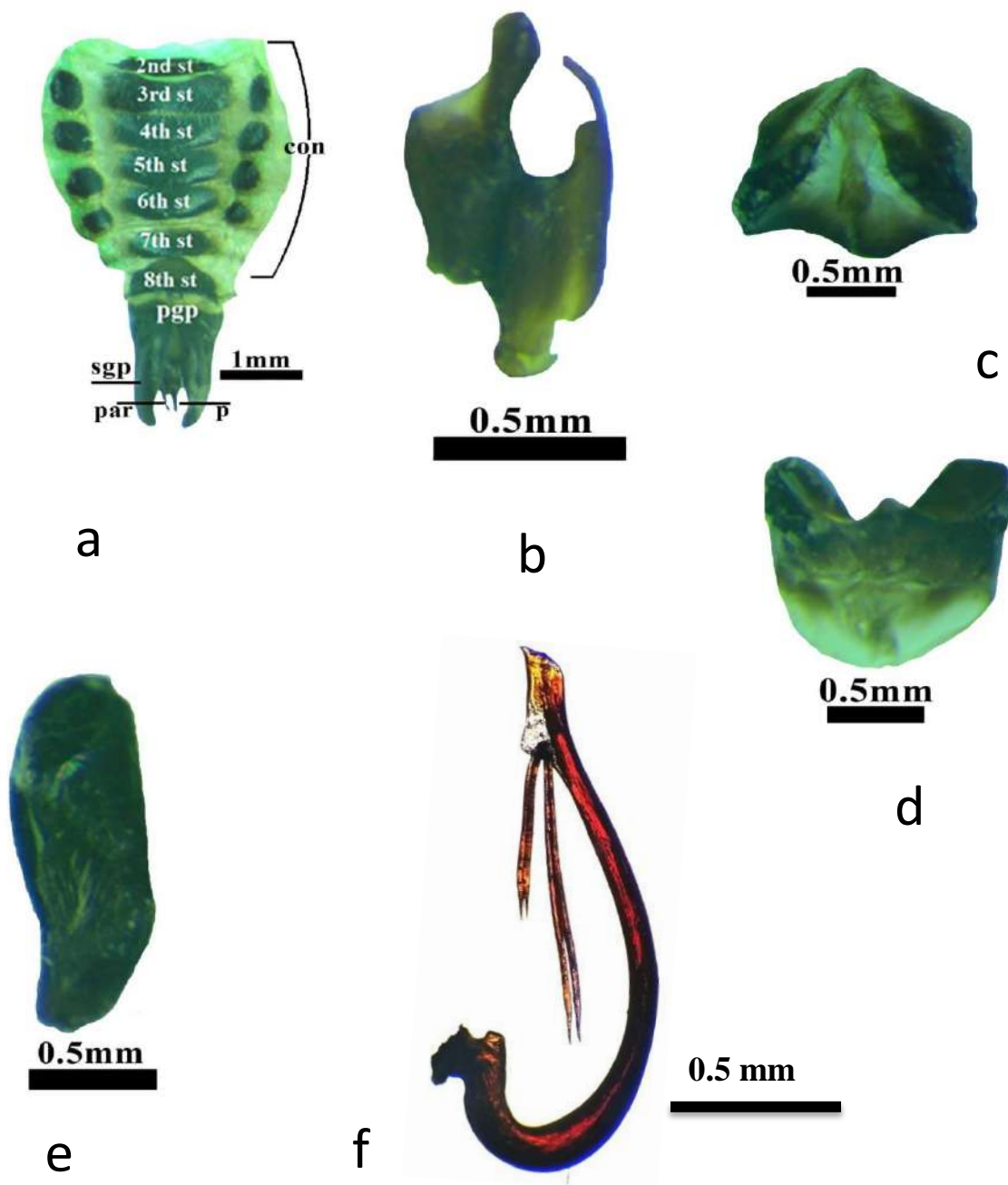
**b. Lateral view**

**c. Ventral vie**



Picture (2) Mouth Parts, Elytra of *Cercopis intermedia*  
 a. Mandible ; b. Maxilla ; c. Antenna; d. Labium (Dorsal view); e. Labium (Ventral view);  
 f. Labium (Lateral view) ; g. Elytra ; 3<sup>rd</sup> as. 3<sup>rd</sup> antennal segment; fl :Flagellum; p. pedicle ;  
 s. Scape;





Picture (3) a. Male Abdomen (Ventral View); b. Paramere (Lateral view); c. . Pygophore (Dorsal view);d. Pygophore (Ventral view);e. Subgenital plate; f. Aedeagus-penis  
 2<sup>nd</sup>: second sternites; P. Penis; Par: Paramere; pgp: Pygophore; Sgp: Subgenital plate

## LITERATURE CITED

- AL-HASNAWY, H. T. & AL-ASADY, H. S. 2015. External Morphology of *Cercopis vulnerata* (Rossi, 1807) (Homoptera: Cercopidae) has been Firstly recorded in Iraq. *Journal of the College of basic education*, 21, 85-92.
- CARVALHO, G. S., SAKAKIBARA, A. M. & WEBB, M. D. 2016. Two new species of the neotropical spittlebug genus *Monecphora* Amyot & Serville (Hemiptera: Cercopidae) with key and notes of species of the genus. *Zootaxa*, 4078, 143-152.
- CARVALHO, G. S. & WEBB, M. D. 2005. Cercopid spittlebugs of the new world (Hemiptera, Auchenorrhyncha, Cercopidae), *Pensoft. Sofia*, 271 pp
- COSTES, D. H. & WEBB, M. D. 2004. Four new species of Neotropical spittlebugs (Hemiptera, Cercopidae, Tomaspidae). *Revista Brasileira de Entomologia*, 48, 391-393.
- DEMIR, E. 2019. BIODIVERSITY AND ZOOGEOGRAPHY OF CICADOMORPHA (EXCL. DELTOCEPHALINAE) SPECIES FROM SOUTHWESTERN TURKEY (INSECTA: HEMIPTERA). *Munis Entomology & Zoology*, 14, 236-243.
- DERWESH, A. I. 1965. preliminary list of identified insects and some arachnids of Iraq. Directorate General of Agriculture Research and Projects, *Baghdad, Bulletin*, 121pp.
- DINARDO-MIRANDA, L. L., PIVETTA, J. P. & FRACASSO, J. V. 2008. Economic injury level for sugarcane caused by the spittlebug *Mahanarva fimbriolata* (Stål)(Hemiptera: Cercopidae). *Scientia Agricola*, 65, 16-24.
- DOLLING, W. R. 1991. Hemiptera, Oxford University Press. *Natural History Museum Pub., Oxford University*, 274pp.
- HAMILTON, K. 1980a. Aphrophorinae of Polynesia (Rhynchota: Homoptera: Cercopidae). *Pacific Insects*, 22, 347-360.
- HAMILTON, K. 1980b. Aphrophorinae of the Solomon Islands Rhynchota: (Homoptera: Cercopidae). *Pacific Insects*, 22, 361-379.
- HAMILTON, K. 1981a. APHROPHORINAE OF NEW CALEDONIA AND THE LOYALTY ISLANDS (RHYNCHOTA: HOMOPTERA: CERCOPIDAE) 12. *Pacific Insects*, 23, 451-464.
- HAMILTON, K. 1981b. Aphrophorinae of the Fiji, New Hebrides and Banks Islands (Rhynchota: Homoptera: Cercopidae). *Pacific Insects*, 23, 465-477.
- HAMILTON, K. A. 2001. A new family of froghoppers from the American tropics (Hemiptera: Cercopoidea: Epipygidae). *Biodiversity*, 2, 15-21.
- HAMILTON, K. A. & MORALES, C. F. 1992. Cercopidae Insecta: Homoptera. *Fauna of New Zealand*, 25, 42.
- HOLZINGER, W. 2008. Die Gemeine Blutzikade (*Cercopis vulnerata*) das Insekt des Jahres 2009 (Hemiptera: Auchenorrhyncha: Cercopidae). *Beiträge zur Entomofaunistik*, 9, 293-303.
- JOHNSON, N. F. & TRIPLEHORN, C. A. 2005. Borror and DeLong's Introduction to the Study of Insects, Thompson Brooks/Cole Belmont, CA.
- LE QUESNE, W. 1969. Handbooks for the identification of British insects Hemiptera (Cicadomorpha-Deltocephalinae). *Royal Entomological Society of London V ol II part 2b, London*.
- MAWLOOD, N. A., HAMAD, M. I. & ABDULLAH, Y. M. 2016. A new record of glaphyrid scarab beetles, *Eulasia vitatta* (Fabricius, 1775)(Coleoptera, Glaphyridae) from Erbil Kurdistan region-Iraq. *Zanco Journal of Pure and Applied Sciences*, 28, 1-4.
- PALADINI, A. & CARVALHO, G. S. 2013. Descriptions of two new species of Sphenorhina (Hemiptera, Cercopidae, Tomaspidae) from the Neotropical region. *Revista Brasileira de Entomologia*, 57, 165-168.
- PECK, D. & THOMPSON, V. 2008. Spittlebugs (Hemiptera: Cercopoidea). *Encyclopedia of entomology*, 2nd ed. Springer, Dordrecht, Netherlands, 3512-3516.

## RESEARCH PAPER

# Swell and Shrinkage Percentages for Various Soil Types and their Prediction from Intrinsic Soil Properties

Haval H. Yousif <sup>1</sup>, Tariq H. Karim <sup>2</sup>, Ismail B. Mohammad <sup>3</sup>

<sup>1</sup> Department of Soil and Water, College of Agricultural Engineering Sciences, Salahaddin University-Erbil, Kurdistan Region, Iraq

<sup>2</sup> Department of Soil and Water, College of Agricultural Engineering Sciences, Salahaddin University-Erbil, Kurdistan Region, Iraq.

<sup>3</sup> Department of Civil Engineering, College of Engineering, Salahaddin University-Erbil, Kurdistan Region, Iraq

### ABSTRACT:

Earthwork construction involves excavation, hauling, placing and compaction of soil, gravel, and other materials that exist on the soil surface. The soil volume varies depending whether the soil is bank, loose or compacted material. Therefore, the final generated volume of earthwork should be adjusted for volume changes during the above states by applying shrinkage and swell-correction percentages. Estimating these correction factors by engineering expertise or selecting predetermined tables without extensive knowledge of the local soils has proven to be costly and may be misleading. Accordingly, the current study was initiated to develop the database of swell/ shrinkage percentages for various soil materials and link them to other soil properties. Standard procedures were applied for determining soil density at different states along with the physical, chemical and geotechnical properties for soils obtained from 39 surveyed projects within and on the outskirts of Erbil city. The obtained data were subjected to different statistical analysis and the results indicated that the swell percentage ranged from 36.10 -55.7% for clays, 18.40 – 69.20% for silts and 11.90 – 54.5% for gravels. Shrinkage percentage ranged from 9.20 – 16.5% for clays, 4.40 – 20.20% for silts and 0.80 - 23.5% for gravel. Overall, within each group, the swell percent was superior to the shrinkage percent. Additionally, the swell percent was characterized by having a higher coefficient of variation compared to that of shrinkage percent. The in situ soil density and clay content have emerged to be the most effective soil properties for predicting swell percent. On the other hand, the influential variables for predicting shrinkage percent were in situ soil density and the maximum dry density. The mean absolute error of prediction of swell and shrinkage percentages were 6.79 and 1.17 respectively, indicating that shrinkage percent can be predicted more accurately compared with swell percent.

KEY WORDS: Soil volume change; Swelling/shrinkage percentages; Bank site; Soil geotechnical properties.

DOI: <http://dx.doi.org/10.21271/ZJPAS.32.6.14>

ZJPAS (2020) , 32(6);123-137 .

### 1. INTRODUCTION :

Earthwork construction involves excavation, hauling, placing and compaction of soil, gravel and other materials that exist on the soil surface (Cole and Harbin, 2006).

There are many unknowns and assumptions required in estimating the earthwork construction and these make this task is at a great risk (Anupriya, 2018).The earthwork projects having two types of constrains, viz., quantitative (cut or fill volumes, swell shrinkage factors, traveling distance/time and unit cost) and qualitative (access to/on site, road condition etc.) (Li and Lu, 2019).

When soil materials are excavated, it undergoes a change in volume and density. As

#### \* Corresponding Author:

Haval H. Yousif

E-mail: [haval.haji.yousif@gmail.com](mailto:haval.haji.yousif@gmail.com)

#### Article History:

Received: 07/07/2020

Accepted: 26/08/2020

Published: 20/12 /2020

material is loosened, air voids increase and gives rise to a decrease soil density. This increase over the original undisturbed volume is termed swell (Uhlik III, 1984). On the other hand, as the soil is compacted in embankment areas it usually occupies less volume than it did in its bank state. The decrease in volume is known as shrinkage. Shrinkage factor is a parameter that represents soil volume changes from the bank state to the compacted state, while swell factor is a parameter represents soil volume change from bank state to the loose state (White *et al.*, 2010).

Soil shrink factors also affect to overall quantity estimation, which depend on the soil type (Burch, 1997). Increase in swelling factor, increases the volume of the embankment and consequently gives rise to an increase in the demand on fuel and energy (Alzoubi *et al.*, 2017). This factor is always greater than 1 depending on the feature of the excavated floor (Sağlam and Bettemir, 2018). By taking swell, compaction and productivity factors into calculations, the total volume of hauling, back filling and other earthworks can be estimated (Najafi and Gokhale, 2005).

It may be misleading to calculate cut-fill volumes without considering the amount of swelling and/or shrinkage (Göktepe *et al.*, 2008). When estimating the amount of cut and fill, the potential for soil shrinkage and swelling must be taken in account; otherwise, volume calculations to and from the site will not be balanced.

Further, Akijje (2013) has shown that where a shrinkage factor of a given soil is known, it could be used in the computation of fill and cut volumes to amend the required net soil materials while calculating mass haul diagram ordinate.

The determination of the soil properties affecting earthwork optimization, such as swelling/shrinkage factor, is highly ambiguous due to the complex behavior of soils (Göktepe *et al.*, 2008). Therefore, for most of the highway designs, swelling/shrinkage factors are selected from predetermined tables according to specific soil types being considered.

Bannister *et al.* (1998) gave typical swell and shrinkage factors for certain materials. Garber and Hoel (2010) claimed that shrinkage used are generally between 1.10 and 1.25 for high fills and between 1.20 and 1.25 for low fills in order to determine the required quantity of fill material. Chopra *et al.* (1999) revealed that adopting factors

without extensive knowledge of the local soils has proven to be costly. Usually, these factors are estimated by local engineering expertise or general values presented in handbooks or texts (Martínez *et al.*, 2014), but when working with large soil movements, the values of these parameters have great impacts on planning of activities and associated costs. Thus, their determination will be interesting.

Burch (1997) revealed that understanding these factors for different soil groups and the factors affecting these parameters are significant for accurately predicting quantities and subsequently costs. The swell/shrinkage factors are influenced by the material type (clay, silt, sand, gravel, etc.), in situ moisture content of the material (dry damp, or wet), final moisture content and density of the material and the type of equipment used for excavation and compaction (Helton, 1992).

Shamo (2013) developed a multivariate model to predict the shrinkage factor and observed that 99.9% of variation in this parameter was attributed to variation in clay content, bulk and densities of the borrow material, and the dry and bulk densities of embankment.

In view of the above facts, the current study was initiated to develop the database for shrink/swell percentages for different soil materials and link them to soil physical and geotechnical properties.

## 2. MATERIALS AND METHODS

### 2.1. Site Selection and Sample Preparation

Thirty-nine projects were surveyed and selected within and on the outskirts of Erbil city Figure 1 The work also includes obtaining and transporting suitable fill material from off-site when suitable on-site material is not available. A representative sample was taken from each site and has been reduced to the proper size by quartering method. Each sample was thoroughly mixed, air dried and kept in polyethylene bags until use. The soil from each project site was subjected to a battery of tests (geotechnical, physical and chemical) using standard methods.

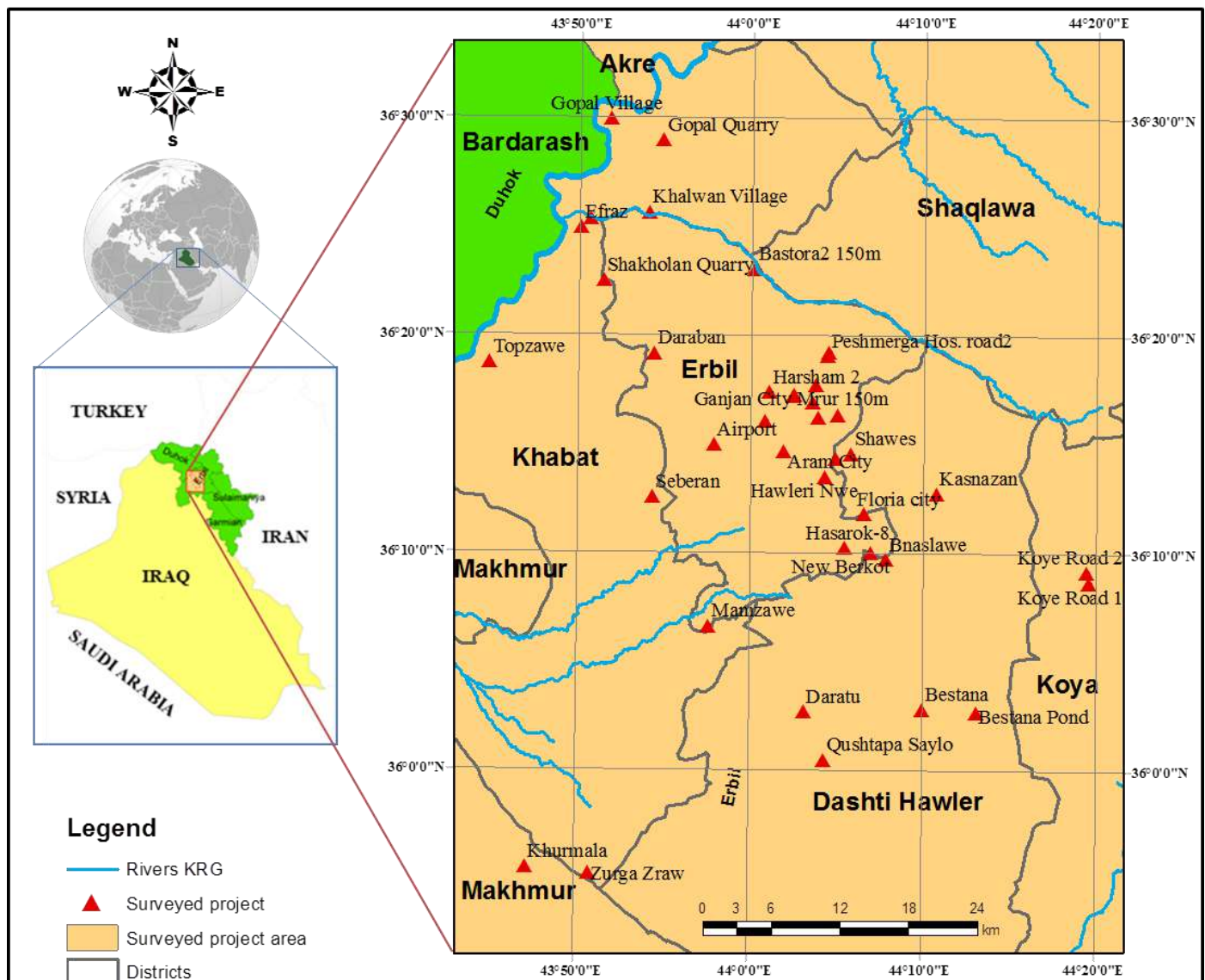


Figure 1: Location map showing the surveyed projects sites

## 2.2. Measurement of Soil Density at Different States

The bank (in situ) site density was determined for each site in 7 replications using core or sand cone method, depending on soil type and soil condition according to Blake and Hartge (1986) and ASTM (D1556-07, 2007). A unit volume box with a volume of exactly 0.31 cubic meter was also used to determine the soil density under loose conditions. On the other hand, the sand cone method was used for measuring soil density in the compacted state according to ASTM (D1556-07, 2007). The soil density measurement at any of the three states was accompanied by soil moisture determination by gravimetric method.

## 2.3. Calculation of Shrink/ Swell percentages

The shrinkage percentages was expressed in terms of dry unit weight of two states of soil as follows (Burch, 1997)

$$SF = \left(1 - \frac{\rho_B}{\rho_C}\right) \times 100 \quad [1]$$

Where

SF = Shrinkage percentages

$\rho_B$  = Density of bank material

$\rho_C$  = Density of compacted material

The swelling (bulkage) was expressed in terms of dry unit weights at loose and in-place states:

$$BF = \left( \frac{\rho_B}{\rho_E} - 1 \right) \times 100 \quad [2]$$

Where:

BF = Bulkage percentages (Swell percentages)

$\rho_B$  = Density of bank material

$\rho_E$  = density of excavated material (in loose state)

## 2.4. Soil Physical, Chemical and geotechnical Analysis

Sufficient quantity of soil materials were taken according to procedure of granular materials ASTM (C136-06, 2006) and (D6913, 2009) for conducting sieve analysis using a nest of sieves (3, 2.5, 2, 1.5, 1, 0.75, 0.5 inches) along with sieve No.4, 8, 10, 40, 50 and 200.

The compaction characteristics of the soils were determined using modified effort in accordance to ASTM (D1557-12, 2012) and (D2216, 2005).

In addition, the California Bearing Ratio (CBR) was used for evaluating subgrade strength as an aid to the design of pavements. The soil samples were compacted at optimum moisture content using 56, 25, 10 blows per layer (if the C.B.R. for soil at 95% of MDD is required) according to ASTM (D1883-16, 2016) method C in which materials coarser than 19mm sieve compensated by material 0.75 inch (19mm) sieve and retained on No. 4 (4.75mm) sieve. The mold into which the soil was placed has a diameter of 152 mm and a depth of 177 mm.

Atterberg limits were determined in accordance with ASTM (D4318, 2010) after passing the soil materials through the No. 40 (0.425mm) sieve.

Particle size distribution for materials passing through a 2-mm sieve was also determined using hydrometer analysis in accordance with ASTM procedure (D422-63, 2007). Test procedure of ASTM (C127, 2015), (D854-14, 2014) and ASTM (C128, 2012). (Specific Gravity and Absorption of Coarse Aggregate) and (Specific Gravity and Absorption of Fine Aggregate) were followed to determine Specific Gravity of the soil samples.

The pH of the soil extract solution was measured by HANNA pH-meter, Model microprocessor pH meter using the procedure of Jackson (1958). Electrical conductivity of the soil extract solution was measured using EC-meter model BC3020 TRANS and adjusted to 25 °C to give an indication of the total dissolved ions in the solution (Hesse, 1971). The calcium carbonate equivalent which involves the dissolution of carbonate in excess of HCl (1N), followed by back titration with (0.5N) NaOH as described in Rowell (2014). Organic matter was determined by the modified (Walkley and Black) method as described by Jackson (1958).

## 2.5. Data Analysis

Pearson's correlation was used to determine the degree of correlation between the dependent variables (Shrinkage and bulkage percentages) and input variables using SPSS program IBM Ver.23. Additionally, linear and non-linear least square techniques were employed to estimate the shrinkage and swell factors from other soil properties using Microsoft Excel 2013 and SPSS.

## 3. RESULTS AND DISCUSSION

### 3.1. General Aspects of the Database

Table 1 and 2 an exhibit physical, geotechnical and chemical properties of the investigated sites (projects) along with the classification of the obtained materials according to Unified and AASHTO classification systems. Close examination of Table 1 indicates that soil materials cover fine grained and coarse grained materials with different proportions of fines.

Table 3 exhibits the summary of some statistical parameters of swell and shrinkage percentages belonging to different soil groups. The swell percent ranged from as low as 11.9% for Daratu project to as high as 69.2% for the Harsham 2 project (Table 2). As a whole the swell percent tends to decrease with an increase in gravel content. This result supports the findings of FHWA (2007). According to these findings, the swell percent of common materials ranging from mud to hard rocks varied from as low as 5% for uniformly graded gravel to as high as 79% for shale. The low soil water content in the field may be responsible for the relatively the high swell percent of the investigated soil materials.

**Table 1** Some geotechnical properties of the soil materials of the surveyed projects

No.	Locations	Atterberg's Limits			Specific gravity	Absorption	Proctor test		C.B.R (%)	According to USCS system				
		Liquid Limit	Plastic Limit	Plastic Index			MDD (Mg m <sup>-3</sup> )	OMC (%)		Gravel (%)	Sand (%)	Fine (%) < 0.075mm	Silt (%)	Clay (%)
1	Shawes	34	23	11	2.638	0.6	2.277	5	110	69	15	16	7	9
2	Future City	43	28	15	2.717	NA	1.731	15.1	4	1	20	79	30	49
3	Hawleri Nwe	40	28	12	2.609	1.2	2.164	6.6	32.7	47	23	30	12	18
4	Floria city	N.L.L	N.P.L.	N.P.I.	2.621	0.7	2.315	4.9	163.8	65	28	7	4	3
5	Kasnazan	21	N.P.L.	N.P.I.	2.654	0.7	2.369	4.1	196.3	68	27	5	3	2
6	Hasarok-8	31	23	8	2.702	NA	1.907	12	7	9	24	67	41	26
7	New Berkot	28	21	7	2.61	1.3	2.239	6.8	39.4	31	24	45	31	14
8	Bnaslawe	N.L.L	N.P.L.	N.P.I.	2.612	0.9	2.328	4.7	180.7	71	25	4	2	2
9	Koye Road 1	37	29	8	2.543	2	2.238	6.1	113	75	19	6	3	3
10	Koye Road 2	46	35	11	2.525	1.5	1.918	13	15.3	11	22	67	41	26
11	Daratu	45	31	14	2.606	1.2	2.154	7	29.5	62	17	21	14	7
12	Bestana	41	30	11	2.622	0.9	2.274	6.1	95.8	68	13	19	10	9
13	Bestana Pond	38	27	11	2.708	NA	1.782	18.3	7.7	5	12	83	48	35
14	Qushtapa Saylo	32	23	9	2.712	NA	1.775	14.7	8.2	2	10	88	52	36
15	Mamzawe	43	26	17	2.705	NA	1.792	16.2	5.5	2	14	84	39	45
16	Zurga Zraw	22	N.P.L.	N.P.I.	2.599	1.4	2.27	5.8	60.4	72	23	5	2	3
17	Khurmala	24	20	4	2.537	1.6	2.203	6.4	52.1	70	21	9	6	4
18	Seberan	46	31	15	2.601	1.1	2.221	6.1	62.2	49	30	21	10	11
19	Airport	40	25	15	2.703	NA	1.88	14.8	9.2	2	14	84	40	44
20	Daraban	42	26	16	2.711	NA	1.797	15.9	3.3	1	11	88	40	48
21	Topzawe	26	16	10	2.66	0.6	2.317	5.2	144.7	77	17	6	4	2
22	Shakholan Quarry	29	20	9	2.616	1	2.267	5.7	85.6	60	26	14	9	5

**Table 1** Continued

No.	Locations	Atterberg's Limits			Specific gravity	Absorption	Proctor test		C.B.R (%)	According to USCS system				
		Liquid Limit	Plastic Limit	Plastic Index			MDD (Mg m <sup>-3</sup> )	OMC (%)		Gravel (%)	Sand (%)	Fine (%) < 0.075mm	Silt (%)	Clay (%)
23	Efraz	26	20	6	2.612	0.7	2.315	5.1	157.2	68	23	9	6	3
24	Gopal Quarry	30	20	10	2.636	0.6	2.304	4.3	134.6	66	28	6	1	5
25	Gopal Village	40	23	17	2.699	NA	1.899	13.4	2.3	8	21	71	30	41
26	Bastora 1	N.L.L	N.P.L.	N.P.I.	2.68	0.3	2.388	3.3	136.8	64	32	4	1	3
27	Khalwan Village	N.L.L	N.P.L.	N.P.I.	2.67	0.2	2.408	3.4	213.5	76	20	4	2	2
28	Bastora2 150m	29	21	8	2.652	1.1	2.328	4.6	121.9	73	18	9	5	4
29	Peshmerga Hosp. road 1	36	25	11	2.714	NA	1.748	18.5	4.9	1	19	80	37	43
30	Peshmerga Hosp. road 2	37	26	11	2.551	1.7	2.078	8.7	12.2	30	17	53	23	30
31	Kalakan Village	49	36	13	2.518	2.2	2.079	8.6	41.2	63	15	22	13	9
32	Mamostayan City	41	29	12	2.713	NA	1.713	17.6	3.3	1	19	80	32	49
33	Kurdistan City	34	24	10	2.547	1.7	2.057	9.3	22.6	40	26	34	15	19
34	Perzin Village	37	24	13	2.613	1.6	2.11	8.7	20.7	63	17	20	11	9
35	Ganjan City	26	19	7	2.663	0.4	2.265	6.2	75.4	56	21	23	10	13
36	Mrur 150m	41	30	11	2.719	NA	1.671	18.5	2.6	0	16	84	36	48
37	Harsham 2	42	31	11	2.723	NA	1.643	18.6	2.2	0	15	85	35	50
38	Libanon Village	35	24	11	2.712	NA	1.796	15.6	3.2	1	17	82	36	46
39	Aram City	42	27	15	2.581	1	2.187	6.9	43.9	63	19	18	9	9
	Minimum	24	16	4	2.518	0.2	1.643	3.3	2.2	0	10	4	1	2
	Maximum	49	36	17	2.72	2.2	2.408	18.6	213.5	77	32	88	52	50
	Average	32.1	21.5	9.3	2.641	1.08	2.082	9.5	62.18	40.8	19.9	39.3	19.3	20.0

N.L.L: Non or without Liquid limit; N.P.L: Non or without Plastic limit and N.P.I: Non or without Plasticity index.



**Table 2** Some geotechnical and chemical properties of the soil materials of the surveyed projects

No.	Locations	In situ (Mg m <sup>-3</sup> )	Loose (Mg m <sup>-3</sup> )	Embankment (Mg.m <sup>-3</sup> )	pH	EC ( $\mu$ S cm <sup>-1</sup> )	CaCO <sub>3</sub> (%)	O.M (%)	According to USDA			Swell (%)	Shrinkage (%)	C <sub>u</sub>	C <sub>c</sub>	Unified system	AASHTO system
									Clay (%)	Silt (%)	Sand (%)						
1	Shawes	1.726	1.405	2.189	7.3	549	33.5	0.096	32	20	48	22.8	21.2	5300	120.75	GC	A-2-6
2	Future City	1.574	0.975	1.675	7.26	341	33	0.186	51	27	22	61.4	6	NA	NA	ML	A-7-6
3	Hawleri Nwe	1.837	1.189	2.052	7.55	275	42	0.114	37	29	34	54.5	10.5	7250	1.21	GM	A-2-6
4	Floria city	2.115	1.613	2.203	7.48	259	31.5	0.087	9	12	79	31.1	4	291	10	GP-GC	A-1-a
5	Kasnazan	2.175	1.665	2.281	7.46	202	31.5	0.078	10	10	80	30.6	4.6	30	4.12	GP-GM	<b>A-1-a</b>
6	Hasarok-8	1.578	1.165	1.794	7.34	567	32	0.159	29	35	36	35.5	12	NA	NA	ML	A-4
7	New Berkot	1.719	1.495	2.027	7.37	491	32	0.132	22	27	51	15	15.2	333	0.19	GC	A-4
8	Bnaslawe	2.128	1.655	2.305	7.66	117.2	37	0.078	7	11	82	28.6	7.7	63	3.71	GP	A-1-a
9	Koye Road 1	1.838	1.545	2.108	7.58	164.6	35	0.15	14	17	69	19	12.8	60	6.29	GP-GM	A-2-4
10	Koye Road 2	1.451	1.226	1.819	7.51	271	35.5	0.15	31	29	40	18.4	20.2	NA	NA	ML	A-7-5
11	Daratu	1.597	1.427	2.024	7.51	276	29	0.132	23	20	57	11.9	21.1	2986	93.28	GM	A-2-7
12	Bestana	1.819	1.488	2.117	7.38	231	36	0.132	35	21	44	22.2	14.1	7500	533.33	GM	A-2-7
13	Bestana Pond	1.405	1.172	1.708	7.25	418	28	0.168	39	38	23	19.9	17.7	NA	NA	ML	A-6
14	Qushtapa Saylo	1.551	1.140	1.709	7.47	431	32.5	0.168	38	28	34	36.1	9.2	NA	NA	CL	A-4
15	Mamzawe	1.537	0.987	1.72	7.45	618	32.5	0.186	47	36	17	55.7	10.6	NA	NA	CL	A-7-6
16	Zurga Zraw	2.167	1.632	2.222	7.54	158.3	29.5	0.096	12	15	73	32.8	2.5	122	5.58	GP-GM	A-1-a
17	Khurmala	1.878	1.596	2.127	7.46	200	27.5	0.123	14	21	65	17.7	11.7	159	6.36	GP-GC	A-1-a
18	Seberan	1.779	1.465	2.136	7.47	493	32.5	0.132	28	19	53	21.4	16.7	4706	36.03	GM	A-2-7
19	Airport	1.597	1.092	1.805	7.5	418	35.5	0.15	46	33	21	46.2	11.5	NA	NA	CL	A-6
20	Daraban	1.617	1.203	1.691	7.52	345	35	0.168	49	30	21	34.4	4.4	NA	NA	ML	A-7-6
21	Topzawe	2.172	1.678	2.217	7.72	152.4	26.5	0.132	11	13	75	29.4	2	67	5.44	GP-GC	A-2-4
22	Shakholan Quarry	2.143	1.629	2.183	7.63	168	31	0.105	14	14	72	31.6	1.8	1059	5.11	GC	A-2-4

Table 2 Continued

No.	Locations	In situ (Mg m <sup>-3</sup> )	Loose (Mg m <sup>-3</sup> )	Embankment (Mg m <sup>-3</sup> )	pH	EC ( $\mu$ S cm <sup>-1</sup> )	CaCO <sub>3</sub> (%)	O.M (%)	According to USDA			Swell (%)	Shrinkage (%)	C <sub>u</sub>	C <sub>c</sub>	Unified system	AASHTO system
									Clay (%)	Silt (%)	Sand (%)						
23	Efraz	2.145	1.636	2.19	7.62	168.6	35.5	0.096	11	14	75	31.1	2.1	481	7.39	GP-GC	A-1-a
24	Gopal Quarry	2.103	1.528	2.214	7.66	185.5	22	0.078	21	10	69	37.6	5	45	2.35	GW-GC	A-2-4
25	Gopal Village	1.5	1.098	1.79	7.29	254	26.3	0.159	47	21	32	36.6	16.2			CL	A-6
26	Bastora 1	2.286	1.786	2.304	7.83	150.8	23	0.06	10	4	86	28	0.8	83	2.55	GW	A-1-a
27	Khalwan Village	2.301	1.926	2.326	7.7	192.5	24.5	0.069	8	8	84	19.5	1.1	65	6.15	GP-GM	A-1-a
28	Bastora2 150m	2.171	1.679	2.215	7.68	163.1	23.8	0.069	22	15	63	29.3	2	267	20.17	GP-GC	A-2-4
29	Peshmerga Hosp. road1	1.516	0.915	1.664	7.41	260	35	0.195	44	29	27	65.7	8.9	NA	NA	ML	A-6
30	Peshmerga Hosp. road2	1.646	1.158	1.909	7.56	345	40.5	0.141	48	28	24	42.1	13.8	NA	NA	GM	A-6
31	Kalakan Village	1.468	1.192	1.919	7.52	227	45.3	0.168	32	39	29	23.2	23.5	4643	139.08	GM	A-2-7
32	Mamostayan City	1.511	0.952	1.615	7.47	301	31.5	0.186	50	32	18	58.7	6.4	NA	NA	ML	A-7-6
33	Kurdistan City	1.618	1.102	1.89	7.51	294	32.5	0.15	39	30	31	46.8	14.4	NA	NA	GM	A-2-4
34	Perzin Village	1.677	1.354	2.034	7.55	279	42	0.132	31	33	36	23.9	17.6	3556	40.14	GC	A-2-6
35	Ganjan City	1.698	1.286	2.141	7.45	340	35.5	0.114	34	19	47	32	20.7	NA	NA	GC	A-2-4
36	Near Mrur 150m	1.505	0.894	1.591	7.46	299	31.5	0.177	49	30	21	68.3	5.4	NA	NA	ML	A-7-5
37	Harsham 2	1.418	0.838	1.603	7.5	296	32.3	0.204	52	27	21	69.2	11.5	NA	NA	ML	A-7-5
38	Libanon Village	1.446	0.962	1.732	7.49	289	29	0.159	49	25	26	50.3	16.5	NA	NA	CL	A-6
39	Aram City	1.684	1.389	2.04	7.59	255	44	0.123	28	37	35	21.2	17.5	4000	31.60	GM	A-2-7
	Minimum	1.4	0.838	1.591	7.25	117.2	22	0.06	7	4	17	11.9	0.8				
	Maximum	2.3	1.926	2.326	7.83	618	45.3	0.204	52	39	86	69.2	23.5				
	Average	1.8	1.337	1.982	7.5	293.9	32.6	0.133	30.1	23.2	46.7	34.9	10.8				

**Table 3** Some Statistical parameters of swelling and shrinkage percentages of the investigated materials during the current study

Soil group	Classification symbol	Parameter	Number of projects	Range	Minimum	Maximum	Mean		Std. deviation	Coefficient of variation	Skewness	Kurtosis
							Statistic	Std. error				
Silt of low plasticity	ML	Shrinkage%	9	15.80	4.40	20.20	10.28	1.87	5.61	54.56	0.85	-0.49
		Swelling %	9	50.80	18.40	69.20	47.94	6.95	20.84	43.47	-0.44	1.40
Clay of low plasticity	CL	Shrinkage%	5	7.30	9.20	16.50	12.80	1.50	3.34	26.13	0.34	-2.85
		Swelling %	5	19.60	36.10	55.70	44.98	3.83	8.57	19.05	0.06	-2.17
Silty gravel	GM	Shrinkage%	8	13.00	10.50	23.50	16.45	1.49	4.22	25.65	0.51	-0.26
		Swelling %	8	42.60	11.90	54.50	30.41	5.37	15.18	49.92	0.61	-1.25
Clayey gravel	GC	Shrinkage%	5	19.40	1.80	21.20	15.30	3.55	7.93	51.83	-1.74	3.16
		Swelling %	5	17.00	15.00	32.00	25.06	3.15	7.05	28.12	-0.50	-0.69
Poorly graded gravel with silt	GP-GM	Shrinkage%	4	11.70	1.10	12.80	5.25	2.62	5.23	99.71	1.57	2.49
		Swelling %	4	13.80	19.00	32.80	25.48	3.62	7.25	28.45	0.08	-5.52
Poorly graded gravel with clay	GP-GC	Shrinkage%	5	9.70	2.00	11.70	4.36	1.87	4.19	96.10	2.02	4.12
		Swelling %	5	13.40	17.70	31.10	27.72	2.54	5.67	20.45	-2.10	4.53
Well graded gravel	GW	Shrinkage%	1				0.80					
		Swelling %	1				28.00					
Poorly graded gravel with clay	GP	Shrinkage%	1				7.7					
		Swelling %	1				28.6					
Well graded gravel with clay	GW-GC	Shrinkage%	1				5					
		Swelling %	1				37.6					

On the other hand, the shrinkage percent varied from a minimum of 0.80 % for Bastora 1 project to a maximum of 23.5 % for Kalakan project. The remaining values were ranged between these values. These observations are in tune with the findings of Nunnally (2011), who observed that the shrinkage percentages for sand and gravel, common earth and clay were 12, 10 and 20%. It is commendable to mention that comparison between the results of the current study to those found in literature is not any easy task. This is due to the fact that different procedures and formulas have been used for determining swell and shrinkage factors (White et al., 2010). As a result the values should be back-calculated using the formulas used in the current study.

Similarly, the shrinkage percent tended to decrease with gravel content. Overall, within each group, the swell percent was superior to the shrinkage percent. Additionally, the swell percent was characterized by having a higher coefficient of variation compared to that of shrinkage percent. By contrast, White et al. (2010), observed that the shrinkage factor varied more than the swell percentages as the shrinkage values are likely influenced by the percent of compaction achieved in the field

It is also evident from Table 3 that the swell percentage ranged from 36.10-55.7% for clays, 18.40-69.20% for silts and 11.90-54.5% for gravels. Shrinkage percentage ranged from 9.20-16.5% for clays, 4.40-20.20% for silts and 0.80-23.5% for gravels. These results are in concordance with the findings of Crooks (2013), who reported that the swell percentage ranged from 30-50 % for clays, 5-40% for gravels. They also indicated that shrinkage percentage ranged from 10-18% for clays, and 5-22% for gravels.

The soil materials of the surveyed projects were categorized into different classes and the results are presented in Figure 2. It is evident from this Figure that the silt of low plasticity has the highest percentage (frequency) and followed by the silty gravel class the second highest. On the other hand, each of poorly graded gravel (GP), well graded gravel and well graded gravel with clayey gravel offered the least percentage (2.56%). Furthermore, no soil material fell in the class of well graded gravel with silty gravel

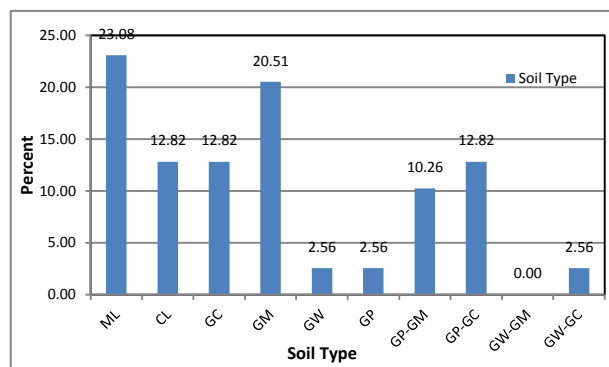


**Figure 2:** Percent of Projects within soil material groups: ML = Silt of low plasticity; CL = Clay of low plasticity; GC = Clayey gravel; GM = Poorly graded gravel with silt; GW = Well graded gravel; GP = Poorly graded gravel with clay; GP-GM = Poorly graded gravel with silt; GP-GC = Poorly graded gravel with clay; GW-GM= Well graded gravel with silt, and GW-GC = Well graded gravel with clay.

Based on swell and shrinkage percentages, the soils were categorized into different classes and the results are presented in Figure 3 and 4. It is apparent from Figure 3 that the swell class of 30-40 offered the highest frequency followed by the swell class of 20-30. Conversely the swell class of 40-50 offered the least frequency. It was also observed that the shrinkage of 0.0-2.5 offered the highest frequency and followed by the shrinkage class of 10.0-12.5 the second highest. Unlike these classes, the shrinkage of class of 22.5-25.0 offered the least frequency (Figure 4).

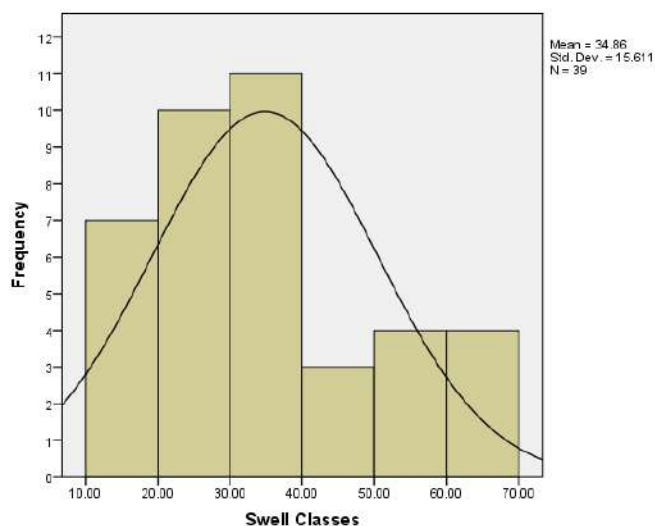


**Figure 3:** Frequency of soil groups within swell classes

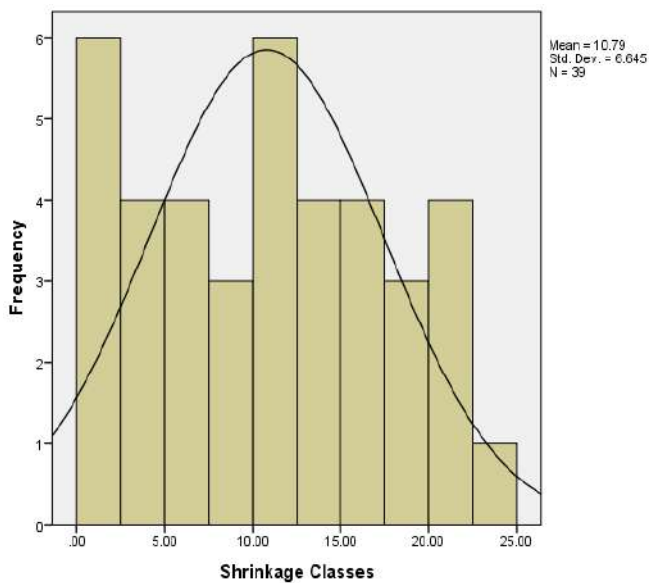


**Figure 4:** Frequency of soil groups within shrinkage classes

A box-whisker plot was also constructed by drawing a box between the upper and lower quartiles (Figure 5). The upper and lower quartiles were used to calculate the interquartile range, from which the inner and outer fences were created. No value of both swell and shrinkage percentages fell beyond the inner and outer fences on both sides, indicating the neither mild nor extreme outlier exists within the swell and shrinkage data.

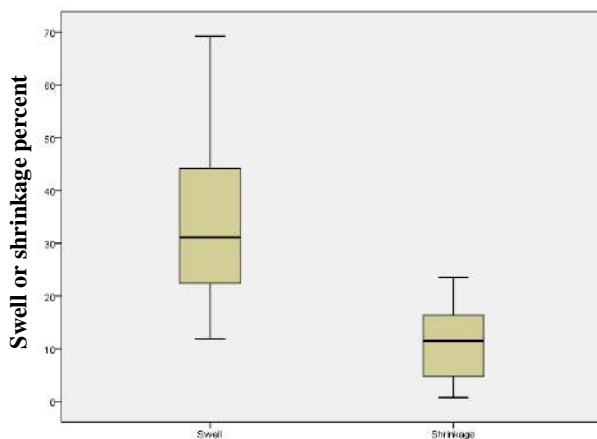


**Figure 5:** Representation of swell and shrinkage percentages data by Box - Whisker plot.

The Kolmogorov-Smirnov test was conducted to test for the normality of swell and shrinkage percentages. The K-S statistics for these two variables were 0.148 and 0.110 respectively. Both of these values were less than the critical D (0.035, 39) = 0.21, indicating these data did not

differ significantly from that which is normally distributed.

Prior to model building for predicting swell and shrinkage percentages, Pearson correlation analyses was conducted as a guide or simple sensitivity analysis to identify the influential factors affecting the overall response variables. Table 4 displays the correlation matrix for the study variables. As it can be seen in this Table, among the study input variables, the in situ soil density was negatively and very high significantly ( $P \leq 0.01$ ) correlated with shrinkage percent, followed by CBR. It can be also noticed from Table 4 that both soil density in the loose state and specific gravity were negatively and high significantly ( $P \leq 0.05$ ) correlated with shrinkage factors. Unlike these input variables, the remaining input variables were not significantly correlated with shrinkage factor. In addition, it was noticed the soil density at the loose state offered the strongest correlation with swell factor ( $r = -0.720$ ) followed by maximum dry density ( $r = -0.666$ ). Similarly, most of the remaining input variables were very high significantly ( $P \leq 0.01$ ) correlated with the swell percent. It is commendable to mention the intercorrelation between the input variable were also displayed as a guide to avoid multicollinearity problem during model calibration.

### 3.2. Model Calibration

A trial was made to predict swell percent and shrinkage percentages separately from other soil attributes using linear multiple regression. The all possible cases algorithm was followed to specify which predictor variables were to be included in the regression equations. The variables which did not give rise to a considerable improvement in the accuracy of prediction were deleted.

It was discerned that among the developed models, Models 1 and 2 offered the best performance for predicting the swell and shrinkage percentages respectively (Not shown here). According to our findings, the in situ soil density and clay content have emerged to be the most effective soil properties for predicting swell percent. On the other hand, the influential variables for predicting shrinkage percent were in situ soil density and the maximum dry density obtained from the laboratory tests.

**Table 4** Correlation matrix showing the relationship among some selected input and response variables

Variables	Variables													
	In situ density (Mg m <sup>-3</sup> )	Loose density (Mg m <sup>-3</sup> )	Embankment density (Mg m <sup>-3</sup> )	Specific gravity	MDD (Mg m <sup>-3</sup> )	OMC (%)	CBR (%)	Gravel (%)	Sand (%)	Fine (< 0.075 mm)	Silt (%)	Clay (%)	Swell (%)	Shrinkage (%)
1. In situ density (Mg m <sup>-3</sup> )	1	0.901**	0.883**	-0.209	0.843**	-0.813**	0.886**	0.779**	0.560**	-0.811**	-0.801**	-0.773**	-0.357*	-0.675**
2. Loose density (Mg m <sup>-3</sup> )	0.901**	1	0.938**	-0.406*	0.923**	-0.892**	0.860**	0.869**	0.473**	-0.880**	-0.798**	-0.903**	-0.720**	-0.379*
3. Embankment density (Mg m <sup>-3</sup> )	0.883**	0.938**	1	-0.480**	0.987**	-0.970**	0.866**	0.939**	0.549**	-0.956**	-0.909**	-0.945**	-0.632**	-0.252
4. Specific gravity	-0.209	-0.406*	-0.480**	1	-0.543**	0.587**	-0.217	-0.603**	-0.296	0.605**	0.529**	0.638**	0.566**	-0.327*
5. MDD (Mg m <sup>-3</sup> )	0.843**	0.923**	0.987**	-0.543**	1	-0.986**	0.834**	0.942**	0.540**	-0.958**	-0.901**	-0.955**	-0.666**	-0.191
6. OMC (%)	-0.813**	-0.892**	-0.970**	0.587**	-0.986**	1	-0.791**	-0.940**	-0.553**	0.958**	0.906**	0.951**	0.653**	0.157
7. CBR (%)	0.886**	0.860**	0.866**	-0.217	0.834**	-0.791**	1	0.788**	0.463**	-0.803**	-0.785**	-0.775**	-0.435**	-0.465**
8. Gravel (%)	0.779**	0.869**	0.939**	-0.603**	0.942**	-0.940**	0.788**	1	0.400*	-0.989**	-0.952**	-0.965**	-0.639**	-0.138
9. Sand (%)	0.560**	0.473**	0.549**	-0.296	0.540**	-0.553**	0.463**	0.400*	1	-0.533**	-0.534**	-0.500**	-0.146	-0.287
10. Fine (< 0.075 mm)	-0.811**	-0.880**	-0.956**	0.605**	-0.958**	0.958**	-0.803**	-0.989**	-0.533**	1	0.966**	0.973**	0.614**	0.174
11. Silt (%)	-0.801**	-0.798**	-0.909**	0.529**	-0.901**	0.906**	-0.785**	-0.952**	-0.534**	0.966**	1	0.880**	0.443**	0.237
12. Clay (%)	-0.773**	-0.903**	-0.945**	0.638**	-0.955**	0.951**	-0.775**	-0.965**	-0.500**	0.973**	0.880**	1	0.730**	0.108
13 Swell (%)	-0.357*	-0.720**	-0.632**	0.566**	-0.666**	0.653**	-0.435**	-0.639**	-0.146	0.614**	0.443**	0.730**	1	-0.268
14. Shrinkage (%)	-0.675**	-0.379*	-0.252	-0.327*	-0.191	0.157	-0.465**	-0.138	-0.287	0.174	0.237	0.108	-0.268	1

\*\* . Correlation is significant at the 0.01 level (2-tailed).

\* . Correlation is significant at the 0.05 level (2-tailed).

To investigate the degree of agreement between the observed and predicted values, the predicted values from each of M1 and M2 were plotted versus the observed values of the swell and shrinkage percentages in relation to line 1:1 (Figure. 6 and 7). As it can be seen from Figure 6 that there is considerable scattering over the whole range of swell percent. The variation in in situ soil density and clay content in Model 1 explained about 64% variation in swell percent. In contrast, there is a limited scattering over the whole range of shrinkage percent (Figure 7). Furthermore, the results indicated that more than 95% of variation in shrinkage percent can be attributed to variations in in situ soil density and maximum dry density. In a similar study by Shamo (2013), it was observed that the bulk bank density, the dry bank density, the dry embankment density and the dry embankment density accounted for 99.5% of variation in shrinkage factor.

Additionally, the plot of residuals of predicted swell from M1 indicated that the employed data were normally distributed (Figure 8). The same conclusion was drawn as the residual of the predicted shrinkage percent values were plotted versus the observed values (Figure 9).

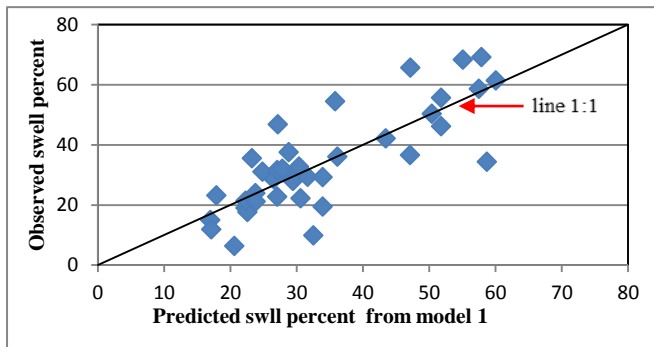


Figure 6: Plot of observe shrinkage percent predicted shrinkage percent from model 1

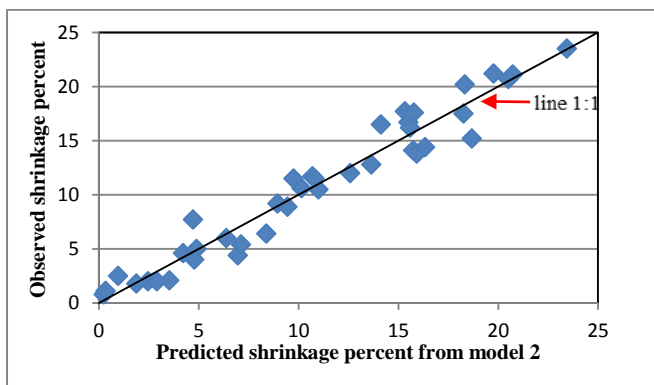


Figure 7: Plot of observed shrinkage factor versus predicted values from model 2

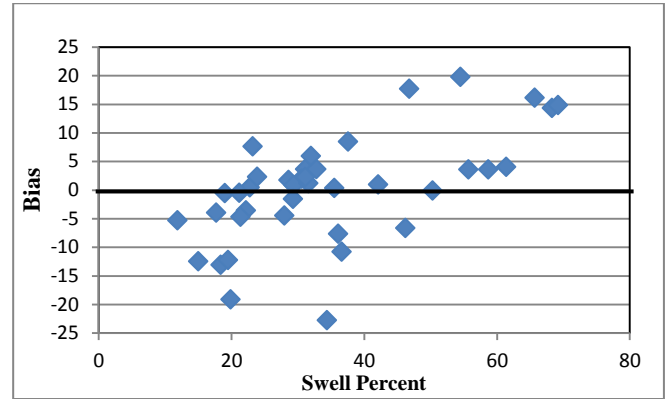


Figure 8: Plot of bias versus observed swell percent

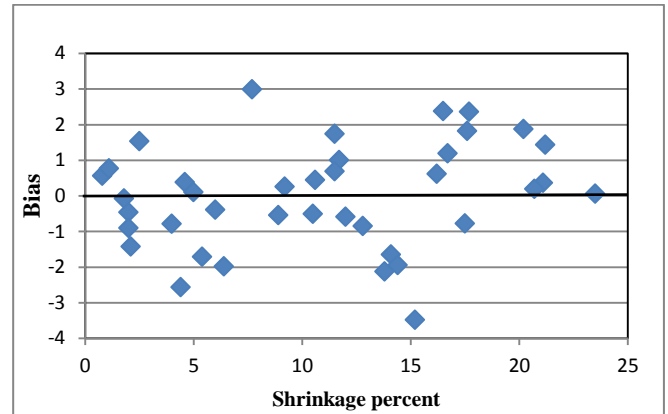


Figure 9: Plot bias versus observed shrinkage percent

### 3.3. Evaluation of the Models Performance

To further confirm the results, a host of performance indicators pertinent with Models 1 and 2 were calculated and depicted in Table 5. It is worth to note that there was a steady increase in R2 with increase in number of regressors beyond 2 (not shown here to save space), but this was not observed for adjusted coefficient of determination ( $R^2_{adj}$ ). The mean absolute error of prediction of swell and shrinkage percentages were 6.79 and 1.17 respectively, indicating that shrinkage percent can be predicted more accurately compared with swell percent.

Close inspection of Table 5 and judging from mean biased error (MBE) and coefficient of residual mass (CRM) indicated that Models 1 very slightly underestimated the overall swell percent, while model 2 neither overestimated nor underestimated the shrinkage percent.

Judging from mean absolute percentage error (MAPE), Models 1 and 2 enlisted in Table 5 fell within the "forecast potentially reasonable" and "forecast potentially good" respectively (Lewis, 1997).

**Table 5** The proposed models for predicting swell and shrinkage percentages of the soil materials along with some selected performance indicators for their evaluation.

Model	Constant	Input variables coefficients			Performance indicators							
		$\rho_{\text{bank}}$ Mg m <sup>-3</sup>	MDD Mg m <sup>-3</sup>	Clay %	R <sup>2</sup>	R <sup>2</sup> adj	MBE	MAE	MAPE	RMSE	CRM	CV
Model 1	-35.28	28.50		0.98	0.64	0.62	0.15	6.79	22.42	9.23	0.00	28.06
Model 2	9.88	-42.04	36.21		0.95	0.95	0.00	1.17	18.77	1.45	0.00	13.42

The MAPE classes for the study percentages are: 20% < MAPE < 30% and MAPE < 20% respectively.

It was also noticed from Table 5 that the root mean square error for the shrinkage percent was substantial lower than that of the swell percent (1.45 versus 9.23).

Smaller root mean square error (RMSE), Mean absolute error (MAE) and MAPE values from a given approach indicate the closeness of the modeled values to the observed ones. The mean absolute percentage error (MAPE) is one of the most widely used measures of forecast accuracy, due to its advantages of scale-independency and interpretability. However, MAPE has the significant disadvantage that it produces infinite or undefined values for zero or close-to-zero actual values (Kim and Kim, 2016).

Based on the classification scheme proposed by Wilding (1985) the coefficient of variability of the predicted and observed shrinkage percentages (CV) for model 2 is low (CV <15%). Model 1 exhibited higher value for CV (28.06%), which fell in the moderate class (15% < CV < 30%).

The higher the CV, the greater the dispersion in the variable. The lower the CV, the smaller the residuals relative to the predicted values and is suggestive of a good model fit.

It is noteworthy to mention that apart to the fact that adding additional variables to the proposed models did not give rise to significant improvement of prediction of swell and shrinkage percentages, insertion of some variables created the problem of multicollinearity. For instance, addition of gravel as a third input variable to

model I created the problem of instability of the model coefficients because this variable is closely related with clay content ( $r = 0.973$ ). Furthermore, it is impractical to add the soil density of the embankment as an additional input variable to Model 1 and 2 because we intend to predict the swell and shrinkage percentages before implementing the projects. In the light of the above results is recommended to perform cost analysis to determine the acceptable percentages of swell and shrinkage percentages.

#### 4. CONCLUSIONS

The results of the current study indicated that the swell percentages of the soil materials of the surveyed projects are characterized by having a wider range compared with shrinkage percentages. There is also the possibility of predicting of these factors with reasonable accuracy in general and the shrinkage percentages in particular.

#### REFERENCES

- AKIJE, I. 2013. An innovative mass haul diagram development for highway earthwork. *Journal of Emerging Trends in Engineering and Applied Sciences*, 4, 38-45.
- ALZOUBI, I., ALALI, F. A. & MIRZAEI, F. 2017. Earthwork Volume Optimization Using Imperialistic Competitive Algorithm to Minimize Energy Consumption of Agricultural Land Leveling. *Journal of Tethys: Vol, 5*, 070-086.
- ANUPRIYA, L. R. C. 2018. Calculation of Cut and Fill of Earthworks with Quantum-GIS. *IJSRD*, 6, 2321-0613.



- BANNISTER, A., RAYMOND, S. & BAKER, R. 1998. Surveying (7th edn). Harlow: Longman, 502.
- BLAKE, G. R. & HARTGE, K. 1986. Bulk density. *Methods of soil analysis: Part 1 Physical and mineralogical methods*, 5, 363-375.
- BURCH, D. 1997. *Estimating excavation*, Craftsman Book Company.
- C127, A. 2015. Standard Test Method for Relative Density (Specific Gravity) and Absorption of a Coarse Aggregate.
- C128, A. 2012. Standard Test Method for Density, Relative Density (Specific Gravity), and Absorption of Fine Aggregate *ASTM International, West Conshohocken, PA. doi*.
- C136-06, A. 2006. Standard test method for sieve analysis of fine and coarse aggregates.
- CHOPRA, M. B., NEGRON, C. A. & KENNETH MORGAN, P. E. 1999. Improved Shrinkage and Bulkage Factors for Cohesionless Soils. *Transportation Research Board Annual Meeting 1999 Washington, D.C.*
- COLE, G. M. & HARBIN, A. L. 2006. Surveyor reference manual. Fourth Edition. Professional publications, Inc., Belmont, CA.
- CROOKS, A. R. 2013. *Application of shrinkage and swelling factors on State Highway Construction*.
- D422-63, A. 2007. Standard test method for particle-size analysis of soils. *ASTM International, West Conshohocken. doi*, 10, 1520.
- D854-14, A. 2014. Standard test methods for specific gravity of soil solids by water pycnometer.
- D1556-07, A. 2007. Standard test method for density and unit weight of soil in place by the sand-cone method.
- D1557-12, A. 2012. Standard test methods for laboratory compaction characteristics of soil using modified effort. *ASTM International, West Conshohocken, PA.*
- D1883-16, A. 2016. Standard test method for California bearing ratio (CBR) of laboratory-compacted soils. *ASTM International West Conshohocken, PA.*
- D2216, A. 2005. Test methods for laboratory determination of water (moisture) content of soil and rock by mass, *ASTM International West Conshohocken, PA, 2005, DOI: 10.1520/D2216-05.*
- D4318, A. 2010. Standard test methods for liquid limit, plastic limit, and plasticity index of soils. *ASTM International, West Conshohocken, PA. doi*, 10.
- D6913, A. 2009. D6913-04.(2009). *Standard test methods for particle-size distribution (gradation) of soils using sieve analysis. West Conshohocken, PA, USA: ASTM international. doi*, 10.
- FHWA, F. H. A. 2007. Geotechnical Technical Guidance Manual. 291.
- GARBER, N. J. & HOEL, L. A. 2010. *Traffic and highway engineering*, Cengage Learning.
- GÖKTEPE, A. B., LAV, A. H., ALTUN, S. & ALTINTAŞ, G. 2008. Fuzzy decision support system to determine swell/shrink factor affecting earthwork optimization of highways. *Mathematical and Computational Applications*, 13, 61-70.
- HELTON, J. E. 1992. *Simplified estimating for builders and engineers*, Prentice Hall, Inc., New Jersey.
- HESSE, P. R. 1971. A textbook of soil chemical analysis.
- JACKSON, M. 1958. Soil chemical analysis prentice Hall. *Inc., Englewood Cliffs, NJ*, 498, 183-204.
- KIM, S. & KIM, H. 2016. A new metric of absolute percentage error for intermittent demand forecasts. *International Journal of Forecasting*, 32, 669-679.
- LEWIS, C. D. 1997. *Demand forecasting and inventory control: A computer aided learning approach*, Routledge.
- LI, D. & LU, M. 2019. Classical Planning Model-Based Approach to Automating Construction Planning on Earthwork Projects. *Computer-Aided Civil and Infrastructure Engineering*, 34, 299-315.
- MARTÍNEZ, G. M. A., ARRÚA, P. A. & EBERHARDT, M. G. 2014. A Topographic Method for Determining the Swelling Factor of Soils by Excavation. *EJGE*, 19, 6627-6634.
- NAJAFI, M. & GOKHALE, S. B. 2005. *Trenchless technology: pipeline and utility design, construction, and renewal*, McGraw Hill Professional, New York, NY.
- NUNNALLY, S. W. 2011. *Construction methods and management*, Prentice Hall.
- ROWELL, D. L. 2014. *Soil science: Methods & applications*, New York : Wiley, 1994, Routledge.
- SAĞLAM, B. & BETTEMIR, Ö. 2018. Estimation of duration of earthwork with backhoe excavator by Monte Carlo Simulation. *Journal of Construction Engineering*, 1, 85-94.
- SHAMO, B. 2013. *Spatial Statistical and Multivariate Regression Approach to Earthwork Shrinkage-Factor Calculation*. North Dakota State University.
- UHLIK III, F. T. 1984. *Optimizing Earthwork Estimating for Highway Construction*. Doctor of Philosophy, AIR FORCE INST OF TECH WRIGHT-PATTERSON AFB OH.
- WHITE, D., VENNAPUSA, P. & ZHANG, J. 2010. Earthwork Volumetric Calculations and Characterization of Additional CFED Soils. *CFED Phase IV*, 44-49.
- WILDING, L. Spatial variability: its documentation, accomodation and implication to soil surveys. Soil spatial variability, Las Vegas NV, 30 November-1 December 1984, 1985. 166-194.

## RESEARCH PAPER

# Alleviating of Lead toxicity using salicylic acid foliar spray in common bean (*Phaseolus vulgaris L.*) plant

Halalal R. Qader<sup>1</sup>, Karim Salih Abdul <sup>2</sup>

1- Department of Environmental science, College of Science, Salahaddin University, Erbil, Kurdistan Region, Iraq.

2. University President of Bayan University

### ABSTRACT

This study was carried out in a greenhouse at the college of science university of salahaddin,erbil, Iraq. Salicylic acid (SA) and Lead (pb) with (0, 50, 100, 200 and 400 ppm) and pb (0, 5 and 10 ppm) are used in a (type of the experiment must be recorded) experiment. Consisting of 10 treatment combinations with 4 replicates. Treatments were compared according to Duncan's multiple range tests at 0.05 level. Some vegetative growth, yield and chemical components were measured. The results notices that SA significantly decreased the harmful effects of Pb on the vegetative growth characteristics such as height of plant number of leaves, number of branches, weight dry of shoot system, also on yield parameters such as number of seeds per pod, dry weight of 100 seeds and on chemical contents such as chlorophyll a and total chlorophyll contents, total protein content of leaves and total sodium.

KEY WORDS: Lead; Toxicity; Salicylic acid; Chlorophyll; Common bean

DOI: <http://dx.doi.org/10.21271/ZJPAS.32.6.15>

ZJPAS (2020) , 32(6);138-149 .

### 1. INTRODUCTION

The common bean(*Phaseolus vulgaris L.*) is a herbaceous annual plant, belongs to leguminous family trained autonomously in old Mesoamerica and now become over wall both for green beans and as dry bean. Among the significant nourishment vegetables the common Bean is the third most significant around the world, after soybean (*Glycine max L.*), and peanut (*Arachis hypogaea L.*) (Zeka, 2007).

The common bean green pods, seeds are the principle source of protein (20–25%) and complex carbohydrates (50–60%) (Martiniz *et al.*, 2011), Vitamins, dietary fiber, mineral nutrients such as phosphorus, zinc, iron and calcium (Carvalho *et al.*, 2012). Bean plants have ability to absorb pollutants from contaminated environments by their roots with other nutrients (Mwstefa and Ahmed, 2019).

Salicylic acid (SA) is the plant hormone, which has fundamental role in the control of most physiological processes in plants. SA has found to assume the significant role in plant growth, and when it combined with other factors is great concern in reactions considerable lot of environmental stresses. Moreover, it play arole in seed germination, plant growth, flowering, fruit yield, glycolysis, ion uptake and stomatal number, transpiration, transport and rate of photosynthetic process, ...etc (Sadeghipour and Aghaei, 2012 A,

#### \* Corresponding Author:

Halalal R. Qader

E-mail: [halala.rahman@gmail.com](mailto:halala.rahman@gmail.com)

#### Article History:

Received:23/12/2019

Accepted: 07/09/2020

Published:20/12/2020

B). It is proved that have primary reactions to a biotic stresses and some reactions of abiotic stress, such as herbicides, heavy metals, salinity, low temperature (Mohsenzadeh *et al.*, 2011), and osmotic stress. Among those stresses, harmful heavy metal stress is a rising and most stress that is effective for major products (Bhardwaj *et al.*, 2009). (Rashid, 2018) reported that salicylic acid corrosive fundamentally increases yield components such as pods weight, pod yield, total yield, seed number per pod, dry weight of hundred seeds, and total seed yield.

Lead (Pb), is one of the heavy metals which is unnecessary discharged into the common habitat from a number of anthropogenic processes (Ekmeççi *et al.*, 2009). When it is discharged, it has harmful effect on plants and animals because of its accumulation in the soil (Kaur *et al.*, 2010). Accumulation of Pb near urban and industrial areas cause a significant increase of Pb in the surface ground layer which effects the cultivated of soil (Hussain *et al.*, 2006). Sullyng of soils with Pb not just influences the number and movement of microorganism but also declines soil fertility, yet additionally directly influence the difference in physiological indices and brings about the reduction of yields (Majer *et al.*, 2002). Pb absorbed by the plants principally through root, leaves and trichomes. Toxicity of Pb cause more problems as decrease in growth, yield, senescence of young leaves, reducing in the absorption of essential elements such as iron and decrease in the rate of photosynthesis. Contamination of Pb in the plant is known to have adverse effects on germination of seed, photosynthesis, seedling growth, respiration, nitrate assimilation and differnt processes (Singh *et al.*, 2003).

Foliar application of SA at doses of 0.1 or 0.2 mM decreased the impact of Pb<sup>+2</sup> on seedling development of two rice (*Oryza sativa* L.) cultivars, SA improve the fresh and dry mass of shoots and roots in the two cultivars under stresses of Pb (Mishra and Choudhuri, 1997). Interaction effect of

SA and Pb increased significantly the height of plant, leaves number, leaf area, fresh and dry weight in contrasted to those treated with Pb in eggplants (Tavakoli *et al.*, 2011)

The principle target of this study was to investigate the ability of SA as foliar spray to decrease the harmful effect of Pb toxicity in the soil.

## 2. MATERIALS AND METHODS

This experiment was conducted in the greenhouse of the College of Science, Salahaddin University-Erbil, during the growing season March 7 2012 to July 5 2012, in order to evaluate the combination impact of lead (Pb) and Salicylic acid (SA) on growth and development of common bean. The study involved 40 plastic pots each pot with 24 and 21 cm diameter and depth respectively. Each contained 7kg dry sandy loam soil of Askikalak area, the soil sieved through 2mm pore size sieves, and 3 seed were sown in each pot. This test comprised of 10 treatment combinations with 4 replicates of foliar spray with different Salicylic acid (SA) concentrations at doses (0, 50, 100, 200, 400ppm) and soil water system of Pb (PbNO<sub>3</sub>) in two doses (0, 5, 10 ppm), and involved 10 treatments with four replications. The following characteristics were taken: height of plant (cm), leaves number.plant<sup>-1</sup>, branches number .plant<sup>-1</sup>, shoot dry weight (g), water content of shoot system, leaf area (cm<sup>2</sup>), stem diameter, yield components such a pods number, seeds number, dry weight of hundred seeds. In addition chemical contents were estimated as photosynthetic pigments, proline, phenol and mineral nutrients of leaves.

Water content of the system of shoot assessed as follows: fresh weight dried in an oven 110°C for an hours and then at 70°C for 24 hours, in an oven. Dry weight of shoot system obtained thirty minutes after cooling at room temperature (He *et al.*, 2005). The following formula was used for the estimation of water content

$$\text{Water content} = \frac{\text{F.wt.} - \text{D.wt.}}{\text{D.wt.}}$$

**F.wt.** =fresh weight

**D.wt. =dry weight**

Chlorophyll content in leaves ( $\text{mg.g}^{-1}$ ) evaluated by taking 0.5g of crisp leaves left in 10 ml of absolute ethanol for 24 hrs. In dull condition, this procedure repeated three times to finish extraction of chlorophyll the last volume arrived 30 ml were spectrophotometrically evaluates on two wavelength 649 and 665 nm as follows (Wintermans and Demote, 1967):

**$\mu\text{g chlorophyll a/ml solution} = (13.70) (A_{665\text{nm}}) - (5.76) (A_{649\text{nm}})$**

**$\mu\text{g chlorophyll b/ml solution} = (25.80) (A_{649\text{nm}}) - (7.60) (A_{665\text{nm}})$**

**Total chlorophyll = chlorophyll a + chlorophyll b**

**A=absorbance**

**m =nanometer**

**Proline content of leaves**

Proline was estimated by the method as depicted by (Bates *et al.*, 1973 and Hassan, 2011).

**3. RESULTS AND DISCUSSION****3.1. Vegetative growth characteristics**

Table (2) shows that SA decreased the adverse impact of Pb on plant height at various development stages which increased significantly ( $p \leq 0.05$ ) by  $\text{Pb}_5\text{SA}_{200}$ ,  $\text{Pb}_5\text{SA}_{400}$ ,  $\text{Pb}_{10}\text{SA}_{400}$  as compared with controls  $\text{Pb}_5\text{SA}_{50}$  and  $\text{Pb}_{10}\text{SA}_{200}$  after 15 days from application. And at  $\text{Pb}_5\text{SA}_{400}$  as compared with  $\text{Pb}_5\text{SA}_0$  after 30 days from application, and at  $\text{Pb}_5\text{SA}_{200}$ ,  $\text{Pb}_5\text{SA}_{400}$  as compared with control  $\text{Pb}_5\text{SA}_0$ ,  $\text{Pb}_{10}\text{SA}_{100}$ ,  $\text{Pb}_{10}\text{SA}_{200}$ ,  $\text{Pb}_{10}\text{SA}_{400}$  as compared with controls  $\text{Pb}_5\text{SA}_0$ ,  $\text{Pb}_{10}\text{SA}_{400}$  after 45 days from application. After 60 days from application at  $\text{Pb}_5\text{SA}_{100}$ ,  $\text{Pb}_5\text{SA}_{200}$ ,  $\text{Pb}_5\text{SA}_{400}$ ,  $\text{Pb}_{10}\text{SA}_{50}$ ,  $\text{Pb}_{10}\text{SA}_{100}$ ,  $\text{Pb}_{10}\text{SA}_{200}$ ,  $\text{Pb}_{10}\text{SA}_{400}$  as compared with  $\text{Pb}_5\text{SA}_0$ ,  $\text{Pb}_{10}\text{SA}_0$ . However, there were significant differences between treatments. The increases in plant height with the increase of

concentrations of SA in the present investigation are in agreement partially with those reported by (Sadeghipour and Aghaei, 2012A). SA treatments showed synergetic effect with endogenous phytohormones auxins, gibberellins and cytokinines, which are cause cell elongation leading to increase of plant height (Mady, 2009).

Table (3) shows that SA decreased the adverse effect of Pb on leaves number at different growth stages, number of leaves increased significantly by the treatment  $\text{Pb}_5\text{SA}_{100}$ ,  $\text{Pb}_5\text{SA}_{400}$ ,  $\text{Pb}_{10}\text{SA}_{200}$  as compared with control after 15 days from application and at  $\text{Pb}_5\text{SA}_0$ ,  $\text{Pb}_5\text{SA}_{400}$ ,  $\text{Pb}_{10}\text{SA}_{200}$ ,  $\text{Pb}_{10}\text{SA}_{400}$  as compared with controls  $\text{Pb}_5\text{SA}_0$ ,  $\text{Pb}_{10}\text{SA}_0$  after 30 days from application. And at  $\text{Pb}_5\text{SA}_{200}$ ,  $\text{Pb}_5\text{SA}_{400}$  as compared with controls  $\text{Pb}_5\text{SA}_0$ ,  $\text{Pb}_{10}\text{SA}_0$  after 45 days from application and after 60 days from application at  $\text{Pb}_5\text{SA}_{200}$ ,  $\text{Pb}_5\text{SA}_{400}$ ,  $\text{Pb}_{10}\text{SA}_{400}$  as compared with  $\text{Pb}_5\text{SA}_0$ ,  $\text{Pb}_{10}\text{SA}_0$  and there were significant differences between treatments. ). These results partially conquered with those got from basil and marjoram plants (Gharib, 2007), common bean plants (Hegazi and El-Shairy, 2007) and pea plants (El-shairy and Hegazi, 2009). SA at 400ppm was the more effect treatments in increasing leaf numbers.

Table (4) indicated thta SA alleviated the effect of Pb stress on the number of branches at different growth stages, which increased significantly by  $\text{Pb}_5\text{SA}_{400}$ ,  $\text{Pb}_{10}\text{SA}_{400}$  as compared with controls  $\text{Pb}_5\text{SA}_0$   $\text{Pb}_{10}\text{SA}_0$  after 15, 30, 45 days from application and at  $\text{Pb}_5\text{SA}_{200}$ ,  $\text{Pb}_{10}\text{SA}_{400}$  as compared with controls  $\text{Pb}_5\text{SA}_0$ ,  $\text{Pb}_{10}\text{SA}_0$  after 60days from application and observed clear significant differences between treatments. these results agreed partially with those obtained by Devi *et al.*, (2011) and Ali and Mahmoud, (2013), who pointed out that SA treatments increased the number of branches. The increase in the number of branches could be due to the suppression of apical dominance, thereby diverting the polar transport of auxins towards the

basal nodes leading to increased branching (Naz, 2006).

**Table 1: Some physical and chemical properties of the soil used in the experiments**

Properties	value
Sand	70.10 %
Silt	24.22 %
Clay	5.68 %
Soil texture	Sandy loam
Soil moisture	3.1 %
Organic matter	0.91 %
PH	7.24
CaCO <sub>3</sub> (Trimetric method)	25.7%
Electrical conductivity (ds m <sup>-1</sup> at 25°C)	0.58
Total nitrogen % (kjeldahl method)	0.4%
Total phosphorus ppm(Olsen method)	118 ppm
Total potassium ppm (flame photometer)	45 ppm
Total calcium ppm (atomic absorption method)	240 ppm
Total lead ppm (atomic absorption method)	9.5 ppm

Means within columns followed with the same letters are not significantly different from each others according to Duncan multiple range test at 5% level

**Table 2: Interaction effects of SA and Pb on plant height at different stages of growth**

Interaction treatments		Plant height (cm) after (days) from application			
Pb mg.Kg <sup>-1</sup>	SA ppm	15 days	30days	45days	60days
5	0	12.62 <sup>b</sup>	15.40 <sup>b</sup>	18.32 <sup>c</sup>	20.62 <sup>c</sup>
	50	13.22 <sup>b</sup>	15.58 <sup>ab</sup>	19.20 <sup>bc</sup>	21.90 <sup>de</sup>
	100	14.30 <sup>ab</sup>	16.14 <sup>ab</sup>	20.17 <sup>bc</sup>	22.64 <sup>cd</sup>
	200	15.17 <sup>a</sup>	17.35 <sup>ab</sup>	22.52 <sup>a</sup>	25.23 <sup>ab</sup>
	400	15.57 <sup>a</sup>	17.92 <sup>a</sup>	21.25 <sup>ab</sup>	24.70 <sup>ab</sup>
	0	12.65 <sup>b</sup>	15.30 <sup>b</sup>	18.70 <sup>c</sup>	21.50 <sup>cd</sup>

	50	14.02 <sup>ab</sup>	15.72 <sup>ab</sup>	20.85 <sup>abc</sup>	23.97 <sup>b</sup>
10	100	13.70 <sup>ab</sup>	16.25 <sup>ab</sup>	21.14 <sup>ab</sup>	24.03 <sup>bc</sup>
	200	13.20 <sup>b</sup>	17.35 <sup>ab</sup>	22.45 <sup>a</sup>	25.87 <sup>a</sup>
	400	15.62 <sup>a</sup>	16.87 <sup>ab</sup>	22.15 <sup>a</sup>	24.92 <sup>bc</sup>

\*Means within columns followed with the same letters are not significantly different from each others according to Duncan multiple range test at 5% level

**Table 3: Interaction effects of SA and Pb on number of leaves at different stages of growth**

Interaction treatments		Number of leaves after (days) from application			
Pb mg.Kg <sup>-1</sup>	SA ppm	15 days	30days	45days	60days
	0	9.00 <sup>b</sup>	11.75 <sup>c</sup>	13.75 <sup>c</sup>	16.00 <sup>b</sup>
	50	9.75 <sup>ab</sup>	12.00 <sup>bc</sup>	15.25 <sup>bc</sup>	17.50 <sup>ab</sup>
	100	11.00 <sup>a</sup>	12.75 <sup>abc</sup>	15.00 <sup>bc</sup>	18.50 <sup>a</sup>
5	200	10.50 <sup>ab</sup>	13.50 <sup>ab</sup>	16.25 <sup>a</sup>	18.25 <sup>a</sup>
	400	11.25 <sup>a</sup>	14.00 <sup>a</sup>	16.00 <sup>a</sup>	19.50 <sup>a</sup>
	0	9.25 <sup>b</sup>	11.50 <sup>c</sup>	13.75 <sup>c</sup>	15.75 <sup>b</sup>
	50	10.50 <sup>ab</sup>	12.00 <sup>bc</sup>	15.25 <sup>bc</sup>	17.50 <sup>ab</sup>
	100	9.75 <sup>ab</sup>	12.75 <sup>abc</sup>	14.25 <sup>bc</sup>	17.50 <sup>ab</sup>
10	200	11.00 <sup>a</sup>	14.00 <sup>a</sup>	15.75 <sup>bc</sup>	17.00 <sup>ab</sup>
	400	10.50 <sup>ab</sup>	14.75 <sup>a</sup>	17.00 <sup>a</sup>	19.25 <sup>a</sup>

\* Means within columns followed with the same letters are not significantly different from each others according to Duncan multiple range test at 5% level

**Table 4: Interaction effects of SA and Pb on number of branches at different stages of growth**

Interaction treatments		Number of branches after (days) from application			
Pb mg.Kg <sup>-1</sup>	SA ppm	15 days	30days	45days	60days
	0	3.25 <sup>b</sup>	5.00 <sup>b</sup>	6.00 <sup>c</sup>	7.50 <sup>c</sup>
	50	3.25 <sup>b</sup>	5.25 <sup>ab</sup>	6.25 <sup>bc</sup>	8.00 <sup>c</sup>
	100	3.50 <sup>b</sup>	5.25 <sup>ab</sup>	6.25 <sup>bc</sup>	8.25 <sup>c</sup>
5	200	3.75 <sup>ab</sup>	5.75 <sup>b</sup>	6.75 <sup>bc</sup>	8.75 <sup>ab</sup>
	400	4.50 <sup>a</sup>	6.00 <sup>a</sup>	7.50 <sup>a</sup>	9.00 <sup>abc</sup>

	0	3.50 <sup>b</sup>	5.25 <sup>ab</sup>	6.50 <sup>c</sup>	8.25 <sup>c</sup>
	50	3.75 <sup>ab</sup>	5.50 <sup>ab</sup>	6.75 <sup>bc</sup>	8.50 <sup>bc</sup>
	100	4.00 <sup>ab</sup>	5.75 <sup>ab</sup>	6.75 <sup>bc</sup>	8.25 <sup>c</sup>
10	200	3.75 <sup>ab</sup>	6.00 <sup>ab</sup>	7.25 <sup>bc</sup>	9.00 <sup>abc</sup>
	400	4.75 <sup>a</sup>	6.75 <sup>a</sup>	8.00 <sup>a</sup>	9.75 <sup>a</sup>

\* Means within columns followed with the same letters are not significantly different from each others according to Duncan multiple range test at 5% level

### 3.2 Yield characteristics

Table (5) shows the combination impact of SA and Pb on yield components. It is observed that

there are no significant differences between treatments.

**Table 5: Interaction effects of SA and Pb on yield characteristics**

Interaction treatments		Yield characteristics		
Pb mg.Kg <sup>-1</sup>	SA ppm	Number of pods .plant <sup>-1</sup>	Number of seeds .pod <sup>-1</sup>	Dry weight of 100 seeds
5	0	14.25 <sup>a</sup>	4.75 <sup>b</sup>	25.63 <sup>b</sup>
	50	15.75 <sup>a</sup>	5.25 <sup>ab</sup>	26.90 <sup>ab</sup>
	100	19.25 <sup>a</sup>	5.75 <sup>ab</sup>	28.25 <sup>ab</sup>
	200	18.50 <sup>a</sup>	5.50 <sup>ab</sup>	29.08 <sup>ab</sup>
	400	20.25 <sup>a</sup>	6.00 <sup>ab</sup>	26.80 <sup>ab</sup>
10	0	12.25 <sup>a</sup>	5.25 <sup>ab</sup>	26.63 <sup>ab</sup>
	50	17.50 <sup>a</sup>	5.50 <sup>ab</sup>	27.25 <sup>ab</sup>
	100	15.75 <sup>a</sup>	5.80 <sup>ab</sup>	28.25 <sup>ab</sup>
	200	14.25 <sup>a</sup>	5.25 <sup>ab</sup>	29.08 <sup>ab</sup>
	400	17.75 <sup>a</sup>	6.25 <sup>a</sup>	31.50 <sup>a</sup>

\* Means within columns followed with the same letters are not significantly different from each others according to Duncan multiple range test at 5% level

### 3.3. Chemical characteristics in leaves

Table (6) indicated that SA diminished the negative impact of Pb on chlorophyll contents of

fresh leaves, which significantly ( $p \leq 0.01$ ) increased chlorophyll a by  $Pb_5SA_{100}$ , as compared with  $Pb_5SA_0$ , and significantly increased by  $Pb_{10}SA_{50}$ ,  $Pb_{10}SA_{400}$  as contrasted with  $Pb_{10}SA_0$ , and there significant differences between 100ppm and 400ppm in total chlorophyll components of leaves. These results somewhat agreed with those conquered by Turkyilmaz *et al.* (2005), who recommended that foliar spray with SA increased chlorophyll a, b, and some photosynthetic pigments in bean in field conditions. The incitement impact of SA on chlorophyll concentration was affirmed by Azooz *et al.* (2011) on broad bean, Fahd and Bano (2012) on maize plants. Table (7) SA treatments decreased the adverse impact of Pb on total protein content of leaves, which increased significantly ( $p \leq 0.01$ ) by  $Pb_{10}SA_{100}$ ,  $Pb_{10}SA_{400}$  as compared with  $Pb_{10}SA_0$ , SA treatments decreased significantly ( $p \leq 0.01$ ) the content of proline under Pb stress by  $Pb_{10}SA_{400}$  as compared with  $Pb_{10}SA_0$ . Data in Table (8) indicated that SA decreased the negative effect of Pb on nitrogen content of leaves. It was observed that there were significant differences between 50ppm with 100 and 400ppm. It is observed that there were significant differences between  $Pb_{10}SA_{50}$  with  $Pb_{10}SA_{100}$ ,  $Pb_{10}SA_{200}$  and  $Pb_{10}SA_{400}$  in potassium content of leaves. The combination impact of SA and Pb on potassium content in leaves, that there were significant differences between  $Pb_5SA_{50}$  with  $Pb_5SA_{400}$ . There were no significant differences between treatments in total zinc, iron, and lead content of leaves. SA treatments increased the contents of K, while decreased Na contents in mung bean plant (Khan *et al.*, 2010). SA caused critical increases in the uptake of elements in tomato plant (Amin *et al.*, 2007). These increases in some mineral content might be associated with the increase in photosynthetic pigments which thusly influence the rate of organic compound assimilation (Abou El-Yazeid, 2011).



**Table 6: Interaction effects of SA and Pb on chlorophyll content of leaves (mg.g<sup>-1</sup>fresh weight)**

Interaction treatments		Photosynthetic pigments (mg.g <sup>-1</sup> fresh weight)		
Pb mg.Kg <sup>-1</sup>	SA ppm	Chlorophyll a	Chlorophyll b	Total chlorophyll
5	0	0.78 <sup>ab</sup>	0.16 <sup>a</sup>	0.95 <sup>abc</sup>
	50	0.69 <sup>ab</sup>	0.27 <sup>a</sup>	0.97 <sup>abc</sup>
	100	0.32 <sup>c</sup>	0.26 <sup>a</sup>	0.58 <sup>bc</sup>
	200	0.88 <sup>a</sup>	0.43 <sup>a</sup>	1.32 <sup>ab</sup>
	400	0.67 <sup>ab</sup>	0.68 <sup>a</sup>	1.35 <sup>a</sup>
10	0	0.45 <sup>bc</sup>	0.10 <sup>a</sup>	0.56 <sup>c</sup>
	50	0.89 <sup>a</sup>	0.43 <sup>a</sup>	1.32 <sup>bc</sup>
	100	0.56 <sup>abc</sup>	0.41 <sup>a</sup>	0.98 <sup>abc</sup>
	200	0.57 <sup>abc</sup>	0.19 <sup>a</sup>	0.76 <sup>abc</sup>
	400	0.83 <sup>a</sup>	0.39 <sup>a</sup>	1.22 <sup>abc</sup>

\* Means within columns followed with the same letters are not significantly different from each others according to Duncan multiple range test at 1% level

**Table 7: Interaction effects of SA and Pb on some biochemical contents of leaves and seeds**

Interaction treatments		Biochemical contents			
Pb mg.Kg <sup>-1</sup>	SA ppm	Protein (%)	Carbohydrate (%)	Proline (µg.g <sup>-1</sup> )	Total phenol (µg.g <sup>-1</sup> )
5	0	26.49 <sup>abc</sup>	48.17 <sup>a</sup>	31.46 <sup>ab</sup>	26.99 <sup>ab</sup>
	50	27.95 <sup>ab</sup>	49.96 <sup>a</sup>	26.97 <sup>ab</sup>	23.96 <sup>ab</sup>
	100	20.17 <sup>c</sup>	53.26 <sup>a</sup>	25.95 <sup>ab</sup>	23.55 <sup>ab</sup>
	200	25.28 <sup>abc</sup>	51.93 <sup>a</sup>	31.97 <sup>ab</sup>	20.16 <sup>ab</sup>
	400	29.41 <sup>a</sup>	48.92 <sup>a</sup>	25.69 <sup>ab</sup>	16.93 <sup>ab</sup>
10	0	20.42 <sup>c</sup>	47.52 <sup>a</sup>	37.43 <sup>a</sup>	28.98 <sup>a</sup>
	50	22.85 <sup>abc</sup>	52.62 <sup>a</sup>	29.79 <sup>ab</sup>	23.33 <sup>ab</sup>
	100	21.15 <sup>ab</sup>	46.10 <sup>a</sup>	26.15 <sup>ab</sup>	15.81 <sup>ab</sup>
	200	25.03 <sup>abc</sup>	45.35 <sup>a</sup>	28.57 <sup>ab</sup>	18.81 <sup>ab</sup>
	400	22.12 <sup>ab</sup>	48.47 <sup>a</sup>	18.76 <sup>b</sup>	24.46 <sup>ab</sup>

\* Means within columns followed with the same letters are not significantly different from each others according to Duncan multiple range test at 1% level

**Table 8: Interaction effects of SA and Pb on some mineral nutrient contents of leaves**

Interaction treatments		Mineral nutrient contents							
		Mg.g <sup>-1</sup>					µg.g <sup>-1</sup>		
Pb mg.Kg <sup>-1</sup>	SA ppm	Nitrogen	phosphorus	Potassium	Sodium	Manganese	Zinc	Iron	Lead
5	0	43.94 <sup>ab</sup>	2.10 <sup>a</sup>	11.65 <sup>b</sup>	2.72 <sup>ab</sup>	25.10 <sup>a</sup>	35.50 <sup>a</sup>	339.55 <sup>a</sup>	103.17 <sup>b</sup>
	50	44.72 <sup>a</sup>	2.65 <sup>a</sup>	12.97 <sup>ab</sup>	2.25 <sup>b</sup>	16.53 <sup>ab</sup>	40.24 <sup>a</sup>	341.62 <sup>a</sup>	174.60 <sup>ab</sup>
	100	32.66 <sup>b</sup>	2.81 <sup>a</sup>	13.19 <sup>ab</sup>	2.99 <sup>ab</sup>	19.90 <sup>ab</sup>	35.61 <sup>a</sup>	353.18 <sup>a</sup>	124.60 <sup>ab</sup>
	200	39.35 <sup>ab</sup>	2.41 <sup>a</sup>	13.76 <sup>ab</sup>	3.08 <sup>ab</sup>	16.12 <sup>ab</sup>	34.76 <sup>a</sup>	489.50 <sup>a</sup>	120.96 <sup>ab</sup>
	400	32.27 <sup>b</sup>	3.09 <sup>a</sup>	13.86 <sup>ab</sup>	3.25 <sup>a</sup>	16.72 <sup>ab</sup>	40.06 <sup>a</sup>	373.41 <sup>a</sup>	141.38 <sup>ab</sup>
10	0	36.55 <sup>ab</sup>	3.25 <sup>a</sup>	14.01 <sup>ab</sup>	2.66 <sup>ab</sup>	14.89 <sup>b</sup>	43.52 <sup>a</sup>	454.43 <sup>a</sup>	184.83 <sup>ab</sup>
	50	34.22 <sup>ab</sup>	3.44 <sup>a</sup>	14.60 <sup>b</sup>	3.21 <sup>a</sup>	15.92 <sup>ab</sup>	36.22 <sup>a</sup>	358.90 <sup>a</sup>	132.90 <sup>ab</sup>
	100	40.44 <sup>ab</sup>	3.55 <sup>a</sup>	14.63 <sup>a</sup>	2.58 <sup>ab</sup>	18.38 <sup>ab</sup>	42.43 <sup>a</sup>	315.20 <sup>a</sup>	254.01 <sup>a</sup>
	200	33.83 <sup>ab</sup>	3.77 <sup>a</sup>	14.72 <sup>a</sup>	2.83 <sup>ab</sup>	21.26 <sup>ab</sup>	35.13 <sup>a</sup>	395.56 <sup>a</sup>	155.53 <sup>ab</sup>
	400	40.83 <sup>ab</sup>	4.03 <sup>a</sup>	15.52 <sup>a</sup>	2.77 <sup>ab</sup>	18.91 <sup>ab</sup>	27.83 <sup>a</sup>	441.13 <sup>a</sup>	153.17 <sup>ab</sup>

\* Means within columns followed with the same letters are not significantly different from each others according to Duncan multiple range test at 1% level

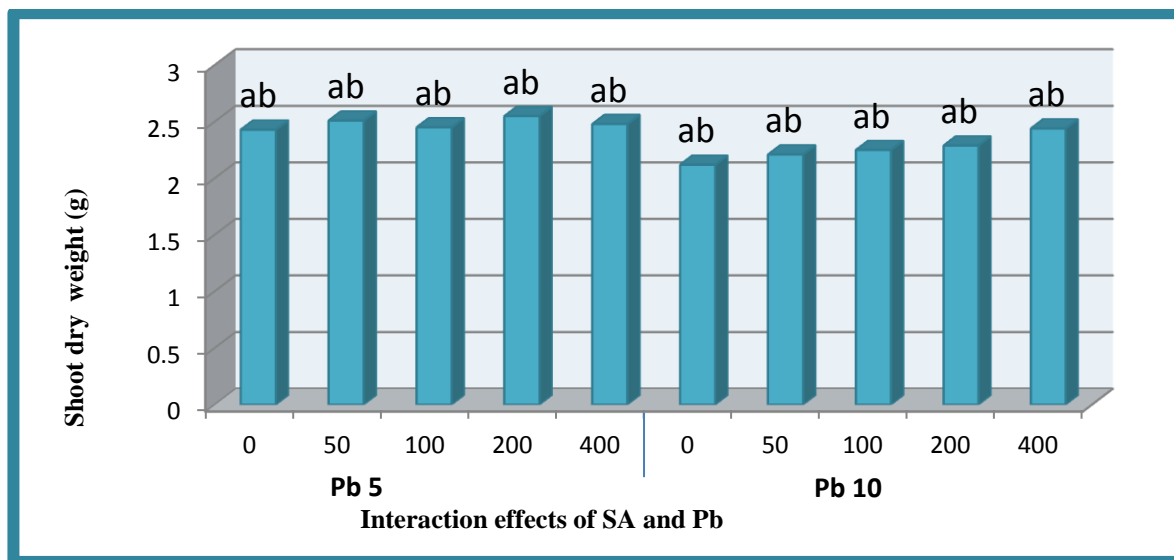


**Figure 1: Interaction effects of SA and Pb on dry weight of shoot system.**

\*Columns followed with the same letters are not significantly different from each other according to Duncan's multiple ranges test at 5% level.

\* Figure Number 1 should be redrawn because the column heights do not represent the reality according to the letters on them

#### 4. CONCLUSIONS

In conclusion the adverse effects of Pb toxicity alleviated by foliar application of SA in common bean plants on vegetative growth such plant height, number of leaves, number of branches, as well as on yield characteristics like number of seeds per pods and dry weight of 100 seeds, further more on and chemical components such as photosynthetic pigments also chemical contents protein, proline, total phenol, mineral nutrients nitrogen, potassium, sodium, and manganese

#### REFERENCES

- A.O.A.C., (2010). Determination of total nitrogen in waste water by steam distillation. Published by Association Official Agriculture Chemists, Washington, D.C., USA.
- A. Abou El-Yazeid. (2011). Effect of Foliar Application of Salicylic Acid and Chelated Zinc on Growth and Productivity of sweet pepper (*Capsicum annuum* L.) Under Autumn Planting. Res. J. of Agric. and Biol. Sci., 7(6): 423-433.
- S.E. Allen. (1974). Chemical Analysis of Ecological Materials. Black well Scientific Publication Osney Mead, Oxford, 565 p.
- E.A.Ali and M. Mahmoud. (2013). Effect of Foliar spray of Salicylic Acid and Zinc concentrations on seed Yield and yield components of Mungbean in Sandy soil. Asian J. of crop Sci., 5(1):33-40.
- M.M. Azooz; A.M. Youssef and P. Ahmad. (2011). Evaluation of salicylic acid (SA) application on growth, osmotic solutes and antioxidant enzyme activities on broad bean seedlings grown under diluted seawater. Int. J. Plant Physiol. & Bioch., 3(14): 253-264.
- P. Bhardwaj; A.K. Chaturvedil and P. Prasadi. (2009). Effect of Enhanced Lead and Cadmium in soil on Physiological and Biochemical attributes of *Phaseolus vulgaris* L. Natural & Sci., 7(8):63-75.

- L.S. Bates; R.P. Waldren and D. Teare. (1973). Rapid determination of free proline for water-stress studies. *Plant and Soil*, 39:205-207.
- L.M. J.Carvalho; M.M. Correa ; E. J. Pereira ; M. R. Nutti ; J.L.V. Carvalho ; E. M. G. Riebeiro and S. C. Freitas. (2012). Iron and Zinc retention in common beans (*Phaseolus vulgaris* L.) after home cooking. *Food & Nut. Res.*, 56:1656-1661.
- P.M.Dey. (1990). *Methods in plant biochemistry. Vol-II. Carbohydrates.* (Publ.) Acad. Press London.
- K.N. Devi; A.K. Vyas and M.S. Singh. (2011). Effect of bioregulators on growth, yield and chemical constituents of Soybean (*Glycine max* L.). *J. of Agric. & Sci.*, 3(4).151-159.
- Y. Ekmekçi; D. Tanyolac and B. Ayhan. (2009). A crop tolerating oxidative stress induced by excess lead: maize. *Acta Physiol. Plant*, 31: 319-330.
- A.M. El-shrai and A.M. Hegazi. (2009). Effect of Acetylsalicylic acid ,Indol-3-Bytric Acid and Gibberellic Acid on plant Growth and Yield of Pea (*Pisum sativum* L.). *Aus. J. of Basic and Applied Sci.*, 3(4):3514-3523.
- S. Fahad and A. Bano. (2012). Effect of salicylic acid on physiological characterization of maize grown in saline area. *Pak. J. Bot.*, 44(4):1433-1438.
- F.A.E. Garib (2007). Effect of salicylic acid on the growth ,metabolic activities and oil content of basil and marjoram . *Int. J. of Agric. & Biol.*, 9(2): 294-301.
- T. M. Hassan. (2011). Role of Salicylic acid on Alleviating Cadmium Toxicity in Pea *Pisum sativum* L. *Plants. M.Sc. Thesis. College of Education-Scientific Department. University of Salahaddin-Iraq.*
- Y. He; Y. Liu; W. Cao; M. Huai; B. Xu and B. Huang. (2005). Effect of salicylic acid on heat tolerance associated with antioxidant metabolism in Kentucky bluegrass. *Am. Crop Sci. Soci.*, 45:988-995.
- A.M. Hegazi and A.M. EL-Shrai. (2007). Impact of salicylic acid and paclobutrazol exogenous application on the growth, yield and nodule formation of common bean. *Aus. J. Basic & Applied Sci.*, 1(4):834-840.
- M. Hussain; M.S.A. Ahmad and A. Kausar. (2006). Effect of Lead and Chromium on growth ,photosynthetic pigments and yield components in Mash bean (*Vigna mungo* L.) Hepper. *Bot.*, 38(5):1389-1396.
- L. Kaur; K. Gadgil and S. Sharma. (2010). Effect of pH and lead concentration on phytoremoval of lead from lead contaminated water by *Lemna minor*. *American-Eurasian. J. Agric. & Environ. Sci.*, 7(5): 542–550.
- A.N.Khan; S. Syeed; A. Masood; R. Nazar and N. Iqbal. (2010). Application of salicylic acid increases contents of nutrients and antioxidative metabolism in mungbean and alleviates adverse effects of salinity stress. *Int. J. of Plant Biol.*, 1(1): 1-8.
- M.A. Mady. (2009). Effect of foliar application with salicylic acid and vitamine E on growth and productivity of tomato (*Lycopersicon esculentum*, Mill.). *Plant J. Agric. Sci. Mansoura Univ.*, 34(6): 6735-6746.
- B.J. Majer; D. Tschерko and A. Paschke. (2002). Effects of heavy metal contamination of soils on micronucleus induction in *Tradescantia* and on microbial enzyme activities: a comparative investigation. *Mutation Res. /Genetic Toxicology and Environmental Mutagenesis*, 515(1-2):111-124.
- M.O. Martiniz; L.A.B. Perez; K.W. Hitney; P.O. Diaz and S. Semik. (2011). Starch characteristics of bean (*Phaseolus vulgaris*) grown in different localities. *Carbohydrate Polymers*, 85(1):54-64.
- A. Mishra and M. A. Choudhuri. (1997). Ameliorating effects of salicylic acid on lead and mercury – induced inhibition of germination and early seedling growth of two rice cultivars. *Seed Sci. Technol.*, 25: 263-270.
- S. Mohsenzadeh; M. Shahrtash and H. Mohabatkar. (2011). Interactive effect of salicylic acid on some physiological response of cadmium-stressed maize seedlings. *Iranian J. of Sci. & Tech.*, 6, 57-60.
- T. Naz (2006). Influence of Salicylic acid and mepiquat chloride on physiology of disease resistance in groundnut (*Arachis hypogaea* L.). *M. Sc. Thesis, department of crop physiology, College of Agriculture, Dharwad University of Agricultural Science. Dharwad. India.*
- J. Rayn; G. Estefon and A. Rashid. (2001). *Soil and plant analysis Labrotory Manual, 2<sup>nd</sup>edition. National Agriculture Research Center (NARC). Islamabad, Pakistan.*
- O. Sadeghipour and P. Aghaei. (2012, A). Impact of exogenous salicylic acid on some traits of common bean (*Phaseolus vulgaris* L.) under water stress conditions. *Int. J. of Agric. & Crop Sci.*, 4(11):685-690.
- O. Sadeghipour, and P. Aghaei. (2012, B). Response of Common bean (*Phaseolus vulgaris* L.) to exogenous application of salicylic acid (SA) under water stress conditions. *Advances in Environ. Biol.*, 6(3):1160-1168.
- G.N. Sharma; S.K. Dubey; N.Sati and J. Sanadya. (2011). Phytochemical Screening and Estimation of Total Phenolic Content in *Aegle marmelos* Seeds. *Int. J. of Pharm. and Clinical Res.*, 3(2): 27-29.
- Singh, R.P.; R.D. Tripathi, S. Dabas ; S.M.H. Rizvi; M.B. Ali; S. K. Shina; D. K. Gupta; S. Mishra and U.N. Rai. (2003). Effect of lead on growth and nitrate assimilation

- of *Vigna radiata* (L) Wilczik seedling in a salt affected environment. Chemosphere. 52(7):1245-1250.
- M. Tavakoli; A.Chehregani; H. L. Yazdi and A. Pakdel. (2011). Study on the effect of different concentrations of Pb and salicylic acid on some growth factors in eggplants (*Solanum melongena* L.). Iranian J. of Plant Biol., 3(7): Abstract.
- B. Türkyılmaz; L.Y. Aktaş and A. Güven. (2005). Salicylic acid induced some biochemical and physiological changes in *Phaseolus vulgaris* L. Science and Engineering J. of Firat Univ., 17(2): 319-326.
- J.F. Wintermans and A. Demote. (1967). Spectrophotometry characteristics of chlorophyll (a) and (b) and their phynophytins in ethanol. Bioch. Biophysiology Acta., 109:448-453.
- D. Zeka. (2007). Inventory of phenotype diversity of landraces of common beans (*Phaseolus vulgaris* L.) in Kosova for a national gene bank.M.Sc.Thesis. Int. Master Programme at the Swedish Biodiversity Centre, pp41.

## RESEARCH PAPER

# Response of Plane Tree (*Platanus orientalis L.*) toward Environmental Pollution of Erbil City

Ismail T. Ahmed<sup>1</sup>, Halmat A. Sabr<sup>2</sup>

1-Department of Soil and water, College of Agricultural Engineering Sciences, Salahaddin University-Erbil, Kurdistan Region, Iraq

2-Department of Forestry, College of Agricultural Engineering Sciences, Salahaddin University-Erbil, Kurdistan Region, Iraq

### ABSTRACT

The objective of the present study was to evaluate the leaves of plane tree (*Platanus orientalis L.*) impaired by traffic pollution. Trees from four locations of Erbil City were investigated. Leaf morphology, leaf and soil heavy metal concentration and leaf pigments were measured from the collected leaf samples. One way ANOVA was used to compare means and determine significant variation among the studied parameters. The highest increase in chlorophyll a and total chlorophyll were obtained in Sami Abul-Rahman Park-whereas, the highest reduction was observed in Ainkawa road. Likewise in case of carotenoid contents, non significant effect was obtained from samples. The study obviously points out that the motor vehicles stimulate air pollution may result in decreases the concentration of photosynthetic pigments in the plane trees exposed to road side air pollution. It is shown that the lowest metal concentrations were detected in Sami Abul-Rahman Park in comparing with the other locations. It is shown that the lowest metal concentrations such as Ni, Zn, Mn and Fe in soil and plant samples were detected in Gulan Street When compared with the other locations. According to the geoaccumulation index ( $I_{geo}$ ), the soils were classified into uncontaminated and uncontaminated to moderately contaminate.

KEY WORDS: Chlorophyll content; Soil heavy metals; Leaf area; Air pollution

DOI: <http://dx.doi.org/10.21271/ZJPAS.32.6.16>

ZJPAS (2020) , 32(6);150-157 .

### 1. INTRODUCTION

Air pollution is a severe problem in many industrialized regions in the world (Kambezidis *et al.*, 1996). Environmental conditions and air pollution expose trees to different stresses and decrease growth. Dineva ,

(2004) believed that urban trees can be used to mitigate the effect of air pollution in areas with polluted environment. In addition, it is mostly documented that planting trees in industrial locations are fundamentally influenced by different pollutants such as particulate matter and gases like HF, Ozone etc. (Dineva, 2004). It has been shown that in many urban areas of the world a major source of air pollution is motor vehicles traffic which contributing 57–75% of total emissions (WHO 2006). Sawidis *et al.* (2001) stated that rural areas have lower pollution than metropolitan areas. Studies showed that plants develop different morphological and anatomical modifications under polluted conditions (Veselkin, 2004).

#### \* Corresponding Author:

Halmat Abubakr Sabr

E-mail: [halmat.sabr@su.edu.krd](mailto:halmat.sabr@su.edu.krd)

#### Article History:

Received: 11/04/2020

Accepted: 08/08/2020

Published: 20/12/2020

One of the most important services of forest trees is regulating services particularly in urban cities. A study conducted by Beckett *et al.*, (2000) showed that air quality through filtering and taking up gases and particles can be improved via trees in the urban environment there is a difference between forest trees species in responding to air pollution. Urban trees are of high essential component in urban areas for the inhabitants, but may also be in danger of extinction by experience to pollution. Plane tree (*Platanus orientalis* L.) is originally native to South Western Asia. It is a large deciduous tree known for its longevity and spreading crown. It can be planted from different elevations up to nearly 2500 meters above sea level (a.s.l) and the species is growing up to 30 m tall. In Erbil city the tree is usually used for the purpose of shading along with the streets and parks. The main objective of the study is to assess

the response of *Platanus orientalis* L. to environmental pollution on in Erbil city.

## 2. MATERIALS AND METHODS

### 2.1. Leaf sample collection

The research was studied leaves from common urban plane tree. The leave samples were collected from four locations during November 2019. Samples were taken randomly from each tree from the south and Northern sides of the crown at about more than 1 m height of every trees from all locations. Overall 120 leaves were gathered from all locations and the number of leaves per tree would be 10 leaves. Tree sampled at each of the four locations: L1 (Sami Abul-Rahman park) as a control, L2 (60 Meter street), L3 (Ainkawa road) and L4 (Gulan street) they had an identical height and growth form the sampling locations (Figure 1).

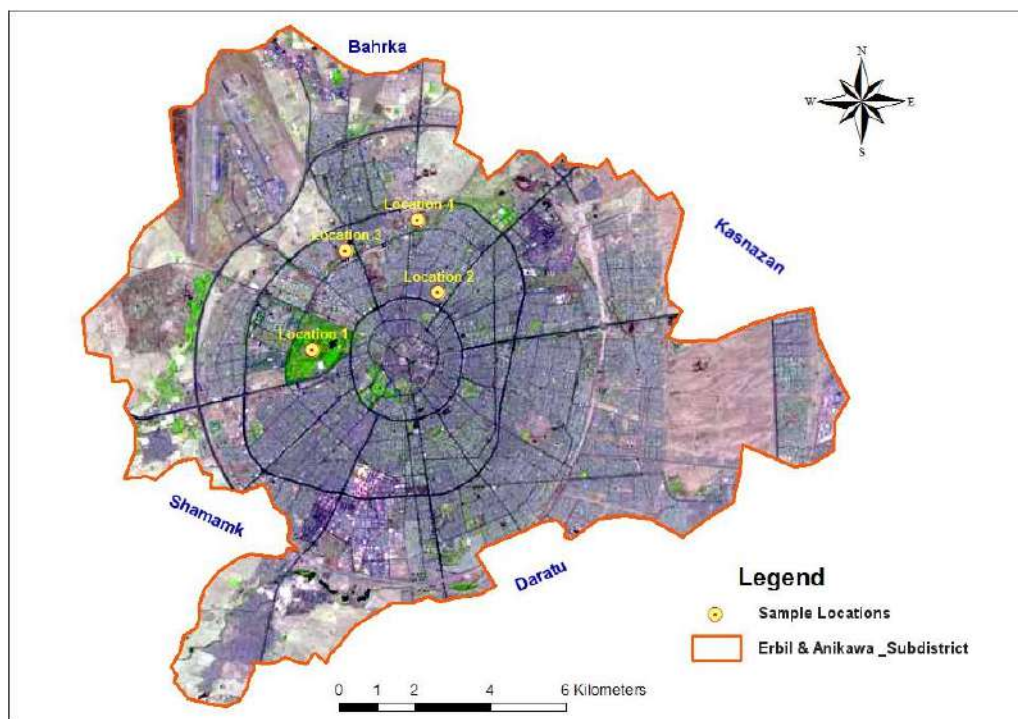


**Figure 1.** Sampling locations of *platanus orientalis* L. tree leaves and soil.

## 2.2 Study parameters

### 2.2.1. Leaf morphology

After cutting leaves from trees immediately they were placed in plastic bags and were imparted on ice to the laboratory. Leaf length and leaf width were measured by a ruler according to method as mentioned by (NeSmith, 1991). Leaf samples were collected from four locations. The leaves were duplicated on A4 sheets with knowing their areas and weight, the leaves were accurately marked and weighed. The area was calculated on portion and portionality scale, to obtain the leave area of whole tree by multiplying the number of leaves by the mean of area one leave (Patton, 1985).

### 2.2.2. Heavy metal concentration in leaves and soil samples ( $\text{mg kg}^{-1}$ )

Leaves and soil samples were directly analyzed by XRF (X-Ray Fluorescence analyzer) method after drying, sieving by 2mm and powdering of the material. Leave and soil samples were analyzed by XRF method and heavy metals were measuring by portable (CIT-300 SMP) (Sitko *et al.*, 2004), in general laboratory -College of Agricultural Engineering Sciences-Salahaddin University. For the evaluation of soil contamination by heavy metals.

Geoaccumulation index ( $I_{geo}$ ), the pollution indices may differ from each other due to several factors that affect their importance (Kowalska *et al.*, 2016).

**Geo-accumulation index ( $I_{geo}$ ) =  $\log_2 C_i / (C_{ig} * 1.5)$ ..... (1)**

Where  $C_i$  is the measured concentration of the studied metal in the surface soil

$C_{ig}$  is the geochemical background concentration or reference value of the metal, and 1.5 is constant that is used for litho logic variations of the heavy metal. Calculation of soil pollution indices needs the evaluated level of the geochemical background (GB). This term was presented to discriminate natural concentrations of heavy metals in the soil from unusual concentrations (Reimann and Garret 2005). Geo-accumulation index ( $I_{geo}$ ) as a single index was primarily defined by (Muller, 1979) to affirm metal contamination. Geo-accumulation index is a simple, precise widely used quantitative

method to assess the pollution level of a single heavy metal in soil by depending on the geological background (BG). Igeo index can compare between the present and past pollution levels. Furthermore, Igeo index uses the multiplication factor of (1.5) to minimize the possible variation of lithogenic effects.

### 2.2.3. Chlorophyll determination

Healthy and uninfected leaves were collected at the stage of maturity; and to avoid mechanical injuries care was also taken into consideration during collecting of leaf samples. Fresh leaf samples were needed to be lotion cautiously first with drinking water and after that by distilled water in the laboratory, kept to dry in room temperature ( $28^\circ\text{C}$ ). The solution mixture was analyzed and spectrophotometric determination absorbance taken at 663.2, 646.8 and 470 nm for analyzing the determination of Chlorophyll-a, Chlorophyll-b and carotenoids contents as presented by Sumanta *et al.*, (2014)

### 2.2.4. Data analysis

SPSS statistical analysis software version 25 was used to perform statistical analysis at  $p < 0.01$  level of significance.

## 3. RESULTS

### 3.1. Leaf growth

From the data obtained in this study, there were differences among the locations ( $97.3$  and  $161.4 \text{ cm}^2$ ) in leave area of *P. orientalis* (Table 1). Mean leaf area of the collected samples in L4 was observed a significant difference in comparison with the mean leaf area of the other locations (Table, 1). Whereas, non significant variations were found between location 1 and other locations respectively. The higher mean of leaf length and leaf width were found in location 1 (control) when compared to other locations, on the other hand, the lowest mean values of them were obtained from location 4 for the same parameters (Table 1), this finding can be explained by entering pollutants in the form of gases such as  $\text{O}_3$  and  $\text{SO}_2$ , throughout openings and closing of leaf stomata. Table (2) shows the significant effect of locations on concentration of photosynthetic pigments in *P.*



*orientalis* L. tree leaves. It is found that the highest increase in chlorophyll 'a' content of the samples collected from location1 in comparison with samples collected from other locations which was obtained in *P. orientalis* L. (1.87 mg g<sup>-1</sup> FW), while the minimum value was observed in location 3 (1.53 mg g<sup>-1</sup> FW). In addition, the elevated mean of total chlorophyll was found in location 1 (control) which was (2.60 mg g<sup>-1</sup> FW) (Table 2).

Heavy metal concentrations in leaf sample compiled were acquired in categorizes to be Mn, Cu, Zn, Ni, Pb and Fe, in that order (for

identification of location numbering see Table 3). Mn concentrations in the leaf samples gathered from control site (L1) was extended from 125.2 to 402.6 (L4), whereas the range was found to be from 0 (L2) to 150.8 (L3). The Cu concentrations were detected as 64.4 (L1), 76.96 (L2), 76.8 (L3), and 76.47 (L4). However, the highest concentration of Zn and Fe were obtained in L2, whereas, maximum concentration of both Ni and Pb were accumulated in the leave samples collected in L3 and L1 (Table 3).

**Table 1.** Leaf morphology of *P. orientalis* L. tree measured at different locations.

Locations	LA (cm <sup>2</sup> )	Leaf length (cm)	Leaf width (cm)
	Mean ± SD	Mean ± SD	Mean ± SD
L1	161.4 ± 34.5 <sup>a</sup>	17.09±1.81 <sup>a</sup>	20.02 ± 2.40 <sup>a</sup>
L2	141.5 ± 41.6 <sup>a</sup>	14.87±2.12 <sup>ab</sup>	15.41 ± 1.97 <sup>bc</sup>
L3	148.1 ± 34.3 <sup>a</sup>	16.3 ± 1.71 <sup>ab</sup>	17.32 ± 2.11 <sup>b</sup>
L4	97.3 ± 8.1 <sup>b</sup>	14.39 ± 1.29 <sup>b</sup>	13.65±2.11 <sup>c</sup>

**Table 2.** Photosynthetic pigments concentration in *P. orientalis* tree leaves at different locations.

Locations	Chlorophyll a (mg g <sup>-1</sup> FW)	Chlorophyll b (mg g <sup>-1</sup> FW)	Total chlorophyll (mg g <sup>-1</sup> FW)	Carotenoids (mg g <sup>-1</sup> FW)
	Mean ± SD	Mean ± SD	Mean ± SD	Mean ± SD
L1	1.87± 0.11 <sup>a</sup>	0.78 ± 0.10 <sup>a</sup>	2.60± 0.11 <sup>a</sup>	0.76 ± 0.12 <sup>a</sup>
L2	1.72 ± 0.07 <sup>ab</sup>	0.73± 0.12 <sup>a</sup>	2.45 ± 0.19 <sup>ab</sup>	0.63 ± 0.07 <sup>a</sup>
L3	1.53± 0.07 <sup>b</sup>	0.56± 0.12 <sup>a</sup>	2.09± 0.19 <sup>b</sup>	0.55 ± 0.12 <sup>a</sup>
L4	1.60± 0.02 <sup>b</sup>	0.63± 0.10 <sup>a</sup>	2.23 ± 0.08 <sup>ab</sup>	0.55± 0.13 <sup>a</sup>

**Table 3.** Metal concentration in mg g<sup>-1</sup>(dw) in leaves of trees at different locations.

Locations	Mn	Cu	Zn	Ni	Pb	Fe
L1	125.2	64.4	42.6	52.3	7.46	3000
L2	ND	76.96	50.86	74.4	6.88	4000
L3	150.8	76.8	33.46	77.8	7.12	3400
L4	402.6	76.47	39.01	77.5	6.17	3200

ND= not determine



## 4. DISCUSSION

### 4.1. Pollution and leaf growth

The main part to determine the response of tree growth in polluted sites is the structure of tree foliage. The data of the study showed that the higher leaf area of the control can be due to trees less exposed to pollutants and differences in characteristic of leaf area give consideration to alter in leaf area index (Kardel *et al.*, 2010). Balasooriya *et al.*, (2009) concluded that there are others studies gained the same results an increase in leaf area of different species, on the other hand measuring leaf anatomy such as stomata density is also a good indicator for comparing influence of polluted and unpolluted sites. A study conducted by Jahan and Iqbal (1992) who found a decrease in leaf morphology such as leaf area, leaf length and width for some woody selected growing in urbanized polluted regions . In addition Gupta and Ghose (1988) documented a diminishing of leaf area for *Euphorbia hirta* plant in smoked environment coal site as compare to the control site and this may support the present finding. Tiwari *et al.*, (2006) observed that improvement of leaf senescence and reducing of foliage can cause a decrease in leaf area. In addition, another reason for leaf area decreasing can be due to reduced irradiation absorption and consequently decreasing in photosynthetic process (Tiwari *et al.*, 2006). Furthermore, encouragement of photosynthetic activity in higher rates of CO<sub>2</sub> in the atmosphere was deterioration by total leaf area reduction (Noormets *et al.*, 2001). Many researchers studied the leaf morphology characters which observed the same results between plants that are growing in air polluted territories.

The most common parameters used to determine effect of increased air pollutants on tree growth is net photosynthetic rate (Woo *et al.*, 2007). It is known that photosynthetic pigments such as carotenoid and chlorophyll a, b are playing a considerable part in photosynthetic process. In the finding study a reduction in chlorophyll a and total chlorophyll may be due to traffic density in the

study sites. Joshi and Chauhan (2009) explained that a reduction of chlorophyll and carotenoid content is mainly caused by restraint of photosynthetic performance in leaves of different plants. The reductions in chlorophyll 'a', chlorophyll 'b' and total chlorophyll owing to air pollution was found in a study by Joshi and Chauhan (2009). A research by Chauhan and Joshi (2009) noticed that pollutant such as particulate matter, SO<sub>2</sub>, NO<sub>x</sub> and CO<sub>2</sub> may lead to a decrease in the concentration of photosynthesis pigments, chlorophyll and carotenoids when above pollutants absorbed by the leaves. When we compared the location 1 as a control to other studied locations, it is essentially carried out by using *P. orientalis* as an identical species, it was observed comparatively differences according to the site and studied species besides the heavy traffic density effects. For the most part of the research acquired a decrease in the concentration of heavy metals in the control samples. However, from leaf samples compiled Pb concentrations in location 1 showed slightly higher compared to the leaf samples with other locations.

### 4.2. Pollution and soil samples

#### 4.2.1. The Effect of different locations on Heavy

#### Metals Concentrations (mg kg<sup>-1</sup>) in Soils

The location 1 which ranked first in total Mn and Fe concentration (ranking Second), and in total Pb, Ni, Cu and Zn concentrations (ranking third), the location (4) showed a low levels of heavy metals present together , this may be due to the accumulation of heavy metals in the soils was probably related to anthropogenic source (Gjoka *et al.*, 2011).The high value of heavy metals may be due to air pollution that contain high amount of metals as a result of dust or smokes of vehicles and industries and this agree with (Fay *et al.*,2005) However some authors prefer to use average shale composition as back ground (Tijani *et al.*, 2004).

#### 4.2.2. Geoaccumulation Index ( $I_{geo}$ )

This Geoaccumulation index has been extensively employed in European trace metal studies. It is shown that originally used for foundation sediments (Muller, 1979), and has been effectively practical to the measurement of soil contamination. This is appropriate if the samples are analyzed for total metal content. In the present study, the soil samples were analyzed for their partial extractable metal content, which represent mainly the mobile fraction of the elements. Table (5) is a diagrammatic presentation of the pollution levels of the various metals at the different sampling locations derived from the geo-accumulation indices. Soils can be described as uncontaminated and uncontaminated to moderately contaminated.

### 5. CONCLUSION

Morphology and physiology as well as heavy metal concentrations in leaves and soil samples of *Platanus orientalis* L. trees were studied to observe influence of high density of traffic roads. It is a species can be successfully planted along road sites and parks as an ornamental tree and ability to assemble the atmospheric pollution this attribute may be used as a biomonitor, as an alternative of using others methods such as costly play a part in pollution monitoring. The outcomes of this research revealed that the pollution level of the various locations within the study area was placed under uncontaminated to moderately contaminate classes, conducting extensive investigations on the sources of air pollution impacts on the environment and increasing public awareness about this serious environmental issue through education and publishing brochures in neighbourhood areas are way to improve this issue.

### ACKNOWLEDGEMENT

The authors are greatly thanks Forestry department, College of Agricultural Engineering Sciences, Salahaddin University and Mr. Ghazi R. Muhammad who is the manager of the central laboratory of the college for conducting this research for the use of the services and place to pursue this work.

### Conflict of Interest

We do not have any conflicts of interests.

### References

- BALASOORIYA, B.L.W.K., SAMSON, R., MBIKWA, F., VITHARANA, W.A.U., BOECKX, P., Van & Meirvenne, M., 2009. Biomonitoring of urban habitat quality by anatomical and chemical leaf characteristics. *Environmental and Experimental Botany Journal*. 65, 386–394.
- BECKETT KP, FREER-SMITH PH, & Taylor G. 2000. Particulate pollution capture by urban trees: effect of species and wind speed. *Global Change Biology Journal*. 6:995–1003
- DINEVA, S.B. 2004. Comparative studies of the leaf morphology and structure of white ash *Fraxinus americana* L. and London plane tree *Platanus acerifolia* Willd growing in polluted area. *Dendrobiology Journal*, 52, pp.3-8..
- FAY, M., WILBUR, S. M. A., ABADIN, H. M. S., INGERMAN, L. & SWARTS, S. G. 2005. Toxicological Profile for Nickel. Nation. *Academic Press of Georgia*: 351pp.
- FORSTNER, U., W. AHLF, & W. CALMANO. 2014. "Sediment quality objectives and criteria development in Germany" *Water Science and Technology Journal*. no. 28, pp. 307.
- GJOKA, F., HENNINGSEN, P. F., WEGENER, H. R., SALILLARI, I & Beqiraj, A.. 2011. Heavy metal in soil from Tarina (Albania). *Environmental Monitoring and Assessment Journal*. 172: 517-527.
- GUPTA, M.C. & GHOUSE A.K.M. 1988. Effects of coal smoke pollutants from different sources in the growth, chlorophyll content, stem anatomy and cuticular traits of *Euphorbia hirta* L. *Environmental Pollution Journal*. 47: 221–230.
- JAHAN, S. & IQBAL M.Z. 1992. Morphological and anatomical studies of leaves of different plants affected by motor vehicles exhaust. *Journal of Islamic Academy of Sciences*. 5: 1, 21–23.
- JOSHI, N., CHAUHAN, A. & JOSHI, P.C. 2009. Impact of industrial air pollutants on some biochemical parameters and yield in wheat and mustard plants. *The Environmentalist Journal*. 29: 398-404.
- KAMBEZIDIS, H. D., ADAMOPOULOS, A. D. & GUEYMARD, C. 1996. Total NO<sub>2</sub> column amount over Athens, Greece in 1996–97. *Atmospheric Research Journal* 57(1), pp.1-8.
- KARDEL, F., WUYTS, K., BABANEZHAD, M., VITHARANA, U.W.A., WUYTACK, T., POTTERS, G., SAMSON, R. 2010. Assessing urban habitat quality based on specific leaf area and stomatal characteristics of *Plantago lanceolata* L. *Environmental Pollution Journal*. 158: 788-794.
- KOWALSKA, J., MAZUREK, R. Ga., SIOREK, M., SETLAK, M., ZALESKI, T. & WAROSZEWSKI, J. 2016 "Soil pollution indices conditioned by medieval metallurgical activity: A case study from Krakow

- (Poland)". *Environmental Pollution Journal*, 218, 1023–1036.
- MULLER, G. 1979. Index of geo-accumulation in sediments of the Rhine River. *Geo Journal*, no. 2, pp.108-118.
- NESMITH, D.S. 1991. Nondestructive leaf area estimation of rabbiteye blueberries. *American Society for Horticultural Science*. 26(10), pp.1332-1332.
- NOORMETS, A., MCDONALD, E.P., Dickson, R.E., Kruger, E.L., Sober, A., Isebrands J.G. & Karnosky, D.F. 2001. The effect of elevated carbon dioxide and ozone on leaf- and branch-level photosynthesis and potential plant-level carbon gain in aspen. *Trees-Structure Function Journal*. 15: 262-270.
- PATTON, L. 1985. Photosynthesis and growth of willows used for short rotation forestry (Doctoral dissertation, Trinity College Dublin).
- REIMANN, C., & GARRET, R. G. 2005. Geochemical background: Concept and reality. *Science of the Total Environment Journal*. 350, 12–27.
- SAWIDIS, T., CHETTRI, M. K., Papaioannou, A., Zachariadis, A. & Stratis, J. 2001. A study of metal distribution from lignite fuels using trees as biological monitors. *Ecotoxicology and Environmental Safety*. 48:27–35.
- SITKO, R., ZAWISZA, B., JURCZYK, J., BUHL, F. & ZIELONKA, U. 2004. Determination of High Zn and Pb Concentrations in Polluted Soils Using Energy-Dispersive X-ray Fluorescence Spectrometry. *Journal of Environmental Studies and Sciences*. 13(1): 91-96.
- SUMANTA, N., HAQUE, C.I., NISHIKA, J. & SUPRAKASH, R. 2014. Spectrophotometric analysis of chlorophylls and carotenoids from commonly grown fern species by using various extracting solvents. *Research Journal of Chemical Sciences* ISSN, 2231, p.606X.
- TIJANI, M. N., Jinno, K. & Hiroshiro, Y. 2004. Environmental impact of heavy metals distribution in water and sediments of Ogunpa River, Ibadan area, Southwestern Nigeria", *Mining and Geology Journal*. 40:73-84.
- TIWARI, S., AGRAWAL M. & Marshall, F.M. 2006. Evaluation of ambient air pollution impact on carrot plants at a sub urban site using open top chambers. *Environmental Monitoring and Assessment Journal*. 119: 15-30.
- VESELKIN D. V. 2004. Anatomical Structure of Ectomycorrhiza in *Abies sibirica* Ledeb. and *Picea obovata* Ledeb. under Conditions of Forest Ecosystems Polluted with Emissions from Copper-Smelting Works Russian. *Journal of Ecology*. (ISSN 1067–4136), Vol. 35: 71.
- WHO (2006) Air quality guidelines for particulate matter, ozone, nitrogen dioxide and sulphur dioxide. Global update 2005. WHO Regional Office for Europe, Copenhagen, Denmark, ISBN 9289 021926.
- WOO, S.Y., Lee, D. K. & Lee, Y.K. 2007. Net photosynthetic rate, ascorbate peroxidase and

glutathione reductase activities of *Erythrina orientalis* in polluted and non-polluted areas. *Journal for Photosynthesis Research*. 45: 293-295

## RESEARCH PAPER

# Transport Parameters and Dielectric Strength of Electrical Discharges in an Arc Discharges in Carbon Dioxide Gas

Idris H. Salih

Tishk International University, KRG, Iraq

### ABSTRACT

The two-term approximation solution of Boltzmann equation analysis has been used to calculate the electron energy distribution function (EEDF), dielectric strength and the electron swarm parameters in carbon dioxide. The electron swarm parameters have been calculated over the wide range of reduced density electric field strength  $E/N$  varying from 0.1 to 1000 Td ( $1\text{Td} = 10^{-17} \text{ V.cm}^2$ ). These parameters, namely electron drift velocity, mean electron energy, electron temperature, characteristic energy, transverse diffusion coefficient, electron mobility, reduced ionization and attachment Townsend coefficients have been compared with the available previous theoretical and experimental results. The values of the critical reduced electric field strength  $(E/N)_{cr}$  from the curves of reduced effective ionization coefficient  $(\alpha-\eta)/N$  are calculated. In addition, excitation rate and fractional power transfer to elastic and inelastic collisions are explained.

KEY WORDS: CO<sub>2</sub> electric discharge, EEDF, dielectric strength, swarm parameters, electron temperature, reduced electric field strength  $(E/N)_{cr}$ .

DOI: <http://dx.doi.org/10.21271/ZJPAS.32.6.17>

ZJPAS (2020) , 32(6);158-175 .

### 1. INTRODUCTION

Carbon dioxide gas play an important role in technological application, atmospheric physics, pulsed-power switching, particle detector, low temperature plasma , CO<sub>2</sub> gas laser (Koushki, Zand, Haghghi, & Neshati, 2015; Uchii et al., 2007) . In high voltage technology carbon dioxide used as admixture for circuit breakers and in health care used as additive to oxygen for medical use as a respiration simulant.

The CO<sub>2</sub> is a man-made and long-lived greenhouse gas with a global warming potential similar to that of CF<sub>3</sub>I (GWP~1) and 23,900 times smaller than that of Sulfur hexafluoride SF<sub>6</sub> (Christophorou, Olthoff, & Van Brunt, 1997). Carbon dioxide at room temperature (300 K) is a colorless, nontoxic, totally non-flammable gas, at low concentrations is odorless, at high concentration has acidic odor, it has a low critical temperature (304.1 K) and high critical pressure (7.3773 MPa), that not deplete the ozone layer. The density of CO<sub>2</sub> is 1.67 times greater than that of dry air (Pierantozzi, 2000).

Several studies have found that Carbon dioxide (CO<sub>2</sub>) is a selected gas for replacing SF<sub>6</sub> in high-voltage switchgear for the transmission and distribution of electricity (Seeger, Avaheden, Pancheshnyi, & Votteler, 2016) at room temperature in the pressure range 0.05-0.5 MPa.

#### \* Corresponding Author:

Idris H. Salih

E-mail: [idrishadi@tiu.edu.iq](mailto:idrishadi@tiu.edu.iq)

#### Article History:

Received:21/06/2020

Accepted: 10/08/2020

Published:20/12/2020

However the dielectric strength of SF<sub>6</sub> (8.9 KV/mm) is greater than that of CO<sub>2</sub> (1.93 KV/mm). When a small amount of oxygen (O<sub>2</sub>) with high dielectric strength add to CO<sub>2</sub> can effectively ameliorate the value of critical reduced electric field strength (E/N)<sub>cr</sub> (Hu Zhao, Deng, & Lin, 2017).

The electron kinetics, the electron energy distribution function (EEDF), rate coefficient, the effect of vibrational excitation and power transfer were studied by (Ogloblina, Tejero-del-Caz, Guerra, & Alves, 2020).

The electron motion at low pressure with mean electron energies in the range of 0.5-3.0 eV are called cold plasma, electron distribution function have non-maxwellian shape due to electron molecule collision processes. The electron swarm parameters, the electron energy distribution function and the percentage of energy loss during the different collision processes may be calculated from a set of collisional cross- sections of CO<sub>2</sub> by using the Monte Carlo Simulation method or the Boltzmann equation. The electron energy distribution function (EEDF) is normalized by  $f(\epsilon) \cdot \epsilon^{1/2} d\epsilon$  (Nighan, 1970), it is difficult to measure experimentally .

The electron transport parameters in CO<sub>2</sub> have been investigated by (Hake Jr & Phelps, 1967) by using Boltzmann equation over the range of E/N varying from 0.02 to 100 Td, and by Monte Carlo simulation methods (Kucukarpaci & Lucas, 1979) within the range 10<E/N<=3000 Td, (where E is the electric field and N gas density, 1Td=10<sup>-17</sup> Vcm<sup>2</sup> , 1 V/cm.Torr=3.0341Td at 293 K). The electron swarm parameters of CO<sub>2</sub> for low E/N<=30 Td were measured by (Elford, 1966; Pack, Voshall, & Phelps, 1962). Moreover, the electron drift velocity and characteristic energy for pure N<sub>2</sub> and CO<sub>2</sub> over the range 10<=E/N<=700 Td have been studied by (Roznerski & Leja, 1984; Saelee, Lucas, & Limbeek, 1977). The electron drift velocity and longitudinal diffusion coefficient of both pure N<sub>2</sub> and CO<sub>2</sub> at room temperature have been measured experimentally in the range 20<=E/N<= 1000 Td using double-shutter drift tube technique by (Hasegawa, Date, Shimozuma, Yoshida, & Tagashira, 1996), ionization and attachment coefficient in CO<sub>2</sub> obtained for 60<=E/N<=152 Td by (Alger & Rees, 1976). The electron transport parameters in pure CO<sub>2</sub> and CO<sub>2</sub>-SF<sub>6</sub> mixtures were measured over the range 100<=E/N<=700 Td by (Hernández-Ávila,

Basurto, & De Urquijo, 2002) using the pulsed Townsend technique.

(Li, Guo, Zhao, Jia, & Murphy, 2015) calculated the critical reduced electric field strength (E/N)<sub>cr</sub> for CO<sub>2</sub> and CO<sub>2</sub>- Cu mixtures using Boltzmann equation at different temperature and pressure 0.4 MPa. Sun et al., 2015 investigated dielectric breakdown of CO<sub>2</sub> at different temperature and pressure using two-term solution of Boltzmann equation. (Grofulović, Alves, & Guerra, 2016) studied the electron swarm motion of CO<sub>2</sub>. (Pietanza, Colonna, D'Ammando, Laricchiuta, & Capitelli, 2016) investigated the role of Superelastic vibration collision on electron energy distribution function (EEDF) and percentage power transfer in cold CO<sub>2</sub> discharge. (Wang & Bogaerts, 2016) studied the effect of inelastic collision on the electron energy distribution function , reduced effective ionization coefficient, critical reduced electric field strength and ion kinetics of CO<sub>2</sub> in the range of temperature varying from 300 K to 5000 K by using Boltzmann equation. (H Zhao, Gu, & Li, 2017) studied the reduced ionization coefficient and critical reduced electric field strength at room temperature of pure CO<sub>2</sub> gas and its mixtures with 10 different gases.

Recently (Jawad & Jassim, 2019), calculated the electron swarm parameters of CO<sub>2</sub>, Xe-CO<sub>2</sub> and Kr-CO<sub>2</sub> mixtures at room temperature over the range of E/P varying from 35 to 350 V/cmTorr. (Grofulovic, 2019) investigated electron swarm parameters of pure CO<sub>2</sub> and rotational Raman in pulsed CO<sub>2</sub>-O<sub>2</sub> and CO<sub>2</sub>-N<sub>2</sub> discharge under non-equilibrium condition.

The electron transport parameters are also calculated in binary gas mixtures, Ar-CO<sub>2</sub> (Yoshiharu Nakamura, 1995), SF<sub>6</sub>-CO<sub>2</sub> (Xiao, Li, & Xu, 2001), CO<sub>2</sub>-Air (De Urquijo et al., 2009), CO<sub>2</sub>-N<sub>2</sub> and CO<sub>2</sub>-O<sub>2</sub> (Yousfi, de Urquijo, Juarez, Basurto, & Hernandez-Avila, 2009), c-C<sub>4</sub>F<sub>8</sub>-CO<sub>2</sub> (Deng, Lu, & Xiao, 2012), CF<sub>3</sub>I-N<sub>2</sub> and CF<sub>3</sub>I-CO<sub>2</sub> (Yun-Kun & Deng-Ming, 2013), CF<sub>3</sub>I-CO<sub>2</sub> (Xiaoling, Juntao, & Dengming, 2016), Fluoronitriles-CO<sub>2</sub> (Nechmi, Beroual, Girodet, & Vinson, 2017),), C<sub>4</sub>F<sub>7</sub>N-CO<sub>2</sub> (Long et al., 2019; Zheng et al., 2019) and CO<sub>2</sub>-CO mixtures (Ogloblina et al., 2019). Furthermore, (Davies, 1978) measured the ionization and attachment coefficients in pure CO<sub>2</sub> and ternary CO<sub>2</sub>-N<sub>2</sub>-He gas mixtures over the range 76.3 Td<=E/N<=98.9 Td,

and (Egüz, Chachereau, Hösl, & Franck, 2019) experimentally measured the electron swarm parameters in ternary  $C_4F_7N-O_2-CO_2$ ,  $C_5F_{10}O-O_2-CO_2$  and  $C_5F_{10}O-O_2-N_2$  mixtures over a wide range of  $E/N$ . (Wedding, 1985) investigated the electron drift velocity, Townsend ionization coefficient and diffusion coefficients both  $D_L$  and  $D_T$  in  $CO_2-N_2-He-CO$  gas mixtures of the ratio 6:34:54:6 by using time-of-flight (TOF) method, over the range of  $E/N$  varying from 100 to 500 Td.

The dielectric breakdown voltage and density reduced critical electric field strength  $(E/N)_{cr}$  of carbon dioxide and its mixtures was calculated at which the balancing electron generation and electron loss are in equilibrium derived from Boltzmann transport equation, this method was used by (Brand & Kopainsky, 1979; Itoh, Shimozuma, & Tagashira, 1980; Laska, Mašek, Krasa, & Peřina, 1984; Hu Zhao et al., 2017). The critical reduced electric field strength  $(E/N)_{cr}$  and breakdown voltage for pure  $CO_2$  and mixtures were analyzed theoretically and experimentally by several authors. (Yousfi et al., 2009) investigated electron drift velocity ( $v_d$ ), longitudinal diffusion coefficient ( $D_L$ ) and effective ionization coefficient ( $(\alpha-\eta)/N$ ) of  $CO_2$ ,  $N_2$ ,  $O_2$  and their mixtures  $CO_2-N_2$  and  $CO_2-O_2$  experimentally (time-resolved pulsed Townsend technique) and theoretically (multi-term Boltzmann equation method), covering the range  $0.01Td \leq E/N \leq 1000 Td$ . (Sun et al., 2015) calculated reduced ionization coefficient ( $\alpha/N$ ), reduced attachment coefficient ( $\eta/N$ ) and the dielectric properties of hot  $CO_2$  at different temperature and pressure by solving Boltzmann equation. (Vass, Korolov, Loffhagen, Pinhao, & Donkó, 2017) were investigated electron swarm parameters and the effective ionization

coefficient  $(\alpha-\eta)/N$  in  $CO_2$  gas experimentally under time-of-flight conditions using scanning drift tube over the range  $15 Td \leq E/N \leq 2660 Td$ , as well as theoretically by solving Boltzmann transport equation and Monte Carlo simulation method. The electron mobility, longitudinal diffusion coefficient and effective ionization rate coefficient of  $CO_2$ ,  $N_2$  and Ar were measured by (Haefliger & Franck, 2018) using pulsed Townsend experiments.

(Beaty, Dutton, & Pitchford, 1980; Dutton, 1975) published a large data on the electron transport parameters in number gases over a wide range of  $E/N$ . We previously reported a detailed explanation to calculate electron swarm parameters by solving two-term solution of the Boltzmann equation (Othman, Taha, & Sailh, 2019; Othman, Taha, & Salih, 2019).

The object of the present article is to calculate the electron swarm parameters, namely (drift velocity, mean electron energy, diffusion coefficient, characteristic energy, electron mobility, ionization and attachment coefficient), reduced effective ionization coefficient, reduced critical electric field strength and mechanisms for fraction power transfer due to collision processes for pure  $CO_2$  over a wide range of reduced electric field strength  $E/N$  varying from 0.1 to 1000 Td by solving two-term solution of Boltzmann equation at temperature 300 K and pressure 1 atm..

## 2. Theory

### 2.1. The Boltzmann Equation

The basic of homogeneous electron Boltzmann transport equation yielding to calculate the electron energy distribution function takes the form (Frost & Phelps, 1962; Holstein, 1946).

$$\frac{E^2}{3} \frac{d}{d\varepsilon} \left( \frac{\varepsilon}{NQ_m^T(\varepsilon)} \frac{df_0(\varepsilon)}{d\varepsilon} \right) + \frac{2m}{M} \frac{d}{d\varepsilon} \left( \varepsilon^2 NQ_m^T(\varepsilon) f_0(\varepsilon) \right) + \frac{2mK_B T_g}{Me} \left( \varepsilon^2 NQ_m^T(\varepsilon) \frac{df_0(\varepsilon)}{d\varepsilon} \right) + \sum_J (\varepsilon + \varepsilon_J) f_0(\varepsilon + \varepsilon_J) NQ_J(\varepsilon + \varepsilon_J) - \varepsilon f_0(\varepsilon) N \sum_J Q_J(\varepsilon) = 0 \quad 1$$

Here,  $K_B$  is the Boltzmann constant,  $T_g$  is the gas temperature,  $m/M$  is the ratio of electronic to atomic mass,  $Q_J(\varepsilon)$  is the cross sections for various excited states,  $\varepsilon_J$  is the threshold energy of the  $J$ th excited

state, and  $Q_m^T(\varepsilon)$  is the total effective momentum transfer cross sections defined as follows,



$$Q_m^T(\varepsilon) = Q_m(\varepsilon) + \sum_j Q_e(\varepsilon) + Q_i(\varepsilon) + Q_a(\varepsilon) \quad 2$$

Where  $Q_m(\varepsilon)$  is momentum transfer cross-section,  $Q_e(\varepsilon)$  is excitation cross-sections (vibration and electronic),  $Q_i(\varepsilon)$  is ionization cross-sections and  $Q_a(\varepsilon)$  is attachment cross-sections. The last term express gain of energy by electrons due to second kind (superelastic) collision. The equation (1) applies to swarm of electron drifting through an gas and mixtures under influence of a uniform dc electric field (E).

## 2.2. Transport parameters

The electron transport coefficient in given gases under the influence of dc applied electric

$$\int_0^{\infty} f_o(\varepsilon) \sqrt{\varepsilon} d\varepsilon = 1 \quad 3$$

the electron energy distribution function was chosen as Maxwellian function at temperature  $T_g$  with mean electron energy  $\langle \varepsilon \rangle = \frac{3}{2} K_B T_g = \frac{3}{2} T_e$  ( $T_e$  is

$$f(\varepsilon) = \frac{2}{\sqrt{\pi}} (K_B T_g)^{-3/2} \exp\left(-\frac{\varepsilon}{K_B T_g}\right) \quad 4$$

the mean electron energy in term of EEDF is expressed as,

$$\langle \varepsilon \rangle = \int_0^{\infty} \varepsilon^{3/2} f_o(\varepsilon) d\varepsilon \quad 5$$

while the reduced electron mobility is given by,

$$\mu_e N = -\frac{1}{3} \sqrt{\frac{2e}{m}} \int_0^{\infty} \frac{\varepsilon}{Q_m^T(\varepsilon)} \frac{\partial f_o(\varepsilon)}{\partial \varepsilon} d\varepsilon \quad 6$$

The drift velocity  $v_d$ , the density transverse diffusion coefficient  $D_T N$  and characteristic energy  $\varepsilon_k$  are given by (Smith & Thomson, 1978),

field, calculated by using a two-term solution of the Boltzmann equation, the resulting solution gives the electron energy distribution function which depend on the reduced electric field strength  $E/N$ , the gas temperature and electron collision cross-sections, and play important parameters for calculation of the electron swarm parameters.

The electron energy distribution function can be normalized by (Morgan & Penetrante, 1990),

electron temperature in eV) is given by (Jiang & Economou, 1993),

$$v_d = -\frac{\bar{E}}{3} \sqrt{\frac{2e}{m}} \int_0^\infty \frac{\varepsilon}{NQ_m^T(\varepsilon)} \frac{\partial f_o(\varepsilon)}{\partial \varepsilon} d\varepsilon \quad 7$$

$$D_T N = \frac{1}{3} \sqrt{\frac{2e}{m}} \int_0^\infty \frac{\varepsilon}{Q_m^T(\varepsilon)} f_o(\varepsilon) d\varepsilon \quad 8$$

$$\varepsilon_k = \frac{eD_T}{\mu_e} \quad 9$$

From the computed drift velocity  $v_d$  the reduced ionization and attachment coefficients are obtained as (Tuan, 2014, 2016),

$$\frac{\alpha}{N} = \frac{1}{v_d} \sqrt{\frac{2e}{m}} \int_i^\infty Q_i(\varepsilon) f_o(\varepsilon) \varepsilon d\varepsilon \quad 11$$

$$\frac{\eta}{N} = \frac{1}{v_d} \sqrt{\frac{2e}{m}} \int_a^\infty Q_a(\varepsilon) f_o(\varepsilon) \varepsilon d\varepsilon$$

12 Where,  $Q_i(\varepsilon)$ ,  $Q_a(\varepsilon)$  are ionization and attachment

The reduced effective ionization is given by (Hu Zhao, Li, Jia, & Murphy, 2013).

$$\bar{\alpha} = \frac{\alpha}{N} - \frac{\eta}{N} = \frac{\alpha - \eta}{N} = 0 \quad 13$$

The rate constant for the  $j^{\text{th}}$  excitation is obtained by the following formula (Y Nakamura & Lucas, 1978),

$$R_{sj} = \left(\frac{2e}{m}\right)^{1/2} \int_0^\infty N Q_{sj}(\varepsilon) f_o(\varepsilon) \varepsilon d\varepsilon \quad 14$$

where  $Q_{sj}$  is electron cross-sections of excitation of level (j) in species (s).

The electron energy loss ( $P_j$ ) is,

$$P_j = \frac{\varepsilon_j R_{sj}}{e \bar{E} v_d} \quad 16$$

Where  $\varepsilon_j$  is the threshold energy for the excitation.

### 3. Collision Cross Section

The electron swarm parameters and EEDF in Carbon dioxide ( $\text{CO}_2$ ) gas calculated from the sets cross-sections (elastic and inelastic) reported by (Kieffer). This sets includes 14 collisional processes: one effective momentum-transfer cross section ( $Q_m$ ), eight vibration excitation ( $Q_{v1}$ -  $Q_{v8}$ ) with threshold energy 0.083, 0.167, 0.252, 0.291, 0.339, 0.422, 0.505 and 2.5 eV respectively and two electronic excitation ( $Q_{ex}$ ) cross-sections with threshold energy of 7.0 and 10.5 eV, one attachment ( $Q_a$ ) and ionization cross-sections with threshold energy 3.85 eV and 13.3 eV respectively and one superelastic de-excitation.

### 4. Results and discussion

The electron cross-sections were explained in section (3) have been used in present calculation to obtain electron swarm parameters and comparison with the previous theoretical and experimental values. The energy range for the  $\text{CO}_2$  cross-sections has been taken from 0.001 eV to 500 eV, which is typical of the dielectric properties and breakdown voltage at room temperature. The necessary condition for the two-term solution to be valid, that the momentum transfer cross-sections is larger than the inelastic cross-sections (Smith & Thomson, 1978; Tanaka, 2004). In the case of  $\text{CO}_2$  molecules the elastic cross-section are large.

Normalized electron energy distribution function (EEDF) in pure  $\text{CO}_2$  for different values of  $E/N$  at temperature 300 K and pressure 1 atm is shown in figure 1. For electron energies  $\leq 2.5$  eV, the maximum value of EEDF decreases as  $E/N$  values increases. However, for electron energies greater than 2.5 eV, the shape of EEDF reversed, the tail of the distribution function is shifted towards high energy which indicates that at high  $E/N$  values the electrons accelerated and increase their kinetic energies and there are only little thermal electrons that have energies greater than the ionization potential. At low electron energies the shape of the EEDF depend on the momentum transfer cross-sections, at high energies the distribution function influenced by the collision frequency for inelastic collisions, for this condition the EEDF play the

important parameters to calculate the swarm parameters.

Figure 2 shows the effect of temperatures on the normalized electron energy distribution function at fixed value of  $E/N=60$  Td and a pressure of 1 atm. For the energy range  $\leq 3.5$  eV, the maximum value of the electron energy distribution function decreases with increasing temperature. However, for temperature above 300 K the shape of EEDF reversed when the energy of electron greater than 3.5 eV. At high temperature  $\text{CO}_2$  molecule begins to dissociate and the kinetic energies of electrons increases with temperature, this is the reason the tail of EEDF shifted toward the right.

Figure 3 shows the effect of pressure on the electron energy distribution function (EEDF) at fixed value of  $E/N= 60$  Td and a temperature of 300 K. For the range of electron energy less than 2 eV the EEDF decreases with increasing pressure, for energies greater than 2 eV, leads to a higher maximum value, this behavior is opposite to that found in Sulfur hexafluoride  $\text{SF}_6$  (Wang, Murphy, Rong, Looe, & Spencer, 2013; Wang, Tu, Mei, & Rong, 2013; Hu Zhao et al., 2013).

Figure 4a and 4b are shown the influence of superelastic collisions on EEDF at reduced electric field strength 1 Td and 70 Td with and without second kind (superelastic) collision respectively. For both cases the effect of superelastic can be seen that superelastic collisions are affect the EEDF at low reduced electric field strength  $E/N$ , but are not important at high  $E/N$  values. At high values of  $E/N$  the electrons gain their energies from the applied d.c electric field. The study of the effect of second kind (superelastic) collisions in Carbone dioxide was explained in literatures of (Pietanza, Colonna, D'Ammando, et al., 2016; Pietanza, Colonna, D'Ammando, Laricchiuta, & Capitelli, 2016).

Figure 5 shows the mean electron energy varying from (0.025 eV to 14.85 eV) for different values of  $E/N$  (0.1 Td to 1000 Td), at high  $E/N$  the mean electron energy sensitive to inelastic collisions. The change of mean electron energy is progressive exponentially, the electron gain all energies from the applied electric field. Comparison has been made with the theoretical results of (Kucukarpaci & Lucas, 1979) and (Jawad, 2015) a good agreement has been observed.

Figure 6 shows calculated electron temperature as a function of  $E/N$  from the relation  $\langle \varepsilon \rangle = (3/2)T_e$ , where  $\langle \varepsilon \rangle$  is mean electron energy and  $T_e$  is electron temperature in unit eV. At  $E/N \geq 4$  Td the variation of electron temperature is more nonlinear this due to large vibrational cross-sections  $\text{CO}_2$  in the energy ranges (3 eV to 5 eV). The theoretical values of (Hu Zhao et al., 2017) are in good agreement compared with the present calculation.

The results of electron drift velocity as a function of  $E/N$  is shown in figure 7 which increases with increasing  $E/N$  values, the results are compare with the theoretical values of (Grofulovic, 2019; Raju, 2018) and experimental values of (Elford & Haddad, 1980; Yoshiharu Nakamura, 1995; Vass et al., 2017). A good agreement has been shown over the entire range of  $E/N$ . The characteristic energy is shown in figure 8 and the agreement is good over the entire range of  $E/N$  when compared with previous values, i.e. it agrees well with the experimental values of (Lakshminarasimha & Lucas, 1977; Rees, 1964) and theoretical values of (Jawad, 2015). In fact, as reported by (Kucukarpaci & Lucas, 1979) the values should be about 10% lower than the present values.

The reduced transverse diffusion coefficient  $D_{\perp}N$  for pure  $\text{CO}_2$  is shown in figure 9, together with theoretical and experimental values for comparison. The present calculation were found in good agreement with theoretical values of (Deng et al., 2012; Grofulovic, 2019) and experimental values of (Hernández-Ávila et al., 2002; Yoshiharu Nakamura, 1995; Vass et al., 2017; Wagner, Davis, & Hurst, 1967). At high  $E/N > 30$ Td the values of (Grofulovic, 2019) lower than the calculated values. In fact, experimental data of (Wagner et al., 1967) and (Yoshiharu Nakamura, 1995) should be higher than the present results. The normalized reduced electron mobility  $\mu_e N$  is shown in figure 10, the calculated values are agree with theoretical values of (Grofulovic, 2019; Raju, 2018) and experimental values of (Elford & Haddad, 1980; Haefliger & Franck, 2018; Yousfi et al., 2009). For low value of  $E/N$  the data of (Yousfi et al., 2009) slightly higher than present calculation. In the case of  $\text{CO}_2$ , when reduced electric field strength ( $E/N$ ) is around (25-30) Td, a maximum values in the reduced electron mobility can be observed, then electron mobility

decreases with increasing  $E/N$ , because during the range  $E/N \geq 30$  Td, the attachment coefficient decrease the number of electrons.

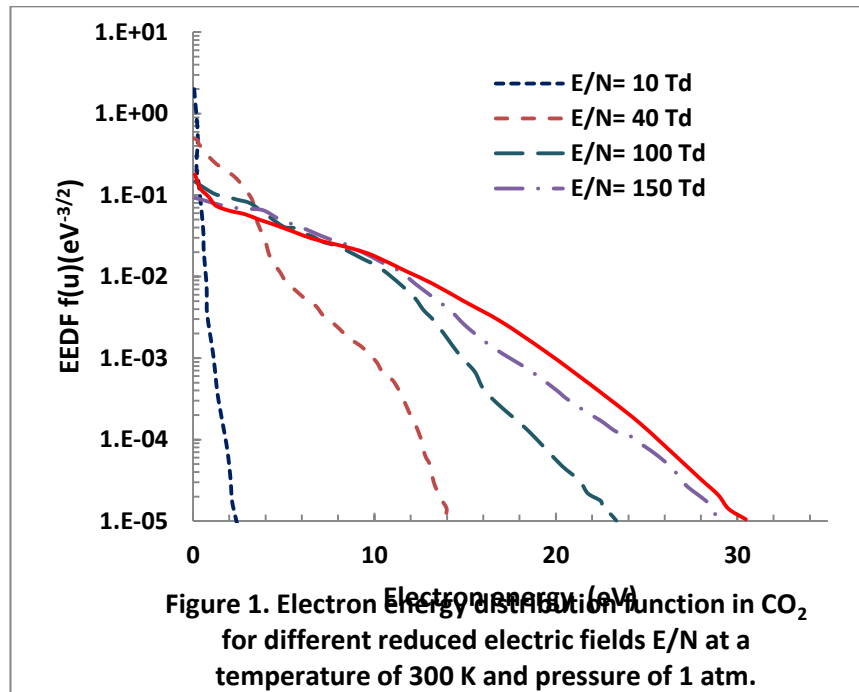
Figure 11, shows the reduced ionization coefficient  $\alpha/N$  in comparison with the experimental data of (Conti & Williams, 1975; Hernández-Ávila et al., 2002; Yoshiharu Nakamura, 1995; Townsend, 1902) as well as the theoretical results of (Grofulovic, 2019; Sun et al., 2015; Hu Zhao et al., 2017). Throughout the range of  $60 \text{ Td} \leq E/N \leq 1000$  Td good agreements has been observed. For  $E/N < 140$  Td, the theoretical values of (Grofulovic, 2019) slightly lower about 8% compare with the present results. In addition, figure 12 shows the comparison of the calculated reduced attachment coefficient  $\eta/N$  in carbon dioxide with the previous literatures. A deviation between the calculated and experimental data of (Alger & Rees, 1976) can be observed due to the cross-sections for the three body attachment, However, the calculated values show in good agreement with theoretical results of (Sun et al., 2015; Hu Zhao et al., 2017) at room temperature.

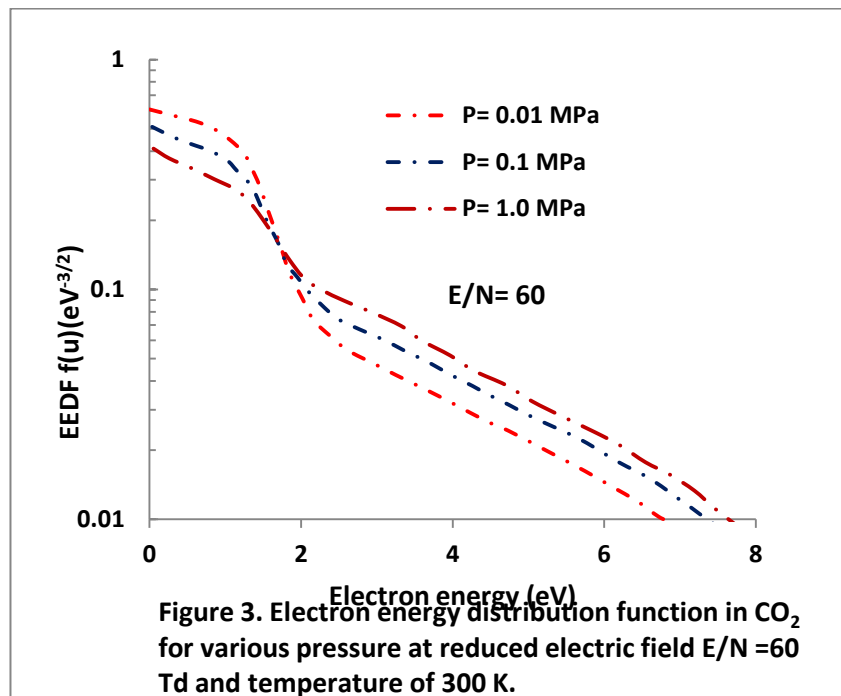
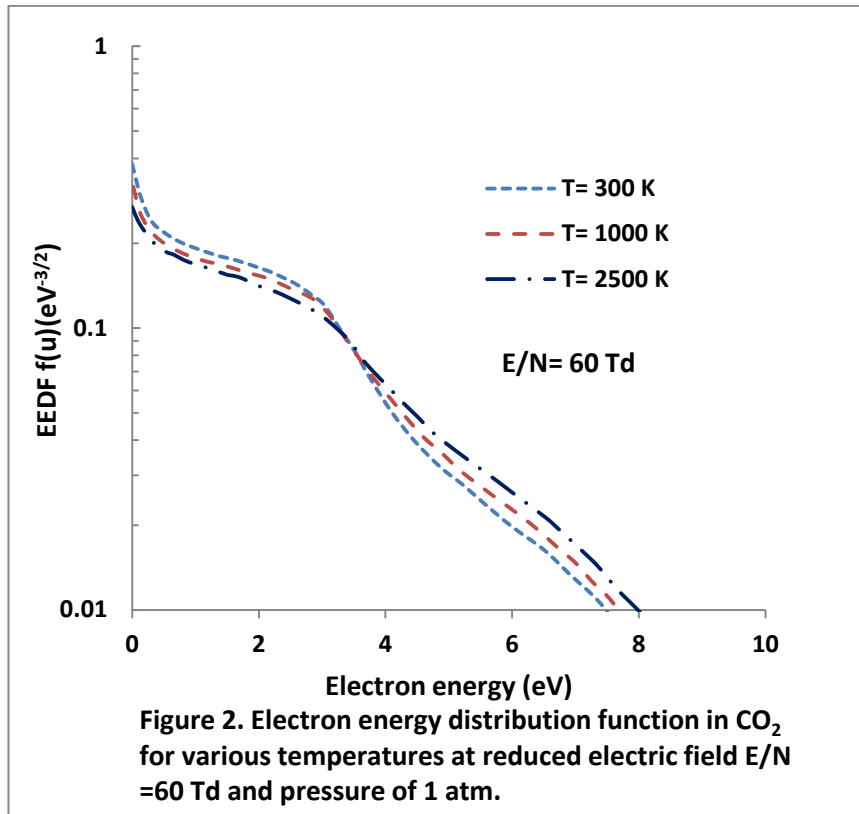
Figure 13 compares the calculated values of the reduced effective ionization coefficient  $(\alpha-\eta)/N$  with experimental values measured at room temperature by (Alger & Rees, 1976; Dahl, Teich, & Franck, 2012; Haefliger & Franck, 2018) and theoretical values calculated by (Sun et al., 2015; Yousfi et al., 2009; Hu Zhao et al., 2017). The present values are in good agreement with previous data. The two-term approximation solution of Boltzmann equation used to calculate the reduced critical electric field strength  $(E/N)_{cr}$ , which is important coefficient for the purpose of identification the insulation performance of gases. From the point of intersection between the density reduced effective ionization coefficient  $(\alpha-\eta)/N$  and the zero line  $E/N$ , the reduced critical electric field strength  $(E/N)_{cr}$  in pure Carbone dioxide molecule were calculated equal to 84 Td. In comparison the dielectric strength of  $\text{CO}_2$  in agreement with the results of (Alger & Rees, 1976) 93 Td, (Dahl et al., 2013) 81 Td, (Sun et al., 2015) 86 Td, and (Haefliger & Franck, 2018) 86 Td, but slightly greater than the results of (Yousfi et al., 2009), 84 Td and (Hu Zhao et al., 2017) 77.3 Td. At low  $E/N \leq 85$  Td, the reduced attachment coefficient dominates and negative values for the effective ionization are observed.

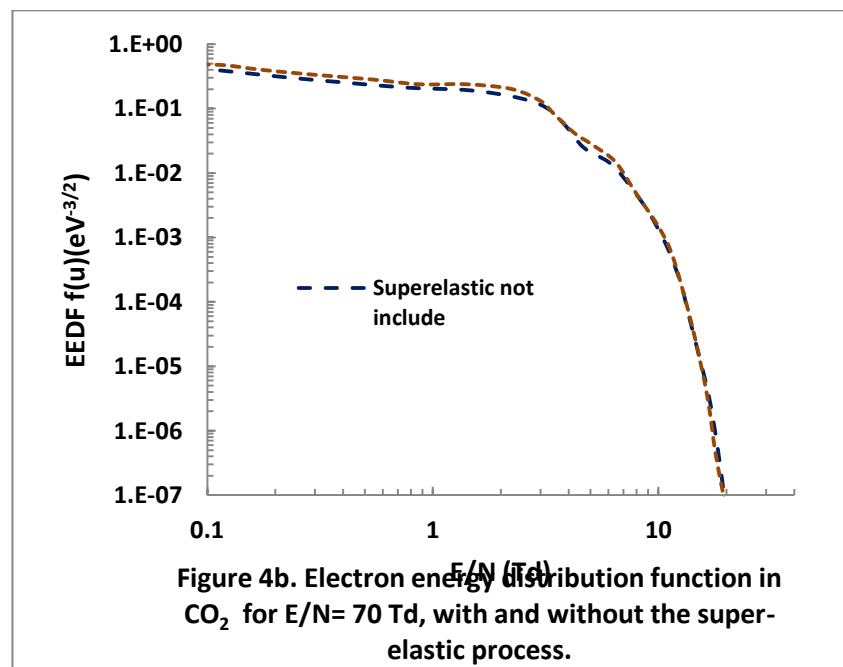
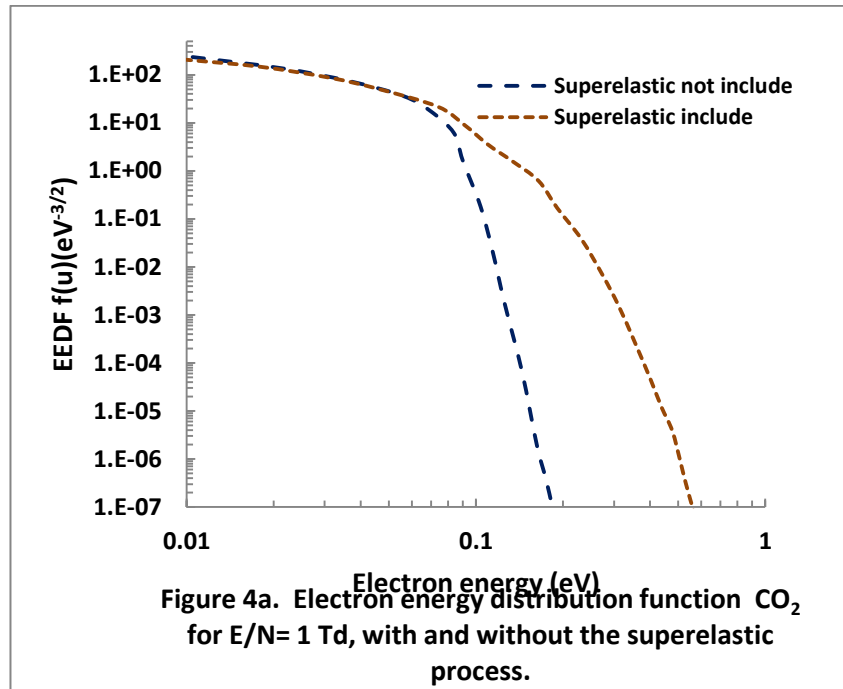
Excitation rates for the vibrational levels 010, 020, 030+110, 001, 200 and 300, with threshold energy of 0.083, 0.0167, 0.252, 0.291, 0.339 and 0.505 eV respectively and electronic excitation of two levels with threshold energy 7 eV and 10.5 eV are calculated according to equation 15, which is shown in figure 14. The excitation rates increases with increasing  $E/N$  up to about 100 Td, where it reach the maximum value then start to decreases monotonically with increasing  $E/N$ , except the electronic level with threshold energy 10.5 eV where it reaches a constant value at high  $E/N$ . In fact, during the inelastic collision processes most of the electron energy will transfer to the electronic levels and ionization.

The mechanism of fraction power transfer to elastic and inelastic processes over the entire  $E/N$

varying from 0.1 Td to 1000 Td is summarized in figure 15. For low range  $0.1 \leq E/N \leq 6$  Td the loss is only by elastic and vibrational collision, for the range  $6 \leq E/N \leq 40$  Td about 98% energy transfers to only vibrational collision. For intermediate  $E/N$  values the vibrational and electronic excitation are the main of energy loss. For high reduced electric field strength  $E/N$  the energy loss are sensitive to the electronic levels having threshold energies of 3.1 eV and 10.5 eV and the ionization processes are the main of energy loss. As shown in figure the energy loss by attachment process is very small.







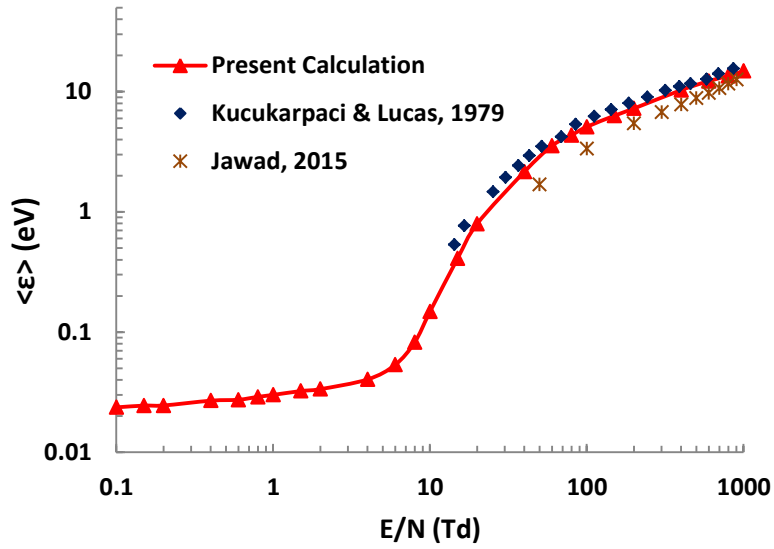


Figure 5. Mean electron energy in  $\text{CO}_2$  as a function of reduced electric field strength  $E/N$ .

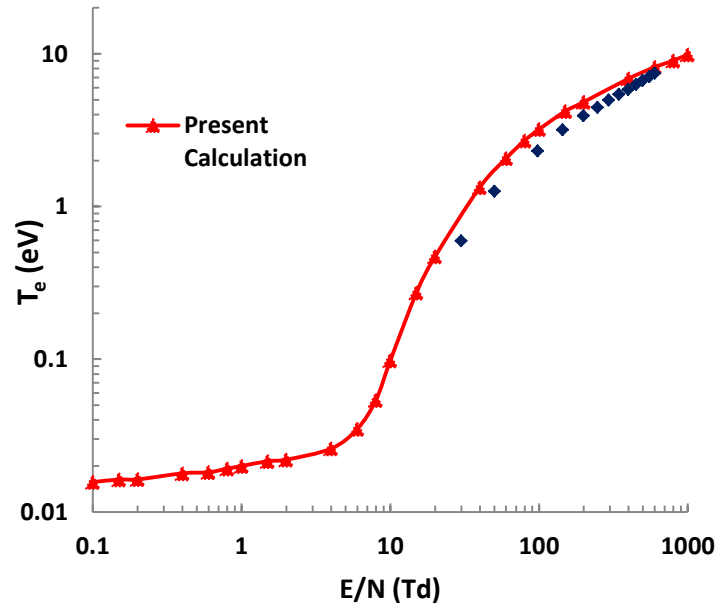
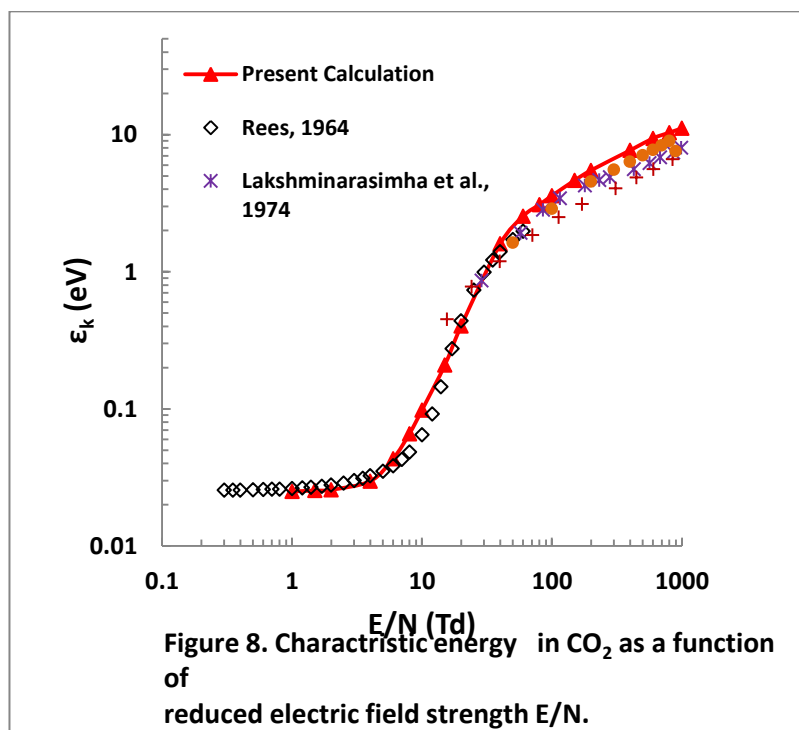
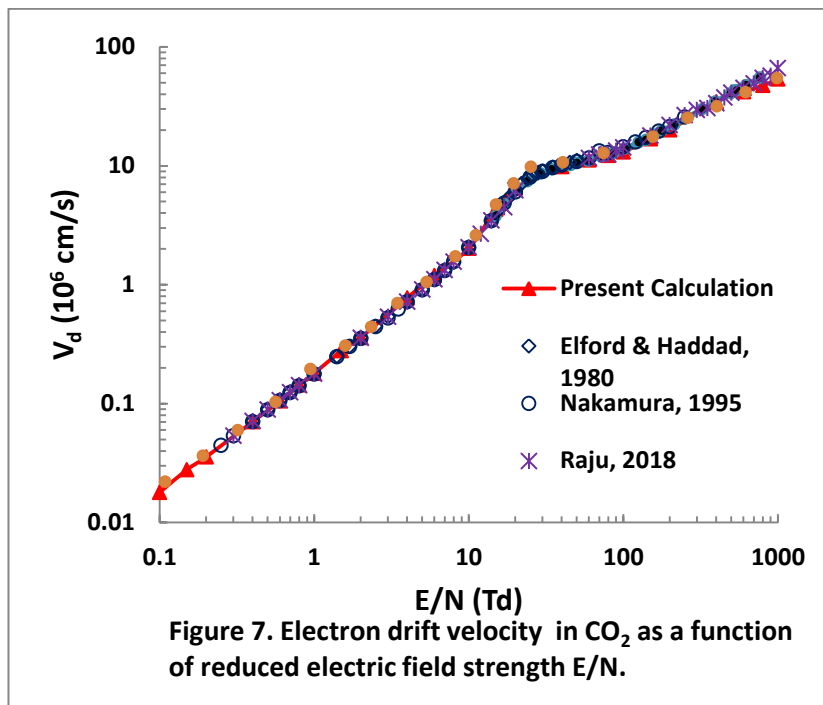
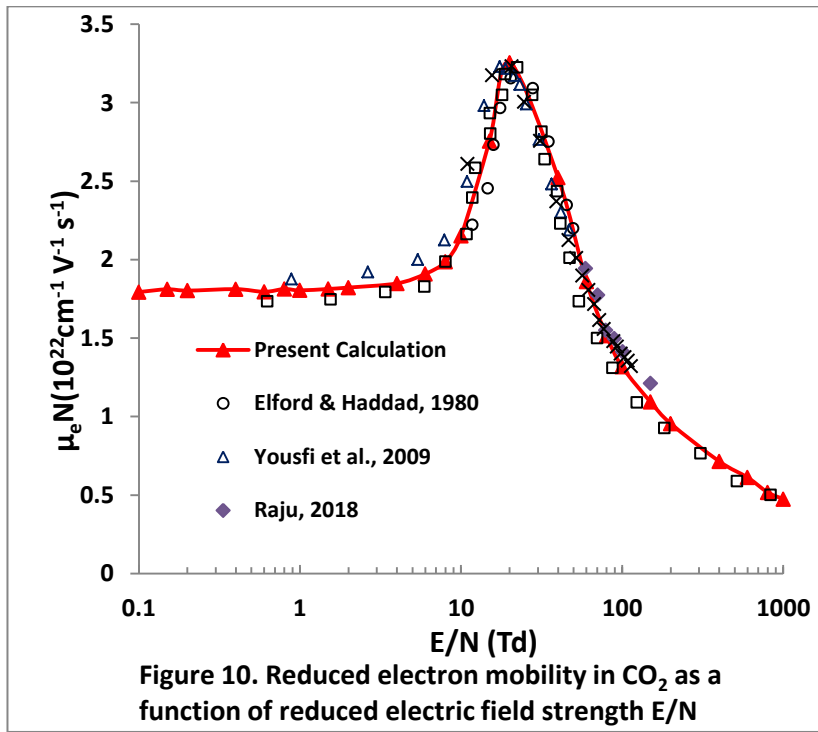
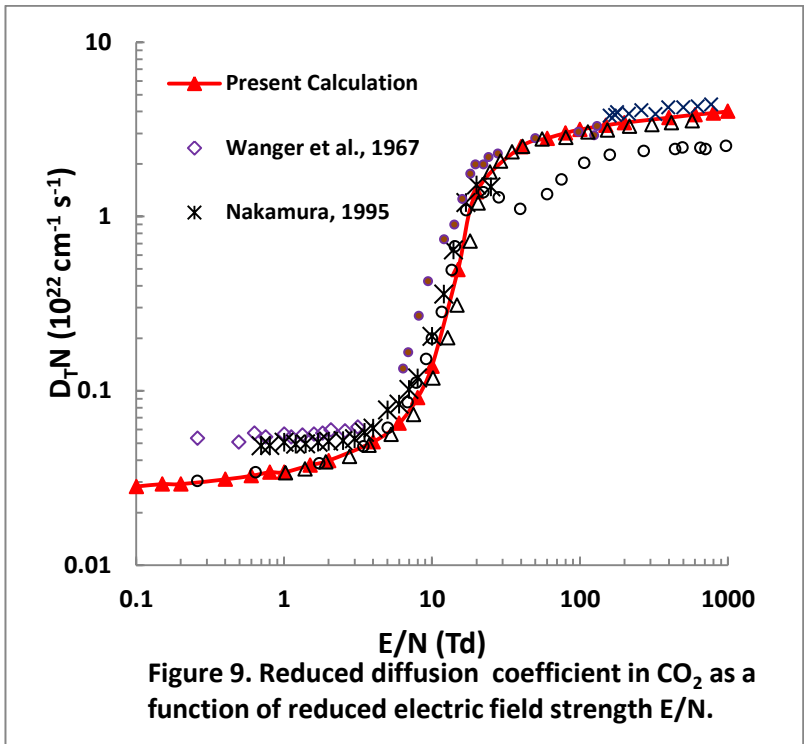
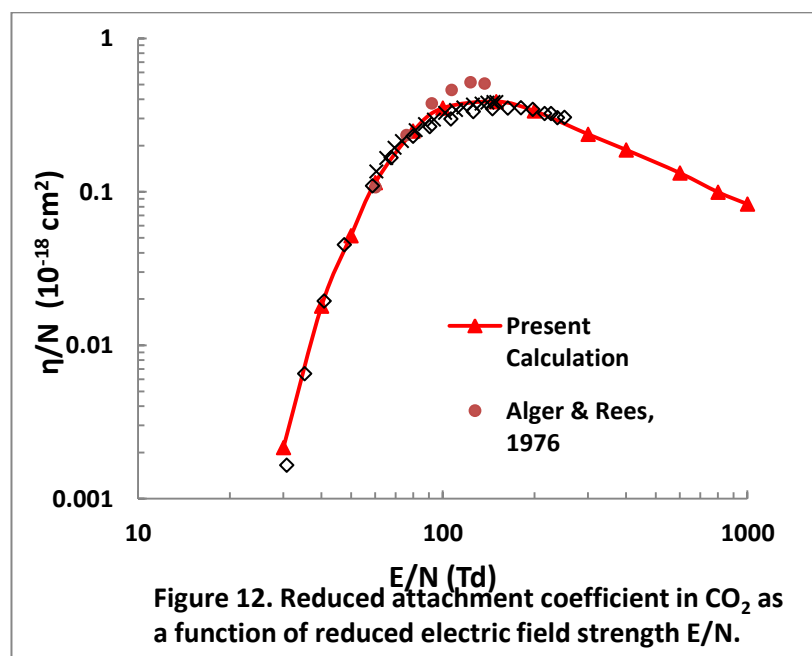
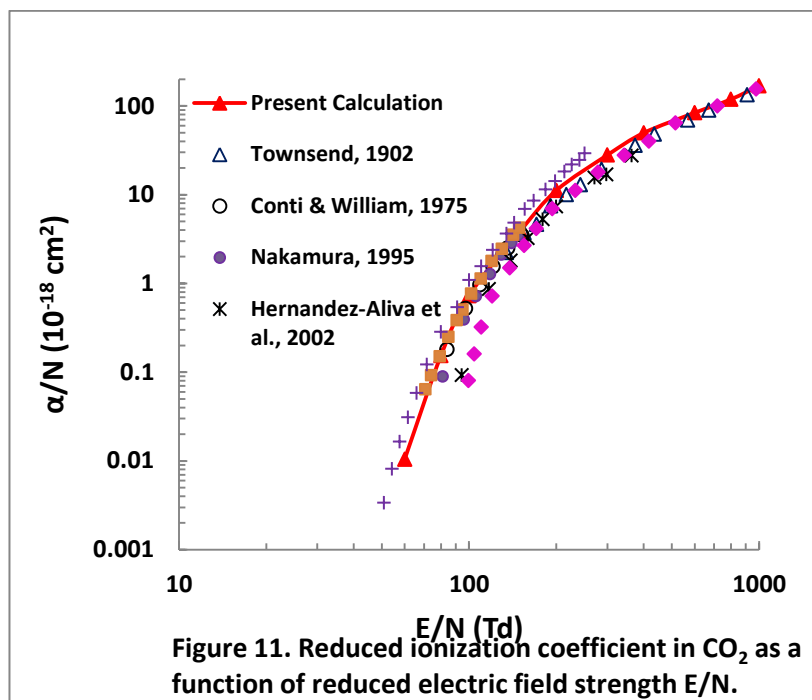


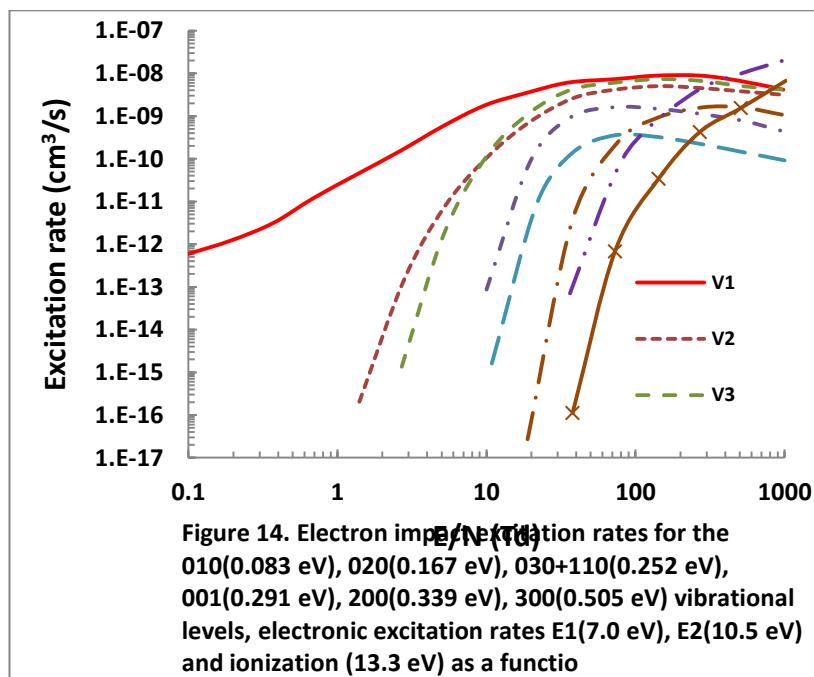
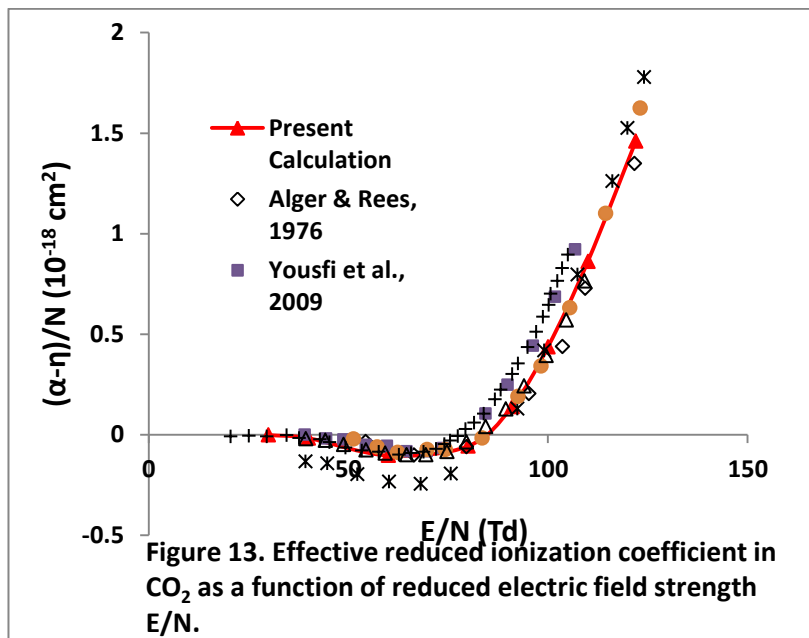
Figure 6. Electron temperature in  $\text{CO}_2$  as a function of reduced electric field strength  $E/N$ .

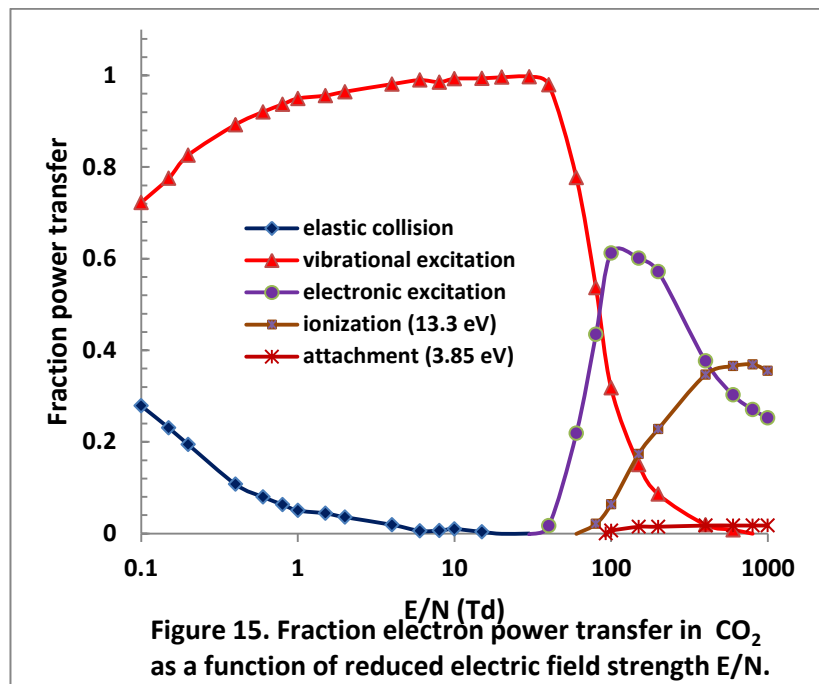












## 5. Conclusion

The electron swarm parameters in Carbon dioxide (CO<sub>2</sub>) have been calculated for an E/N range from 0.1 to 1000 Td using two term-resolution of Boltzmann equation method, in which the influence of ionization and attachment coefficient taken into account. These parameters, namely (electron drift velocity, mean electron energy, electron temperature, characteristic energy, electron mobility and transverse diffusion coefficient) have been compared with the previous theoretical and experimental values. Also the effect of E/N, temperature and pressure on EEDF was studied. Moreover, the reduced ionization coefficient ( $\alpha/N$ ), reduced attachment coefficient ( $\eta/N$ ) and reduced effective ionization coefficient ( $(\alpha-\eta)/N$ ) were derived from EEDF. Then the reduced critical electric field strength  $(E/N)_{cr}$  are obtained from the effective ionization curve. In addition, the excitation rate and the fraction power transfer to different types of elastic and inelastic collision has been explained.

## References

- Alger, S., & Rees, J. (1976). Ionization, attachment and negative ion reactions in carbon dioxide. *Journal of Physics D: Applied Physics*, 9(16), 2359.
- Beatty, E., Dutton, J., & Pitchford, L. (1980). Electron swarm data relevant to high-voltage insulation. In *Gaseous Dielectrics II* (pp. 25-31): Elsevier.
- Brand, K., & Kopainsky, J. (1979). Breakdown field strength of unitary attaching gases and gas mixtures. *Applied physics*, 18(4), 321-333.
- Christophorou, L. G., Olthoff, J. K., & Van Brunt, R. J. (1997). Sulfur hexafluoride and the electric power industry. *IEEE Electrical Insulation Magazine*, 13(5), 20-24.
- Conti, V., & Williams, A. (1975). Ionization growth in carbon dioxide. *Journal of Physics D: Applied Physics*, 8(18), 2198.
- Dahl, D. A., Teich, T. H., & Franck, C. M. (2012). Obtaining precise electron swarm parameters from a pulsed Townsend setup. *Journal of Physics D: Applied Physics*, 45(48), 485201.
- Davies, D. K. (1978). Ionization and attachment coefficients in CO<sub>2</sub>: N<sub>2</sub>: He and pure CO<sub>2</sub>. *Journal of Applied Physics*, 49(1), 127-131.
- De Urquijo, J., Yousfi, M., Juárez, A., Bekstein, A., Basurto, E., Benhennis, M., & Merbahi, N. (2009). *Electron Swarm Coefficients in CO<sub>2</sub>-Air Mixtures*. Paper presented at the International Conference on Phenomena in Ionised Gases.
- Deng, Y., Lu, C., & Xiao, D. (2012). Electron swarm parameters in c-C<sub>4</sub>F<sub>8</sub> and CO<sub>2</sub> gas mixtures from Boltzmann equation analysis. *IEEE Transactions on Plasma Science*, 40(10), 2671-2677.
- Dutton, J. (1975). A survey of electron swarm data. *Journal of Physical and Chemical Reference Data*, 4(3), 577-856.

- Egüz, E. A., Chachereau, A., Hösl, A., & Franck, C. (2019). *Measurements of Swarm Parameters in C<sub>4</sub>F<sub>7</sub>N: O<sub>2</sub>: CO<sub>2</sub>, C<sub>5</sub>F<sub>10</sub>O: O<sub>2</sub>: CO<sub>2</sub> and C<sub>5</sub>F<sub>10</sub>O: O<sub>2</sub>: N<sub>2</sub> Mixtures*. Paper presented at the 19th International Symposium on High Voltage Engineering (ISH 2019).
- Elford, M. (1966). The drift velocity of electrons in carbon dioxide at 293° K. *Aust. J. Phys.*, 19, 629.
- Elford, M., & Haddad, G. (1980). The drift velocity of electrons in carbon dioxide at temperatures between 193 and 573 K. *Australian Journal of Physics*, 33(3), 517-530.
- Frost, L., & Phelps, A. (1962). Rotational excitation and momentum transfer cross sections for electrons in H<sub>2</sub> and N<sub>2</sub> from transport coefficients. *Physical Review*, 127(5), 1621.
- Grofulovic, M. (2019). Energy storage and transfer in non-equilibrium CO<sub>2</sub> plasmas.
- Grofulović, M., Alves, L. L., & Guerra, V. (2016). Electron-neutral scattering cross sections for CO<sub>2</sub>: a complete and consistent set and an assessment of dissociation. *Journal of Physics D: Applied Physics*, 49(39), 395207.
- Haefliger, P., & Franck, C. (2018). Detailed precision and accuracy analysis of swarm parameters from a pulsed Townsend experiment. *Review of Scientific Instruments*, 89(2), 023114.
- Hake Jr, R., & Phelps, A. (1967). Momentum-Transfer and Inelastic-Collision Cross Sections for Electrons in O<sub>2</sub>, CO, and C O<sub>2</sub>. *Physical Review*, 158(1), 70.
- Hasegawa, H., Date, H., Shimozuma, M., Yoshida, K., & Tagashira, H. (1996). The drift velocity and longitudinal diffusion coefficient of electrons in nitrogen and carbon dioxide from 20 to 1000 Td. *Journal of Physics D: Applied Physics*, 29(10), 2664.
- Hernández-Ávila, J., Basurto, E., & De Urquijo, J. (2002). Electron transport and swarm parameters in CO<sub>2</sub> and its mixtures with SF<sub>6</sub>. *Journal of Physics D: Applied Physics*, 35(18), 2264.
- Holstein, T. (1946). Energy distribution of electrons in high frequency gas discharges. *Physical Review*, 70(5-6), 367.
- Itoh, H., Shimozuma, M., & Tagashira, H. (1980). Boltzmann equation analysis of the electron swarm development in SF<sub>6</sub> and nitrogen mixtures. *Journal of Physics D: Applied Physics*, 13(7), 1201.
- Jawad, E. A., & Jassim, M. (2019). Studying the effect of adding buffer gases to CO<sub>2</sub> gas on the electron transport parameter. *Energy Procedia*, 157, 117-127.
- Jiang, P., & Economou, D. J. (1993). Temporal evolution of the electron energy distribution function in oxygen and chlorine gases under dc and ac fields. *Journal of applied physics*, 73(12), 8151-8160.
- Kieffer, L. *A Compilation of Electron Collision Cross-Section Data for Modeling Gas Discharge Lasers, 1973*. Retrieved from
- Koushki, A., Zand, M., Haghighi, H., & Neshati, R. (2015). Numerical solution of Boltzmann's transport equation to predict characteristics of TEA CO<sub>2</sub> lasers. *Optik*, 126(23), 3601-3604.
- Kucukarpaci, H., & Lucas, J. (1979). Simulation of electron swarm parameters in carbon dioxide and nitrogen for high E/N. *Journal of Physics D: Applied Physics*, 12(12), 2123.
- Lakshminarasimha, C., & Lucas, J. (1977). The ratio of radial diffusion coefficient to mobility for electrons in helium, argon, air, methane and nitric oxide. *Journal of Physics D: Applied Physics*, 10(3), 313.
- Laska, L., Mašek, K., Krasa, J., & Peřina, V. (1984). Dielectric properties of SF<sub>6</sub> mixtures containing oxygen and other gases. *Czechoslovak Journal of Physics B*, 34(10), 1038-1047.
- Li, X., Guo, X., Zhao, H., Jia, S., & Murphy, A. B. (2015). Prediction of the critical reduced electric field strength for carbon dioxide and its mixtures with copper vapor from Boltzmann analysis for a gas temperature range of 300 K to 4000 K at 0.4 MPa. *Journal of Applied Physics*, 117(14), 143302.
- Long, Y., Guo, L., Shen, Z., Chen, C., Chen, Y., Li, F., & Zhou, W. (2019). Ionization and attachment coefficients in C<sub>4</sub>F<sub>7</sub>N/N<sub>2</sub> gas mixtures for use as a replacement to SF<sub>6</sub>. *IEEE Transactions on Dielectrics and Electrical Insulation*, 26(4), 1358-1362.
- Morgan, W., & Penetrante, B. (1990). ELENDF: A time-dependent Boltzmann solver for partially ionized plasmas. *Computer Physics Communications*, 58(1-2), 127-152.
- Nakamura, Y. (1995). Drift Velocity and Longitudinal Diffusion Coefficient of Electrons in CO<sub>2</sub>/Ar Mixtures and Electron Collision Cross Sections for CO<sub>2</sub> Molecules. *Australian Journal of Physics*, 48(3), 357-364.
- Nakamura, Y., & Lucas, J. (1978). Electron drift velocity and momentum cross-section in mercury, sodium and thallium vapours. II. Theoretical. *Journal of Physics D: Applied Physics*, 11(3), 337.
- Nechmi, H. E., Beroual, A., Girodet, A., & Vinson, P. (2017). Effective ionization coefficients and limiting field strength of fluoronitriles-CO<sub>2</sub> mixtures. *IEEE Transactions on Dielectrics and Electrical Insulation*, 24(2), 886-892.
- Nighan, W. L. (1970). Electron Energy Distributions and Collision Rates in Electrically Excited N<sub>2</sub>, CO, and CO<sub>2</sub>. *Physical Review A*, 2(5), 1989.
- Ogloblina, P., Tejero-del-Caz, A., Guerra, V., & Alves, L. L. (2020). Electron impact cross sections for carbon monoxide and their importance in the electron kinetics of CO<sub>2</sub>-CO mixtures. *Plasma Sources Science and Technology*, 29(1), 015002 (16pp).
- Othman, M. M., Taha, S. A., & Sailh, I. H. (2019). Solving of the Boltzmann transport equation using two-term approximation for pure electronegative gases (SF<sub>6</sub>, CCl<sub>2</sub>F<sub>2</sub>). *ZANCO Journal of Pure and Applied Sciences*, 31(s4), 7-25.
- Othman, M. M., Taha, S. A., & Salih, I. H. (2019). Analysis of Electron Transport Coefficients in SiH<sub>4</sub> Gas Using Boltzmann Equation in the Presence of Applied Electric Field. *ZANCO Journal of Pure and Applied Sciences*, 31(1), 77-88.

- Pack, J., Voshall, R., & Phelps, A. (1962). Drift velocities of slow electrons in krypton, xenon, deuterium, carbon monoxide, carbon dioxide, water vapor, nitrous oxide, and ammonia. *Physical Review*, 127(6), 2084.
- Pierantozzi, R. (2000). Carbon dioxide. *Kirk-Othmer Encyclopedia of Chemical Technology*.
- Pietanza, L., Colonna, G., D'Ammando, G., Laricchiuta, A., & Capitelli, M. (2016). Electron energy distribution functions and fractional power transfer in "cold" and excited CO<sub>2</sub> discharge and post discharge conditions. *Physics of Plasmas*, 23(1), 013515.
- Pietanza, L., Colonna, G., D'Ammando, G., Laricchiuta, A., & Capitelli, M. (2016). Non equilibrium vibrational assisted dissociation and ionization mechanisms in cold CO<sub>2</sub> plasmas. *Chemical Physics*, 468, 44-52.
- Raju, G. G. (2018). *Gaseous electronics: tables, atoms, and molecules*: CRC Press.
- Rees, J. (1964). Measurements of Townsend's energy factor  $k_1$  for electrons in carbon dioxide. *Australian Journal of Physics*, 17(4), 462-471.
- Roznerski, W., & Leja, K. (1984). Electron drift velocity in hydrogen, nitrogen, oxygen, carbon monoxide, carbon dioxide and air at moderate E/N. *Journal of Physics D: Applied Physics*, 17(2), 279.
- Saelee, H., Lucas, J., & Limbeek, J. (1977). Time-of-flight measurement of electron drift velocity and longitudinal diffusion coefficient in nitrogen, carbon monoxide, carbon dioxide and hydrogen. *IEE Journal on Solid-State and Electron Devices*, 1(4), 111-116.
- Seeger, M., Avaheden, J., Pancheshnyi, S., & Votteler, T. (2016). Streamer parameters and breakdown in CO<sub>2</sub>. *Journal of Physics D: Applied Physics*, 50(1), 015207.
- Smith, K., & Thomson, R. M. (1978). *Computer modeling of gas lasers*: Springer.
- Sun, H., Rong, M., Wu, Y., Chen, Z., Yang, F., Murphy, A. B., & Zhang, H. (2015). Investigation on critical breakdown electric field of hot carbon dioxide for gas circuit breaker applications. *Journal of Physics D: Applied Physics*, 48(5), 055201.
- Tanaka, Y. (2004). Prediction of dielectric properties of N<sub>2</sub>/O<sub>2</sub> mixtures in the temperature range of 300–3500 K. *Journal of Physics D: Applied Physics*, 37(6), 851.
- Townsend, J. S. (1902). LXVI. The conductivity produced in gases by the aid of ultra-violet light. *The London, Edinburgh, and Dublin Philosophical Magazine and Journal of Science*, 3(18), 557-576.
- Tuan, D. A. (2014). Calculations of electron transport coefficients in Cl<sub>2</sub>-Ar, Cl<sub>2</sub>-Xe and Cl<sub>2</sub>-O<sub>2</sub> mixtures. *Journal of the Korean Physical Society*, 64, 23-29.
- Tuan, D. A. (2016). Analysis of electron transport coefficients in binary mixtures of TEOS gas with Kr, Xe, He and Ne gases for using in plasma assisted thin-film deposition. *Journal of Electrical Engineering and Technology*, 11(2), 455-462.
- Uchii, T., Hoshina, Y., Kawano, H., Suzuki, K., Nakamoto, T., & Toyoda, M. (2007). Fundamental research on SF<sub>6</sub>-free gas insulated switchgear adopting CO<sub>2</sub> gas and its mixtures. *ISETS07*.
- Vass, M., Korolov, I., Loffhagen, D., Pinhao, N., & Donkó, Z. (2017). Electron transport parameters in CO<sub>2</sub>: scanning drift tube measurements and kinetic computations. *Plasma Sources Science and Technology*, 26(6), 065007.
- Wagner, E., Davis, F., & Hurst, G. (1967). Time-of-Flight Investigations of Electron Transport in Some Atomic and Molecular Gases. *The Journal of Chemical Physics*, 47(9), 3138-3147.
- Wang, W., & Bogaerts, A. (2016). Effective ionisation coefficients and critical breakdown electric field of CO<sub>2</sub> at elevated temperature: effect of excited states and ion kinetics. *Plasma Sources Science and Technology*, 25(5), 055025.
- Wang, W., Murphy, A. B., Rong, M., Looe, H. M., & Spencer, J. W. (2013). Investigation on critical breakdown electric field of hot sulfur hexafluoride/carbon tetrafluoride mixtures for high voltage circuit breaker applications. *Journal of Applied Physics*, 114(10), 103301.
- Wang, W., Tu, X., Mei, D., & Rong, M. (2013). Dielectric breakdown properties of hot SF<sub>6</sub>/He mixtures predicted from basic data. *Physics of Plasmas*, 20(11), 113503.
- Wedding, A. B. (1985). Electron swarm parameters in a CO<sub>2</sub>: N<sub>2</sub>: He: CO gas mixture. *Journal of Physics D: Applied Physics*, 18(12), 2351.
- Xiao, D., Li, X., & Xu, X. (2001). Swarm parameters in SF<sub>6</sub> and CO<sub>2</sub> gas mixtures. *Journal of Physics D: Applied Physics*, 34(24), L133.
- Xiaoling, Z., Juntao, J., & Dengming, X. (2016). Breakdown Electric Field of Hot 30% CF<sub>3</sub>I/CO<sub>2</sub> Mixtures at Temperature of 300–3500 K During Arc Extinction Process. *Plasma Science and Technology*, 18(11), 1095.
- Yousfi, M., de Urquijo, J., Juarez, A., Basurto, E., & Hernandez-Avila, J. L. (2009). Electron Swarm Coefficients in  $\text{CO}_2$ – $\text{N}_2$  and  $\text{CO}_2$ – $\text{O}_2$  Mixtures. *IEEE Transactions on Plasma Science*, 37(6), 764-772.
- Yun-Kun, D., & Deng-Ming, X. (2013). The effective ionization coefficients and electron drift velocities in gas mixtures of CF<sub>3</sub>I with N<sub>2</sub> and CO<sub>2</sub> obtained from Boltzmann equation analysis. *Chinese Physics B*, 22(3), 035101.
- Zhao, H., Deng, Y., & Lin, H. (2017). Study of the synergistic effect in dielectric breakdown property of CO<sub>2</sub>–O<sub>2</sub> mixtures. *AIP Advances*, 7(9), 095102.
- Zhao, H., Gu, W., & Li, X. (2017). Study of the Insulating and Arc-quenching Performance of CO<sub>2</sub> and Its Mixtures: A Brief Review. *PLASMA PHYSICS AND TECHNOLOGY*, 4(1), 91-94.
- Zhao, H., Li, X., Jia, S., & Murphy, A. B. (2013). Dielectric breakdown properties of SF<sub>6</sub>–N<sub>2</sub> mixtures at 0.01–1.6 MPa and 300–3000 K. *Journal of Applied Physics*, 113(14), 143301.
- Zheng, Y., Yan, X., Chen, W., Zhou, W., Hu, S., & Li, H. (2019). Calculation of electrical insulation of C<sub>4</sub>F<sub>7</sub>N/CO<sub>2</sub> mixed gas by avalanche characteristics of pure gas. *Plasma Research Express*, 1(2), 025013.

## RESEARCH PAPER

### Finite Element Modeling of High Strength Self-Compacting Concrete T-Beams under Flexural Load Reinforced by ARFP

Sinan Abdulkhaleq Yaseen<sup>1</sup> & Muhammad Ali Ihsan<sup>2</sup>

<sup>1,2</sup>Department of Civil Engineering, College of Engineering, Salahaddin University-Erbil, Kurdistan Region, Iraq

#### ABSTRACT:

A finite element models were constructed for comparison self-compacted concrete (SCC) T-beams to study a behavior change of these that reinforced with aramid fiber reinforced polymer (AFRP) and steel bars when compared with experimental data. Nine T-beam specimens reinforced with ARFP and three beams reinforced with steel bars were modeled and analyzed. The key variables were different high strength self-compacted concrete compressive strength, different ratios of AFRP and conventional steel bars for comparison. The comparison for output of flexural strain, load-deflection relationship and crack propagation are taken into consideration. The FE models by using (ANSYS) software show good agreement with the experimental data from previous study by (Yaseen, 2020). The numbers of cracks were reduced in all FE models while the final crack spacing was smaller than experimental samples by maintain the final deflection. Beams reinforced steel bars show better load capacity than those reinforced by AFRP. The FE models were stiffer than the experimental beams. The overall trend of analytical and experimental beam capacity vs reinforcement ratio, shows that the ANSYS response was conservative compared with experimental data of SCC AFRP reinforced beams.

KEY WORDS: FE T-Beam, FEA Method, Flexural behavior, Aramid fiber reinforced polymers, and Self-compacting concrete.

DOI: <http://dx.doi.org/10.21271/ZJPAS.32.6.18>

ZJPAS (2020) , 32(6);176-184

#### INTRODUCTION:

The precast or cast in-situ reinforced concrete is widely used for constructing structural element. Reinforced concrete T-section beam is one of these elements used in bridge construction, and in most cases the reinforced concrete T-section may be monolithically built in which a part of the slab close to the beam section help in resisting the flexural load. The cast in-situ elements are cast in a prepared molds, so the slab and beams work as monolithic reinforced concrete structure to resist higher load capacities (Ofonime & Ndifreke, 2016; Nabil et al, 2013).

Among several concrete types, Self-compacting concrete (SCC), found to be a special one in its high performance, segregation resistance, excellent deformability and it doesn't need vibration to fill small detailed corners during placing process. The SCC is used instead of conventional concrete when the ongoing properties are needed in casting any structural members (Yasser, 2012; Kamal et al, 2001). Durability of reinforced element has the most point of importance. Using steel bars in bridges, chemical industry buildings and construction near the coastal region causes a corrosion for existing reinforcement bars. Therefore, a need for alternative bars come out to fill the weakness of concrete structure in tension. Aramid fiber reinforced polymers (AFRP), fiber-reinforced polymers (FRP), and glass fiber reinforced polymers (GFRP), are a high-performance reinforcement that have high strength-to-weight ratio and corrosion resistance were used instead of conventional steel bars (Guowei, 2011; Rolland,

---

#### \* Corresponding Author:

Sinan Abdulkhaleq Yaseen

E-mail: [sinan.yaseen@su.edu.krd](mailto:sinan.yaseen@su.edu.krd)

#### Article History:

Received: 23/12/2019

Accepted: 15/08/2020

Published: 20/12/2020



2014). This work is aiming at FE modeling, supported by experimental work, to use it in analyzing the flexural behavior of T-sectioned beam that are constructed by using self-consolidation concrete and ARFP bars, since very little work was found on finite element modeling of the related experimental work. Subramani et al. (Subramani et al, 2017) recorded that ultimate tensile strength, the modulus of elasticity of the used bars and beam width was the most affected parameters by changing the applied load, so the modeling must be controlled. Ofonime and Ndifreke (Ofonime and Ndifreke, 2016) studied the effect of increasing the flange width on beam stiffness, the initial crack load, and the load deflection curve. The beam samples were simulated accurately by using LS DYNA software. Buyukkaragoz et al. (Buyukkaragoz et al., 2013) made a numerical study of concrete beams reinforced with AFRP bars to focus on the flexural behavior. The loads on the beams found by FE analysis were close to those from the effective moment of inertia expressions, and the numerical ultimate moments also correlated well with the analytical values of concrete stress-strain models. Numerical analyses, which hardly predict the sudden reduction in the flexural rigidity of FRP-reinforced concrete beams due to the crushing of cover concrete, were shown to provide somewhat conservative deflection estimates. Yaseen (Yaseen, 2020) experimentally investigated the flexural behavior of T-beams made by self-compacting concrete and reinforced with ARFP.

In this study, a total of 9 T-sectioned beams were modeled to see the agreement of FE model beams with experimental data for beams having the same properties and same loading condition (ACI 440.1R, 2006). The material definitions were made for SCC to work as a matrix and ARFP reinforced bars to work as a fiber in the simulation of these T-beams.

The paper objective is to use FE model for estimation an accurate stresses and to see the response of structural components (having slab-beam action) when used in long span members, bridges and other similar applications. Constructing FE models to compare with an experimental data from Yaseen's study (Yaseen, 2020), for find behavior change in flexural using p-delta curve, mode of failure, and crack pattern, due to change in SCC strength and reinforcement

ratio using ARFP bars. A simulation of simply supported SCC T-beams, covering significant key variables, and loaded by static loading is made using ANSYS 18 program (ANSYS, 2018; Srinivasan & Sathiya, 2010).

## 1. FINITE ELEMENT MODEL SIMULATION

As mentioned previously, the ANSYS computer program was used to analyze all the tested beams, the FE analysis of these models is not dedicated for T-Beam SCC casted models which have the same hardened property as a normal concrete to conform the T-Beam SCC casted

experimental results. ANSYS has a ability to build a finite element model and simulate the actual boundary condition of the beam elements. The finite element technique is used to simulate the behavior of self-compacted concrete T-beams reinforced with AFRP bars. The matrix and fiber definition were utilized to construct the FEM. These models were the integration of the three phases of finite element analysis that involve defining the model, boundary conditions and loadings, then the preprocessing, solution, and post-processing.

### 1.1. AFRP Reinforced Concrete Element Definition

The material and element specification of AFRP reinforced Concrete must be defined in any used modeling software to be able to show the interaction between concrete and reinforcement and represent concrete cracking, and crushing. The width reduction of crack growth and the ability of transferring flexural stress after first crack occurs can be found by the interaction between concrete and reinforcement. An eight-node three-dimensional solid element is used to represent the AFRP Reinforced Concrete, called (Solid65) Fig. (1). Each node had three degrees of freedom (u, v, and w, in three direction x, y, and z respectively). The element has ability of plastic deformation and is used to investigate failures in flexural deficit beams.

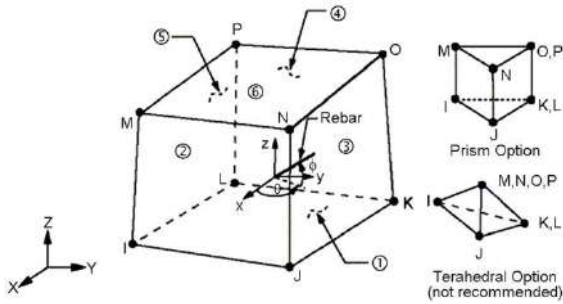


Figure 1: Three-dimensional eight-node solid element

### 1.2. AFRP and steel Stirrup Reinforcement Modeling

The definition of AFRP and stirrup steel bar with their property, can actualize in finite element method by techniques called, discrete, embedded, and smeared representations Fig. (2). A two-node individual representation of main flexural bars (AFRP bars) and shear reinforcement (steel bars) were modeled using 3-D spar elements (Link180), which allow the elastic–plastic response of reinforcing bars (ANSYS, 2011). It is merged with 8 nodal element that represent the reinforced concrete. Some assumptions taken in to consideration, the perfect bond between the nodes of (AFRP and Steel) bars elements and the corresponding nodes for the concrete elements, and the two type of bars carry axial load only.

The difference between the material properties (concrete, AFRP, steel bars) lead to necessities of connecting these distinct elements to allow for the best transforming the load, stresses and strains among them. It means that they share the same nodes. The actual stress–strain curve adopted from the tensile tests is used to determine stress–strain relationship of all type of reinforcement.

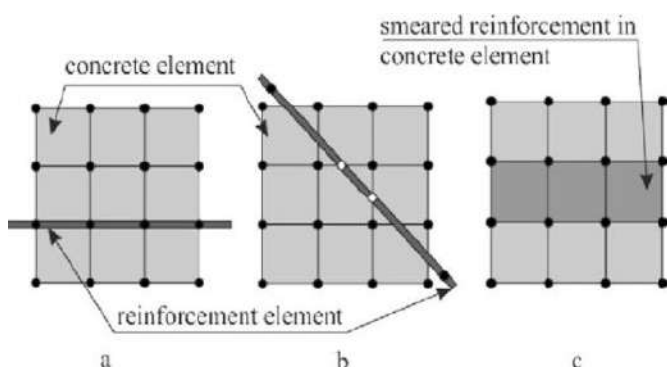


Figure 2: Reinforced concrete model representations (a) Discrete; (b) Embedded; and (c) Smeared

### 1.3. Load transferring bearing plates

A bearing plate is needed under load point connection with the beams. To prevent any stress accumulation at certain points, 10 mm-thick

plates were placed under two points (third-point loading test). This will reduce and distribute the stress to prevent crushing near the supporting point. Solid 185 elements were used to identify the base plate (ANSYS, 2018).

## 2. MATERIAL PROPERTIES MODELLING

### 2.1. Self-compacted Concrete Modeling

Concrete is a quasi-brittle material with different compression and tension behaviors. It is assumed to be homogeneous and initially isotropic. The compressive uniaxial stress–strain relationship for the concrete model is given by Fig.3

The behavior of normal concrete under compression is illustrated in a typical uniaxial stress-strain curve, as shown in Fig. 3, and consists of two parts, linear and nonlinear. The limit of the linear portion is defined as 30% of the maximum compressive strength, the modulus of elasticity ( $E_c$ ) and Poisson’s ratio (calculated from the linear portion). The nonlinear elastic behaviors of concrete can be defined by the multi-linear stress-strain relationships, as illustrated in Fig. 3.

Used material properties are described below:

Two material models were given: material 1 for concrete, material 2 for AFRP, material 3 for steel, under the linear isotropic material definition.

a) Self compacted concrete with varied strengths:

$$\hat{f}_c = 60 \text{ MPa}, \hat{f}_c = 80 \text{ MPa}, \hat{f}_c = 100 \text{ MPa}.$$

Modulus of elasticity,  $E_c = 42.49 \text{ GPa}$ , Ultimate Strain = 0.003, Poisson’s ratio,  $\nu = 0.2$ .

b) AFRP bars:

Modulus of elasticity,  $E_a = 50 \text{ GPa}$ ,  $f_u = 1200 \text{ MPa}$ , Ultimate Strain = 0.023, Poisson’s ratio,  $\nu = 0.28$ .

c) Steel bars

Modulus of elasticity,  $E_s = 200 \text{ GPa}$ ,  $f_y = 420 \text{ MPa}$ , yield Strain = 0.002, Poisson’s ratio,  $\nu = 0.30$ .

the self-compacted concrete mix proportion and the fresh test results are shown in Table (1) and (2).

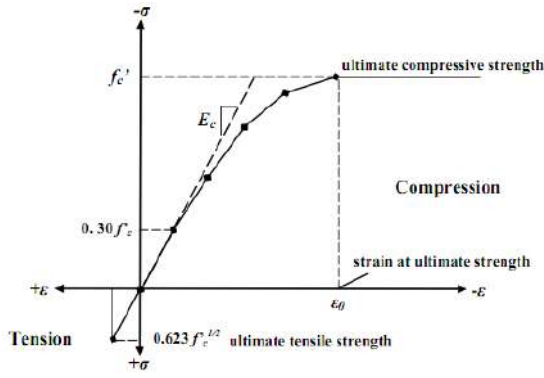


Figure 3: compressive uniaxial stress – strain curve of concrete (ACI, 2016b)

Table (1) Self-compacted concrete mix proportion

Mix No.	Cement kg/m <sup>3</sup>	Gravel kg/m <sup>3</sup>	Sand kg/m <sup>3</sup>	Silica Fume kg/m <sup>3</sup>	Stone Powder kg/m <sup>3</sup>	%Super plasticizer By weight of cement	Free water kg/m <sup>3</sup>	SCC strength at 28 day $\hat{f}_c$ (MPa)
Mix 1	380	850	900	38	57	1.40	155	60
Mix 2	440	800	900	44	66	1.20	165	80
Mix 3	480	900	720	48	72	2.10	139	100

Table (2) Fresh self-compacted concrete test results

Mix No.	Slump Flow (mm)	T <sub>50</sub> (sec)	V-Funnel (sec)	L-Box (H1/H2)
Mix 1	645	4.45	9.65	0.88
Mix 2	675	3.12	8.4	0.91
Mix 3	565	6.85	12.32	0.8

2.2. Geometrical Detail of T-beams

The 12 casted beams were of length 1100mm, over all height 200mm, flange width 200 mm, flange thickness 50mm and web thickness 75mm. (effective depth d=176.3 mm). The beams were simple supported and loaded statically under universal loading machine. The test program includes fabrication of T-beams with three different compressive strengths of self-compacted concrete 60, 80, and 100 MPa, and using AFRP as main longitudinal reinforcement with different reinforcements ratios (less than  $\rho_{bFRP}$ , between balance and  $1.4\rho_{bFRP}$  ratio, and more than  $1.4\rho_{bFRP}$ ).

Also, three beams were casted using conventional steel bars with normal steel balanced reinforcement ratio ( $\rho_b$ ) to be compared with FE model sample defined by normal steel bar, as a reference. Fig. 4 and Table (3 & 4) present the properties and details of the tested specimens (Yaseen, 2018). Half of the full beam was used for modeling by taking advantage of the symmetry of the beams. This approach reduced computational time and computer disk space requirements significantly.

Table (3) Tested beam Detail

G. No.	Sample	SCC strength $\hat{f}_c$ (MPa)	Rein.Ratio $\rho$	No. of main bars	Stirrups	Details
1	TS-11	60	0.83	2-Ø8mm	Ø5.5@75 mm	$\rho_b$
	TA-12		0.55	1-Ø5mm		$\rho < \rho_b$
	TA-13		1.09	2-Ø5mm		$\rho_b < \rho < 1.4\rho_b$
	TA-14		1.64	3-Ø5mm		$\rho > 1.4\rho_b$
2	TS-21	80	0.97	2-Ø10mm	Ø5.5@75 mm	$\rho_b$
	TA-22		0.82	2-Ø5mm		$\rho < \rho_b$
	TA-23		1.23	3-Ø5mm		$\rho_b < \rho < 1.4\rho_b$
	TA-24		1.64	4-Ø5mm		$\rho > 1.4\rho_b$
3	TS-31	100	0.78	2-Ø10mm	Ø5.5@75 mm	$\rho_b$
	TA-32		0.66	3-Ø5mm		$\rho < \rho_b$
	TA-33		1.31	4-Ø5mm		$\rho_b < \rho < 1.4\rho_b$
	TA-34		1.64	5-Ø5mm		$\rho > 1.4\rho_b$

Table (4) Tested Beam Detail

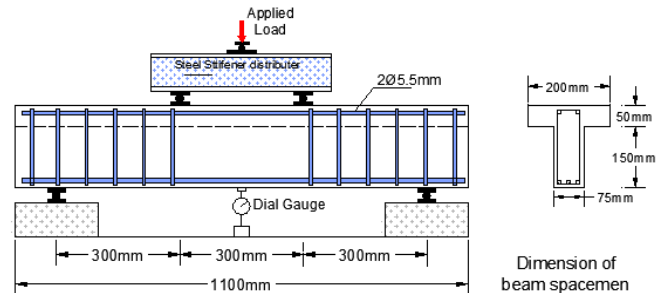
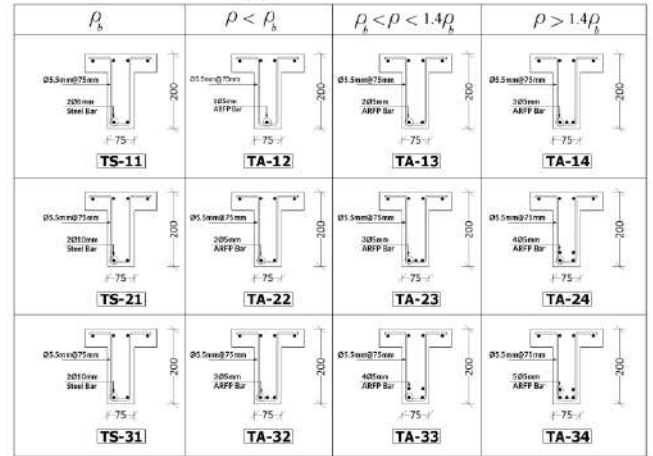


Figure 4: T-Beam geometrical detail with loading

3. LOADING AND BOUNDARY CONDITION

The symmetry allows the use of only half of the beam instead of full sample. A simple supported beam boundary condition was entered. The direction perpendicular to the plane of symmetry must be restrained against displacement. A base plate placed under point load position to prevent the accumulation of stress and it was defined as

steel material with elastic properties. The perfect merge between the nodes is checked to gain the fully interaction between the three material (concrete, AFRP, and steel). In the contact definition, concrete is specified as the master surface while the steel plate is the slave surface. All top nodes of the steel plate at the loading point are pushed down following a prescribed time-displacement curve while ensuring that dynamic effect is negligible, to mimic a quasi-static loading. Figs. 5 & 6 show the one-half finite element model of the reinforced concrete T-beam with reinforcement detail.

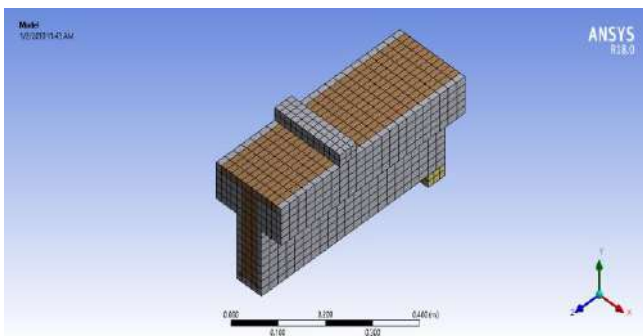


Figure 5: Typical steel reinforcement locations for the half-size beams

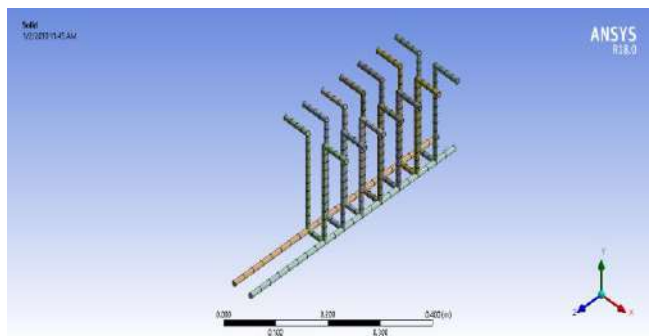


Figure 6: Reinforcement locations for the half-size beams

#### 4. PREDICTED RESULTS FROM THE FINITE ELEMENT MODEL (FEM)

The results of all specimens with their 1<sup>st</sup> cracking load (The first cracking load from the finite element analysis is the load step where the first signs of cracking occur in concrete elements (solid65)), deflection, ultimate load (ultimate load is the last converge load step  $P_u$ ), and their final deflections are summarized in Table 5.

##### 4.1. First Cracking Load

A behavior recording of all loading steps is taken by ANSYS. Cracking became visible on the sides of the FE Modeled beam at 12-18% of the failure

Sp.No.	G.No.	Samples	SCC strength $f'c$ (MPa)	Experimental Result				Mode of Failure
				First Crack load kN	Deflection at first crack mm	Failure load kN	Deflection mm	
1	G1	TS-11	60	21.07	1.4	52.67	5.99	Compresion
2		TA-12		7	3.17	33.6	79.11	Tension
3		TA-13		8.64	5.9	60.45	87.26	Compresion
4		TA-14		9.82	6.2	70.7	91.61	Compresion
5	G2	TS-21	80	22.69	0.91	75.64	5.96	Compresion
6		TA-22		4.76	2.9	65.03	80.55	Tension
7		TA-23		6.86	3.8	84.38	83.06	Compresion
8		TA-24		10.16	5.27	94	89.15	Compresion
9	G3	TS-31	100	23.47	0.91	78.25	5.03	Compresion
10		TA-32		8.08	1.22	95.35	81.98	Tension
11		TA-33		9.13	3.2	107.57	85.19	Compresion
12		TA-34		9.37	3.53	119.93	91.2	Compresion

Sp.No.	G.No.	Samples	SCC strength $f'c$ (MPa)	FE Model Result				Mode of Failure
				First Crack load kN	Deflection at first crack mm	Failure load kN	Deflection mm	
1	G1	TS-11	60	19.66	1.2	55.3	6.13	Compresion
2		TA-12		6.55	2.78	35.1	79.68	Tension
3		TA-13		8.14	5.6	62.3	87.48	Compresion
4		TA-14		9.23	5.82	72.5	91.23	Compresion
5	G2	TS-21	80	20.03	0.61	78.3	6.32	Compresion
6		TA-22		4.12	2.62	67.3	80.66	Tension
7		TA-23		6.22	2.65	86.2	82.47	Compresion
8		TA-24		9.16	5.22	96.12	91.35	Compresion
9	G3	TS-31	100	22.12	0.73	80.71	6.51	Compresion
10		TA-32		7.89	1.02	97.61	82.12	Tension
11		TA-33		8.99	3.09	119.65	85.24	Compresion
12		TA-34		9.07	3.23	128.32	91.78	Compresion

load in beams of 60 MPa strength and 6-9% in beams of 80 and 100 MPa strength, while these ratios were a bit larger in experimental data. The first sign cracks were flexural crack occurred at mid-span length of the T-beam specimens, starting at the bottom when the applied load reached the loads shown in result table. The flexural failing pattern seen in all beams. The number of cracks from the ANSYS-FEM analysis is smaller than that observed in the experimental test, see Fig. 7. No more than three cracks can be predicted in each Solid65 element for the FEM. Therefore, the number of cracks shown is affected by the size of the mesh. Using a large mesh size for Solid65 elements would result in few elements and minimal cracks, whereas using a small mesh size would result in the opposite conditions.

The overall first crack load was larger in Finite element model compared with the experimental data. This is due the compatibility between the material definitions making an enhancement in load transferring between the materials and that the cracking load in the experimental test was the load at which the first visible flexural crack appeared, whereas the theoretical cracking load is the load step in which one of the principal stresses in the concrete element reached the maximum limit. The specimens reinforced with steel need very larger loads to reach the first crack when compared with AFRP reinforced samples. Increasing SCC strength from 60 to 100 MPa led to increase the first crack load in same groups of reinforcement ratios.

Table (5) FE model and experimental testing results

The final deflections of AFRP beam were ranged between 79-92 mm, while the deflection in the corresponding beams reinforced with steel were 6-7 mm. The final crack spacing was smaller than experimental samples, mainly because of assuming SCC to be a homogenous isotropic material in FE model which's make the load of first crack be less and the number and crack opening less than experimental. The corresponding strain intensity for the beam sample shown in Fig. 8.

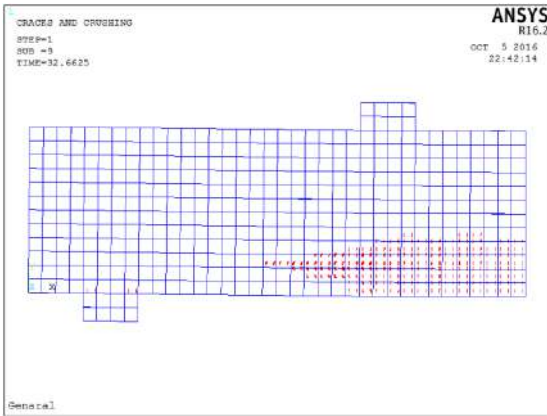


Figure 7: Flexural crack pattern for T-beam

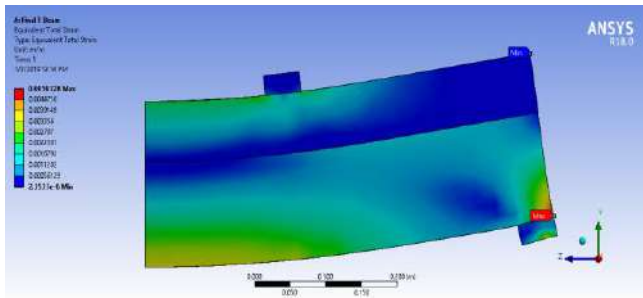


Figure 8: Strain intensity for beam sample by ANSYS

### 4.2. Compressive Strength Effects on Ultimate Capacity

The influence of self-compacted concrete can be seen for the same reinforcement ratio groups. A small increase of ultimate load capacity is seen for  $\rho < \rho_b$  of AFRP ratio, while a larger load carrying capacity is seen for,  $\rho_b < \rho < 1.4\rho_b$  and  $\rho > 1.4\rho_b$  of AFRP ratio when the strength changed from 60MPa, to 80MPa, and then to 100MPa, Table 1. The T-beams reinforced with steel bars were stiffer by carrying more load when compared with AFRP reinforced beams. The ultimate load capacity of the steel reinforced beam differs by 57.54%, 16.34%, and -17.31% than aramid reinforced beams for same group of concrete strength. These ratios are seen to be more than the experimental data by 0.84%, 1.01%, and 0.65% respectively. This increase in results is occurred because that the concrete was taken as

homogenous material, so more interlocking between the meshes and higher results are occurred. Ultimate load capacity is increased by 41.60% for steel reinforced beams when strength increased from 60MPa to 80MPa. However, ultimate load capacity is increased by 3.07% when strength increased from 80MPa to 100MPa which shows that the effect of strength change is more in low strengths. These ratios coincide with those of the experimental data.

### 4.3. AFRP Reinforcement Ratio Effect

The change in reinforcing ratio effect for the same strength group made an improvement in ultimate load capacity. The enhancement found to be 77.49%, 28.08%, and 22.57% for 60, 80, and 100MPa strength groups when the ratio increased from  $\rho < \rho_b$  to  $\rho_b < \rho < 1.4\rho_b$ , and the increases were 16.37%, 11.5%, and 7.24% for 60, 80, and 100MPa strength groups when the ratio increased from  $\rho_b < \rho < 1.4\rho_b$  to  $\rho > 1.4\rho_b$  as shown in Fig. 9. The predicted load of ANSYS model versus the experimental beam data shows a convergence to be ranged from 97-99% for small reinforcement ratios  $\rho < \rho_b$  to  $\rho_b < \rho < 1.4\rho_b$  and 90% for larger ratios ( $\rho_b < \rho < 1.4\rho_b$  to  $\rho > 1.4\rho_b$ ), this is thereby an indication of perfect calibration of FEM model to perform the simulations close to reality.

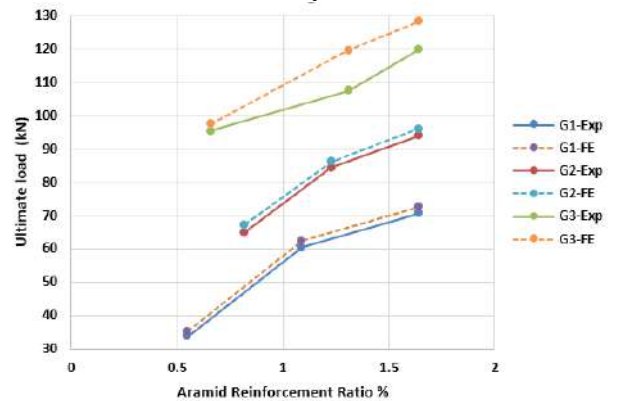


Figure 9: FE model and experimental beam capacity vs. reinforcement ratio

### 4.4. Load Displacement Relations

The loading stages with the corresponding displacement were recorded. Because of putting displacement transducer at mid span of the experimental tested beam, so the deflections were taken in the same location in FE model at the bottom of the mid span as indicated in Fig. 10. The load-deflection comparison curves of FE models and experimental tested beams are presented in Fig. 11, 12, and 13, for 60-, 80-, and

100-MPa self-compacted concrete respectively. The FE model ultimate load capacity shows slight increase in deflection with respect to the experimental data for all strengths and AFRP ratios. This is an indication of agreement of the constructed model with the experimental beams. The number of cracks were reduced in all FE models. The models were stiffer than the experimental beams because of the non-consideration of the micro-cracks in concrete (because of drying shrinkage), the bond slip of the reinforcement and the assumed perfect bond between the concrete and the reinforcement bar in the FE model, which may not be true for actual beams. The first cracking loads obtained from the ANSYS-FEM is lower than those from the experimental results in the pre-cracking stages. The low modulus of elasticity of AFRP bars made their effect of changing reinforcement ratio be small on reducing the beam mid-span deflection. The deflection of T-beams with steel bars were much smaller than the AFRP reinforced beam, and having more ultimate load capacity due to deform bar effect and transferring high tensile stress at high strain levels. The increase of AFRP ratio within each group led to more load carrying capacity of T-beams. Specimens with  $\rho < \rho_b$  ratio of AFRP were compared when the strength changes from 60 to 80MPa and from 80 to 100MPa. The enhancements in ultimate load capacity were 91.73% and 45.03% respectively. For  $\rho_b < \rho < 1.4\rho_b$  The enhancements were 33.54% and 38.80%, and for  $\rho > 1.4\rho_b$  were 32.57% and 33.49% respectively. Analytical and experimental beam capacity vs. reinforcement ratio for groups 1, 2, 3 are shown in Fig.14, 15, 16. However, the overall trend of the ANSYS response is compared to experimental results.

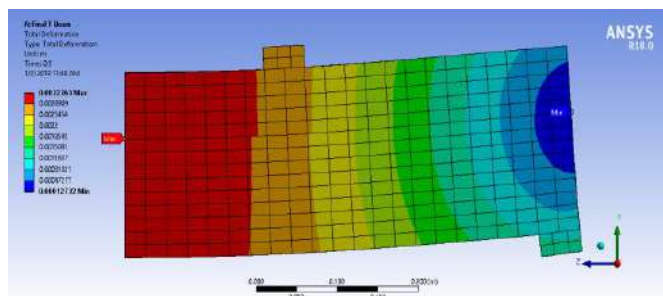


Figure 10: Deflected beam shape for beam sample by ANSYS

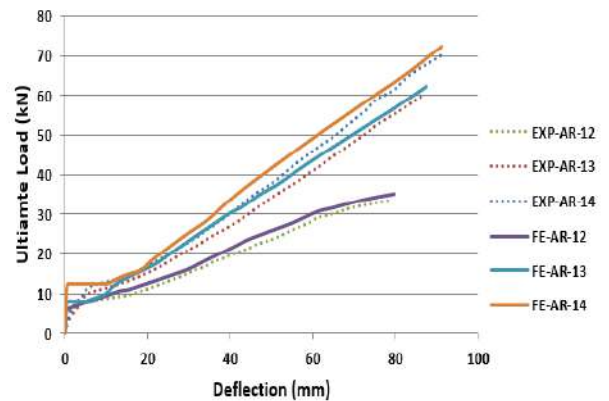


Figure 11: FE model vs experimental load-deflection curve for 60MPa strength group

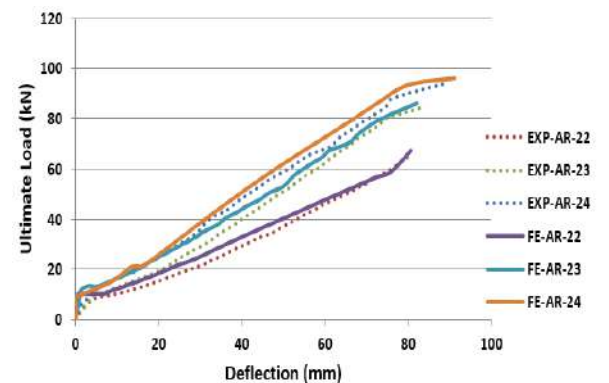


Figure 12: FE model vs experimental load-deflection curve for 80MPa strength group

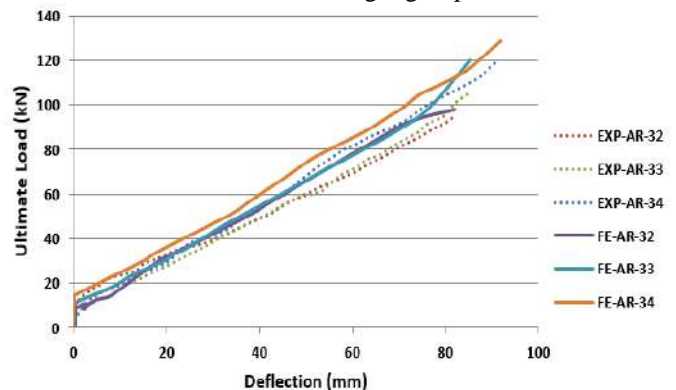


Figure 13: FE model vs experimental load-deflection curve for 100MPa strength group

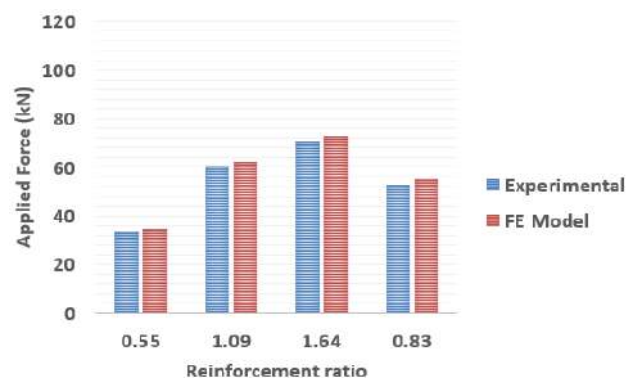


Figure 14: Analytical and experimental beam capacity vs Reinforcement Ratio for Group-3 ( $f_c=60\text{MPa}$ )

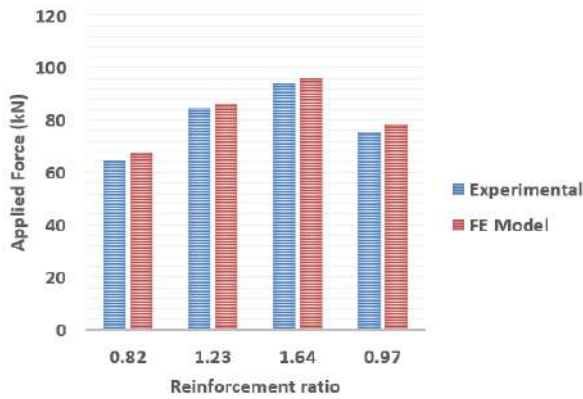


Figure 15: FE and experimental beam capacity vs Reinforcement Ratio for Group-2 ( $f_c=80\text{MPa}$ )

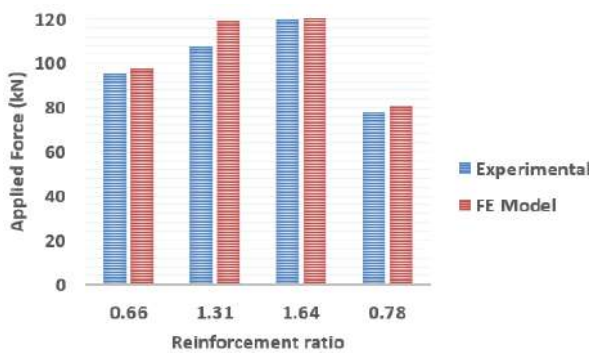


Figure 16: Analytical and experimental beam capacity vs Reinforcement Ratio for Goup-3 ( $f_c=100\text{MPa}$ )

5. INFLUENCES OF MAJOR PARAMETERS

The aforementioned beam test results were used to investigate the reasons behind the weak representation of design equations for predicting the beam capacity of the reinforced concrete T-beams reinforced with different type bars. To do this, table (6) were prepared showing finite element and experimental crack load ratio and finite element and experimental ultimate (failure) load ratio. And accordingly, it is seen that the crack loads for finite element is so close to 1 and for the ultimate load they are more than 1. This is the indication of accuracy of Finite element models so the load capacity pattern is too close.

Table (6) FE and experimental  $P_{cr}$  and  $P_u$  load ratio

Sp.No	G.No.	Samples	SCC strength $f_c$ (MPa)	Finite Element First Crack load kN	Experimental First Crack load kN	Pcr FE/Pcr Exp	Finite Element Pu load kN	Experimental Pu load kN	Pu FE/Pu Exp
1	G1	TS-11	60	19.66	21.07	0.933	55.3	52.67	1.050
2		TA-12		6.55	7	0.936	35.1	33.6	1.045
3		TA-13		8.14	8.64	0.942	62.3	60.45	1.031
4		TA-14		9.23	9.82	0.940	72.5	70.7	1.025
5	G2	TS-21	80	20.03	22.63	0.883	78.3	75.64	1.035
6		TA-22		4.12	4.76	0.866	67.3	65.03	1.035
7		TA-23		6.22	6.86	0.907	86.2	84.38	1.022
8		TA-24		9.16	10.16	0.902	96.12	94	1.023
9	G3	TS-31	100	22.12	23.47	0.942	80.71	78.25	1.031
10		TA-32		7.89	8.08	0.976	97.61	95.35	1.024
11		TA-33		8.99	9.13	0.985	119.65	107.57	1.112
12		TA-34		9.07	9.37	0.968	128.32	119.93	1.070

6. CONCLUSION

1-The FE model ultimate load capacity shows slight increase in deflection with respect to the experimental data for all strengths and AFRP ratios. The T-beams reinforced with steel bars show very small deflection compared with AFRP reinforced beams. This is an indication of agreement of the constructed model with the experimental beams. The number of cracks were reduced in all FE models.

2- An increase of AFRP ratio within each group led to more load carrying capacity of T-beams. For  $\rho < \rho_b$  the enhancements in ultimate load capacity were 91.73% and 45.03% for (TA-13 and TA-14) respectively over (TA-12). For  $\rho_b < \rho < 1.4\rho_b$  the enhancements were 33.54% and 38.80% for (TA-23 and TA-24) respectively over (TA-22), while, it was 32.57% and 33.49% for (TA-33 and TA-34) respectively over (TA-32) for  $\rho > 1.4\rho_b$ .

3- The steel reinforced beam differs by 57.54%, 16.34%, and -17.31% than aramid reinforced beams for same group of concrete strength in term of final deflection, in which they had balanced reinforcement ratio.

4- The final crack spacing was smaller than experimental samples (which is mean higher number of cracks), taking concrete element (solid65) to be homogenous isotropic material in FE model make the occurrence of first crack be less in number and crack opening less than experimental for the three ratios respectively.

5- The ultimate load capacity of the steel reinforced beam differs by 57.54%, 16.34%, and 17.31% than aramid reinforced beams for same group of concrete strength. These ratios are seen to be more than the experimental data by 0.84%, 1.01%, and 0.65% respectively, this increase in results occurred because that the concrete was taken as homogenous material, so more interlocking between the meshes and higher results is found.

6- For steel reinforced beams of 60MPa and 80MPa strength, ultimate load capacity increases by 41.60%, while for 80MPa and 100MPa strength groups, ultimate load capacity increase by 3.07% showing that the effect of strength change is more in low strengths. These ratios coincide with those of the experimental data.

6- The predicted load of ANSYS model versus the experimental beam data shows a convergence to be ranged from 97-99% for small reinforcement

ratios  $\rho < \rho_b$  to  $\rho_b < \rho < 1.4\rho_b$  and 90% for larger ratios ( $\rho_b < \rho < 1.4\rho_b$  to  $\rho > 1.4\rho_b$ ), this is thereby an indication of perfect calibration of FEM model to perform the simulations close to reality.

7- The models were stiffer than the experimental beams. This came from the non-consideration of the micro-cracks in concrete (because of drying shrinkage), the bond slip of the reinforcement and the assumed perfect bond between the concrete and the reinforcement bar in the FE model, which may not be true for actual beams, and the first cracking loads obtained from the ANSYS-FEM being lower than those from the experimental results in the pre-cracking stages.

8- Analytical and experimental beam capacity vs. reinforcement ratio relations are plotted for all groups. Noting that the overall trend of the ANSYS response is conservative when applied on SCC AFRP reinforced beams compared to experimental data.

## Reference

- ABDULLAH A. H., ABDUL KADIR M.R. (2016), Reinforcement for Strengthening Reinforced Concrete Beams-Overview, ZANCO Journal of Pure and Applied Sciences, 28(2), 178-200.
- ACI 440.1R-06. (2006). ACI Committee 440 Guide for the Design and Construction of Concrete Reinforced with FRP Bars, American Concrete Institute, Farmington Hills, Michigan.
- ACI 2013b. CT-13. (2013). ACI Concrete Terminology. ACI STANDARD.
- ANSYS, (2018). ANSYS User's Manual Revision 5.5. Canonsburg, Pennsylvania: ANSYS, Inc.
- BUYUKKARAGOZ, A., KALKAN, I., & LEE, J. H. (2013). A Numerical Study of the Flexural Behavior of Concrete Beams Reinforced with AFRP Bars. Strength of Materials journal, 45(6), 716–729.
- GUOWEI, N., BO, L., XIAO L., & WENSHANG, Y. (2011). Experimental Study on Concrete T-Beams Strengthened with Carbon Fiber Reinforced Polymer (CFRP) Sheets on Three Sides. Systems Engineering Procedia, 1, 69–73.
- KAMAL, H. K., PATRICK, P., AND STEPHAN T. (2001). Structural Performance and In-Place Properties of Self-Consolidating Concrete Used for Casting Highly Reinforced Columns. Materials Journal, 98(5), 371-378.
- NABIL, G., ASCE, M., KENICHI, U., PRINCE, B., AND MENA B. (2013). Flexural Behavior of a Carbon Fiber-Reinforced Polymer Prestressed Decked Bulb T-Beam Bridge System. Journal of Composites for Construction. 17(4).
- OFONIME, A. H., & NDIFREKE, E. U. (2016). Effect of Flange Width on Flexural Behavior of Reinforced Concrete T-Beam. Civil and Environmental Research, 8(8).

- ROLLAND, A., CHATAIGNER, S., BENZARTI, K., QUIERTANT, M., ARGOUL, P., & PAUL, J-M. (2014). Mechanical behaviour of aramid fiber reinforced polymer (AFRP) rebar/concrete interfaces. Transport Research Arena, Paris.
- SRINIVASAN, R. & SATHIYA K. (2010). Flexural behavior of reinforced concrete Beams using finite element analysis (elastic Analysis). Buletin of the political institute in Iași. Technical university "gheorghe asachi" iasi. Tom lvi (Ix), fasc. 4.
- SUBRAMANI, T., MOHAMMED ALI, A., KARTHIKEYAN, R., PANNER SELVAN, E., & PERIYASAMY, K. (2017). Analytical Study Of T-Beam Using ANSYS. International Journal of Emerging Trends & Technology in Computer Science. 6(3).
- YASEEN, S.A. (2020). Flexural Behavior of Self Compacting Concrete T-Beams Reinforced With ARFP. ZANCO Journal of Pure and Applied Sciences, 32(3).
- YASSER S. (2012). Structural performance of Self-Consolidating Concrete used in reinforced concrete beams. KSCE Journal of Civil Engineering, 16(4), 618–626.



## RESEARCH PAPER

# Minimizing Time and Cost in The Iraqi AEC industry by Adopting Building Information Modeling (BIM) Technique.

Mahmood Maad Mahdi<sup>1\*</sup>, Khalil Ismail Wali<sup>2</sup>, Burog Abdullhalim Yuosif<sup>3</sup>

<sup>1</sup>MSc Candidate in Civil Engineering Department, College of Engineering, Salahaddin University-Erbil, Kurdistan Region, Iraq

<sup>2</sup> Department of Civil Engineering, College of Engineering, Salahaddin University-Erbil, Kurdistan Region, Iraq

<sup>3</sup>MSc. In public management, a consultant at the Ministry of Planning, Baghdad, Iraq

### ABSTRACT:

The Architectural, Engineering, and Construction (AEC) industry is essential for its direct influence on the development of any country, particularly in terms of economy. Thus, problems related to cost and time arise as a global phenomenon in this industry, particularly in the third world countries like Iraq. The Building information modeling (BIM) technique is considered as the most adequate technique that overcomes the problems facing the AEC industry. This paper aimed to assess the causes of cost issues and time delays in the Iraqi AEC industry and to outline the BIM concept and the benefits of its application for solving these problems. This paper consists of two parts; the first one is the quantitative approach, which was adopted for data collection through a specially designed questionnaire form; these questionnaires were spread among 50 of the top and middle management in different construction companies, and other experts in the arena of AEC industry. The results of the statistical analysis showed that the highest influential factors on cost and time overrun are: inadequate planning and scheduling, selecting inefficient contractors, change orders, and the errors and mistakes in preparing the bill of quantities and materials (BOQ/BOM) with relative importance index (RII) of 0.98, 0.87, 0.83 and 0.82 respectively. The second part of this paper reviewed the benefits of applying BIM and highly recommend this technology to improve the local AEC industry. The application of the BIM technique will lead to more sustainable design, construction, and project delivery in the Iraqi projects. This paper presents a significant set of recommendations that demonstrate how BIM technique can be applied to overcome the challenges of the AEC industry in Iraq. It unlocks the door for further authentic researches on the adoption of BIM technique as an influential and exceptional tool to point out the issues related to time and cost in the AEC industry in Iraq.

KEYWORDS: Building Information Modeling, Construction Management, Cost overrun, Sustainability, Time overrun.

DOI: <http://dx.doi.org/10.21271/ZJPAS.32.6.19>

ZJPAS (2020) , 32(6);185-196.

### 1. INTRODUCTION:

The Architectural, Engineering, and Construction (AEC) industry stands as a very essential for its direct influence on the development of any country, particularly in terms of economy. From an economic point of view, it contributes to the development of the overall gross domestic product (GDP) of a country significantly. On the other hand, it improves life quality by providing necessary infrastructures like schools and hospitals, for instance, and other

essential and basic services (Cantarelli, 2009, Olawale and Sun, 2010). Therefore, its deeply critical to complete the projects successfully within the determined time, cost, and the required quality. Nevertheless, the AEC industry, at all times, facing recurrent challenges like cost overrun, time overrun, low productivity and poor quality, as well as construction waste and others for it is a complicated, miscellaneous industry that based on time tables and schedules (Abdul Rahman et al., 2013).

Cost overrun arises as a global phenomenon in the AEC industry, and there are

#### \* Corresponding Author:

Mahmood Maad Mahdi

E-mail: [Mahmood.mahdi@su.edu.krd](mailto:Mahmood.mahdi@su.edu.krd) or [MahmoodM.mahdi@Gmail.com](mailto:MahmoodM.mahdi@Gmail.com)

#### Article History:

Received: 16/12/2019

Accepted: 26/08/2020

Published: 20/12/2020

very rare projects that are accomplished within the planned budget (Flyvbjerg et al., 2003). In terms of costs transport infrastructure projects, a worldwide study showed that costs transport does not perform as promised, cost-related issues were recognized as the main challenge where almost 9 of 10 projects experienced cost-related issues in around 50% to 100%. Countries like Malaysia are also dealing with a serious cost-related problem in the building industry where about 37.2% of the private sector projects and around 46.8% of public sector building projects were completed within the planned budget (Abdullah et al., 2009, Razak Bin Ibrahim et al., 2010, Sambasivan and Soon, 2007). The AEC industry in developed countries such as the UK, dealing with these problems as well, where approximately one-third of the client complain that their projects exceed the assigned financial plan (Olawale and Sun, 2010). All that increases the need for new solutions to hold on and control these problems. On the other hand, the construction industry is always improving to overcome the challenges facing the projects' performance and other issues related to the industry. It has witnessed a paradigm shift in the direction of raising productivity, efficiency, sustainability, quality, the value of infrastructures, and in the direction of reducing duplications, overall lifecycle cost besides reducing the time (Arayici et al., 2009). This is consistent with the words of Azhar (2011) as he pointed out that construction projects tend to implement new methods that decrease the project's cost, increase the project's productivity and reduce the project's time, which increases the value of the project. While Mahdi and Ali (2019) highly recommended the use of advanced technologies such as the BIM technique to reduce problems of wastage in construction materials along with Wali and Othman (2019), who recommended the use of advanced technologies to reduce risks in the AEC industry in Iraq.

Building information modeling (BIM) is one of these techniques. BIM is a revolutionary technology and process that transformed and developed the way of design, planning, construction, and operation of buildings (Hardin and McCool, 2015). BIM technique has been defined as the application of a software program for simulating the building and the operation of a project. This model is a digital representation of the project which is rich of the project's data, where the data can be isolated and analyzed to generate the needed information to meet the needs

of different users, which will be used to improve decision making and improve the delivery process (AGC, 2005). BIM technique is the most vital sustainable approach to manage and deliver the project within its designed time, cost, and quality (Eastman et al., 2011).

The aim of the research is to present a study explaining the value of BIM technology and its effect in developing the AEC industry, overcoming AEC problems, and to determine the necessity of applying this technology to minimizing time and cost in the AEC industry in Iraq.

## 2. LITERATURE REVIEW

### 2.1. COST AND TIME RELATED ISSUES

Abdul Rahman et al. (2013) aimed in their paper to recognize the highly influential causes for cost problems in large Malaysian building projects. Their designed questionnaire contains thirty-five of the main frequent factors causes cost problems, and these factors were classified into seven groups. The findings showed that the highest three signs of cost issues are the cash flow and financial problems tackled the contractors, the variation in the prices of the materials, and the inadequate management and supervision which goes under the group of contractor's site and financial management.

On the other hand, Doloi (2012) aimed to provide more understanding of the cost-related problems and different methods of management by conducting a survey study. The survey was designed to investigate the experiences of the contractors, the clients, and the consultants in the building industry. Also, to recognize the main acute factors that influence the performance of costs and expenses by ranking these factors reliant on the relative importance weight (RIW). They also used a multivariate regression assessment to investigate and analyze these influential factors considering the duties and responsibilities of the stakeholders. The gained regression analysis illustrates the impact of 5 key-factors on the expenses operations, and these factors are: accurate planning of the project and sufficient monitoring, as well as design adequacy along with the efficient site management, efficient communication, and the efficiency of contractor's performance.

Moreover, Enshassi et al. (2009) aimed to assess the factors that lead to issues related to costs (expenses overrun) and time problems (delays) in the AEC projects in Gaza Strip, Palestine. They selected around 110 factors/causes related to delays, and 42 cost-related factors classified into 12 major groups. All these factors were based on previous studies, along with factors that arise in different circumstances occurring in the strip of Gaza. The importance level of all these factors was calculated and ranked according to their importance indexes based on the contractors, consultants, and owner's perspectives. The results indicate that there is a general agreement between the three major parties in construction (i.e., the owner, consultant, and contractor). The major delay factors appeared to be related to the general situation in the Gaza strip, materials availability, and procurement, etc. Furthermore, the major causes of cost-related issues were inflation, the fluctuations in the prices of materials, delays in delivering the material, and the equipment by the contractors.

Assaf and Al-Hejji (2006) investigated the roots of delays in megastructure projects. They also tested the importance degree of delay factors to analyze the differences based on the perceptions of the three major parties in the construction industry (i.e., the owners, the consultants, and the contractors). Based on a comprehensive literature review, they presented seventy-three causes of delays. A questionnaire form was made for data collection, and the results show that "change order" is the most significant cause of construction delays. Furthermore, around 76% and 56% of both of the contractors and the consultants respectively indicated that the percentage of time delays varies from (10 to 30)% of the project's estimated duration. Finally, they concluded that around 70 % of the projects did not progress according to the planned schedule correctly for that they found that from the 76 selected projects in this study, 45 projects were considered as a delayed project.

## 2.1. THE BENEFITS OF BIM TECHNIQUE

It must be mentioned that there are many dedicated researchers who studied the benefits of the application the building information modeling in the AEC industry. One of these scholars is Azhar (2011). He determined eight different types of benefits: more effective and faster processes,

improved designs, controlled overall expenses and data, improve the quality, better service for customers, accurate geometrical representation, and lifecycle data. He also presents four case studies to show the benefits of BIM technology by illustrating the cost and time savings, project planning, designing, pre-construction, and construction stages. By calculating the return on investment (ROI), the results show that the average ROI of BIM for the selected projects found to be around 634%, which illustrates the potential benefits of implementing BIM in terms of economy. On the other hand, Eastman et al. (2011) also discuss the benefits of applying BIM technique in the AEC industry at all of the stages of the main four construction phases, which are: the pre-construction phase, the design phase, construction, and building phase, and the post-construction phase. Moreover, some of these benefits were determined and discussed as expected benefits of BIM technique gained through the development of this technology in the future.

Jernigan (2007), in his practical approach to BIM technique, he illustrates that in the several case studies of construction projects he investigated, show that there were around 8 to 15% cost savings on the new projects and up to 35% cost savings on reiterated projects that apply the technique of BIM. These recognized savings are the result of the proper use of information, improved decision making, and better assessments in the early phase of the project.

Hamada et al. (2016) investigated twenty potential BIM benefits as motivation factors to adopt BIM technique along with twelve factors that stand as barriers against implementing BIM in Iraq. They stated that the major benefit of BIM is minimizing the cost of the project. On the other hand, Hasan and Rasheed (2019) investigated the benefits of implementing 5D BIM in the construction industry. They determined that the significant benefits of adopting 5D BIM are that it increases the collaboration among the working teams, better estimation of cost and time, visual tracking and monitoring, Reduce change orders, and better quantity estimation.

According to global statistics in Britain, America, Finland, and Denmark, the most important business benefits for owners who are using BIM technology in construction projects

are: reduce rework by 36%, reduce errors in documenting, reduce omissions and oversight by 61%, reducing the cost of construction by 30%, reduce the duration of the project delivery by 22%, and reduce litigations and disputes by 17% (AUTODESK, 2014). Despite all other benefits,

cost and time are related to all of them in a way or another. The previous researches illustrated that the application of the BIM technique endures the following benefits in terms of cost and time saving, see Table 1.

**Table (1):** Benefits of BIM According to Previous Studies

Organization or Researcher	Benefits
(Yan and Demian, 2008)	<ul style="list-style-type: none"> <li>• reduce the cost and time by 25% of the UK's projects</li> <li>• USA projects reduce cost by 16% &amp; time by 26% of USA projects</li> </ul>
(Gilligan and Kunz, 2007)	<ul style="list-style-type: none"> <li>• reducing costs and improving the accuracy and speed of cost estimates</li> <li>• reduction in projects' time by around 7%</li> </ul>
(Azhar et al., 2008)	<ul style="list-style-type: none"> <li>• Cost estimation accuracy within 3%.</li> <li>• Reduction in time up to 7%</li> </ul>
(CIFE, 2007, Innovation, 2007, Azhar, 2011)	<ul style="list-style-type: none"> <li>• A savings of up to 10% of the contract value through clash detections.</li> <li>• Up to 80% reduction in time taken to generate a cost estimate.</li> <li>• Up to 40% elimination of unbudgeted change.</li> <li>• Up to 10% reduction in project time.</li> </ul>
(Azhar, 2011)	<ul style="list-style-type: none"> <li>• Elimination of 40% of unbudgeted change</li> <li>• Accuracy cost estimation with 3% as compared to the traditional way</li> <li>• Reducing the time taken in cost estimation by 80%</li> <li>• Saving 10% of the contract value due to clash detection</li> <li>• reducing the project time by 7%</li> </ul>
(Gerges et al., 2017)	<ul style="list-style-type: none"> <li>• Increase the collaboration and coordination between stakeholders</li> <li>• The calculation of accurate estimates</li> <li>• Managing the sequence of the activities through the 4D model</li> </ul>
(Ali, 2015, Osman, 2016)	<ul style="list-style-type: none"> <li>• Increase design efficiency</li> <li>• Improve the construction process</li> <li>• Reduction and saving the cost of the project</li> <li>• Saving in cost and time due to clash detection</li> </ul>
(Bryde et al., 2013)	<ul style="list-style-type: none"> <li>• Control and reduce the cost &amp; the time of the project</li> <li>• Risk reduction</li> <li>• Improve communication and coordination</li> <li>• Increase the quality of the project</li> <li>• Increase clients satisfactory</li> <li>• Improve the owner's experience and satisfaction</li> <li>• Increase the profit margin</li> </ul>

### 3. METHODOLOGY

A questionnaire form is used as the main source of data in order to fulfill this paper's objective. This survey form was organized and created based on the academic study of the topic, including a comprehensive literature review of published scientific researches and articles related to the subject of this study as well as one-to-one interviews with experts involved and some

academic personnel engrossed in the process of the AEC industry in Iraq.

As for the design of this survey, it was written with a clear English language supported by a good Arabic translation. It provided with a well-written cover letter that explains the objectives of the survey study, how to respond to the questions, and clarifies the security information security in order to encourage the respondents.

All of the needed information that supports to achieve the objectives of this paper were collected, assessed, and formalized to be appropriate for the survey and easy to understand by the respondents. Furthermore, after several phases of brainstorming, accessing, revising, and evaluating performed by the author, the questionnaire form was formed with two sections.

The first section of the questionnaire form is associated with the respondent's profile. This part is used to determine the experience, knowledge of respondents, etc. While the second part of this survey investigates the factors that influencing the project performance, and that might cause time & cost to overrun in AEC projects. It covers thirty factors categorized into different seven groups. The answers would be telling the importance of each factor based on three-point scale as recommended by experts. These three points are (3 = high), (2 = moderate) and (1 = low).

Regarding the questionnaire distributed, it has been distributed to 50 members of the top and middle management in different construction companies, site engineers, consultants, and other experts in the field of the AEC industry. The researchers were dedicated to make a one on one interview with respondents discussing and explaining each factor in the questionnaire to gain the most accurate response. The valid received and analyzed questionnaires were only 42.

In terms of data analysis, the statistical package for the Social Science (SPSS 25) software is used, and Microsoft Excel for the data manipulating and analysis. The relativity importance index (RII) will be adopted to rank (R) each factor in the questionnaire. The relative importance index will be calculated for the data collected based on the formula used by Saleh (2015) below:

$$RII = \frac{\sum W}{A * N} \dots \dots \dots (1)$$

Where  $W$  represents the weight assumed by the respondents for each question, ranging from one to three; while  $A$  stand for the maximum weight which is three in this case; and  $N$  correspond to the number of the respondents.

#### 4. RESULTS AND DISCUSSION

In order to assist the reader to have a clear understanding of the data, it has been discussed and presented within three sections where the first section deals with the profile of the respondents while the second section is dedicated to discussing the statistical reliability of the questionnaire survey. Finally, the third part is devoted to review the core of the research where it shows the responses of the participants on the questionnaire, the calculations as well as the comparison of the results with previous researches.

##### 4.1. RESPONDENTS' PROFILE

The characteristics of respondents are presented in Table 2 gives the percentage of each category, while Figure 1 shows the percentage of respondents who know BIM and who don't.

Table 2 describes the participants in this study. The obtained results show that 59.5% of respondents working in the public sector, 16.7% work in the private sector while the rest of them work in both industries. Males represent 81% of the respondents, 44.7% of the participants were aged (31 – 40) years old, 78.6% have a bachelor's degree, 69% were civil engineers while the around 21.4% were Architects, 26.2% were consultants, and 52.4% have a (6 – 15) years of experience. The survey showed that about 10% of participants use BIM technology; in other words, only a few parts of the BIM technique like cost estimation and clash detection. Only 6% used REVIT architecture, 3.6% used REVIT structural, and 7% used ARCHICAD, which are software for BIM.

**Table (2):** Respondent Profile

Information	Categories	Percentage (%)	Information	Categories	Percentage (%)	
Sector	Public	59.5	Group (Job)	Designer	19.0	
	Private	16.7		Consultant	26.2	
	both sectors	23.8		Project manager	7.1	
Gender	Male	71.4		Site engineer	42.9	
	Female	28.6		Other	4.8	
Age (years)	21 – 30	9.5		Use of BIM	yes	9.5
	31 – 40	47.6			no	90.5
	41 – 50	19.0	Use of CAD	Don't use the CAD	9.5	
	More than 51	23.8		Use only 2D CAD	69.0	
				Use only 3D CAD	2.4	
Academic qualification	Diploma	2.4	Use both 2D & 3D	19.0		
	Bachelor	78.6	Software	Autodesk AutoCAD	44.0	
	Master	4.8		SKETCH UP	10.7	
	Ph.D.	11.9		MS EXCEL	23.8	
	Other	2.4		MS PROJECT	3.6	
				PRIMAVERA	1.2	
Specialization	Architect	21.4	REVIT structural	3.6		
	Civil	69.0	REVIT architecture	6.0		
	Electrical	2.4				
	Mechanical	7.1	ARCHICAD	0		
Practical experience	≤ 5	7.1	3D MAX	7.1		
	6 – 15	52.4				
	16 – 25	23.8				
	More than 26	16.7				

By asking the respondent, “have you ever heard of the applications and solutions of BIM?” the results showed that only 29% of them know

about BIM, see Figure 1. How respondents got their knowledge about BIM and their Suggestions to promote BIM in Erbil are shown in Table 3.

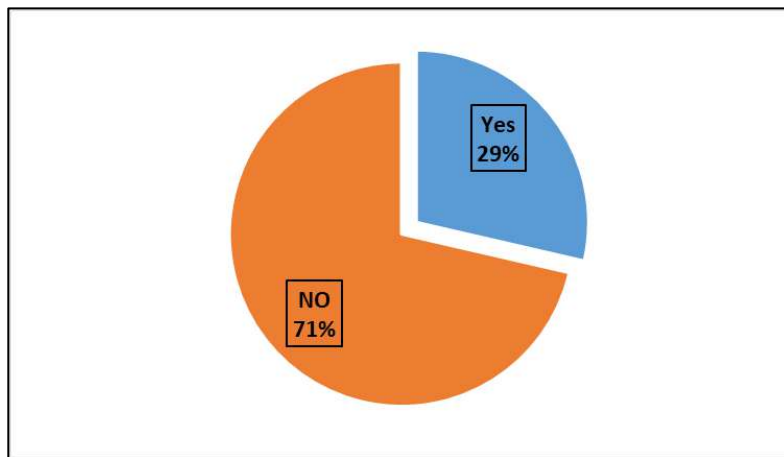


**Figure (1):** Do Respondents Have Knowledge About BIM?

**Table (3):** Respondents’ source of knowledge about BIM and suggestions to promote BIM

<b>How Respondents’ get their information about BIM</b>	Read researches related to BIM	50.00%
	participated in conferences or meetings related to BIM	16.70%
	part dealt with in my university	11.10%
	I am training on the use of the BIM programs individually	16.70%
	Other	5.60%
<b>Respondents’ Suggestions to promote BIM</b>	Promote local awareness of BIM benefits through workshops and courses.	35.60%
	Improving the role of the local Engineers Union.	28.80%
	To be included in the curriculum	33.90%
	Other	1.70%

### 4.2. STATISTICAL RELIABILITY

One of the basic requirements in any research paper is maintaining accurate measurements and acceptable results. So, a 25 sized pilot survey was performed to check the questionnaire’s validity and reliability before starting the main survey study. The researcher performed an internal consistency with the aim of testing the statistical validity. The questionnaire’s internal consistency giving the values of the Spearman’s Rho correlation and the p-values as shown in table 6. The correlation coefficients for Part (II) of the survey varied from 0.311 to 0.750 and the p-value for all of the questions were below 0.05, which means that all of the questions are valid to start the survey. For measuring internal consistency, the researcher used Cronbach’s alpha as it is an effective important common method for testing reliability (Yockey, 2017). Table 4 shows the classifications of reliability, according to Cronbach’s alpha value. By conducting this method to test the questionnaire reliability, the result showed that the Cronbach’s alpha is on the Excellent scale, as shown in Table 5 and Table 6 below, which confirm the questionnaires’ reliability.

**Table (4):** Cronbach's alpha Reliability Classifications (Yockey, 2017)

Cronbach's alpha	Degree of reliability
$\alpha \geq 0.9$	Excellent
$0.9 > \alpha \geq 0.8$	Good
$0.8 > \alpha \geq 0.7$	Acceptable
$0.7 > \alpha \geq 0.6$	Questionable (Moderate)
$0.6 > \alpha \geq 0.5$	Poor
$0.5 > \alpha$	Unacceptable

**Table (5):** Case Processing Summary of Cronbach's alpha Reliability Test

Case Processing Summary		N	%
Cases	Valid	42	100.0
	Excluded <sup>a</sup>	0	.0
	Total	42	100.0

a. Listwise deletion based on all variables in the procedure.

**Table 6:** Cronbach's alpha Reliability

Reliability Statistics	
Cronbach's Alpha	N of Items
.912	30

**Table (7):** Questionnaire's Internal Consistency

Factor	Correlation Coefficient	Sig. (2-tailed)	Factor	Correlation Coefficient	Sig. (2-tailed)
Q1	.547**	0.00	Q16	.494**	0.00
Q2	.492**	0.00	Q17	.443**	0.00
Q3	.520**	0.00	Q18	.560**	0.00
Q4	.517**	0.00	Q19	.462**	0.00
Q5	.548**	0.00	Q20	.494**	0.00
Q6	.618**	0.00	Q21	.333*	0.04
Q7	.412**	0.01	Q22	.348*	0.03
Q8	.426**	0.00	Q23	.494**	0.00
Q9	.750**	0.00	Q24	.590**	0.00
Q10	.700**	0.00	Q25	.382*	0.03
Q11	.664**	0.00	Q26	.697**	0.00
Q12	.679**	0.00	Q27	.482**	0.00
Q13	.468**	0.00	Q28	.515**	0.00
Q14	.509**	0.00	Q29	.595**	0.00
Q15	.311*	0.04	Q30	.567**	0.00

\*\*Correlation is significant at the 0.01 level (2-tailed).

\*Correlation is significant at the 0.05 level (2-tailed).

### 4.3. FACTORS THAT CAUSE DELAY AND COST TO OVERRUN IN THE AEC PROJECTS

The mean and the standard deviation values for all of the 29 factors are shown in Table 8, as well as their rankings, which is based on the values of the relative importance index (RII) along with the RII values for each group of factors. The top five factors in this survey are Q2, Q19, Q26, Q7, and Q18, with RII of 0.98, 0.87, 0.85, 0.83, and 0.82, respectively. These factors are inadequate planning and scheduling; selection of inefficient contractors in administrative and financial terms; selection of contractors with limited technical competence; frequent changes in design (change orders); the selection of a project team that is inefficient in administrative and financial terms, and errors and mistakes in the preparation of bill of quantities and materials (BOQ/BOM) are the most influential factors on the cost and time-related problems in the

construction projects. This is related to the bad practices, lack of experience and the poor technique used in the construction industry, as well as the corruption in most governmental departments, which strongly stand against the development of the AEC industry in Iraq. This corruption caused several projects to be delayed, implemented with poor quality and high costs, which dramatically reduce the value as well as the economic feasibility of the project.

In terms of the values of the mean and standard deviation, the mean values were ranged from 1.81 to 2.93; the highest value of mean is for Q2, obviously as it ranked first. The values of standard deviation were all below one, which indicates a good relationship between the collected data.

Similar findings were obtained by Frimpong et al. (2003), Assaf and Al-Hejji (2006), Le-Hoai et al. (2008), Alinaitwe et al. (2013), and Btoush and Harun (2017).

**Table (8):** Factors Affecting cost and Time overrun in Construction Projects

Group	RII	No.	Items	Mean	SD	RII	Rank
Contractor's site management factors	0.79	Q1	Poor site management and supervision	2.38	0.764	0.79	9
		Q2	Inadequate planning and scheduling	2.93	0.707	0.98	1
		Q3	Inaccurate time and cost estimation	2.33	0.721	0.78	11
		Q4	Delay in providing instructions/responding to contractor's requests for information	2.07	0.712	0.69	22
		Q5	Lack of follow up by the contractor's home	2.17	0.794	0.72	17



			office				
<i>Design related factors</i>	0.78	Q6	Mistakes and errors in design	2.26	0.734	0.75	14
		Q7	Frequent changes in design (change orders)	2.5	0.595	0.83	4
		Q8	Bad preparing of shop drawings	2.29	0.636	0.76	13
<i>Information and communication related factors</i>	0.69	Q9	Lack of coordination between parties	2.12	0.803	0.71	19
		Q10	Slow information flow between parties	1.98	0.78	0.66	27
		Q11	weak communications and misunderstanding between parties	2.07	0.808	0.69	23
		Q12	Low harmony between the contractor team and the owner team which may lead to a controversy between both of them	2.12	0.772	0.71	20
<i>Project management related factors</i>	0.69	Q13	Poor project management	2.24	0.692	0.75	15
		Q14	Delays in decision making	1.95	0.764	0.65	28
		Q15	Major disputes and negotiations	2.05	0.697	0.68	24
		Q16	The absence of continuous tracking for the project time schedule	2	0.796	0.67	26
		Q17	Weak Definition of the roles and responsibilities that fit the organization's structure according to the project and its characteristics	2.14	0.647	0.71	18
<i>Administration related factors</i>	0.84	Q18	The selection of a project team that is inefficient in administrative and financial terms	2.45	0.705	0.82	5
		Q19	Selection of inefficient contractors in administrative and financial terms	2.6	0.701	0.87	2
<i>Legislative problems and errors</i>	0.70	Q20	The contracts are not well drafted, due to the lack of experience in contracting.	2.12	0.861	0.71	21
		Q21	The duration of the project must be in the years and months, not the number of days that are explained by working days	1.81	0.862	0.60	30
		Q22	There is no legislation on the use of modern technologies in building projects, according to international standards	2.33	0.65	0.78	12
<i>Technical related factors</i>	0.78	Q23	Method of transferring project data and information such as (soil examination report, site maps, and survey works)	2.05	0.764	0.68	25
		Q24	Preparation of architectural, structural, mechanical and electrical designs without a general coordinator for the design team, causing frequent conflicts.	2.43	0.668	0.81	8
		Q25	The difficulty of conducting electronic checks of designs because they are placed in hundreds of files for each department.	2.24	0.726	0.75	16
		Q26	Selection of contractors with limited technical competence	2.55	0.739	0.85	3
		Q27	Errors and mistakes in the preparation of bill of quantities and materials (BOQ/BOM)	2.45	0.633	0.82	6
		Q28	Change orders and their consequences	2.38	0.623	0.79	10
		Q29	Wrong implementation methods due to the lack of design and working schemes	2.45	0.633	0.82	7

		Q20	Frequent conflicts with other projects implemented in advance due to not having the documents of these projects for not giving documents the proper attention.	1.9	0.79	0.63	29
--	--	-----	--	-----	------	------	----

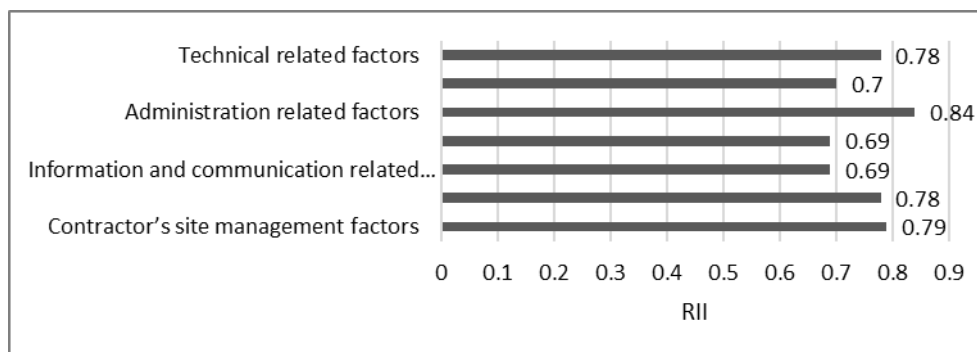


Figure (2): Relative Importance Index (RII) for Factor Groups

Figure 2 shows the values of RII for each group factor, which ranged from 0.69 to 0.84. These values are based on the results shown in Table 8 as they represent the average of factors of each group. The group of administration-related factors is in the first position among all groups with an RII of 0.84. The second position is for contractor's site management related factors is with RII of 0.79 then closely followed by the technical-related group and design-related group with RII of 0.78 each. The group factors of the information and communication and the group of project management come at the last position with RII of 0.69 each.

Similar findings were obtained by Assaf and Al-Hejji (2006), While Le-Hoai et al. (2008), and Alinaitwe et al. (2013) regarding the contractor related factors for coming in the first position. While Btoush and Harun (2017) revealed that technical related issues along with the information and communication-related influences are the essential factors in terms of time delays in the AEC projects.

## 5. CONCLUSION AND RECOMMENDATIONS

This paper investigates the cost and time-related problems in the AEC industry of Iraq as well as reviewing the benefits of BIM technology in solving these issues through a deep literature review. The results of the survey prepared for the purpose of the study were analyzed, and it concluded that inadequate planning and

scheduling, choosing an inefficient contractor, change orders, the mistakes and errors occurring during the preparation of the bill of quantities and the bill of materials (BOQ/BOM) are the most influential factors on the cost and time overrun. It is concluded that poor experience, as well as poor practices and techniques used in the AEC industry, along with the corruption in most governmental departments, plays a vital role in the rising of these issues. It's been concluded that the Administration, contractors, design, and technical related factors are the most influential factor groups with RII of 0.84, 0.79, and 0.78, respectively. This indicates the low technology and the poor management practices used in the AEC industry in Iraq.

The best solution to overcome time and cost issues in the AEC industry is building information modeling technique. It is essential to improve the AEC industry by putting more effort into taking BIM into implementation. The application of BIM technology will contribute to reduce the expenses and the time required to deliver the projects and therefore, it has a significant impact on the economy and resources (i.e., the application of BIM technology is significant and it will cooperate in developing the sustainability of Iraqi AEC industry).

Based on those previously identified conclusions, the results obtained from this research, and the comments of respondents

through interviews and the questionnaire survey, the following points can be recommended:

- Developing systems and laws to meet the highest international standards in order to develop the level of services and optimal use of modern technology.
- Instructing all governmental departments in the country that have construction projects to use this technology and obligate them to make designs according to BIM technology for its benefits in solving all of projects problems.
- Imposing rules on implementing BIM in large projects.
- Giving more attention to the sustainability of the construction projects.
- The use of (employ) experts and consultants to assist ministries and government departments in preparing the appropriate plan for the implementation of BIM technology.
- Participation and Organizing events, conferences, and exhibitions that promote this technology locally and improving the role of the local Engineers Union.
- Including this technology in the curriculum of engineering colleges.
- Conducting visits and working meetings with the organizations working with BIM technology in USA, UK, UAE, and Qatar as they are among the leading countries in this field.

### Acknowledgements

the Author acknowledges with many thanks and gratitude to *Prof. Dr. Maad Mahdi Shalal* and *Al-Qatif Engineering Bureau* and its director consultant Engineer *Mr. Ali Salman*, for their guidance, advice, and cooperation which have made the accomplishment of this paper possible.

### References

ABDUL RAHMAN, I., MEMON, A. H., KARIM, A. & TARMIZI, A. 2013. Significant factors causing

- cost overruns in large construction projects in Malaysia. *Journal of Applied Science*, 13, 286-293.
- ABDULLAH, M., AZIS, A. A. & RAHMAN, I. A. 2009. Potential effects on large mara construction projects due to construction delay. *International Journal of Integrated Engineering*, 1.
- AGC, A. 2005. The contractors guide to BIM. URL: <http://iweb.agc.org/iweb/Purchase/ProductDetail.aspx>.
- ALI, H. B. M. 2015. Benefits of building Information Modeling for Construction in Sudan. Sudan University of Science and Technology.
- ALINAITWE, H., APOLOT, R. & TINDIWENSI, D. 2013. Investigation into the causes of delays and cost overruns in Uganda's public sector construction projects. *Journal of Construction in Developing Countries*, 18, 33.
- ARAYICI, Y., KHOSROWSHAHI, F., PONTING, A. M. & MIHINDU, S. Towards implementation of building information modelling in the construction industry. *Proceedings of The Fifth International Conference on Construction in the 21st Century (CITC-V) "Collaboration and Integration in Engineering, Management and Technology"*, May 20-22, 2009, Istanbul, Turkey., 2009. 1342-1351.
- ASSAF, S. A. & AL-HEJJI, S. 2006. Causes of delay in large construction projects. *International journal of project management*, 24, 349-357.
- AUTODESK. 2014. The Value of BIM for Owners: Save Time and Money During the Building Lifecycle [Online]. Available: [http://damassets.autodesk.net/content/dam/autodesk/www/solutions/bim/BIM\\_for\\_Owners.pdf](http://damassets.autodesk.net/content/dam/autodesk/www/solutions/bim/BIM_for_Owners.pdf). [Accessed 23-Dec 2018].
- AZHAR, S. 2011. Building information modeling (BIM): Trends, benefits, risks, and challenges for the AEC industry. *Leadership and management in engineering*, 11, 241-252.
- AZHAR, S., NADEEM, A., MOK, J. Y. & LEUNG, B. H. Building Information Modeling (BIM): A new paradigm for visual interactive modeling and simulation for construction projects. *Proc., First International Conference on Construction in Developing Countries (ICCIDC-I)*, Karachi, Pakistan; 08/2008, 2008. 435-446.
- BRYDE, D., BROQUETAS, M. & VOLM, J. M. 2013. The project benefits of building information modelling (BIM). *International journal of project management*, 31, 971-980.
- CANTARELLI, C. C. Cost overruns in Dutch transportation infrastructure projects. Delft University of Technology. Conference Presentation, 2009. Citeseer, 19-20.
- CIFE. 2007. CIFE Technical Reports [Online]. Available: <https://cife.stanford.edu/Publications/index.html> [Accessed 23-Dec 2018].
- DOLOI, H. 2012. Cost overruns and failure in project management: Understanding the roles of key stakeholders in construction projects. *Journal of construction engineering and management*, 139, 267-279.
- EASTMAN, C., TEICHOLZ, P., SACKS, R. & LISTON, K. 2011. BIM handbook: A guide to building information modeling for owners, managers,

- designers, engineers and contractors, John Wiley & Sons.
- ENSHASSI, A., AL-NAJJAR, J. & KUMARASWAMY, M. 2009. Delays and cost overruns in the construction projects in the Gaza Strip. *Journal of Financial Management of Property and Construction*, 14, 126-151.
- FLYVBJERG, B., SKAMRIS HOLM, M. K. & BUHL, S. L. 2003. How common and how large are cost overruns in transport infrastructure projects? *Transport reviews*, 23, 71-88.
- FRIMPONG, Y., OLUWOYE, J. & CRAWFORD, L. 2003. Causes of delay and cost overruns in construction of groundwater projects in a developing countries; Ghana as a case study. *International Journal of project management*, 21, 321-326.
- GERGES, M., AUSTIN, S., MAYOUF, M., AHIKWO, O., JAEGER, M., SAAD, A. & GOHARY, T.-E. 2017. An investigation into the implementation of Building Information Modeling in the Middle East. *Journal of Information Technology in Construction (ITcon)*, 22, 1-15.
- GILLIGAN, B. & KUNZ, J. 2007. VDC use in 2007: significant value, dramatic growth, and apparent business opportunity. TR171, 36.
- HAMADA, H., HARON, A., ZAKIRIA, Z. & HUMADA, A. 2016. Benefits and Barriers of BIM Adoption in the Iraqi Construction Firms. *International Journal of Innovative Research in Advanced Engineering*, 3, 76-84.
- HARDIN, B. & MCCOOL, D. 2015. BIM and construction management: proven tools, methods, and workflows, John Wiley & Sons.
- HASAN, A. N. & RASHEED, S. M. 2019. The Benefits of and Challenges to Implement 5D BIM in Construction Industry. *Civil Engineering Journal*, 5, 412-421.
- INNOVATION, C. C. 2007. Adopting BIM for facilities management: Solutions for managing the Sydney Opera House. Cooperative Research Center for Construction Innovation, Brisbane, Australia.
- JERNIGAN, F. 2007. BIG BIM little bim: The practical approach to building information modeling, edn. 4 Site Press, Salisbury, Maryland, United States.
- LE-HOAI, L., DAI LEE, Y. & LEE, J. Y. 2008. Delay and cost overruns in Vietnam large construction projects: A comparison with other selected countries. *KSCE journal of civil engineering*, 12, 367-377.
- MAHDI, M. M. & ALI, N. S. 2019. Reducing Waste of Construction Materials in Civil Engineering Projects In Iraq. *J ZANCO Journal of Pure Applied Sciences*, 31, 257-263.
- OLAWALE, Y. A. & SUN, M. 2010. Cost and time control of construction projects: inhibiting factors and mitigating measures in practice. *Construction management and economics*, 28, 509-526.
- OSMAN, M. K. 2016. Implementation and potential benefits of building information modeling (BIM) in Sudan construction industry. *Sudan University of Science and Technology*.
- RAZAK BIN IBRAHIM, A., ROY, M. H., AHMED, Z. & IMTIAZ, G. 2010. An investigation of the status of the Malaysian construction industry. *Benchmarking: An International Journal*, 17, 294-308.
- SALEH, M. A. D. 2015. Barriers and Driving Factors for Implementing Building Information Modelling (BIM) in Libya. Eastern Mediterranean University (EMU)-Doğu Akdeniz Üniversitesi (DAÜ).
- SAMBASIVAN, M. & SOON, Y. W. 2007. Causes and effects of delays in Malaysian construction industry. *International Journal of project management*, 25, 517-526.
- WALI, K. I. & OTHMAN, S. A. 2019. Schedule Risk Analysis Using Monte Carlo Simulation for Residential Projects. *J ZANCO Journal of Pure Applied Sciences*, 31, 90-103.
- YAN, H. & DEMIAN, P. 2008. Benefits and barriers of building information modelling.
- YOCKEY, R. D., (2017). *SPSS Demystified: A Simple Guide and Reference*, 2nd ed. 2017, United Kingdom: Taylor & Francis, (2017). [https://books.google.iq/books?id=m6Q5DwAAQB\\_AJ](https://books.google.iq/books?id=m6Q5DwAAQB_AJ)

## RESEARCH PAPER

# Performance Analysis of WRIM Drive System Operating under Distorted and Unbalanced Supply: A Survey

Hilmi Fadhil Ameen , Fadhil Toufick Aula

Department of Electrical Engineering, College of Engineering, Salahaddin University-Erbil, Kurdistan Region, Iraq

### ABSTRACT:

The development of technology in power semiconductor devices leads to the increasing use of a static switching device in wound rotor induction motor (WRIM) controller systems. Supply voltage and current always contain harmonics and in the same circumstances unbalanced supply voltages. The low power quality has detrimental effects on the motor characteristics in the form of derating the output power and increasing torque pulsation. The static rotor resistance chopper controller (SRRCC) and slip power recovery drive (SPRD) are used in many applications. This survey presents a comprehensive review of many studies of SRRCC and SPRD operating with distorted and unbalanced supply, and their effects on the wound rotor induction motor performance. Starting from various techniques of control methodologies of SRRCC, SPRD, harmonic analysis, unbalanced supply and distorted unbalance supply simultaneously. Contributions from various researchers in this field have been presented, reviewed, and assessed.

KEY WORDS: Wound Rotor Induction Motor (WRIM), Slip power Recovery Drive (SPRD), Static Rotor Resistance Chopper Control (SRRCC), Harmonic Analysis, Distorted Supply, Unbalance Supply, Performance Analysis of WRIM

DOI: <http://dx.doi.org/10.21271/ZJPAS.32.6.20>

ZJPAS (2020) , 32(6);197-216 .

## 1. INTRODUCTION

Studies have shown that two-thirds of the global electricity is consumed by the electrical motors, about 8% is consumed by DC motors, the remaining 92% is consumed by the AC motors, and the majority of them that are used in industries are induction motors. In the past, induction motors were considered as a constant speed motor, but with the advanced development in power semiconductor technologies the variable speed induction motor drives have been developed.

These technologies made WRIM having a wide applications such as in mills, conveyors, cooling pumps, steel drives, paper drives, cranes, elevators, cement factories, ventilation pumps [(Von Jouanne and Banerjee 2001)].

The characteristic of speed control by the capability of inserting additional circuits to the rotor terminals makes WRIM superior to other commercial squirrel cages IMs [(Sen and Ma 1975)]. **Figure 1** shows a block diagram of the control scheme of WRIM. The improved starting characteristics are obtained by connecting an external resistance in series with the rotor windings as shown in **Figure 2**. The bridge rectifier can be connected through a DC link to the inverter and feedbacks slip power to the main as shown in **Figure 3**. The speed-torque curve of WRIM can be controlled by rotor resistance

---

### \* Corresponding Author:

Hilmi Fadhil Ameen

E-mail: [Hilmi.Ameen@su.edu.krd](mailto:Hilmi.Ameen@su.edu.krd)

### Article History:

Received: 04/08/2020

Accepted: 07/09/2020

Published:2 0/12 /2020

through the chopper circuit or by changing the firing angle of the inverter.

AC slip power of the rotor is converted to DC power through a bridge rectifier and consumed by the chopper resistance as depicted in **figure 2**, or this power can be recovered and return to the main through using inverter and transformer this is known as (SPRD). However, as slip power is taken from the rotor to the AC main in a unidirectional, the control of the speed will be in a sub-synchronous speed range. If a diode bridge rectifier is replaced by a controlled bridge, the slip power flow can be controlled in two directions (Scherbius Scheme), **figure 3**, and the speed can be controlled in both regions, sub-synchronous and super-synchronous speed.

Despite the increasing demand for using WRIM in the industries but the appearance of the disturbance, such as unbalance and voltage harmonic distortion, in the main causes the derating of its performance.

In general, most of the electrical devices are designed to operate under symmetrical and sinusoidal supply voltage conditions. However, voltages and currents in the electrical power system are infrequently sinusoidal and balanced. Induction motors like all other devices, they are designed to work under sinusoidal and balanced supply voltages. Any change in main or unbalanced supply voltage lead to deteriorated the characteristics of the induction machines (IM) [(El-Kharashi and Massoud 2017)].

There are many studies available in the literature review that have analyzed and evaluated these problems and proposed different types of solutions, in which this work is devoted to reviewing them. It has been noted that SPR drive system has replaced the conventional rotor resistance control, but the problem in the value of power factor and total harmonic distortion of the supply. Our work summarizes researches on the performance analysis of WRIMD, harmonic effect, unbalance supply effect, and harmonic with unbalance effect on the drive performance. Besides, more than ninety publications are reviewed and organized including WRIM mathematical model, static chopper resistance control, slip power recovery drive system, the effect of harmonic distortion, the effect of voltage unbalance on WRIM, and finally the conclusion and references.

This paper is organized as follows: following the introduction in section one, speed control techniques are presented in section two. Section three and four include the details of static rotor resistance chopper control and slip power recovery drive system. The effects of harmonics, unbalanced, and distorted supply voltage of the operation and performance for WRIM are given in sections five and six respectively. Finally, sections seven and eight are the latest trend and future development and conclude this survey paper.

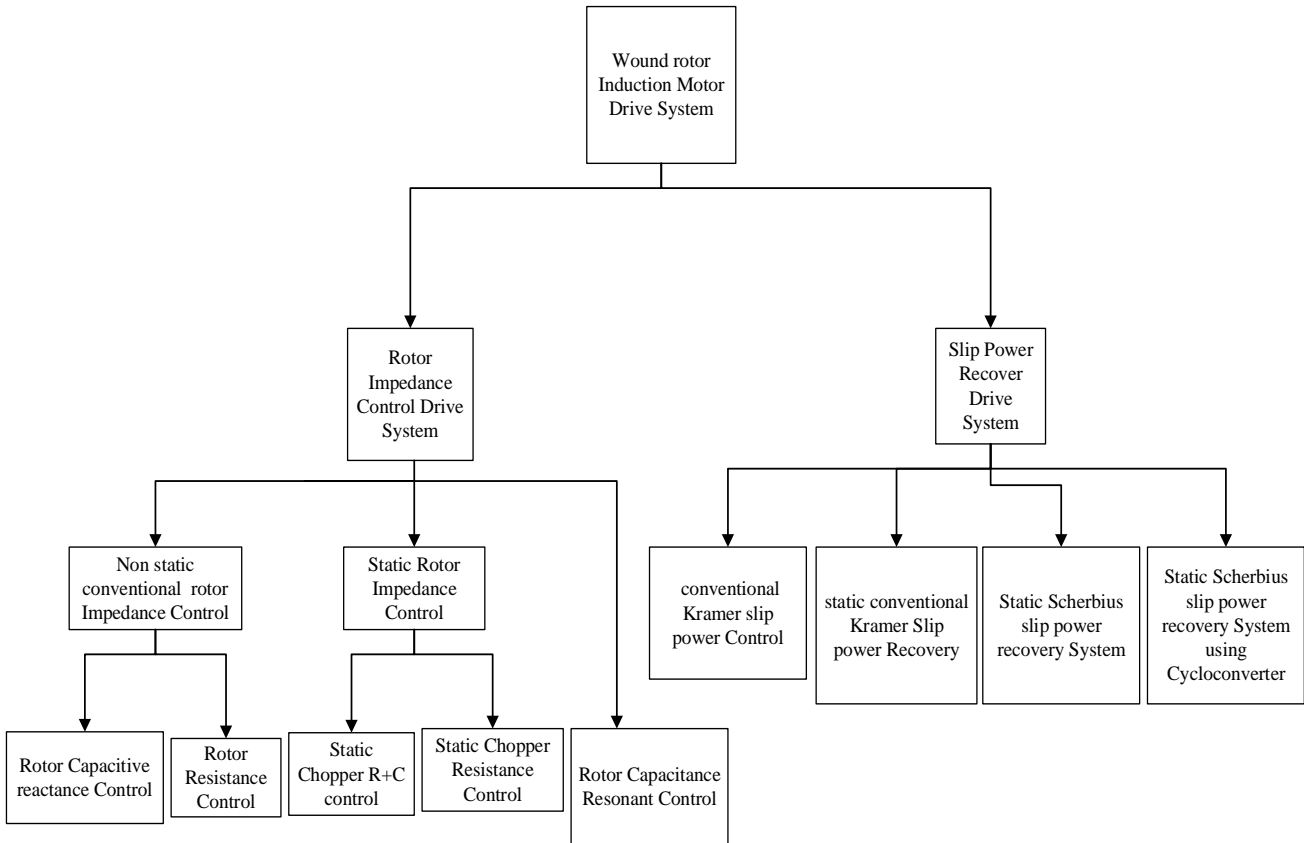


**Figure 1:** Control Scheme of Various WRIM Drive System

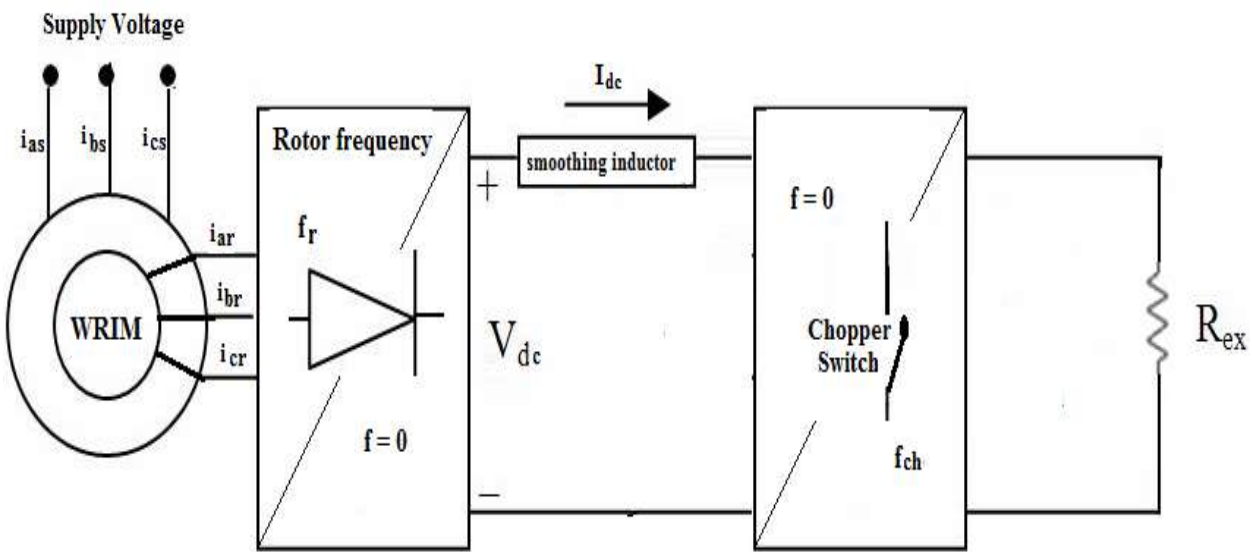


**Figure 2:** Static Rotor Resistance Chopper Control of WRIM [(Ameen 2011)]

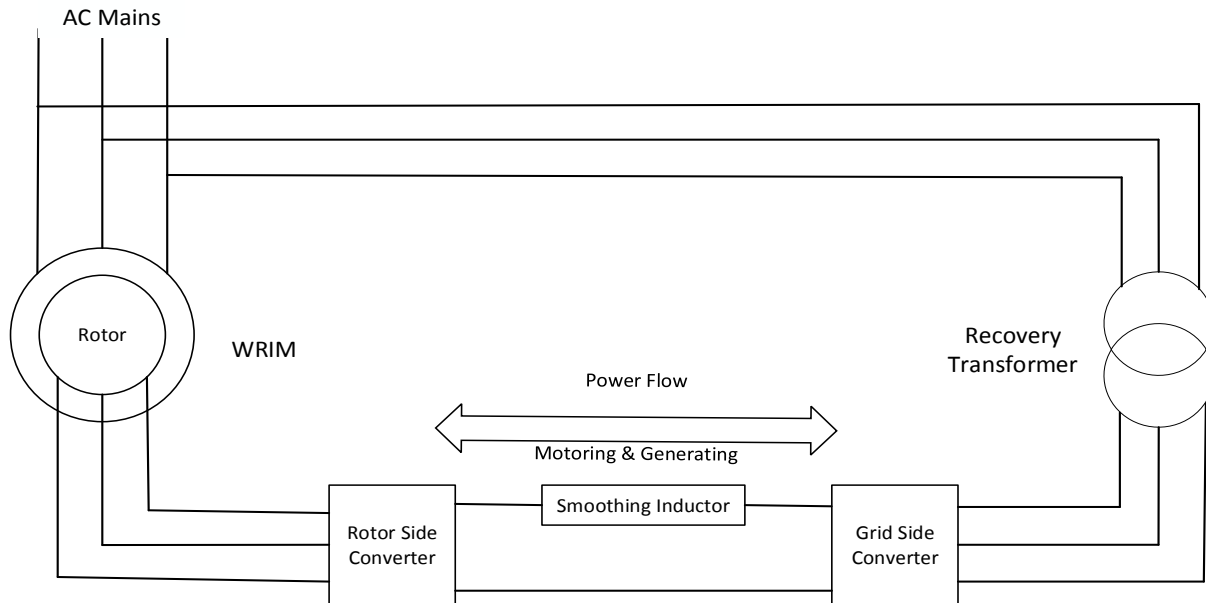


**Figure 3:** Static Scherbius SPR Scheme Block Diagram of WRIM [(Datta and Ranganathan 2013)]

## 2. WRIM Speed Control Techniques

A simple method of speed control of WRIM includes a mechanical variation of rotor circuit resistance as shown in **figure 4**. Based on

$$Te = \frac{3V^2 R' / s}{\omega_s \left[ \left( R_s + \frac{R'}{s} \right)^2 + (X_s + X_r)^2 \right]} \quad (1)$$

Where  $R' = R_{ex} + R'_r$ , and  $V$  is the per phase voltage. The speed of WRIM is controlled by the variations of the external resistances at the rotor terminals. Since  $Te \propto \frac{s}{R_r}$ , therefore, the speed is decreased with increasing rotor resistance. The torque-speed characteristics for varying rotor resistance  $R_r$  of WRIM, as calculated in (1) is shown in **figure 5**. The drawbacks of this technique include the inherent disadvantage of the variations in the resistances and slip power energy is wasted in the rotor resistances. However, reducing the starting inrush current, high power factor, smooth and wide range speed-torque control without producing harmonics are major advantages of this technique.

the approximate equivalent circuit model of three phase induction motor, the electromagnetic torque developed can be written as

## 3- Static Rotor Resistance Chopper Control (SRRCC)

### 3.1-Mathematical Model OF DC CIRCUIT

In basic SRRCC, the rotor slip power is rectified by a full bridge diode rectifier. A filter and an external resistance  $R_{ex}$  are connected with a diode bridge rectifier in different configurations as shown in **figure 6**. Assuming that the rotor rectified current  $I_{dc}$  is a ripple free and rotor phase current is a square pulse of  $(2\pi/3)$  duration, therefore, from both rectifications and chopping process the rms value of rotor phase current  $I_r$  is given by

$$I_r = \sqrt{\frac{2}{3}} I_{dc} \quad (2)$$



The rotor rectified voltage of the rotor is

$$V_{dc} = \frac{3\sqrt{6}}{\pi} \cdot s \cdot \frac{V}{n} \tag{3}$$

From the DC equivalent circuit which is shown in **figure 7**, when either chopper frequency or smoothing inductor or both are high then the average DC current  $I_{dc}$  is given by the following expression[(Sen and Ma 1975)].

$$I_{dc} = \frac{V_{dc}}{R_s + R_{ex}(1-\delta)} \tag{4}$$

where  $\delta$  is duty cycle of chopper circuit (on period/ chopper period), then the electromagnetic torque developed based from the dc model is given by

$$T_e = \frac{1}{s} \left\{ \left[ V_{dc} - \frac{3s(X'_s + X_r)I_{dc}}{\pi} \right] I_{dc} - 2sR'_s I_{dc}^2 \right\} \tag{5}$$

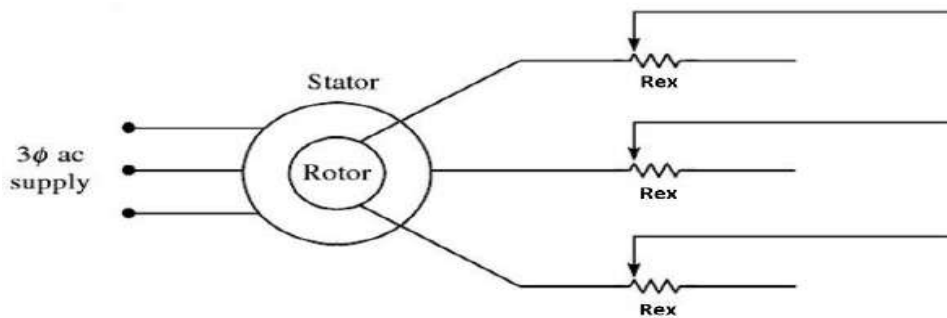


**Figure (4):**Conventional Rotor Resistance Control of WRIM

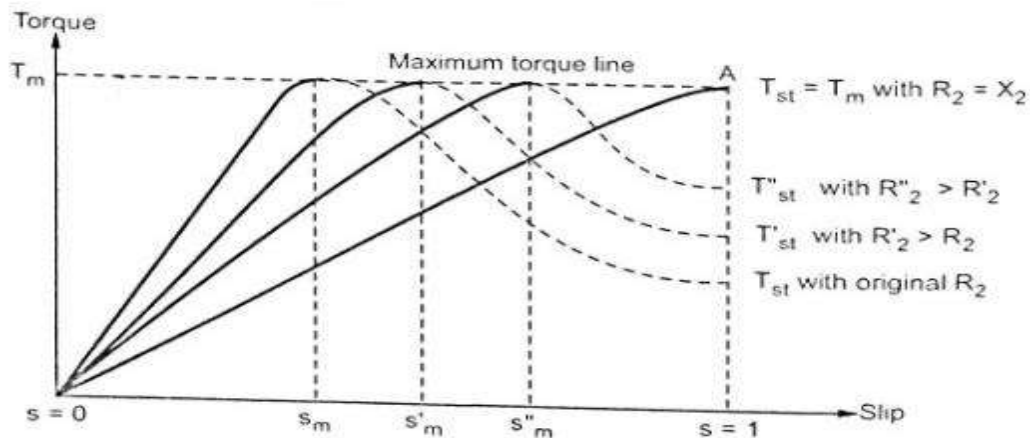


**Figure (5):** The Effect of Rotor Resistance on the Torque-Slip Characteristics of WRIM

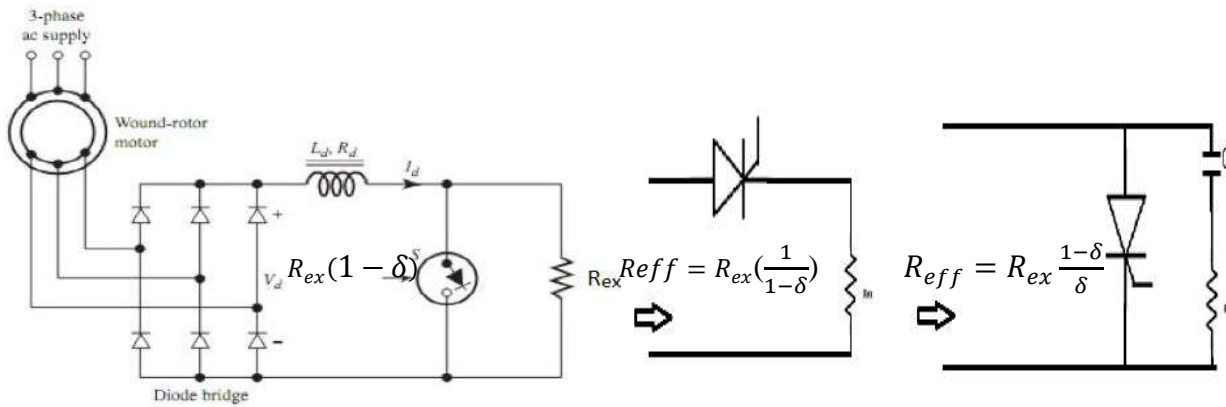


**Figure 6:** Different static chopper resistance control configuration

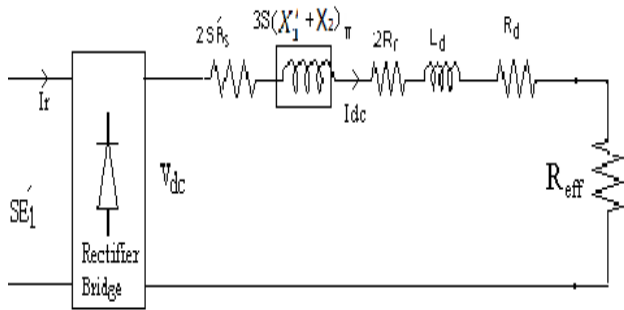


**Figure 7** The dc circuit model of static chopper resistance control of WRIM

### 3.2 Mathematical Model of AC Circuit

By neglecting the commutation overlap of bridge rectifier due to motor leakage reactance, therefore,

$$P_e = \frac{1}{3} I_{dc}^2 (R_d + R_{eff}) \tag{6}$$

This power is equivalent to the dissipated power which is caused by the flow of rotor current  $I_r$  in resistance and is equal to  $0.5(R_d + R_{eff})$  in each of

$$R_{eff}^* = \frac{1}{2} (R_d + R_{eff}) \tag{7}$$

The per phase equivalent circuit is shown in **figure 8**, in which the drive circuit referred to the

$$E'_1 I_{rf} \cos \theta_r = (R_h + \frac{R_f}{s}) I_{rf}^2 \tag{8}$$

And the electromagnetic torque developed based on AC equivalent model is [(Sen and Ma 1975)]

$$T_e \cong 3 I_{rf}^2 (R'_h + \frac{R'_f}{s}) / \omega_s \tag{9}$$

the total rotor resistance across the diode bridge rectifier is  $(R_d + R_{eff})$  and the per phase power consumed,  $P_e$  is,

the rotor phases. Hence the effective per phase value of AC resistance is given by [(Lavi and Polge 1966)].

stator side and the mechanical power developed can be written as

Where  $R_h = \left(\frac{\pi^2}{9} - 1\right) (R_r + R_{eff}^*)$ ,  $R_f = (R_r + R_{eff}^*)$  and  $I_{rf} = \left(\frac{3}{\pi}\right) I_r$

(Sen and Ma 1975)] analyzed the SRRCC scheme using the time ratio technology, and derived the DC and AC equivalent model. while

[(Ramamoorthy and Wani 1978)] have investigated a small signal dynamic model with a thyristorized chopper control closed loop and improving the

speed and current feedback loops. The electromagnetic torque-speed characteristics and Torque against rotor rectified current of SRRC of WRIM with varying the chopper duty cycle for 2hp, 4-pole, 50Hz wound rotor IM are shown in **figure 9 and 10**, respectively.

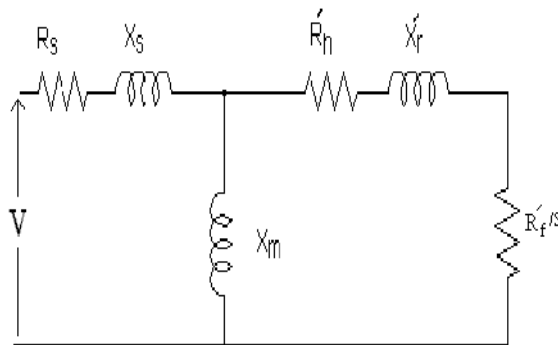


**Figure 8** The AC circuit model of static chopper resistance control

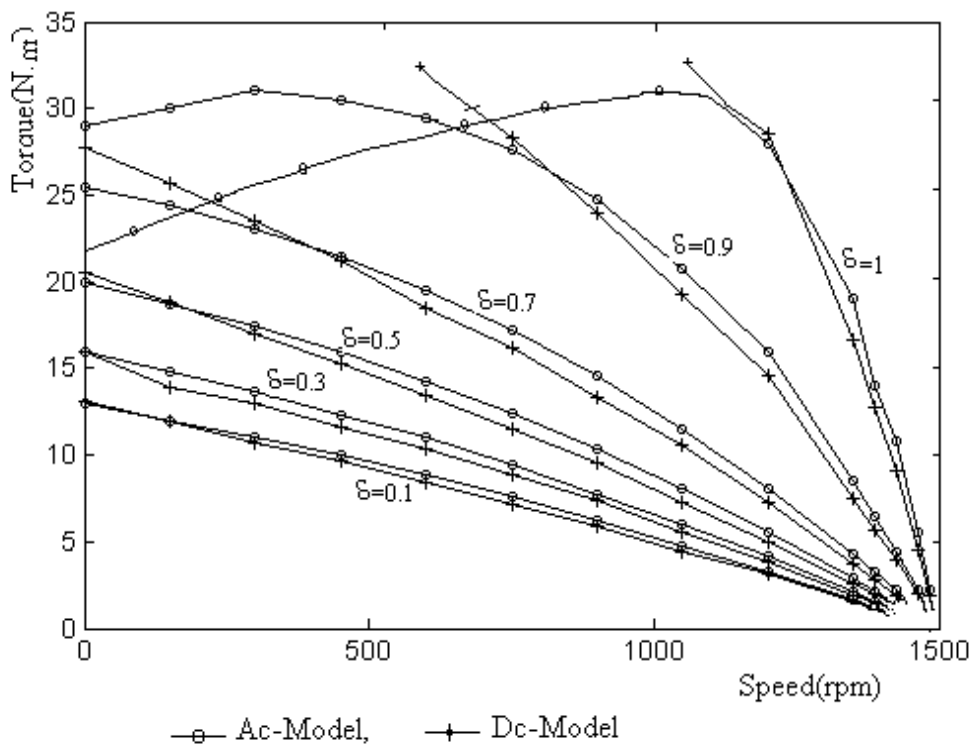


**Figure 9:** Torque-speed characteristics of SRRCC

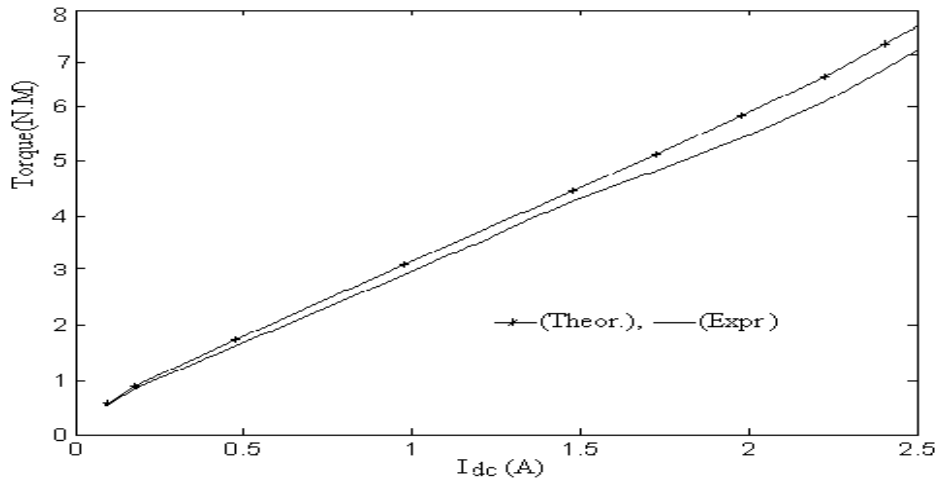


**Figure10:** Torque-rotor rectified current of of SRRCC

**4. Slip Power Recovery Drive System (SPRDS)**  
**4.1 Mathematical Model of SPRD**

The slip power recovery provides the speed control for WRIM below and above the synchronous speed. There are two bridge rectifiers in the slip power recovery system, in which a portion of the power of the rotor is converted into DC by the first diode bridge rectifier, while the second converter works as an inverter that converts the slip power back to AC mains. In a slip power recovery system, the rotor slip power is feedback to mains unlike static chopper resistance control when is wasted in external resistors, such a method has higher efficiency than SRRCC.

The drive input power is equal to the difference between motor input power and the power

$$V_i = \frac{3\sqrt{6} V \cos\alpha}{m \pi}$$

$$V_{dc} + V_i = 0$$

$$s = -\frac{n}{m} \cos\alpha$$

If stator to rotor turn ratio (n) is equal to the grid side to inverter side turn ratio of recovery transformer (m), then the slip will be varying from 0 to 1, and the motor speed can be controlled from synchronous speed to the standstill. Thus, the motor speed can be controlled in the subsynchronous region by controlling the inverter

returned back to the supply. The reactive input power is the sum of motor and inverter reactive powers. Therefore, the drive has a poor power factor during its operation.

**Figures 11 and 12** show the static Kramer and Scherbius slip power recovery scheme of WRIM drive system, respectively. In the Kramer scheme, the speed will be controlled below the synchronous speed, while in the Scherbius scheme the speed will be controlled below and above synchronous speed and [(Taniguchi and Mori 1986) and (Al Zahawi, Jones, et al. 1987)].

In either scheme, the inverter terminal voltage  $V_i$  is given by

$$(10)$$

In an ideal case, where the smoothing inductor resistance is neglected, the voltage equation in DC loop can be written as,

$$(11)$$

The slip as a function of inverter firing angle according to (3) and (11) can be written as,

$$(12)$$

firing angle. In Scherbius scheme the bridge 2 in **Figure 12** works as a rectifier while bridge 1 acts as an inverter and the speed can be controlled above the synchronous speed.

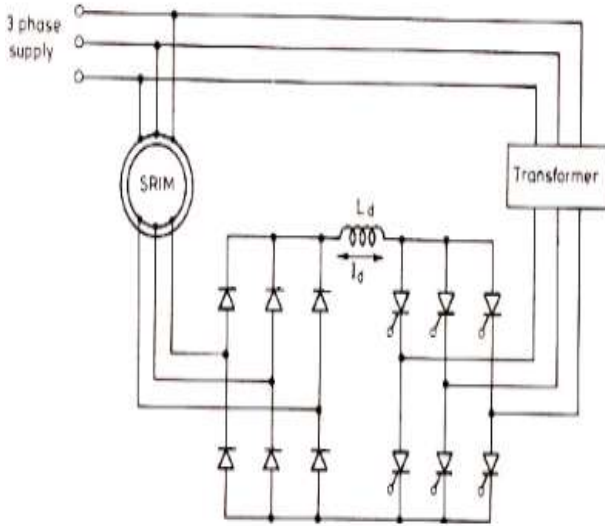


Figure 11: The Static Kramer Scheme

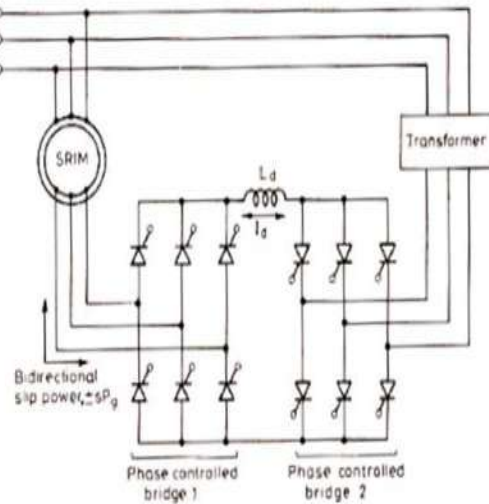


Figure 12: The Scherbius Scheme

4.2 DC Model of SPRD System

The rotor current of the SPRD ideally has six-stepped waves if the commutation effect of the rectifier is neglected and assuming that the link dc current is ripple free, and neglecting the rectifier

$$\text{Slip power} = (V_{dc} - sX_a I_{dc} - 2sR'_s I_{dc})I_{dc} \tag{13}$$

where  $X_a = 3\omega_s(L'_s + L_r)/\pi$ ,  $\omega_s$  is synchronous speed, then the motor developed torque can be written as

$$T_e = [(V_{dc} - sI_{dc}(X_a + 2R'_s)I_{dc})]I_{dc}/s\omega_s \tag{14}$$

4.3 AC Equivalent Circuit Model of SPRDs

The slip power recovery drive is analyzed under the assumption that the rotor phase current is a square pulse of  $2\pi/3$  radians duration in six pulses,

$$P_g = 3E_{rf}I'_{rf}\cos\theta_{rf} \tag{15}$$

where  $\theta_{rf}$  is the phase angle between  $E_{rf}$  and  $I'_{rf}$ . The total power consumed in the rotor circuit will be the sum of mechanical power

$$P_r = -V_i I_d = -\frac{3V I_{rf}}{m} \cos\alpha \tag{16}$$

The electromagnetic torque developed based on AC model is given by [(Lavi and Polge 1966)]

$$T_e = \frac{3}{s\omega_s} [I'^2_{rf}R'_d + V'_c I'_{rf}] \tag{17}$$

where  $R'_d = n^2(R_r + 0.5R_f)$ ,  $R_h = (\frac{\pi^2}{9} - 1)(R_r + 0.5R_f)$  and  $V'_c = -\frac{n}{m}V\cos\alpha$

The AC equivalent circuit indicates that the speed and torque of the machine can be controlled by controlling the counter emf with the firing angle  $\alpha$  as shown in figure 15.

and inverter bridge converter voltage drop. The DC equivalent circuit of the slip power recovery is shown in figure 13. The slip power ( $sp_g$ ) of the slip power recovery drive system is given by

therefore the flux can be assumed sinusoidal. In the fundamental equivalent circuit, as shown in figure 14, the power transferred across the air gap is given by

( $P_m$ ), rotor copper loss ( $P_{cr}$ ), and power feedback by the inverter ( $P_r$ ).

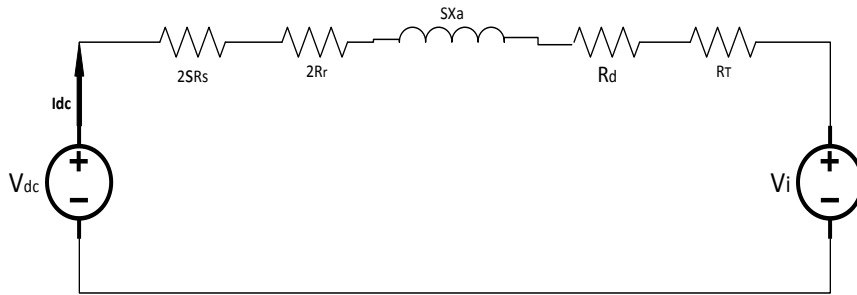


**Figure 13:** DC Equivalent circuit of the SPRD

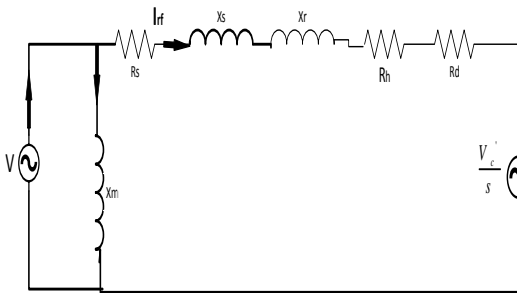


**Figure 14:** The AC Equivalent Circuit of SPRD

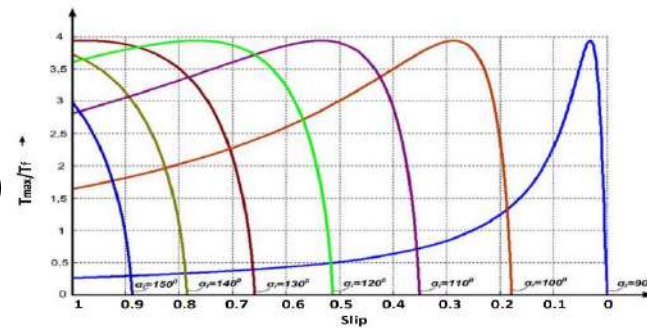


**Figure 15:** The torque slip characteristics of SPRD at Different Firing Angle

## 5. The Effect of Distorted Supply on the WRIM Operation and Performance

A chopper circuit, high-speed static semiconductor devices, is inserted between the diode and inverter bridge as shown in **figure 16**. This chopper converts the constant DC input voltage into variable DC output voltage directly. It controls the output of the inverter by duty cycle and fixing the inverter firing angle to take the minimum reactive power from the supply [(Kumar, Aggarwal et al. 2011)]. The chopper control technology also is used to improve the power factor of SPRDS and to improve the quality of power supply as well. Reducing harmonics in SPRDS is necessary for high power rating applications. Many researchers have contributed in the field of harmonic analysis and harmonic reduction techniques of SPRDS and chopper resistance of WRIM.

[(Mi 1968)] found that the inverter improves the power factor of WRIMDS by the time ratio control of inverter and provides smooth speed control. [(Pillai and Desai 1977)] proposed the static scherbius with drive chopper circuit in which the required speed control was obtained by the duty cycle control of the chopper circuit. For constant firing angle inverter, they concluded that in the absence of the recovery transformer the current distortion in the supply system would increase.

More investigations using chopper power in SPRDS with improving the performance of the conventional system and improving power factor significantly had been presented by [(Doradla, Chakravorty et al. 1985) and (Taniguchi and Mori 1986)]. [(Al Zahawi, Jones et al. 1987)] investigated the effect of rotor rectifier on motor characteristics in SPRDS including the effect of overlap angle and diode voltage drop effect. In meantime [(Taniguchi, Takeda et al. 1987)] demonstrated the performance of static scherbius drive using DC and AC model circuits to improve the power factor and reducing the harmonic ripple current and the torque pulsation.

[(Akpınar, Pillay et al. 1992) and (Akpınar, Pillay et al. 1992)] presented and discussed in detail the starting transient in SPRD, by allowing the resistor develops maximum torque at starting, as well as the effect of overlap angle in rotor rectifier and harmonics reflected by the inverter. [(Baghzouz and Azam 1992)] proposed a technique using a hybrid d-q/abc model to evaluate harmonic distortion in SPRD, taking into account the commutation overlap and DC current ripple. Their technique predicted the voltage and current waveform accurately and computed the individual harmonic components.

The analytical technique to determine the overlap angle of rectifier voltage and the harmonic

prediction was investigated by [(Akpinar, Pillay et al. 1993)]. (Pillay and Refoufi 1994) proposed two new circuit configurations for calculating the performance of the chopper controlled of SPRD. [(Refoufi and Pillay 1994)] compared the harmonic analysis of SPRD generated by rectifier and inverter as well as chopper control techniques to reducing it. [(Zakaria, Shaltout et al. 1996) and (Zakaria, Alwash et al. 1996)] developed the simulation model and carried out the harmonic analysis of a double rotor circuit WRIM to enhance the performance of SPRDS, but with the presence of two rotor circuits and their interaction have increased the complexity of the model.

[(Refoufi, Al Zahawi et al. 1999)] analyzed and compared the results obtained from the hybrid d-q model of DFIG using reference frame theory. [(Marques 1996) &(Marques 1999)] introduced a boost chopper control circuit to improve the performances and control the reactive power based on the rectifier theory. [(Marques and Verdelho 1996)] implemented the series resonant converter based SPRDS as a variable speed drive of WRIM and variable speed constant frequency in DFIG to maintain the rotor current sinusoidal with a unity power factor.

[(Marques and Verdelho 2000)] presented a simple method configuration for a slip power recovery system by connecting a boost chopper between the diode bridge rectifier to the DC link voltage. This method simplified the controller and minimized the cost in comparison with other configurations. [(Panda, Benedict et al. 2001)] described a novel machine side converter and control strategy of DFIM, which consists of a thyristor bridge and boost-buck-boost dc-to-dc converter. In this scheme, the speed is controlled in both region super and sub synchronous speed beside it works as an active filter to compensate any additional harmonics that are injected by the stator of the machine to the utility. The harmonic current of the stator and rotor, the electromagnetic torque pulsation of the SPRD considering harmonics produced by the bridge rectifier, and inverter have been examined by [(Papathanassiou and Papadopoulos 2001)].

[(Tunyasrirut, Kanchanathep et al. 1999, Tunyasrirut, Ngamwiwit et al. 2002)] presented various chopper control methods using fuzzy logic and voltage source inverter for SPRD. In addition to evaluation of the THD in stator current and, it reduced to less than the standard limit,

Using the artificial neural network for controlling the speed and limiting the rotor current of static chopper resistance control of WRIM proposed by [(Abdelfattah and Ahmed 2002)].

[(Lee, Leeb et al. 2005)] proposed a voltage source drive power estimation method to find the relation between fundamental and high harmonic content in the stator current. [(Jarocho 2005)] studied the simulation and experimental test results base on the modified sub-synchronous speed and they found that the new model has a higher power factor and lower THD. [(El-Kholy, Mahmoud et al. 2006)] introduced a new technique for induction motor drive based on the current control space vector to get optimal voltage control and minimum THD.

The steady state analysis of SPRD using the microcontroller technique with increasing efficiency as shown in **figure 17** of the motor presented by [(Dalal, Syam et al. 2006)]. (Altun and Sunter 2007)] have developed the simulation model of slip power and matrix converter to improve the quality of power and conversion efficiency, while the current signal of SPRDS through discrete wavelet transform and harmonic reduction using active power filters have been investigated [(Alwash, Al-Chalabi et al. 2006)].

[(Ameen 2007)] analyzed the effect of duty cycle and switching frequency on the performance of WRIM and torque pulsation, and analyzed harmonics of stator and rotor current waveforms. [(Yang, Xi et al. 2008)] introduced a technique to improve the line power factor of a cascade speed control in WRIM drives by applying power factor correction into cascade speed control.

[(Ameen, K. et al. 2010)] proposed a boost chopper in a static rotor resistance control system in which the stator and rotor current distortion have been reduced to about 2.9%. [(Joksimović 2010)] made the analysis expression of stator current harmonics frequencies in the spectrum of saturated cage and WRIM based on the mmf permeance wave approach. [(Tunyasrirut, Kinnares et al. 2010) and (Tunyasrirut and Kinnares 2013)] presented the line harmonic current reduction by the voltage source inverter and improving the power factor of the drive by applying a boost in which the THD is reduced to below the standard limits and power factor to about 0.85 at half of the rated speed. [(Ameen 2011)] analyzed the dynamic and steady state performance of SRRCC of WRIM using reference frame theory, further, he studied the effect of duty cycle on the performance of the

motor. The injection of the third harmonic technique to the rotor circuit of chopper resistance control was done by [(Ameen 2011), it has been observed that the THD of the proposed technique and its power factor improved by 3.12% and 0.84 respectively.

[(Jaiswal, Joshi et al. 2012)] demonstrated the harmonic characteristics of currents and voltages of SPRDS with a comparison of harmonic contents of drive waveforms over a wide range of operating speed based on THD criteria. [(Hernández and Madrigal 2013)] developed a DFIM model for steady state harmonic analysis by taking into account the non-sinusoidal voltage source on the stator and rotor side of the machine, the results showed that harmonics of current exist on both sides of the machine depend on the slip and fundamental frequency of both voltage sources. [(Ajabi-Farshbaf and Azizian 2014)] introduced an SPRD consisting of a diode rectifier, a boost chopper, and three T-type converters to improve power factor and reducing the voltage output THD of WRIM in industrial applications.

[(Pardhi, Yadavalli et al. 2014),(Manoliu 2014) and (Ram, Rahi et al. 2015)] presented the study of SPRD with DC voltage intermediate circuit and the three types of PWM techniques. It has been observed that THD is reduced by 3.4%. [(Chen and Jiang 2015)] developed a double field model for steady state harmonic analysis taking into consideration the distorted supply source on the stator and rotor side of the machine. The effect of the stator supply harmonics of WRIM and DFIM on the pulsating torque and additional frame vibration have been investigated [(Djurović, Vilchis-Rodriguez et al. 2015)].

[(Lerch and Rad 2016)] demonstrated the power loss results in IM supplied with distorted voltage

considering the effect of each of core losses, windage losses, and additional losses are resulting from distorted power supply conditions. [(Yao, Cosic et al. 2015)] studied the WRIM with a novel concept of the rotor fed by a converter, it has been obtained that the power factor and efficiency improved significantly. [(Yao and Sadarangani 2016)] proposed a novel idea of a rotating converter on the rotor of WRIM, and it is found that the efficiency and power factor improved significantly.

[(Sarma and Tuohy 2018)] studied the effect of voltage grid harmonics on the stator current of WRIMDS by using finite element time-stepping transient model and conductor distribution function. [(Bajjuri and Jain 2018)] presented torque ripple estimation and reduction in a vector controlled double inverter fed of WRIM by employing different pulse width modulation techniques applied to both stator and rotor side voltage source inverter. [(Beleiu, Maier et al. 2020)] analyzed the effect of voltage waveform distortion on IM, mechanically and electrically, by applying the negative and positive sequence harmonics as a percentage of the fundamental, as well as the level of the stator current harmonics, and its effect on the electromagnetic torque, power factor and efficiency have been considered.

From the previous researches' results, it has been found that the different techniques of reducing harmonic distortion are used, depending on the slip and the fundamental frequency of the supply. Moreover, the negative effect of harmonics on the speed, torque, and power factor have been investigated.

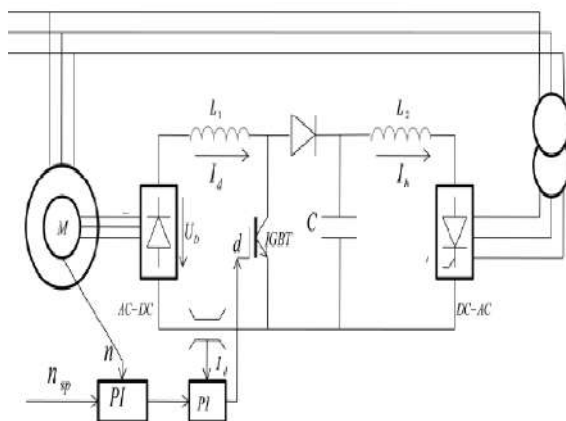


**Figure 16 :** Control scheme of SPR with chopper

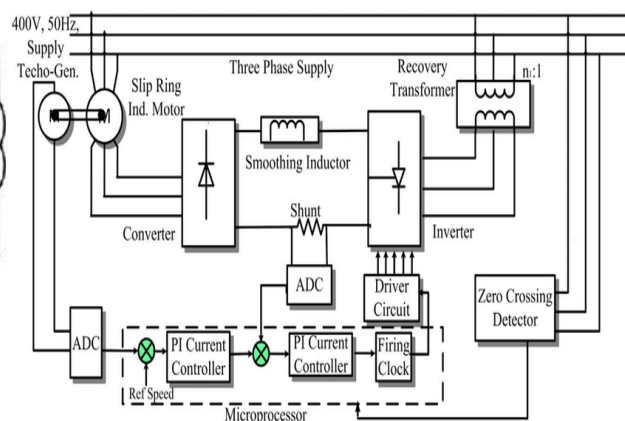


**Figure 17:** Closed loop SPRD



## 6. The Effect of Unbalance Supply Voltage on the performances of IM and WRIMD

The electrical machines are designed to operate under symmetrical and sinusoidal supply voltage conditions. However, voltage and current in the electrical power system are asymmetry and distorted by the effect of the non-linear loads. Induction motors like all other machines are designed to work under sinusoidal and balanced supply voltage. **Figures 18 and 19** show the derating of the efficiency and increase in the losses with increasing with a voltage unbalance

$$\%VUF = \frac{V_n}{V_p} \cdot 100 \quad (18)$$

$$\%LVUR = \frac{\text{Max Voltage Deviation from the Avg Line Voltage}}{\text{Avg Line Voltage}} \cdot 100 \quad (19)$$

$$\%PVUR = \frac{\text{Max Voltage Deviation from the Avg Phase Voltage}}{\text{Avg Phase Voltage}} \cdot 100 \quad (20)$$

where  $V_n$ ,  $V_p$ , and Avg are the negative sequence component, positive sequence component, and the average voltage, respectively.

In the literature review, many researchers have studied induction machines operating under an unbalanced voltage supply and its performance based on the positive and negative equivalent circuit as shown in **figure 20**. [(Woll 1975)] demonstrated that the effect of the unbalanced supply voltage is quite detrimental to successful motor operation, farther, it has been seen that an extremely serious loss of insulation life can be expected even with a voltage unbalance as low as 2%. [(Kersting 2000)] proposed a simple system using two transformers connections in order to find how these connections contribute to the voltage unbalance. [(Pillay, Hofmann et al. 2002) and (Wang 2001)] examined the proper application of IM in the presence of a combination of unbalance voltage and over voltage or under voltages and addressed the impact on the derating curve established.

[(Siddique, Yadava et al. 2004)] studied the effect of different voltage magnitude unbalance with the same voltage unbalance factor on the stator and rotor copper losses of three classes of three phase IM, while [(Pillay and Manyage 2006)] studied the loss of life of IM when supplied by unbalanced voltages, also, it has been estimated the motor life based on the thermal model parameters. [(Anwari and Hiendro 2010, Kostic and Nikolic 2010) studied the effect of unbalance supply on the IM performance considering the

factor [(Von Jouanne, 2001)]. Any quantities of unbalance will make the motor temperature rise and derating the power output. As per NEMA guidelines, operating a motor for any period of time at voltage unbalance above 5% is not recommended.

The general definition of voltage unbalance according to different principles are the IEC definition VUF, NEMA definition LVUR and IEEE definition PVUR [(Von Jouanne, 2001) ].

skin effect, and introducing the new unbalance factor for over and under rated voltage respectively. [(Singh, Singh et al. 2012)] proposed a new algorithm to determine the phase angle of voltage unbalance factor from the line voltage. Moreover, the presented the economic analysis for the different conditions of voltage index and it was shown that economical loss is more in the case under voltage condition in comparison to over voltage and equal voltage condition. [(Guasch-Pesquer, Youb et al. 2012) analyzed the effect of voltage unbalance on torque and current of IM at different unbalanced situations.

[(Youb 2014) and (Patil and Chaudari 2015)] investigated the negative effect of unbalance voltage on the performance parameters of IM, and verified their results by using MATLAB simulation. They concluded that the current unbalance factor is equal to 6 to 10 times the percent voltage unbalance factor. [(Quispe, Gomez et al. 2015)&(Kumar, Celliah et al. 2015)] presented the impact of unbalanced supply voltage on the energy-efficient of squirrel cage induction motors and on double field induction generators, respectively. [(Guasch-Pesquer, Jaramillo-Matta et al. 2017) and (Sudasinghe, Perera et al. 2018)] presented the effect of voltage unbalance in both complex current unbalance factor and torque ripple factor of three phase IM. From the simulation, they showed that only the voltage unbalance factor and positive voltage sequence parameters have a big influence in torque ripple factor and current unbalance factor. The detailed analysis of the impact of positive and negative

sequence voltage components and the angle between them on the motor behavior has been presented by [(Quispe, López et al. 2018)]. [(Adekitan and Abdulkareem 2019) and (Adekitan, Ogunjuyigbe et al. 2019)] have revealed the significance of the manner of variation of the positive sequence voltage component on the motor losses, output power, and sensitivity of parameters of three phase IM. [(El-Kharashi, Massoud et al. 2019)] investigated and studied the performance and efficiency of two types of motors where they are mechanically combined and have been operated under balanced

and unbalanced supply voltages. [(Donolo, Pezzani et al. 2020)] have presented the comparison of derating factor that has been provided by standards IEEE and NEMA to maintain the losses at rated value.

From the above, we can see that the voltage asymmetry appears to be much more harmful to the IM performance than distorted voltage. The effect of harming includes overheating, line current unbalance, derating of output power, torque pulsation, low efficiency (increasing losses), etc.

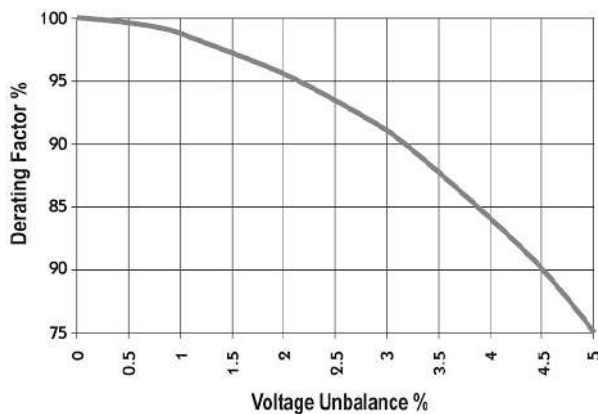


**Figure 18:** The Derating Factor against the voltage unbalance ratio

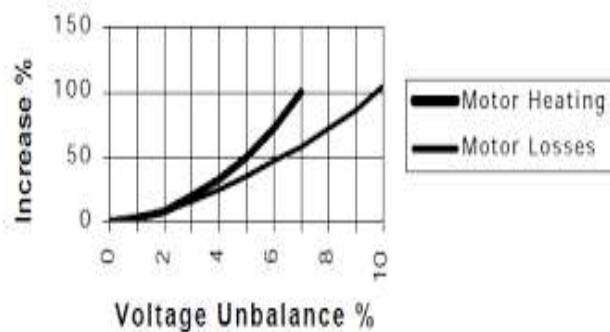


**Figure 19:** The Loss increasing with increasing the voltage unbalance ratio

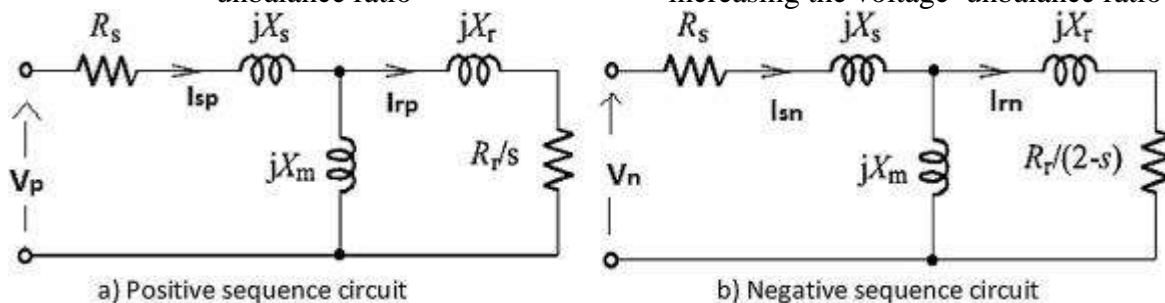


**Figure 20:** The positive and negative sequence equivalent circuit of IM under unbalance supply

## 7. The Effect of Distorted and Unbalance Supply Voltage on The WRIM Performance

The three-phase WRIM is operated below rated power when it is supplied by voltage networks that are unbalanced and distorted, that is because of an increase in losses. **Figure 21** shows the distorted balanced supply while **figure 22** shows the distorted unbalanced supply waveforms applied on the same three phase IM.

(Eguiluz, Lavandero et al. 1999) presented the behavior of an induction motor supplied by non-sinusoidal and unbalanced networks, and they investigated those additional losses caused to induction motor when supplied by such systems.

[(de Abreu and Emanuel 2000) studied the effect of voltage unbalance and distortion upon thermal aging of IM insulation based on three dimensional modeling of heat transfer flow and monitored the temperature of hot spots of the insulation materials. [(Quispe, Gonzalez et al. 2004)] investigated the proper application of IM when subjected to unbalance and harmonic voltages, and they proposed a technique that showed a poor quality voltage have a bad impact on the motor characteristics, losses, temperature rise, derating of output power, efficiency, noise, current in bearing, and reliability of the machine.

A detailed analysis study on the effect of unbalance voltage in mains on the harmonic injected by three phase AC to DC rectifier with a new term named as phase total harmonic distortion unbalance factor (PTHDF) have been introduced by [(Singh, Singh et al. 2006)]. [(Ramos, Martins et al. 2007)] presented and proposed a controller for minimizing the effect of unbalanced and distorted stator voltage on the rotor current and overall motor performance of the DFIG. [(Khoobroo, Fahimi et al. 2008)] investigated the combined effect of unbalance and harmonics on the electromagnetic performance of IM. They also studied in their work the relation between harmonics existence and unbalanced operating conditions to measurable parameters such as voltage, current, and harmonics.

[(Duarte and Kagan 2010)] discussed the need for simultaneously monitoring voltage unbalance and harmonic distortion and a new power quality index has been proposed to combine the effect of voltage unbalance and harmonic distortion. [(Sousa, Viego et al. 2015)] proposed a new method based on the equivalent circuits of IM fed with harmonics and unbalanced supply voltages simultaneously and they calculated parameters by applying Bacterial Forging Algorithm as a technique of evolutionary search. The behavior of torque and efficiency of three phase IM when simultaneously supplied with imbalance voltage and harmonic distortion have been investigated by (Neves, de Mendonça et al. 2016)]. In meantime, [(Donolo, Bossio et al. 2016)] presented the effect of unbalance and harmonic voltage distortion on power factor, torque, and vibration of IM. Their results showed that vibrations are only presented during high level voltages' unbalance and harmonic distortion.

[(Al-Badri, Pillay et al. 2017)] proposed an algorithm for in situ efficiency estimation of an induction motor operating under distorted unbalance voltages by using genetic algorithm procedures. Further proposed techniques to identify rotor harmonics from slip frequency, are determined by using the space time symmetrical characteristics of IM [(Zhang, An et al. 2017)].

[(Deleanu, Iordache et al. 2019)] studied the operation of the three phase IM when energized from an unbalanced voltage supply with the presence of harmonics with considering the skin effect due to the higher frequency harmonics on the overall motor performance. [(Donolo, Pezzani et al. 2020)] presented the voltage unbalance and harmonic distortion effect on the losses of IM in different efficiencies classes and it has been seen that IM losses due to voltage unbalance and harmonic distortion are greater in high efficiency class and derating factors are not enough to avoid overload on high efficiency class IMs.

From the above studies, we detected that analyzing the WRIM stator resistance chopper control and SPRDS when supplied by distorted and unbalanced supply voltage simultaneously require more investigations and researches. The presence of a rotor bridge rectifier and inverter, in addition to the low-quality supply, led to more power derating and loss of life of IM insulations.

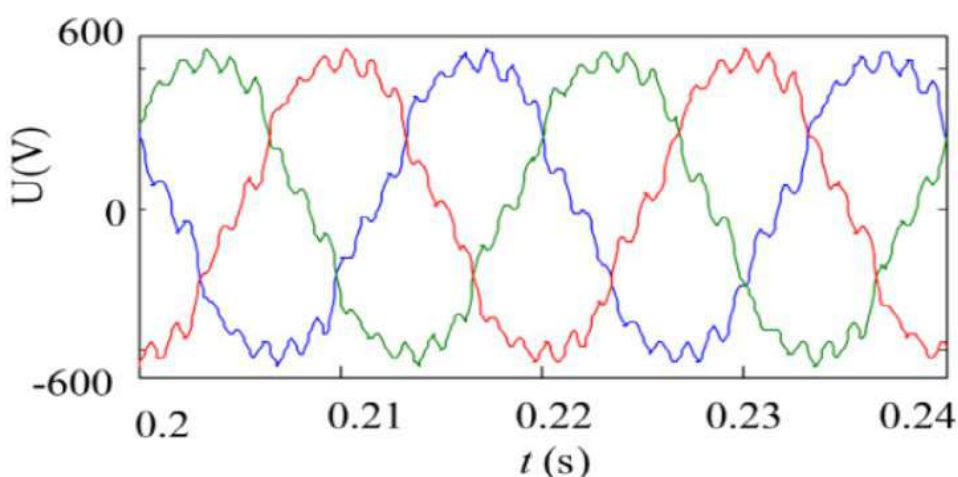


**Figure 21:** Voltage wave form with balance and THD of 10%

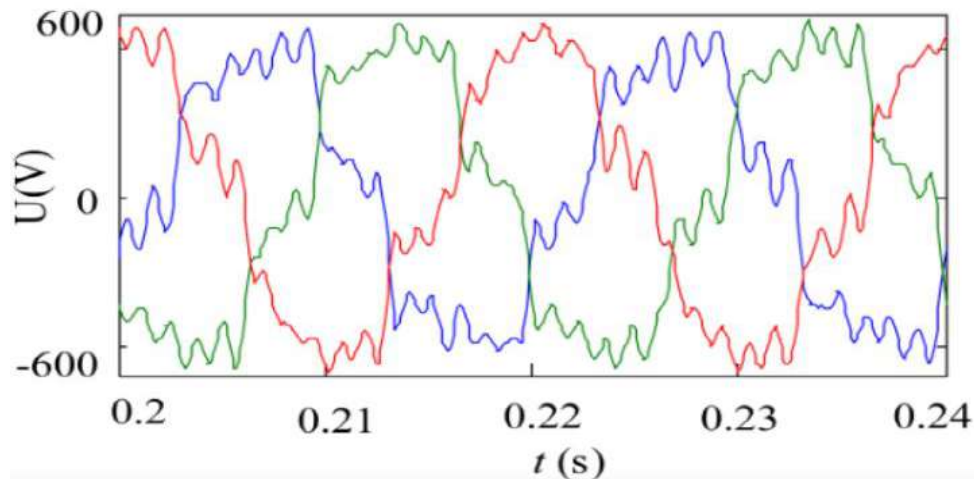


**Figure 22:** Voltage waveform with CVUF (5%) and THD of 20%

### 8- The Latest Trends and Future Developments in WRIM Drive System

The WRIM drive system specifically the SPRD system was developed and utilized in vast applications in the range of a few kilowatts to megawatt machine sizes. Such system adopts with advanced electronic subsystems such as converters, Rotor rectifier, DC link smoothing inductor, and recovery transformer. However, there are new developments in the ac-dc-ac converter for further improvements in their performance such as , increasing chopper frequency, boost chopper, buck boost chopper, multi-level inverter, PWM types inverter, and increasing the smoothing inductor value. These converters improvement provide improved power quality and WRIM drive system performance like a power factor, THD, efficiency of the system, speed, and torque pulsation.

The aim of this survey is to outline the study of the performance of WRIM drive system under unbalance supply voltage and combination of the unbalanced and distorted supply voltage simultaneously. The lack of researches in this field and low power quality in nowadays due to increasing in nonlinearity of loads, make the mains have distorted and unbalanced.

### 9. Conclusion

The intensive investigations spread in the last decades indicate the visibility of using adjustable speed drive to WRIM control in the rotor side with various methodologies and control techniques. Most of researches published in the harmonic analysis and performance improvement, static rotor resistance control, and SPRDS. A few papers have been presented the effects of the unbalanced supply of squirrel cage IM, and some papers have been dealt with the effect of distorted

supply waveforms and unbalance supply voltage on the performance of IM.

It is found that the converters in the rotor side of WRIM drive system inject harmonic to the power supply, resulting in low power factor, and increasing the torque and speed pulsation. Various methods have been suggested by several authors to overcome these problems. Each technique has advantages and disadvantages with respect to power quality, complexity, cost, size, and applications. It is concluded that the multi-level inverters produce output voltage with very low distortion components in SPRD system. The brief history of beginning the speed control of WRIM during the last five decades has been outlined without taking into consideration the effect of unbalance supply voltage and unbalance supply voltage combined with distorted supply on the performance and operation of WRIM drive system.

This survey has focused on several areas and the current status of research of WRIMDS as well as an extension for the future work in the area of the impact of unbalanced supply voltage and distorted supply voltage simultaneously on the performance of SRRCC of and SPRD of WRIM. The objective and future outcome of this survey are to find out the effect of supply voltage asymmetry and distortion in separate and simultaneously on the performance of WRIM drive system.

### REFERENCES

- Abdelfattah, M. and M. Ahmed (2002). An artificial neural network-based chopper-controlled slip-ring induction motor. 11th IEEE Mediterranean Electrotechnical Conference (IEEE Cat. No. 02CH37379), IEEE.
- Adekitan, A., et al. (2019). "The impact of supply phase shift on the three phase induction motor operation."

- Engineering Review: Međunarodni časopis namijenjen publiciranju originalnih istraživanja s aspekta analize konstrukcija, materijala i novih tehnologija u području strojarstva, brodogradnje, temeljnih tehničkih znanosti, elektrotehnike, računarstva i građevinarstva **39**(3): 270-282.
- Adekitan, A. I. and A. Abdulkareem (2019). "The significance of the mode of voltage imbalance on the operation and energy losses of a 3-phase induction motor." Engineering and Applied Science Research **46**(3): 200-209.
- Ajabi-Farshbaf, R. and M. R. Azizian (2014). Slip power recovery of induction machines using three-Level T-type converters. The 5th Annual International Power Electronics, Drive Systems and Technologies Conference (PEDSTC 2014), IEEE.
- Akpinar, E., et al. (1992). "Starting transients in slip energy recovery induction motor drives. I. Formulation and modeling." IEEE Transactions on Energy Conversion **7**(1): 238-244.
- Akpinar, E., et al. (1992). "Starting transients in slip energy recovery induction motor drives. II. Flowchart and performance." IEEE Transactions on Energy Conversion **7**(1): 245-251.
- Akpinar, E., et al. (1993). "Calculation of the overlap angle in slip energy recovery drives using ad, q/abc model." IEEE Transactions on Energy Conversion **8**(2): 229-235.
- Al-Badri, M., et al. (2017). "A novel in situ efficiency estimation algorithm for three-phase induction motors operating with distorted unbalanced voltages." IEEE Transactions on Industry Applications **53**(6): 5338-5347.
- Al Zahawi, B., et al. (1987). "Effect of rotor rectifier on motor performance in slip recovery drives."
- Altun, H. and S. Sunter (2007). Application of matrix converter to doubly-fed induction motor for slip energy recovery with improved power quality. 2007 International Aegean Conference on Electrical Machines and Power Electronics, IEEE.
- Alwash, S., et al. (2006). "Closed-loop control of a double-circuit-rotor slip energy recovery drive system." Electric Power Components and Systems **34**(1): 61-78.
- Ameen, H. F. (2007). "Stator Current Harmonic Analysis and Torque Pulsation of Wound Rotor Induction Motor Speed Control by Chopper Resistance in Rotor Circuit " Zanco Journal of pure and Applied Science **19**(1): 123-134.
- Ameen, H. F. (2011). "Computer simulation and mathematical modelling of static rotor resistance chopper control of WRIM by reference frame theory." Procedia Computer Science **3**: 1009-1017.
- Ameen, H. F. (2011). "Minimizing Rotor Current Distortion and Power Factor Improvement of WRIM Chopper Resistance Control Using Third Harmonic Current Injection " Zanco Journal of pure and Applied Science **23**(2): 23-37
- Ameen, H. F., et al. (2010). "Total Harmonic Reduction of Wound Rotor Induction Motor Chopper Resistance Control Using Three Phase Boost Rectifier in Rotor Circuit " Zanco Journal of pure and Applied Science **22**(3): 10-22.
- Anwari, M. and A. Hiendro (2010). "New unbalance factor for estimating performance of a three-phase induction motor with under-and overvoltage unbalance." IEEE Transactions on Energy Conversion **25**(3): 619-625.
- Baghzouz, Y. and M. Azam (1992). "Harmonic analysis of slip-power recovery drives." IEEE Transactions on Industry Applications **28**(1): 50-56.
- Bajjuri, N. K. and A. K. Jain (2018). "Torque Ripple Reduction in Double-Inverter Fed Wound Rotor Induction Machine Drives Using PWM Techniques." IEEE Transactions on Industrial Electronics **66**(6): 4250-4261.
- Beleiu, H. G., et al. (2020). "Harmonics Consequences on Drive Systems with Induction Motor." Applied Sciences **10**(4): 1528.
- Chen, W.-L. and B.-Y. Jiang (2015). "Harmonic suppression and performance improvement for a small-scale grid-tied wind turbine using proportional-resonant controllers." Electric Power Components and Systems **43**(8-10): 970-981.
- Dalal, A. K., et al. (2006). Use of matrix converter as slip power regulator in doubly-fed induction motor drive for improvement of power quality. 2006 IEEE power India conference, IEEE.
- Datta, R. and V. Ranganathan (2013). "Rotor side control of grid-connected wound rotor induction machine." Journal of the Indian Institute of Science **80**(5): 437.
- de Abreu, J. P. G. and A. E. Emanuel (2000). Induction motors loss of life due to voltage imbalance and harmonics: a preliminary study. Ninth International Conference on Harmonics and Quality of Power. Proceedings (Cat. No. 00EX441), IEEE.
- Deleanu, S., et al. (2019). The Induction Machine Operating from a Voltage Supply, Unbalanced and Polluted with Harmonics: A Practical Approach. 2019 15th International Conference on Engineering of Modern Electric Systems (EMES), IEEE.
- Djurović, S., et al. (2015). "Supply induced interharmonic effects in wound rotor and doubly-fed induction generators." IEEE Transactions on Energy Conversion **30**(4): 1397-1408.
- Donolo, P., et al. (2016). "Voltage unbalance and harmonic distortion effects on induction motor power, torque and vibrations." Electric power systems research **140**: 866-873.
- Donolo, P. D., et al. (2020). "Derating of induction motors due to power quality issues considering the motor efficiency class." IEEE Transactions on Industry Applications **56**(2): 961-969.
- Doradla, S., et al. (1985). A new slip power recovery scheme with improved supply power factor. 1985 IEEE Power Electronics Specialists Conference, IEEE.
- Duarte, S. X. and N. Kagan (2010). "A power-quality index to assess the impact of voltage harmonic distortions and unbalance to three-phase induction motors." IEEE Transactions on Power Delivery **25**(3): 1846-1854.
- Eguiluz, L., et al. (1999). Performance Analysis of a three-phase induction motor under non-sinusoidal and unbalanced conditions. IEEE International Symposium on Diagnostic for electrical machines,

- power electronics and drives. Gijón, España, Citeseer.
- El-Kharashi, E., et al. (2019). "The impact of the unbalance in both the voltage and the frequency on the performance of single and cascaded induction motors." Energy **181**: 561-575.
- El-Kholy, E., et al. (2006). "Analysis and implementation of a new space vector current regulation for induction motor drives." Electric Power Components and Systems **34**(3): 303-319.
- Guasch-Pesquer, L., et al. (2017). Analysis of Current Unbalance and Torque Ripple Generated by Simulations of Voltage Unbalance in Induction Motors. Workshop on Engineering Applications, Springer.
- Guasch-Pesquer, L., et al. (2012). Effects of voltage unbalance on torque and current of the induction motors. 2012 13th International Conference on Optimization of Electrical and Electronic Equipment (OPTIM), IEEE.
- Hernández, E. and M. Madrigal (2013). "A step forward in the modeling of the doubly-fed induction machine for harmonic analysis." IEEE Transactions on Energy Conversion **29**(1): 149-157.
- Jaiswal, K., et al. (2012). Harmonic analysis of slip power recovery drives. 2012 IEEE 5th India International Conference on Power Electronics (IICPE), IEEE.
- Jarochoa, R. (2005). Comparison of the modified subsynchronous cascade drive. 2005 European Conference on Power Electronics and Applications, IEEE.
- Joksimović, G. (2010). Stator current harmonics in saturated cage and wound rotor induction motors. The XIX International Conference on Electrical Machines-ICEM 2010, IEEE.
- Kersting, W. (2000). Causes and effects of unbalanced voltages serving an induction motor. 2000 Rural Electric Power Conference. Papers Presented at the 44th Annual Conference (Cat. No. 00CH37071), IEEE.
- Khoobroo, A., et al. (2008). Effects of system harmonics and unbalanced voltages on electromagnetic performance of induction motors. 2008 34th Annual Conference of IEEE Industrial Electronics, IEEE.
- Kostic, M. and A. Nikolic (2010). "Negative consequence of motor voltage asymmetry and its influence to the unefficient energy usage." WSEAS transactions on circuits and systems **9**(8): 547-552.
- Kumar, A., et al. (2011). "Performance analysis of a microcontroller based slip power recovery drive." International Journal of Engineering, Science and Technology **3**(3).
- Kumar, N., et al. (2015). "Analysis of Doubly-Fed Induction Machine operating at motoring mode subjected to symmetrical voltage sag."
- Lavi, A. and R. Polge (1966). "Induction motor speed control with static inverter in the rotor." IEEE Transactions on Power Apparatus and Systems(1): 76-84.
- Lee, K. D., et al. (2005). "Estimation of variable-speed-drive power consumption from harmonic content." IEEE Transactions on Energy Conversion **20**(3): 566-574.
- Lerch, T. and M. Rad (2016). "Influence of higher harmonics on losses in induction machines." Czasopismo Techniczne **2016**(Elektrotechnika Zeszyt 3-E 2016): 13-24.
- Manoliu, V. (2014). Mathematical modeling of an induction motor with chopper-controlled rotor resistance. 2014 International Symposium on Fundamentals of Electrical Engineering (ISFEE), IEEE.
- Marques, G. (1996). Performance evaluation of the slip power recovery system with a DC voltage intermediate circuit and a LC filter on the rotor. Proceedings of IEEE International Symposium on Industrial Electronics, IEEE.
- Marques, G. (1999). "Numerical simulation method for the slip power recovery system." IEE Proceedings-Electric Power Applications **146**(1): 17-24.
- Marques, G. and P. Verdelho (1996). Control of a slip power recovery system with a DC voltage intermediate circuit. PESC Record. 27th Annual IEEE Power Electronics Specialists Conference, IEEE.
- Marques, G. D. and P. Verdelho (2000). "A simple slip-power recovery system with a DC voltage intermediate circuit and reduced harmonics on the mains." IEEE Transactions on Industrial Electronics **47**(1): 123-132.
- Mi, P. N. (1968). "The through-pass inverter and its application to the speed control of wound rotor induction machines." IEEE Transactions on Power Apparatus and Systems(1): 234-239.
- Neves, A. B. F., et al. (2016). Effects of voltage unbalance and harmonic distortion on the torque and efficiency of a Three-Phase Induction Motor. 2016 17th International Conference on Harmonics and Quality of Power (ICHQP), IEEE.
- Panda, D., et al. (2001). A novel control strategy for the rotor side control of a doubly-fed induction machine. Conference Record of the 2001 IEEE Industry Applications Conference. 36th IAS Annual Meeting (Cat. No. 01CH37248), IEEE.
- Papathanassiou, S. and M. Papadopoulos (2001). "On the harmonics of the slip energy recovery drive." IEEE Power Engineering Review **21**(4): 55-57.
- Pardhi, C., et al. (2014). A study of slip-power recovery schemes with a buck dc Voltage intermediate circuit and reduced harmonics on the mains by various PWM techniques. International Conference on Computation of Power, Energy, Information and Communication.
- Patil, R. U. and H. Chaudari (2015). "Behavior of Induction Motor at Voltage Unbalanced." Int. J. Eng. Res. Tech.(IJERT) **4**(05): 1344-1348.
- Pillai, S. and K. Desai (1977). "A static Scherbius drive with chopper." IEEE Transactions on Industrial Electronics and Control Instrumentation(1): 24-29.
- Pillay, P., et al. (2002). "Derating of induction motors operating with a combination of unbalanced voltages and over or undervoltages." IEEE Transactions on Energy Conversion **17**(4): 485-491.
- Pillay, P. and M. Manyage (2006). "Loss of life in induction machines operating with unbalanced supplies." IEEE Transactions on Energy Conversion **21**(4): 813-822.

- Pillay, P. and L. Refoufi (1994). "Calculation of slip energy recovery induction motor drive behavior using the equivalent circuit." *IEEE Transactions on Industry Applications* **30**(1): 154-163.
- Quispe, E., et al. (2004). Influence of unbalanced and waveform voltage on the performance characteristics of three-phase induction motors. International Conference on Renewable Energies and Power Quality, Barcelona.
- Quispe, E. C., et al. (2015). Impact of Voltage Unbalance on the Energy Performance of Three-Phase Single Cage Induction Motors, 9th Energy Efficiency in Motor Driven Systems (EEMODS'15), Helsinki, Finland.
- Quispe, E. C., et al. (2018). "Unbalanced voltages impacts on the energy performance of induction motors."
- Ram, S., et al. (2015). "Performance analysis of slip power recovery scheme employing two inverter topologies."
- Ramamoorthy, M. and N. Wani (1978). "Dynamic model for a chopper-controlled slip-ring induction motor." *IEEE Transactions on Industrial Electronics and Control Instrumentation*(3): 260-266.
- Ramos, C., et al. (2007). Rotor current controller with voltage harmonics compensation for a DFIG operating under unbalanced and distorted stator voltage. IECON 2007-33rd Annual Conference of the IEEE Industrial Electronics Society, IEEE.
- Refoufi, L., et al. (1999). "Analysis and modeling of the steady state behavior of the static Kramer induction generator." *IEEE Transactions on Energy Conversion* **14**(3): 333-339.
- Refoufi, L. and P. Pillay (1994). "Harmonic analysis of slip energy recovery induction motor drives." *IEEE Transactions on Energy Conversion* **9**(4): 665-672.
- Sarma, N. and P. M. Tuohy (2018). Investigation of grid supply harmonic effects in wound rotor induction machines. 2018 5th International Conference on Electrical and Electronic Engineering (ICEEE), IEEE.
- Sen, P. C. and K. Ma (1975). "Rotor chopper control for induction motor drive: TRC strategy." *IEEE Transactions on Industry Applications*(1): 43-49.
- Siddique, A., et al. (2004). Effects of voltage unbalance on induction motors. Conference Record of the 2004 IEEE International Symposium on Electrical Insulation, IEEE.
- Singh, A. K., et al. (2006). Evaluation of harmonic distortion under unbalanced supply conditions. 2006 IEEE International Conference on Industrial Technology, IEEE.
- Singh, S. B., et al. (2012). Assessment of induction motor performance under voltage unbalance condition. 2012 IEEE 15th International Conference on Harmonics and Quality of Power, IEEE.
- Sousa, V., et al. (2015). Estimating induction motor efficiency under no-controlled conditions in the presences of unbalanced and harmonics voltages. 2015 CHILEAN Conference on electrical, electronics engineering, information and communication technologies (CHILECON), IEEE.
- Sudasinghe, P., et al. (2018). Revisiting the effects of supply voltage unbalance on the losses of three phase induction motors. 2018 Australasian Universities Power Engineering Conference (AUPEC), IEEE.
- Taniguchi, K. and H. Mori (1986). Applications of a power chopper to the thyristor Scherbius. IEE Proceedings B (Electric Power Applications), IET.
- Taniguchi, K., et al. (1987). High-performance slip-power recovery induction motor. IEE Proceedings B (Electric Power Applications), IET.
- Tunyasrirut, S., et al. (1999). Fuzzy logic control for speed of wound rotor induction motor with slip energy recovery. SICE'99. Proceedings of the 38th SICE Annual Conference. International Session Papers (IEEE Cat. No. 99TH8456), IEEE.
- Tunyasrirut, S. and V. Kinnarees (2013). "Speed and power control of a slip energy recovery drive using voltage-source PWM converter with current controlled technique." *Energy Procedia* **34**: 326-340.
- Tunyasrirut, S., et al. (2010). "Performance improvement of a slip energy recovery drive system by a voltage-controlled technique." *Renewable Energy* **35**(10): 2235-2242.
- Tunyasrirut, S., et al. (2002). Fuzzy logic controlled inverter-chopper for high performance of slip energy recovery system. Proceedings of the 41st SICE Annual Conference. SICE 2002., IEEE.
- Von Jouanne, A. and B. Banerjee (2001). "Assessment of voltage unbalance." *IEEE Transactions on Power Delivery* **16**(4): 782-790.
- Wang, Y.-J. (2001). "Analysis of effects of three-phase voltage unbalance on induction motors with emphasis on the angle of the complex voltage unbalance factor." *IEEE Transactions on Energy Conversion* **16**(3): 270-275.
- Woll, R. (1975). "Effect of unbalanced voltage on the operation of polyphase induction motors." *IEEE Transactions on Industry Applications*(1): 38-42.
- Yang, X.-h., et al. (2008). Research on the application of PFC technology in cascade speed control system. 2008 3rd IEEE Conference on Industrial Electronics and Applications, IEEE.
- Yao, Y., et al. (2015). "Power factor improvement and dynamic performance of an induction machine with a novel concept of a converter-fed rotor." *IEEE Transactions on Energy Conversion* **31**(2): 769-775.
- Yao, Y. and C. Sadarangani (2016). Optimum operating point of an induction machine using a rotor integrated converter with a floating capacitor. 2016 IEEE 8th International Power Electronics and Motion Control Conference (IPEMC-ECCE Asia), IEEE.
- Youb, L. (2014). "Effects of unbalanced voltage on the steady state of the induction motors." *International Journal of Electrical Energy* **2**(1): 34-38.
- Zakaria, W., et al. (1996). "A novel double-circuit-rotor balanced induction motor for improved slip-energy recovery drive performance. I. Modeling and simulation." *IEEE Transactions on Energy Conversion* **11**(3): 556-562.
- Zakaria, W., et al. (1996). "A novel double-circuit-rotor balanced induction motor for improved slip-energy recovery drive performance. II. Experimental verification and harmonic analysis." *IEEE*

Transactions on Energy Conversion **11**(3): 563-569.

Zhang, D., et al. (2017). "Effect of voltage unbalance and distortion on the loss characteristics of three-phase cage induction motor." IET Electric Power Applications **12**(2): 264-270.